LITHOSPHERIC STRUCTURE OF PROTEROZOIC-PHANEROZOIC AUSTRALIA AND PAPUA NEW GUINEA.

by

DOUGLAS McKNIGHT FINLAYSON

A thesis submitted for examination under the terms and conditions applying for the award of the Higher Degree of

DOCTOR of SCIENCE (D.Sc.)
in the
UNIVERSITY of EDINBURGH

December 1983

SUMMARY

This thesis contains twenty-nine published papers relevant to a greater understanding of lithospheric structure in central and eastern Australia and in Papua New Guinea. Most of the papers contain research involving the application of explosion seismic methods to the determination of structures down to depths not greater than 100 km from the Earth's surface, and the subsequent interpretation of these structures in terms of the known geology of the various geological provinces.

No attempt has been made to summarise separately the results of the the papers because such reviews are contained in some of the papers submitted. The papers collectively make a significant contribution to knowledge of the deep geology and lithospheric structure of continental Australia and its outer margins to the northeast, adjacent to the Pacific lithospheric plate.

All the papers have been subject to the normal refereeing proceedures of the Bureau of Mineral Resources, Geology and Geophysics and of the journals within which they have been published.

CONTENTS

Submitted papers:

1. Finlayson, D.M. & Collins, C.D.N., 1980 - A brief description of BMR portable seismic tape recording systems. Aust. Soc. Expl. Geophys. Bull., 11, 75-77.
2. Finlayson, D.M., Cull, J.P., Wiebenga, W.A., Furumoto, A.S. & Webb, J.P., 1972 - New Britain - New Ireland crustal seismic refraction investigations 1967 and 1969. Geophys. J. Roy. Astr. Soc., 29, 245-253.
3. Finlayson, D.M. & Cull, J.P., 1973 - Structural profiles in the New Britain - New Ireland region. J. Geol. Soc. Aust., 20, 37-48.
4. Finlayson, D.M. & Cull, J.P., 1973 - Time-term analysis of New Britain - New Ireland island arc structures. Geophys. J. Roy. Astr. Soc., 33, 265-280.
5. Brooks, J.A., Connelly, J.B., Finlayson, D.M. & Wiebenga, W.A., 1971 - St George's Channel - Bismarck Sea trough. Nature Phys. Sci., 229, 205-207.
6. Finlayson, D.M.,Muirhead, K.J., Webb, J.P., Gibson, G., Furumoto, A.S., Cooke, R.J.S. & Russell, A.J., 1976 - Seismic investigation of the Papuan Ultramafic Belt. Geophys. J. Roy. Astr. Soc., 44, 45-60.
7. Finlayson, D.M., Drummond, B.J., Collins, C.D.N. & Connelly, J.B., 1977 - Crustal structures in the region of the Papuan Ultramafic Belt. Phys. Earth & Planet. Int., 14, 13-29.
8. Finlayson, D.M., 1977 - Seismic travel-times to east Papua from USSR nuclear explosions. BMR J. Aust. Geol. & Geophys., 2, 209-216.
9. Finlayson, D.M., Drummond, B.J., Collins, C.D.N. & Connelly, J.B., 1976 - Crustal structure under the Mount Lamington region of Papua New Guinea. In, Volcanism in Australasia (ed. R.W. Johnson), Elsevier, Amsterdam, 259-274.

10. Finlayson, D.M., 1975 - Crustal variations in the Solomon - Papua New Guinea region based on seismic investigations. Aust. Soc. Expl. Geophys. Bull., 6, 61.

11. Finlayson, D.M., Cull, J.P. & Drummond, B.J., 1974 - Upper mantle structure from the Trans-Australia Seismic Survey (TASS) and other seismic refraction data. J. Geol. Soc. Aust., 21, 447-458.

12. Muirhead, K.J., Cleary, J.R. & Finlayson, D.M., 1977 - A long-range seismic profile in southeastern Australia. Geophys. J. Roy. Astr. Soc., 48, 509-519.

13. Finlayson, D.M., 1968 - First arrival data from the Carpentaria Region Upper Mantle Project (CRUMP). J. Geol. Soc. Aust., 15, 33-50.

14. Finlayson, D.M., Prodehl, C. & Collins, C.D.N., 1979 - Explosion seismic profiles and their implications for crustal evolution in southeastern Australia. BMR J. Aust. Geol. & Geophys., 4, 243-252.

15. Finlayson, D.M., Collins, C.D.N. & Denham, D., 1980 - Crustal structure under the Lachlan Fold Belt, southeastern Australia. Phys. Earth & Planet. Int., 21, 321-342.

16. Finlayson, D.M. & McCracken, H.M., 1981 - Explosion seismic studies of crustal structure under the Sydney Basin and northern Lachlan Fold Belt. J. Geol. Soc. Aust., 28, 177-190.

17. Finlayson, D.M., 1981 - Reconnaissance of upper crustal seismic velocities within the Tennant Creek Block. BMR J. Aust. Geol. & Geophys., 6, 245-252.

18. Finlayson, D.M., 1982 - Seismic structure of the Proterozoic North Australian Craton between Tennant Creek and Mount Isa. J. Geophys. Res., 87, 10569-10578.

19. Finlayson, D.M., 1979 - The Australian continental crust: explosion seismic studies in Archaean, Proterozoic and Palaeozoic provinces. In, IASPEI Program and Abstracts for the IUGG XVII General Assembly, Canberra, Australia, 3-15 Dec. 1979, 84-85.

20. Finlayson, D.M., 1982 - Velocity differences in the middle-lower crust across the Proterozoic North Australian Craton. In, proceedings of International Symposium on Archean and Early Proterozoic Geologic Evolution and Metallogenesis, Salvador, Bahia, Brasil, 3-11 Sept. 1982, Revista Brasileire de Geociencias, 12(1-3), 132-134.

21. Finlayson,D.M., Collins, C.D.N. & Lock, J., 1984 - P-wave velocity features of the lithosphere under the Eromanga Basin, eastern Australia, including a prominent mid-crustal (Conrad?) discontinuity. Tectonophysics, 101, in press.

22. Spence, A.G. & Finlayson, D.M., 1982 - The resistivity structure of the crust and upper mantle in the central Eromanga Basin, Queensland, using magnetotelluric techniques. J. Geol. Soc. Aust., 30, 1-16.

23. Finlayson, D.M., 1983 - The mid-crustal horizon under the Eromanga Basin, eastern Australia. Tectonophysics, 100, in press.

24. Finlayson, D.M. & Mathur, S.P., 1983 - Seismic features of the lithosphere under the central Eromanga Basin - a contrast with adjacent tectonic provinces. Geol. Soc. Aust. Abstract Series No. 9, 6th Australian Geological Convention, Theme: Lithospheric Dynamics and Evolution of Continental Crust, 9-11.

25. Lock, J., Collins, C.D.N. & Finlayson, D.M., 1983 - Basement structure and velocities under the central Eromanga Basin from seismic refraction data. In, Eromanga Basin Symposium Papers (ed. P.S.Moore), Geol. Soc. Aust. Special Publn.

26. Finlayson, D.M., 1982 - Geophysical differences in the lithosphere between Phanerozoic and Precambrian Australia. Tectonophysics, 84, 287-312.

27. Finlayson, D.M. & Mathur, S.P., 1983 - Seismic refraction and reflection features of the lithosphere in northern and eastern Australia, and continental growth. In, proceedings of ICL Symposium 1, Structure, Composition and Dynamics of the Continental Lithosphere, IUGG XVIII General Assembly, Hamburg, FGR, 15-27 Aug. 1983 (eds. C.Froidevaux & K.Fuchs), Annales Geophysicae, in press.

28. Finlayson, D.M. & Collins, C.D.N., 1983 - Seismic ray tracing through the ZURICH-1 model. In, Seismic wave propogation in laterally heterogeneous structures, interpretations of Data Set-1 presented at the IASPEI Commission on Controlled Source Seismology meeting at Einsiedeln, Switzerland, August 1983, (eds. D.M.Finlayson & J.Ansorge), Bur. Miner. Resour., Geol. & Geophys. Aust. Report, in press.

29. Finlayson, D.M., 1973 - Isomagnetic maps of the Australian region for epoch 1970.0. Bur. Miner. Resour., Geol. & Geophys. Aust. Report 159.

STATEMENT ON CANDIDATE'S CONTRIBUTION TO THE PAPERS SUBMITTED

The comments contained below on the contribution by the various authors to the papers submitted in this thesis are made under four general headings; 1) contributions to field work and organisation, 2) contributions to the interpretation of data, 3) contributions to scientific management, and 4) written contributions and scientific emphasis.

In all papers where the candidate, D.M.Finlayson, is the first author, unless otherwise stated below, it should be assumed that the candidate was solely responsible for writing the paper, for the scientific emphasis placed on the interpretation, for satisfying referees' comments on the paper and that the candidate played the major role in the interpretation of the data.

All the papers submitted were written while the candidate was employed by the Australian Commonwealth Government in the Bureau of Mineral Resources, Geology and Geophysics (BMR), Canberra. The candidate acknowledges the general organisational, scientific and technical support from colleagues within BMR. Where such support can be identified it is acknowledged in the various individual papers.

There is also a greater level of support given by close scientific colleagues, who work in specialist discipline areas for the common interest of projects as a whole. Such work involves the mutual cooperation in field work, data retrieval and computer program development. This close common interest support is recognised by inclusion as co-authors on the papers from particular projects, even though these co-authors generally have had little to do with the interpretation of the data, geological interpretation or the writing of the paper. Such is the case for the following papers (as listed by number in the Contents); Nos. 2,4,6,7,11,15,16,21 and 28.

In paper 1, co-author Collins contributed by conducting calibration tests on BMR seismic tape recording systems. In paper 3, co-author Cull was responsible for the interpretation of gravity data. In paper 5, the data analysis and writing of the paper was done solely by the candidate (DMF) who, at the time, was working under the supervision of first author Brooks. Co-authors Connelly and Wiebenga were involved in the

organisation and execution of marine work.

In paper 9, co-authors Drummond and Collins greatly assisted in field work and co-author Connelly was responsible for the compilation and interpretation of the magnetic data. In paper 12, the candidate was the principal EMR scientist responsible for the survey as a whole. In paper 14, co-author Prodehl contributed to the interpretation and co-author Collins contributed to field work and computer programming.

In paper 22, first author Spence was responsible for field data acquisition, data processing and modelling. The candidate (DMF) made a major contribution to the geophysical interpretation and wrote the paper. In paper 25, the candidate was the senior scientist resposible for field operations and scientific management of the project. In papers 24 & 27, co-author Mathur was responsible for the compilation of seismic profiling data.

The candidate is the sole author on the remaining submitted papers (Nos. 8,10,13,17,18,19,20,23,26 and 29) and any general assistance rendered is acknowledged in these papers.

To the best of my knowledge, the above statement is a fair and true representation of my contribution to the submitted papers. No papers contain scientific results which have been used in the award of any other degree at any university or similar institution.

Douglas McKnight Finlayson

December 1983

INTRODUCTION

The continental crust in the Australian region has some of the oldest known rocks on Earth near Mount Narryer in the West Australian Shield where zircons dated at 4200 m.y. old have been found (Compston,1983), and some of the youngest in the active volcanic arcs of the Papua New Guinea region (Johnson,1976). Any study aimed at contributing significantly to the examination of lithospheric structure of continental Australia must recognise therefore that it is attempting to describe structures resulting from evolutionary and dynamic processes which have operated for over 90% of the Earth's existence.

Geophysical methods must play an important role in any attempt to examine the three-dimensional structure of a continent. Prior to 1965 only isolated attempts had been made to characterise the Australian continental lithosphere using gravity, magnetic and seismic methods. However, since 1965 there has been a considerable effort on the part of Australian earth scientists to conduct a systematic research program aimed at determining the deep structure of the continent. A major role has been played by the research and survey work of the Bureau of Mineral Resources, Geology and Geophysics, Canberra.

This thesis presents twenty-nine published papers which contribute significantly to the study of the lithospheric structure of continental Australia. One paper represents a major accomplishment in the field of geomagnetism with the establishment of the first 1st-order network of regional magnetic stations in the region and the compilation of iso-magnetic maps for the epoch 1970.0 based on data from that network. The remaining twenty-eight papers are based largely on explosion seismic investigations of the continental crust and upper mantle throughout central/eastern Australia and Papua New Guinea.

Geology

Plumb(1979) has described the tectonic evolution of Australia and Papua New Guinea, derived from surface geology, in terms of major crustal blocks, each of which has its own history and tectonic style. These are shown in Fig. 1. Generally, the tectonic development of the continent has

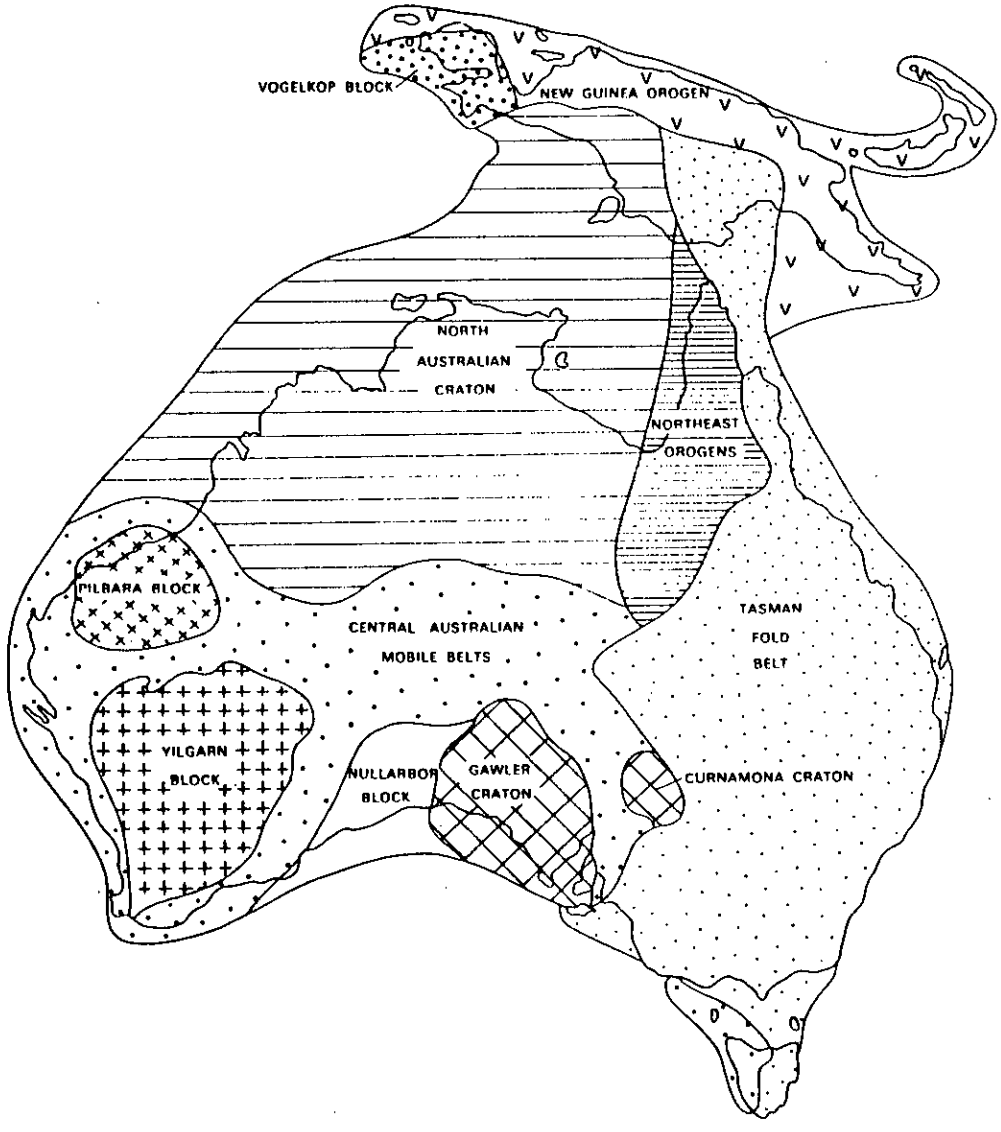

Fig. 1 Major crustal subdivisions of continental Australia (from Plumb, 1979)

progressed from west to east. The Archaean Pilbara and Yilgarn blocks were cratonised more than 2500 m.y.B.P. and are overlain in places by the early Proterozoic West Australian Platform Cover. Stratigraphic equivalents are thought to underlie much, if not all, of the younger North Australian and Gawler Cratons.

The early Proterozoic North Australian Craton has been relatively stable since 1700 m.y.B.P. and is overlain by elements of the mid-Proterozoic North Australian Platform Cover and the late Proterozoic Cental Australian Platform Cover. The Northeast Orogens developed at the edge of the North Australian Craton concurrent with the deposition of the North Australian Platform Cover. They may be considered as the youngest component of the North Australian Orogenic Province which resulted in the North Australian Craton.

The Central Australian Orogenic Province has a long history of tectonic development throughout the Proterozoic culminating in the deposition of the Central Australian Platform Cover. The Gawler and Curnamona Blocks were cratonised by about 1450 m.y.B.P. but tectonic activity continued within the Central Australian Mobile Belts. These were successively cratonised from about 1400 to 900 m.y.B.P. The concealed Nullarbor Block is identified from its gravity expression and its tectonic history is still uncertain.

The Australian Precambrian craton assumed its final form by about 900 m.y.B.P. The Palaeozoic Tasman Fold Belt and the New Guinea Orogen, beginning in the Mesozoic-Tertiary and still active, may be considered marginal to the Precambrian craton.

Plumb(1979) considers there are significant parallels in the tectonic processes which operated during Precambrian and Phanerozoic times. In both he sees elements of a progression from geosynclinal deposition and orogenesis (precratonic tectonism), through transitional tectonism to cratonisation and deposition of platform cover.

Rutland(1982) envisages the development of the present continental structure being the result of global thermal (chelogenic) cycles during which large areas of continental crust were stabilised as shield areas. At 2400 and 1000 m.y.B.P. cratonic areas were at their maximum extent; these were remobilised and reached their minimum during peaks of geothermal flux from the mantle at 1900-1700 and 400-200 m.y.B.P.,

analogous to Palaeozoic Hercynotype development in Europe. The present-day continental crust is seen as developing through a multi-stage process of deformation and plutonic episodes in pre-existing continental crust. Underplating of the crust from basaltic sources in the mantle is also seen as contributing to the present-day continental structure (Ewart et al., 1980; Wass & Hollis,1983).

Elements of crustal evolution in Phanerozoic Australian have been described in terms of plate tectonic models for the currently active, western Pacific region (Crook,1980). Crook recognises many of the elements of western Pacific tectonics in ten arc terrains which he sees as having been successively accreted onto the margin of the Australian Precambrian craton or continental fragments. However, the dating of the older components of S-type granites as being 1100 m.y. old (Compston & Chappell,1979) indicates that reworking of older cratonic fragments is a major factor in the present-day lithospheric structure of eastern Australia.

The convergence of the Australian and Pacific lithospheric plates in the Papua New Guinea region has resulted in the youngest additions of continental material. The collision zone is not simple but comprises a broad area of interacting micro-plates, each of which has identifiable boundaries as spreading centres, transform faults or as subduction zones (Dow,1977; Johnson,1979). The collision of continental Australia with the island arc and oceanic terrains of the New Guinea region has resulted in crustal shortening and thickening along the main island of New Guinea. The deformation has resulted in the spectacular mountains of the main island, but, despite this, the original tectonic relationships of the various rock assemblages can still be identified. The history of this region emphasises the relatively short time span over which some tectonic episodes can occur (a few tens of millions of years). The tectonic history of continental Australia must undoubtedly contain many such episodes in a complex history involving reworking of old terrains and convergent tectonics.

Seismic Investigations of the Australian Crust and Upper Mantle prior to 1965

Seismic methods of investigating the structure of the crust and upper mantle, because of the relatively short wavelengths involved, generally provide a better image of deep geology than other geophysical methods. Hence their widespread use for such investigations (Prodehl,1983). Prior

to 1965 there were a few isolated attempts to estimate the gross structure of various parts of the continent using both earthquake and explosive sources. Cleary(1973) described some of the results in a paper presented at the 1971 IUGG General Assembly in Moscow and Dooley(1970) summarised results at the 1970 Second Symposium on the Upper Mantle Project in Hyderabad.

In southeastern Australia, large explosions associated with the Snowy Mountains hydro-electric dam project were recorded during 1956-57 at a number of widely spaced seismic stations (Doyle et al.,1959). During 1953-56 atomic explosions detonated at Maralinga and Emu were recorded towards the west and southeast (Doyle,1957; Bolt et al.,1958; Doyle & Everingham,1964) and during 1959 Bolt(1962) used quarry blasts near Sydney to determine local crustal velocities.

A number of papers were written based on the seismic observatory recordings of both earthquakes and atomic explosions at teleseismic distances (Doyle & Webb,1963; Cleary,1966; Sutton & White,1966; Bolt,1959). These studies sought to determine travel-time differences from the standard Jeffreys-Bullen tables and thus detect relative velocity/structural differences across the continent. This data was used mostly to determine models for locating continental earthquakes, which were then recognised as being a hazard to the cities of Adelaide and Sydney and the Snowy Mountains hydro-electric scheme.

Surface waves were also used to estimate the gross velocity features of the crust and upper mantle of continental Australia (De Jersey,1946; Officer,1955; Bolt,1957,1959; Bolt & Niazi,1964; Cooney,1962). However, the resulting surface wave models could only provide, at best, an image of the crust overlying a mantle averaged over large tracts of Australia.

Thus, seismic studies, prior to 1965, gave indications of continental structure in only the most general terms and could not be used to describe the detail required in a study of deep geology. Since 1965 there has been a systematic research program to apply explosion seismic methods to the determination of the structure of the continental lithosphere in all the major crustal sub-divisions described earlier by Plumb(1979). The author (DMF) is pivileged to have played a role in most of these surveys.

Seismic Techniques

The majority of the published papers submitted in this thesis use explosion seismic techniques as the basis for determining the deep structure of the continent. It is appropriate, therefore, to comment on the reasons behind the use of these techniques.

The theoretical basis for seismic investigations is set out in many texts (Aki & Richards,1980; Pilant,1979). The key to the application of seismic methods to the detailed exploration of the continent is the use of seismic phases which can be reliably recorded and have wavelengths comparable with the dimensions of the geological structures being investigated. In explosion seismology, the frequences of the seismic waves generated at the source and recorded to any great distance are usually in the range 1 to 50 Hz. Taking the crustal P-wave velocities to be in the range 2.5 to 7 km/s, the wavelengths of the P-waves will be in the range 50 m to 7 km, comparable with the dimensions of major geological features observed at the surface and expected to be common also in sub-surface geology.

It is a desireable goal in explosion seismology to include as many phases as possible in the data set to be interpreted so that models derived by different methods can be cross-checked. However, this goal has been limited by the types of recorders which have been available for field use and the ability of interpretation and modelling techniques to image the continental crust in geological terms.

Giese et al. (1976), Olsen(1983) and Prodehl(1983) have given summaries of the techniques used in the development of seismic refraction recording and interpretation. Seismic vertical reflection recording is also coming into more widespread use in the determination of the deep structure of continents (Oliver et al.,1983) as developments in recording and data processing techniques improve. It is now recognised that a merging of the two techniques is highly desireable to achieve a more complete image of deep lithospheric processes and structures. This strategy is evident in some of the more recent papers submitted in this thesis.

However, the interpretations of most seismic data in this thesis are

largely based on the analysis of the following phases, illustrated diagramatically in a reduced travel-time plot in Fig. 2.

Ps - P-waves refracted through near-surface low-velocity sediments. The fine structural detail in these sedimentary layers is better defined by seismic vertical incidence recording.

Pg - P-waves refracted through the upper crustal basement and usually having an apparent velocity of about 6 km/s.

Pc or P* - Refracted (diving) waves observed from upper or middle crustal depths where there are prominent increases in velocity. There apparent velocity is commonly in the range 6.4 to 7.2 km/s.

Pn - P-waves critically refracted at the crust/mantle boundary and usually having an apparent velocity of 7.8 to 8.3 km/s. This phases is sometimes followed by larger amplitude diving waves which result from structure below the crust/mantle boundary. Their prominence is also affected by the velocity/depth structure at this latter boundary.

P7P or PxP - Sub- and super-critical reflections from horizons within the crust and their travel-time branches are asymptotic to those for Pc(P*) phases at the critical refraction distance.

PmP - Sub- and super-critical reflections from the crust/mantle boundary; their travel-time branch is asymptotic to that of Pn phases at the critical refraction distance.

The ability to record these phases on portable instruments in the remote areas of Australia and Papua New Guinea is crucial to any systematic investigation of deep geology. It is for this reason that the first published paper submitted in this thesis deals with equipment.

In the period 1965 to 1970 the projects in which the author was involved in southeastern Australia (Underwood,1969), in southwestern Australia (Mathur,1974), in New Britain - New Ireland (Finlayson et al.,1972) and northeastern Australia (Finlayson,1968) all used a large variety of portable recording systems. These ranged from engineering refraction spreads, through ad hoc paper recorders, to photographic drum recorders. Few of the systems were calibrated and none recorded in a medium which could be used for post-survey processing of data. An operator was usually required at the

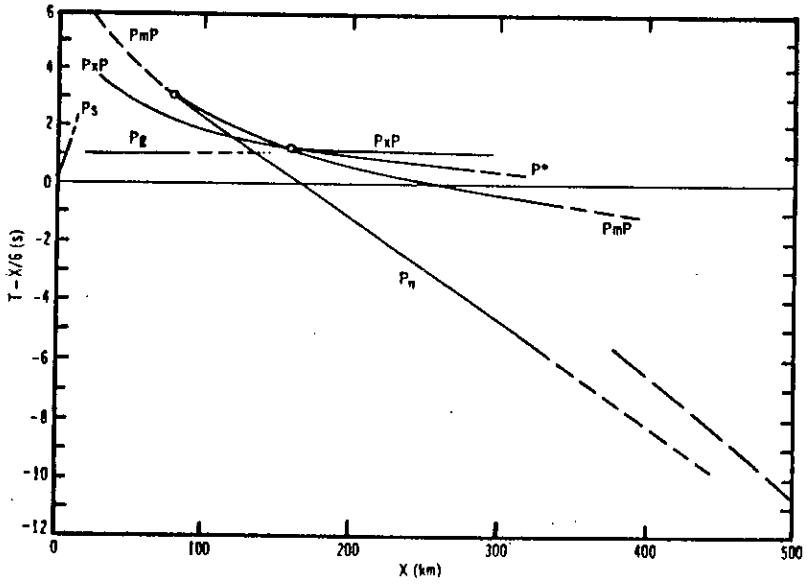

Fig. 2. Schematic P-wave travel-time diagram showing approximate trends of onsets for several compressional seismic phases important in the interpretation of continental crustal structures. See text for identification and discussion of various phases. The time axis is plotted using a reducing velocity of 6.0 km/s. Open circles indicate the approximate coordinates for critical reflection of P-waves from the Moho (PmP) and a midcrustal velocity discontinuity (PxP).

(adapted from Olsen, 1983)

recording site.

This poor equipment situation was recognised and rectified in the period 1970-72 with the development of the BMR remote seismic tape recording systems for explosion seismology. The half-inch tape recording systems were first put into the field by the author during 1971 for an investigation of upper mantle structure using a 500 t blast at the site of the Ord River Dam (Denham et al.,1972). The quarter-inch tape recording systems were subsequently developed and first used in the field during 1973 in the Bowen Basin (Collins,1978).

The limitations inherent in using only P-waves in the interpretations is recognised. S-waves, although evident on some vertical component recordings, are more difficult to detect precisely within the coda of explosion seismic records. Hence, although surveys in many countries have made the effort to record horizontal as well as vertical components, there are relatively few interpretations which determined a detailed S-wave structure (Prodehl,1983).

Submitted Papers

Twenty-nine published papers are submitted in this thesis. They are not arranged in chronological order of publication but are mostly grouped according to the geological provinces which have been the subject of research.

As indicated earlier in this Introduction, paper 1 describes the equipment developed for explosion seismic investigations of deep geology. Papers 2 to 10 are all related to the structure and tectonics of Papua New Guinea. Papers numbered 11 and 12 relate to the seismic structure of the upper mantle of continental Australia and papers 13 to 16 examine the structure and tectonics of southeastern Australia. Papers numbered 17 to 20 are relevant to the structure of the Precambrian craton.

Papers numbered 21 to 25 stem from research into the deep structure under the Eromanga Basin in eastern Australia and papers 26 and 27 are comparative studies into the seismic structure of the lithosphere in Australia. Paper 28 is a contribution to the IASPEI Commission on Controlled Source Seismology 1983 Symposium and paper number 29 is a compilation of geomagnetic data into the first iso-magnetic maps of Australia controlled by 1st-order regional magnetic stations. Three papers (Nos. 10,

19 and 24) are abstracts submitted to symposia but have been included because they have contributed to reviews of regional seismic structure or have contained ideas which have been subsequently developed in full papers.

ACKNOWLEDGEMENTS

I should like to thank Dr.M.W.McElhinny, Chief of the Division of Geophysics in the Bureau of Mineral Resources, Geology and Geophysics (BMR) who encouraged me to submit this thesis. I should also like to thank many colleagues in BMR who have been associated with the explosion seismic program and in particular Barry Drummond, Clive Collins, David Denham, Ian Everingham, John Moss, Jim Dooley, Jim Cull and Bill Wiebenga (deceased). In Australian universities, I have received much encouragement from Dr.John Cleary (deceased), Dr.Ken Muirhead and Prof.Anton Hales at Australian National University, Dr.John Webb and Dr.Jack Rynn at the University of Queensland, and from Dr.Hugh Doyle at the University of Western Australia; all have been valued colleagues in Australian explosion seismic research since my arrival in Australia in 1965. This thesis is submitted with the approval of the Director, Bureau of Mineral Resources, Geology and Geophysics, Canberra.

REFERENCES

Aki,K. & Richards,P.G.,1980 - Quantitative Seismology, Vols. I & II. W.H.Freeman and Co., San Francisco.

Bolt,B.A.,1957 - Velocity of the seismic waves Lg and Rg across Australia. Nature, 180, 495.

Bolt,B.A., Doyle,H.A. & Sutton,D.J.,1958 - Seismic observations from the 1956 atomic explosions in Australia. Geophys. J. Roy. Astr. Soc., 1, 135-145.

Bolt.B.A.,1959 - Seismic travel times in Australia. J. & Proc. Roy. Soc. NSW., 91, 64.

Bolt.B.A.,1962 - A seismic experiment using quarry blasts near Sydney. Aust. J. Phys., 15, 293-300.

Bolt,B.A. & Niazi,1964 - Dispersion of Rayleigh waves across Australia. Geophys. J. Roy. Astr. Soc., 9, 21-35.

Cleary,J.R.,1966 - P amplitudes from Longshot at Australian stations. Nature, 211, 954.

Cleary,J.R.,1973 - Australian crustal structure. Tectonophysics, 20, 241-248.

Collins,C.D.N.,1978 - Crustal structure of the central Bowen Basin, Queensland. BMR J. Aust. Geol. & Geophys., 3 203-209.

Compston,W. & Chappell,B.W.,1979 - Sr-isotope evolution of granitoid source rocks. In, The Earth, Its Orogin, Structure and Evolution, (ed. M.W. McElhinny), Academic Press, London-New York-San Francisco.

Compston,W.,1983 - Very early Archean rocks in the Yilgarn Block, W.A. Paper presented to the Geological Society of Australia (Territories Div.), 18 Oct. 1983.

Cooney,G.H.,1962 - The New South Wales earthquake of May 22, 1961. Aust. J. Phys., 15, 536-548.

Crook,K.A.W.,1980 - Fore-arc evolution in the Tasman Geosyncline: the origin of the southeast Australian continental crust. J. Geol. Soc. Aust., 27, 215-232.

De Jersey,N.J.,1946 - Seismological evidence bearing on crustal thickness in the southeast-west Pacific. Paper of the Dept. of Geol., Uni. of Qld.

Denham,D.,Simpson,D.W.,Gregson,P.J. & Sutton,D.J.,1972 - Travel times and amplitudes from explosions in northern Australia. Geophys. J. Roy. Astr. Soc., 28, 225-235.

Dooley,J.C.,1970 - Seismological studies of the upper mantle in the Australian region. Proceedings of the Second Symposium on the Upper Mantle Project, Hyderabad, 113-146.

Dow,D.B.,1977 - A geological synthesis of Papua New Guinea. Bur. Miner. Resour., Geol. & Geophys. Bull. 201.

Doyle,H.A.,1957 - Seismic recordings of atomic explosions in Australia. Nature, 180, 132.

Doyle,H.A.,Everingham,I.B. & Hogan,T.K.,1959 - Seismic recordings of large explosions in south-eastern Australia. Aust. J. Phys., 12, 222-230.

Doyle,H.A. & Webb,J.P.,1963 - Travel times to Australian stations from Pacific nuclear explosions in 1958. J. Geophys. Res., 68, 1115-1120.

Doyle,H.A. & Everingham,I.B.,1964 - Seismic velocities and crustal structure in southern Australia. J. Geol.Soc. Aust., 11, 141-150.

Ewart,A.,Baxter,K. & Ross,J.A.,1980 - The petrology and petrogenesis of the Tertiary anorogenic mafic lavas of southern and central Queensland, Australia - possible implications for crustal thickening. Contrib. Mineral. Petrol., 75, 129-152.

Finlayson,D.M.,1968 - First arrival data from the Carpentaria Region Upper Mantle Project (CRUMP). J. Geol. Soc. Aust., 15, 33-50.

Finlayson,D.M.,Cull,J.P.,Wiebenga,W.A.,Furomoto,A.S. & Webb,J.P.,1972 - New Britain - New Ireland crustal seismic refraction investigations 1967 and 1969. Geophys. J. Roy. Astr. Soc., 29, 245-253.

Giese,P.,Prodehl,C. & Stein,A.,(editors),1976 - Explosion Seismology in Central Europe. Springer-Verlag, Berlin-Heidelberg-New York.

Johnson,R.W.,(editor),1976 - Volcanism in Australasia. Elsevier, Amsterdam-Oxford-New York.

Johnson,R.W.,1979 - Geotectonics and volcanism in Papua New Guinea: a review of the late Cainozoic. BMR J. Aust. Geol. & Geophys., 4, 181-207.

Mathur,S.P.,1974 - Crustal structure in southwestern Australia from seismic and gravity data. Tectonophysics, 24, 151-182.

Officer,C.B.,1955 - Southwest Pacific crustal structure. Trans. Am. Geophys. Un., 36, 449-459.

Oliver,J.,Cook,F. & Brown,L.,1983 - COCORP and the continental crust. J. Geophys. Res., 88, 3329-3347.

Olsen,K.H.,1983 - The role of seismic refraction data for studies of the origin and evolution of continental rifts. Tectonophysics, 94, 349-370.

Pilant,W.L.,1979 - Elastic Waves in the Earth. Developments in Solid Earth Geophysics, Vol. 11, Elsevier, Amsterdam-Oxford-New York.

Plumb.K.A.,1979 - The tectonic evolution of Australia. Earth Science Reviews, 14, 205-249.

Prodehl,C.,1983 - Structure of the earth's crust and upper mantle. In, Geophysics of the Solid Earth, the Moon and the Planets, (editors K.Fuchs and H.Soffel), Springer-Verlag, Berlin-Heidelberg-New York.

Rutland,R.W.R.,1982 - On the growth and evolution of continental crust: a comparative tectonic approach. J. & Proc. Roy. Soc. NSW., 115, 33-60.

Sutton,D.J. & White,R.E.,1966 - A study of P travel-times from some Australian earthquakes. Aust. J. Phys., 19, 157-166.

Underwood,R.,1969 - A sesmic refraction study of the crust and upper mantle in the viscinity of Bass Strait. Aust. J. Phys., 22, 573-587.

Wass,S.Y. & Hollis,J.D.,1983 - Crustal growth in southeastern Australia - evidence from lower crustal eclogite and granitic xenoliths. J. Metamorphic Geol., 1, 25-45.

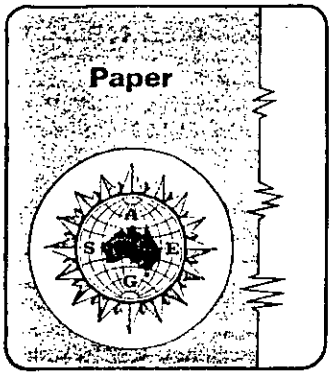

A Brief Description of BMR Portable Seismic Tape Recording Systems

D. M. Finlayson & C.D.N. Collins

Bureau of Mineral Resources Geology and Geophysics, P.O. Box 378, Canberra City, ACT 2601

Current methods of interpreting seismic data from earthquake or explosion sources in terms of geological structures use both the kinematic and dynamic information in the data. This requires that the characteristics of the systems used for recording and analysing ground motion be well known, and in recent years this requirement has been allied with the many developments in electronic engineering and tape recording to produce a generation of field equipment which is both portable and rugged (Dibble, 1964; Mereu & Kovach, 1970; Muirhead & Simpson, 1972; Crowe, 1973; Long, 1974). Most of this equipment has been designed and built by research groups and therefore was not easily available for purchase. Those systems which were available commercially were generally very expensive for the tasks required of them.

About 1970, therefore, the Bureau of Mineral Resources, Geology and Geophysics (BMR) decided to produce a system for its own purposes. The general requirement was for a seismic recording system which was portable, rugged, and would have an unattended endurance of about one week on an intermittent basis. The recording system had to be capable of use in any of the climatic conditions likely to be encountered in Australia and Papua New Guinea. The systems had to produce high quality recordings of ground motion which could subsequently be digitised and accessed to a digital data storage and retrieval system.

Twenty one sets of seismic tape recording equipment were subsequently built by BMR, each containing a seismometer, amplifier, modulator, calibrator, crystal clock, radio time signal receiver, and four-track tape deck. The systematics of the recording and playback facilities are illustrated in Figure 1 and the field recording equipment is shown in Figure 2. This Technical Note briefly describes the characteristics required by the seismologist for field operation and interpretation of ground motion, but does not attempt to describe the electronic design and circuitry.

Since 1971 these seismograph systems have been used extensively on explosion seismic surveys in the Australian region (Denham & others, 1972; Finlayson & others, 1974, 1977, 1979, 1980; Collins, 1978; Drummond, 1979). The ability to maintain essentially the same characteristics in all recording systems, coupled with the frequency modulated tape recording system, enables the recovery of reliable ground motion data from widely separate locations. This is essential for any interpretation involving the relative amplitudes along recording station lines which may be 300-500 km in length.

Seismometers and amplifier

Willmore Mk II or Mk IIIA short-period seismometers are used with the free period adjusted to 0.7 s. A calibration coil and magnet have been fitted to the indicator rod of each Mk II seismometer; a calibration coil wound concentrically with the signal coil is used on the Mk IIIA seismometers.

The seismometer amplifier is a BMR type TAM5 very low frequency AC coupled amplifier with a maximum gain of 120 dB (10^6) switchable in 6 dB steps from 48 dB to 120 dB. The amplifier has two outputs, the high-gain as selected and the low-gain 24 dB below the selected level. Five switched bandpass filter settings are available: 0.01-0.2 Hz, 0.01-20.0 Hz, 0.1-10 Hz, 1.0-5.0 Hz, and 1.0-100.0 Hz. For explosion seismic recording the bandpass filter is usually set in the range 0.01-20.0 Hz.

The frequency responses of the TAM5 amplifier itself, and of the seismometer plus amplifier system, are shown in Figure 3. The displacement magnification of the seismometer plus amplifier as a function of frequency is shown in Figure 4. The average sensitivity of the Mk II seismometers is 5.7 V per $m.s^{-1}$ and for the Mk IIIA seismometers is 5.05 V per $m.s^{-1}$. The damping factor of the seismometer is typically 0.52. At 7.5 Hz, the predominant frequency in quarry blast signals, the displacement magnification is 2.6×10^7 volts per metre for a TAM5 set at 72 dB with a bandpass filter setting of 0.01-20.0 Hz and a Willmore Mk II seismometer. The system performance in the field can be assessed using pulses from a BMR type SSC–1 calibrator applied to the seismometer.

Modulation and recording

The two gain levels from the TAM5 amplifiers are frequency modulated (fm) for recording on slow-speed tape recorders. Two types of recorders are used: highly modified Akai ¼-inch tape recorders, and Precision Instrument (PI) type 5107 ½-inch tape recorders. Both types record at a tape speed of 1.488 mm/s (15/256 in/s) with a fm centre frequency of 105.5 Hz. A maximum frequency deviation of ± 40% is produced with a signal of ± 1.4 V to the modulator input. The frequency response of the modulation-

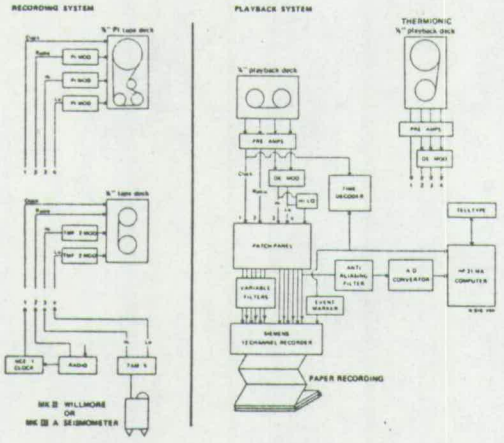

FIGURE 1
BMR portable seismic tape recording systems and playback systems.

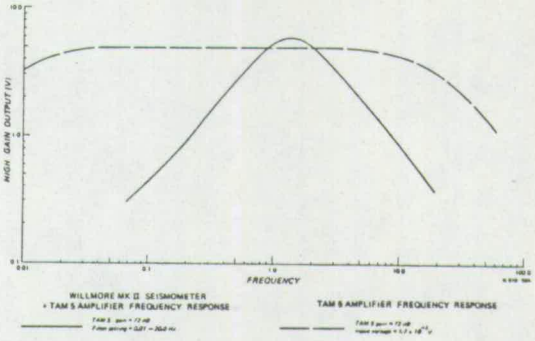

FIGURE 3

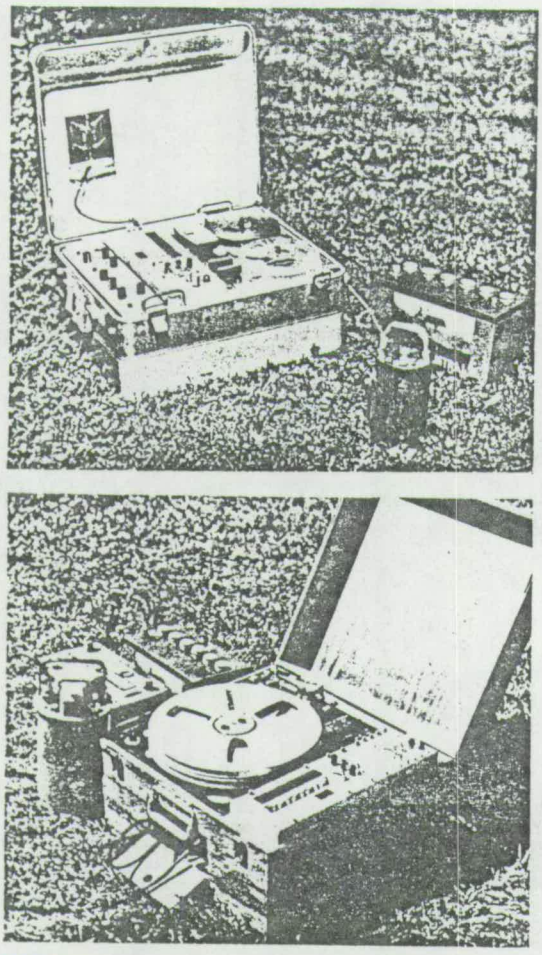

FIGURE 2
BMR portable seismic tape recorders, a) ¼-inch tape system, b) ½-inch tape system.

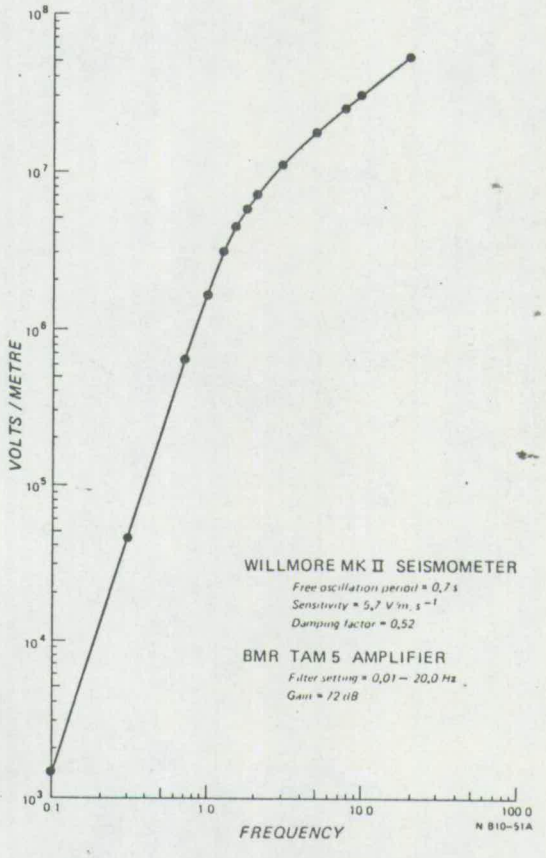

FIGURE 4
Displacement magnification of BMR seismic tape recording systems, with respect to frequency.

record-demodulation system is flat within the range DC – 19.5 Hz. The modified Akai recorders use BMR type TMF-2 modulators; the PI recorders use modulators built in by the manufacturers.

Crystal Clock

A BMR type NCE-1 crystal controlled clock is incorporated in each set of equipment, and an IRIG serial time code is recorded on a third tape channel. The frequency standard is derived from a Vectron temperature compensated crystal oscillator (TCXO), and this provides a 50 Hz carrier frequency for tape recording; the time code is an amplitude-modulated signal superimposed on the carrier. An accuracy of ± one part in 10^7 (± 8 ms per day) in the temperature range 0-50°C is typical for the clock. An LED display, in addition to showing days, hours, minutes, and seconds, also shows the difference between the clock time code and a radio derived time signal. Clock time can be synchronised with the radio time-signal using advance and retard buttons.

The clock can also be programmed to switch on and off the recorder and radio to extend the endurance of field recording. This facility is used when survey staff either detonate their own shots or know the time periods within which quarries fire shots.

Radio time-signal receiver

The fourth recorder channel is used to record a standard radio time-signal transmitted on 4.5, 7.5, and 12.0 MHz by station VNG operated by Telecom Australia from Lyndhurst in southeast Australia (Australian Post Office, 1973). The signal is received by a modified Labtronics type 21B time-signal receiver which is crystal locked to the selected frequency.

Power requirements

The power for the systems is provided from 12V lead-acid batteries. The equipment which uses the modified Akai tape deck requires a current of 0.6 A when only the clock is functioning, and an additional 0.4 A when recording is in progress. Thus, when two 80 Ah batteries and a 548 m (1800 ft) tape are used, the endurance for recording 12 hours per day is about 8.3 days. Planned improvements to the clock and tape-drive systems should reduce power consumption to about 15% of its present level.

Playback system

Playback of the ¼-inch tapes is achieved through BMR design playback equipment. Playback tape speed is possible at 4, 8, 16, and 32 times the recording tape speed and can be locked to the 50 Hz clock signal on the tape to make allowance for small variations in recording speeds. The clock time code on tape is continuously decoded and displayed through a BMR type NTD1 decoding unit. Signals from tape are amplified, the seismic channels are demodulated, and all channels are fed to a patch-panel and hence to a Siemens Oscillomink 12-channel analogue chart recorder (Fig. 1). Tape jitter on recorders can be eliminated by subtracting the low-gain seismic signal from the high-gain signal. Signals can also be filtered using a bank of Rockland Model 452 dual HI/LO variable filters. The playback of ½-inch tapes is achieved at 4 times the nominal recording speed through a Racal Thermionics type T8300 tape reproducer, and signals are fed to the patch panel mentioned above.

One seismic channel from the patch panel can be fed through an anti-aliasing filter to an analogue-to-digital converter and hence to a BMR data acquisition system incorporating an HP 21MX computer. Data files are created for each event being interpreted, each file containing a header which incorporates all relevant survey information about shot number, recorder number, distance, gain, etc. With ¼-inch recordings, playback speed is commonly 8 times record speed, and usually about 3 minutes of record is digitised with a sampling interval of 2 ms. A suite of programs exists to edit data files and compile seismic record sections.

Acknowledgements

The design responsibility for the BMR recording and playback facilities was undertaken by K. J. Seers, D. Kerr, B. Liu, and A. J. Barlow. Development and production of the systems was completed by technical staff of the BMR Engineering Services Branch. This paper is published with the permission of the Director, Bureau of Mineral Resources, Geology and Geophysics, Canberra.

References

AUSTRALIAN POST OFFICE, 1973. Standard frequency and time signal service VNG. Research Laboratories, Melbourne.

COLLINS, C.D.N., 1978. Crustal structure of the central Bowen Basin, Queensland. *BMR Journal of Australian Geology and Geophysics*, 3, 203-209.

CROWE, W.A., 1973. Listening to the earth. *Electronic Engineering*, July 1973, 51-53.

DENHAM, D., SIMPSON, D.W., GREGSON, P.J., & SUTTON, D.J., 1972. Travel times and amplitudes from explosions in northern Australia. *Geophysical Journal of the Royal Astronomical Society*, 28, 225-235.

DIBBLE, R.R., 1964. A portable slow motion magnetic tape recorder for geophysical purposes. *New Zealand Journal of Geology and Geophysics*, 7, 455-65.

DRUMMOND, B.J., 1979. A crustal profile across the Pilbara and northern Yilgarn Blocks, Western Australia. *BMR Journal of Australian Geology and Geophysics*, 4, 171-180.

FINLAYSON, D. M., CULL, J. P., & DRUMMOND, B. J., 1974. Upper mantle structure from the Trans-Australia Seismic Survey (TASS) and other seismic refraction data. *Journal of the Geological Society of Australia*, 21, 447-458.

FINLAYSON, D.M., DRUMMOND, B.J., COLLINS, C.D.N., & CONNELLY, J.B., 1977. Crustal structures in the region of the Papuan Ultramafic Belt. *Physics of the Earth and Planetary Interiors*, 14, 13-29.

FINLAYSON, D.M., PRODEHL, C., & COLLINS, C.D.N., 1979. Explosion seismic profiles and crustal structure in southeastern Australia. *BMR Journal of Australian Geology and Geophysics*, 4, 243-252.

FINLAYSON, D.M., COLLINS, C.D.N., & DENHAM, D., 1980. Crustal structure under the Lachlan Fold Belt, southeastern Australia. *Physics of the Earth and Planetary Interiors*, 21, 321-342.

LONG, R. E., 1974. A compact portable seismic recorder. *Geophysical Journal of the Royal Astronomical Society*, 37, 91-98.

MEREU, R.F., & KOVACH, R.J., 1970. A portable inexpensive seismic system for crustal studies. *Bulletin of the Seismological Society of America*, 60, 1607-13.

MUIRHEAD, J.J., & SIMPSON, D.W., 1972. A three-quarter watt seismic station. *Bulletin of the Seismological Society of America*, 62, 985-90.

Geophys. J. R. astr. Soc. (1972) 29, 245–253

New Britain—New Ireland Crustal Seismic Refraction Investigations 1967 and 1969

D. M. Finlayson, J. P. Cull, W. A. Wiebenga, A. S. Furumoto and J. P. Webb

(Received 1972 June 26)*

Summary

The initial interpretation of deep seismic refraction data in the New Britain–New Ireland region has resulted in generalized crustal cross-sections in six areas being defined. In the south-east Bismarck Sea a single layer crust with a P seismic velocity of $6{\cdot}9\ \mathrm{km\ s^{-1}}$ overlies $8{\cdot}0\ \mathrm{km\ s^{-1}}$ mantle at 20 km depth. The crust thickens under the Gazelle Peninsula to 32 km in a two-layer crustal model and this thickness is maintained out to the islands east of New Ireland. In central New Britain a two-layer crust 29 km thick at the Solomon Sea margin thins to 25 km under Central New Britain with high crustal seismic velocities indicating a high density crust. Further examination of the large amount of data now available in the region is under way and should reveal detailed structure in the upper crust.

Introduction

'The Melanesian archipelago is generally conceded to be the most complicated tectonic province bordering the Pacific basin' (Hayes & Ewing 1970) and for this reason has been the focus of a number of geophysical and geological investigations in recent years. The Australian Bureau of Mineral Resources (BMR) has taken an active part in promoting such surveys in the New Guinea region and this paper gives an account of the 1967 and 1969 crustal surveys in the New Britain–New Ireland region and presents preliminary results.

The major geophysical studies conducted during 1967 and 1969 consisted of seismic refraction and regional gravity surveys (Brooks 1971; Finlayson 1972). Associated work included a geological survey of New Britain and New Ireland and marine sparker and magnetic profiling in surrounding waters. The success of these surveys was assisted greatly by the active support of the University of Queensland, the Hawaii Institute of Geophysics, the Australian National University and the staff of the Rabaul Vulcanological Observatory.

The tectonic setting of the survey area has been outlined by a number of authors (Denham 1969, 1971; Johnson & Molnar 1972; Krause 1972) all of whom use the concept of plate tectonics to account for seismicity and earthquake focal mechanism data from the area (Fig. 1). Their investigations necessitate the existence of three small sub-plates (Solomon Sea plate, South Bismarck plate and North Bismarck plate) interacting between the major Indian–Australian and Pacific plates.

Other geophysical investigations which add considerably towards our knowledge of crustal structures in the survey area are the marine surveys conducted by BMR and the Hawaii Institute of Geophysics (Willcox 1971; Brooks *et al.* 1971; Rose, Woollard & Malahoff 1968; Furumoto *et al.* 1970; Brown & Webb 1971).

*Received in original form 1972 March 6.

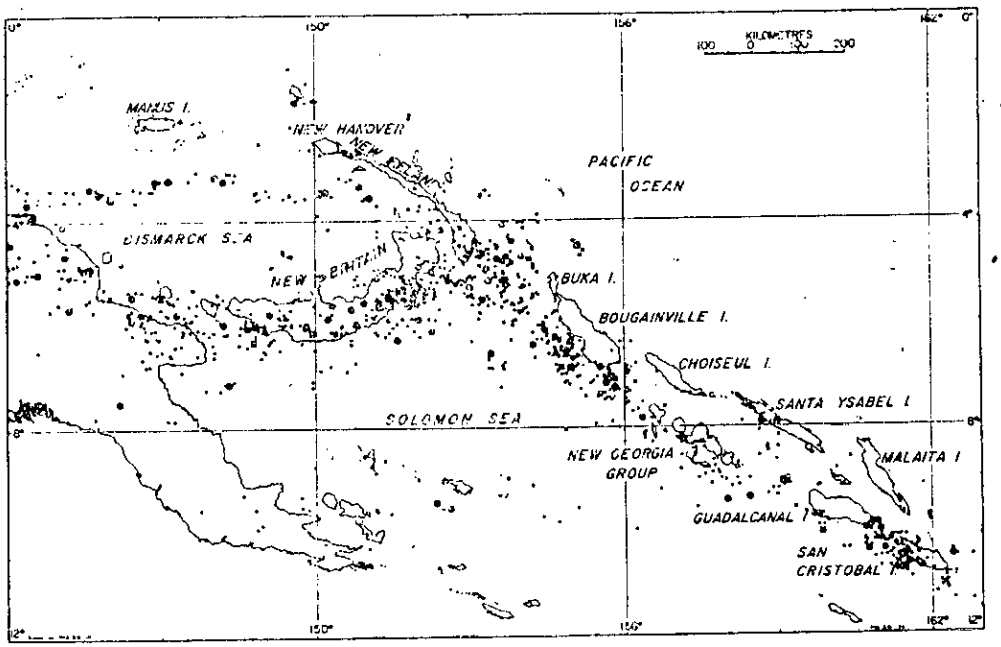

FIG. 1. Seismicity of the Bismarck Sea–Solomon Sea region to December 1970 (Denham 1971)

1967–1969 seismic refraction surveys

Against a background of continuing active tectonic evolution the problems involved in conducting and interpreting a seismic refraction survey to define crustal boundaries are clearly considerable.

The pattern of shots and stations for the combined 1967 and 1969 survey work is indicated in Fig. 2. The 1967 programme involved recording 44 shots at 26 stations (Finlayson 1972). In 1969, 54 shots were recorded at 47 stations over a larger range of distances than during the 1967 survey (Brooks 1971). Both surveys were shot in a number of stages, the recording stations being moved during the course of the survey in order to give wider coverage of New Britain and New Ireland.

Explosive charges varied in size up to 1 ton of TNT, and were detonated electrically at depths down to 107 m from a shooting ship positioned by Decca Hi-fix in some areas and by radar bearings/distances and land sightings in the remaining areas.

Recordings were made at distances up to 300 km on a variety of photographic and pen recording instruments coupled to 1·0–4·5 Hz geophones or seismometers (Fig. 3). Timing was derived uniformly from signals transmitted from Rabaul Volcanological Observatory. Station co-ordinates were generally derived to accuracies better than 100 m.

All original records, after being checked in the field, were re-read by two or three observers in BMR Canberra and an accuracy category and subjective quality were assigned to each arrival. The resulting travel times were computer plotted to give various configurations of time–distance plots with times adjusted to substitute a 4·0 km s^{-1} layer for the depth of water. Complete listings of time–distance data are given in Brooks (1971) and Finlayson (1972), and copies of the time–distance plots are available from BMR on request.

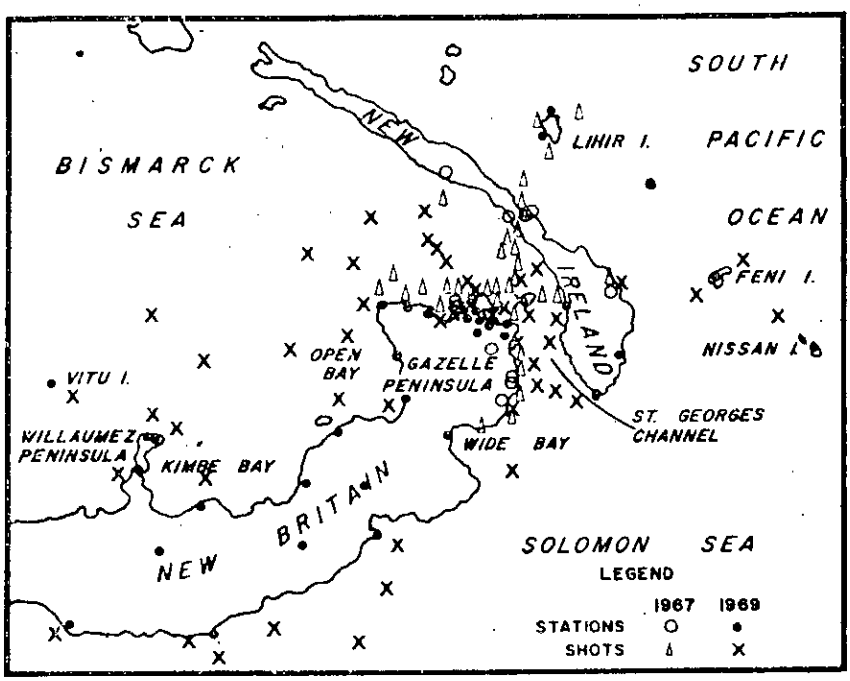

FIG. 2. Combined shot and recording station distribution for 1967 and 1969 seismic refraction surveys. Detail in Rabaul area not shown.

Refractor identification

It is by no means obvious from the comprehensive time–distance plots what refractors can be identified. Steinhart & Meyer (1961) and Bott (1971), among others, have pointed out some of the subjective implications in identifying seismic arrivals with particular refractors, and the task in the New Britain–New Ireland region is not made any easier by the variety of apparent velocities on common shot and common station time–distance plots. The positive identification of second and subsequent seismic arrivals is not at all to be relied upon when one considers the further complicating factors of possible sub- and super-critical reflections and the bifurcation and triplication of time–distance plots.

Drake & Nafe (1968) have pointed out the ' increase in diversity of structure from ocean basins to young orogenic belts '. In their examination of world wide crustal and upper mantle velocities, they divided the measured velocities into four groups: (1) 4·5–6·5 km^{-1}, (2) 6·5–7·2 km s^{-1}, (3) 7·2–7·7 km s^{-1} and (4) 7·9–8·5 km s^{-1}. The group (3) velocities, in particular, were identified with young orogenic belts and it was suggested that the materials with such velocities were of a transient nature associated with the build-up of continental type crust.

As the first step in the 1967 and 1969 survey data analysis, an examination of first arrivals only was made for all reduced time–distance plots on an individual common shot and common station basis. It is important to identify all refractors correctly in order to determine accurate crustal sections. Dowling (1970) has shown that, although uncertainties in upper crust velocities do not propagate very strongly downwards in seismic refraction calculations, if dips are present the uncertainties may significantly increase, and this is likely to be the case in the present interpretation.

A large proportion of the arrivals identified were for shots at distances between 10 and 100 km. Thus, it is possible to determine with a fair degree of accuracy the

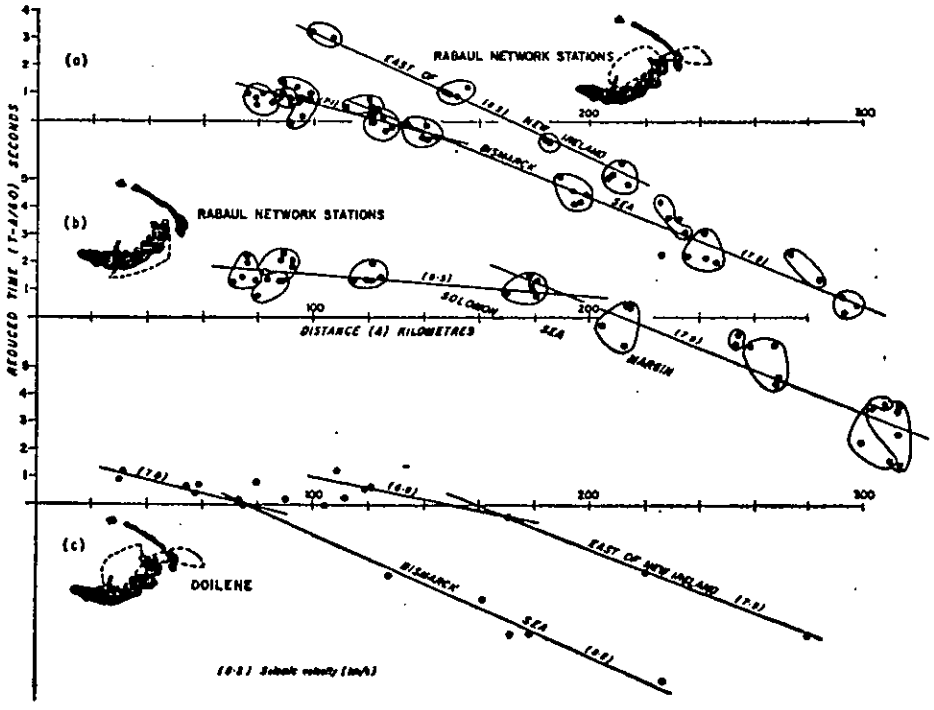

FIG. 4. (a) Reduced time–distance plot, Rabaul Network; (b) Reduced time–distance plot, Rabaul Network; (c) Reduced time–distance plot, Doilene.

velocities in the upper crust. The apparent velocities were determined by approximating the data by straight line segments, using least squares methods. Weights were attached to points in the ratios 5:3:1 according to the subjective qualities ' good, fair and poor ' assigned to the seismic arrivals during reading of the original records.

Only in a few cases were combinations of various shot or station plots useful in indicating velocities, but for a number of stations it was possible to group arrivals into various azimuth windows, and in other cases, to consider the shot-station distribution as a reversed profile.

The problem of determining the true velocities at greater depths was much more difficult because of the larger distances over which seismic energy must travel to be recorded as a first arrival from deep refractors, with the consequent reduction in the quality of data. Estimates of apparent velocities for deeper refractors were made in two ways, (a) be weighted least squares methods, as applied at distances 10–100 km, and (b) by fitting straight line segments by eye with no weighting.

In all, 171 time–distance plots were examined in an attempt to obtain typical refractor velocities and to assess regional variations in the parameters. The following are representative examples: (Figs 4 and 5).

(i) RABAUL NETWORK from shots to the east of New Ireland and in the Bismarck Sea:—this demonstrates the relatively high crustal apparent velocities in the Bismarck Sea and suggests that intercepts for the refractor of velocity close to 8 km s^{-1} are significantly less in the Bismarck Sea area than in the region to the east of New Ireland (Fig. 4(a)).

(ii) RABAUL NETWORK observations of shots in the Solomon Sea region—evidence for upper crustal apparent velocities of approximately 6·3 km s^{-1}, and a sub-Moho velocity close to 8 km s^{-1} (Fig. 4(b)).

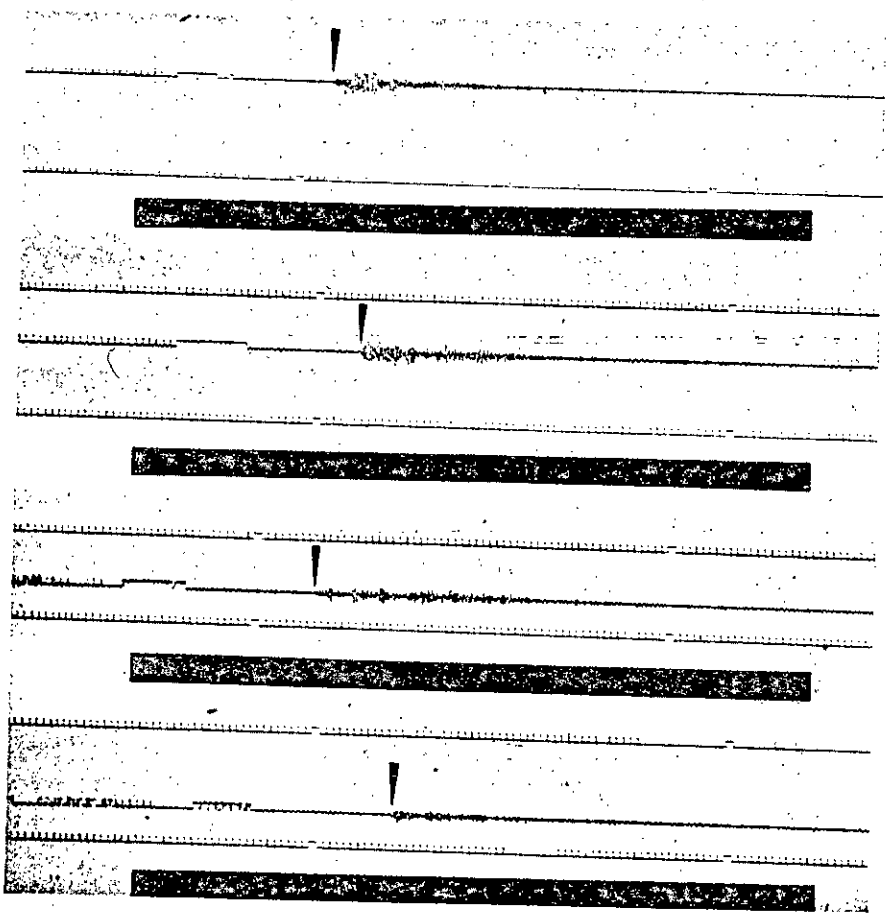

FIG. 3. Example of good recordings made at station RBL in the 50–150 km range.

facing page 248

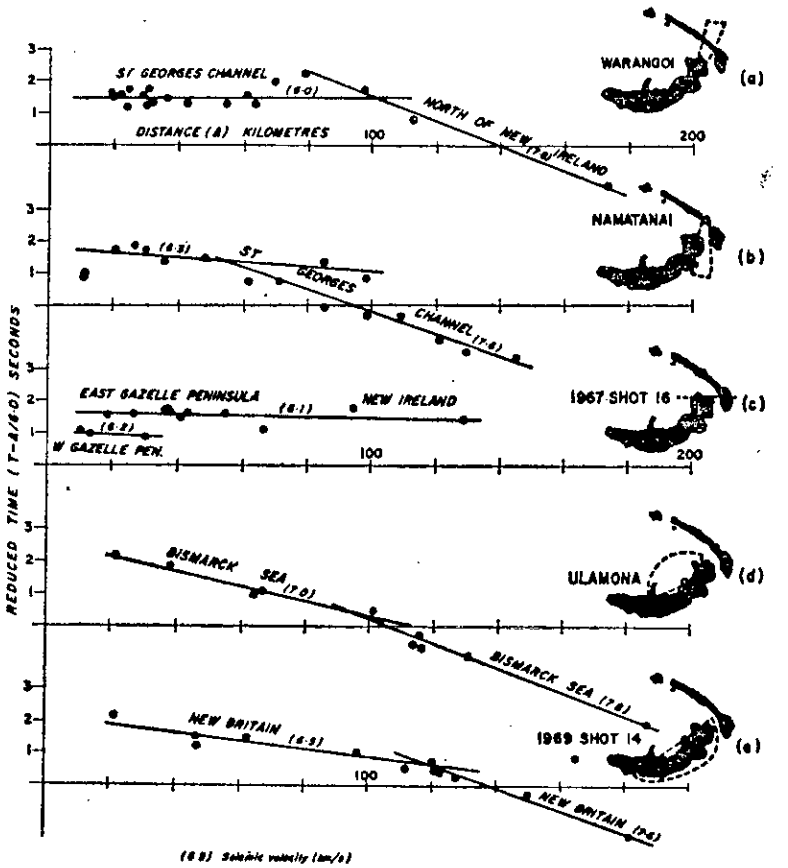

FIG. 5. (a) Reduced time–distance plot, Warangoi; (b) Reduced time–distance plot, Namatanai; (c) Reduced time–distance plot, Shot 16 (1967); (d) Reduced time–distance plot, Ulamona; (e) Reduced time–distance plot, Shot 14 (1969).

(iii) DOILENE observations of shots to the west across the Bismarck Sea and east of New Ireland:— demonstrates the high apparent velocities in the upper crust in the Bismarck Sea region and indicates that intercepts for the deeper refractor are smaller for the Bismarck Sea than for the region to the east of New Ireland (Fig. 4(c)).

(iv) WARANGOI from shots to the north across St Georges Channel and New Ireland:— illustrates upper crustal velocities close to 6 km s^{-1} in the northern Gazelle Peninsula, and a deeper refractor with apparent velocity of approximately 8 km s^{-1} (Fig. 5(a)).

(v) NAMATANI from shots to the south:— indicates apparent velocities of 6·2 km s^{-1} and 7·6 km s^{-1} (Fig. 5(b)).

(vi) SHOT 16 (1967) observed to the west and to the east along the northern Gazelle Peninsula:— demonstrates the presence of an upper crustal layer with apparent velocities near 6 km s^{-1}, and indicates that intercepts are smaller towards the west than to the east (Fig. 5(c)).

(vii) ULAMONA from shots in the Bismarck Sea:— illustrates the relatively high crustal velocities in the Bismarck Sea area and, in particular, the absence of an upper layer with velocities near 6 km s^{-1} (Fig. 5(d)).

(viii) SHOT 14 (1969) observed to the south in central New Britain:— demonstrates the relatively high apparent crustal velocities in central New Britain (Fig. 5(e)).

Discussion

Summaries of the straight-line parameters for the range 10–100 km, determined for time-distance plots, are given in Tables 1, 2 and 3. From these tables it is seen that in the northern and eastern Gazelle Peninsula, New Ireland and islands to the east and in the Willaumez Peninsula region the refractor velocities are within the range 6·12–6·23 km s^{-1}, but in other areas the velocities are significantly greater. In central and southern New Britain and in the Solomon Sea margin the velocity is in the range 6·36 to 6·56 km s^{-1} and in the Bismarck Sea is 6·78±0·13 km s^{-1}.

The data for deep crustal and upper mantle velocities are given in Tables 4 and 5. The existence of a deep crustal refractor with a velocity of approximately 7 km s^{-1} is evident from first arrivals only in the range 80–140 km, but supporting evidence is available from second arrivals in other ranges. Subjective judgement does enter into the interpretation when it is decided to assign arrivals to particular refractors and, as has been pointed out before (Steinhart & Meyer 1961), the least squares errors indicated in the tables of data give, at best, an indication of the minimum uncertainty.

It is evident from Tables 4 and 5 that there is not a great variation in the mean velocities measured in the lower crust and upper mantle in the various regions, so that

Table 1

Mean common station time–distance parameters: 10–100 *km approx.*

Station area	Shot area	No. of station T–D Plots		Mean velocity (km s^{-1})	Mean intercept (s)
Rabaul Region	Northward	6		6·02±0·14	1·54±0·20
Rabaul Region	Southward	7		5·96±0·13	1·51±0·24
Rabaul Region	Eastward	6		6·03±0·13	1·52±0·21
Rabaul Region	Westward	8		6·52±0·14	1·89±0·15
			Mean	6·13±0·14	1·62±0·20
Rabaul Region	All azimuths	14		6·11±0·10	1·70±0·14
E. Gazelle Pen.	Northward	2		5·90±0·15	1·31±0·18
	Southward	2		5·92±0·12	1·52±0·16
	Westward	2		6·07±0·38	1·66±0·44
			Mean	5·98±0·20	1·50±0·25
E. Gazelle Pen.	All azimuths	7		6·13±0·11	1·54±0·12
N.W. Gazelle Pen.	All azimuths	3		6·12±0·15	1·24±0·20
New Ireland and Islands to East	All azimuths	8		6·22±0·17	1·76±0·31
Willaumez Pen. Area	All azimuths	3		6·14±0·21	1·91±0·35
N. Coast New Britain	All azimuths	3		6·78±0·13	2·35±0·20
S. Coast New Britain	All azimuths	3		6·36±0·09	2·28±0·16

Table 2

Mean common shot time–distance parameters 10–100 *km approx.*

Shot area	Station area	No. of shot T–D plots	Mean velocity (km s^{-1})	Mean intercept (s)
E. of New Ireland	All azimuths	3	6·27±0·18	1·77±0·36
St Georges Channel and E. Bismarck Sea	Gazelle Pen. and New Ireland	40	6·12±0·15	1·51±0·23
Bismarck Sea	Central New Britain	6	6·52±0·12	2·14±0·20
Solomon Sea	Central New Britain	4	6·61±0·12	3·07±0·20

Table 3

Mean Time–Distance parameters: 10–100 *km Approx.*

Region	No. of T–D plots	Velocity (km s^{-1})	Intercept (s)
N. Gazelle Peninsula	64	6·12±0·13	1·54±0·20
New Ireland and Pacific Is.	11	6·23±0·17	1·76±0·32
Bismarck Sea	3	6·78±0·13	2·35±0·20
Willaumez Peninsula	3	6·14±0·21	1·91±0·35
Central New Britain	10	6·56±0·12	2·51±0·22
Solomon Sea	3	6·36±0·09	2·28±0·16

Table 4

Mean time–distance parameters for lower crustal arrivals

Region	No. of plots used	Velocity (km s^{-1})	Intercept (s)
Gazelle Peninsula	18	7·05±0·23	3·47±0·46
Bismarck Sea	6	6·96±0·16	2·39±0·20
Central New Britain	33	7·03±0·16	3·49±0·53
Solomon Sea	2	7·30	4·80
New Ireland and Pacific Islands	14	7·09±0·14	3·56±0·32

Table 5

Mean time–distance parameters for upper mantle arrivals

Region	No. of plots used	Velocity (km s^{-1})	Intercept (s)
Gazelle Peninsula, New Ireland, Pacific Islands	12	8·04±0·30	6·41±0·64
Bismarck Sea	14	7·98±0·18	4·64±0·43
Solomon Sea	2	7·96±0·18	6·33±0·40
Central New Britain	19	8·09±0·31	5·68±0·70

the greatest differences in crustal composition appear to be in the upper crust, as is evident from Table 3. In the Bismarck Sea the velocities of the lower crust (Table 4) are not significantly different from the velocities measured in the range 10–100 km (Table 3). Thus it appears that the first refractor velocity evident in the Bismarck Sea can be taken as 6·9 km s^{-1}, and this suggests the existence of a quite different crustal structure in this portion of the region.

As is evident from Tables 3, 4 and 5, parameters for determining crustal structure have been obtained for six regions in the survey area. In deriving these, an effort was made to limit estimates to seismic ray paths wholly within the various regions, so that an assessment of significant differences in average crustal structure can be obtained. The measured parameters were then used in simple horizontal layer models to obtain the average structural sections shown in Fig. 6. What little evidence there is from surface rocks indicates that the value for the velocity of the uppermost layer of 4·0 km s^{-1} used in the models is not unreasonable. If the least squares errors are used to determine errors in depths, then the uncertainty in the depth to Moho is 1·2 km; however, as pointed out earlier, this must be regarded as the minimum uncertainty

The features of the structure illustrated in Fig. 6 which are important are as follows: (i) the lack of material with velocity 5·8–6·5 km s^{-1} in the Bismarck Sea, indicating similarity with other marginal seas. (ii) the small thickness of 6·14 km s^{-1} material in the Willaumez Peninsula area, perhaps indicating its comparative youth,

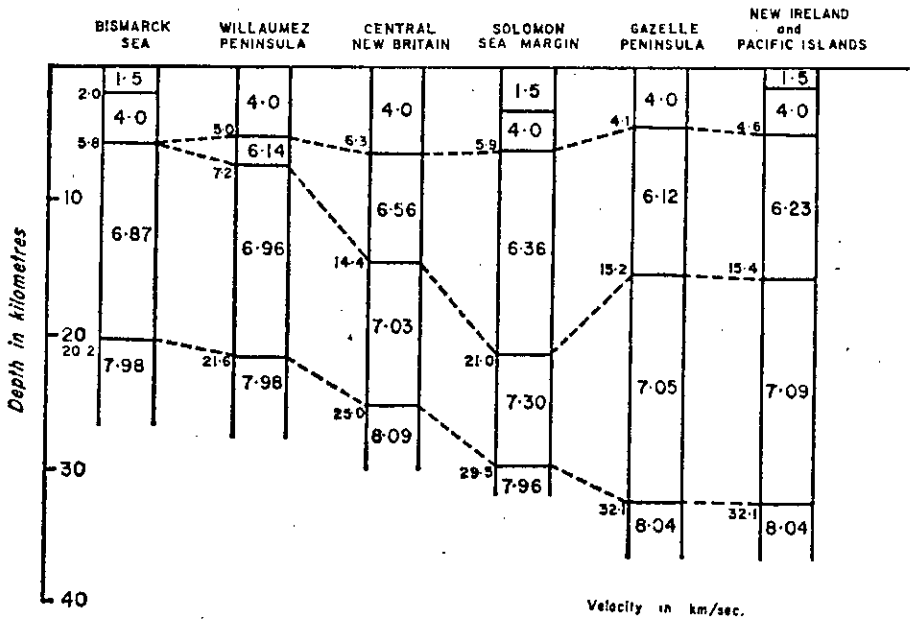

FIG. 6. Average crustal sections for the New Britain–New Ireland region.

(iii) the similarity of structure beneath the Gazelle Peninsula and New Ireland and the indication that this structure possibly extends to the islands to the east, (iv) the shallow Moho and the higher velocities evident in the upper crust under central New Britain, and (v) the thickening of upper crustal material towards the Solomon Sea, where it is still evident on the landward side of the deep ocean trench.

The present discussion represents only a first approach to the data available. More detailed interpretations on the structure and geological history of this complex region are in preparation.

Acknowledgments

The authors wish to thank the many people and organizations taking part in the 1967 and 1969 field operations, and to colleagues who have provided helpful discussions and suggestions on aspects of the interpretation. Assistance with field expenses for University of Queensland personnel, provided by the Bureau of Mineral Resources is gratefully acknowledged. Participation in the surveys by staff of the Hawaii Institute of Geophysics was made possible through support by the United States Navy, Office of Naval Research, Grant No. 083603.

Three of us (D. M. Finlayson, J. P. Cull, W. A. Wiebenga) wish to thank the Director, Bureau of Mineral Resources, Geology and Geophysics for permission to publish this paper.

D. M. Finlayson, J. P. Cull and W. A. Wiebenga:
Bureau of Mineral Resources, Geology and Geophysics, Canberra

A. S. Furumoto:
Hawaii Institute of Geophysics, Honolulu.

J. P. Webb:
University of Queensland, Brisbane

References

Bott, M. H. P., 1971. *The interior of the Earth*, Edward Arnold, London.

Brooks, J. A., editor, 1971. Investigations of crustal structure in the New Britain–New Ireland region 1969; *Geophysical and Geological Data. Bur. Min. Resour. Aust.* Record 1971/131 (unpublished).

Brooks, J. A., Connelly, J. B., Finlayson, D. M. & Wiebenga, W. A., 1971. St George's Channel—Bismarck Sea trough, *Nature Phys. Sci.*, **229**, 205.

Brown, A. R. & Webb, J. P., 1971. Oceanographic investigations in Melanesia by the Hawaii Institute of Geophysics—*Equipment and Operations. Bur. Min. Resour. Aust.* Record 1971/32 (unpublished).

Denham, D., 1969. Distribution of earthquakes in New Guinea–Solomon Islands region, *J. geophys. Res.*, **74**, 4290.

Denham, D., 1971. The seismicity of the south-west Pacific and new global tectonics, Proc. 12th Pacific Science Congress 1972, Canberra.

Dowling, J. J., 1970. Uncertainties in velocities determined by seismic refraction, *J. geophys. Res.*, **75**, 6690.

Drake, C. L. & Nafe, J. E., 1968. The transition from ocean to continent from seismic refraction data, *Am. Geophys. Union, Geophys. Mono* 12.

Finlayson, D. M., editor, 1972. Investigations of crustal structure in the Rabaul region, 1967; logistics and seismic data, *Bur. Min. Resour. Aust.*, Record, in preparation.

Furumoto, A. S., Hussong, D. M., Campbell, J. F., Sutton, G. H., Malahoff, A., Rose, J. C. & Woollard, G. P., 1970. Crust and upper mantle structure of Solomon Islands as revealed by seismic refraction survey of Nov.-Dec. 1966, *Pacific Science*, **24**, 3.

Hayes, D. E. & Ewing, M., 1970. *The Sea*, Vol. 4, Pt 2, ed. A. E. Maxwell, Wiley Interscience.

Isacks, B., Oliver, J. & Sykes, L. R., 1968. Seismology and the new global tectonics, *J. geophys. Res.*, **73**, 5855.

Johnson, T. & Molnar, P., 1972. Focal mechanisms and plate tectonics of the south-west Pacific, *J. geophys. Res.*, in press.

Krause, D. C., 1972. Crustal plates of the Bismarck and Solomon Seas, in press.

Rose, J. C., Woollard, G. P. & Malahoff, A., 1968. Marine gravity and magnetic studies of the Solomon Islands, *Am. geophys. Union, Geophys. Mono.* **12.**

Ryburn, R. J., 1971. Investigations of crustal structure in the New Britain–New Ireland region 1969; Geophysical and geological data, *Bur. Min. Resour. Aust.* Record 1971/131 (unpublished), editor J. A. Brooks.

Steinhart, J. S. & Meyer, R. P., 1961. Explosion studies of continental structure, *Carnegie Inst. of Washington, Publ.* 622.

Willcox, J. B., 1971. Preliminary results of the marine geophysical survey in the Bismarck Sea, *Abstracts ANZAAS Congress*, Brisbane 1971.

STRUCTURAL PROFILES IN THE NEW BRITAIN / NEW IRELAND REGION

By D. M. FINLAYSON & J. P. CULL

(with 10 Text-Figures)

(Received 25 September 1972; revised MS received 7 November 1972)

ABSTRACT

Seismic interpretations along lines of shots and stations in the New Britain/New Ireland region have revealed structural detail in this tectonically complex region. When correlated with marine and land gravity measurements, they indicate a comparatively uniform crust 18 km thick in the eastern Bismarck Sea, thickening to between 30 and 40 km approximately under New Britain and New Ireland. The interpretations indicate crustal thinning of the order of 8 km under the gravity high of central New Britain, and it is suggested that this is upwarping due to north-south compressional forces. The gravity data indicate that a similar structure could apply to other islands in the Solomon chain. Shear forces seem to dominate the geological structure in the region of the Gazelle Peninsula and southern New Ireland, and the 30 km thick crust there contrasts sharply with an 18 km Bismarck Sea crust along the west coast of the Peninsula. The crustal thickness under New Ireland is the same as that under the islands to the east. The seismicity of the region indicates a multiple junction of crustal plates in the Rabaul area, and the structural characteristics are predominantly a result of a lithospheric subduction zone under New Britain and a multiple shear zone extending across the Bismarck Sea.

INTRODUCTION

In their initial examination of seismic refraction data obtained from the 1967 and 1969 crustal surveys in the New Britain/New Ireland region by the Australian Bureau of Mineral Resources, Geology & Geophysics (BMR) and co-operating universities, Finlayson *et al.* (1972) produced generalized crustal sections

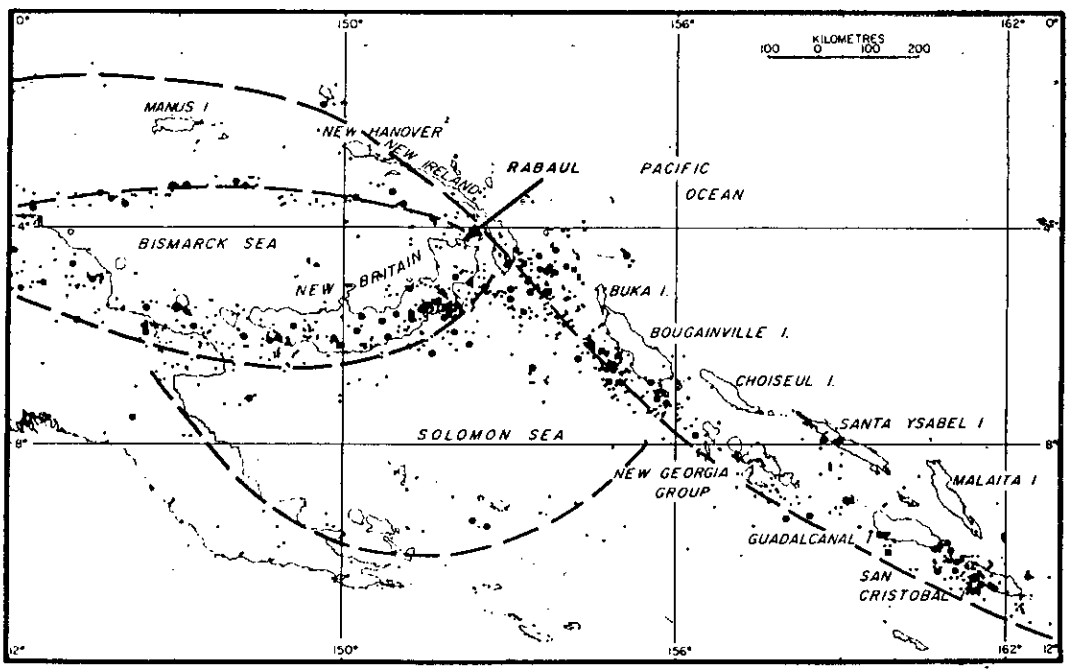

Fig. 1. Seismicity of the Solomon/Bismarck Sea region 1956/70 and inferred crustal plate boundaries (Denham, 1971).

for six areas within the survey region. This interpretation can be improved by examining the data in more detail along profiles of shots and stations, and by making use of gravity readings in the same area to establish a correlation between gravity and seismic data which may be applied to other islands in the Bismarck and Solomon Seas.

Other authors have examined the seismicity and earthquake focal mechanism data in the region and provided models of current tectonic activity using the concepts of plate tectonics (Denham, 1969, 1971; Johnson & Molnar, 1972; Krause, in press; Milsom, 1970). Their interpretations outline the existence of three small plates—the Solomon Sea plate, the South Bismarck plate and the North Bismarck plate —interacting between the larger Indian-Australian and Pacific plates. The multiple junction of four of these plates in the vicinity of Rabaul can be expected to result in complex crustal structures (Fig. 1).

SURVEYS AND DATA

The area covered by the 1967 and 1969 seismic refraction surveys is illustrated in Figure 2. Details of the work have been given in un-

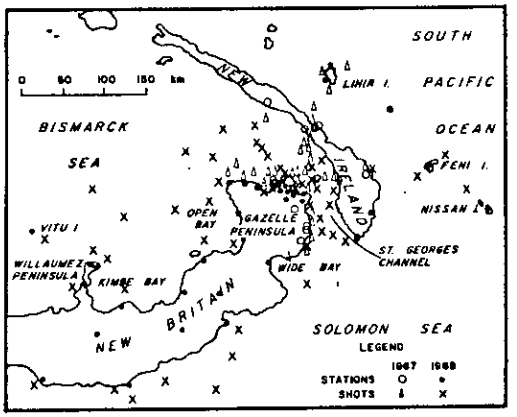

Fig. 2. Shot and station locations for the 1967 and 1969 seismic refraction surveys. Detail in the Rabaul area is not shown.

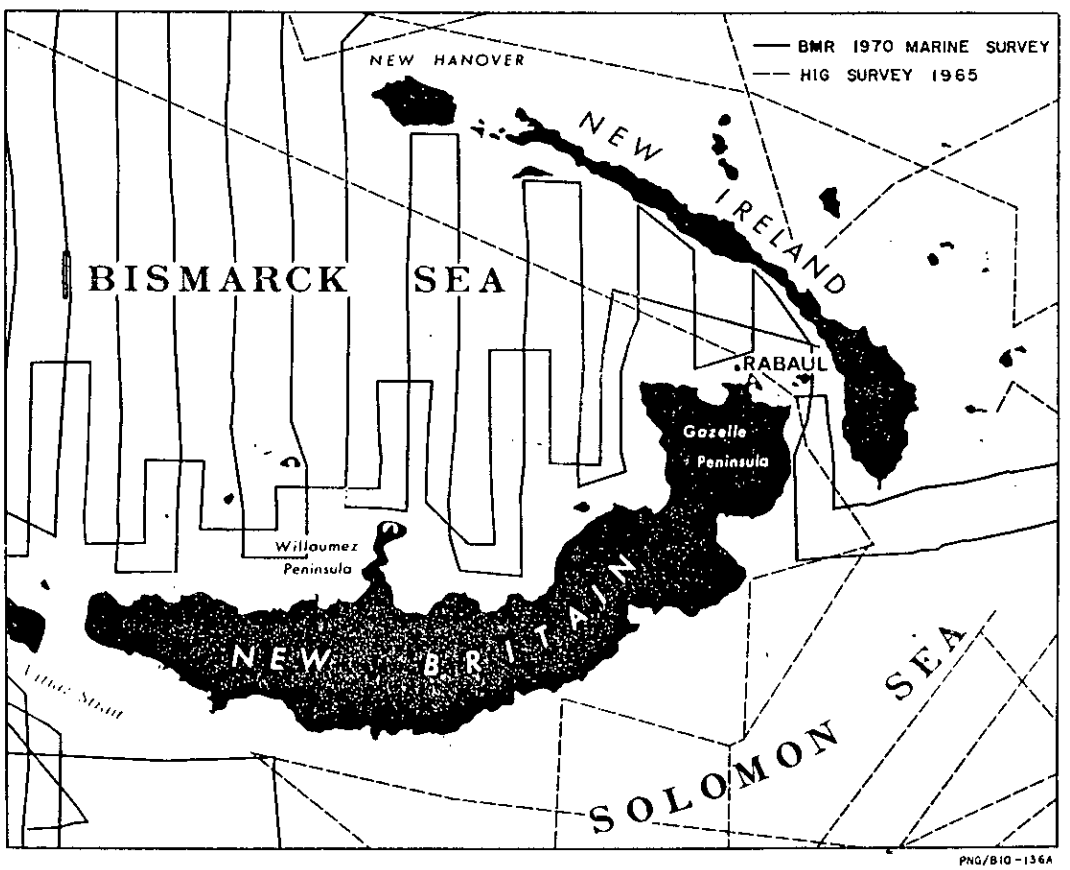

Fig. 3. Marine gravity traverses in the New Britain /New Ireland region conducted during 1965 by the Hawaii Institute of Geophysics and during 1970 by the Bureau of Mineral Resources.

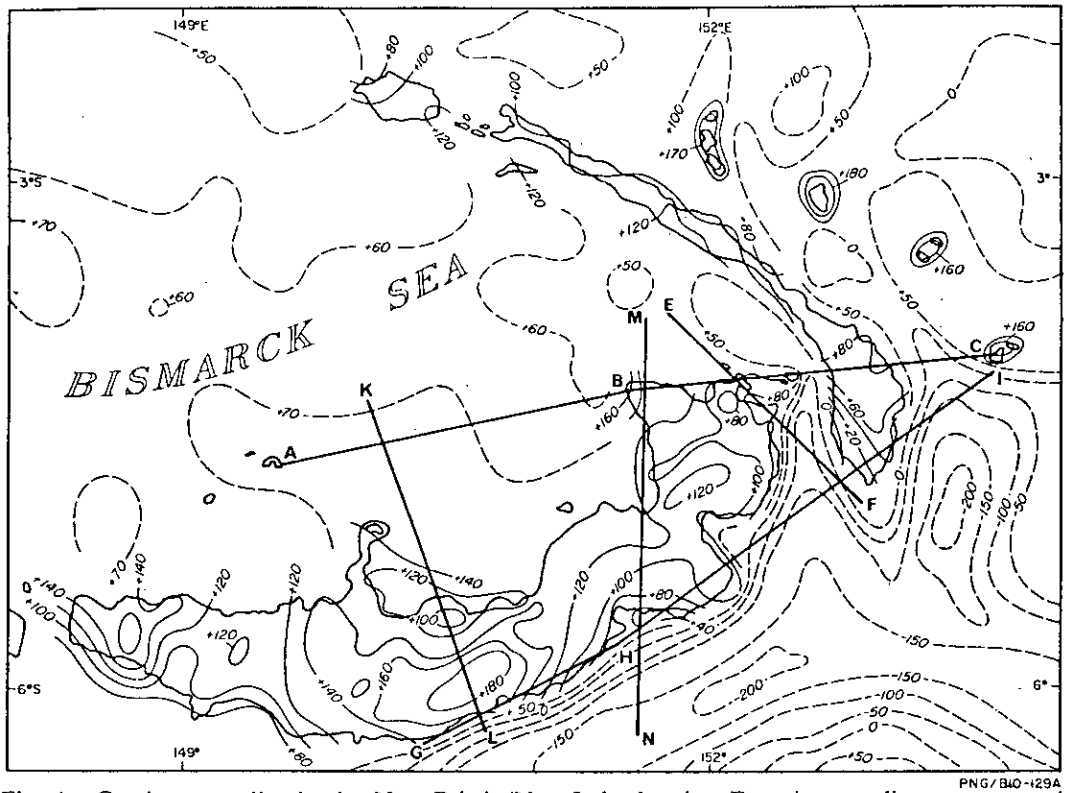

Fig. 4. Gravity anomalies in the New Britain/New Ireland region. Free-air anomalies are contoured at sea; Bouguer anomalies are contoured on land from BMR 1969 survey using crustal density of 2.67 g/cm^3.

published reports by Brooks (1971), Finlayson (1972) and Finlayson *et al.* (1972). In this paper the 1969 survey data, which provides the information for interpretation of structures down to the M discontinuity (Moho), are used to maintain seismic control of gravity interpretations.

During 1969 BMR conducted a helicopter reconnaissance gravity survey of New Britain and New Ireland to supplement the other geological and geophysical information in the area (Brooks, 1971). Whenever possible a station interval of 15 km was maintained; a higher station density was achieved in the Rabaul area. The gravity observations were made with a LaCoste & Romberg gravity meter and tied to existing 'isogal' reference stations, of which there are six in the area (Barlow, 1970). Height was determined by using microbarometers and bench marks, and latitude and longitude by using aerial photography and the mapping network. The corrected gravity values are estimated to be accurate within 1 milligal.

The marine gravity surveys in the area were conducted by the Hawaii Institute of Geophysics (HIG) during 1965 (Rose & Tracy, 1971; Rose *et al.*, 1968) and by BMR during 1970 (Willcox, in prep.). The combined marine traverses are illustrated in Figure 3.

In Figure 4 the results of the three gravity surveys have been combined in a composite map, which illustrates the free-air gravity anomalies over the sea and simple Bouguer anomalies on land, calculated using a crustal density of 2.67 g/cm^3.

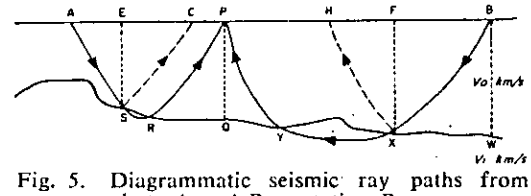

Fig. 5. Diagrammatic seismic ray paths from shots A and B to station P.

ANALYSIS OF SEISMIC PROFILES

Five lines of shots and stations were chosen for profile analysis, and these are shown in Figure 4. Lines KL and EF were selected because they were approximately normal to the geological trends; lines MN, ABC, and GHI were chosen to show structural variations

across the various regions along convenient lines of shots and stations. At each end of the chosen lines, a station (or shot) was selected and its time-distance plot was produced from those shots (or stations) which were situated within an azimuth of about 10° on either side of the line, so that apparent velocities could be determined with little ambiguity. The two plots produced for each line were considered as a reversed profile, and time depths were obtained at several points on the line by the reciprocal method of seismic refraction interpretation outlined below (Hawkins, 1961).

Referring to Figure 5, at point P the *time depth* (td_p) is defined as

$$td_p = \tfrac{1}{2}(t_1 + t_2 - T_R) \quad \ldots\ldots (1)$$

where t_1 and t_2 are the times taken to travel the refraction paths ASRP and BXYP, and T_R (the *reciprocal time*) is the time taken to travel the path ASXB. Because t_1 and t_2 in equation 1 cannot be measured in the regions AC and BH respectively, such time depths can be obtained only in the range CH. For refraction at the Moho the offset distances AE and BF are of the order of 40 km, and AC and BH of the order of 80 km.

To derive crustal structure closer to the extremities of the lines it is necessary to use the concept of delay times. Referring to the path BXYP of Figure 5 the delay time (DT) at B is known from refraction theory as:

$$DT_B = BX/V_0 - WX/V_1 \quad \ldots\ldots (2)$$

where V_0 and V_1 are the seismic velocities in the upper and lower layers respectively and are assumed constant.

If the delay time at P (DT_p) is known, then equation (2) can be rewritten as:

$$DT_B = t_2 - DT_p - PB/V_1 \quad \ldots\ldots (3)$$

It should be noted that DT_p is not unique. In Figure 5 it can be defined as either

$$DT_p = PY/V_0 - QY/V_1 \quad \ldots\ldots (4)$$

$$\text{or } DT_p = PR/V_0 - RQ/V_1 \quad \ldots\ldots (5)$$

Equations (4) and (5) give equivalent results for DT_p only if the points R and Y are at the same depth. However, averaging equations (4) and (5) we get

$$\text{av. } DT_p = \tfrac{1}{2}(PY + PR)/V_0 - (QY + RQ)/V_1) \quad \ldots\ldots (6)$$

Comparing the right hand sides of equations (1) and (6) we see that

$$td_p = \text{av. } DT_p \quad \ldots\ldots (7)$$

As an approximation, equation (7) can be substituted in equation (3) so that the delay time at B is defined as

$$DT_B = t_2 - PB/V_1 - td_P \quad \ldots\ldots (8)$$

For the selected seismic profiles (Figure 4) equation (1) was used to calculate as many time depths (td_p) as possible, and these were used in equation (8) to calculate the delay times at the end points of the lines. The end-point delay times were then used in equation (3) to calculate delay times for points along the line at which time depths could not be determined. Offset distances were calculated where appropriate.

An example of the time-distance plots across the Bismarck Sea is illustrated in Figure 6. The velocities identified from all the travel-time plots are denoted by P_0, P_1, P_2, and P_n, which respectively represent the velocities 4.0, 6.2 ± 0.4, 7.1 ± 0.4, and 8.2 ± 0.4 km/s. The near-surface P_0 velocities were in general not well defined, but for the purpose of constructing the sections little error is introduced to the gross structure by assuming a velocity of 4.0 km/s. The P_n information obtained from shots at larger distances is well defined for the sections chosen; apparent velocities ranged between 7.8 and 8.5 km/s, with an average of 8.13 km/s.

The P_1 velocities were determined reliably when azimuth restrictions were removed, but only along the sections GHI and EF could they be accurately determined when azimuth limits were imposed. Elsewhere the average velocities derived by Finlayson *et al.* (1972) were used as a basis for computation. The P_2 velocities were well determined if some second and subsequent arrivals were used to define the line segments; they range between 6.6 and 7.4 km/s, with an average of 7.0 km/s.

The parameters for the linear segments fitted to the travel-time plots were computed, and the sections shown in Figures 8 and 9 were derived from these parameters.

The principles used in the interpretation are commonly used in this type of survey work, namely: (a) seismic data alone were used as a basis for the interpretation models and at a later stage geological and gravity considerations were taken into account to test the adequacy of the model; and (b) the models derived from the interpretation were to be as simple as possible, introducing the least number of assumptions to account adequately for the data.

GRAVITY CORRELATION

The derived seismic structures can to a certain extent be substantiated by comparing the gravity profiles computed from the seismic cross-sections with the observed gravity anomalies (Figure 4).

The gravity modelling of the seismic profiles was carried out using a computer gravity program designed for arbitrary two-dimensional structures (Cull, in prep.). The approximation to two-dimensional models is reasonable

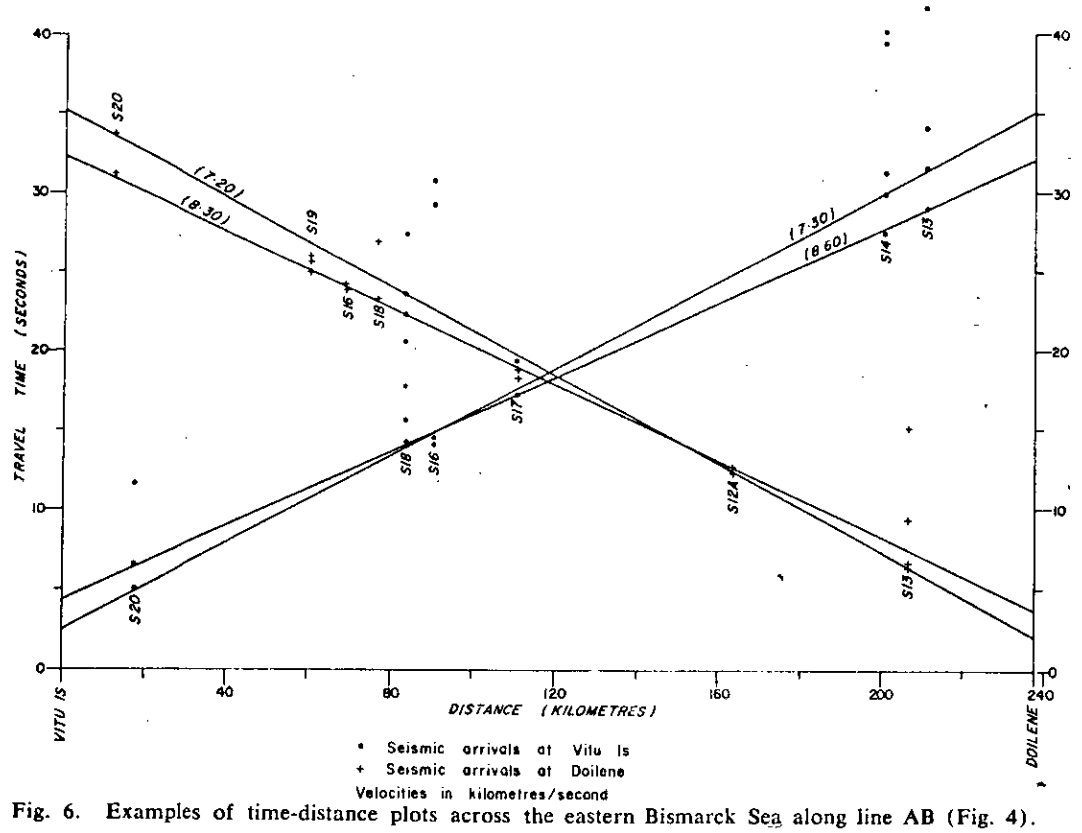

Fig. 6. Examples of time-distance plots across the eastern Bismarck Sea along line AB (Fig. 4).

in all profiles except GHI, where the profile is not approximately normal to the geological trends. The modelling principles are similar to those of Talwani, Sutton, & Worzel (1959) and Mueller & Talwani (1971). The modelling procedure adopted for the profiles uses free-air anomalies in sea areas and simple Bouguer anomalies over the land.

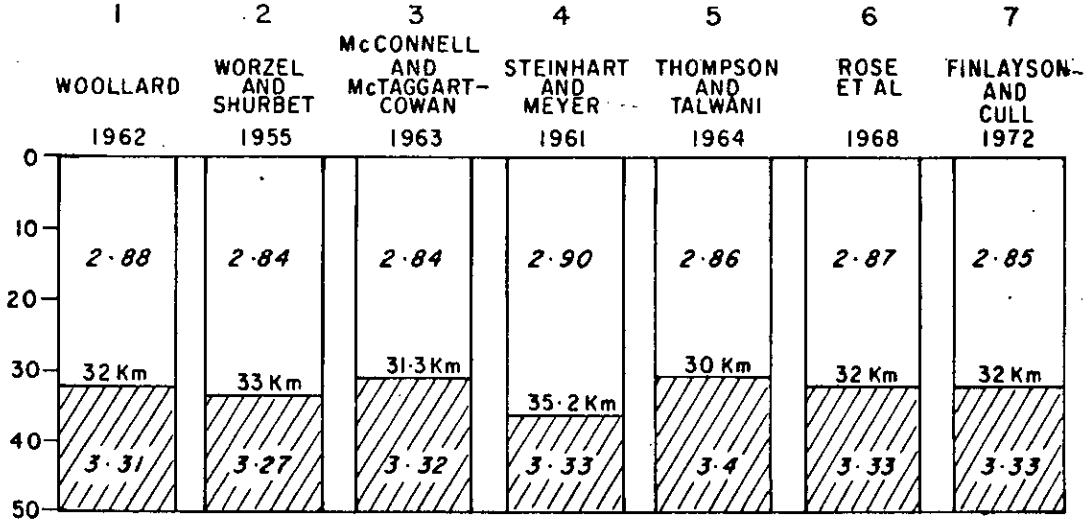

Fig. 7. Standard crustal sections used by various authors for gravity interpretations; 1972 represents standard section used in present interpretation.

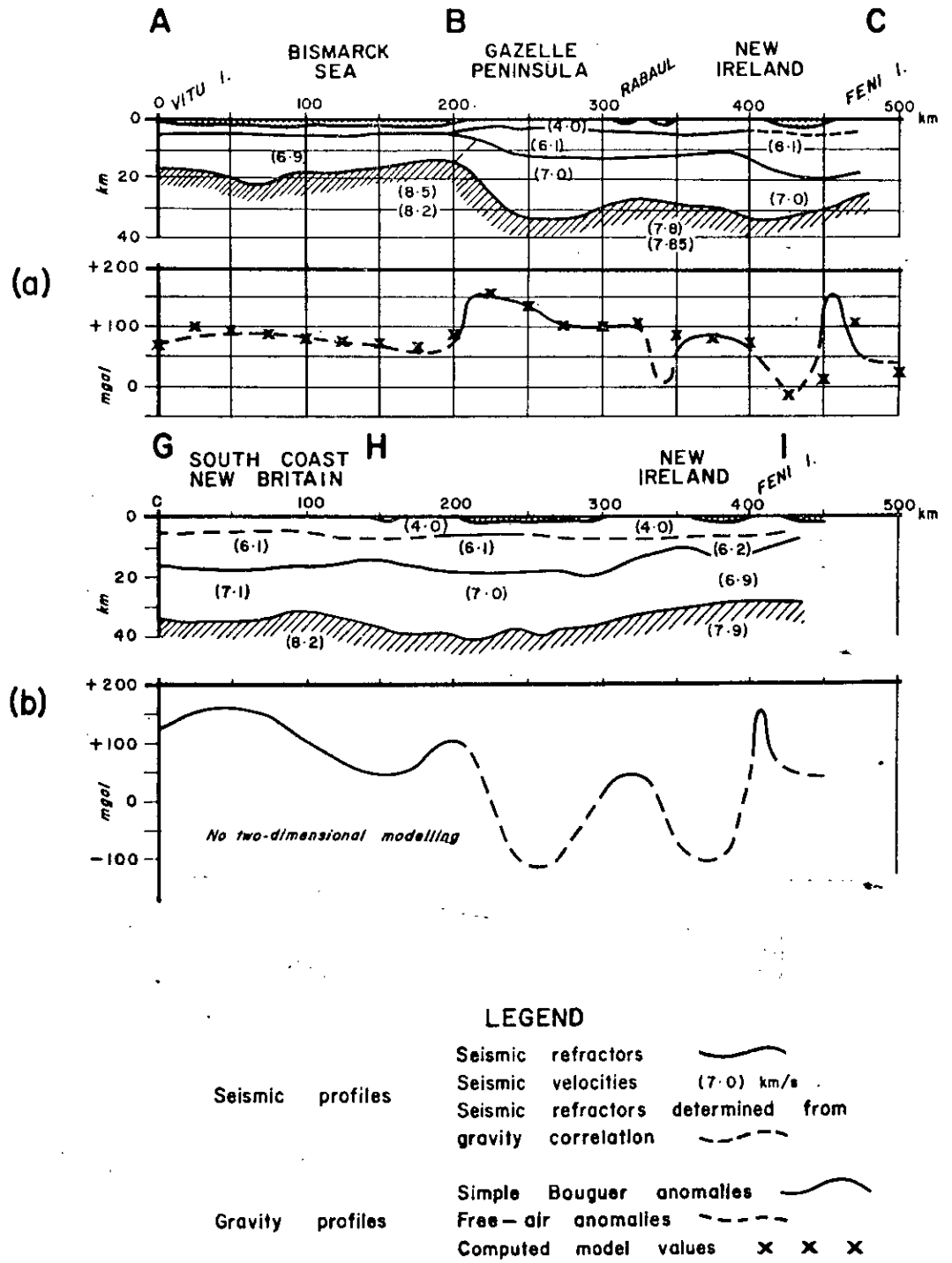

LEGEND

Seismic profiles	Seismic refractors	
	Seismic velocities	(7·0) km/s
	Seismic refractors determined from gravity correlation	
Gravity profiles	Simple Bouguer anomalies	
	Free–air anomalies	
	Computed model values	× × ×

Fig. 8. Seismic and gravity profiles along lines ABC and GHI.

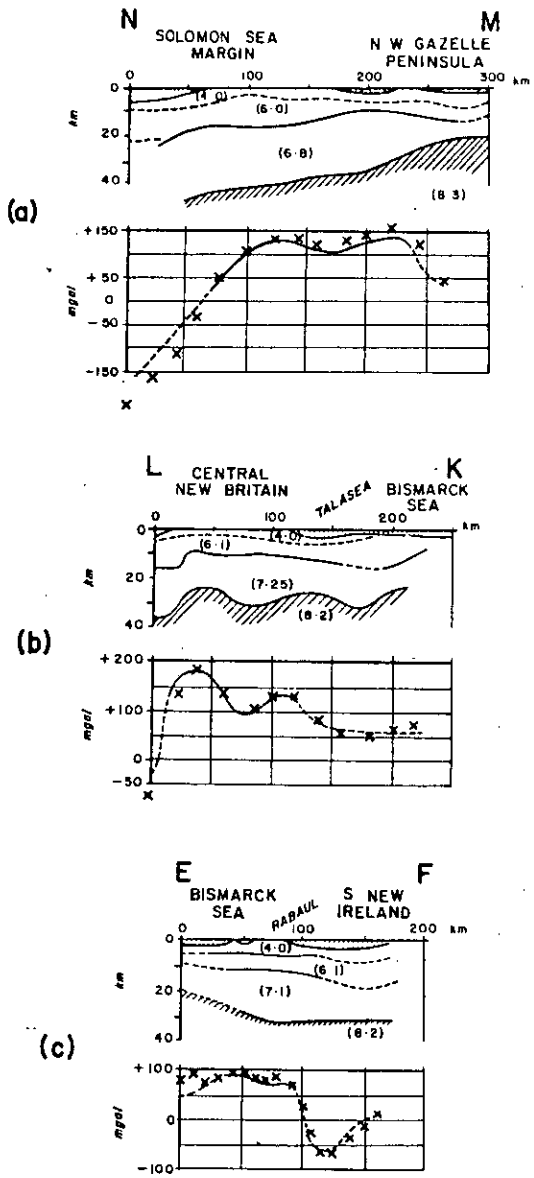

Fig. 9. Seismic and gravity profiles along lines NM, LK, and EF.

Densities measured on rock samples from the land survey areas ranged between 2.60 and 2.85 g/cm^3 on average, and consequently the simple Bouguer anomalies over central New Britain may be in error by about 10 mgal. However, terrain corrections (typically 5-10 mgal but going up to 40 mgal in extreme cases) if applied would have the opposite sense to errors introduced by underestimating the density, and thus to a certain extent these cancel each other out.

In the mountainous regions of New Britain and New Ireland the free-air anomalies have a direct correlation with topography. This is caused by the proximity of the surface mass distribution; although isostatic compensation may take place for average regional values of elevation, the compensation mass distribution at depth is remote relative to the surface mass distribution. The simple Bouguer anomalies used for modelling are in large measure free of the local topographic effect as the correction for the included mass above sea level incorporates the bulk of the effect of topographic variations (Woollard, 1967).

Computer models were used to calculate the gravity effect of a proposed crustal cross-section, but to relate this to measured gravity values it is necessary to determine the gravity effect of a standard crustal section selected to provide a datum level for reconstruction. As noted by Smith *et al.* (1966), discrepancies of up to 100 mgal can occur owing to incorrect choice of standard sections. Several sections used in gravity analyses in recent years are illustrated in Figure 7. For the New Britain/New Ireland region a standard crustal density was derived by plotting Bouguer anomalies against Moho depth calculated from seismic data and applying a least-squares fit to obtain the empirical relation

$$BA = (20.0 \pm 3.5)D + (720 \pm 120) \quad (9)$$

where BA=Bouguer anomaly in mgal and D=Moho depth in km.

From (9) we get

$$d(BA)/dD = 20.0 \pm 3.5 \quad (10)$$

and from the Bouguer plate equation

$$d(BA)/dD = 41.85\ \Delta\rho \quad (11)$$

where $\Delta\rho$ is the density difference

Hence from (10) and (11) $\Delta\rho = 0.48$ g/cm^3.

If an upper mantle density of 3.33 g/cm^3 is used, then the average crustal density is

$$\rho = 3.33 - \Delta\rho = 2.85 \pm 0.08 \text{ g/cm}^3 \quad (12)$$

The standard section used in the analysis given in this paper is shown in Figure 7 for comparison with other sections; it is very similar to the section that Rose *et al.* (1968) used for interpretation of gravity in the Solomon Sea region.

The velocities and densities measured on geological samples collected in New Britain were in good accord with the empirical velocity-density curve of Nafe & Drake (Talwani *et al.*, 1959) which was used to compute the gravity profiles from the seismic sections (Figures 8 and 9).

The fit between the observed and computed gravity anomalies based on the seismic models

is generally good, and any differences can be attributed to a coarseness in the modelling of the sea bottom in areas of extreme relief and to deviations of the true structure from the two-dimensional models.

The New Britain gravity anomalies are very similar in size to those described by Laudon (1968) along the Solomon Island chain (Figure 10). Along central New Britain, free-air anomalies greater than +200 mgal and Bouguer anomalies up to +190 mgals have been measured. On Buka Island at the northern end of the Solomon Island chain, the Bouguer gravity maximum of +240 mgals is associated with basic volcanics, and on adjoining Bougainville Island the coastal Bouguer gravity values of +170 mgal probably indicate values greater than +200 mgal in the interior of the island. Similar high values are observed farther south along the island chain, and the free-air anomaly attains its highest value of about +300 mgal in the mountains on Guadalcanal and San Cristobal.

Thus in common with the major Solomon Islands, New Britain is characterized by large positive free-air and Bouguer anomalies, and considerable local departures from isostasy are indicated by the regional association between elevation and Bouguer anomaly value. These departures from isostasy can be attributed to high-density crustal material, especially ultrabasic intrusives in the basement, or to upwarping of the base of the crust (Laudon, 1968), or both. Geological investigations in New Britain and the seismic refraction evidence substantiate both these ideas.

Local large anomalies in Late Tertiary and Quaternary volcanic areas are attributable to the crust's supporting accumulated volcanic piles without isostatic compensation. This probably applies to the islands east of New Ireland, where Bouguer values of +160 and +180 mgal are observed. In the Rabaul region Laudon (1968) associates the volcanic craters with the local gravity highs and suggests that the present volcanic activity is associated with intersecting fracture zones filled with crystalline material intruding the lighter predominantly pyroclastic material. One of us (J.P.C.) has modelled the detailed gravity in the area and finds that a prism of high-density material extending to considerable depth under Rabaul fits the local gravity picture superimposed on the regional trend. Although a highly idealistic model, it substantiates Laudon's suggestion mentioned above.

The Bouguer gravity anomalies along New Ireland do not reach the very high values observed on New Britain but have maxima of +120 mgal with the trends running parallel to the axis of the island. Farther along the island chain, at Manus Island in the northern Bismarck Sea, the Bouguer values are somewhat less, in the range +70 to +100 mgal (Laudon, 1968). In southern New Ireland a steep gravity gradient parallel to the Weitin River Fault indicates the importance of this fault in the tectonic interpretation of the area.

Significantly all the islands in the Bismarck/Solomon Archipelago with high Bouguer anomaly values (greater than about +120 mgal) have adjacent ocean trenches and high seismicity. Thus the tectonic situation revealed by the seismic results in New Britain—upwarping of the base of the crust to produce high gravity values—could apply also to Buka, Bougainville, Guadalcanal, and San Cristobal around the perimeter of the Solomon Sea, and Choiseul and Santa Ysabel with their associated embryo trench on the Pacific side of the Solomon Island chain. The notable absence of a trench and of major seismicity in the New Georgia Island group, and the fact that the corresponding Bouguer anomaly values do not exceed +100 mgal on a regional scale (Figure 10), seem to substantiate this idea. Similarly the lower Bouguer anomaly maxima observed on New Ireland and Manus Island can be associated with relative tectonic quiescence.

DISCUSSION

The sections illustrated in Figures 8 and 9 are in broad agreement with the conclusions derived from adopting average crustal areas (Finlayson *et al.*, 1972); however, some further details have been brought out which are worth noting.

Along section ABC the major transition from the Bismarck Sea structure to the Gazelle Peninsula structure is re-emphasized. There is a slight thinning of the crust under the St Georges Channel, west of New Ireland and under New Ireland itself, but the average crustal thickness out to Feni Islands is maintained at about 30 km by an increase in the thickness of the upper crustal layer.

The section GHI demonstrates the thickening of the crust along the south coast of New Britain on the landward side of the ocean trench. Sections KL and NM again bring out this feature; however, the most obvious feature of the section LK is the thinning of the crust in the region of the gravity high in central New Britain. The gradients interpreted in the Moho structure in the central New Britain region can be up to 20° from the horizontal, and the existence of oblique angle refractions along

sections parallel to the strike, e.g. section GHI, would lead to migration of the refraction points by as much as 15 km up-dip.

Along the section EF through the Rabaul caldera there do not appear to be any gross crustal changes, but undoubtedly further interpretation of the close refraction work in that region will reveal more complicated structure in the upper crust.

The significance of the refracting horizons and velocities in terms of current tectonic processes is more difficult to define. The 7.2 to 7.7 km/s velocities which Drake & Nafe (1968) associated with orogenic belts have not been identified in this survey; we recognise only two crustal velocities below basement.

As mentioned in the introduction, the seismicity pattern in the region is taken as the most

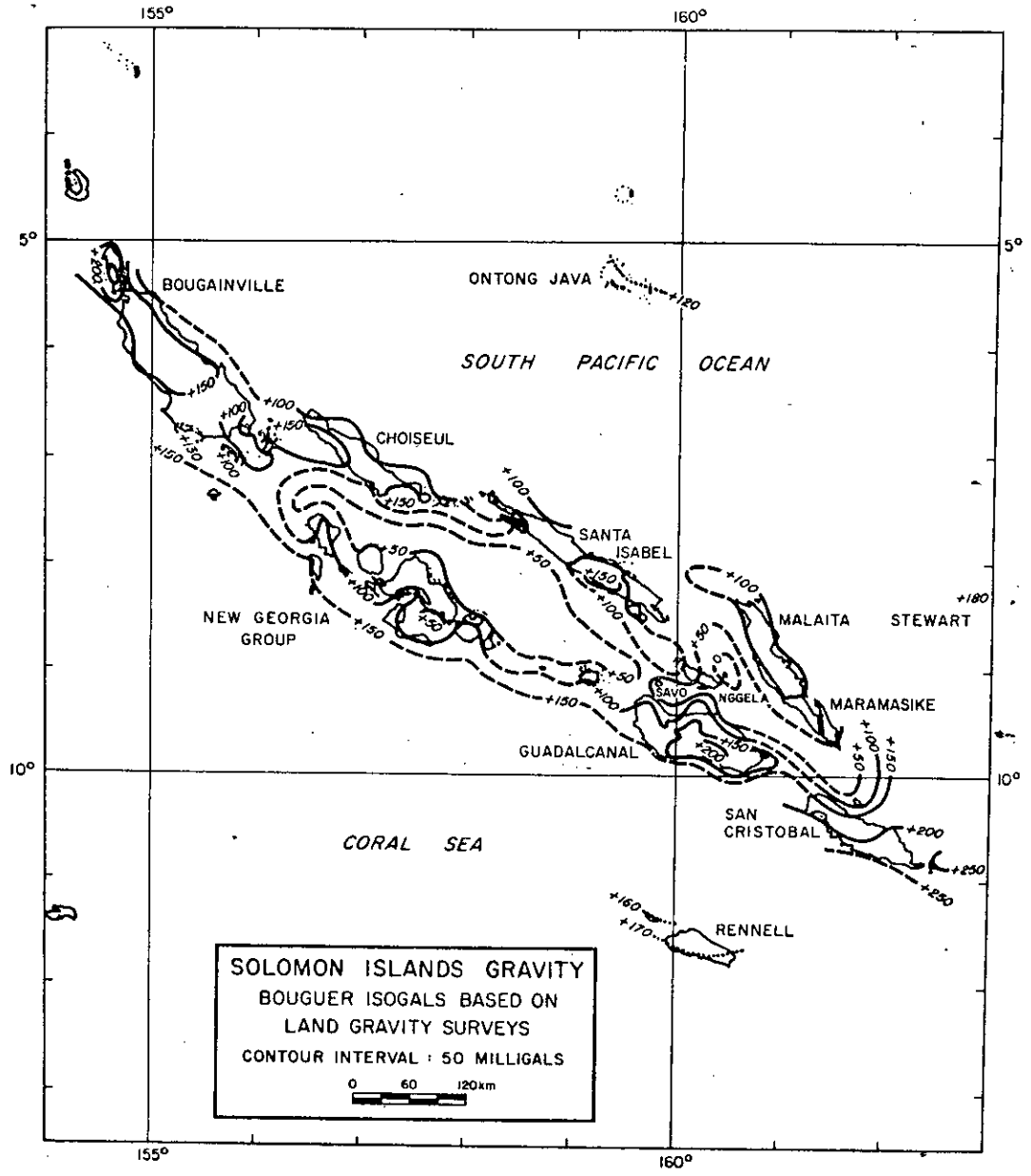

Fig. 10. Solomon Islands regional Bouguer anomaly contours interpreted from Bouguer maps of the individual islands (after Laudon, 1968).

significant indicator of current tectonics and it suggests a multiple junction of crustal blocks in the neighbourhood of Rabaul. Recently Wiebenga (1971) has advanced the idea that the crustal structural features in the area are a result of tensional stresses across the region from the Tertiary until the present. However, the arguments for such a tectonic hypothesis ignore the substantial evidence to the contrary provided by seismicity and focal mechanisms (Denham, 1971; Johnson & Molnar, 1972; Krause, in press).

The preferred emphasis in the present interpretation is that the crustal structure in central New Britain results from north-south compressional forces which have produced a northward-dipping Benioff zone with upwarping of the Moho and a surface geological expression of block faulting and local tensional features, regional uplift, and volcanism which is still active. In the region of the Gazelle Peninsula and southern New Ireland large-scale multiple shearing seems to be associated with the Bismarck Sea seismicity zone; the surface pattern of northwest-trending faults and local seismic lineaments substantiates this idea. The submarine topography along the zone of high seismicity and in the St Georges Channel (Brooks *et al.*, 1971) indicates that the shear zones are a source of volcanic extrusive material.

ACKNOWLEDGMENTS

The authors would like to thank all those who have taken part in the recent geophysical and geological surveys in the New Britain/New Ireland region and those who have provided helpful discussions and suggestions on aspects of the interpretation. This paper is published with the permission of the Director of the Bureau of Mineral Resources, Geology and Geophysics.

REFERENCES

BARLOW, B. C., 1970: National report on gravity in Australia, July 1965-June 1970. *Bur. Miner. Resour. Aust. Rec.* 1970/62 (*unpubl.*).

BROOKS, J. A., 1971: Investigations of crustal structure in the New Britain—New Ireland region 1969; geophysical and geological data. *Bur. Miner. Resour. Aust. Rec.* 1971/131 (unpubl.).

———, CONNELLY, J. B., FINLAYSON, D. M., and WIEBENGA, W. A., 1971—St Georges Channel-Bismarck Sea trough. *Nature Physical Science, 229* (7), p. 205.

CULL, J. P., (in prep.): A Fortran program for calculating the gravity effect of arbitrary two dimensional bodies. *Bur. Miner. Resour. Aust. Rec.*

DENHAM, D., 1969: Distribution of earthquakes in the New Guinea—Solomon Islands region. *J. geophys. Res., 74,* p. 4290.

———, 1971: The seismicity of the southwest Pacific and new global tectonics. *Proc. 12th Pacif., Sci. Congr., Abstr.* Also *Univ. W.Aust. Press* (*ed. P. J. Coleman*), in press.

DRAKE, C L., & NAFE, J. E., 1968: The transition from ocean to continent from seismic refraction data. *Amer. geophys. Un., geophys. Monogr. 12,* pp. 174-186.

FINLAYSON, D. M., 1972: Investigations of crustal structure in the Rabaul region 1967—logistics and data. *Bur. Miner. Resour. Aust. Rec.* 1972/45 (unpubl.).

———, CULL, J. P., WIEBENGA, W. A., FURUMOTO, A. S., & WEBB, J. P., 1972: New Britain—New Ireland crustal refraction investigations 1967 and 1969. *Geophys. J. R. Astr. Soc., 29,* p. 245.

HAWKINS, L. V., 1961: The reciprocal method of routine shallow seismic refraction investigations. *Geophysics, 26* (6), p. 806.

JOHNSON, T., & MOLNAR, P., 1972: Focal mechanisms and plate tectonics of the southwest Pacific. *J. geophys. Res., 77,* pp. 5000-5032.

KRAUSE, D. C., in press: Crustal plates of the Bismarck and Solomon Seas.

LAUDON, T. S., 1968: Land gravity survey of the Solomon and Bismarck Islands. *Amer. geophys. Un., Geophys. Monogr. 12,* pp. 279-295.

MCCONNEL, R. K., & MCTAGGART-COWAN, G. H., 1963: Crustal seismic refraction profiles—a compilation. *Inst. Earth Sci., Univ. Toronto, Earth Sci. Rep.* 8.

MILSOM, J. S., 1970: Woodlark Basin, a minor center of sea-floor spreading in Melanesia. *J. geophys. Res., 75,* pp. 7335-7339.

MUELLER, S., & TALWANI, M., 1971: A crustal section across the eastern Alps. *Pure appl. Geophys., 85,* p. 226.

ROSE, J. C., & TRACY, R. W., 1971: Gravity results in the Solomon Islands region, aboard H.M.S. Dampier in 1965. *Hawaii Inst. Geophys. Data Rep. 17,* HIG-71-2.

———, WOOLLARD. G. P., & MALAHOFF, A., 1968: Marine gravity and magnetic studies of the Solomon Islands. *Amer. Geophys. Un., Geophys. Monogr. 12,* pp. 379-410.

SMITH, T. J., STEINHART, J. S., & ALDRICH, L. T., 1966: Lake Superior crustal structure. *J. geophys. Res., 71,* p. 1141.

STEINHART, J. S., & MEYER, R. P., 1961: Explosion studies of continental structure. *Carneg. Inst. Wash. Publ.* 622.

TALWANI, M., SUTTON, G. H., & WORZEL, J. L., 1959: A crustal section across the Puerto Rico Trench. *J. geophys. Res., 64,* p. 1545.

THOMPSON, G. A., & TALWANI, M., 1964: Geology of the crust and mantle, western United States. *Science, 146,* pp. 1539-1549.

WIEBENGA, W. A., 1971: Crustal structure of the New Britain—New Ireland region. *Proc. 12th Pacif. Sci. Cong. Abstr.* Also *Univ. W.Aust. Press (ed. P. J. Coleman)*, in press.

WILLCOX, J. B., 1971: Preliminary results of the BMR marine geophysical survey in the Bismarck Sea. *ANZAAS Cong., Brisbane, 1971, Abstr.*

———, in prep: Bismarck Sea and Gulf of Papua marine geophysical survey 1970; interpretation of Bismarck Sea region. *Bur. Miner. Resour. Aust. Rec.*

WOOLLARD, G. P., 1962: The relation of gravity anomalies to surface elevation, crustal structure and geology. *Univ. Wisconsin, Geophys. polar Res. Center, Res. Rep.* 62-9.

———, 1967: *International Dictionary of Geophysics, 1,* p. 688. Pergamon Press.

WORZEL, J. L., & SHURBET, G. L., 1955: Gravity interpretations from standard oceanic and continental crustal sections. *Geol. Soc. Am. spec. Pap. 62,* pp. 87-100.

D. M. Finlayson
J. P. Cull
Bureau of Mineral Resources, Geology and Geophysics,
Canberra, Australia.

Geophys. J. R. astr. Soc. (1973) **33**, 265–280

Time-Term Analysis of New Britain–New Ireland Island Arc Structures

D. M. Finlayson and J. P. Cull

(Received 1973 March 16)

Summary

Seismic data from the New Britain–New Ireland region are interpreted by the time-term method to give depths to four refractors: (a) the near-surface refractor in the area of the Rabaul Caldera; (b) the basement refractor under the Gazelle Peninsula–southern New Ireland area; (c) the intra-crustal refractor; and (d) the Moho refractor under New Britain, New Ireland, and surrounding waters. The respective least-squares velocities are $4{\cdot}64 \pm 0{\cdot}08\ \mathrm{km\,s^{-1}}$, $6{\cdot}11 \pm 0{\cdot}02\ \mathrm{km\,s^{-1}}$, $6{\cdot}84 \pm 0{\cdot}03\ \mathrm{km\,s^{-1}}$, and $7{\cdot}92 \pm 0{\cdot}05\ \mathrm{km\,s^{-1}}$, with the residuals indicating that there is a wider divergence of structure at the Moho boundary than at the upper three refractors.

Introduction

The combined distribution of shots and recording stations for seismic refraction surveys conducted during 1967 and 1969 in the New Britain–New Ireland region of Melanesia (Brooks 1971; Finlayson 1972; Finlayson *et al.* 1972; Finlayson & Cull 1973) provides an opportunity for applying the time-term interpretation techniques of Scheidegger & Willmore (1957) to an island arc structure (Fig. 1). The tectonic complexity of the Bismarck and Solomon Sea region has made it the focus of a number of geophysical investigations in recent years (Rose, Woollard & Malahoff 1968; Furumoto *et al.* 1970; Denham 1969, 1973; Johnson & Molnar 1972; Krause 1973; Willcox, in preparation) and the seismic refraction interpretation presented in this paper gives a structural basis for some of that work. The interpretations published so far from the refraction data (Finlayson *et al.* 1972; Finlayson & Cull 1973; Wiebenga 1973) do not provide the overall picture of crustal structure obtained by using the time-term technique.

Data and analysis

The data from the 1967 and 1969 seismic refraction surveys conducted by the Bureau of Mineral Resources, Geology & Geophysics (BMR) and co-operating universities are listed in various reports (Brooks 1971; Finlayson 1972) and are sufficient to provide the sound statistical basis essential for the time-term interpretation method. A description of the surveys and the methods used is given by Finlayson *et al.* (1972). Briefly, 44 marine shots were recorded in 1967 on 17 sets of land based recording equipment and 54 marine shots were recorded in 1969 on 24 sets

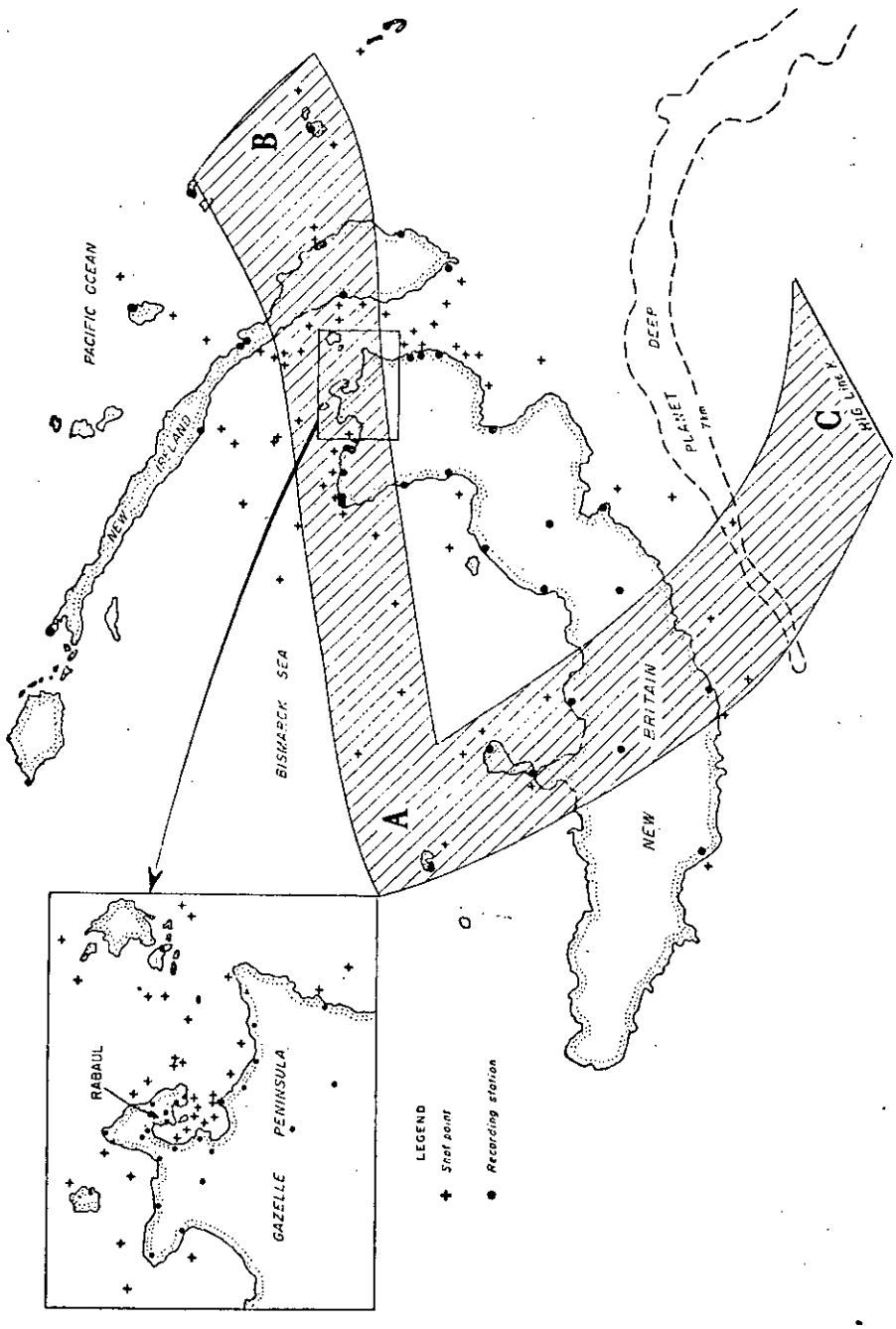

FIG. 1. Combined shot and station locations for the 1967 and 1969 seismic refraction surveys and location of sections illustrated in Fig. 9.

of equipment. The equipment was relocated during various stages of the survey, to provide readings at 28 sites in 1967 and 48 sites in 1969. Altogether, 1074 seismic first arrivals were recorded at distances less than 100 km and 396 at distances greater than 100 km; all arrivals were allotted a subjective ' quality ' and an ' accuracy ' for use in subsequent weighting of the data.

The distribution of shots and stations (Fig. 1) largely satisfies the criteria that should be incorporated in any survey using the time-term interpretation method (Scheidegger & Willmore 1957; Willmore & Bancroft, 1960), namely:

1. Shot and station locations must form extended patterns to provide adequate determination of the velocity in the marker layer.

2. Where the most accurate interpretation is required (which in this case is the Rabaul area) there must be an adequate number of stations and shots connected to other survey points in several directions.

3. Recording stations should not be moved too frequently, so that a statistically significant quantity of data is recorded at each station.

4. To determine a unique solution it is important to have several locations at which shots and stations are near-coincident.

The method has been applied to crustal investigations in a number of areas: the Lake Superior survey (Berry & West 1966; Smith, Steinhart & Aldrich 1966), various Australian surveys (Finlayson 1968; Underwood 1969), and the Continental Margin Refraction Experiment (Bamford 1971). Unfortunately these surveys were not really designed with time-term interpretation in mind, as is evident from the linear arrangements of shots and stations, and the weaknesses of applying a time-term analysis to such experiments have been described by O'Brien (1968).

The mathematical method used for the interpretation of data in this paper is that of Berry & West (1966) and is described only in outline here.

Assuming that there is a refracting boundary with seismic velocity V_1 above and V_2 below, the theoretical travel-time for the critically refracted head wave between sites i and j can be written

$$t_{ij} = D_{ij}/V_2 + a_i + a_j \tag{1}$$

where

D_{ij} = distance separating the ith and jth sites

If a_i and a_j = time terms at the i-th and j-th sites (i.e. at the shot-point and recording station)

T_{ij} = observed travel time for head wave, the residual difference between the theoretical and observed travel times can be written

$$R_{ij} = T_{ij} - t_{ij} \tag{2}$$

$$= X_{ij} - a_i - a_j \tag{3}$$

where

$$X_{ij} = T_{ij} - D_{ij}/V_2. \tag{4}$$

Assuming that the sites i and j are from a total of N shot and recording station sites, there should therefore be, at most, a total of $N(N-1)$ equations of the form (3) if there were both a shot and a station at each site. There will, however, be only $N+1$ unknowns—the N time terms and the refractor velocity V_2. The statistical criterion taken to give the best-fit solution is that the sum of the squares of the residuals (R_{ij}^2) shall be a minimum.

Berry & West (1966) give details of the method used to derive the set of linear equations in the unknown time terms a_r (where $r = 1 \ldots N$) and velocity V_2, which can be solved by matrix methods readily available at computer centres. They also describe the data handling method in the practical situation where there are not shots

and stations at each site. The authors adapted the method for use on a CDC 3600 computer. In practical survey operations it is often impossible to satisfy the condition of coincident shots and stations, and therefore a set of time terms can only be determined subject to the value of a constant (α) which is of opposite sign for shot and station sites. In the present interpretation a unique solution is achieved by using values of the constant α determined from several pairs of near-coincident shots and stations. Table 1 lists the adjacent stations and shots (e.g. recording station Tavui and shot 1969/31) used to find the average value of α for the four refractors analysed in this paper.

In a multi-layer model, time terms can be determined for successive refractors, and the depths to these refractors can be written

$$H_n = \sum_{p=1}^{n} h_p$$

$$= \sum_{p=1}^{n} \left(a_p - \sum_{q=1}^{p-1} h_q / K(V_{p+1}, V_q) \right) K(V_{p+1}, V_p) \qquad (5)$$

Table 1

Pairs of adjacent recording stations and shot sites used to determine unique time-term solutions

		Time-term constant α
4·64 km s^{-1} Refractor		
Tavui	& 1969/31	0·64
Nonga	& 1969/31	0·68
Praed Pt	& 1967/D	0·45
Burma Rd	& 1969/32	0·48
Vulcan	& 1969/34	0·72
		Average 0·60
6·11 km s^{-1} Refractor		
Doilene	& 1967/19	0·94
Kabiara	& 1969/45	0·95
Ravalien	& 1969/37	1·04
Kabanga	& 1967/30	1·02
Muliama	& 1967/47	1·02
Uluputor	& 1967/27	1·04
Namatanai	& 1967/37	0·90
Sum Sum	& 1967/33	0·81
Kilinwata	& 1969/46	0·92
		Average 0·96
6·84 km s^{-1} Refractor		
Doilene	& 1969/47	0·84
Manga	& 1969/4	0·35
Bulumuri	& 1969/19	1·07
Talasea	& 1969/21	1·10
Lindenhafen	& 1969/23	0·71
Palmalmal	& 1969/8	0·59
Vitu I.	& 1969/20	0·68
Powell HB.	& 1969/12	0·96
		Average 0·79
7·92 km s^{-1} Refractor		
Manga	& 1969/4	3·40
Vitu I.	& 1969/20	3·40
Bulumuri	& 1969/16	2·96
Lindenhafen	& 1969/23	3·54
Palmalmal	& 1969/8	3·32
Lambom	& 1969/40A	3·30
		Average 3·29

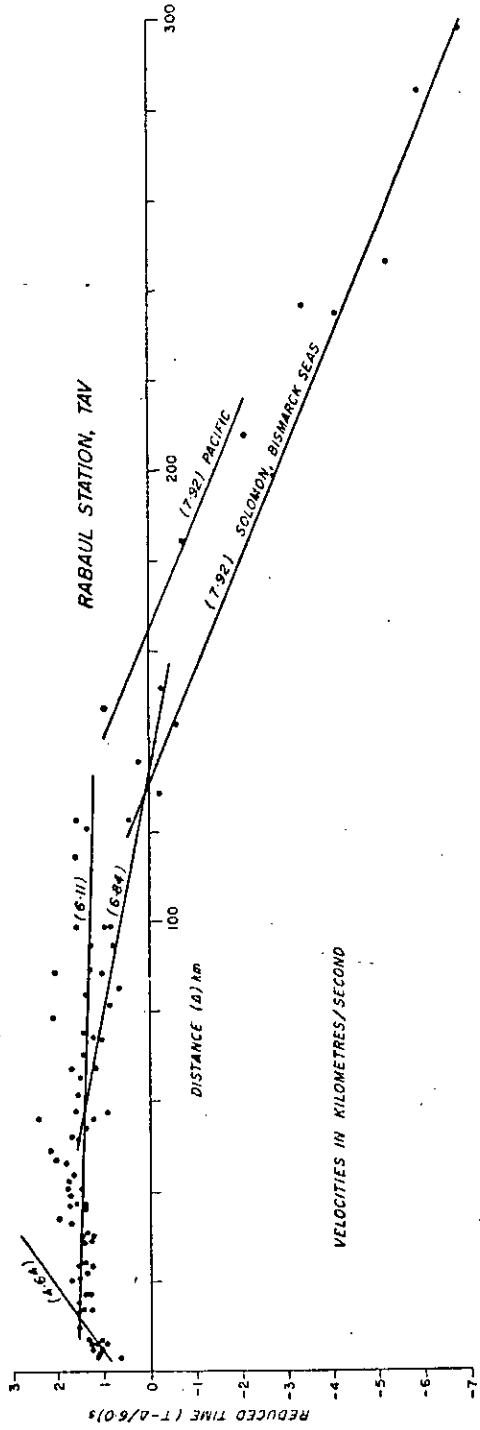

FIG. 2. Example of reduced time-distance plot.

where

n = number of layers above bottom refractor;

H_n = total depth to critical refractor;

h_p = thickness of layer with velocity V_p;

a_p = time-term to critical refractor V_{p+1};

and

$$K(V_{p+1}, V_p) = \frac{V_{p+1} V_p}{(V_{p+1}^2 - V_p^2)^{\frac{1}{2}}} \text{ etc.}$$

The standard deviation of the residuals R_{ij} is used to derive a measure of the statistical uncertainty of the time terms and of the velocity determined by the time-term method.

The identification of the refractors in the New Britain–New Ireland region to which time-term analyses could be applied has been described by Finlayson *et al.* (1972). The data used in the least-squares analyses in that paper provide the basis for data selection for the time-term analysis of four refractors: (a) the near-surface refractor in the region of the Rabaul volcanic caldera; (b) the basement refractor in the Gazelle Peninsula–southern New Ireland region; (c) the intra-crustal refractor; and (d) the Moho refractor over the whole survey area. The refractor velocities are illustrated in the example of a reduced time-distance plot shown in Fig. 2.

The allocation of data to a particular refractor is necessarily a subjective process, especially at distances in the cross-over regions of time-distance plots. Thus some data may well be included in the analyses of two refractors if there is no geophysical justification for limiting them to one refractor or another. All the time-term analyses finally adopted are the results of an iterative process in which the residuals from each individual observation were examined at each cycle and those rejected which were thought to be grossly distorting the solution.

Local Structures in the Rabaul Caldera

A total of 131 seismic first-arrival data points (approx. 85 per cent of recorded data) at distances out to 16 km are used to determine the time terms at 30 locations (16 shots and 14 recording stations) in the vicinity of the Rabaul caldera (Fig. 3). In a preliminary study of the caldera in 1966, Cifali *et al.* (1969) established near-surface velocities of approximately 2·5 km s^{-1} from refraction results. Therefore in the present interpretation around the Rabaul caldera, corrections are applied to the observed travel times by replacing the depth of water at the shot-points with a pseudo-layer with velocity 2·5 km s^{-1} for the purpose of the analysis.

The time-term computations give a velocity of 4·64 ± 0·08 km s^{-1} for the material in the critically refracting layer, and the resultant time terms for the various sites are computed using this velocity. Space limitations preclude the listing of detailed time-term values for all analyses in this paper but these may be obtained from the authors on request. Depths to the refractor are determined using equation (5) in a one-layer model with 2·5 km s^{-1} material overlying 4·64 km s^{-1} material, and these are contoured in Fig. 3. The distribution of residuals is illustrated in Fig. 4 with those for other refractors; the standard deviation of the residuals is 0·12 s, giving an uncertainty in depth of ±0·4 km using the velocity model determined above.

From Heming's geological description (in preparation), the 2·5 km s^{-1} refractor probably contains rocks consisting of lava flows, tuff, tuffite, coral limestone, and volcanic ash while the 4.64 km s^{-1} refractor contains older metamorphosed sedimentary rocks, lava flows, and intrusions; consequently the velocity transition is

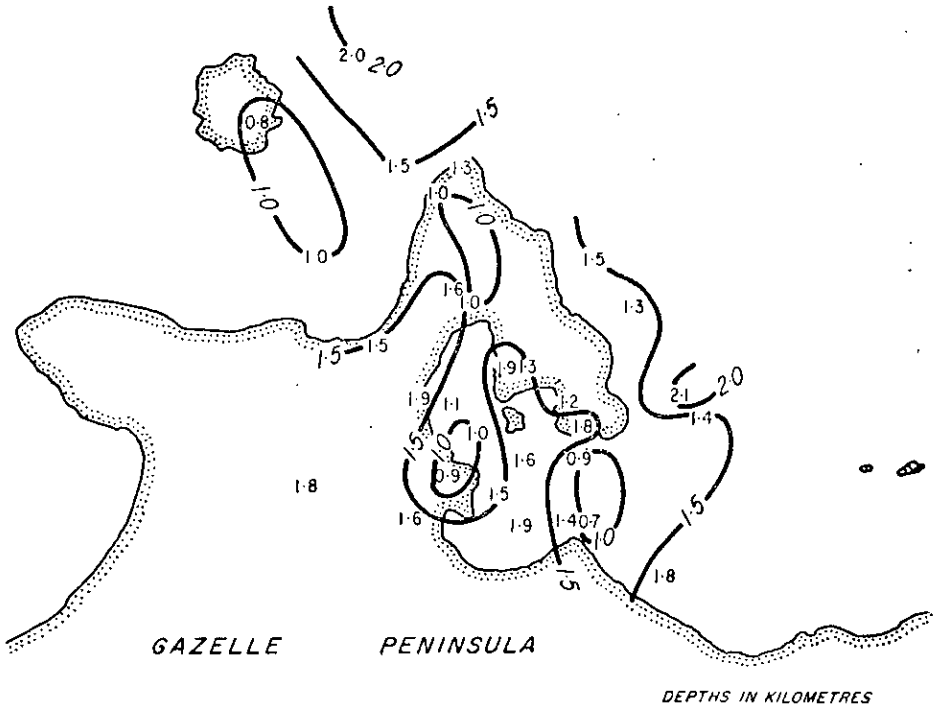

FIG. 3. Shot and station locations and depths to 4·64 km s^{-1} refractor in the region of the Rabaul Caldera.

probably complex. It is also evident that the dense rocks (presumably of high velocity) expected near the surface by Laudon (1968) on the basis of his gravity work are not apparent in the seismic results. However, dense surface rocks can have low seismic velocity because of weathering and fracturing (Lort & Mathews 1972), and thus the low velocity does not necessarily prove the non-existence of dense rocks.

Basement structure

The presence of a refractor with velocity of approximately 6·1 km s^{-1} in the Gazelle Peninsula–southern New Ireland area is evident from preliminary examination of the data (Finlayson *et al.* 1972). This refractor (defined as basement) is interpreted as the upper boundary of a thick pile of volcanic, pyroclastic, and intrusive rocks formed by lower and middle Tertiary island arc magmatism. These rocks are exposed in some parts of the Gazelle Peninsula and New Ireland but are generally overlain by younger, less consolidated rocks.

Most of the first-arrival data at distances less than 100 km were recorded in this area, and they are well suited to time-term analysis. Data from 736 seismic arrivals (approx. 95 per cent of recorded data) are compiled to give time terms at a total of 118 shot-points, and recording stations. For interpreting basement structure and deeper refractors, a water correction velocity of 4·0 km s^{-1} is adopted, based on the meagre information available from the Rabaul caldera and engineering refraction surveys in the Gazelle Peninsula (Cifali, Milson & Polak 1968; Cifali *et al.* 1969).

The velocity for the basement refractor determined from the analysis is $6{\cdot}11 \pm 0{\cdot}02$ km s^{-1}. The time terms computed with this velocity are used to calculate depths from a single-layer model with 4·0 km s^{-1} rock overlying a 6·11 km s^{-1} basement. The results are contoured in Fig. 5. The residual distribution

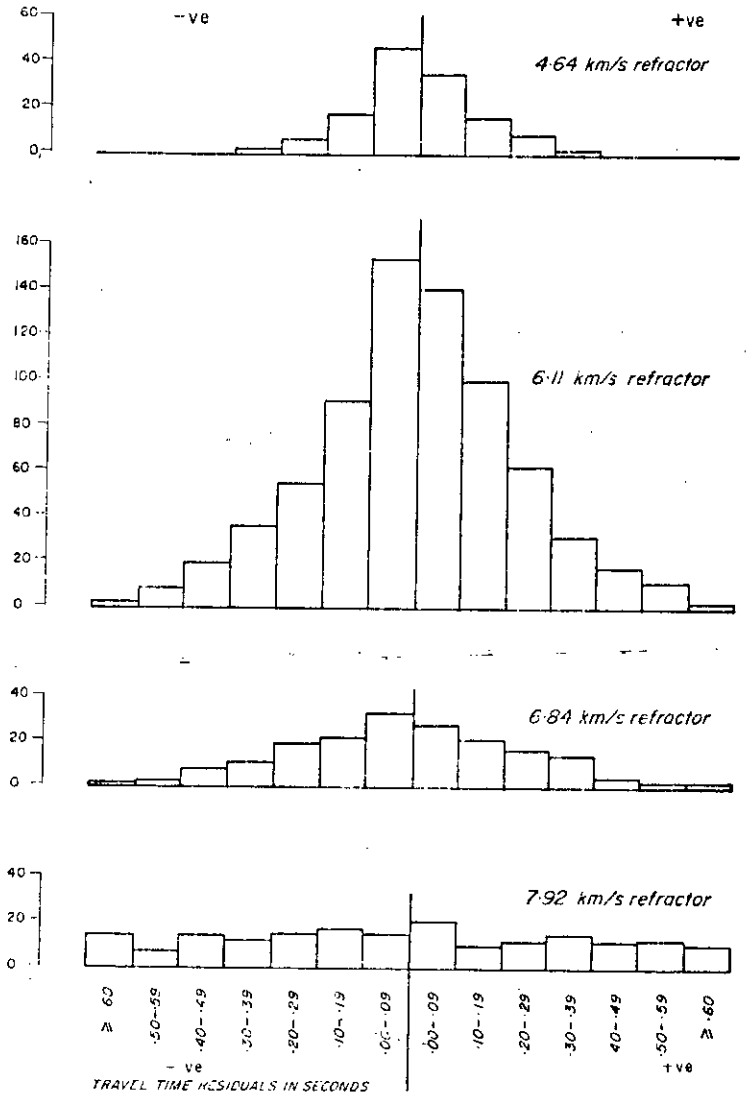

FIG. 4. Histograms of residuals from time-term analyses of (*a*) 4·64 km s^{-1}, (*b*) 6·11 km s^{-1}, (*c*) 6·84 km s^{-1} and (*d*) 7·92 km s^{-1} refractors.

is shown in Fig. 4 and the standard deviation is 0·22 s, giving an uncertainty of 1·16 km from the model adopted for the depth computations.

Some of the features of structure are illustrated in an east–west section through Rabaul (Fig. 6). The following features of the interpretation deserve special mention:

1. The shallow basement in the north-west of the Gazelle Peninsula.

2. The rapid increase in depth at a point half-way along the north coast of the Gazelle Peninsula.

3. The deep basement under the eastern St Georges Channel.

4. The much shallower basement under central than under southern New Ireland.

5. The deep basement east of New Ireland.

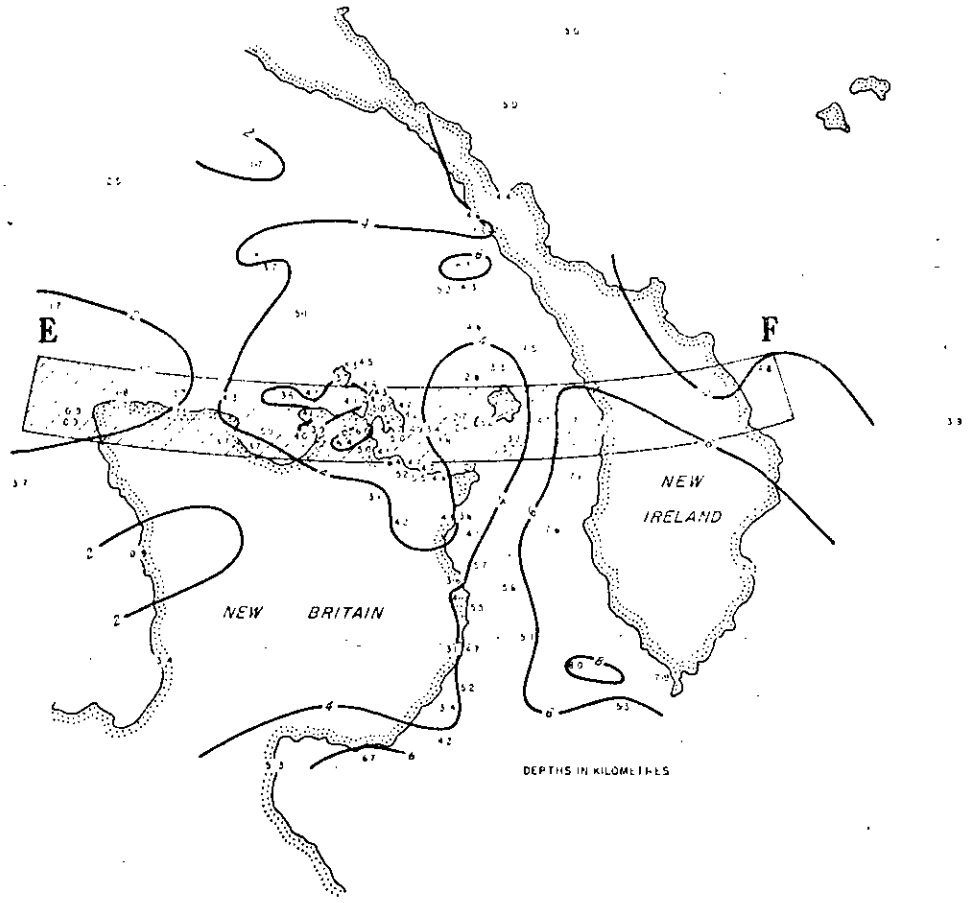

FIG. 5. Depths to basement (6·11 km s^{-1}) refractor in the Gazelle Peninsula—southern New Ireland region and location of section illustrated in Fig. 6.

Intra-crustal structure

The difficulties of identifying any structure within the crust above the Moho are many, and it may be that the interpretation here, representing a step in velocity from 6·11 km s^{-1} to between 6·8 and 6·9 km s^{-1}, is an over-simplification of the variation of velocity with depth. However, careful examination of first-arrival data in the range 80–150 km seems to indicate clearly the presence of a refractor, and with the added evidence from subsequent arrivals outside this range the case for the refractor improves.

The refractor is mostly easily identified in the Bismarck Sea, where there is clear evidence that the first velocity identified is 6·78 km s^{-1} and there is little evidence of a velocity near 6·1 km s^{-1}.

For the time-term analysis, 191 data points (approx. 80 per cent of recorded data) are used to give time terms at 64 places (25 recording stations and 39 shot-points). Iteration of the data analysis procedure to eliminate arrivals which were of doubtful interpretation indicates a velocity which does not deviate far from 6·8 km s^{-1}. The final solution adopted gives a velocity of $6{\cdot}84 \pm 0{\cdot}03$ km s^{-1} and the time terms and consequent depths are computed using this velocity. The distribution of residuals (Fig. 4) seems to substantiate the idea of a distinct intra-crustal refractor, since the

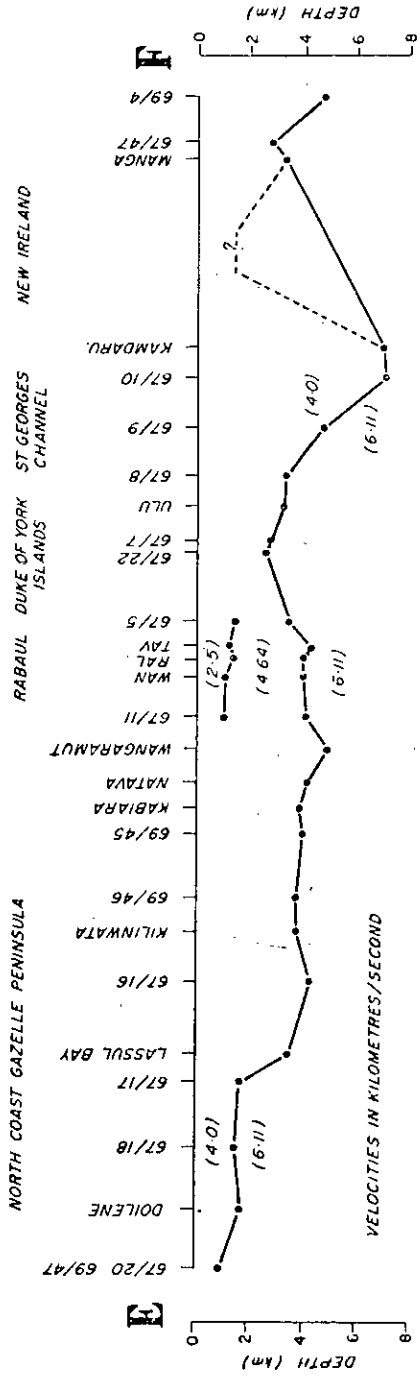

FIG. 6. East–west section through Rabaul illustrating basement structure.

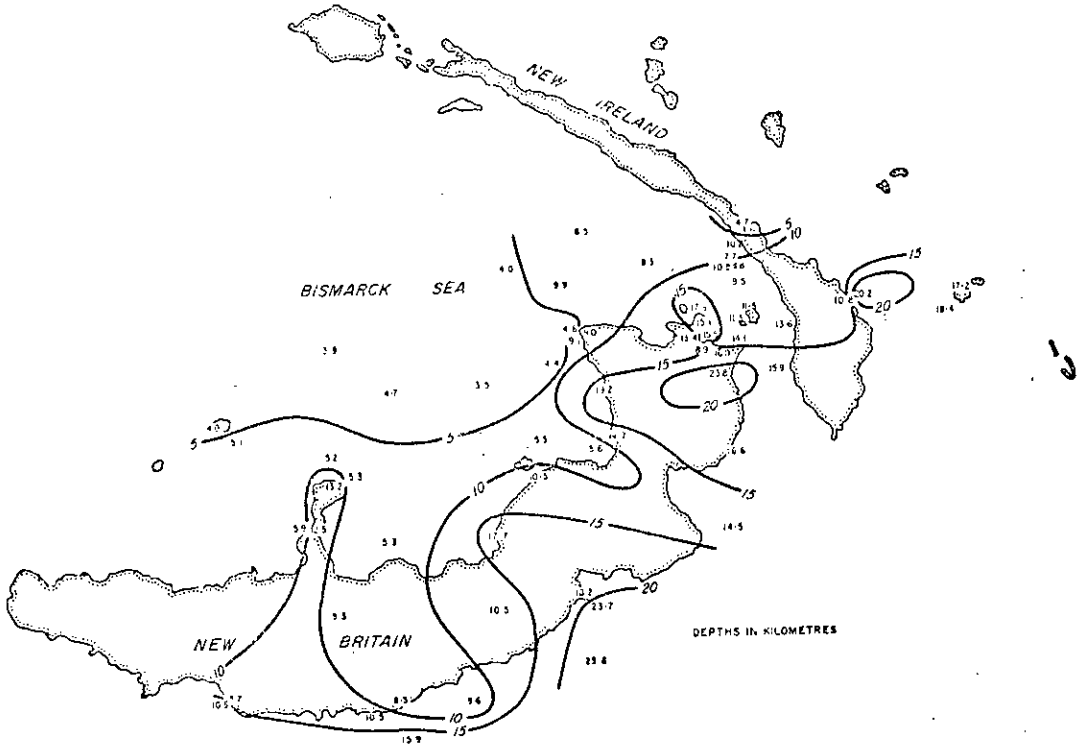

FIG. 7. Depths to intra-crustal (6·84 km s^{-1}) refractor.

number of data used represents a large percentage of those available for interpretation. The standard deviation of the residuals is 0·26 s.

The depth determinations are made using equation (5) and the data available from the time-term interpretation of the basement refractor. Where there are deficiencies in the information available for depth calculations, estimates have been made from the least-squares analysis of Finlayson *et al.* (1972). The depths are contoured in Fig. 7, and the following features may be noted:

1. Depths in the Bismarck Sea are generally less than 5 km, and the 6·84 km s^{-1} refractor is the first detected below the sea bed.

2. Other depths range up to 25 km, with average depths of approximately 15 km in the Rabaul area.

3. In central New Britain there seems to be an area where the refractor shallows to less than 10 km corresponding with an area of high Bouguer gravity anomalies (Brooks 1971).

4. The depths under central New Ireland (approximately 5 km) are much shallower than under the southern part of the island (10–15 km).

Moho structure

Most methods of interpreting seismic refraction data make various assumptions about the existence of refractors, continuity over a certain area near shot-points and recording stations, reversal of ray paths, lateral uniformity over a certain distance, and increasing velocity with depth, which are the logical extension of experience in

sedimentary basins. In crustal investigations, especially in island arc areas, there must always be some doubt about making such assumptions when one considers that island arc tectonism involves large vertical movements, magmatism, metamorphism, phase changes, large-scale horizontal shear and consequent discontinuities and large boundary gradients.

The interpretation of Moho structure in an area such as New Britain/New Ireland is inevitably difficult and is not helped by the added complication that the seismic arrivals from the greater distances required for the interpretation contain a greater proportion of poor results. In the present time-term interpretation an attempt is made to include as many data as possible even though the scatter of residuals is high.

In all, 188 datum points (approx. 90 per cent of recorded data) have been used to determine the time terms at 51 sites (28 shot points and 23 recording stations). The velocity computed from the final analysis is $7{\cdot}92 \pm 0{\cdot}05\ \mathrm{km\,s^{-1}}$ and in the iteration process, the most probable velocity for the region was always found to be approximately $7{\cdot}9\ \mathrm{km\,s^{-1}}$. The distribution of residuals (Fig. 4) clearly demonstrates that although $7{\cdot}92\ \mathrm{km\,s^{-1}}$ is the most probable velocity for the region as a whole, there is likely to be a good deal of variation within the region. The standard deviation of the residuals is $\pm 0{\cdot}44$ s. The velocity determined is in agreement with the evidence from marine refraction work in the Solomon Sea Basin by Furumoto *et al.* (1970) of velocities ranging between 7·7 and $8{\cdot}0\ \mathrm{km\,s^{-1}}$.

The distribution of residuals is likely to be influenced also by anisotropy in the crustal layers and upper mantle. Christensen (1972) has summarized the argument for anisotropy in the oceanic layer 3, backed by laboratory evidence that velocities vary from 6·2 to $7{\cdot}1\ \mathrm{km\,s^{-1}}$ along the different axes of rock samples. Keen & Barrett

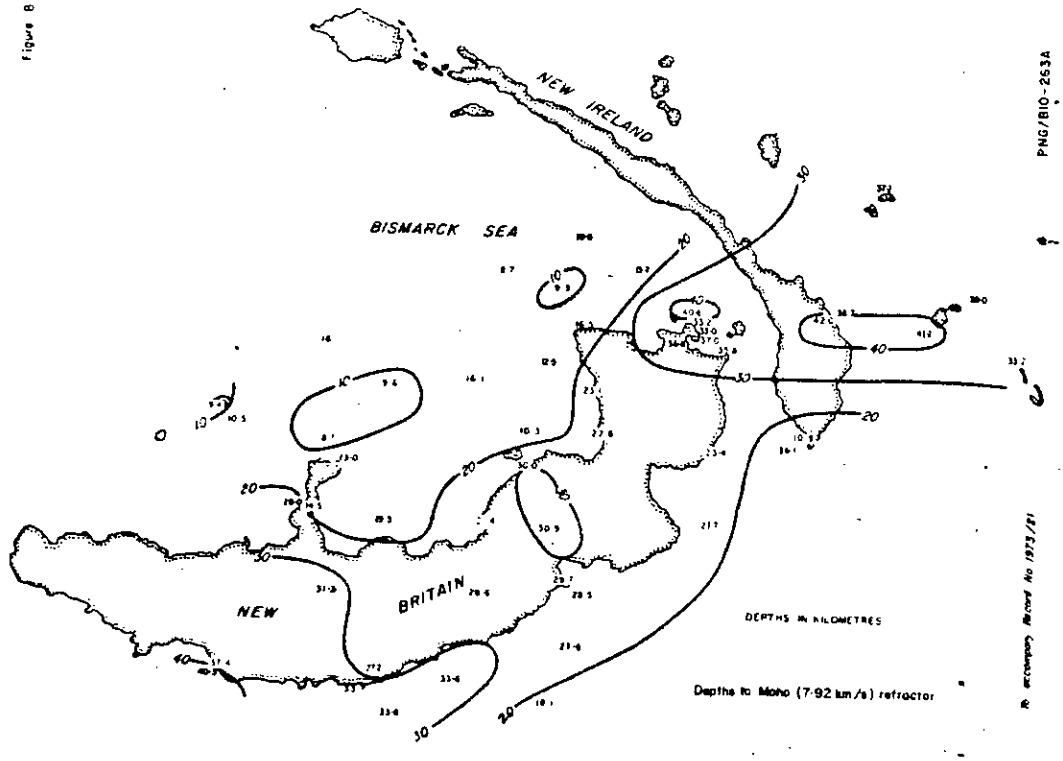

FIG. 8. Depths to Moho ($7{\cdot}92\ \mathrm{km\,s^{-1}}$) refractor.

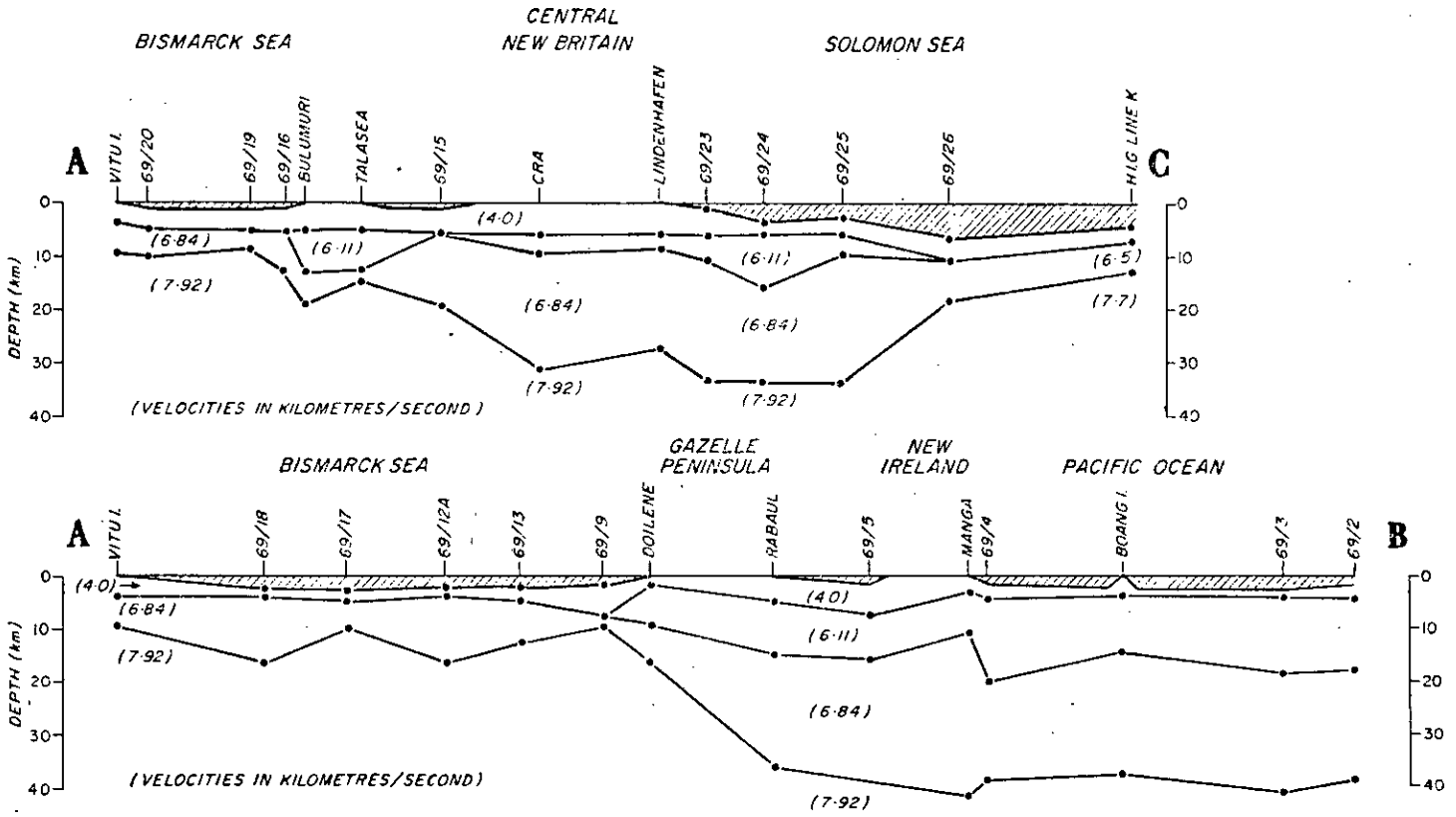

FIG. 9. Representative crustal cross-sections from time-term analyses in the New Britain–New Ireland region.

(1971) found 8 per cent seismic anisotropy in the upper mantle from survey work in the Pacific Ocean Basin off British Columbia.

The time terms are computed using the least squares velocity and the depth contours are illustrated in Fig. 8. The depths under the Bismarck Sea generally increase from 10 to 20 km going from NW to SE, and a large increase in depth under the north New Britain coast indicates a major structural feature. The differences between the depths under the south coast of New Britain and the Solomon Sea margin are not nearly so great. The shallower depths in central New Britain probably reflect the similar structure in the intra-crustal depth contours. From the results of Furumoto *et al.* (1970), depth to Moho is 12–13 km under the Solomon Sea Basin.

The depths to the Moho under the Gazelle Peninsula are generally less than 25 km increasing to approximately 35 km in the Rabaul area. Southern New Ireland has a Moho depth in excess of 30 km except for the area in the south-west of the island. East of New Ireland the depths are consistently greater than 30 km, indicating that the structure in that area is not that of typical oceanic crust. Two representative crustal cross-sections in the region are illustrated in Fig. 9.

Discussion

Seismicity and earthquake focal mechanism studies have shown that Rabaul lies at a triple junction of lithospheric plates: the Pacific Plate including the ill-defined north Bismarck Plate, the south Bismarck Plate and the Solomon Plate (Denham 1969, 1973; Johnson & Molnar 1972; Krause 1973). Using the nomenclature of McKenzie & Morgan (1969) the junction is of the TTR type and is stable, since the transcurrent fault across the Bismarck Sea would seem to be tangential to the Solomon Islands subduction zone. The continuity of the fault in the St Georges Channel is not well defined from earthquake locations, probably owing to crustal weakness and volcanism having prevented the build-up of strain energy.

The seismic refraction interpretations of crustal structure given in this paper help to describe the structural differences across the plate boundaries. The Bismarck Sea crust, which increases in thickness from approximately 10 km to over 20 km (including 2 km of water), as the New Britain coast is approached, is slightly thicker on average than the Solomon Sea crust (Furumoto *et al.* 1970), which is approximately 12 km thick (including about 5 km of water). The crustal thickness of the Pacific Plate east of New Ireland is between 35 and 40 km and is consistent with the suggestions by Kroenke (1972) that the Ontong Java Plateau area north-east of the Solomon Islands has a crust of considerable thickness (Furumoto *et al.* 1971).

The crustal structures under the islands of New Britain and New Ireland show a diversity to be expected in active or latent island arc systems, but there is no gross structural difference across the boundary between the two. This conclusion seems to be substantiated by the fact that data from under the two islands can be included in the same time-term analyses without obvious disparity.

One of the reasons for conducting the BMR crustal investigations in the region was to provide information that would permit the precise location of earthquakes and magmatic activity associated with the active Rabaul volcanic complex and thus assist with safeguarding of the Rabaul community. Within the assumptions made in seismic refraction interpretation, the near-surface and basement structures in the Rabaul area are determined; but the interpretation does not define magma chambers or conduits, although they probably contribute to the spread of the travel-time residuals. The broad aspects of the overall intra-crustal and Moho structures are defined.

Acknowledgments

The authors wish to thank those in BMR, Australian National University, University of Queensland, and Hawaii Institute of Geophysics who have encouraged and assisted with all aspects of the survey work. This paper is published with the permission of the Director of the Bureau of Mineral Resources.

Bureau of Mineral Resources,
Box 378,
Canberra City, ACT 2601,
Australia.

References

Bamford, S. A. D., 1971. An interpretation of first-arrival data from the Continental Margin Refraction Experiment. *Geophys. J. R. astr. Soc.*, **24**, 213.

Berry, M. J. & West, G. F., 1966. An interpretation of the first arrival data of the Lake Superior Experiment by the time-term method. *Bull. seism. Soc. Amer.*, **56**, 141.

Brooks, J. A., editor, 1971. Investigations of crustal structure in the New Britain–New Ireland region, 1969; geophysical and geological data. *Bur. Miner. Resour. Aust. Rec.* 1971/131, unpublished.

Christensen, N. I., 1972. Seismic anisotropy in the lower oceanic crust. *Nature*, **237**, 450.

Cifali, G., Milsom, J. & Polak, E. J., 1968. Warangoi dam site geophysical survey, New Britain, PNG, 1966. *Bur. Miner. Resour. Aust. Rec.* 1968/96.

Cifali, G., D'Addario, G. W., Polak, E. J. & Wiebenga, W. A., 1969. Rabaul preliminary crustal seismic test, New Britain, 1966. *Bur. Miner. Resour. Aust. Rec.* 1969/125, unpublished.

Denham, D., 1969. Distribution of earthquakes in New Guinea–Solomon Islands Region, *J. geophys. Res.*, **74**, 4290.

Denham, D., 1973. The seismicity of the southwest Pacific and new global tectonics. *Proc. 12th Pacific Science Congress* 1971, Canberra, Perth, University W. Aust. Press (ed. P. J. Coleman).

Finlayson, D. M., 1968. First arrival data from the Carpentaria Region Upper Mantle Project (CRUMP). *J. geol. Soc. Aust.*, **15**(1), 33.

Finlayson, D. M., (editor), 1972. Investigations of crustal structure in the Rabaul region 1967; logistics and seismic data, *Bur. Miner. Resour. Aust. Rec.* 1972/45, unpublished.

Finlayson, D. M. & Cull, J. P., 1973. Structural profiles in the New Britain–New Ireland region, *J. geol. Soc. Aust.*, **20** (1), 37.

Finlayson, D. M., Cull, J. P., Wiebenga, W. A., Furumoto, A. S. & Webb, J. P., 1972. New Britain–New Ireland crustal seismic refraction investigations 1967 and 1969, *Geophys. J. R. astr. Soc.*, **29**, 245–53.

Furumoto, A. S., Hussong, D. M., Campbell, J. F., Sutton, G. H., Malahoff, A., Rose, J. C. & Woollard, G. P., 1970. Crustal and upper mantle structure of the Solomon Islands as revealed by seismic refraction survey of November–December 1966, *Pacific Science*, **24**, 3.

Furumoto, A. S., Wiebenga, W. A. & Webb, J. P., 1971. Seismic refraction studies in Melanesia, an area of crustal convergence. Proc. Joint Oceanogr. Assembly (Tokyo, 1970), IAPSO, IABO, CMC, SCOR, 'The Ocean World' (ed. M. Uda), *Japan Society for the Promotion of Science.*

Johnson, T. & Molnar, P., 1972. Focal mechanisms and plate tectonics of the southwest Pacific, *J. geophys. Res.*, **77**, 5000.

Keen, C. E. & Barrett, D. L., 1971. A measurement of seismic anisotropy in the northeast Pacific, *Can. J. earth Sci*, **8**, 1056.

Krause, D. C., 1973. Crustal plates of the Bismarck and Solomon Seas, in press.

Kroenke, L. W., 1972. Geology of the Ontong Java Plateau, *Hawaii Institute of Geophysics Report HIG-72-5.*

Laudon, T. S., 1968 Land gravity survey of the Solomon and Bismarck Islands, *Am. geophys. Un., geophys. Monogr.* 12,

Lort, J. M. & Mathews, D. H., 1972. Seismic velocities measured in rocks of the Troodos igneous complex, *Geophys. J. R. astr. Soc.*, **27**, 383.

McKenzie, D. P. & Morgan, W. J., 1969. Evolution of triple junctions, *Nature*, **224**, 125.

O'Brien, P. N. S., 1968. Lake Superior crustal structure. A reinterpretation of the 1963 seismic experiment, *J. geophys. Res.*, **73**(8), 2669.

Rose, J. C., Woollard, G. P. & Malahoff, A., 1968. Marine gravity and magnetic studies of the Solomon Islands, *Am. geophys. Un., geophys. Monogr.*, **12**, 379.

Scheidegger, A. E. & Willmore, P. L., 1957. Use of a least square method for the interpretation of data from seismic surveys, *Geophysics*, **22**, 9–22.

Smith, T. J., Steinhart, J. S. & Aldrich, L. T., 1966. Crustal structure under Lake Superior, *Am. geophys. Un., geophys. Monogr*, **10**, 181.

Underwood, R., 1969. A seismic refraction study of the crust and upper mantle in the vicinity of Bass Strait, *Aust. J. Phys.*, **22**, 573.

Wiebenga, W. A., 1973. Crustal structure of the New Britain–New Ireland region. *Proc. 12th Pacific Science Congress*, 1971, Canberra. Perth, Univ. W. Aust. Press (ed. P. J. Coleman).

Willmore, P. L. & Bancroft, A. M., 1960. The time-term approach to refraction seismology, *Geophys. J. R. astr. Soc.*, **3**, 419.

(*Reprinted from Nature Physical Science, Vol. 229, No. 7, pp. 205–207, February 15, 1971*)

St George's Channel–Bismarck Sea Trough

DURING 1969 the Australian Bureau of Mineral Resources, Geology and Geophysics, in conjunction with the University of Queensland, Australian National University and the Hawaii Institute of Geophysics, carried out a survey of the crustal structure in the New Britain–New Ireland region of the Territory of Papua and New Guinea. This area, being situated in a tectonically complex region, has interested many Earth scientists in recent years.

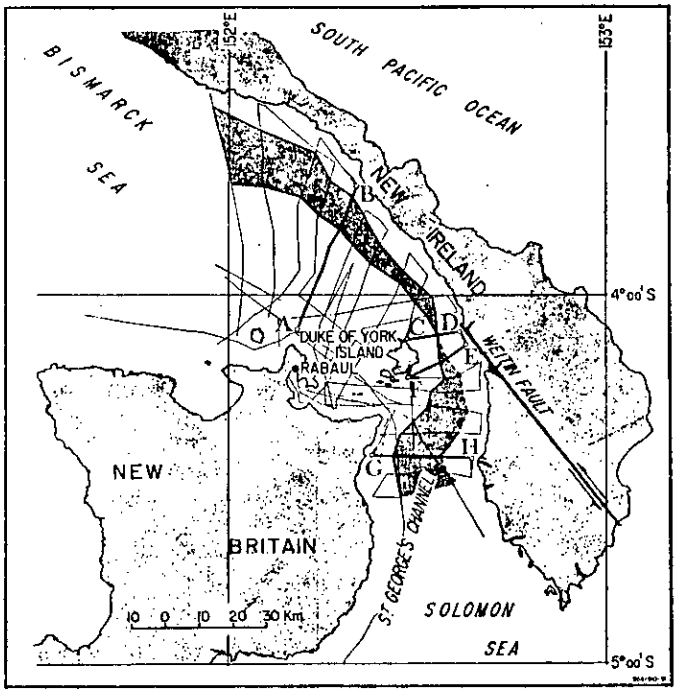

Fig. 1 The survey of New Britain/New Ireland in 1969 by the Australian Bureau of Mineral Resources, Geology and Geophysics showing marine sparker traverses and the extent of the floor of the submarine trough (heavily shaded area).

As part of the 1969 survey several marine seismic reflexion (sparker) traverses were recorded on board MV Coral Queen in the channel between New Britain and New Ireland (Fig. 1). The traverse spacing was between 5 and 10 km and position control was estimated to be approximately ±1 km on average but varied above and below this figure, depending on the availability of radar and visual land sightings. A 7,000 J Edgerton, Germeshausen and Grier sparker system was used which gave a penetration of the order of 100 m in the bottom sediments that were encountered.

The outstanding feature of the submarine topography revealed by the survey is the pronounced trough, 2,000 m deep and extending through St George's Channel into the eastern Bismarck Sea (Fig. 1). Previous bathymetric maps[1] of the region have not suggested such a prominent deep water feature. The area indicated in Fig. 1 is the approximate extent of the floor of the trough. The central section north-east of the Duke of York Islands is very narrow and the trough can be divided into northern and southern sectors. Examples of profiles across the area are shown in Figs. 2, 3 and 4.

At the wider sections the trough floor is relatively flat and smooth with a distinct angle of contact between the floor and the walls of between 10° and 25°. The topography becomes more disturbed toward the narrower section. In some places the sides of the trough show block faulting.

In the central part of the northern sector the topography indicates intrusives forming the south-west boundary of the trough floor (Fig. 2). These intrusives would post-date the formation of the trough and therefore are responsible for its narrowing north-west of the Duke of York Islands. Hence it can be inferred that the original trough was at least as wide as the present maximum width.

The method by which the trough was formed originally has not been determined, and so the feature has not been described as a rift, trench, or canyon which implies particular methods of formation.

Both New Britain and New Ireland have experienced volcanism and tectonism from the Lower Tertiary period onwards and geologically speaking resemble the Solomon and New Hebrides Islands. New Britain has many characteristics of an island arc structure with an oceanic trench more than 8,000 m deep along the south coast and extending along the west coast of Bougainville Island (Planet Deep). A belt of active volcanoes extends along the north coast of New Britain but there are no active volcanoes on New Ireland. A zone of earthquake foci dips steeply northward under New Britain and towards the north-east off the southern tip of Ireland[2]. Also a weak shallow seismic zone extends in an arc across the Bismarck Sea from

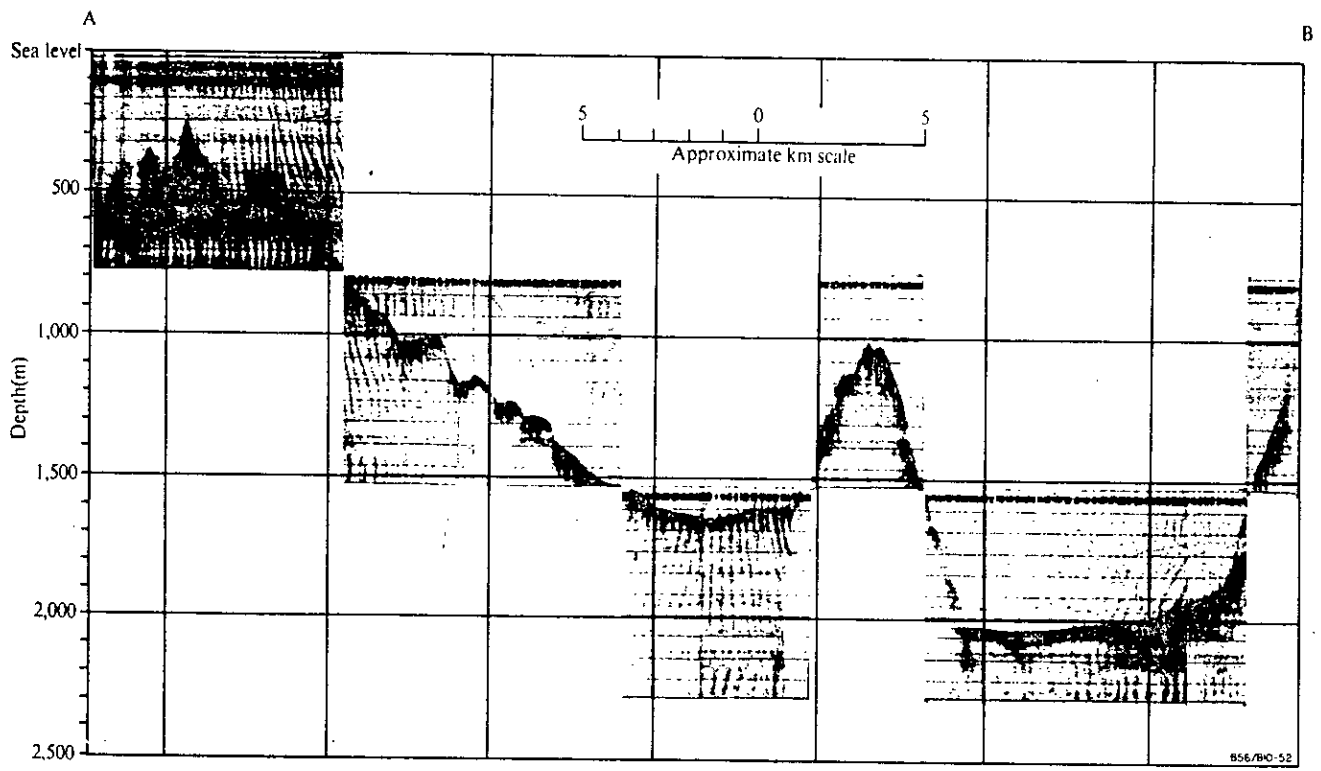

Fig. 2 Sparker traverse A–B in Fig. 1.

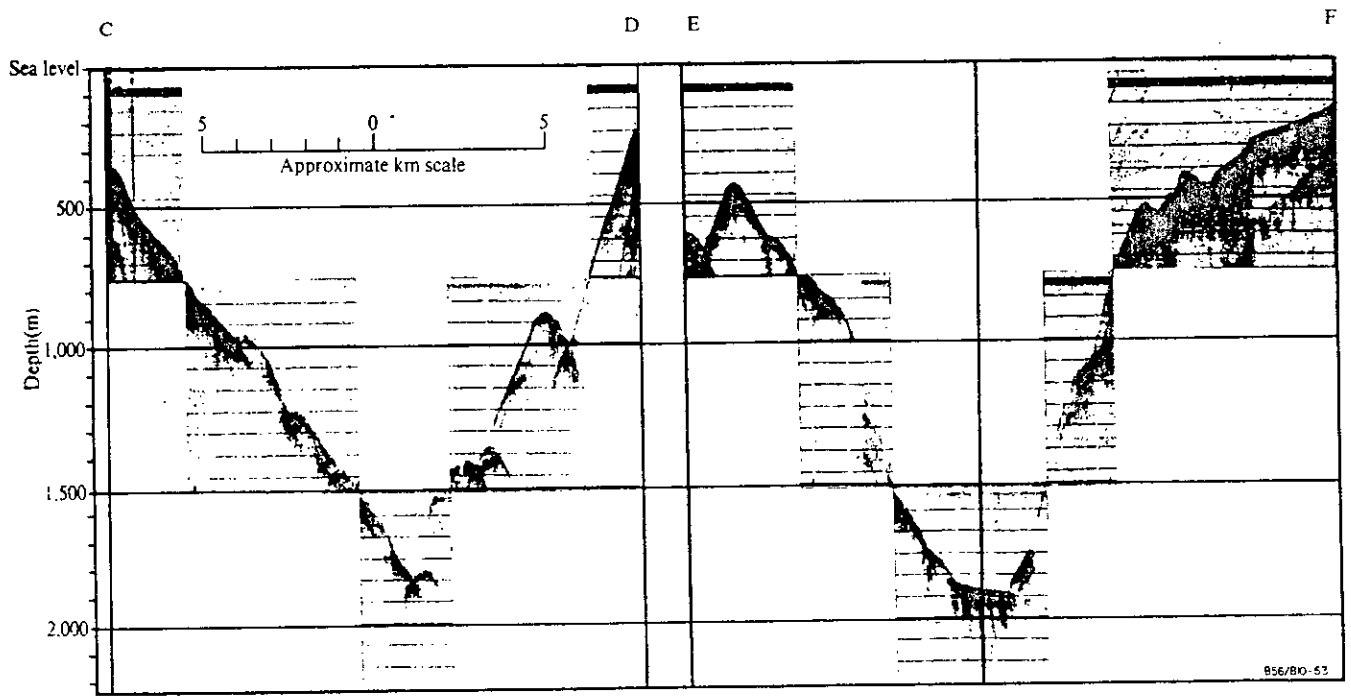

Fig. 3 Sparker traverse C–D–E–F in Fig. 1.

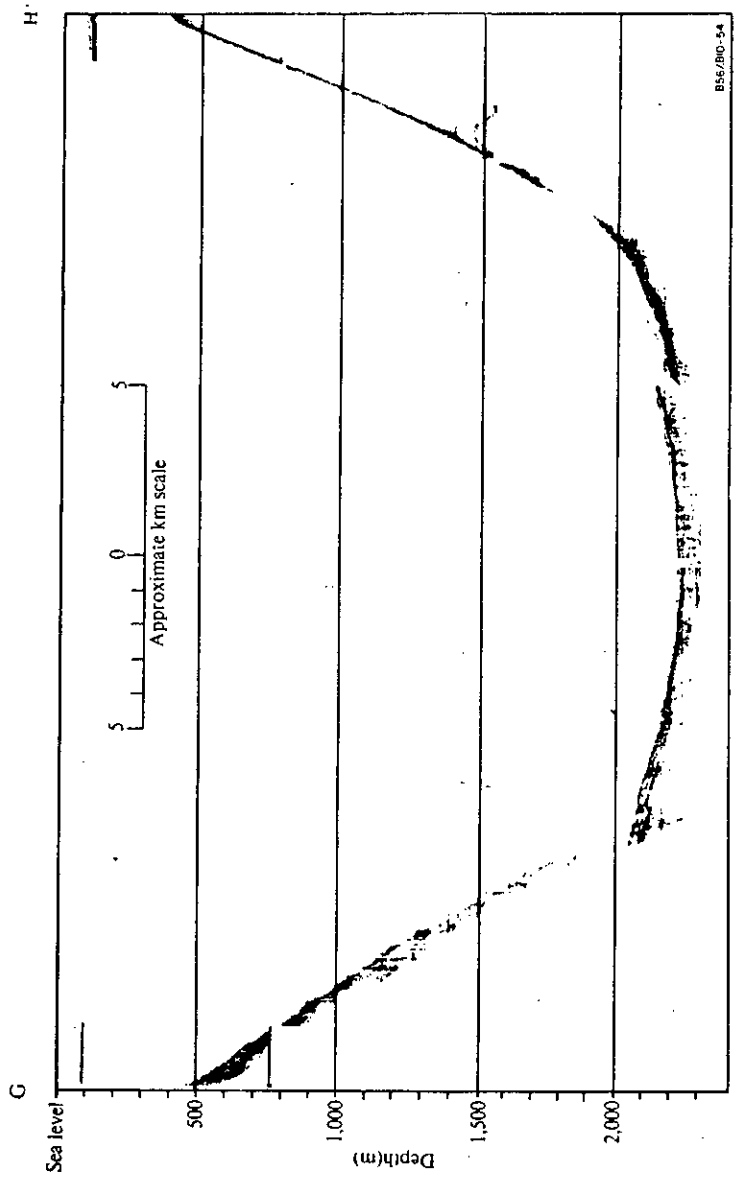

Fig. 4 Sparker traverse G–H in Fig. 1.

north of Rabaul to the New Guinea mainland coast at Wewak.

A major geological feature of southern New Ireland is the Weitin River Fault which French (unpublished) regarded as indicating sinistral transcurrent movement. The north-west extension of this fault is cut by several sparker profiles (Fig. 3) and runs into the northern boundary of the trough's northern sector. The profiles are not detailed enough, however, to show whether or not the two features are structurally related to each other.

Isolated profiles in other waters off New Britain suggest that other prominent submarine features may be present and we feel that the 1970 sparker profiling programme in the Bismarck Sea by the Bureau of Mineral Resources, Geology and Geophysics will be a further useful contribution to our understanding of the region.

J. A. Brooks
J. B. Connelly
D. M. Finlayson
W. A. Wiebenga

Bureau of Mineral Resources, Geology and Geophysics, Canberra

Received January 19, 1971.

[1] Rose, J. C., Woollard, G. P., and Malahoff, A., *Amer. Geophys. Un., Geophys. Mono. No. 12*, 379 (1968).
[2] Denham, D., *J. Geophys. Res.*, 74, 4290 (1969).

Printed in Great Britain by Fisher, Knight & Co., Ltd., St. Albans.

Geophys. J. R. astr. Soc. (1976) **44**, 45–59.

Seismic Investigation of the Papuan Ultramafic Belt

D. M. Finlayson, K. J. Muirhead, J. P. Webb, G. Gibson, A. S. Furumoto, R. J. S. Cooke and A. J. Russell

(Received 1975 July 21)*

Summary

Seismic survey data from a profile along the north-east Papuan peninsula coast indicate velocities which can be correlated with those of oceanic layers 1, 2 and 3, but with a crustal thickness of between 20 and 25 km. Distinct differences in the crustal layering are determined between the region where the Papuan Ultramafic Belt crops out along the coast and the region of the Trobriand Platform. The crustal thickness is more than twice the total thickness of gabbro and basalt components of the ophiolite suite exposed inland. Later seismic arrivals suggest the presence of a low-velocity zone below the Moho and a return to upper mantle velocities at depths of about 50 km.

Introduction

The ophiolite suite of rocks in eastern Papua described by Davies (1971) is widely considered to be a classic example of a fragment of oceanic crust and upper mantle obducted on to a continental mass during orogenesis in an area of continent/island arc convergence (Coleman 1971; Moores & Vine 1971; Moores 1973). Dewey & Bird (1970) have stressed the importance of the study of such rock sequences in the development of mountain belts and indicate that ophiolites are present in many of the major intra-continental orogenies such as those in the Urals and in the Appalachian–Caledonian belts (Dewey & Bird 1971). The time–space relationships of the younger ophiolite belts therefore play an important role in placing constraints on interpretations of continental interaction and accretion at plate boundaries.

The East Papua Crustal Survey conducted during October–December 1973 was a seismic investigation of the major structures in the region of the Papuan Ultramafic Belt and was designed to add more definitive geophysical constraints to interpretations of the nature and evolution of the Belt. The results presented in this paper are some initial observations which are of importance in providing a framework for more detailed interpretation.

Papuan Ultramafic Belt

Davies (1971) and Davies & Smith (1971) described the Papuan Ultramafic Belt and its geological setting in the Papuan peninsula in some detail. The belt is a peridotite-gabbro-basalt complex which crops out over a length of 400 km and width of 40 km to the north-east of the Owen Stanley Range which runs the length of the Papuan peninsula (Fig. 1). The complex comprises, from top to bottom, some

* Received in original form 1975 June 9.

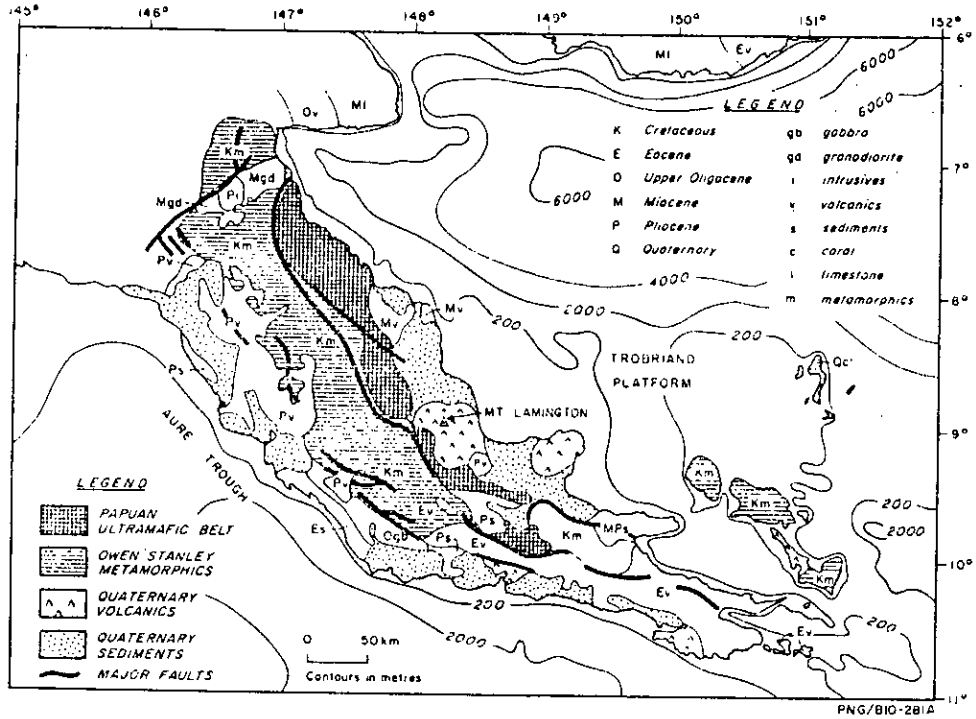

FIG. 1. Simplified geology and bathymetry of the Papuan peninsula region.

4–6 km of basalt and spilite in massive form and as pillow lavas with some dacite, 4 km of high-level gabbro, granular gabbro, and cumulates, and 4 to 8 km of ultramafic rocks of which up to 0·5 km are cumulates and the remainder are non-cumulate harzburgite, dunite, and orthopyroxenite. The basalt, gabbro and cumulate ultramafics probably crystallized in the Cretaceous and were intruded by tonalite in the Eocene. The ophiolites were emplaced in Eocene or Oligocene time.

Mesozoic schist and gneiss of varied metamorphic grade form the sialic core of eastern Papua and abut the ultramafic suite along the Owen Stanley Fault system. The metamorphics were formed during the Eocene from Cretaceous or older sediments derived from continental Australia, the most common grade being greenschist facies; lawsonite occurs in the metamorphic rocks along the entire length of the Owen Stanley Fault.

Regional gravity observations have been made throughout the Papuan peninsula (St John 1970; Milsom 1973; Finlayson, in preparation). Milsom (1973) has made a detailed interpretation of the gravity data and considered the constraints on the emplacement of the ophiolites and their possible origin. The data are compatible with the ophiolites being slabs of oceanic or frontal-arc overthrusts with dip angles of 25°–60°, but the means of emplacement is still not uniquely determined. The dips are much larger than those determined by seismic work (13°–19°) by Finlayson *et al.* (1976). Milsom (1973) has considered other modes of emplacement for the ophiolite structure in eastern Papua and regards the ' orogenic thickening ' hypothesis (Rabinowitz & Ryan 1970) and the ' pluto-volcanic ' hypothesis as unlikely. He regards it as possible that the overthrust material may be derived from a marginal basin rather than normal oceanic crust.

The structures to the south-west of Papua in the Coral Sea Basin have been investigated by Ewing, Hawkins& Ludwig (1970), Mutter (1975) and Gardner (1970). These

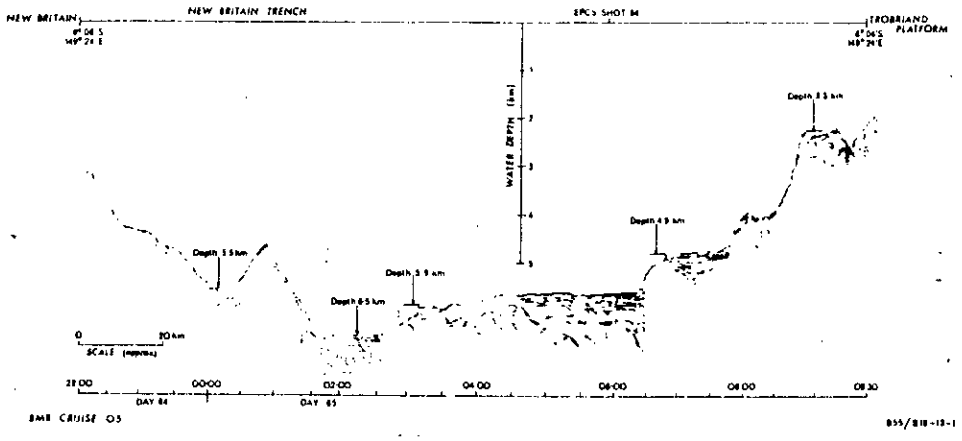

FIG. 2. Seismic sparker traverse across the Solomon Sea from the Trobriand Platform to New Britain (location shown in Fig. 3).

demonstrate that crust of oceanic thickness is present in the Basin between the Coral Sea Plateau and the Papuan Platform. Crustal extension during the early Eocene is proposed to account for formation of the Basin (Davies & Smith 1971). In the north-west Coral Sea a Mesozoic and Tertiary sedimentary section more than 10 km thick (St John 1970) overlies a predominantly continental type crust extending north-east from Australia (Finlayson 1968; Brooks 1969).

North-east of Papua the central part of the Solomon Sea Basin has a crust of oceanic thickness (11–14 km) but the upper mantle velocities (7·7–8·0 km s^{-1}) tend to be low (Furumoto *et al.* 1970). Profiling records from the Basin show it is characterized by rough topography (Fig. 2) with pockets of sediments. The free-air gravity values in the centre of the Basin are predominantly positive (0–100 mGal) with considerable variation in the areas of high structural relief at its margins (Rose, Woollard & Malahoff 1968).

The tectonic framework of the region has been studied, mainly on the basis of seismicity, by a number of authors (Denham 1969; Milsom 1970; Ripper 1970; Johnson & Molnar 1972; Krause 1973; Luyendyk, MacDonald & Bryan 1973; Curtis 1973). The Melanesian region is regarded as an area of convergence between the Pacific and Indian–Australian lithospheric plates with the smaller North Bismarck, South Bismarck and Solomon plates in the interaction zone. Minor seismicity at shallow and intermediate depth occurs along the eastern Papuan peninsula, and the formal solution to plate motions requires a transition in this area between a spreading centre in the Woodlark Basin and the Benioff zones along northern New Guinea and New Britain (Krause 1973). Vertical movements also have played, and continue to play, an important role in the tectonics of the peninsula, both upwards in its eastern part (Smith 1970; Davies & Smith 1971) and downwards as is evident along the drowned coastline where the Ultramafic Belt crops out on the coast (von der Borch 1972).

In the southern part of the Ultramafic Belt large Pliocene and Quaternary strato-volcanoes occur in the Mount Lamington–Hydrographer Range–Managalase province round seismic station LMG (Fig. 3), and in the Mount Victory–Mount Trafalgar area round the seismic station at Tufi (Fig. 3). Mount Lamington (Taylor 1958) and Mount Victory (Smith 1969) have been active in the last hundred years. The tectonic significance of the volcanology of eastern Papua has been discussed by many authors (Jakes & White 1969; Jakes & Smith 1970; Johnson, Mackenzie & Smith 1970;

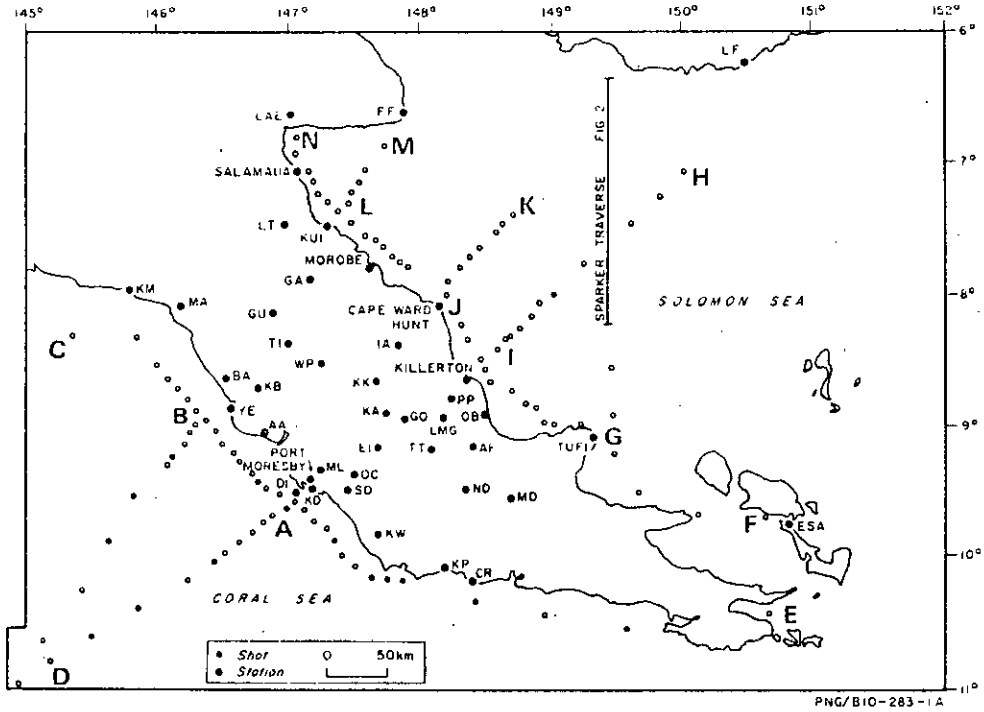

FIG. 3. East Papua Crustal Survey: shot and recording station locations, and position of sparker traverse shown in Fig. 2.

Smith 1973; Finlayson *et al.* 1976), and the structure of the Trobriand Platform (Fig. 1) has been reviewed by Bickel (1974).

Seismic survey

The Australian Bureau of Mineral Resources, Geology and Geophysics conducted the East Papuan Crustal Survey during October–December 1973 in co-operation with the Australian National University, the University of Queensland, the Geological Survey of Papua New Guinea, the University of Hawaii, Preston Institute of Technology and Warrnambool Institute of Advanced Education (Finlayson, in preparation). One-hundred and eleven shots were fired in the Coral and Solomon Seas and recordings were made at 42 seismic stations in Papua New Guinea (Fig. 3). The shots were mostly of two sizes, 180 kg and 1000 kg, detonated 100 m below the water surface where depth of water permitted. A timing accuracy of 0·01 s tied to the VNG Australian Post Office radio time signals was achieved for most shot instants and a positional accuracy of 0·1 minutes of arc was aimed at, using an extended SHORAN navigation system.

All seismic stations recorded VNG radio time signals for use as their time standard. Station positions were determined prior to seismic field work using a Decca trisponder trilateration network tied to the Australian Map Grid. Four seismic recording stations were part of the permanent PNG seismic observatory network and recorded on photographic or smoked paper recorders. Most of the remaining stations used high-gain seismic amplifiers coupled to slow-speed tape recorders, the majority operating unattended, either continuously (Muirhead & Simpson 1972) or programmed to operate for the first quarter of an hour every hour when shot firing was scheduled. Analogue

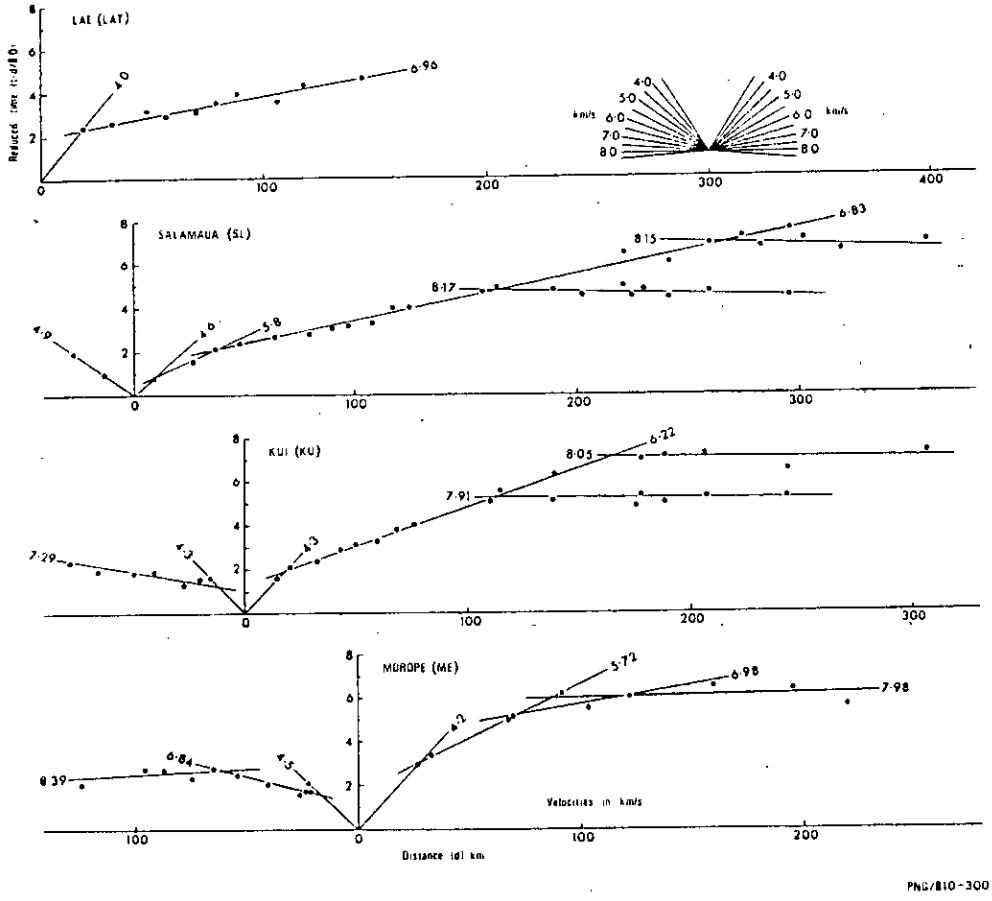

FIG. 4. Reduced travel-time plots for recording stations Lae, Salamaua, Kui and Morobe from shots along the north-east Papuan peninsula coast.

records were subsequently produced from all tapes and significant arrival times were picked by two or more seismologists. The details of the survey operations and data from the survey have been described by Finlayson (in preparation).

Seismic recording along the north-east Papuan coast

An initial interpretation has been made of data recorded along the north-east Papuan coast from Lae to Tufi (Fig. 3). Several recording stations (Salamaua, Kui, Morobe) along this line are closely associated with outcrops of Papuan Ultramafic Belt rocks. This line was chosen so that structures normal to the geological strike would have their least effect on the interpretation and water depth corrections to the seismic travel times would be small (water replacement velocity = $4{\cdot}0\,\mathrm{km\,s^{-1}}$).

Figs 4 and 5 are reduced travel-time plots of the first-arrival data recorded at the seven recording stations along the north-east coast; Lae (LAT), Salamaua (SL), Kui (KU), Morobe (ME), Cape Ward Hunt (CW), Killerton (KL), and Tufi (TI). In a few instances, subsequent seismic arrivals are plotted where they are important for this interpretation. Examples of records from Salamaua are shown in Fig. 6. The travel-time data have been plotted according to the approximation that the shots and stations can be considered as reversed profiles between Lae and Tufi, an approximation which

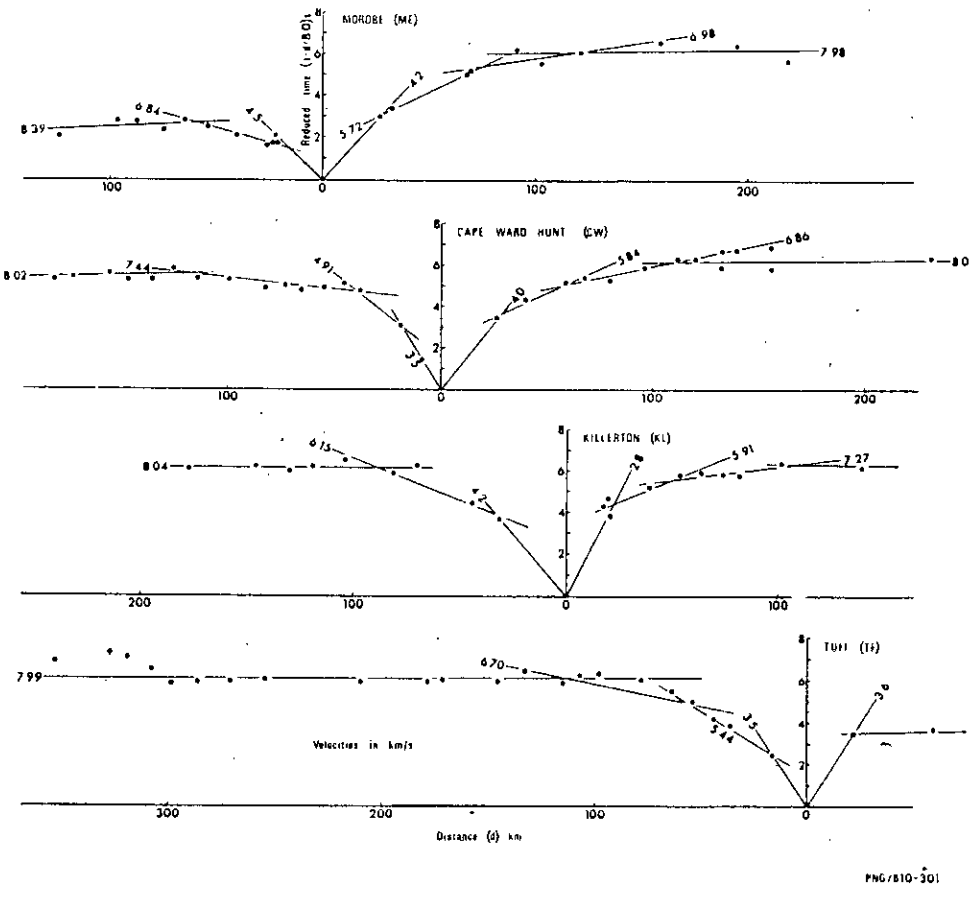

FIG. 5. Reduced travel-time plots for recording stations Morobe, Cape Ward Hunt, Killerton and Tufi from shots along the north-east Papuan peninsula coast.

is reasonable except at the shorter shot-to-station distances. Least-squares straight-line fits were applied to sets of data points where it was thought that refracting horizons had been identified. The data were weighted according to a subjective 'quality' attributed to each arrival when the records were read; the weights were 5, 3, or 1 according to whether the arrivals were judged good, fair, or poor (Finlayson, in preparation). The least-squares parameters are listed in Table 1 and the velocities so determined are indicated in Figs 4 and 5. An estimate of the velocity in the uppermost layer is obtained by constraining lines through the datum points from the nearest shots to the origin.

The travel-time plots indicate a difference in character between the data plotted north-west of Morobe towards Lae and those plotted south-east of Morobe towards Tufi. This major difference is attributed to changes in crustal structure in the Morobe region, where the shooting line crosses the boundary between the Papuan Ultramafic Belt and the Trobriand Platform.

A prominent intracrustal refractor with a velocity of approximately 7 km s^{-1} is identified between Lae and Morobe (Fig. 4); the small intercepts associated with this refractor indicate its relatively shallow depth. The cross-over distance between the 7 km s^{-1} refractor and the travel-time branch associated with arrivals directly recorded through the near-surface layers is, in most cases, between 20 and 25 km. From the data available an average velocity for these layers is 4·4 km s^{-1}.

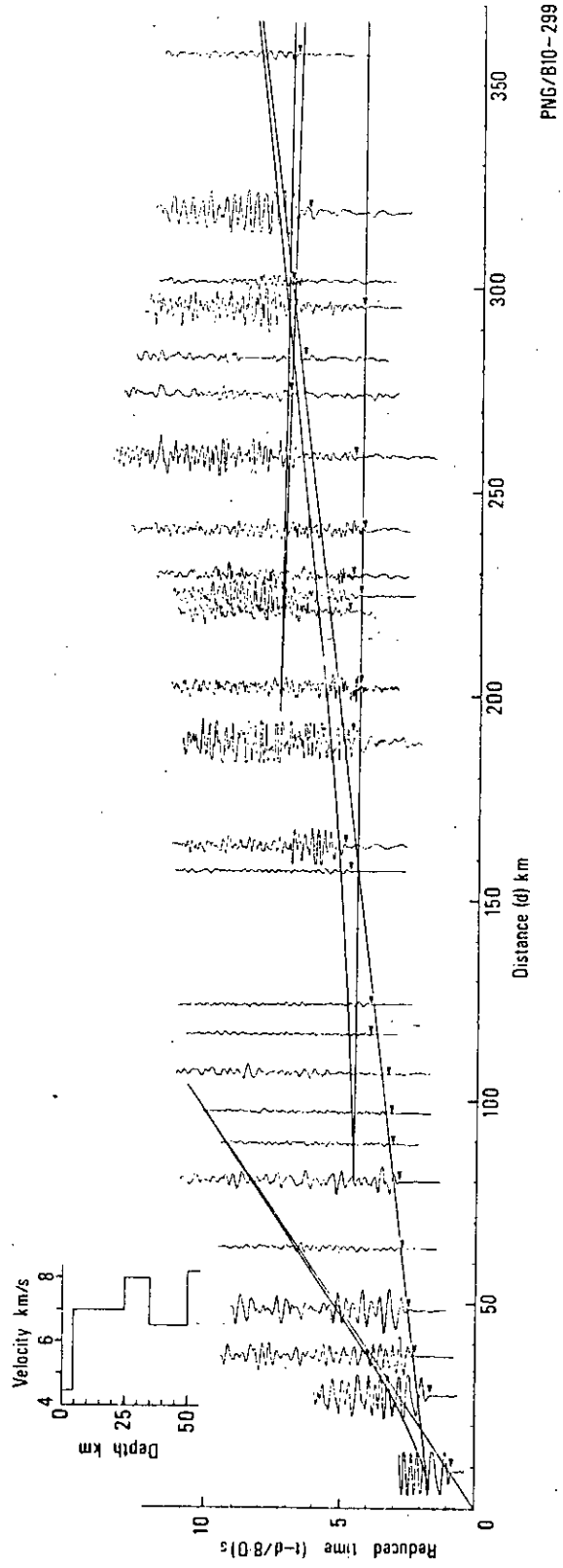

FIG. 6. Un-normalized record sections at Salamaua from shots south-east along the Papuan peninsula coast, together with the travel-time curve for the PUB-1 crustal model.

Table 1

Least-squares velocities and intercepts from stations along the north-east Papuan coast

Station	Direction	Velocity (km s^{-1})	Intercept (s)	No. of data	Rms residual (s)
Lae	SE	6·96±0·09	1·99±0·14	10	0·21
Salamaua	SE	5·80±0·02	0·33±0·04	5	0·04
		6·83±0·03	1·27±0·10	16	0·21
		8·17±0·09	5·21±0·30	10	0·17
		8·15±0·18	7·52±0·83	6	0·22
Kui	NW	7·29±0·18	1·24±0·16	7	0·17
	SE	6·22±0·04	1·24±0·09	11	0·13
		7·91±0·12	4·83±0·33	7	0·15
		8·05±0·25	7·22±0·88	5	0·31
Morobe	NW	6·84±0·22	1·31±0·18	7	0·17
		8·39±0·37	3·00±0·46	6	0·24
	SE	5·72±0·08	1·61±0·14	5	0·10
		6·98±0·37	3·91±0·73	6	0·33
		7·98±0·26	5·96±0·52	6	0·38
Cape Ward Hunt	NW	4·91±0·20	1·60±0·30	3	0·09
		7·44±0·14	4·38±0·21	9	0·19
		8·02±0·20	5·47±0·44	8	0·20
	SE	5·84±0·19	2·36±0·28	4	0·12
		6·86±0·07	3·75±0·16	10	0·16
		8·00±0·35	6·20±0·80	5	0·35
Killerton	NW	6·15±0·10	2·69±0·21	4	0·13
		8·04±0·17	6·24±0·31	7	0·20
	SE	5·91±0·41	3·40±0·39	5	0·29
		7·27±0·19	4·91±0·26	7	0·24
Tufi	NW	5·44±0·12	1·58±0·22	6	0·16
		6·70±0·26	3·64±0·48	8	0·39
		7·99±0·05	6·03±0·15	14	0·22

Between Morobe and Tufi the 7 km s^{-1} refractor is not such an obvious feature on the travel-time plots (Fig. 5) but can still be seen in the range 50–100 km with arrival times affected considerably by the sedimentary structure of the Trobriand Platform. At distances between 20 and 50 km a refractor can be identified with apparent velocities ranging between 4·9 and 6·1 km s^{-1} and having a mean of 5·66 km s^{-1}. The shots nearest to the recording stations indicate a mean apparent velocity of 3·7 km s^{-1} but at Killerton arrivals with an apparent velocity of 2·8 km s^{-1} are recorded from shots over a sediment sequence greater than 3 km thick, and this velocity is taken to be the velocity of direct recorded waves. The 3·7 km s^{-1} mean velocity probably corresponds to the minimum velocity in acoustic basement, which may be correlated with magnetic basement determined by CGG (1971) for the Trobriand Platform.

Apparent velocities of the order of 8 km s^{-1} are not seen as first arrivals on the time–distance plots at distances less than 100 km except at Morobe, where data distribution is not good. The reliable data from all stations indicate that apparent velocities are in the range 7·91–8·17 km s^{-1}. An interesting feature of the arrivals at Salamaua and Kui is that there appears to exist a later branch of the travel-time plot with an apparent velocity slightly greater than 8 km s^{-1}, the delay being about 2·0–2·5 s (Fig. 4). The increased amplitude of the later arrivals would suggest that they may be wide-angle reflections; a decrease in the energy of the first refracted arrivals is also apparent. Thus a retrograde branch of the travel-time curve may be inferred which leads to a subsequent, higher-velocity, refracting branch.

Structural interpretation

The arrival data plotted in Figs 4 and 5 have been interpreted by using routine time-depth methods on as many pseudo-reversed profiles of shots and stations as possible. The approximations associated with the assumed coincidence of shot and stations 10–15 km apart at each end of the reversed profiles became evident when reciprocal times could not be matched closely in all cases; however, the interpretation attaches greater importance to those profiles where reciprocal times matched to better than 0·3 s. The wavefront method of Schenck (1967) and the time-term method of Willmore & Bancroft (1960) were also applied to various data sets along the profile. Identification of arrivals at some stations was assisted by the compilation of seismic record sections (Fig. 6).

The sedimentary structure has been estimated from the aeromagnetic work conducted by BMR over the Papuan peninsula (CGG 1969, 1971, 1973) and the BMR marine sparker traversing conducted along the north-east Papuan Shelf (von der Borch 1972) and Trobriand Platform (Tilbury, 1975).

The shots between Lae and Morobe were fired offshore from the shelf area, which extends seaward for between 11 and 16 km. Acoustic basement offshore was identified with Papuan Ultramafic Belt rocks, which appear to have been stable and slowly subsiding since the early Pliocene (von der Borch, 1972). The shelf break occurs at between 109 and 117 m depth and sediments are present on the 1:6 gradient slope with a two-way reflection time of at most 0·25 s, i.e. a thickness of approximately 0·2–0·4 km. Aeromagnetic interpretation of the slope seaward of the Papuan Ultramafic Belt indicates that magnetic basement follows the seabed depths closely and no great thickness of sediment exists (CGG 1969).

South-east of Morobe magnetic basement depth is estimated at 1–2 km to beyond Cape Ward Hunt, then increasing to about 3 km in the Killerton region and decreasing again towards Tufi (Fig. 7). Magnetic basement is associated with the basaltic component of the ophiolite suite of rocks at Morobe and with the possible extension of this component under the Trobriand Platform (Finlayson *et al.* 1976). The 2·8 km s^{-1} seismic velocity measured at Killerton from the nearest shots is taken to indicate the velocity of the sedimentary sequence.

The 4·4 km s^{-1} velocity indicated for the uppermost layer between Salamaua and Morobe is associated with the near-surface rocks of the Papuan Ultramafic Belt, which are shown to continue offshore at shallow depth (von der Borch 1972). The 3·7 km s^{-1} velocity indicated from shots close to most of the stations south-east of Morobe is less than that for the near-surface ophiolite suite rocks and may indicate the sequence of Pliocene to Recent volcanics associated with the Trobriand Platform (Smith 1973). It may in fact not represent a single rock type but rather a series of rocks which are undistinguished by magnetic interpretation methods (CGG 1971).

The 5·66 km s^{-1} horizon is evident at depths of 3–7 km on the Trobriand Platform. The widely ranging apparent velocities determined on the travel-time plots may be associated with a layer of non-uniform velocity resulting from the rapid decrease in compressibility caused by the closure of cracks and grain boundaries at 1–2 kb pressures. Manghnani & Woollard (1968) have demonstrated the wide range of velocities apparent in laboratory tests on basalts at these pressures, and it is probable that the 5·66 km s^{-1} layer under the Trobriand Platform shallows in the Morobe region and becomes the surface layer with velocity 4·4 km s^{-1} between Morobe and Salamaua. It is also possible that a thin 5·66 km s^{-1} layer is not detected from first arrival data in that region.

The refractor with velocity 6·8–7·0 km s^{-1} is identified at depths of 3–6 km between Salamaua and Morobe, the shallower depths being interpreted in the Salamaua region (Fig. 7). The refractor deepens markedly south-east of Morobe under the Trobriand Platform. Depths in the Cape Ward Hunt to Killerton region are

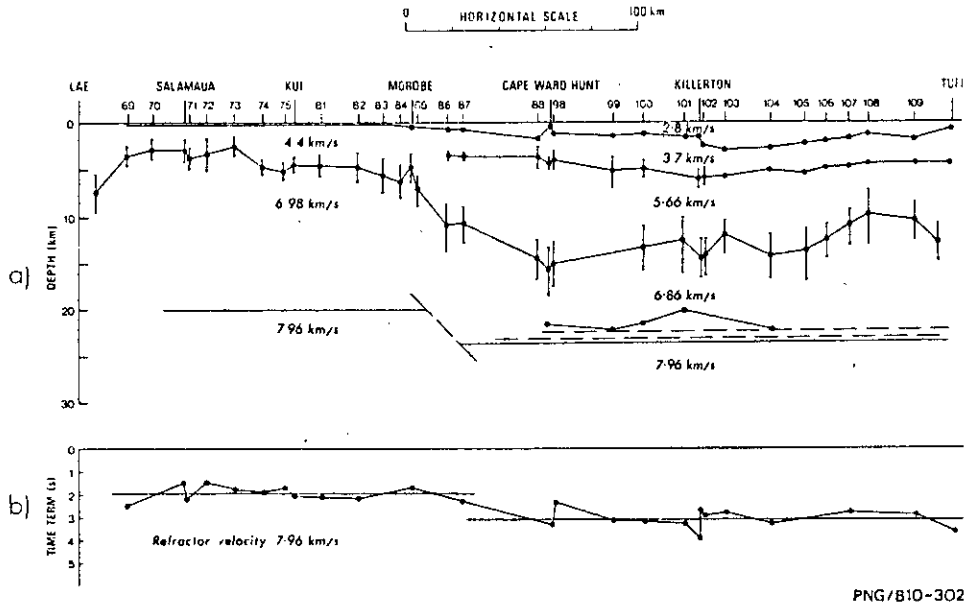

FIG. 7. (a) Crustal structure along the Lae-Tufi profile. (b) Time-terms to the 7·96 km s^{-1} refractor.

about 13–15 km, shallowing into the range 10–13 km towards Tufi. The bars on the plotted datum points in Fig. 7 indicate the extremities of depths interpreted from various data sets using different interpretation methods.

The depth to the 8 km s^{-1} refractor is more difficult to interpret because of the greater distances required to observe refractions as first arrivals and the crustal structure changes which occur half way along the profile, therefore a simple interpretation is presented at this time.

Time-depth interpretations have been made from data across the Trobriand Platform between Morobe and Tufi and the depths are indicated in Fig. 7. The good data sets from Morobe, Cape Ward Hunt, Killerton and Tufi indicate velocities in the range 7·98–8·02 km s^{-1} with no significant dip. Simple layered modelling indicates an average depth of 22–23 km.

Finlayson *et al.* (1976) have shown how the depth to this refractor decreases to about 8 km along a profile between Killerton and Mount Lamington (LMG), demonstrating the gradients (approximately 19°) to be expected in this refracting horizon normal to the geological strike. Along the strike, however, it is expected that the gradients would not be as great, and a time-term interpretation was sought by constraining the refractor velocity to 7·96 km s^{-1}, the mean of all apparent velocities along the profile. The resultant time-terms are plotted in Fig. 7 and it is evident that the average for the Salamaua–Morobe region (1·92 a) was 1·14 s smaller than the average for the Trobriand Platform (3·06 s). Computation of the average depths indicates that under the north-west part of the profile the refractor is at 20·0 km and under the Trobriand Platform at 23·7 km.

The later arrivals evident on some of the seismic traces can be used as additional evidence for the interpretation along the profile. Simple ray-tracing methods were applied to layered models to try to account for the prominent later arrivals at Salamaua (Fig. 6) from shots beyond 200 km mentioned earlier in this paper. The characteristics of seismic traces from various velocity-depth profiles have been described by many

Table 2

Seismic velocities (km s^{-1}) *from the Papuan Ultramafic Belt and Cyprus*

Formation	Outcrop	Cyprus in formation	Laboratory 0–2 kbar	At sea	Oceanic crust	Along profile	Papuan Ultramafic Belt	Laboratory
Upper sediments	—	—	—	2·1	Layer 1	2·8		
Pillow lavas	2·9	3·3	2·9–4·3	3·3	Layer 2	3·7, 4·4		
	3·7	—	—	4·4–4·5	—	—		
Basal group	4·8	5·1	—	4·4	—	—		
Diabase	4·9–5·1	6·4	4·9–5·7	5·5	Layer 3	5·66		
Gabbro	5·5	—	6·6–7·0	6·5	—	6·86–6·98	Gabbro	7·44–7·45 2–3 kbar
					Upper mantle	7·91–8·17	Cumulate ultramafics	7·37–8·06 3 kbar
							Non-cumulate ultramafics	8·01–8·17 3–4 kbar
	Lort & Gray 1974					East Papua Crustal Survey		Kroenke *et al.* (1974)

authors (Fuchs & Müller 1971). To achieve the characteristics of the profile recorded at Salamaua a deeper refractor was introduced with a velocity of about 8·2 km s^{-1} and a low-velocity zone above it, not only to account for the substantial delay in the arrival of reflections but also to approximate the relative amplitude features. The PUB–1 model and travel-time curve superimposed on Fig. 6 is one model which can be used.

Discussion

Berry (1971), among others, has drawn attention to the uncertainties in interpretation of first-arrival seismic data and indicated that the depths to a refractor for some velocity-depth models consistent with the travel-time plots may be 20 per cent greater than those from the simplest consistent model. No attempt therefore has been made to relate the statistical uncertainties indicated in Table 1 to structural uncertainties; the errors should be taken merely as an indication of the fit of the datum points to the least-squares straight lines.

The velocities along the Lae-Tufi profile can be compared with laboratory velocity measurements on Papuan Ultramafic Belt rocks by Kroenke *et al.* (1974), Their results, together with results from the Cyprus ophiolite complex (Lort & Gray 1974), are listed in Table 2. The Cyprus velocity data are correlated with oceanic crustal structure of Moores & Vine (1971) and the velocities found in eastern Papua are similar to those data. However, the layer thicknesses found in ocean basins are commonly 1–2 km for layer 2 and 4–6 km for layer 3, giving a total thickness of solid crust of about 8 km (Drake & Nafe 1968) compared with a thickness greater than 20 km along the Lae-Tufi profile. The 22–23 km depth determined off the Killerton coast is in broad agreement with Milsom's (1975) coastal value of 25 km based on gravity data. Further seismic analysis is required, however, to determine the detailed structure of the ophiolite sequence over the whole of the region. The total crustal thickness along the Lae-Tufi profile is considerably greater than 10 km, which is thickness of the basalt and gabbro components of the ophiolite suite exposed at the surface farther inland.

Finlayson *et al.* (1976) have drawn attention to the structures below the Moho demonstrated by the PUB–1 model fitted to Salamaua data (Fig. 6). Similar seismic features can be seen in the recordings beyond 150 km (Fig. 3) at Musa (MU), Cape Rodney (CR), Kupiano (KP), and Kwikila (KW) from shots along the north-east coast. The time-delay and amplitude data associated with deeper refractors seem to be satisfied only by introducing a low-velocity zone of the proportions of that in the PUB–1 model. It may be speculated that the material for such a low-velocity zone is derived from the Mesozoic north-east margin of the Australian continent, but this will clearly require further investigation.

Acknowledgments

The authors wish to acknowledge the large contribution to field survey work and data reduction by B. J. Drummond, C. D. N. Collins, J. B. Connelly, M. L. Broyles, P. M. T. Ryan and J. M. W. Rynn. Other survey personnel who greatly contributed to the success of the field operations were P. E. Mann, A. G. Spence, R. Cherry, D. A. Coutts, I. D. Ripper, J. R. Cleary, B. Carr, V. Dent, V. Ingham and J. Hyslop.

We also wish to thank all survey logistic support personnel, PNG Government Administration staff, and persons resident in the survey area for their assistance with survey operations. The University of Queensland, the Warrnambool Institute of Advanced Education and the Preston Institute of Technology wish to acknowledge the financial support from BMR to enable participation in the survey, and the participa-

tion of the University of Hawaii was funded by US Office of Naval Research Project NR 083-603. BMR wishes to acknowledge the assistance rendered to crustal investigations in the Australian region by West Australian Petroleum Pty Ltd, who donated the explosives. This paper is published with the permission of the Director of the Bureau of Mineral Resources and the Chief Geologist, Geological Survey of PNG.

D. M. Finlayson:
Bureau of Mineral Resources, Geology and Geophysics, Canberra

K. E. Muirhead:
Australian National University, Canberra

J. P. Webb:
University of Queensland, Brisbane

G. Gibson:
Preston Institute of Technology, Preston, Victoria

A. S. Furumoto:
Hawaii Institute of Geophysics, University of Hawaii, Honolulu

R. J. S. Cooke:
Volcanological Observatory, Geological Survey of Papua, New Guinea, Rabaul

A. J. Russell:
Warrnambool Institute of Advanced Education, Warrnambool, Victoria

References

Berry, M. J., 1971. Depth uncertainties from seismic first-arrival refraction studies, *J. geophys. Res.*, **76**, 6464–6468.

Bickel, R. S., 1974. Reconnaissance geology of Cape Vogel Basin, Papua New Guinea; *Bull. Am. Ass. petrol. Geol.*, **58**, 2477–2489.

Brooks, J. A., 1969. Rayleigh waves in southern New Guinea. II: A shear velocity profile, *Bull. seism. Soc. Am.*, **59**, 2017–2038.

Coleman, R. G., 1971. Plate tectonic emplacement of upper mantle peridotites along continental edges, *J. geophys. Res.*, **76**, 1213–1222.

Compagnie Generale de Geophysique (CGG), 1969. Papuan Basin and Basic Belt aeromagnetic survey, Territory of Papua and New Guinea, *Bur. Miner. Resour. Aust. Rec.*, 1969/58 (unpubl.).

Compagnie Generale de Geophysique (CGG), 1971. Eastern Papua aeromagnetic survey. Part 1. North-eastern portion (mainly offshore) flown in 1969, *Bur. Miner. Resour. Aust. Rec.*, 1971/67 (unpubl.).

Compagnie Generale de Geophysique (CGG), 1973. Eastern Papua aeromagnetic survey. Part 2. Southwestern panel (onshore) flown in 1970–71, *Bur. Miner. Resour. Aust. Rec.*, 1973/60 (unpubl.).

Curtis, J. W., 1973. Plate tectonics and the Papua New Guinea—Solomon Islands region, *J. geol. Soc. Aust.*, **20,** 21–36.

Davies, H. L., 1971. Periodotite-gabbro-basalt complex in eastern Papua: an overthrust of oceanic mantle and crust, *Bur. Miner. Resour. Aust. Bull.*, **128.**

Davies, H. L. & Smith, I. E., 1971. Geology of eastern Papua, *Bull. geol. Soc. Am.*, **82,** 3299–3312.

Denham, D., 1969. Distribution of earthquakes in the New Guinea–Solomon Islands region, *J. geophys. Res.*, **74,** 4290–4299.

Dewey, J. F. & Bird, J. M., 1970. Mountain belts and the New Global Tectonics, *J. geophys. Res.*, **75,** 2625–2647.

Dewey, J. F. & Bird, J. M., 1971. Origin and emplacement of the Ophiolite Suite: Appalachian ophiolites in Newfoundland, *J. geophys. Res.*, **76,** 3179–3206.

Drake, C. L. & Nafe, J. E., 1968. The transition from ocean to continent from seismic refraction data. In, *The Crust and Upper Mantle of the Pacific Area,* eds L. Knopoff, C. L. Drake, P. J. Hart, *Am. Geophys. Un. Monog.*, **12.**

Ewing, M., Hawkins, L. V. & Ludwig, W. J., 1970. Crustal structure of the Coral Sea, *J. geophys. Res.*, **75,** 1953–1962.

Finlayson, D. M., 1968. First arrival data from the Carpentaria Region Upper Mantle Project (CRUMP), *J. geol. Soc. Aust.*, **15,** 33–50.

Finlayson, D. M., 1975. East Papua Crustal Survey, Oct-Dec 1973: operational report, *Bur. Miner. Resour. Aust. Rec.*, in preparation.

Finlayson, D. M., Drummond, B. J., Collins, C. D. N. & Connelly, J. B., 1976. Crustal structure under the Mount Lamington region of Papua New Guinea. In, *Volcanism in Australasia,* ed. R. W. Johnson, Elsevier, in press.

Fuchs, M. & Müller, G., 1971. Computation of synthetic seismograms with the reflectivity method and comparison with observations, *Geophys. J. R. astr. Soc.*, **23,** 417–433.

Furumoto, A. S., Hussong, D. M., Campbell, J. F., Sutton, G. H., Malahoff, A., Rose, J. C. & Woollard, G. P., 1970. Crustal and upper mantle structure of the Solomon Islands as revealed by seismic refraction survey of Nov-Dec 1966, *Pacific Science,* **24,** 315–332.

Gardner, J. V., 1970. Submarine geology of the western Coral Sea, *Bull. geol. Soc. Am.*, **81,** 2599–2614.

Jakes, P. & Smith, I. E., 1970. High potassium calc-alkaline rocks from Cape Nelson, eastern Papua, *Mineral. Petrol.*, **28,** 259–271.

Jakes, P. & White, A. J. R., 1969. Structure of the Melanesian arcs and correlation with distribution of magma types, *Tectonophys.*, **8,** 223–236.

Johnson, R. W., Mackenzie, D. E. & Smith, I. E., 1970. Short papers on Quaternary volcanic areas in Papua New Guinea, *Bur. Miner. Resour. Aust. Rec.*, 1970/72. (unpubl.).

Johnson, T. & Molnar, P., 1972. Focal mechanisms and plate tectonics of the southwest Pacific, *J. geophys. Res.*, 77, 5000–5032.

Krause, D. C., 1973. Crustal plates of the Bismarck and Solomon Seas. In, *Oceanography of the south Pacific,* ed. R. Fraser, New Zealand National Commission for UNESCO, Wellington, 271–280.

Kroenke, L. K., Manghnani, M. H., Rai, C. S., Ramananantoandro, R. & Fryer, P., 1974. Elastic properties of ultramafic rocks from Papua-New Guinea: composition and structure of the upper mantle. In, International Woollard Symposium; the Geophysics of the Pacific Ocean Basin and its Margin. University of Hawaii & Interunion Commission on Geodynamics.

Lort, J. H. & Gray, F., 1974. Cyprus: Seismic studies at sea, *Nature,* **248,** 745–747.

Luyendyk, B. P., MacDonald, K. C. & Bryan, W. B., 1973. Rifting history of the Woodlark Basin in the south-west Pacific, *Bull. geol. Soc. Am.*, **84,** 1125–1134.

Manghnani, M. H. & Woollard, G. P., 1968. Elastic wave velocities in Hawaiian rocks at pressures to ten kilobars, In, *The crust and upper mantle of the Pacific Area,* eds L. Knopoff, C. L. Drake & P. J. Hart, *Am. geophys. Un. Monog.*, **12,** 501–516.

Milsom, J. S., 1970. Woodlark Basin, a minor center of sea-floor spreading in Melanesia, *J. geophys. Res.*, **75,** 7335–7339.

Milsom, J. S., 1973. Papuan Ultramafic Belt: gravity anomalies and the emplacement of ophiolites, *Bull. geol. Soc. Am.*, **84,** 2243–2258.

Moores, E. M., 1973. Geotectonic significance of ultramafic rocks, *Earth-Sci. Rev.*, **9,** 241–258.

Moores, E. M. & Vine F. J., 1971. The Troodos Massif, Cyprus and other ophiolites as oceanic crust: evaluation and implications, *Phil. Trans. R. Soc. Lond.*, **A, 268,** 443–466.

Muirhead, K. J. & Simpson, D. W., 1972. A three-quarter watt seismic station, *Bull. seism. Soc. Am.*, **62,** 985–990.

Mutter, J. C., 1975. A structural analysis of the Gulf of Papua and northwest Coral Sea region, *Bur. Miner. Resour. Aust. Rep.*, **179.**

Rabinowitz, P. D. & Ryan, W. B. F., 1970. Gravity anomalies and crustal shortening in the eastern Mediterranean, *Tectonophysics*, **10,** 585–608.

Ripper, I. D., 1970. Global tectonics and the New Guinea-Solomon Islands region, *Search*, **1,** 226–232.

Rose, J. C., Woollard, G. P. & Malahoff, A., 1968. Marine gravity and magnetic studies of the Solomon Islands. In, *Am. geophys. Un. Monog.*, **12,** 379–410, eds L. Knopoff, C. L. Drake, & P. J. Hart.

Schenck, F. L., 1967. Refraction solutions and wavefront targeting. In, *Seismic refraction prospecting*, ed. A. W. Musgrave, *Soc. Expl. Geophys.*, 416–425.

Smith, I. E., 1969. Notes on the volcanoes Mount Bogana and Mount Victory, TPNG, *Bur. Miner. Resour. Aust. Rec.*, 1969/12 (unpubl.).

Smith, I. E., 1970. Late Cainozoic uplift and geomorphology in southeastern Papua. *Search*, **1,** 222–225.

Smith, I. E., 1973. Late Cainozoic volcanism in the south-east Papuan islands, *Bur. Miner. Resour. Aust. Rec.*, 1973/67 (unpubl.).

St John, V. P., 1970. The gravity field and structure of Papua and New Guinea. *Aust. Petrol. Expl. Ass. (APEA) Journal*, 41–55.

Taylor, G. A. M., 1958. The 1951 eruption of Mount Lamington, Papua, *Bur. Miner. Res. Aust. Bull.*, **38.**

Tilbury, L. A., 1975. Geophysical results from the Gulf of Papua and Bismarck Sea, *Bur. Miner. Resour. Aust. Rec.*, 1975/115 (unpubl.)

Von der Borch, C. C., 1972. Marine geology of the Huon Gulf region of New Guinea, *Bur. Miner. Resour. Aust. Bull.*, **127.**

Willmore, P. L. & Bancroft, A. M., 1960. The time-term approach to refraction seismology, *Geophys. J. R. astr. Soc.*, **3,** 419–432.

Physics of the Earth and Planetary Interiors, 14 (1977) 13–29

CRUSTAL STRUCTURES IN THE REGION OF THE PAPUAN ULTRAMAFIC BELT

D.M. FINLAYSON, B.J. DRUMMOND, C.D.M. COLLINS and J.B. CONNELLY

Bureau of Mineral Resources, Geology and Geophysics, Canberra, A.C.T. (Australia)

(Received September 6, 1976; accepted for publication September 27, 1976)

Finlayson, D.M., Drummond, B.J., Collins, C.D.M. and Connelly, J.B., 1977. Crustal structures in the region of the Papuan Ultramafic Belt. Phys. Earth Planet. Inter., 14: 13–29.

Geophysical interpretation of crustal structures in the region of the Papuan Ultramafic Belt shows that the belt consists of a major dipping layered structure with velocities similar to those found in Alpine ophiolite sequences. However, the thickness of crustal material seaward of the belt is probably too great to be oceanic in origin, a feature it has in common with the Ivrea and Troodos ophiolite complexes. Seismic travel times demonstrate the continuity of a high-velocity slab of rock dipping northeast at angles of between 13 and 25° and exclude the presence of a host sialic rock which would reduce average crustal velocities. Seismic record sections indicate that a low-velocity zone under the dipping slab is likely. The thickness of crustal material offshore ranges from 33 km in the area of the Huon Gravity Low in the western Solomon Sea, to 27 km in the area north of the Trobriand Platform, decreasing to 13 km in the central Solomon Sea. It is speculated that the crust under the Trobriand Gravity High contains an ophiolite rock suite similar to that comprising the Papuan Ultramafic Belt, and displaced from that belt during episodes of Cainozoic crustal extension which formed the Trobriand Platform. The Solomon Sea crust and lithosphere west of 150°E has undergone considerable deformation, and the thick crust under that region may be a result of imbrication in a marginal basin crust. The Eastern Fields Marginal Plateau in the northwest Coral Sea has a crust about 22 km thick and is subcontinental in character. It is separated from the Papuan peninsula by a zone of crust about 18 km thick, possibly formed during crustal extension coinciding with the formation of the ocean-floor basalts exposed in the east of the peninsula. The crustal thickness of about 30 km along the southwest Papuan peninsula coast increases only slightly inland by 3–5 km until underthrusting takes place in the area of the Papuan Ultramafic Belt.

1. Introduction

The Papuan Ultramafic Belt (Fig. 1) is a relatively undeformed peridotite–gabbro–basalt layered complex which crops out over a length of 400 km along the Papuan peninsula of Papua New Guinea (Davies, 1971; Davies and Smith, 1971). A number of geophysical surveys have been conducted in the region to determine the crustal structure; these have been summarised by Finlayson et al. (1976a, b) in their initial reports of the explosion seismic survey conducted in 1973. Further interpretation and modelling studies have been conducted on data from that survey and these are presented in this paper combined with interpretations from recently compiled gravity and magnetic data.

During the 1973 East Papua Crustal Survey (Finlayson et al., 1976a) 111 marine shots were detonated on both the Coral Sea and Solomon Sea sides of the Papuan peninsula and these were recorded at 39 sites shown in Fig. 2. The data available have been described by Finlayson (1976). Regional gravity data have been obtained from many different sources and compiled for the production of a gravity map of Melanesia (Connelly, 1976). Fig. 3 shows the simple Bouguer anomalies on land (Bouguer density 2.67 t m^{-3}) and free-air anomalies at sea in the region of the Papuan peninsula and surrounding waters. High-level aeromagnetic data are available from surveys conducted for the Australian Bureau of Mineral Resources, Geology and Geophysics (CGG, 1971).

14

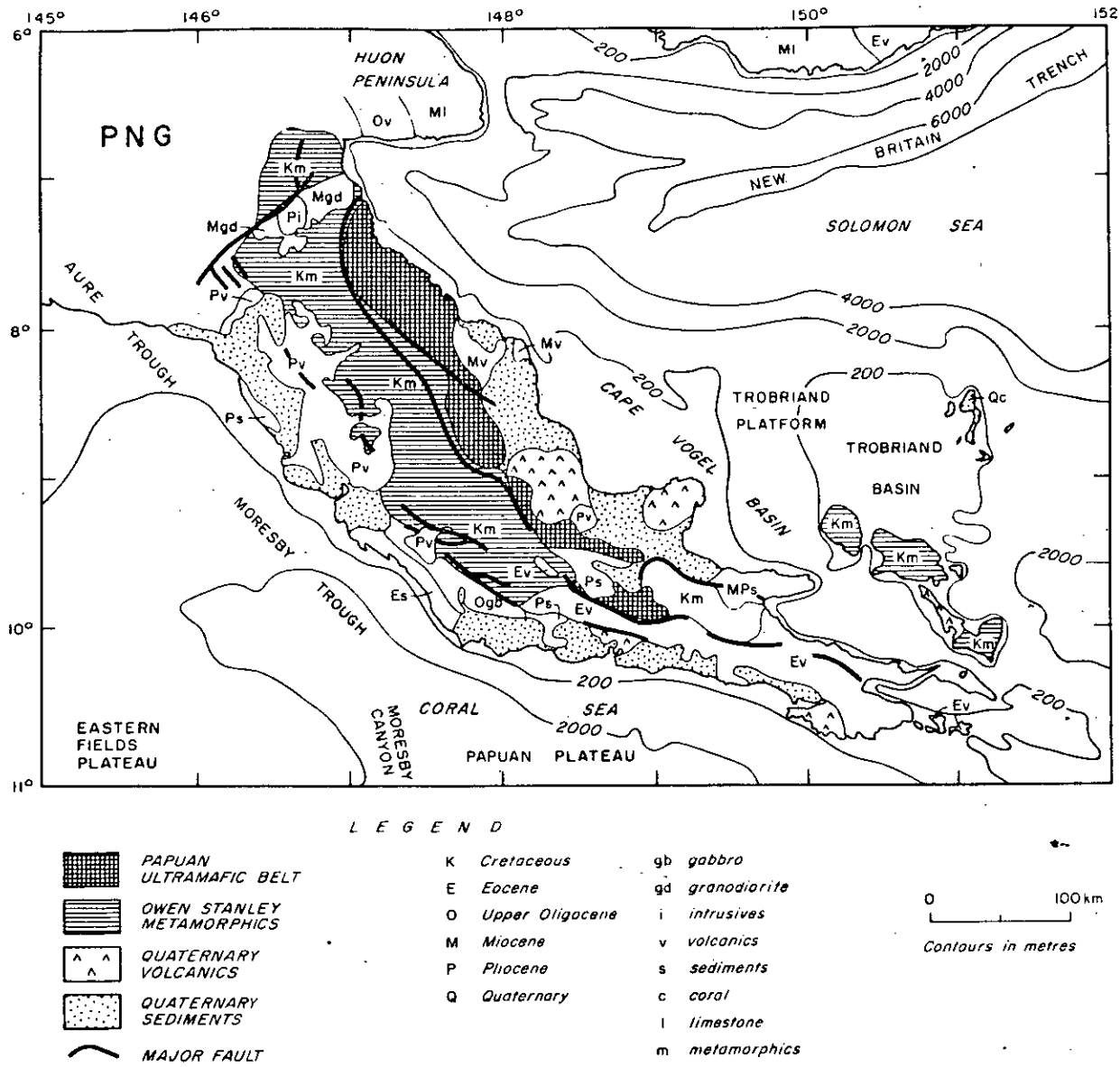

Fig. 1. Simplified geology and bathymetry of the east Papua region.

2. Structural interpretation

The interpretation of the seismic data along the northeast and southwest coasts of the Papuan peninsula has been used to control seismic and gravity modelling of gross tectonic features at right angles to the geological strike.

2.1. Northeast Papuan peninsula coast

On the northeast side of the peninsula, the seismic record sections for Salamaua (*SL*), Kui (*KU*) and Lake Trist (*LT*) are shown in Fig. 4, and those from Tufi (*TF*) and Musa (*MD*) are shown in Fig. 5. We have assumed, in making interpretations along this line, that

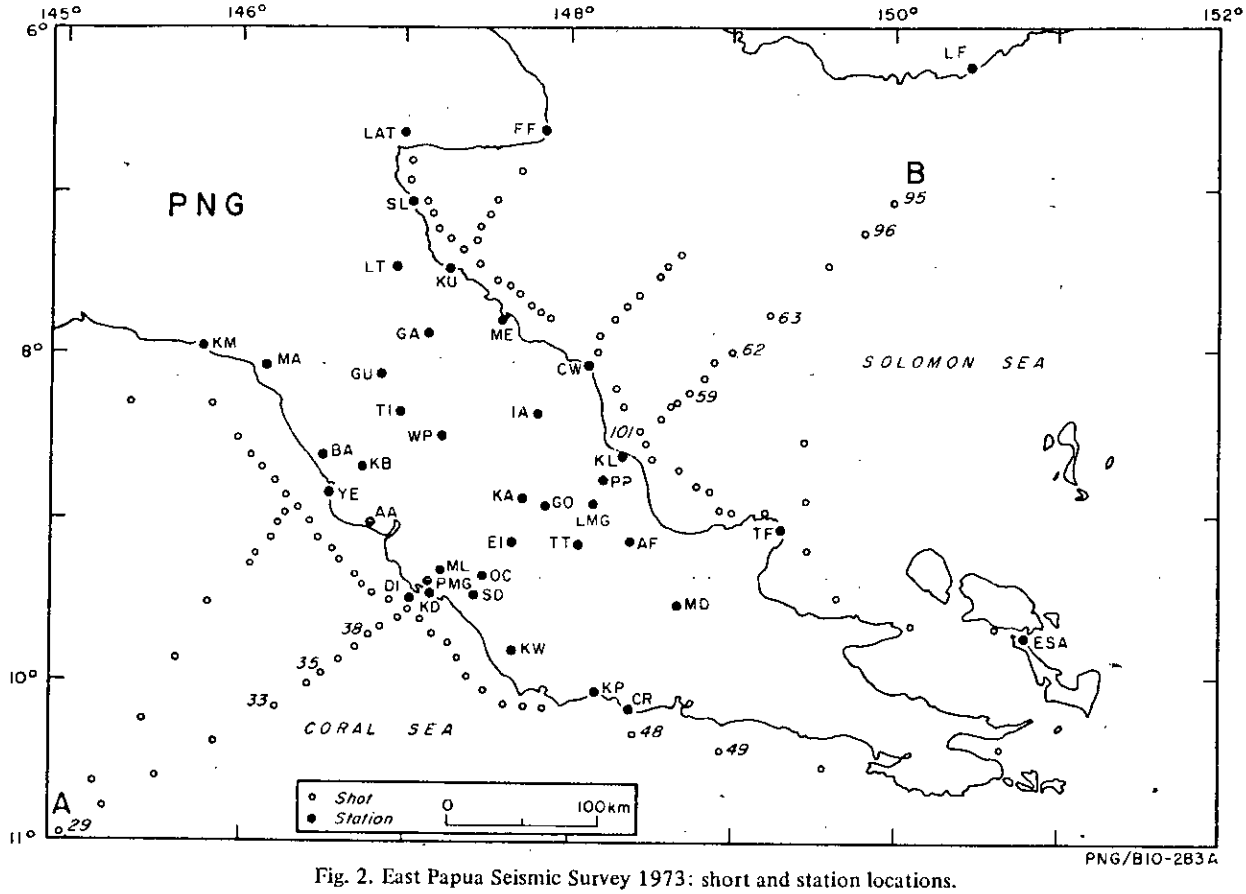

Fig. 2. East Papua Seismic Survey 1973: short and station locations.

there are no extreme structural changes such as those expected across the geological strike, and that the seismic refractors are reasonably continuous. The NW–SE-trending gravity and magnetic anomalies (Finlayson et al., 1976b) associated with various components of the Papuan Ultramafic Belt support this assumption.

The interpretation of Finlayson et al. (1976a) in the region between Salamaua (*SL*) and Morobe (*ME*) comprises a two-layer crust 20 km thick, consisting of a 3–5 km upper basaltic layer with velocity 4.4 km s^{-1} overlying a gabbroic layer with velocity about 7.0 km s^{-1}. In the region between Cape Ward Hunt (*CW*) and Tufi (*TF*) the crust thickens to 23–24 km and consists of a sedimentary section with velocity 2.8 km s^{-1}, two upper crustal layers with velocities of 3.7 and 5.7 km s^{-1} and a lower crustal layer with velocity 6.9 km s^{-1}. The velocity of the upper mantle is about 8.0 km s^{-1} along the whole coast.

The interpretation of deeper structures along the northeast Papuan coast depends on the identification of significant subsequent arrivals in the record sections (Figs. 4 and 5). Finlayson et al. (1976a) proposed an average model structure from the Salamaua (*SL*) results and the travel-time curve for their PUB-1 model is shown in Fig. 4a. The model requires a low-velocity zone beneath the uppermost mantle material. This model is not unique and other possibilities, models PUB-2 and PUB-3, are shown in Figs. 4b, c, and 5, together with their travel-time curves.

The minimum velocity used in the low-velocity zone for all models is 6.5 km s^{-1} which is not as low as the 4.0 km s^{-1} interpreted for the sialic material under the Ivrea ophiolite complex in the European Alps. That sialic material is considered to be partly molten (Giese et al., 1967; Giese, 1968). Velocities of about 4.7 km s^{-1} have been measured in lithified sediments

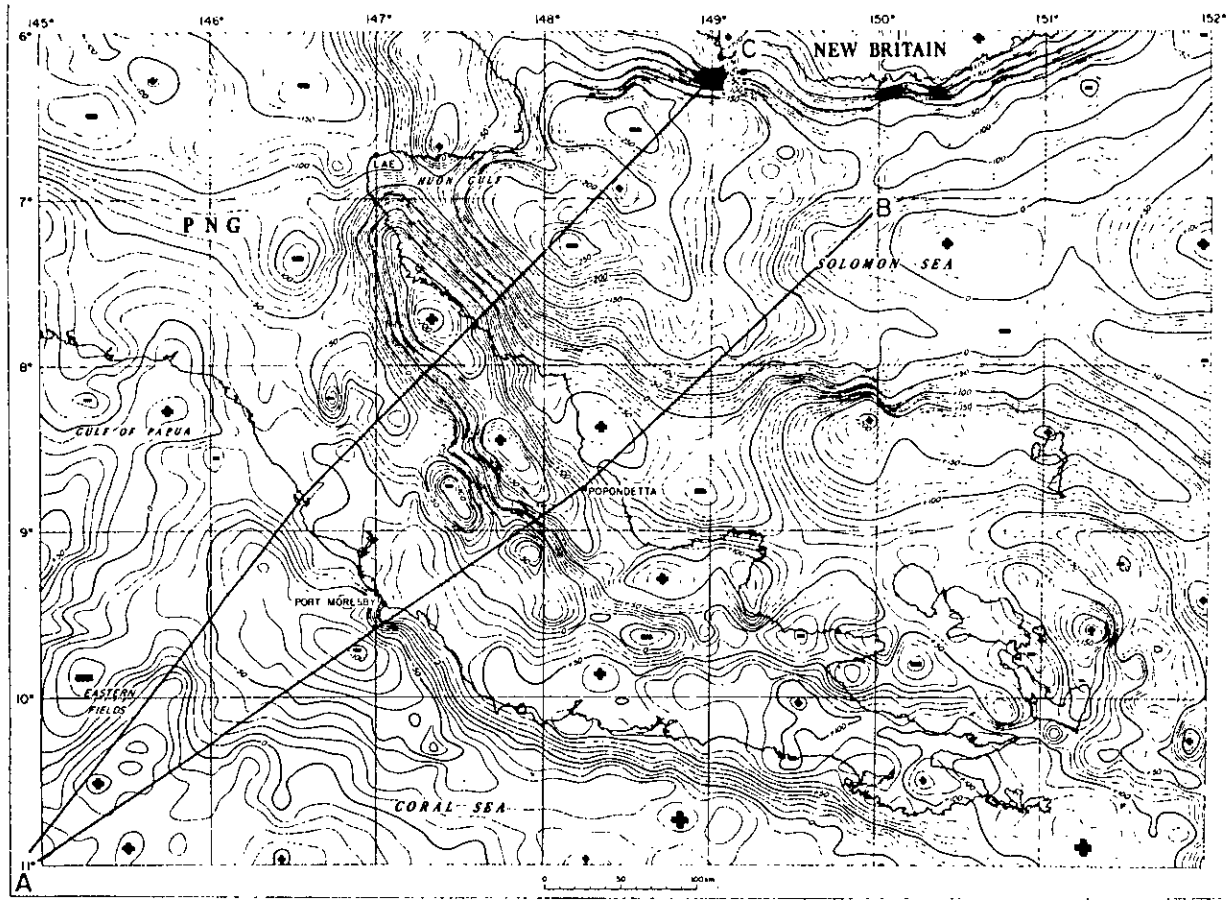

Fig. 3. Gravity map of the east Papua region showing free-air anomalies at sea and simple Bouguer anomalies on land (Bouguer density 2.67 t m^{-3}).

of the Aure and Moresby troughs (Fig. 1) at depths of less than 10 km (Tallis, 1975; Brown et al., 1975), and the upper crustal material along the southwest coast of the Papuan coast, described later in this paper, has a minimum velocity of about 5.9 km s^{-1}. We therefore consider it unlikely that a low-velocity zone under the ophiolite material has a velocity of less than 6.0 km s^{-1}.

The PUB-2 model of the Tufi record section (Fig. 5) contains the upper crustal structure under the Trobriand Platform region. At distances less than 150 km the differences between the PUB-2 travel-time curve and the Musa record section in Fig. 5 are attributable to the breakdown in the two-dimensional model assumptions when applied to stations remote from the coast. Seismic rays consequently encounter dipping structures across the geological strike. The modelling of seismic travel time across the strike of steeply dipping structures will be discussed later in this paper; it is sufficient to indicate at this point that apparent velocities can differ greatly from refractor velocities. The general trend in all the proposed models seems to indicate the existence of upper-mantle material between approximately 23 and 35 km with a velocity of about 8.0 km s^{-1}, underlain by lower-velocity material (about 6.5 km s^{-1}) down to about 50 km.

2.2. Southwest Papuan peninsula coast

The crustal structure along the southwest coast of the Papuan peninsula differs greatly from that along the northeast coast. Finlayson et al. (1976b) have already pointed out that the differences in the travel-

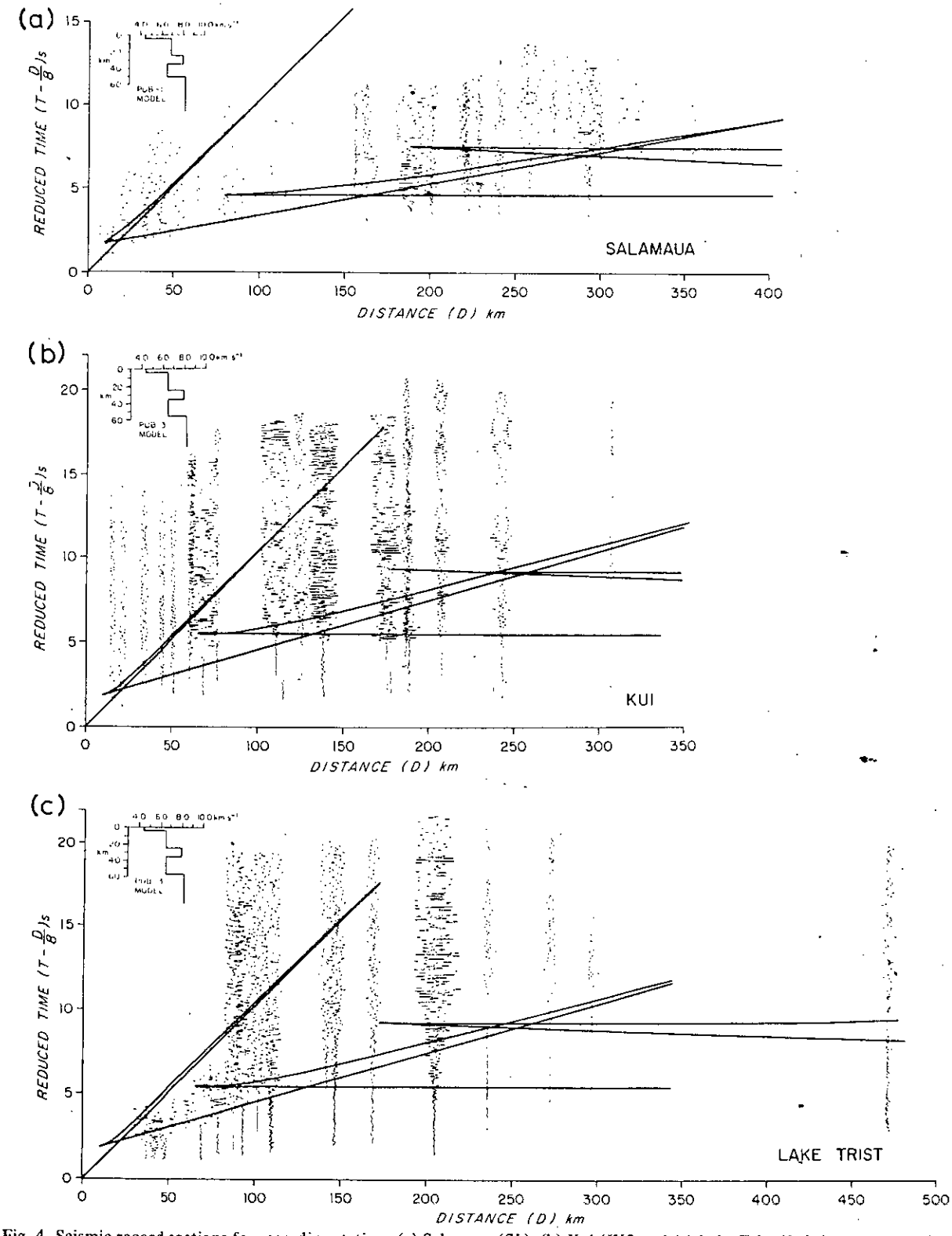

Fig. 4. Seismic record sections for recording stations (a) Salamaua (*SL*), (b) Kui (*KU*) and (c) Lake Trist (*LT*) from shots to the southeast along the NE Papuan coast. PUB-1 and PUB-3 velocity–depth models and their computed time–distance plots are superimposed on the record sections.

18

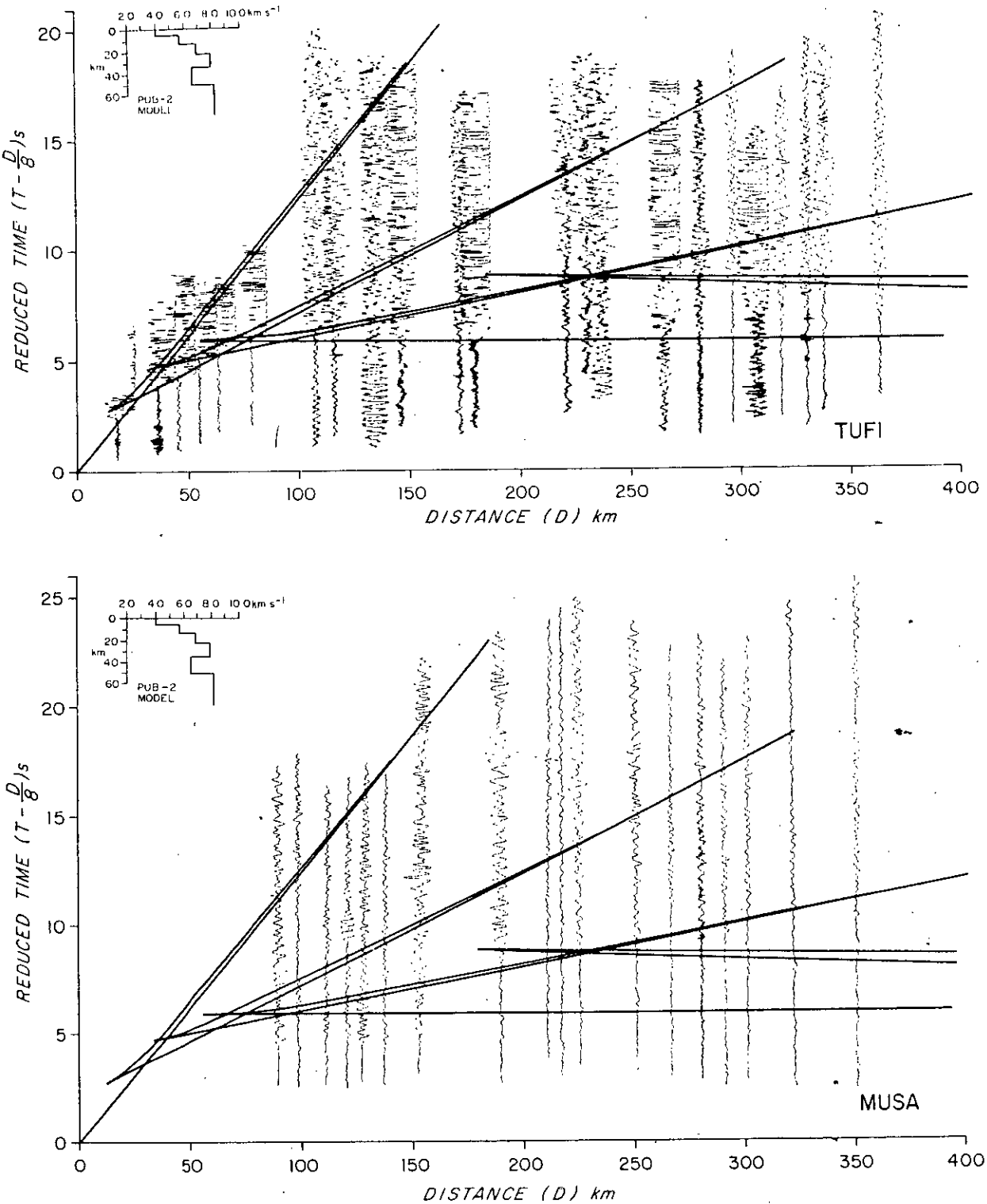

Fig. 5. Seismic record sections for recording stations Tufi (*TF*) and Musa (*MD*) from shots northwest along the NE Papuan coast. The PUB-2 velocity–depth model and its computed time–distance plot are superimposed on the record sections.

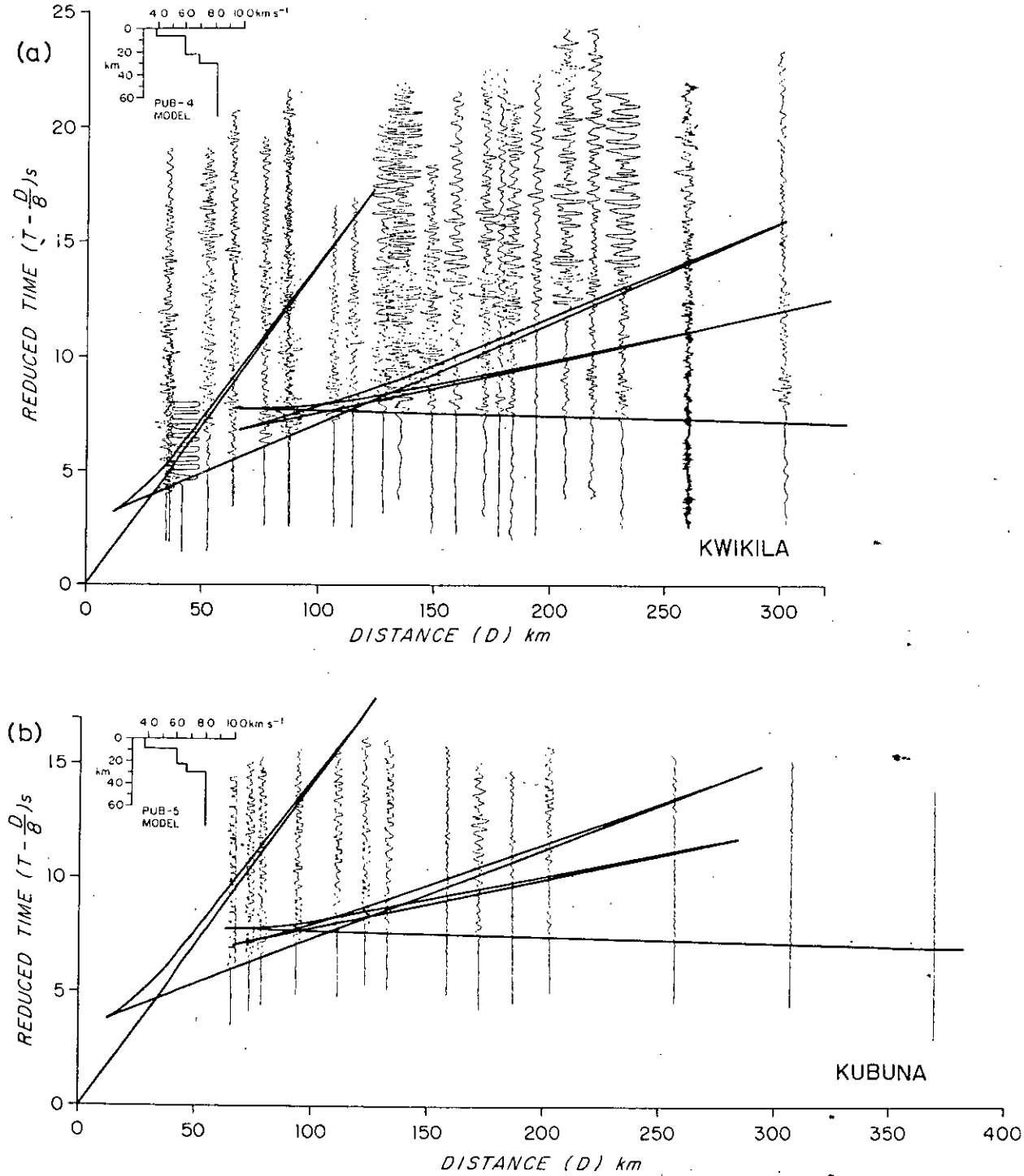

Fig. 6. Seismic record sections (a) for recording station Kwikila (*KW*) from shots to the northwest along the SW Papuan coast and (b) for recording station Kubuna (*KB*) from shots to the southeast along the SW Papuan coast. The PUB-4 and PUB-5 velocity–depth models and their computed time–distance plots are shown in (a) and (b), respectively.

time curves from shots in the Coral Sea and Solomon Sea are considerable. Their preliminary estimate of crustal thickness along the Coral Sea coast was 26 km.

Fig. 6 illustrates seismic record section from Kwikila (*KW*) and Kubuna (*KB*) along the southwest Papuan coast, and also shows PUB-4 and PUB-5 models and travel-time curves for crustal structure under the coast. Velocities ranging from 3.0 to 4.7 km s^{-1} are associated with sediments of the Aure and Moresby troughs (Brown et al., 1975; Tallis, 1975). A velocity of about 5.9 km s^{-1} is determined for the upper crust, and a lower crustal layer with velocity of about 6.8 km s^{-1} is evident from subsequent arrivals on the record sections. These velocities are higher than those proposed by Finlayson et al. (1976b) in their preliminary interpretation, and the revised average crustal thickness in the PUB-4 model of 30 km is consequently greater.

2.3. Profile across the Papuan peninsula

The major features of the Papuan ophiolite suite of rocks are evident only when profiles across the Papuan peninsula are considered. The determination of seismic structure at right angles to the geological strike is complicated by the possible existence of large dips and abrupt changes in velocity. The assumptions of low dips and continuity of refractors normally associated with delay-time and time-term analyses would almost certainly not apply across the Papuan peninsula. Hence a computer modelling program which directs seismic rays from a source through a structure was applied to determine travel times. Models were compiled along the line *A–B* (Fig. 2) from shot *29* in the Coral Sea through Port Moresby (*PMG*) and Popondetta (*PP*) to shot *95* in the Solomon Sea. Control on velocities and depths was available from the seismic profiles parallel to the northeast and southwest coasts of the Papuan peninsula and from the interpretations of fan shoots on both the northeast and southwest coasts (Finlayson et al., 1976b).

Fig. 7 shows record sections from four shots in the Solomon Sea as recorded at stations along profile *A–B*, and Fig. 8 shows record sections from three shots in the Coral Sea recorded at the same stations.

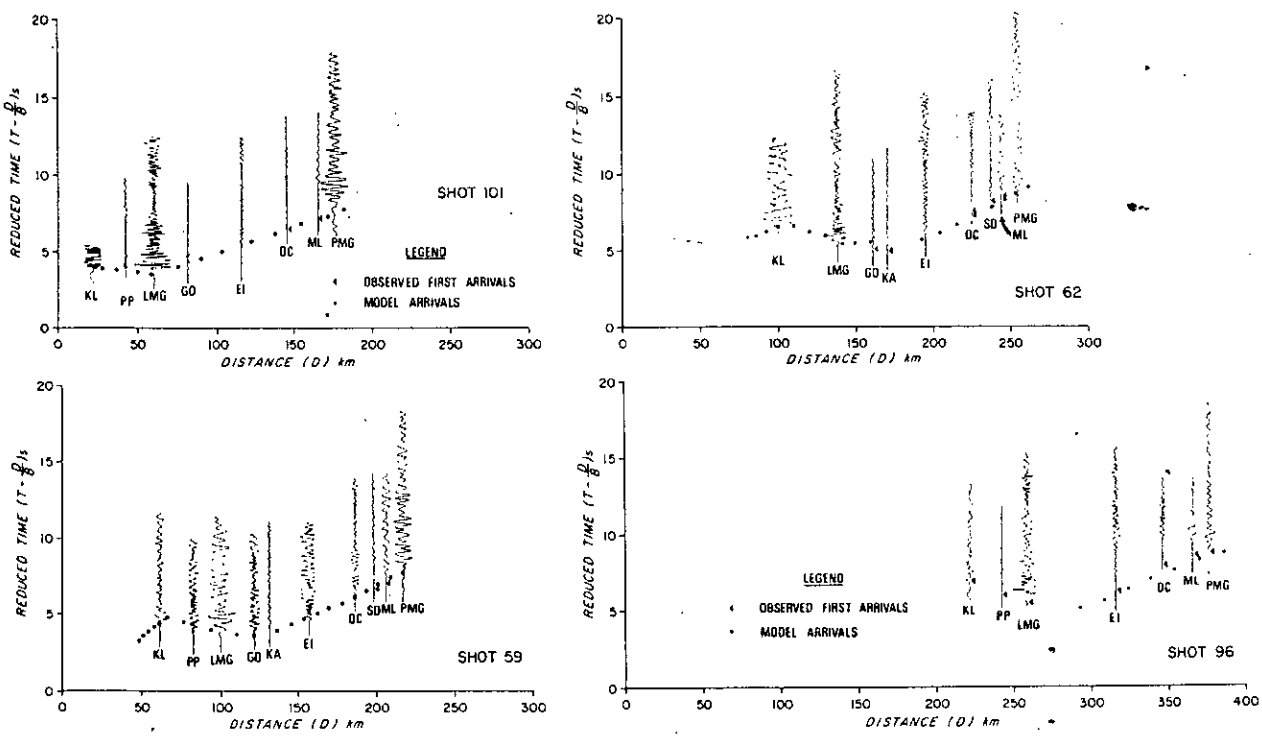

Fig. 7. Seismic record sections from shots numbers *101, 59, 62* and *96* in the Solomon Sea to recording stations along profile *A–B*, together with computed arrivals from the seismic model shown in Fig. 9a.

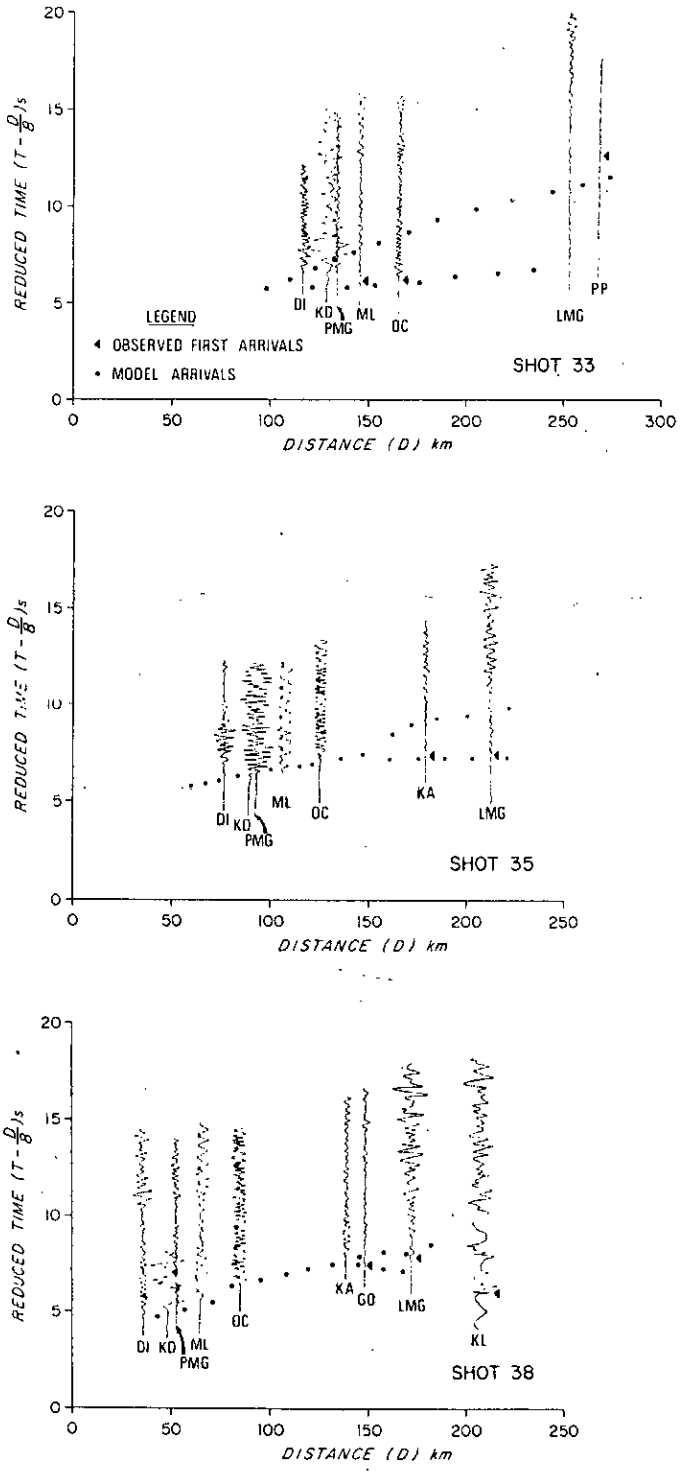

Fig. 8. Seismic record sections from shots *33*, *35* and *38* in the Coral Sea to recording stations along profile $A-B$, together with arrivals from the seismic model shown in Fig. 9a.

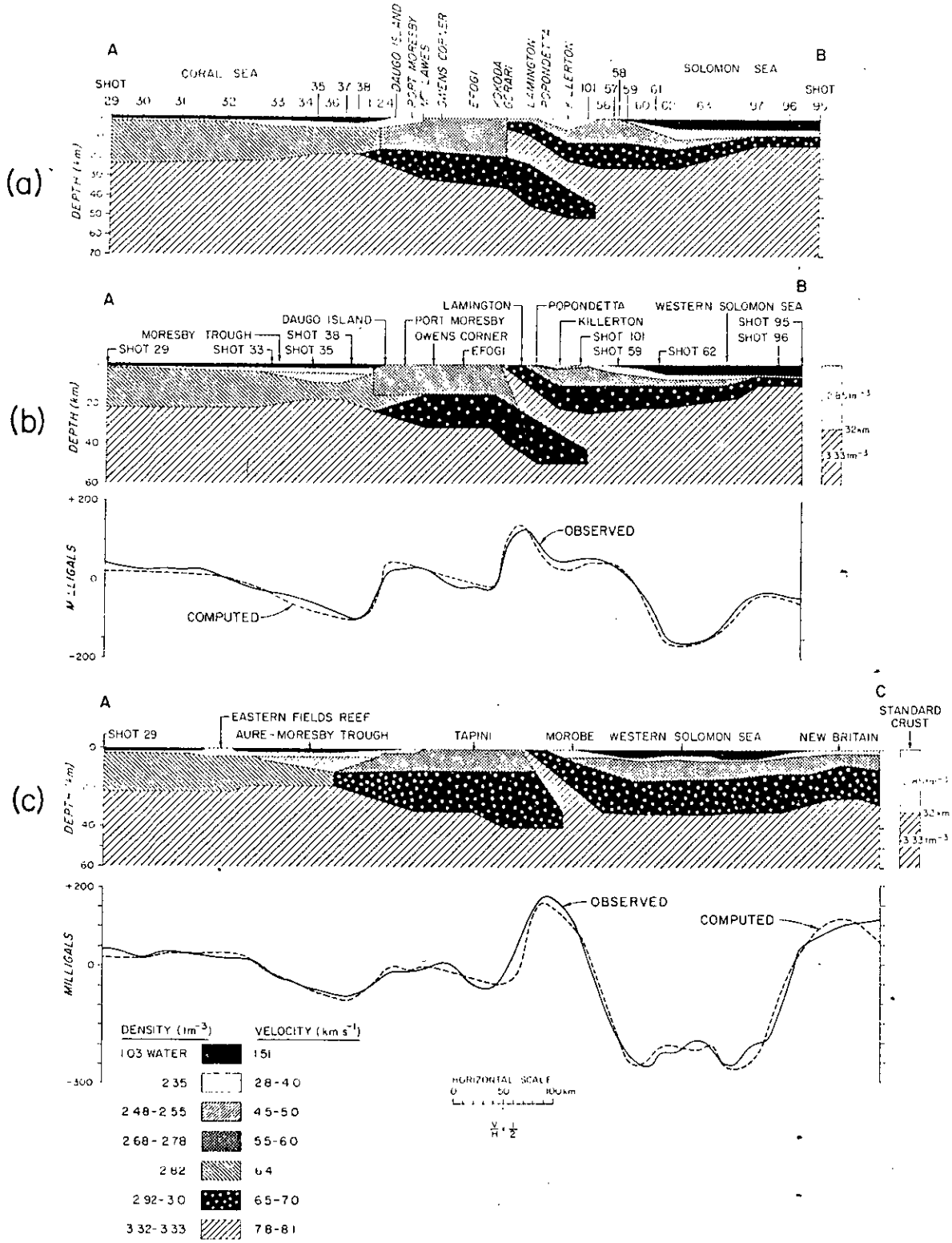

Fig. 9. a. Seismic model along the profile $A-B$ shown in Fig. 2.
b. Gravity model along the profile $A-B$, together with observed simple Bouguer values and computed gravity values.
c. Gravity model along the profile $A-C$, together with observed simple Bouguer values and computed gravity values.

The first arrivals from the model shown in Fig. 9a are indicated in Figs. 7 and 8.

Features of the model which deserve special mention are as follows. On the Solomon Sea side of the peninsula a series of high-velocity layers with dips up to 20° is necessary to account for the observed travel times. Apparent velocities between stations can be very high. The continuity of the dipping layers is evident in the observed results from the array of stations between the northeast coast and Gorari (*GO*). The possibility of the high-velocity material having intruded sialic host rocks was considered but is not consistent with the data: a low velocity in the host rock would reduce the average velocity in the crust, but the data indicate that high-velocity material predominates in the crustal rocks of the northeast side of the Papuan peninsula.

Near the Solomon Sea coast along profile *A–B*, the upper crustal layers consist of Miocene to Holocene sediments of what is variously called the Cape Vogel Basin (Bickel, 1974) or the Trobriand Basin (Tjhin 1976). The crustal thickness along the coast near Killerton (*KL*) according to the seismic data is approximately 23 km. Farther offshore, the crustal thickness increases to a maximum of 27 km beneath shot *62*, which is above the bottom of the slope from the Trobriand Platform into the Solomon Sea basin about 110 km from the shoreline. Beyond this distance the crust thins to about 13 km under shots *95–97*. The seismic travel times to Esa Ala (*ESA*) and Lindenhafen (*LF*) support this thinning. The crust is of similar thickness to that measured by Furumoto et al. (1970) approximately 200 km east of shot *96* in the central Solomon Sea. The Moho dips at approximately 10° between shots *97* and *63*, consistent with the 9.05-km s^{-1} apparent velocity clearly measured between these two shots at six stations across the Papuan peninsula.

As described earlier, the PUB-1, -2 and -3 models include a low-velocity zone under the uppermost mantle refractor; this is difficult to recognise in the interpretation of record sections across the geological strike. The shape of the deep crustal 6.5–7.0 km s^{-1} zone under the Papuan peninsula shown in Fig. 9a is largely a result of the requirements of the gravity interpretation discussed later in this paper.

The structure along the *A–B* profile from shots in the Coral Sea is difficult to determine uniquely in the absence of reversed shooting. Thus only apparent refractor velocities are available. However, the interpreted profile along the southwest Papuan coast constrains the possible structures. The sediments of the Aure and Moresby troughs have been described by Tailis (1975) and Brown et al. (1975). Basement depth has not yet been determined by seismic exploration methods along the profile *A–B* (Fig. 2), but it is estimated that the maximum sediment depth must be over 10 km.

Values for the depths and velocities of the crustal layers beneath the Eastern Fields basement high near point *A* in Fig. 2 can be estimated only from subsequent arrivals in the record sections because first arrivals are predominantly refracted waves travelling through the upper mantle. An average crustal velocity of 6.4 km

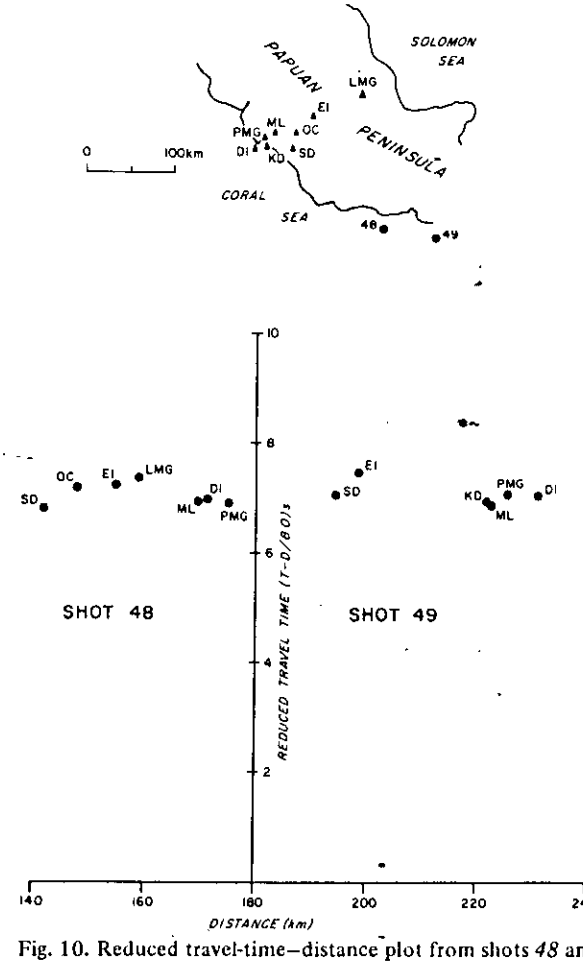

Fig. 10. Reduced travel-time–distance plot from shots *48* and *49* on the SW Papuan peninsula coast to stations between Daugo Island (*DI*) and Efogi (*EI*).

s^{-1} has been adopted largely on the basis of crustal investigations across the central Coral Sea by Ewing et al. (1970) and in the northwest Coral Sea by Finlayson (1968). Also Denham (1968) proposed a crust 30–32 km thick with an average velocity of 6.4 km s^{-1} under Port Moresby, from interpretation of the spectral characteristics of teleseismic wave trains. The resulting depths to the Moho using the 6.4 km s^{-1} crustal velocity, decreases from approximately 30 km beneath the Papuan coast to 18 km under the deepest sediments, and increases to approximately 22 km under the Eastern Fields basement high.

The travel times from shots *48* and *49* (Fig. 2) to stations along profile *A–B* between Daugo Island (*DI*) and Efogi (*EI*) do not increase greatly (Fig. 10). This is interpreted as an indication that the Moho depth along that part of the profile does not increase greatly.

3. Gravity modelling

The gravity field in the Papuan peninsula region is dominated by: (a) the gravity high in the area of the Papuan Ultramafic Belt (simple Bouguer anomaly values of over +200 mGal); (b) a similar high over the northern margin of the Trobriand Platform; and (c) the extremely low-free-air gravity anomaly of −250 mGal in the western Solomon Sea.

On the Coral Sea side of the Papuan peninsula the gravity variations are comparatively mild and controlled largely by the bathymetry of the Coral Sea, the topography of the Owen Stanley Ranges, and the depth of sediment in the Aure and Moresby Troughs, which exceeds 10 km in places (Tallis, 1975; Brown et al., 1975).

The seismic interpretation has been used to construct gravity models along two profiles *A–B* and *A–C* indicated in Fig. 3. As mentioned earlier, simple Bouguer anomalies have been contoured on land (Bouguer density 2.67 t m^{-3}) and free-air anomalies at sea. Milsom (1973a, b) has produced terrain-corrected Bouguer anomalies in the region of the Papuan Ultramafic Belt using different Bouguer densities for the various rock units; this increased the simple Bouguer maxima by about 10 mGal. Most areas of high topographic relief lie in the region southwest of the Ultramafic Belt. In the land areas as a whole, 74% of stations had terrain corrections less than 5 mGal, 20% had corrections between 5 and 20 mGal and the remaining 6% had corrections greater than 20 mGal. These figures give some idea of the allowances to be made when fitting model structures to the simple Bouguer data used in this paper. Since only the broader features of the structure are being modelled here, care must be taken not to attach too much significance to fine detail which can be used to achieve a better fit than the interpretation method warrants. Milsom (1973a) has already pointed out some finely detailed models that fit the data but are unrealistic structurally.

Fig. 9b and c contains the observed and modelled gravity data along profiles *A–B* and *A–C* together with the details of the models used. Constraints have been placed on the models where seismic interpretations are available along the northeast and southwest Papuan peninsula coasts and along profile *A–B*. Densities were obtained from the seismic velocities using the data compiled by Nafe and Drake (after Talwani et al., 1959). A 32 km thick standard crust was used with a crustal density 2.85 t m^{-3} and an upper-mantle density 3.33 t m^{-3}. This is the same as that used by Finlayson and Cull (1973) for the New Britain–New Ireland region and virtually the same as that used by Rose et al. (1968) for the crust under the Solomon Sea (crustal density 2.87 t m^{-3}, upper-mantle density 3.33 t m^{-3}). The modelling procedure assumes that structures are approximately two dimensional across the geological strike. In areas of high relief near Efogi in Fig. 9b, the gravity values calculated from the model should be reduced by about 15 mGal to correct for average crustal geology above sea level.

Fig. 9b indicates that all essential features of the structure interpreted from seismic data can be accommodated in a gravity model which fits the observed gravity along the profile *A–B*. This therefore generates further confidence in the gravity model along profile *A–C* where seismic control is less rigorous.

The principal difference of profile *A–C* from profile *A–B* is the substantial deepening of the gravity low in the western Solomon Sea to about −260 mGal (Huon Gravity Low) in a depth of water less than that along profile *A–B*. The region of the gravity low is traversed by the Markham Canyon (Von der Borch, 1972), the channel through which large quantities of sediment are transported to the western extremity of the New Britain Trench. However, the canyon itself has a rugged topography and a significant minimum slope of 1–2°

and is not an area of sediment accumulation. It is therefore unlikely that the low gravity values are due to a large thickness of recent low-density sediment.

There are few indications from other sources of the origins and structure of the crust under the western Solomon Sea. The crustal material may be associated with the Palaeogene volcanic arcs formed in the New Britain and Finisterre areas and the subsequent attachment of the Finisterre area to mainland New Guinea in the Neogene (Bain, 1973). Various unpublished Bureau of Mineral Resources marine profiling records in the Huon Gulf area show a rugged sea bottom. The bathymetric ridge which extends eastwards from the Huon peninsula to about 149°30'E (Finlayson et al., 1976a, fig. 2) at the western end of the New Britain Trench is not prominent on magnetic profiles; it may be structurally similar to Karig's (1973) "mid-slope basement high" on the volcanic arc side of the trench. However, as discussed later in this paper, Johnson (1976) interprets the feature as the surface expression of a dipping slice of crust (Vitiaz Slice).

The crust under the Huon Gravity Low is interpreted here as having a thickness of about 33 km. This is consistent with the significantly longer seismic travel times measured from the shots in the area of the deep gravity low. The Solomon Sea crustal structure west of 150°E must be significantly different from the oceanic crust found by Furumoto et al. (1970) in the central Solomon Sea, where there are regional free-air gravity values of about +100 mGal in similar water depths.

The profile $A-C$ model on the Coral Sea side of the Papuan peninsula does not differ greatly from that along profile $A-B$. In the region of the Aure and Moresby troughs the depth of sediment largely determines the gravity model. Inland from Yule Island (*YE*) to Tapini (*TI*) the seismic delay times from upper mantle arrivals do not differ greatly, indicating no great increase in the crustal thickness.

4. Discussion

4.1. Papuan Ultramafic Belt

The Papuan Ultramafic Belt is classified, in composition and mode of emplacement, as an Alpine ophiolite complex (Moores, 1973). Milsom (1973a) has compared some of the gravity features of the Papuan peninsula with those of the Troodos complex on Cyprus and the Ivrea complex in the European Alps (Gass and Masson-Smith, 1963; Berckhemer, 1968; Giese, 1968; Kaminski and Menzel, 1968). In these three cases the interpretations of the gravity highs are compatible with dipping slabs of high-density material of the order of 9–15 km thick dipping at angles of 15–25°. The complexes are regarded as being overthrust slices of oceanic crust and mantle (Moores and Vine, 1971), although Miyashiro (1975) regards the Troodos complex as being of island-arc origin, a conclusion that is strongly contested by Gass et al. (1975).

In east Papua, the seismic data substantiate the continuity of layering in the ophiolite suite and also require the thickness of crust above the high-density mantle material to be considerably greater than that found in oceanic crust. Thus there must still exist some doubts, as Milsom (1973a) points out, regarding the origin of the overthrust material. In the region of the Troodos and Ivrea complexes, the crustal-material downdip of the high-velocity slabs is similarly much thicker than normal oceanic crust. Estimates of crustal thickness in the eastern Mediterranean in the Cyprus region vary from 25 km (Rabinowitz and Ryan, 1970) to 32 km (Gass and Masson-Smith, 1963; Woodside and Bowin, 1970), and in the Ivrea-area crustal thickness is estimated at 49–51 km (Kaminski and Menzel, 1968). Lort et al. (1974) have suggested that the eastern Mediterranean is more likely to be continental than oceanic in structure.

4.2. Western Solomon Sea

In the Solomon Sea west of 150°E there are anomalous geophysical features in addition to the −250-mGal gravity low. Denham (1969) and Johnson and Molnar (1972) have mapped the distribution of earthquakes in the Papua New Guinea region and shown that the western Solomon Sea is the location of a triple plate junction. Johnson and Molnar (1972) discussed the possibility of there being nearly vertical and overturned lithospheric material under the region. Denham (1975) has pointed out a major discontinuity at depth which occurs just west of the 150° meridian under New Britain, there being no deep earthquakes west of there. Johnson (1976) has presented geochemi-

cal data to show that Late Cainozoic volcanoes of the South Bismarck Sea can be separated into western and eastern arcs with a boundary on New Britain near 150°E (Fig. 11). Johnson (1976) has also drawn attention to the termination of the New Britain Trench in a divided structure west of 150°E. He invokes the concept of a slice of overriding crust and upper mantle (Vitiaz Slice) dipping under western New Britain, to explain the bathymetric high where the trench splits and also the change in tectonic environment required to account for the volcanic geochemistry.

The post-Miocene crustal shortening and uplift, which produced the coastal ranges of the Huon peninsula and north coast New Guinea ranges, probably resulted in crustal thickening under the western Solomon Sea after the emplacement of the Papuan Ultramafic Belt in the Early Eocene. Rabinowitz and Ryan (1970) invoke an imbricated crustal structure in the eastern Mediterranean to account for crustal shortening, and it is possible that some similar type of structure accounts for the crustal features of the western Solomon Sea. The possibility that the crustal material originated in a marginal basin must also be considered likely since a three- to four-fold increase in thickness of normal oceanic crust by imbrication seems unlikely.

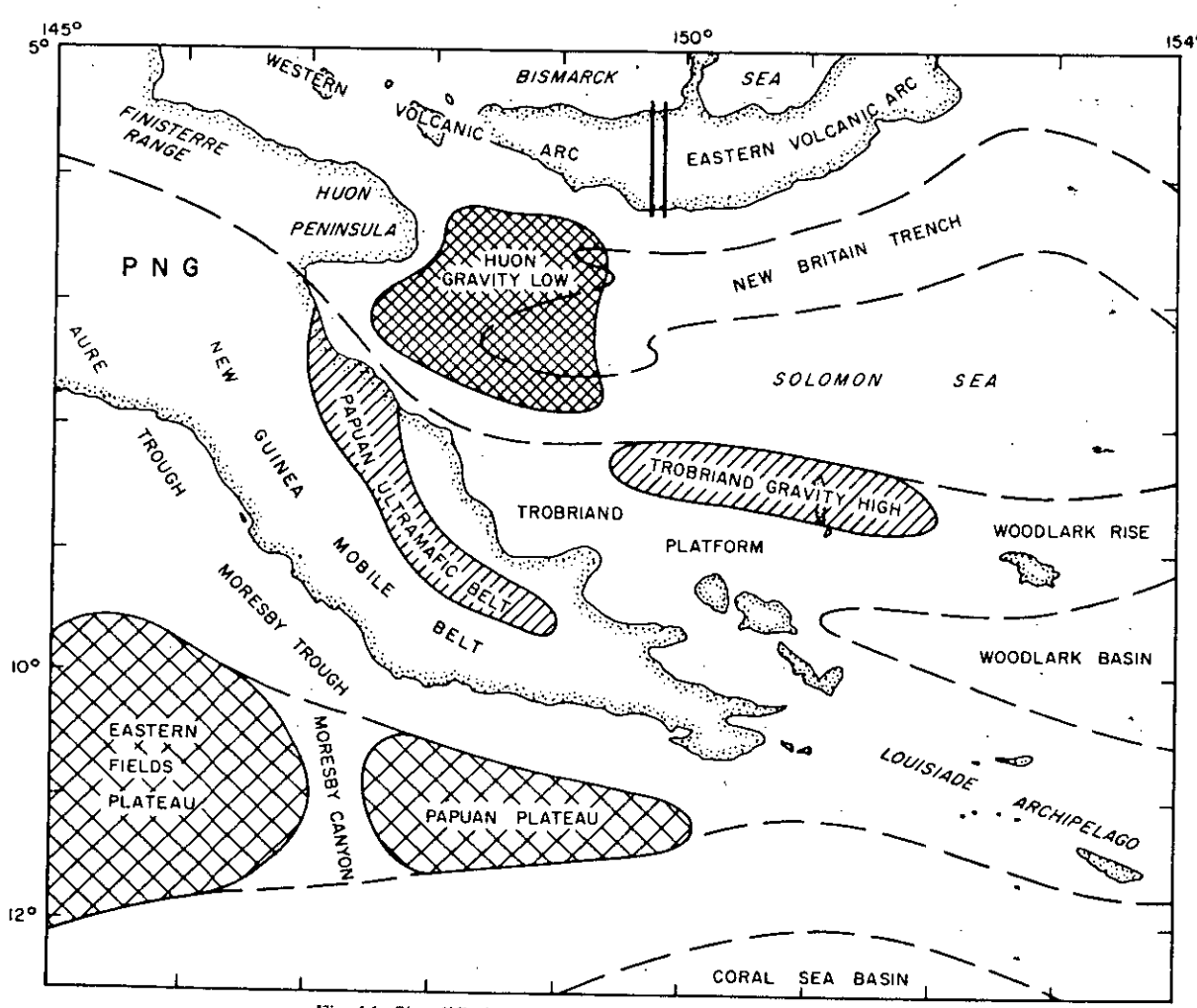

Fig. 11. Simplified tectonic features in the east Papuan region.

4.3. Trobriand Platform

The Trobriand Platform is a shallow-water area of thick crust extending north and east from mainland Papua. At its eastern extremity, it adjoins the Woodlark Basin which is recognised as an area of crustal extension and rifting (Milsom, 1970; Luyendyk et al., 1973). Tjhin (1976) indicates that the Trobriand Basin in the centre of the Platform, with up to 5 km of sediments, is probably the result of an E–W-trending graben structure. Smith (1975) has drawn attention to the nature of the volcanism at the eastern margin of Papua and indicated that several episodes of both compression and extension must have occurred during the Cainozoic. Calc-alkaline volcanism appears to have migrated westward from the Louisade Archipelago (in the Late Miocene) to the active volcanoes on mainland Papua in recent times, possibly indicating an episode of limited subduction which is no longer active. Milsom and Smith (1975) indicate that the Papuan peninsula east of 149°E consists predominantly of Upper Cretaceous and Middle Eocene tholeiitic basalt, but that the mechanism for the formation of the thick crust in the area is not clear. Their favoured mechanism is that it was formed at least in part by mantle differentiation and diapirism in a Middle Miocene tensional environment.

The major gravity high (Trobriand Gravity High) on the northern edge of the Trobriand Platform (Figs. 3 and 11), as mentioned earlier, is another of the striking features of the region. Observations were made near sea level on the islands in the shallow-water area of the Platform and were supplemented offshore with marine gravity data in the deeper waters to the north and east. Smith (1973) has shown that there are Pliocene–Pleistocene volcanics on the islands at the northern edge of the Trobriand Platform, but the mass excess required to produce the gravity values indicates some additional tectonic features. Connelly (in Finlayson et al., 1976b) has drawn attention to the magnetic lows associated with the gabbroic and peridotitic components of the Papuan Ultramafic Belt, and similar lows are found on the outer margin of the Trobriand Platform (CGG, 1971), where they are not associated with the Trobriand Basin sediments. Unfortunately the seismic refraction data do not extend along the gravity feature. However, we speculate that the feature is caused by an ophiolite complex similar in age and extent to the Papuan Ultramafic Belt and separated from it by those tectonic episodes which formed the extensional features of eastern Papua and the Woodlark Basin.

4.4. Northwest Coral Sea

In the northwest Coral Sea crustal thinning is demonstrated between the New Guinea Mobile Belt (Bain, 1973, fig. 1) and the Eastern Fields marginal plateau, although the precise extent of thinning is masked partly by the sediments of the Aure and Moresby troughs. The lithification of the deep sediments, however, will result in physical properties not greatly different from those of basement rocks, and thus the interpreted crustal thickness under the Moresby Trough and Eastern Fields Plateau of 18 and 22 km, respectively, cannot be varied greatly. This interpretation agrees with that of Mutter (1975a, b) who classifies the plateaux marginal to the Coral Sea as being sub-continental in character. Taylor (1975) envisages the Aure and Moresby troughs as being the result of crustal rifting or extension during the Early Eocene antedating the emplacement of the Papuan Ultramafic Belt and coinciding with the formation of sea-floor basalts in southeast Papua. He regards the Papuan and Eastern Fields plateaux as being one tectonic unit, and Mutter (1975a) interprets the Moresby Canyon between these two plateaux as an erosional feature. However, there is evidence in the seismic travel times to suggest a basement feature on the northward extension of the Canyon near the Papuan coast.

Acknowledgements

The authors wish to acknowledge the major contributions to the 1973 investigations of crustal structure in the east Papuan region by the Australian National University, the Universities of Queensland and Hawaii, the Geological Survey of Papua New Guinea, the Preston Institute of Technology, and the Warrnambool Institute of Advanced Education. We also wish to thank Western Australia Petroleum Pty. Ltd. for donating explosives to the survey. This paper is published with the permission of the Director of the Bureau of Mineral Resources, Geology and Geophysics.

References

Bain, J.H.C., 1973. A summary of the main structural elements of Papua New Guinea. In: P.J. Coleman (Editor), The Western Pacific, Island Arcs, Marginal Seas, Geochemistry, University of Western Australia Press, Perth, W.A., pp. 147–161.

Berckhemer, H., 1968. Topographie des "Ivrea-Korpers" abgeleitet aus seismischen und gravimetrischen Daten. Schweiz. Mineral. Petrogr. Mitt., 48: 235–246.

Bickel, R.S., 1974. Reconnaissance geology of Cape Vogel Basin, Papua New Guinea. Bull. Am. Assoc. Pet. Geol., 58: 2477–2489.

Brown, C.M., Pieters, P.E. and Robinson, G.P., 1975. Stratigraphic and structural development of the Aure Trough and adjacent shelf and slope areas. Aust. Petrol. Explor. Assoc., J., pp. 61–71.

CGG (Compagnie Générale de Géophysique), 1971. Eastern Papua aeromagnetic survey, Part 1: Northeastern portion (mainly offshore) flown in 1969. Aust., Bur. Miner. Resour., Rec., 1971/67 (unpublished).

Connelly, J.B., 1976. Preliminary gravity map of Melanesia. Aust., Bur. Miner. Resour., Map PNG/B2-58.

Davies, H.L., 1971. Periodotite–gabbro–basalt complex in eastern Papua: an overthrust plate of oceanic mantle and crust. Aust., Bur. Miner. Resour., Bull., 128.

Davies, H.L. and Smith, I.E., 1971. Geology of Eastern Papua. Bull. Geol. Soc. Am., 82: 3299–3312.

Denham, D., 1968. Thickness of the earth's crust in Papua New Guinea and the British Solomon Islands. Aust. J. Sci., 30 (7): 277.

Denham, D., 1969. Distribution of earthquakes in the New Guinea–Solomon Islands region, J. Geophys. Res., 74: 4290–4299.

Denham, D., 1975. Distribution of underthrust lithospheric slabs and focal mechanisms – Papua New Guinea and Solomon Islands region. Aust. Soc. Explor. Geophys., Bull., 6(2/3): 78–79.

Ewing, M., Hawkins, L.V. and Ludwig, W.J., 1970. Crustal structure of the Coral Sea. J. Geophys. Res., 75: 1953–1962.

Finlayson, D.M., 1968. First arrival data from the Carpentaria Region Upper Mantle Project (CRUMP). J. Geol. Soc. Aust., 15: 33–50.

Finlayson, D.M. (Editor), 1976. East Papua Crustal Survey, October–December 1973; Operational Report. Aust., Bur. Miner. Resour., Rec., 1975/177.

Finlayson, D.M. and Cull, J.P., 1973. Structural profiles in the New Britain/New Ireland region. J. Geol. Soc. Aust., 20(1): 37–48.

Finlayson, D.M., Muirhead, K.J., Webb, J.P., Gibson, G., Furumoto, A.S., Cooke, R.J.S. and Russell, A.J., 1976a. Seismic investigation of the Papuan Ultramafic Belt. Geophys. J.R. Astron. Soc., 44: 45–60.

Finlayson, D.M., Drummond, B.J., Collins, C.D.N. and Connelly, J.B., 1976b. Crustal structure under the Mount Lamington region of Papua New Guinea. In: R.W. Johnson (Editor), Volcanism in Australasia, Elsevier, Amsterdam, pp. 259–274.

Furumoto, A.S., Hussong, D.M., Campbell, J.F., Sutton, G.H., Malahoff, A., Rose, J.C. and Woollard, G.P., 1970. Crustal and upper mantle structure of the Solomon Islands as revealed by seismic refraction survey of Nov.–Dec. 1966. Pac. Sci., 24: 315–332.

Gass, I.G. and Masson-Smith, D., 1963. Geology and gravity anomalies of the Troodos Massif, Cyprus. R. Soc. London Philos. Trans., Ser. A, 255: 417–467.

Gass, I.G., Neary, C.R., Plant, J., Robertson, A.H.F., Simonian, K.O., Smewing, J.D., Spooner, E.T.C. and Wilson, R.A.M., 1975. Comments on *The Troodos ophiolite complex was probably formed in an island arc* by A. Miyashiro, and subsequent correspondence by A. Hynes and A. Miyashiro. Earth Planet. Sci. Lett., 25(2): 236–238.

Giese, P., 1968. Die Struktur der Erdkruste im Bereich der Ivrea-Zone. Schweiz. Mineral. Petrogr. Mitt., 48: 261–284.

Giese, P., Prodehl, C. and Behnke, C., 1967. Ergebnisse refraktionsseismischer Messungen 1965 zwischen dem französischen Zentralmassiv und den Westalpen. Geophys., 33(4): 215–261.

Johnson, R.W., 1976. Late Cainozoic volcanism and plate tectonics at the southern margin of the Bismarck Sea, Papua New Guinea. In: R.W. Johnson (Editor), Volcanism in Australasia. Elsevier, Amsterdam, pp. 101–116.

Johnson, T. and Molnar, P. 1972. Focal mechanisms and plate tectonics of the south-west Pacific. J. Geophys. Res., 77: 5000–5032.

Kaminski, W. and Menzel, H., 1968. Zur Deutung der Schwereanomalie des Ivrea-Korpers. Schweiz. Mineral. Petrogr. Mitt., 48(1): 255–260.

Karig, D.E., 1973. Comparison of island arc–marginal basin complexes in the northwest and southwest Pacific. In: P.J. Coleman (Editor), The Western Pacific, Island Arcs, Marginal Seas, Geochemistry, University of Western Australia Press, Perth, W.A., 355–364.

Lort, J.M., Limond, W.Q. and Gray, F., 1974. Preliminary seismic studies in the eastern Mediterranean. Earth Planet. Sci. Lett., 21: 355–366.

Luyendyk, B.P., Macdonald, K.C. and Bryan, W.B., 1973. Rifting history of the Woodlark Basin in the south-west Pacific. Bull. Geol. Soc. Am., 84: 1125–1134.

Milsom, J.S., 1970. Woodlark Basin, a minor center of sea-floor spreading in Melanesia. J. Geophys. Res., 75: 7335–7339.

Milsom, J.S., 1973a. Papuan Ultramafic Belt: gravity anomalies and the emplacement of ophiolites. Bull. Geol. Soc. Am., 84: 2243–2258.

Milsom, J.S., 1973b. Gravity field of the Papuan peninsula. Geol. Mijnbouw, 52: 13–20.

Milsom, J.S. and Smith, I.E., 1975. Southeastern Papua: generation of thick crust in a tensional environment? Geology, 3(3): 117–120.

Miyashiro, A., 1975. Classification, characteristics and origin of ophiolites. J. Geol., 83(2): 249–282.

Moores, E.M., 1973. Geotectonic significance of ultramafic rocks. Earth-Sci. Rev., 9: 241–258.

Moores, E.M. and Vine, F.J., 1971. The Troodos Massif, Cyprus and other ophiolites as oceanic crust: evaluation and implications. Philos. Trans. R. Soc. London, Ser. A, 268: 443–466.

Mutter, J.C., 1975a. A structural analysis of the Gulf of Papua and northwest Coral Sea region. Aust., Bur. Miner. Resour., Rep., 179.

Mutter, J.C., 1975b. Basin evolution and marginal plateau subsidence in the Coral Sea. Aust. Soc. Explor. Geophys., Bull., 6(2/3): 35–37.

Rabinowitz, P.D. and Ryan, W.B.F., 1970. Gravity anomalies and crustal shortening in the eastern Mediterranean. Tectonophysics, 10: 585–608.

Rose, J.C., Woollard, G.P. and Malahoff, A., 1968. Marine gravity and magnetic studies of the Solomon Islands. In: L. Knopoff, C.L. Drake and P.J. Hart (Editors), Am. Geophys. Union, Monogr. 12: 379–410.

Smith, I.E., 1973. Late Cainozoic volcanism in the south-east Papuan islands. Aust., Bur. Miner. Resour., Rec., 1973/67 (unpublished).

Smith, I.E., 1975. Southeastern Papua – evolution of volcanism on a plate boundary. Aust. Soc. Explor. Geophys., Bull., 6(2/3): 68–69.

Tallis, N.C., 1975. Development of the offshore Papuan Basin. Aust. Petrol. Explor. Assoc., J., pp. 55–60.

Talwani, M., Sutton, G.H., and Worzel, J.L., 1959. A crustal section across the Puerto Rico Trench, J. Geophys. Res., 64: 1545.

Taylor, L.W.H., 1975. Depositional and tectonic patterns in the western Coral Sea. Aust. Soc. Explor. Geophys., Bull., 6(2/3): 33–35.

Tjhin, K.T., 1976. Trobriand Basin exploration, Papua New Guinea. Aust. Petrol. Explor. Assoc., J., pp. 81–90.

Von der Borch, C.C., 1972. Marine geology of the Huon Gulf region of New Guinea. Aust., Bur. Miner. Resour., Bull., 127.

Woodside, J. and Bowin, C., 1970. Gravity anomalies and inferred crustal structure in the eastern Mediterranean Sea. Geol. Soc. Am. Bull., 81: 1107–1122.

BMR Journal of Australian Geology & Geophysics, 2 (1977) 209-216

Seismic travel-times to east Papua from USSR nuclear explosions

D. M. Finlayson

Recordings of P seismic waves from a Novaya Zemlya nuclear explosion at 26 sites on the east Papuan peninsula show that there are significant apparent departures (residuals) from travel-times calculated using average earth models. The residual at Port Moresby (PMG) differs by between +0.3 and +0.5 seconds from previous attempts to assign a station effect there. Without precise times and locations of the Novaya Zemlya events it is not possible to determine the proportions of the residual due to source effects and velocity anomalies in the mantle. It is shown that complex crustal structure in the east Papuan region accounts for a significant proportion of the station residuals, which differ from the PMG residual by between −0.72 seconds and +1.41 seconds. There is a tendency towards more negative residuals on the northeast side of the Papuan peninsula.

Introduction

During the 1973 investigation of crustal structure in the east Papuan region (Finlayson and others, 1976) some 42 seismic stations were deployed to record 111 shots fired in the Solomon and Coral Seas from the L/V "Sir Allan". At 06h 59 min 57.37 ± 1.00s U.T. on 27 October 1973 (USGS, 1973), during that survey, the USSR detonated a nuclear device on Novaya Zemlya, and it was successfully recorded at 26 stations in east Papua (Fig. 1). These recordings have been used to determine seismic travel-time residuals, i.e. departures from the Herrin (1968) seismological travel-time tables, for P phases. The residuals were then analysed with respect to interpreted crustal models derived from the local explosion seismic and gravity observations (Finlayson and others, 1976, 1977).

Freedman (1967) has discussed the problems associated with trying to determine station residuals which apply to all azimuths and sources . She points out that small location errors and azimuth varying source residuals make the use of a world-wide distribution of sources essential for the determination of an average station residual. This was not possible with most of the east Papua stations because recording times were usually limited to those required for the local explosion seismic work, thus severely limiting the usable sources. Only at the permanent Papua New Guinea seismic stations are other source data available. The detonation of the 27 October 1973 USSR nuclear device

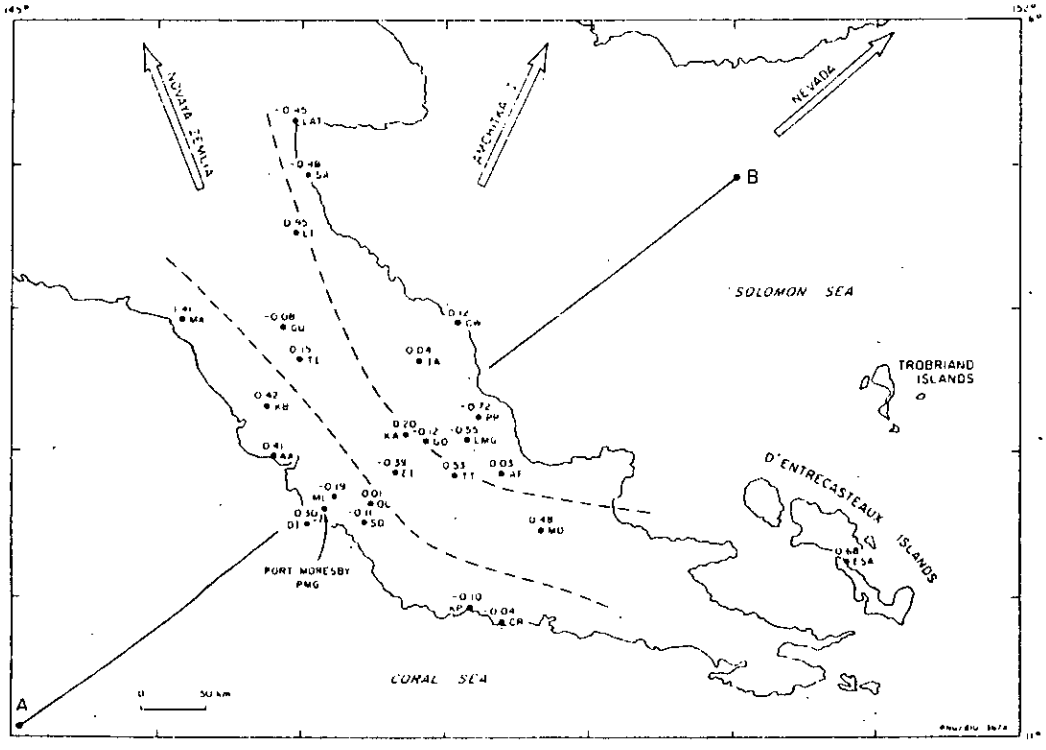

Figure 1. Location of seismic stations on the east Papuan peninsula and residual differences (in seconds) from Port Moresby. Three letter mnemonics indicate permanent stations; dashed lines indicate station groupings discussed in text; A-B indicates location of crustal profile shown in Figure 4; arrows indicate the azimuths of various nuclear explosion sites from Port Moresby.

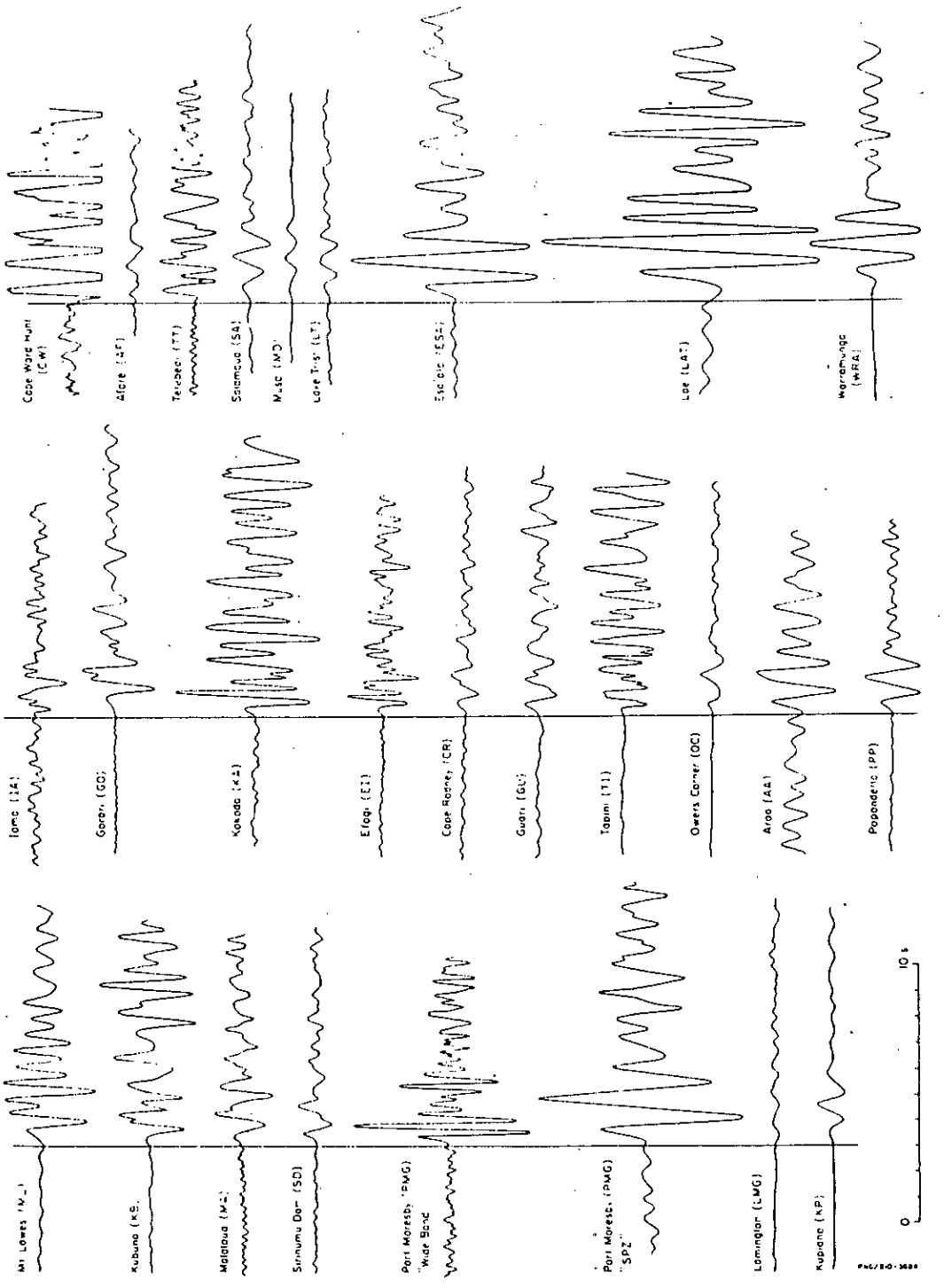

Figure 2. Recordings of the Novaya Zemlya nuclear explosion of 27 October 1973 at seismic stations on the east Papuan peninsula, and a processed record from the Novaya Zemlya nuclear explosion of 27 October 1966 recorded at Warramunga seismic array (Weight & Mulrhead, 1969, fig. 2). The onset used to compute residuals is indicated on each record.

while many instruments were recording was purely fortuitous. Even with a single event, however, some comments can be made on the residuals within the survey area relative to a standard station, which, in this case, was taken as the World-Wide Standard Seismograph Network (WWSSN) station at Port Moresby (PMG).

Seismic recordings

Four of the stations (PMG, LAT, LMG and ESA) in Figure 1 that recorded the USSR explosion, were part of the Papua New Guinea permanent seismic observatory network, and the remaining sites were occupied temporarily by field recording equipment. A typical set of field equipment consisted of a Willmore Mk. 2 vertical seismometer, amplifier, long-endurance tape recorder, internal crystal clock, and radio time-signal receiver locked to the Australian standard frequency and time-signal tranmission VNG.

Reproductions of the recordings for the stations are contained in Figure 2. The replayed records have not been filtered and the reproductions of observatory records were made from photographic enlargements. Despite some differences in the recording characteristics of the equipment, the character of the first three seconds of the wave train could generally be recognised in most records. On some reproductions from tape recording systems, signal saturation is evident by folding of the high amplitude peaks. However, the basic form of the initial wave train is seen plainly in the reproductions from Port Morseby, Esa-ala, Kupiano, Popondetta and Salamaua.

Much has been written on the waveforms to be expected from underground nuclear explosions. Thirlaway (1966) has indicated that in general the first few seconds of wave forms from the same site are similar with minor variations resulting from variations in depth of burial. Carpenter and others (1967) have determined amplitude-distance curves from various nuclear explosions, and the initial wave forms of their examples of records from French and Russian explosions are strikingly similar to the 1973 recordings made in east Papua. For comparison purposes, Figure 2e also shows the initial wave form of a Novaya Zemlya nuclear explosion on 27 October 1966 as recorded at the Warramunga seismic array in northern Australia (Wright & Muirhead, 1969). This basic wave-form has been used to ensure that the onsent time is identified correctly on all east Papuan records.

The observed travel-times are listed in Table 1 together with other data, and an estimate has also been made of the observational uncertainty in the onset times which takes into account the instrumental factors connected with clock errors, parallax errors, etc. The components of possible error classified by Freedman (1966) as miscounts, misidentifications and instrumental errors are deemed to have been eliminated by independent examination of records by at least two geophysicists.

The positions of the seismic stations were determined, using a Decca trisponder system, to within the 0.1 minute of arc in latitude and longitude required for the local seismic survey. The location and time of the USSR explosion are taken from the US Geological Survey Earthquake Data Report 65-73 (USGS, 1973). The angular distances of the stations from the shot point, with ellipticity corrections, were in the range 97.17° to 101.32°. Using the Herrin (1968) model of the earth, the angle of emergence (angle from the vertical) of P waves at these distances is 14.5 ± 0.1° (Pho & Behe, 1972). The seismic rays can therefore be considered as emerging almost vertically through the upper mantle and crustal structure of east Papua.

The angular distances at which the east Papua records were made puts them at the outer limit of direct P wave observation. Figure 3 shows the Herrin (1968) P and PcP phases converging beyond 80°. Beyond 97.5° the travel-time curve is substantially straight with a gradient of 4.56 seconds per degree. Jeffreys & Bullen (1948) travel-times are between 1.7s and 1.8s greater than those of Herrin (1968) in the range between 95° and 100°. There are three Papuan stations that are between 100° and 101° and one station at 101.32° and it is possible that some diffraction at the core-mantle boundary may have occurred. However Wright & Muirhead (1969) consider the differences from the linear

1 *Station*	2 *Mnemonic*	3 *Angular distance degrees*	4 *Observed travel-time* min. s.	5 *Elevation correction* s.	6 *Corrected travel-time* min. s.	7 *Herrin (1968) travel-time* min. s.	8 *Residual (R)* s.	9 *R-R* (PMG)* s.
Port Moresby	PMG	99.80	13 45.97 ± .10	−.01	13 45.96	13 45.64	0.32	—
Daugo Island	DI	99.86	13 46.63 ± .05	0	13 46.63	13 45.94	0.69	0.30
Arua	AA	99.33	13 44.34 ± .03	0	13 44.34	13 43.54	0.80	0.41
Kubuna	KB	99.00	13 42.76 ± .01	−.01	13 42.75	13 41.94	0.81	0.42
Malalaua	MA	98.22	13 40.24 ± .02	0	13 40.24	13 38.44	1.80	1.41
Guari	GU	98.51	13 40.33 ± .03	−.38	13 39.95	13 39.64	0.31	−0.08
Efogi	EI	99.73	13 45.53 ± .05	−.19	13 45.34	13 45.34	0.0	−0.39
Tapini	TI	98.76	13 41.63 ± .01	−.15	13 41.48	13 40.94	0.54	0.15
Lumington	LMG	99.67	13 45.28 ± .10	−.20	13 45.08	13 45.04	0.04	−0.55*
Kupiano	KP	100.76	13 50.43 ± .05	0	13 50.43	13 50.14	0.29	−0.10
Cape Rodney	CR	100.93	13 51.29 ± .03	0	13 51.29	13 50.94	0.35	−0.04
Gurari	GO	99.58	13 44.99 ± .01	−.08	13 44.91	13 44.64	0.27	−0.12
Atore	AF	99.96	13 46.98 ± .10	−.12	13 46.86	13 46.44	0.42	0.03
Tetebedi	TT	99.87	13 47.13 ± .10	−.17	13 46.96	13 46.04	0.92	0.53
Kokoda	KA	99.50	13 44.90 ± .01	−.07	13 44.83	13 44.24	0.59	0.20
Popondetta	PP	99.56	13 44.23 ± .01	−.02	13 44.21	13 44.54	−0.33	−0.72
Owers Corner	OC	99.87	13 46.43 ± .01	−.09	13 46.34	13 45.94	0.40	0.01
Ioma	IA	99.04	13 42.48 ± .10	−.01	13 42.47	13 42.04	0.43	0.04
Mount Lawes	ML	98.76	13 45.80 ± .01	−.06	13 45.74	13 45.54	0.20	−0.19
Sirinumu Dam	SD	99.96	13 46.79 ± .01	−.07	13 46.72	13 46.44	0.28	−0.11
Salamaua	SL	97.56	13 35.43 ± .10	0	13 35.43	13 35.34	0.09	−0.48
Lae	LAT	97.17	13 34.03 ± .10	−.01	13 34.02	13 33.54	0.48	−0.45*
Esa'ala	ESA	101.32	13 53.73 ± .10	−.01	13 53.72	13 52.54	1.18	0.68*
Lake Trist	LT	97.93	13 38.73 ± .10	−.25	13 38.48	13 37.14	1.34	0.95
Musa	MD	100.43	13 49.48 ± .10	−.02	13 49.46	13 48.59	0.87	0.48
Cape Ward Hunt	CW	98.86	13 41.95 ± .10	0	13 41.95	13 41.44	0.51	0.12

*Data from Table 3, Residual A.

Table 1. Observed and calculated data from east Papuan seismic stations of the Novaya Zemlya nuclear explosion, 27 October 1973, 06h 59 min 57.37s U.T.

section of the travel-time curve to be negligible out as far as 106°, the distance at which they recorded the October 1966 Novaya Zemlya event at Warramunga. Herrin & Taggart (1968a) use data out to 105° in their investigations of regional variations in P travel-times.

Travel-time residuals

The travel-time residuals (observed travel-time minus travel-time derived from the Herrin (1968) tables for P phases) for the east Papuan stations are listed in Table 1, column 8. Station elevation corrections are applied according to the method of Engdahl & Gunst (1966), using a velocity of rock above sea level of 5.8 km/s. Although the explosion source is listed in the Earthquake Data Report 65-73 (USGS, 1973) as being at zero depth, this is unlikely. Robinson & Iyer (1976) used a source depth of 1 km for the same USSR event and this is the value used here. Herrin (1968) used an average crustal model consisting of 15 km with velocity 6.0 km/s, overlying 25 km with velocity 6.75 km/s, for correcting shallow focus travel-times. The correction to the Herrin travel-time for the depth of the shot is −0.16s, and has been applied to all data in Table 1 column 7. The validity of applying this correction to the data is discussed later in connection with the station residual for Port Moresby.

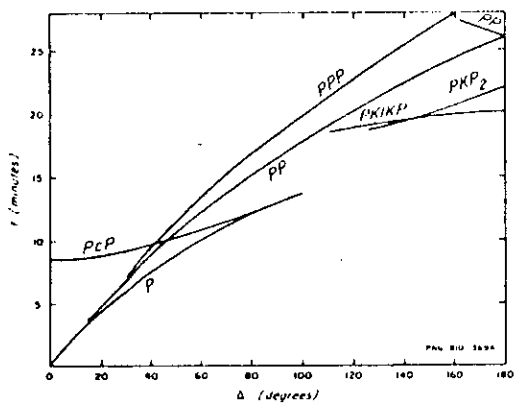

Figure 3. Travel-time curves (surface focus) from the 1968 Seismological Tables for P phases (Herrin 1968, fig. 1).

Permanent recording station residuals

Some comment can be made about the value of the travel-time residuals at the permanent seismic stations. As mentioned earlier, azimuth variations in the crust and upper mantle beneath the stations affect station residuals. Thus observations are required from many sources, in all azimuths, to determine a statistically significant value of the residual at any particular station.

The PMG station is the only one in east Papua for which such a study has been undertaken and has been included in a number of world-wide investigations of P wave travel-time analyses (Cleary & Hales, 1966; Cleary, 1967; Carder, Gordon & Jordon, 1966; Herrin & Taggart, 1968a; Lilwall & Douglas, 1970; Sengupta & Julian, 1976). Cleary (1967) derived a station residual of −0.84s for PMG based on 10 events relative to the Cleary & Hales (1966) revision of the Jeffreys & Bullen (1948) travel-time curve for P waves. This value was determined using data mostly from the azimuth of Japan and the Aleutian Islands, to the north and northeast of PMG.

Herrin & Taggart (1968a) determined azimuthally dependent station residuals relative to the Herrin (1968) travel-time curves for 321 world-wide seismic stations including PMG. Their data for PMG were determined using 122 arrivals and the residual (R) was given by the equation

$$R = -0.38 + 0.29 \sin(Z + 340) \text{ along azimuth } Z.$$

This gives PMG residual values of between approximately −0.2s and −0.5s for events to the north and northeast, and a value of −0.55s for events in the azimuth of the October 1973 Novaya Zemlya nuclear explosion (approx. 338°). A residual value for PMG of −0.28 ± 0.45s has been determined recently by Sengupta & Julian (1976). These authors have reduced the standard deviation of their value to about half that of previous authors by using deep-focus earthquakes, which eliminates source effects due to crustal and upper mantle structure, and by tight control of data quality. The value determined in this paper from the observation of the October 1973 USSR explosion (Table 1) is +0.32s; the difference between this and the Herrin & Taggart (1968a) or the Sengupta & Julian (1976) value is considerable, and, clearly, further comment is required on the possible sources of travel-time corrections.

The timing and positioning tolerance on the data from east Papua preclude any significant systematic error from instrumental sources at all 26 stations operating independently. Residual differences between PMG station and temporary stations in the vicinity, e.g. Mount Lawes (ML), Daugo Island (DI), Sirinumu Dam (SD), (Fig. 1), are consistent with the Port Moresby local geology, as will be shown later in this paper. Six other observations of Novaya Zemlya nuclear explosions on PMG records were also considered; the residuals for these are listed in Table 2. The average of these residuals is 0.43s, which substantially agrees with the value of 0.32s in Table 1, considering the reading error of the observatory WWSSN records of about ±0.1s. The difference between the Sengupta & Julian (1976) or the Herrin & Taggart (1968a) PMG residual value and the observed October 1973 value cannot therefore be explained in terms of observational inaccuracy.

Permanent recording station data consistency

The consistency of the PMG data with respect to other permanent stations in the region was also examined. The residuals at Lae (LAT), Lamington (LMG), Esa'ala (ESA), and Manton (MTN) near Darwin for a number of Novaya Zemlya events are listed in Table 2. These have been determined using the arrival times listed in U.S. Geological Survey Earthquake Data Reports, as were the PMG residuals listed in Table 2. The averages for LAT, LMG and ESA were +0.21s, −0.46s and +1.04s respectively, compared with the values in Table 1 of +0.48s, +0.04s and +1.18s respectively. The consistency of the LAT and LMG residuals can clearly be questioned.

The residual differences between MTN and the four Papua New Guinea stations were also determined. The MTN and PMG data were consistent within a standard deviation of ±0.10s. Those LAT and LMG residuals which were not consistent with either the MTN or PMG data within ±0.2s were rejected; these data are marked with an asterisk in Tables 1 and 2. Also, it was noted that those nuclear explosions with a magnitude (m_b) less than 6.5 were less reliably recorded, so the PMG residuals from three Novaya Zemlya explosions have been rejected (marked by asterisk in Table 2). The resultant mean residuals from

Station	Mnemonic	Event	Date	Origin Time U.T. h	min	s	Angular distance, degrees	Residual Observed—Herrin (1968) s	Magnitude m_b	Azimuth (approx)
Port Moresby	PMG	Novaya Zemlya	14 Oct '70	05	59	57.1	99.52	0.51	6.7	338°
Port Moresby	PMG	Novaya Zemlya	27 Sept '71	05	59	55.18	99.54	0.74*	6.4	338°
Port Moresby	PMG	Novaya Zemlya	28 Aug '72	05	59	56.51	99.54	0.59*	6.3	338°
Port Moresby	PMG	Novaya Zemlya	12 Sept '73	06	59	54.33	99.52	0.28	6.8	338°
Port Moresby	PMG	Novaya Zemlya	2 Nov '74	04	59	56.70	99.84	0.46	6.7	338°
Port Moresby	PMG	Novaya Zemlya	23 Aug '75	08	59	57.90	99.67	0.03*	6.4	338°
Port Moresby	PMG	Nevada	26 Mar '70	19	00	00.2	100.64	1.49*	6.4	50°
Port Moresby	PMG	Nevada	12 Feb '71	14	45	00.2	100.67	−1.14*	6.2	50°
Port Moresby	PMG	Amchitka Island	6 Nov '71	22	00	00.1	66.61	−0.15	6.8	25°
Lae	LAT	Novaya Zemlya	12 Sept '73	06	59	54.33	96.96	−0.18	6.8	338°
Lae	LAT	Novaya Zemlya	2 Nov '74	04	59	56.70	97.21	0.05	6.7	338°
Lae	LAT	Novaya Zemlya	23 Aug '75	08	59	57.90	97.01	0.75*	6.4	338°
Lae	LAT	Nevada	12 Feb '76	14	45	00.2	99.20	2.06*	6.2	338°
Lae	LAT	Amchitka Island	6 Nov '71	22	00	00.1	64.18	−0.22	6.8	25°
Lamington	LMG	Novaya Zemlya	12 Sept '73	06	59	54.33	99.39	−0.37	6.8	338°
Lamington	LMG	Novaya Zemlya	2 Nov '74	04	59	56.70	99.69	−0.54*	6.7	338°
Manton	MTN	Novaya Zemlya	12 Sept '73	06	59	54.13	98.29	−0.27	6.8	342°
Manton	MTN	Novaya Zemlya	27 Oct '71	06	59	57.37	97.87	−0.11	6.9	342°
Manton	MTN	Novaya Zemlya	2 Nov '74	04	59	56.70	97.84	0.16	6.7	342°
Manton	MTN	Novaya Zemlya	23 Aug '75	08	59	57.90	98.39	−0.24	6.4	342°
Esa'ala	ESA	Novaya Zemlya	14 Oct '70	05	59	57.1	100.89	1.07	6.7	338°
Esa'ala	ESA	Novaya Zemlya	27 Sept '71	05	59	55.18	100.96	1.27	6.4	338°
Esa'ala	ESA	Novaya Zemlya	28 Aug '72	05	59	56.51	101.03	1.02	6.3	338°
Esa'ala	ESA	Novaya Zemlya	12 Sept '73	06	59	54.33	100.94	0.81	6.8	338°
Esa'ala	ESA	Amchitka Island	6 Nov. '71	22	00	00.1	65.68	−1.52	6.8	25°

* Rejected data

Table 2. Residuals at east Papua and Manton seismic stations using Novaya Zemlya, Nevada and Amchitka Island nuclear explosions.

reliably recorded Novaya Zemlya explosions for PMG, LAT, LMG, ESA and MTN, using the Herrin (1968) tables for P waves are listed in Table 3 (Residual A).

Source uncertainties

USSR does not publish precise location and timing data for their nuclear explosions and therefore these data must be obtained by normal earthquake-inversion modelling. Robinson & Iyer (1976), in their analysis of temporal as well as spatial variations of travel-time residuals in the Californian region, clearly consider the origin time of the October 1973 event to be more precise than the USGS standard deviation of ±1.0s indicates. The data from that event are consistent with travel-times from 7 other nuclear explosions in the Novaya Zemlya region. Their average standard deviation of residuals from the means at 107 stations was ±0.06s using 8 Novaya Zemlya events. However the Robinson & Iyer average residual in the area of the Berkeley (BKS) WWSSN station is about +0.12s whereas the average value determined from four world-wide studies listed by Sengupta & Julian (1976) is +0.59s. Thus the seismic P phases from Novaya Zemlya explosions seem to arrive early in the California region (about 70° from the sources), whereas in east Papua they arrive late. Hence although the Robinson & Iyer data indicate that the USGS origin times are consistent, there may still be a systematic bias.

Subsequent recomputation of revised data by the International Seismological Centre, Edinburgh (ISC) indicates that the USGS origin time for the October 1973 event was 0.23s early. This trend is seen in other recomputed data (ISC, 1970-1974). Hence a correction of between −0.20s and −0.25s may be applied to the residuals listed in Table 3 to obtain better estimated values. This correction results in a PMG station residual of between +0.14s and +0.19s.

The validity of applying a source-depth correction of 0.16s may also be questioned, bearing in mind the statistical techniques applied in determining the origin time. It is probable that the convergence of the origin time is little affected by small variations in depth of about 1 km at the source and therefore the depth correction should not be applied. If no source depth correction is applied the PMG residual in Table 3 is further altered to between −0.02s and +0.03s. This is still significantly different from the Herrin & Taggart (1968), and the Sengupta & Julian (1976), values of −0.55s and −0.28s respectively.

Table 3 contains values of the residuals at the permanent east Papuan stations with an origin time correction of 0.23s applied and without a source-depth correction (Residual B).

Source bias at the Novaya Zemlya nuclear test site is clearly another factor to be considered in trying to account for travel-time variations from average earth models. Reported results, from World Wide Standard Seismograph Stations at Guam (GUA), Hong Kong (HKC), Manila (MAN) and Lembang (LEM), of the two 1973 Novaya Zemlya explosions were used to investigate whether there was any systematic lag in P arrivals in the general direction of Port Moresby. Unfortunately there was considerable scatter in the data and no clear bias was indicated.

Other indications of source bias are not available. There are few seismic observatories in USSR whose records are available for scrutiny and the precise origin times of USSR nuclear explosions are not published. Sengupta & Julian (1976) among others have evaluated the residuals in the northern Scandinavian shield area as being between 0s and

Station	Residual A	Residual B*	Difference from PMG
Port Moresby (PMG)	+0.39s	0.0s	
Lae (LAT)	−0.06s	−0.45s	−0.45s
Lamington (LMG)	−0.16s	−0.55s	−0.55s
Esa'ala (ESA)	1.07s	0.68s	+0.68s
Manton (MTN)	−0.12s	−0.51s	−0.51s

* Residual A with −0.23s origin time correction applied, and without source depth correction (see text).

Table 3. Residuals, using Herrin (1968) tables, for east Papuan permanent stations and Manton from Novaya Zemlya explosions.

−1.0s, but this is probably not representative of Novaya Zemlya, which is considered an extension of the Ural Mountain chain, a zone of inactive continental collision. For lack of other evidence there is assumed to be no source bias at Novaya Zemlya due to crustal and upper mantle structure.

Permanent station data from other sources

Some data from nuclear explosions along azimuths from PMG other than Novaya Zemlya were examined. Table 2 contains the residuals at PMG, LAT and ESA using nuclear explosions on Amchitka Island in the Aleutian Islands. ("Cannikin" explosion), and in Nevada. Unfortunately the Nevada explosions are not large enough for the onsets to be picked reliably and these data have therefore been rejected.

The Cannikin explosion gave residuals of −0.15s, −0.22s, and −1.52s at PMG, LAT and ESA respectively (azimuth approx. 25°). The magnitude of this explosion(m_b = 6.8), and the shorter distances, preclude rejecting these results. The difference between these residuals and those in Table 3 from Novaya Zemlya explosions illustrates the caution which must be exercised in the interpretation of residuals from different azimuths. In the case of the Cannikin nuclear explosion, it is probable that shot-point corrections differ considerably from the average because of major tectonic activity along the Aleutian Island chain (Herrin & Taggart, 1968b).

Residual differences

The uncertainties in the determination and interpretation of the residuals shown in the preceding sections do not preclude their use for the determination of residual differences which can be used to comment on crustal structure. Generally, the onset of the P arrivals at the temporary stations was more reliably and precisely determined than at the permanent stations. The spread of the stations over a small angular distance from the source (4.15°) encouraged the assumption made in this paper that all residual differences could be due to variations in crust and upper mantle structure beneath the east Papuan peninsula.

Hales and others (1968), in their studies of residuals in North America and Australia, concluded that the major part of regional residual variations could be attributed to small velocity variations in the mantle at depths of between 100 km and 600 km. However the results by Cleary and others (1972) of their recordings of the Cannikin explosion across eastern Australia clearly indicate that, as well as a regional effect, there is also a local component of station residuals which can be attributed to crustal and upper mantle structure. This component has been shown to be quite large (1-2 seconds) at recording stations in sedimentary basins (Everingham, 1969). In tectonically active areas this may even be the major component.

The values of the residual differences listed in Table 3 for LAT, ESA and LMG have been quoted in Table 1, column 9. The other east Papuan station residual differences from PMG, i.e. station residual minus PMG residual (Table 1, column 9), have been determined using a PMG residual value of +0.39s. The resultant residual differences ranged from +1.41s at Malalaua to −0.72s at Popondetta. Their spatial distribution is shown in Figure 1. The range of residual differences in east Papua, 2.13s, is greater than that found in California by Robinson & Iyer (1976), 1.48s; and that found across eastern Australia by Cleary and others (1972), 1.53s.

The angle of emergence of the seismic rays recorded at east Papuan stations is less than 15° from the vertical, using the Herrin (1968) earth model. In order to obtain the magnitude of the effects of crustal structure on the travel-times it has been assumed that rays are travelling vertically through the crust. Figure 4 shows the crustal structure along the line A-B shown in Fig. 1, interpreted by Finlayson and others (1977). The sedimentary structure has been derived from interpretations by Tallis (1975), and Brown and others (1975) for the southwestern coast, and by Davies & Smith (1971) for the northeast coast.

Coral Sea Coast

The residual differences along the southern and southwestern coasts are considered first. Three stations, Malalaua (MA), Kabuna (KB), and Aroa (AA), lie within the unstable eastern shelf area of Brown and others (1975); the stations from Port Moresby towards the southeast lie within their southeastern Papua Volcanic province.

In the unstable eastern shelf area, there is a sequence above seismic basement which is probably more than 10 km thick. It consists of clastic sediments of the Cainozoic Papuan Geosyncline unconformably overlying a sequence of deformed, faulted and metamorphosed Mesozoic to Lower Tertiary rocks. The three seismic stations were situated on surface alluvium.

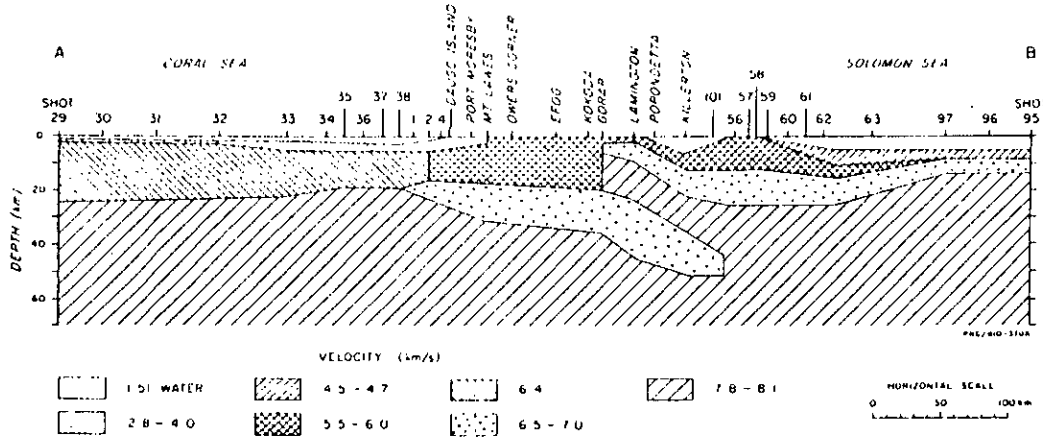

Figure 4. Crustal cross-section along line A-B indicated in Figure 1 (Finlayson and others, 1977).

Estimates of the interval velocities above seismic basement under MA, KB and AA can be made from various oil-drilling and exploration activities (Tallis, 1975). In this way it is possible to make estimates of travel-time differences due to the sedimentary sequence. For seismic rays arriving vertically the effects of variation in the depth of the Moho from Port Moresby of about 5 km are small (approx. 0.02 s/km) compared with the considerable delays introduced nearer the surface. Using velocities varying from 2.0 km/s to 5.0 km/s for the various sedimentary layers under MA, KB and AA, the residual differences can be adequately explained. Similarly the residual difference at Daugo Island of 0.30s can be reasonably explained using a low-velocity sequence about 0.8 km thick.

The residual differences at Mount Lawes (−0.19s), Sirinumu Dam (0.11s), Kupiano (−0.10s) and Cape Rodney (−0.04s) are all consistent with their location within the southeast Papua volcanic province of Brown and others (1975). Drummond and others (in prep.) interpret very little change in crustal structure between Port Moresby and Cape Rodney. The near-surface volcanic rocks are likely to have only a slightly higher seismic velocity than the Eocene marine clastic sedimentary rocks, cherts and limestone on which the PMG station is located.

Owers Corner (OC) is situated on pyroclastics, lavas and clastic sedimentary rocks which overlie Owen Stanley low-grade metamorphic rocks. The residual difference of +0.01s is slightly more positive than the values at ML (−0.19s) and SD (−0.11s). This can readily be accounted for by the near-surface geological differences; Finlayson and others (1977) do not interpret any significant difference in Moho depth under these three stations.

Central Papuan Peninsula

The second group of results are those residual differences at stations located along the centre of the Papuan peninsula (Fig. 3). The stations at Lake Trist (LT), Kokoda (KA), Tetebedi (TT) and Musa (MD) are located on or close to outcropping rocks of the Papuan Ultramafic Belt (Davies, 1971), but all have significant positive residual differences, +0.95s, +0.20s, +0.53s and +0.48s respectively. It is clear, therefore, that although these stations are associated with surface rocks with a high seismic velocity, the underlying rocks of the crust must have lower velocities compared with those under Port Moresby. Up to 0.3s could be accounted for by the morphology of the crust-mantle interface of Finlayson and others (1977). The balance at KA, TT and MD can reasonably be attributed to underlying metamorphic rocks with a velocity structure similar to that under Owers Corner (OC). The balance at Lake Trist (LT) requires a thickness of underlying low-velocity rocks of about 10 km if a velocity contrast from Port Moresby upper crustal rocks of about 1.5 km/s is assumed.

The residual difference at Guari (GU) and Tapini (TI) are not very large, +0.08s and +0.15s respectively. Because of the location of the stations, these values support the argument that the larger positive residual differences at MA, KB and AA are entirely due to near-surface geology. The residual difference at Efogi (EI), of −0.39s, is anomalous when viewed in terms of known surface geology, since positive values close to those at Owers Corner (OC), Kokoda (KA), and Tetebedi (TT) might be expected. It is therefore concluded that the surface geology must mask unrecognised deeper geological features which include high velocity rocks.

The station at Esa'ala (ESA) has a residual difference of +0.68s and may be considered within this group of stations because crustal rocks which make up the core of the Papuan peninsula, extend offshore (Davies & Smith, 1971). The high positive residual difference does not seem to indicate any great reduction in crustal thickness under Esa'ala compared with stations onshore. However the volcanic activity in the D'Entrecasteaux Islands probably has an effect on the seismic velocities in the area and thus may alter this inferred crustal structure.

Solomon Sea Coast

The third group of stations are those on or near the Solomon Sea coast. The stations at Ioma (IA) and Cape Ward Hunt (CW) have residual differences of +0.04s and +0.12s respectively. Davies & Smith (1971) report several thousand metres of basaltic pyroclastic shallow-marine sediments and limestone in the region of these stations. Substituting a higher velocity for the low velocity material at the surface will result in negative residual differences of −0.1s to −0.3s, which are close to residual differences at other stations on the Solomon Sea coast. The value at Afore (AF) of +0.03s is also positive only because of surface Quaternary lavas and pyroclastics.

The trend towards negative residual differences on the northeast side of the Papuan peninsula can be attributed to the lack of crustal rocks with velocities in the range 5.5-6.0 km/s in the crustal models (Fig. 4) interpreted by Finlayson and others (1977). The small negative residual difference at Gorari (GO) of −0.12s probably implies that a thin layer of high velocity surface rock of the Papuan Ultramafic Belt is underlain by lower velocity material.

The residual difference at Lae (LAT) of −0.45s is close to those for stations on the northeast Papuan peninsula coast. The crustal structure north-northwest of LAT is not likely to be the same as that towards the southeast but there is little other geophysical data to speculate on a crustal model.

Conclusions

The following conclusions can be drawn from the data presented:

The value of the residual at Port Moresby as determined from Novaya Zemlya explosions is apparently significantly different from previous evaluations, but the location of the velocity variation along the ray path leading to the travel-time difference cannot be determined without precise data on shot times and locations.

The residual differences from Port Moresby seismic station at other stations throughout the Papuan peninsula can reasonably be explained in terms of variations in crustal structures in this tectonically complex area.

A regional crustal effect which can be recognised is a tendency towards negative residual differences on the northeast side of the peninsula.

The determination of regional residual values from widely spaced observatories must take into consideration the sometimes considerable crustal effects. This would best be achieved by operating small seismic networks rather than single observatory sites.

Acknowledgements

The author wishes to thank the following organisations for data and records contributed towards this study: Research School of Earth Sciences, Australian National University; Geophysical Observatory, Port Moresby; Vulcanological Observatory, Rabaul; Department of Terrestrial Magnetism, Carnegie Institute of Washington, USA. The figures were drawn by Brett Holden, Geophysical Drawing Office, BMR.

References

BROWN, C. M., PILLERS, P. E., & ROBINSON, G. P., 1975—Stratigraphic and structural development of the Aure Trough and adjacent shelf and slope areas. *Australian Petroleum Exploration Association Journal*, **15**, 61-71.

CARDER, D. S., GORDON, D. W., & JORDAN, J. N., 1966—Analysis of surface-focus travel times. *Bulletin of the Seismological Society of America*, **56**, 815-40.

CARPENTER, E. W., MARSHALL, P. D., & DOUGLAS, A., 1967—The amplitude—distance curve for short period teleseismic P-waves. *Geophysical Journal of the Royal Astronomical Society*, **13**, 61-70.

CLEARY, J. R., 1967—P times to Australian stations from nuclear explosions. *Bulletin of the Seismological Society of America*, **56**, 773-81.

CLEARY, J. R., & HALES, A. L., 1966—An analysis of the travel times of P waves to north American stations, in the distance range 32° to 100°. *Bulletin of the Seismological Society of America*, **56**, 467-89.

CLEARY, J. R., SIMPSON, D. W., & MUIRHEAD, K. J., 1972—Variations in Australian upper mantle structure, from observations of the Cannikin explosion. *Nature*, **236**, 111-12.

DAVIES, H. L., 1971—Peridotite-gabbro-basalt complex in eastern Papua: an overthrust plate of oceanic mantle and crust. *Bureau of Mineral Resources, Australia—Bulletin* **128**.

DAVIES, H. L. & SMITH, I. E., 1971—Geology of eastern Papua. *Geological Society of America—Bulletin*, **82**, 3299-312.

DRUMMOND, B. J., COLLINS, C. D. N., & GIBSON, G., in prep.—Crustal structure of the Coral Sea and southwestern Papuan peninsula.

ENGDAHL, E. R., & GUNST, R. H., 1966—Use of a high speed computer for the preliminary determination of earthquake hypocenters. *Bulletin of the Seismological Society of America*, **56**, 325-36.

EVERINGHAM, I. B., 1969—P-wave residuals at Australian seismograph stations. *Bureau of Mineral Resources, Australia, Record* **1969/22** (unpublished).

FINLAYSON, D. M., MUIRHEAD, K. J., WEBB, J. P., GIBSON, G., FUROMOTO, A. S., COOKE, R. J. S., & RUSSELL, A. J., 1976—Seismic investigation of the Papua Ultramafic Belt. *Geophysical Journal of the Royal Astronomical Society*, **44**, 45-60.

FINLAYSON, D. M., DRUMMOND, B. J., COLLINS, C. D. N., & CONNELLY, J. B., 1977—Crustal structures in the region of the Papua Ultramafic Belt. *Physics of the Earth and Planetary Interiors*, **14**, 13-29.

FREEDMAN, H. W., 1966—The 'little variable factor'. A statistical discussion of the reading of seismograms. *Bulletin of the Seismological Society of America*, **56**, 593-604.

FREEDMAN, H. W., 1967—A statistical discussion of P residuals from explosions. Part II. *Bulletin of the Seismological Society of America*, **57**, 545-61.

HALES, A. L., CLEARY, J. R., DOYLE, H. A., GREEN, R., & ROBERTS, J., 1968—P-wave station anomalies and the structure of the upper mantle. *Journal of Geophysical Research*, **73**, 3885-96.

HERRIN, E., 1968—1968 Seismological tables for P phase. *Bulletin of the Seismological Society of America*, **58**, 1193-241.

HERRIN, E., & TAGGART, J. N., 1968a—Regional variations in P travel times. *Bulletin of the Seismological Society of America*, **58**, 1325-37.

HERRIN, E., & TAGGART, J. N., 1968b—Source bias in epicenter determinations. *Bulletin of the Seismological Society of America*, **58**, 1791-96.

INTERNATIONAL SEISMOLOGICAL CENTRE (ISC), 1970-1974—Monthly bulletins of seismic data.

JEFFREYS, H., & BULLEN, K. E., 1948—SEISMOLOGICAL TABLES. *British Association for the Advancement of Science, Gray Milne Trust, London*.

LILWALL, R. C., & DOUGLAS, A., 1970—Estimation of P-wave travel times using joint epicentre method. *Geophysical Journal of the Royal Astronomical Society*, **19**, 165-81.

PHO, H., & BEHE, L., 1972—Extended distances and angles of incidence of P-waves. *Bulletin of the Seismological Society of America*, **62**, 885-902.

ROBINSON, R., & IYER, H. M., 1976—Temporal and spatial variations of travel time residuals in central California for Novaya Zemlya events. *Bulletin of the Seismological Society of America*, **66**, 1733-47.

SENGUPTA, M. K., & JULIAN, B. J., 1976—P-wave travel times from deep earthquakes. *Bulletin of the Seismological Society of America*, **66**, 1555-79.

TAITT, N. C., 1975—Development of the Tertiary offshore Papuan Basin. *Australian Petroleum Exploration Association Journal*, **15**, 55-60.

THIRLAWAY, H. I. S., 1966—Interpreting array records: explosion and earthquake P wavetrains which have traversed the deep mantle. *Proceedings of the Royal Society of London, Series A*, **290**, 385-95.

UNITED STATES GEOLOGICAL SURVEY (USGS), 1973—Earthquake data report **65-73**, December 5, 1973.

WRIGHT, C., & MUIRHEAD, K. J., 1969—Longitudinal waves from the Novaya Zemlya nuclear explosion of October 27, 1966, recorded at the Warramunga seismic array. *Journal of Geophysical Research*, **74**, 2034-48.

Reprinted from *Volcanism in Australasia*, R. W. Johnson (Editor)
Elsevier Scientific Publishing Company, Amsterdam — Oxford — New York 1976

CRUSTAL STRUCTURE UNDER THE MOUNT LAMINGTON REGION OF PAPUA NEW GUINEA

D.M. FINLAYSON, B.J. DRUMMOND, C.D.N. COLLINS, and J.B. CONNELLY

Bureau of Mineral Resources, P.O. Box 378, Canberra City, A.C.T. 2601

ABSTRACT

The Mount Lamington stratovolcano in eastern Papua is underlain by the ophiolite suite of rocks which make up the Papuan Ultramafic Belt and is situated near a north-south magnetic anomaly offset which marks the western limit of current volcanic activity on the Papuan peninsula. The Moho in the region shallows from depths of about 21 km under the northeast Papuan coast to 8 km under Mount Lamington. The crustal layers are interpreted as having P-wave velocities of 2.8, 3.7, 5.66, and 6.86 km/s, which are similar to those found for oceanic layers 1, 2, and 3. However, the total crustal thickness along the coast is about twice that of normal oceanic crust. The crustal layers dip towards the Solomon Sea at angles between 13° and 19°, which are higher than the 9° dip determined from magnetic models but much less than the 25°-60° dips used in previous gravity modelling. The Moho depth along the southwest Papuan coast is about 26 km, decreasing towards the Coral Sea. There is evidence for a low-velocity zone under the Mount Lamington region at depths between 35 and 50 km. Deeper lithospheric processes are responsible for the calcalkaline volcanism of Mount Lamington and may be related to the minor earthquake activity at shallow and intermediate depth, possibly associated with a fossil Benioff zone.

INTRODUCTION

Mount Lamington (1585 m) is one of a number of large Quaternary stratovolcanoes which lie northeast of the Owen Stanley Range in eastern Papua (Fig. 1). Until 1951 it had been regarded as dormant because there was no history or legend of activity, but in January of that year a catastrophic Peléan-type eruption occurred which caused considerable loss of life and property damage (Taylor, 1958). A seismic monitoring system was subsequently set up on the northern slopes of the mountain to detect earth tremors. Data are telemetered to a recording station in Popondetta for immediate inspection.

In 1973, the Mount Lamington station was one of the recording stations operating during the East Papua Crustal Survey, a regional seismic survey designed to investigate some of the major structural features of the Papuan peninsula (Finlayson, in prep.). Preliminary interpretations of crustal structure in the Mount Lamington region have been derived from data recorded at stations in that region. These interpretations, together with those of unpublished aeromagnetic work (CGG, 1969, 1971, 1973), enable basic structures under Mount Lamington to be outlined.

REGIONAL GEOLOGY

The geology and structure of eastern Papua (Fig. 1) have been discussed by Davies (1971), Davies & Smith (1971), Milsom (1973), and St John (1970). The Mount Lamington volcanic region lies on the Solomon Sea side of the Papuan Ultramafic Belt. This Belt is an ophiolite suite of rocks regarded as the surface exposure of a dipping slab of Jurassic oceanic crust and mantle, which has been obducted on to sialic crust during an episode of crustal convergence in the late Eocene (Davies, 1971; Dewey & Bird, 1970; Coleman, 1971; Moores, 1973). During this episode, the Owen Stanley Metamorphics were formed from Cretaceous sediments deposited at the northeastern margin of continental

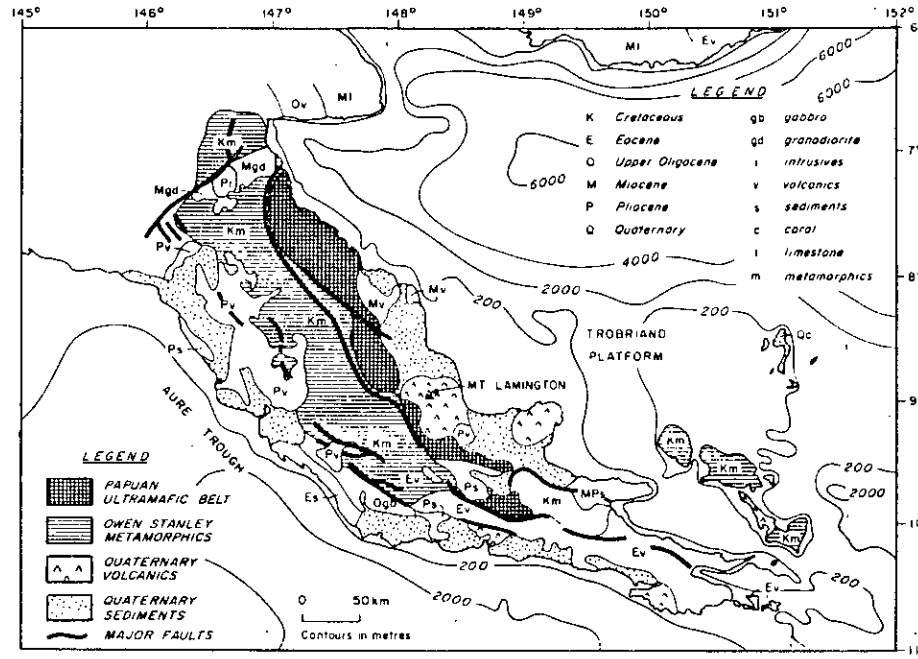

Fig. 1: Simplified geological map of eastern Papua.

Australia and rifted from Australia during the opening of the Coral Sea prior to separation of Australia from Antarctica in the early Eocene. The metamorphics now form the mountainous spine of the Papuan peninsula. Milsom (1973) has discussed the various proposed methods of emplacement of the ophiolite suite and concluded that there is a possibility that it may represent crust of a marginal basin type rather than a true oceanic type.

After emplacement of the Papuan Ultramafic Belt, volcanism took place in the late Miocene and Pliocene on the Papuan peninsula and offshore islands and continued through the Quaternary to the present time (Johnson et al., 1973; Smith, 1973; Taylor, 1958). It is difficult to relate the present episode of volcanism to the Tertiary tectonic episode which resulted in the emplacement of the ophiolite rocks. However, Mount Lamington and the other active volcanoes lie on the northeast margin of the Indian-Australian lithospheric plate where it abuts on a series of contrasting crustal types in a region of crustal convergence between the Indian-Australian and Pacific plates. The tectonic development of this northeast margin has continued since the separation of Australia from Antarctica in an episodic manner.

This development is illustrated in recent times by the pattern of earthquake activity (Denham, 1969) and volcanic activity (Johnson et al., 1973) in the region. The shallow and intermediate seismicity of the Papuan peninsula is minor compared with the major earthquake zones to the north and east but it is significant, and some form of left-lateral strike-slip movement in the general direction of the Owen Stanley Fault is essential to the tectonic synthesis of the

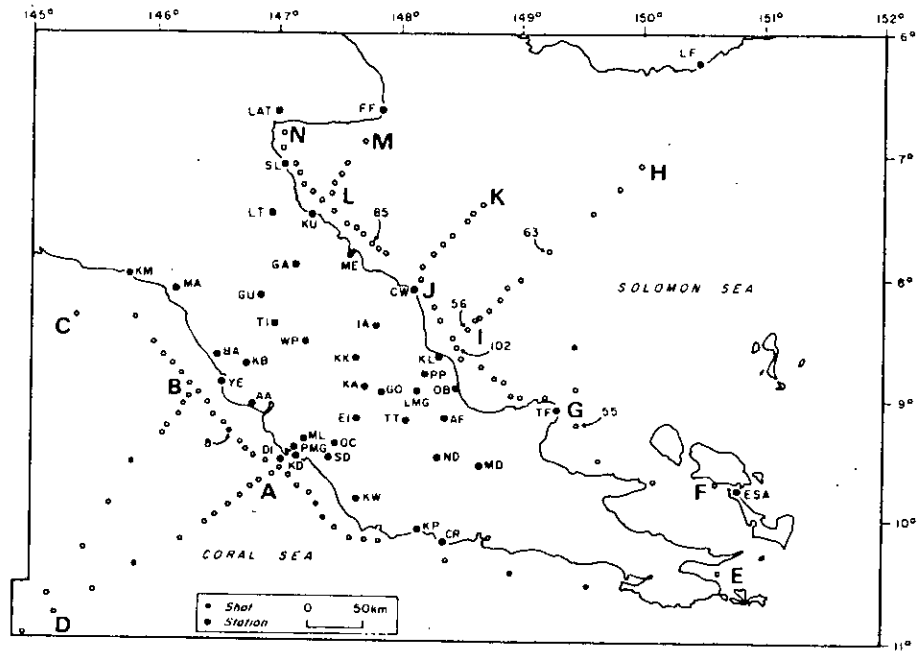

Fig. 2: East Papuan Crustal Survey 1973, shot and recording station locations.

Papua New Guinea region as a whole (Johnson & Molnar, 1972; Krause, 1973; Luyendyk et al., 1973; Milsom, 1970). Ripper (in prep.) has computed focal mechanism solutions for two earthquakes off the tip of the Papuan peninsula, one of which indicates strike-slip movement parallel to the geological strike and the other rifting.

SURVEY OPERATIONS AND DATA

The operational details of the East Papua Crustal Survey have been described by Finlayson (in prep.). Briefly, 111 shots were fired at sea (5 were small test shots) and 42 recording stations were positioned as shown in Figure 2. The stations were operated by the following institutions: Bureau of Mineral Resources (24), Australian National University (9), University of Queensland (3), Warrnambool Institute of Advanced Education and Preston Institute of Technology (3), PNG Geological Survey (3) and the University of Hawaii (1). The shots were usually either 1 tonne or 180 kg and were fired at approximately 100 m depth; a water replacement velocity of 4.0 km/s was used for shot-point corrections. Most of the recording stations were equipped with high-gain, slow-speed, automatic tape recorders but the permanent stations in the region (denoted by a 3-letter mnemonic in Fig. 2) were equipped with either photographic or smoked-paper drum recorders. Mount Lamington station (LMG) was of the latter type and was successful in recording 101 of the 111 shots, a performance bettered by only one other station (Mount Lawes, ML).

The regional gravity coverage of the Papuan peninsula was also completed during the 1973 survey period by helicopter, and this enabled a composite picture

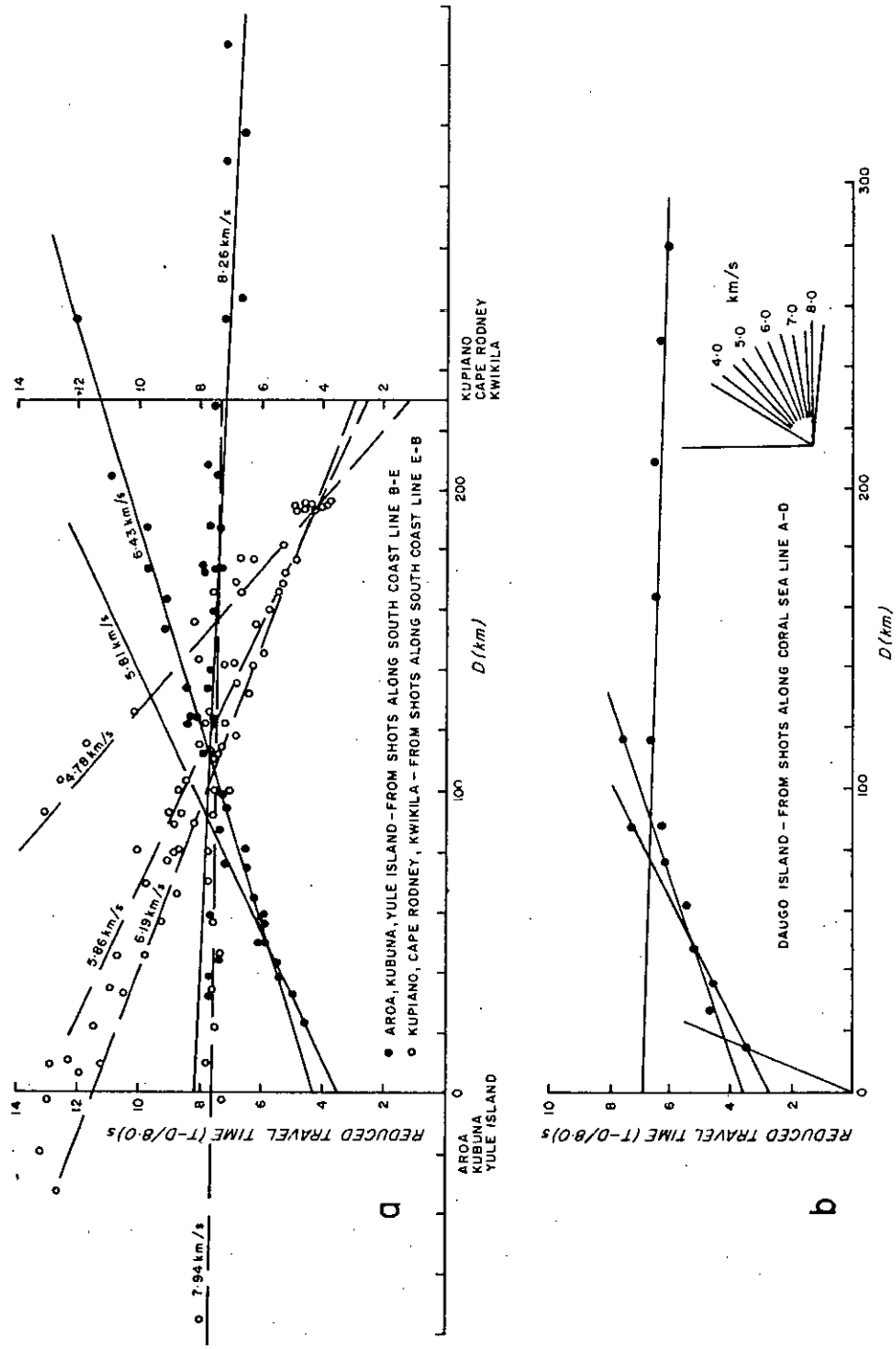
REDUCED TRAVEL TIME (T−D/8·0)s
D (km)
AROA
KUBUNA
YULE ISLAND
KUPIANO
CAPE RODNEY
KWIKILA
8·26 km/s
6·43 km/s
5·81 km/s
4·78 km/s
5·86 km/s
6·19 km/s
7·94 km/s
● AROA, KUBUNA, YULE ISLAND – FROM SHOTS ALONG SOUTH COAST LINE B-E
○ KUPIANO, CAPE RODNEY, KWIKILA – FROM SHOTS ALONG SOUTH COAST LINE E-B
a
km/s
4·0
5·0
6·0
7·0
8·0
DAUGO ISLAND – FROM SHOTS ALONG CORAL SEA LINE A-D
b

of the gravity field to be compiled using the BMR preliminary marine data (Tilbury, in prep.) and the land stations. Milsom (1973) has interpreted the regional gravity data straddling the Ultramafic Belt and constructed models to fit the observed values. The general gravity trends are consistent with the geological synthesis for the area, but the gravity models require a thicker crustal section. Much of the detail in the gravity models must be regarded as speculative at the survey station spacing used.

As described later in this paper, high-level aeromagnetic coverage of the Gulf of Papua, Papuan peninsula, and Trobriand Platform has also been completed (CGG, 1969, 1971, 1973), enabling depths to magnetic basement to be determined in these areas and some of the tectonic provinces to be delineated.

CRUSTAL STRUCTURE SOUTHWEST OF MOUNT LAMINGTON

Shots along line CBAE (Fig. 2) were recorded at several stations along the southwestern coast of the Papuan peninsula, giving approximately reversed profiles between Yule Island (YE) and Cape Rodney (CR). Unfortunately it was not possible to reverse the two lines of shots into the Coral Sea (lines AD and BD).

Representative time-distance plots from two groups of stations along the south coast are shown in Figure 3. Yule Island (YE), Kubuna (KB), and Aroa (AA) are grouped together, as are Cape Rodney (CR), Kupiano (KP), and Kwikila (KW). Also shown in Figure 3 is a time-distance plot of data from shots along line AD recorded at Daugo Island (DI). All travel-time data plots presented in this paper have been reduced by the shot-to-station distance divided by 8.0, which highlights changes in the apparent velocities near 8.0 km/s (parallel to the horizontal axis).

The data from the stations in Figure 3 and also from Mount Lawes (ML) were used to derive a simple three-layer crustal model along the southwest coast (Fig. 4). The uppermost layer has been assigned a velocity of 4.0 km/s. Survey design did not enable the recording of energy from this layer as first arrivals although it is sometimes present as later arrivals, as in Figure 3, where a refractor of 4.78 km/s is evident. Using 4.0 km/s as an average velocity, the uppermost layer appears to have an almost uniform thickness of 6-7 km along the southeast half of line CBAE, but thickens to approximately 10 km in the northwest. This coincides with the sediment distribution in the Aure Trough indicated by Mutter (1975) and CGG (1969).

Profiles both along the coast and in the Coral Sea indicate that velocities for the deeper crustal layers lie within the ranges 5.6-5.85 km/s and 6.0-6.45 km/s. Compilation of composite seismic record sections is necessary to define these velocities accurately because energy from the deeper layers commonly occurs as later arrivals. The velocities of 5.75 km/s and 6.3 km/s indicated in Figure 3 are considered representative of these refractors. From north to south the 5.75 km/s layer appears to thicken and the 6.3 km/s layer thins.

Fig. 3 (opposite): Seismic travel-time plots (reduced by shot-to-station distance/8.0) for stations along the southwest Papuan peninsula coast from (a) shots along the coast, and (b) shots out in the Coral Sea.

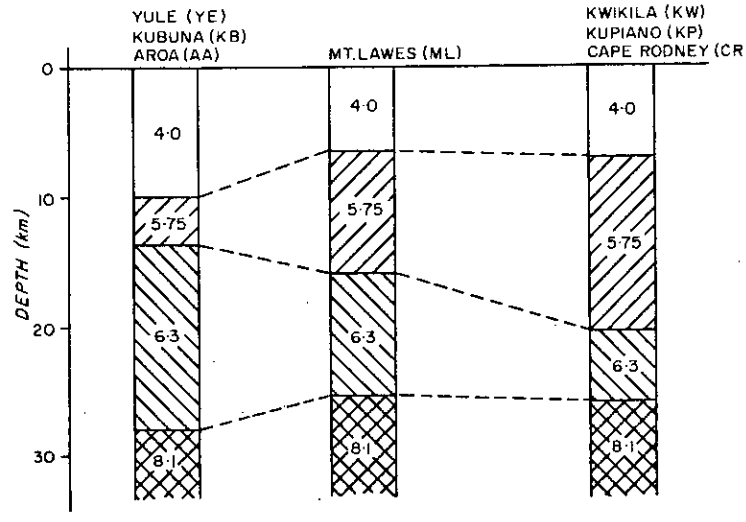

Fig. 4: Simplified crustal structure along the southwest Papuan peninsula coast (velocities in km/s).

Crustal information from the Coral Sea lines is available only near the coast, so it is necessary to interpret the Coral Sea structure by extrapolation using the data along the single-ended refraction lines AD and BD. An increase in the delay times of shots within 100 km of the coast implies an increase in the sediment thickness in the Aure Trough and its southeastern extension. The data are in good agreement with the model proposed by Mutter (1975) on the basis of gravity data, in which the sediments increase in thickness to about 7 km within the Trough. This model requires the mantle depth to decrease by about 6 km beneath the thickest part of the sedimentary pile to achieve isostatic equilibrium.

A mantle velocity of 8.1 km/s is found along the southwest coast, giving Moho depths under Cape Rodney (CR) and Mount Lawes (ML) of 25-26 km. The Moho dips to about 28 km below the northern coastal stations. An apparent Moho velocity of 8.2 km/s from shooting lines out into the Coral Sea suggests that the crust thins from the southwest Papuan peninsula coast towards the Coral Sea.

The crustal structure illustrated in Figure 4 is derived from simple plane layered models, but it is recognised that a more complex velocity/depth relation is likely and this is being investigated.

SEISMIC TRAVEL-TIME FEATURES THROUGH THE MOUNT LAMINGTON REGION

Two sets of shot and station data have been selected to illustrate the dominant features of seismic travel-times traversing the Mount Lamington region.

The first is illustrated by a seismic travel-time plot of recordings made at all stations from shots 56 and 8, on the northeast and southwest coasts of the Papuan peninsula respectively (Fig. 5).

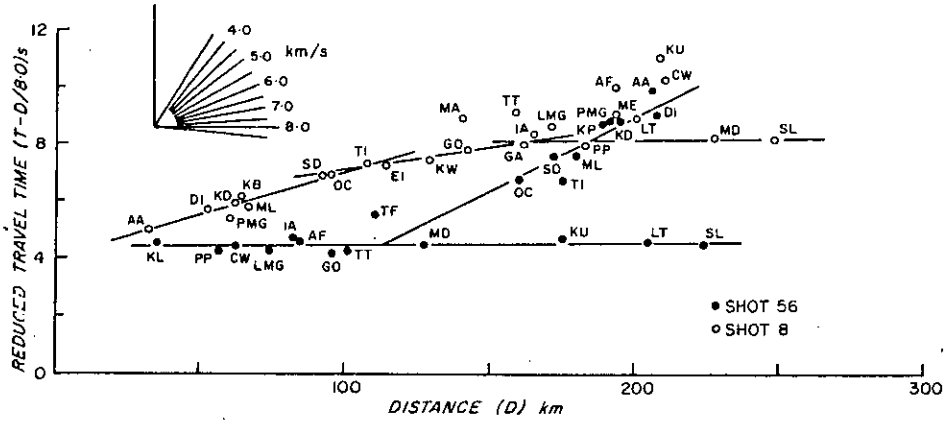

Fig. 5: Reduced seismic travel-times to all recording stations from shots 8 and 56.

The most pronounced feature of the plot is the asymmetry of the travel-times from the two shots. The arrivals from shot 8 on the southwest coast to all stations along azimuths ranging over 180° indicate successive increases in apparent velocity as distance from the shot-point is increased. The departure of some travel-times from the approximately fitted lines detracts only slightly from the overall trend, and many of the departures are readily explained.

The travel-time plot of data recorded from shot 56 on the northeast coast, however, exhibits entirely different characteristics. Over an azimuth range of 180°, a high apparent velocity (8 km/s) is evident from distances less than 50 km out to distances of over 200 km. The departures from the approximately fitted line are small. The stations that indicate this high velocity at an intercept of approximately 4.5 s are all located northeast of the Owen Stanley Fault. The same stations that recorded shot 8 from the southwest coast indicate similar apparent velocities, but with intercepts greater than 8.0 s, demonstrating that a considerably longer ray path is required in traversing the peninsula from southwest to northeast.

A longer travel-time is also evident in the data from shot 56 recorded at stations southwest of the Owen Stanley Fault. It is not until the shooting distance is about 180 km, however, that the travel-times from the two shots are similar. The asymmetry is undoubtedly due to greatly differing crustal structure on the northeast and southwest coasts of the Papuan peninsula. A simplified interpretation of crustal structure for the southwest coast and Coral Sea is presented earlier in this paper, and an interpretation along the northeast coast is presented by Finlayson et al. (in prep.) and is summarised here.

There are distinct differences in the crustal structure between the areas where the Papuan Ultramafic Belt crops out along the northeast coast and the region of the Trobriand Platform. Between Salamaua (SL) and Morobe (ME), surface-layer P-wave velocities of 4.4 km/s are recorded and a prominent refractor with a velocity of 6.98 km/s is interpreted at depths between 2.5 and 6.0 km. The Moho is interpreted at 20 km depth with an upper mantle velocity of 7.96 km/s. Between Morobe (ME) and Tufi (TF) across the Trobriand Platform, upper crustal layers

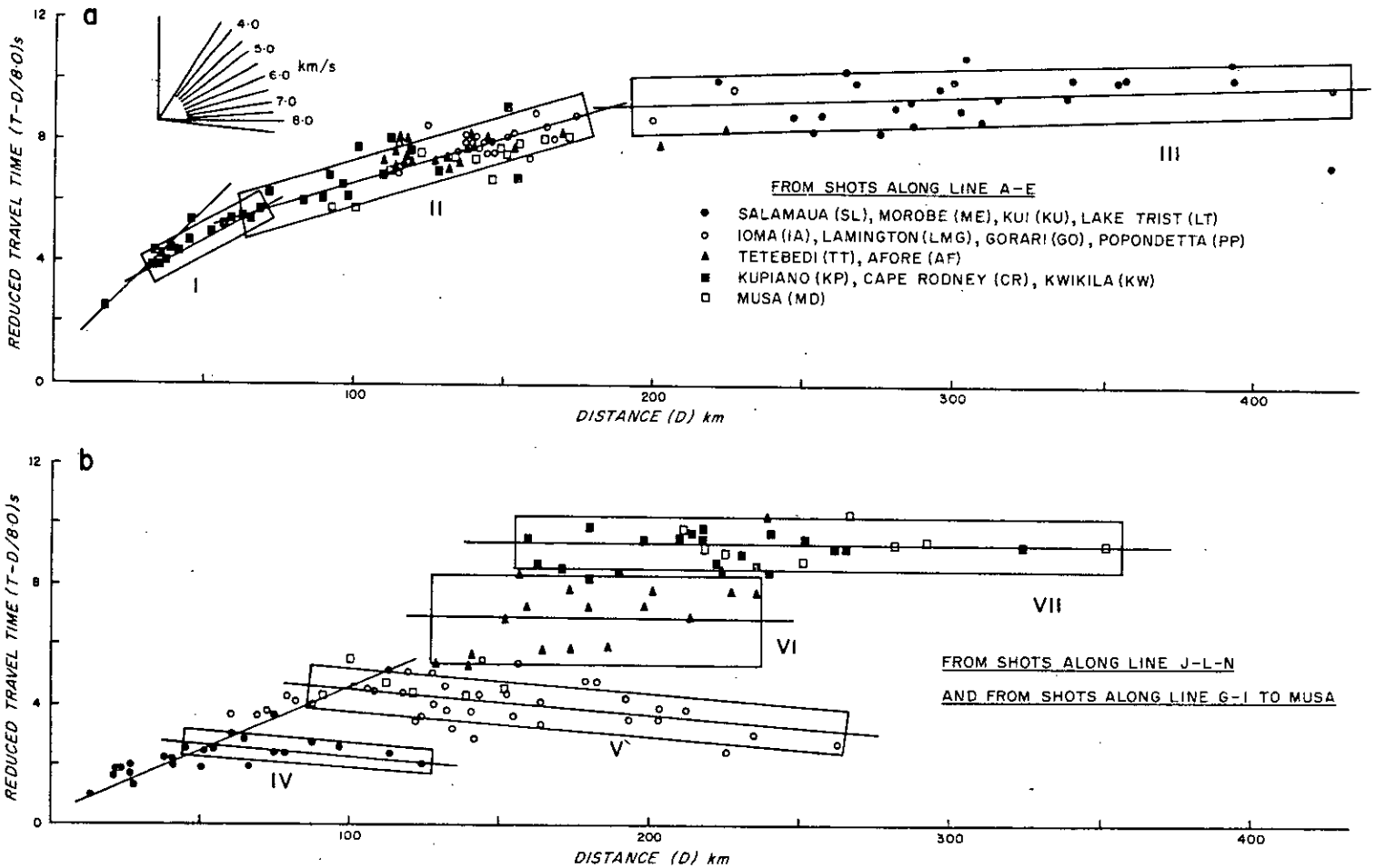
a
REDUCED TRAVEL TIME (T-D/8·0)s
DISTANCE (D) km
4·0
5·0
6·0
7·0
8·0
km/s
I
II
III
FROM SHOTS ALONG LINE A-E
SALAMAUA (SL), MOROBE (ME), KUI (KU), LAKE TRIST (LT)
IOMA (IA), LAMINGTON (LMG), GORARI (GO), POPONDETTA (PP)
TETEBEDI (TT), AFORE (AF)
KUPIANO (KP), CAPE RODNEY (CR), KWIKILA (KW)
MUSA (MD)
b
REDUCED TRAVEL TIME (T-D/8·0)s
DISTANCE (D) km
IV
V
VI
VII
FROM SHOTS ALONG LINE J-L-N
AND FROM SHOTS ALONG LINE G-I TO MUSA

with velocities of 2.8, 3.7, and 5.66 km/s and total thickness between 10 and 15 km are interpreted, overlying lower crustal material with velocity 6.86 km/s. The Moho is interpreted as lying at depths between 20 and 23 km and the upper mantle velocity is 7.96 km/s. Computer modelling along the northeast coast indicates the existence of a low velocity zone at depths between 35 and 50 km.

The second set of data is illustrated in Figure 6(a and b), which shows two travel-time plots, one from shots along traverse A-E (Fig. 2) and the other from shots along traverse J-L-N (and traverse G-I to Musa), with common recording stations along the zone between the sets of shots. The time-distance plot in Figure 6(a) displays similar characteristics to that in Figure 5 from shot 8. The envelopes of the data sub-sets I, II, and III in Figure 6(a) are consistent with the seismic ray paths traversing a crust with velocities similar to those determined along the southwest coast (Fig. 4).

The data plotted in Figure 6(b) can be grouped into various sub-sets IV, V, VI, and VII, all with the apparent velocities near 8 km/s. Sub-set IV is from stations on the Papuan Ultramafic Belt and is clearly associated with high-velocity material relatively near the surface and steeply dipping refractors. Data sub-set V has a similar apparent velocity, but the seismic travel-times are influenced by the onshore structures of the Trobriand Platform's southern margin on which the recording stations Ioma (IA), Lamington (LMG), Gorari (GO), and Popondetta (PP) are situated. The arrivals recorded at Tetebedi (TT) and Afore (AF) are largely contained in sub-set VI and display a much less well defined trend than the other data sub-sets. Sub-set VI is similar to the transition data at distances between 150 and 180 km in Figure 5. The interesting point, however, is that the ray paths are all in the region northeast of the Owen Stanley Fault. Sub-set VII contains recordings from Musa (MD), which is also northeast of the Owen Stanley Fault, as well as data from KW, KP, and CR, southwest of the Fault, and no further offset in the time-distance plot is apparent on crossing the Fault.

Thus it appears that longer (and presumably deeper) ray paths from shots along traverse J-L-N are evident under the Mount Lamington region as recorded at stations southeast of Mount Lamington. This feature is not apparent in data recorded at Tufi (TF) from the same shots but may be inferred from recordings made at Salamaua (SL) and Kui (KU) from shots along line G-N (Finlayson et al., in prep.). It is also apparent from the data recorded at Musa (MD) from shots along traverse G-I that they fit into data set E in Figure 6(b). Thus the evidence for a deep 8 km/s layer described by Finlayson et al. (op. cit.) is substantiated and is certainly present under the Mount Lamington region.

An approximate model for the crustal structure under Mount Lamington can be determined by treating the line of stations Gorari (GO), Lamington (LMG), Popondetta (PP), Killerton (KL) and shots out from the coast along traverse I-H (Fig. 2) as a fan-shooting pattern. Morobe (ME) and shot 85 have been chosen as one pair of reference points, and in the opposite direction Tufi (TF) and shot 55 have been chosen as the other pair. The travel-times from these reference points are

Fig. 6 (opposite): Reduced seismic travel-times from shots along (a) shooting line A-E, and (b) shooting line J-L-N.

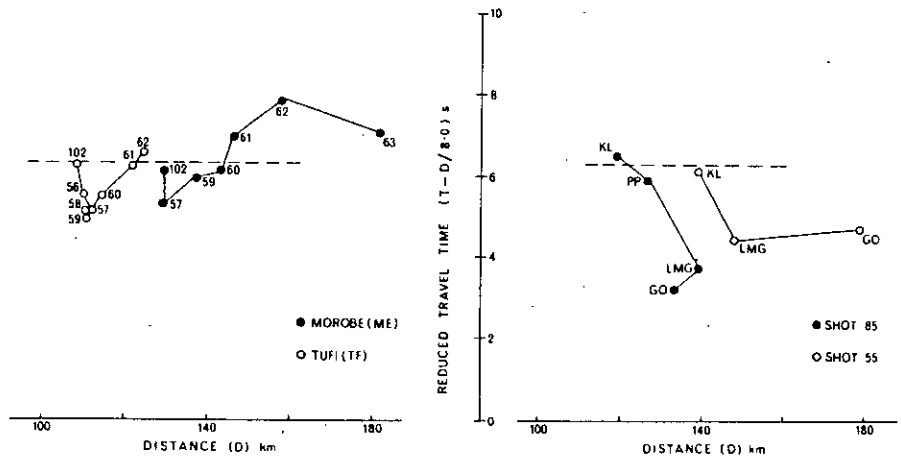

Fig. 7: Delay-time differences along a line of stations and shots normal to the northeast Papuan peninsula coast.

illustrated in Figure 7. The distances involved are all over 100 km, and the ray paths can be regarded as being from a refractor with a velocity of approximately 8.0 km/s (Finlayson et al., in prep.).

It is apparent from Figure 7 that Killerton (KL) and shot 102 (closest shot to KL) have approximately the same delay-times to the '8.0' refractor. The delay-times decrease as one moves along the line of shots out from Killerton (KL). At shots 57, 58, and 59 the delay times are a minimum and the 1.1 s delay-time difference from shot 102 can be attributed to thinning of the near-surface layer as the basement high is approached at the edge of the Trobriand Platform (CGG, 1971). The travel-times from shots in deeper water (60, 61, 62) indicate increasing delay-times, and these may be attributed to the structures on the submarine slope down from the Trobriand Platform to the floor of the Solomon Sea Basin (Finlayson et al., in prep.).

The right-hand side of Figure 7 illustrates the considerable decrease in the delay-times going from Killerton (KL) inland to Gorari (GO), the delay-time difference between Killerton (KL) and Lamington (LMG) being approximately 2.2 s. Aeromagnetic interpretation (CGG, 1971) indicates that sediment thickness decreases from approximately 3 km to zero along this line. The delay-time difference introduced by the near-surface layers can be taken as approximately the same as that in the zone extending offshore to the basement high referred to above, viz. 1.1 s. Interpretation of the aeromagnetic data later in this paper indicates that the basaltic province associated with the Papuan Ultramafic Belt extends under the Quaternary cover of the Trobriand Platform and the onshore areas northeast of the Owen Stanley Ranges, and that Mount Lamington is near its southwest boundary.

If the remaining 1.1 s delay-time difference between Killerton (KL) and Lamington (LMG) is attributed to a thinning of the basaltic and gabbroic layers and if the seismic velocity used for the volcanic pile is similar to that determined at Rabaul, i.e. 4.6 km/s (Finlayson & Cull, 1973), the structure under Mount

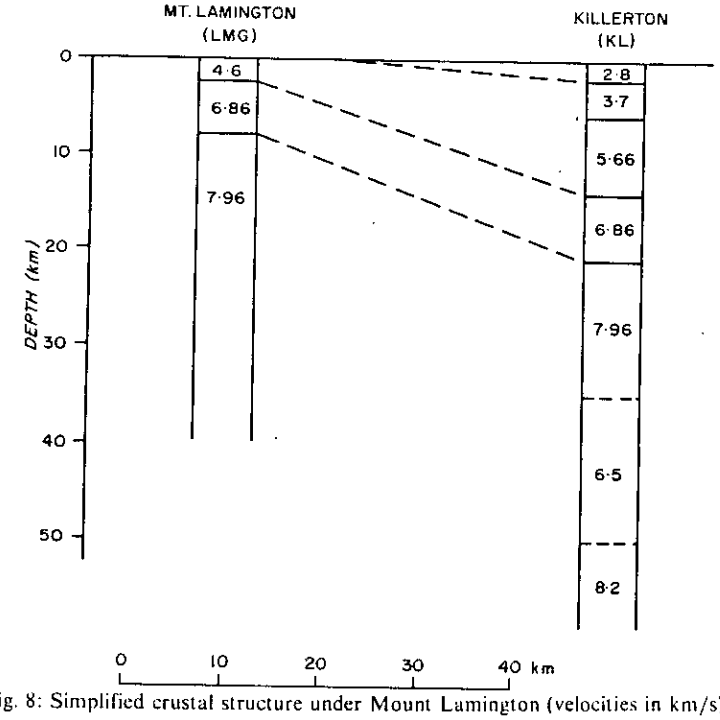

Fig. 8: Simplified crustal structure under Mount Lamington (velocities in km/s).

Lamington can be extrapolated from the crustal structure under Killerton (KL) as shown in Figure 8. The depth to the deep '8.0' refractor can be approximated from apparent velocities and intercepts of data sub-sets III and VII in Figure 6, but detailed analysis of the low velocity layer between the '8.0' refractors will be required in order to resolve the structure more accurately. Refractors may also dip considerably across the strike of the gross structures; if so, the refractor depths indicated would be offset from positions directly under Mount Lamington.

The first-arrival data from shot 56 to recording stations Killerton (KL), Popondetta (PP), Mount Lamington (LMG), and Gorari (GO) in Figure 5 have an apparent velocity of 8.4-8.5 km/s. This is the velocity to be expected if the 5.66/6.86 km/s interface dips at 13°-14° towards the Solomon Sea. However, seismic modelling indicates that the velocity/depth distribution may vary from the simple layered section indicated in Figure 8 to one of smoothly varying velocity increase with depth for the layers above the 6.86 km/s refractor. The apparent velocity indicates that the dip of this refractor is slightly less than the 16° obtained from Figure 8. This is much less than the 25°-60° dips used by Milsom (1973) in his gravity models for the dipping structures of the Papuan Ultramafic Belt.

Seismic first arrivals from shots along traverse I-H (Fig. 2) at distances greater than 100 km towards the same recording station array mentioned above (KL, PP, LMG, GO) give apparent velocities of 9.4-9.7 km/s. Modelling indicates that such velocities would be apparent from the 6.86/7.96 km/s interface at dip angles of 12°-15°, which are less than the 19° indicated in Figure 8. Further analysis will undoubtedly modify the simple dipping structures used in this paper.

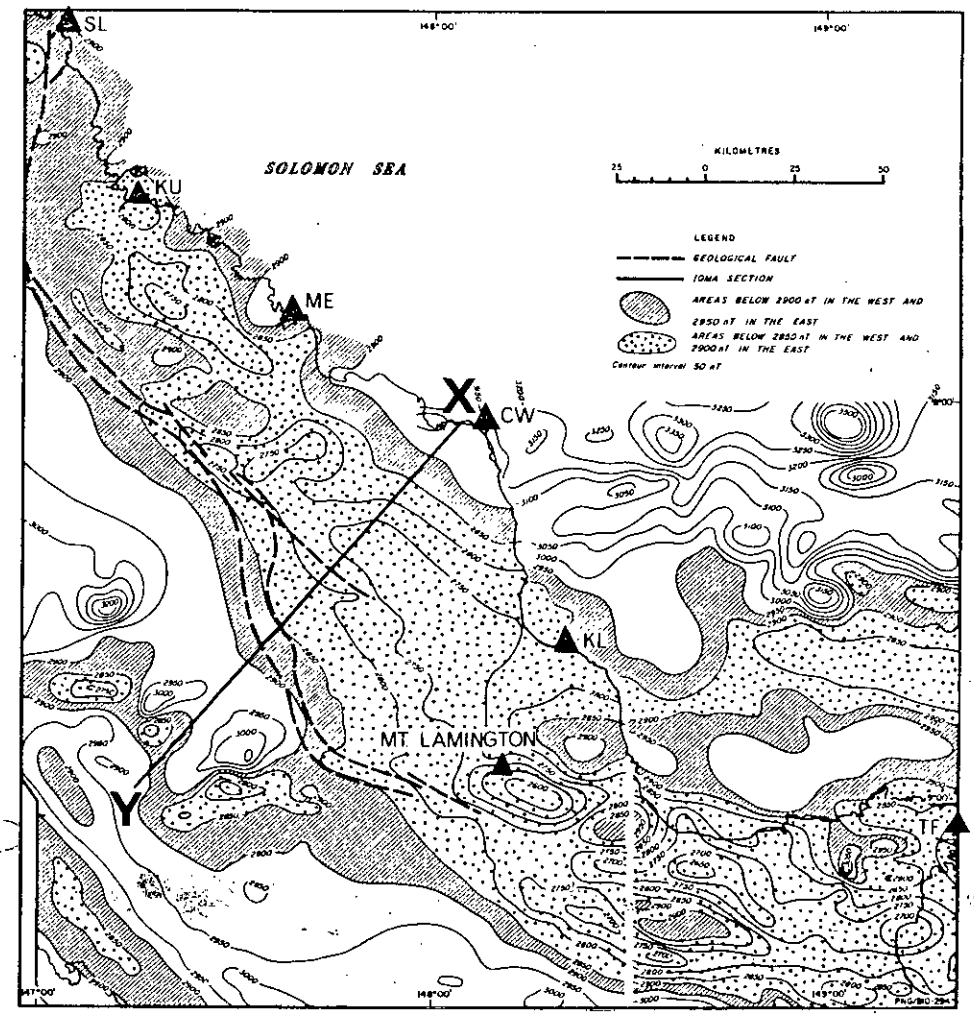

Fig. 9: Aeromagnetic anomaly map of the Mount Lamington region.

MAGNETIC EXPRESSION IN THE MOUNT LAMINGTON AREA

Aeromagnetic surveys covering the eastern Papuan peninsula, the Gulf of Papua and the Trobriand Platform have been undertaken by BMR (CGG 1969, 1971, 1973). Figure 9 shows a composite map of these surveys over the Papuan Ultramafic Belt in the Mount Lamington region and includes the major geological faults. The eastern half was flown at 2400 m and the western half at 4600 m. The regional gradient used to produce the contour map was that given by Parkinson & Curedale (1962) for the epoch 1957.5, but the contour values are not tied to any reference field. The dip, declination, and magnitude of the Earth's magnetic field in this region are approximately -31°, +6°E, and 42500 nT respectively (Finlayson, 1973).

The most obvious feature of the magnetic map is the prominent negative anomaly which is closely associated with the Papuan Ultramafic Belt particularly

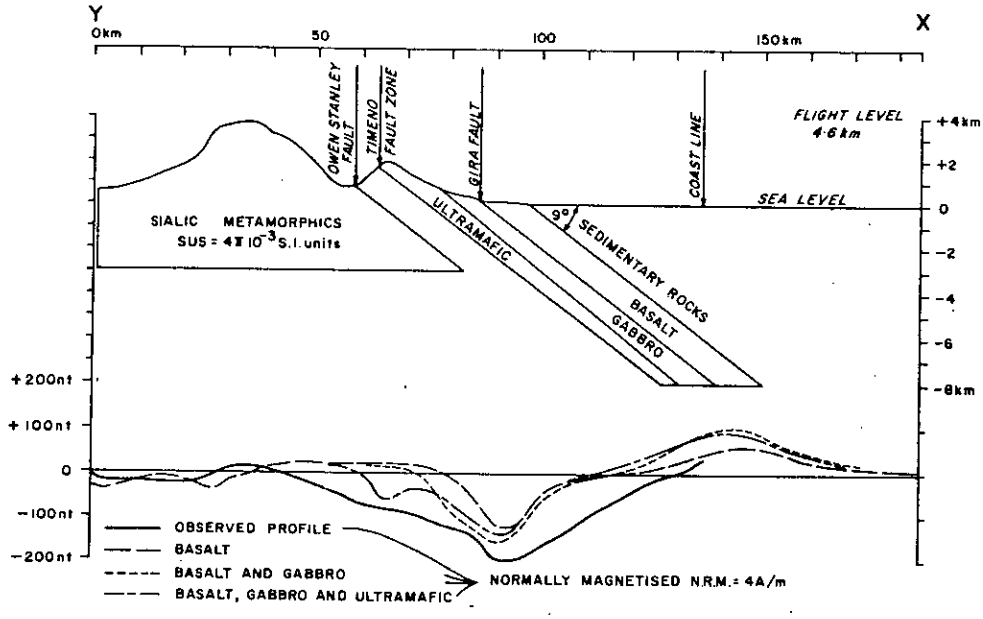

Fig. 10: Magnetic models along the line X-Y shown in Fig. 9.

from Kui (KU) to Mount Lamington (LMG). Immediately south Kui (KU) the negative anomaly is near the coast, and between Morobe (ME) and Cape Ward Hunt (CW) it is closer to the Owen Stanley Fault and shows rather irregular relief. South from Cape Ward Hunt it reflects the trends of the major faults indicated in Figure 9. The northernmost section of the Belt, which trends towards the coast near Salamaua (SL), is expressed by lack of relief in the magnetic contours.

In the region of Mount Lamington the anomaly is offset some 30 km to the south and its trend alters from southeast to east. The anomaly is very prominent in this area and the trend continues towards the east, but the relief of the anomaly is more irregular here than to the north of the offset. The magnetic expression of the Owen Stanley metamorphic zone southwest of the Papuan Ultramafic Belt is generally small except for a number of circular anomalies attributable to local intrusives.

In the northern part of the Belt the negative anomaly correlates well with two rock units mapped by Davies (1971) as the gabbroic and basaltic components of the ophiolite suite of rocks. Most of the areas mapped as being occupied by these two units have associated negative anomalies. Between Kui (KU) and Morobe (ME), however, the anomaly is rather irregular and does not correlate well with the large area of gabbro mapped in the region, an effect probably caused by the presence of numerous diorite intrusions in the area. The absence of magnetic expression in the most northerly part of the Belt reflects the absence of basalt and gabbro in this area and provides convincing evidence that the ultramafic component of the ophiolite suite has a very small magnetic effect.

Figure 10 shows three two-dimensional magnetic models along the profile XY (Fig. 9). The models show the effects of three layers with dip angles of about 9° and a natural remanent magnetism of 4 A/m in the direction of the Earth's present field. The terrain effects of the Owen Stanley Range are also included in the models. The three models illustrate the magnetic effects of the basalt, the basalt and gabbro, and the basalt, gabbro, and ultramafic rocks with layer thicknesses corresponding to the measured surface exposures.

Although none of the fits is good, that produced by the basalt and gabbro model is closest. The observed anomaly has a longer-wavelength component than the calculated anomalies, indicating that an accurate magnetic model of the Papuan Ultramafic Belt must differ from Figure 10. Detailed magnetic studies of oceanic crust (Talwani et al., 1971; Atwater & Mudie, 1973) indicate that the magnetic material may not be uniformly distributed within the oceanic layers 2 and 3, and the non-uniqueness of magnetic interpretation methods makes it difficult to construct detailed models based solely on magnetic observations.

The depth to the basalt layer at the coastline in Figure 10 is 6 km, which agrees with the depth to the 5.66 km/s layer indicated in Figure 8 but is 2 km deeper than that indicated by Finlayson et al. (in prep.) for the Cape Ward Hunt (CW) region. The dip of 9° is less than the dip of the 6.86 km/s refractor in the Mount Lamington region determined from seismic work described earlier in this paper and within the range of topographic dips (5°-15°) on the sea-floor towards the Solomon Sea basin (Finlayson et al., in prep.).

East of the magnetic anomaly offset mentioned earlier, outcrops of basalt and gabbro associated with the Ultramafic Belt are sparse and the main surface rock units are Quaternary volcanics and alluvium. However, the continuation of the regional negative magnetic anomaly suggests strongly that the basalt and gabbro units are present under the Quaternary cover. Their presence in this region has been postulated by Davies (1971) on geological evidence and by Milsom (1973) from the gravity modelling studies. The Quaternary volcanics have a relatively subdued magnetic expression. This may possibly be explained if they are composed of interlayered reversely and normally magnetised lava flows which would render them effectively non-magnetic. This effect was found in parts of Iceland (Piper, 1971).

The offset in the magnetic anomaly near Mount Lamington represents a boundary, possibly a north-south shear zone along which the Ultramafic Belt has been offset. Quaternary volcanics are prevalent east of the offset but absent to the west.

DISCUSSION

In eastern Papua the contemporary suites of calcalkaline and high-K calcalkaline lavas (Johnson et al., 1973) associated with recent volcanism cannot be associated with any currently active well defined Benioff zone in accordance with the model that Jakeš & White (1969) have proposed for island-arc areas. Such lavas are usually associated with magma generation at depths greater than 150 km. The lithospheric structures at such depths cannot be determined from the seismic and magnetic survey work interpreted in this paper. The simplified crustal

structure proposed here indicates that the concept of a slice of crust and upper mantle obducted on to a less dense crust is substantially correct in the Mount Lamington region, but the development of the thicker crustal section (twice that of normal oceanic crust) along the northeast Papuan peninsula coast (Finlayson et al., in prep.) requires further investigation.

The crustal shortening required to generate the Papuan Ultramafic Belt structures in the Eocene-Oligocene (40 m.y. B.P. approximately) cannot be directly related to present-day volcanism in eastern Papua. However, the whole Melanesian region demonstrates episodic development since that time and is still a major interaction zone between the Australian and Pacific lithospheric plates. Thus it is possible that some latent geochemical separation has been maintained until the present to account for the current volcanic activity. A subduction episode of only 1-2 m.y. duration under east Papua would be sufficient to enable oceanic crust to descend to the 150 km depth which is generally considered necessary to generate calcalkaline volcanics. It may be speculated that this has occurred since the emplacement of the Papuan Ultramafic Belt. A few earthquakes and hypocentres in the depth range 70 to 300 km have been detected in the Mount Lamington area and also in the Ioma (IA) area, indicating that there is current lithospheric activity under east Papua.

ACKNOWLEDGEMENTS

The authors wish to acknowledge the contribution of the following institutions to the field work during the East Papua Crustal Survey: Research School of Earth Sciences, Australian National University; Department of Geology and Mineralogy, University of Queensland; Warrnambool Institute of Advanced Education; Preston Institute of Technology; Hawaii Institute of Geophysics, University of Hawaii; and Geological Survey of Papua New Guinea. The staff of the Papua New Guinea District Administration and many individuals rendered invaluable assistance with the logistic operations connected with the field work; the authors wish to thank them for their help towards the overall success of the survey. We also wish to pay tribute to the volcanological work of Tony Taylor who, with others, was instrumental in promoting and encouraging the deep seismic investigation of the Mount Lamington region of eastern Papua. This paper is published with permission of the Director of the Bureau of Mineral Resources, Geology & Geophysics.

REFERENCES

Atwater, T., & Mudie, J.D., 1973: Detailed near bottom geophysical study of the Gorda Rise. *J. geophys. Res., 78 (35)*, pp. 8665.

Coleman, R.G., 1971: Plate tectonic emplacement of upper mantle peridotites along continental edges. *J. geophys. Res., 76 (5)*, pp. 1213.

Compagnie General De Geophysique (CGG), 1969: Papuan Basin and Basic Belt aeromagnetic Survey, Territory of Papua and New Guinea 1967. *Bur. Miner. Resour. Aust. Rec.* 1969/58 (unpubl.).

Compagnie General De Geophysique (CGG), 1971: Eastern Papua aeromagnetic survey, Part 1: northeastern portion (mainly offshore) flown in 1969. *Bur. Miner. Resour. Aust. Rec.* 1971/67 (unpubl.).

Compagnie General De Geophysique (CGG), 1973: Eastern Papua aeromagnetic survey, Part 2: southwestern panel (onshore) flown in 1970-71. *Bur. Miner. Resour. Aust. Rec.* 1973/60 (unpubl.).

Davies, H.L, 1971: Peridotite-gabbro-basalt complex in eastern Papua: an overthrust of oceanic mantle and crust. *Bur. Miner. Resour. Aust. Bull. 128.*

Davies, H.L., & Smith, I.E., 1971: Geology of eastern Papua. *Bull. Geol. Soc. Am., 82*, pp. 3299.
Denham, D., 1969: Distribution of earthquakes in the New Guinea-Solomon Islands region. *J. geophys. Res., 74*, pp. 4290.
Dewey, J.F., & Bird, J.M., 1970: Mountain belts and the New Global Tectonics. *J. geophys. Res., 75 (14)*, pp. 2625.
Finlayson, D.M., 1973: Isomagnetic maps of the Australian region for epoch 1970.0. *Bur. Miner. Resour. Aust. Rep. 159.*
Finlayson, D.M., & Cull, J.P., 1973: Time term analysis of New Britain-New Ireland island arc structures. *Geophys. J. Roy astr. Soc., 33*, pp. 265.
Finlayson, D.M. (ed.), in prep.: East Papua Crustal Survey 1973, operational report. *Bur. Miner. Resour. Aust. Rec.*
Finlayson, D.M., Muirhead, K.J., Webb, J.P., Gibson, G., Furumoto, A.S., Cooke, R.J.S., & Russell, A.J., in prep.: Seismic investigation of the Papuan Ultramafic Belt. *Geophysics. J. Roy. astr. Soc.*
Jakeš, P., & White, A.J.R., 1969: Structure of the Melanesian arcs and correlation with distribution of magma types. *Tectonophysics, 8*, pp. 223.
Johnson, R.W., Mackenzie, D.E., Smith, I.E., & Taylor, G.A.M., 1973: Distribution and petrology of late Cenozoic volcanoes in Papua New Guinea. In *The Western Pacific Island Arcs, Marginal Seas. Geochemistry* (ed. P.J. Coleman) *Perth University of Western Australia Press.*
Johnson, T., & Molnar, P., 1972: Focal mechanisms and plate tectonics of the southwest Pacific. *J. geophys. Res., 77*, pp. 5000.
Krause, D.C., 1973: Crustal plates of the Pacific and Solomon Seas. In *Oceanography of the South Pacific* (ed. R. Fraser) *New Zealand National Commission for UNESCO, Wellington.*
Luyendyk, B.P., Macdonald, K.C., & Bryan, W.B., 1973: Rifting history of the Woodlark Basin in the southwest Pacific. *Bull. Geol. Soc. Am., 84*, pp. 1125.
Milsom, J.S., 1970: Woodlark Basin, a minor center of sea-floor spreading in Melanesia. *J. geophys. Res., 75*, pp. 7335.
Milsom, J.S., 1973: Papuan Ultramafic Belt: gravity anomalies and the emplacement of ophiolites. *Geol. Soc. Am. Bull., 84*, pp. 2243.
Moores, E.M., 1973: Geotectonic significance of ultramafic rocks. *Earth Sci. Rev., 9*, pp. 241.
Mutter, J.C., 1975: A structural analysis of the Gulf of Papua and northwest Coral Sea region. *Bur. Miner. Resour. Aust. Rep. 179.*
Parkinson, W.D. & Curedale, R.G., 1962: Isomagnetic maps of eastern New Guinea for the epoch 1957.5. *Bur. Miner. Resour. Aust. Rep. 63.*
Piper, J.D.A., 1973: Interpretation of some magnetic anomalies over Iceland. *Tectonophysics, 16*, pp. 163.
Ripper, I.D., in prep.: Seismicity, earthquake focal mechanisms, volcanism and tectonics of the New Guinea Solomon Island region. *Bur. Miner. Resour. Aust. Rep.*
Smith, I.E., 1973: Late Cainozoic volcanism in the southeastern Papuan Islands. *Bur. Miner. Resour. Aust. Rec.* 1973/67 (unpubl.).
Smith, I.E., 1975: Eastern Papua, evolution of volcanism on a plate boundary. *Aust. Soc. Explor. Geophys., 6*, pp. 68-69.
St John, V.P., 1970: The gravity field and structure of Papua and New Guinea. *Aust. Petrol. Explor. Ass. (APEA) Journal. 41.*
Talwani, M., Windisch, C.C., & Langseth, M.G. Jr, 1971: Reykjanes Ridge crest: a detailed geophysical study. *J. geophys. Res., 79 (2)*, pp. 473.
Taylor, G.A.M., 1958: The 1951 eruption of Mount Lamington, Papua. *Bur. Miner. Resour. Aust. Bull. 38.*
Tilbury, L.A., in prep.: Geophysical results from the Gulf of Papua and Bismarck Sea. *Bur. Miner. Resour. Aust. Rec.*

CRUSTAL VARIATIONS IN THE SOLOMON–PAPUA–NEW GUINEA REGION BASED ON SEISMIC INVESTIGATIONS

D.M. Finlayson,
Bureau of Mineral Resources, Canberra, A.C.T.

Explosion seismic investigations provide the definition required to enable the variations in gross crustal structure over quite small areas to be outlined. Typifying the crustal structure in any particular area may however be misleading. A number of seismic surveys have now been conducted which outline the variations in crustal structure between the Barkley Tablelands of northern Australia and the Ontong Java Plateau of the western Pacific. These surveys involved a number of different shooting/recording configurations; land shooting and recording, marine shooting/land recording and marine shooting and recording.

The upper mantle is usually taken to begin where the P wave velocity approaches 8 km/s but over the region this is shown to vary between 7.7 and 8.6 km/s and occur at depths ranging from less than 5 km to 43 km. Some crustal thicknesses in "continental" Australia (27 km) appear to be much thinner than those on the Ontong Java Plateau (43 km) with considerable variation throughout the region in between. The parameters controlling the stability or otherwise of a region would therefore appear not to be those of the crust but those of the deeper mantle.

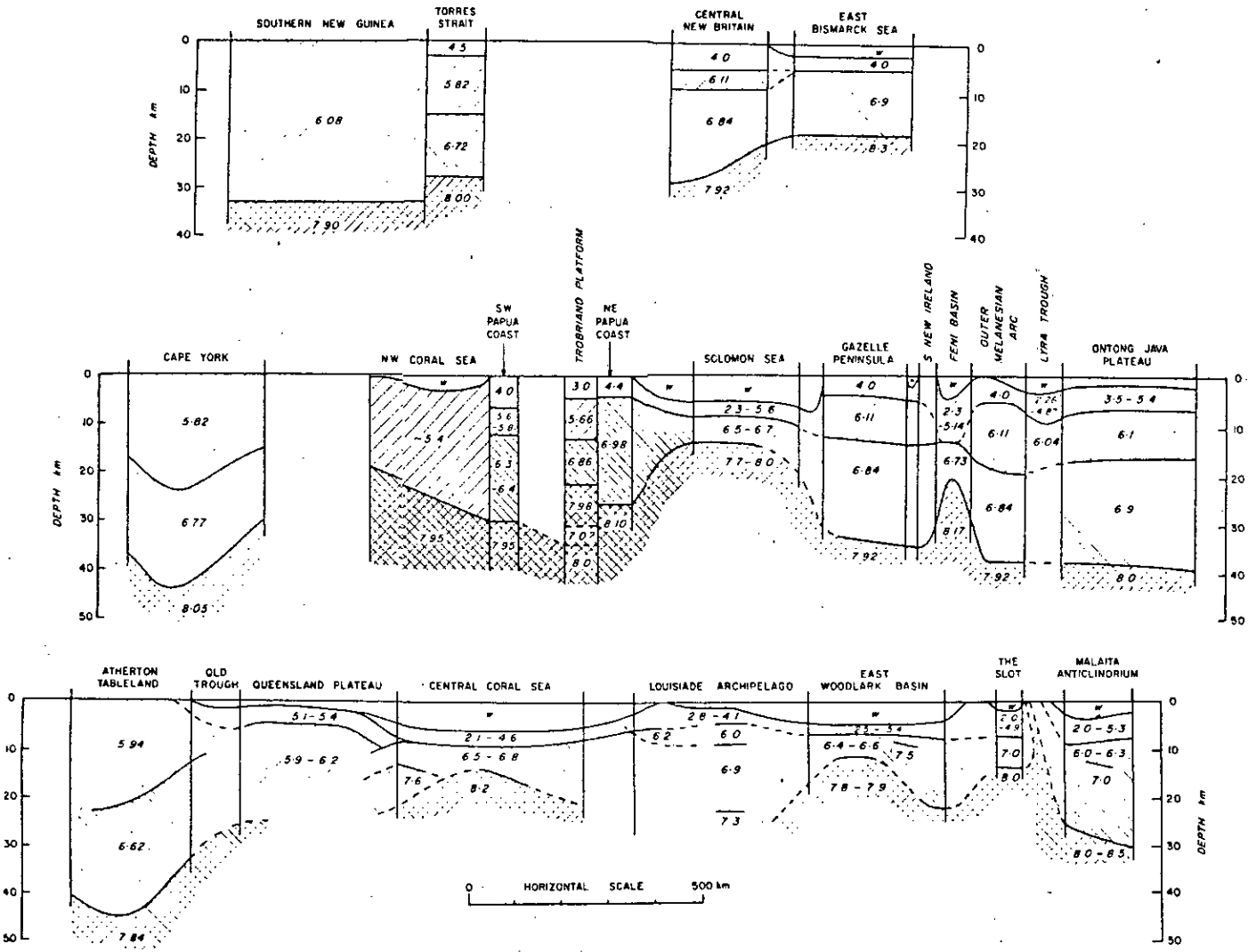

AUSTRALIAN-PACIFIC PLATE BOUNDARY
CRUSTAL THICKNESS VARIATIONS

UPPER MANTLE STRUCTURE FROM THE TRANS-AUSTRALIA SEISMIC SURVEY (TASS) AND OTHER SEISMIC REFRACTION DATA

By D. M. FINLAYSON, J. P. CULL, and B. J. DRUMMOND

(With 3 Tables and 8 Figures)

(MS received 27 June 1974; revised MS received 5 September 1974)

ABSTRACT

The recordings made during 1972 from large explosions at Kunanalling (W.A.), Mount Fitton (S.A.), and Bass Strait have added considerably to seismic refraction data measured over distances of 1000 km in continental Australia. Taken together with data from the 1956 Maralinga atomic bomb and 1970-71 Ord Dam explosions they show the existence of a refractor with apparent P-wave velocity in the range 8.26-8.29 km/s, which is interpreted as the Moho under shield regions, at a depth of 34 km under Kalgoorlie and deepening eastward to 39 km under Maralinga. In northern South Australia and farther north and east this refractor is evident as a sub-Moho refractor at a depth of about 60 km; the Moho refractor is also evident, with an apparent P velocity of 8.04 ± 0.04 km/s at a depth of 40 km. Two computer models (TASS-1a and 2a) match the observed data. The subsequent arrivals recorded are consistent with the velocity of 8.53 km/s in a refractor at 165 km depth interpreted from the Ord Dam; there is little conclusive evidence for a low-velocity zone above this depth.

INTRODUCTION

During 1972 the Bureau of Mineral Resources, Geology & Geophysics (BMR) detonated three large explosions as energy sources for seismic refraction observations out to distances greater than 1000 km. The explosions were at Mount Fitton in the north Flinders Ranges, at Kunanalling near Kalgoorlie, and in Bass Strait south of Orbost (Fig. 1). BMR combined with the Australian National University and the University of Adelaide to set up recording stations across the Nullarbor Plain, across New South Wales, from Port Augusta (S.A.) to Alice Springs (N.T.), and north of Meekatharra (W.A.). These recording lines, together with the permanent recording networks throughout Australia, were designed to give results that would supplement earlier long-distance seismic refraction information obtained from the atomic bomb tests at Maralinga during 1956 (Bolt, Doyle, & Sutton, 1958; Doyle & Everingham, 1964) and the Ord River explosions of 1970-71 (Denham *et al.*, 1972; Simpson, 1973).

THE EXPLOSIONS

In 1971 BMR received a gift from West Australian Petroleum Pty Ltd (WAPET) of 355 tonnes of Du Pont Nitramon WW explosive that was surplus to their requirements, and it was decided to use some of this explosive to further knowledge of the upper mantle structure of the Australian continent by seismic refraction methods. Details of the seismic operation are given by Finlayson & Drummond (1974). The Western Australian and South Australian Departments of Mines assisted in locating suitable sites for two land explosions.

The *Mount Fitton South Copper Mine* is at the northern end of the Mount Painter Metallogenic Province of the north Flinders Ranges in South Australia (Coats & Blissett, 1971), and was worked from 1889 until 1922. The mine workings cut through a series of sheared and jointed coarse-grained granites of Carpentarian age into Precambrian crystalline basement, which consisted of metamorphosed Proterozoic sediments intruded by several generations of granite.

Eighty tonnes of explosive packed in 30 kg cans was loaded into the end of the main adit, which went horizontally into the hillside for 100 m. Priming charges of AN 60 gelignite with no delays were placed throughout the explosive, and a multiple-detonation cord was run to the adit portal. The main adit was sandbagged up to half-way along its length, and the open stopes above the main adit were filled with broken rock. The explosive was detonated electrically, and the shot time was measured by recording VNG radio time signals, the signal from a geophone near the adit portal, and a chronometer signal on a multi-channel recorder. Details of the shot-point data of all three shots are given in Table I.

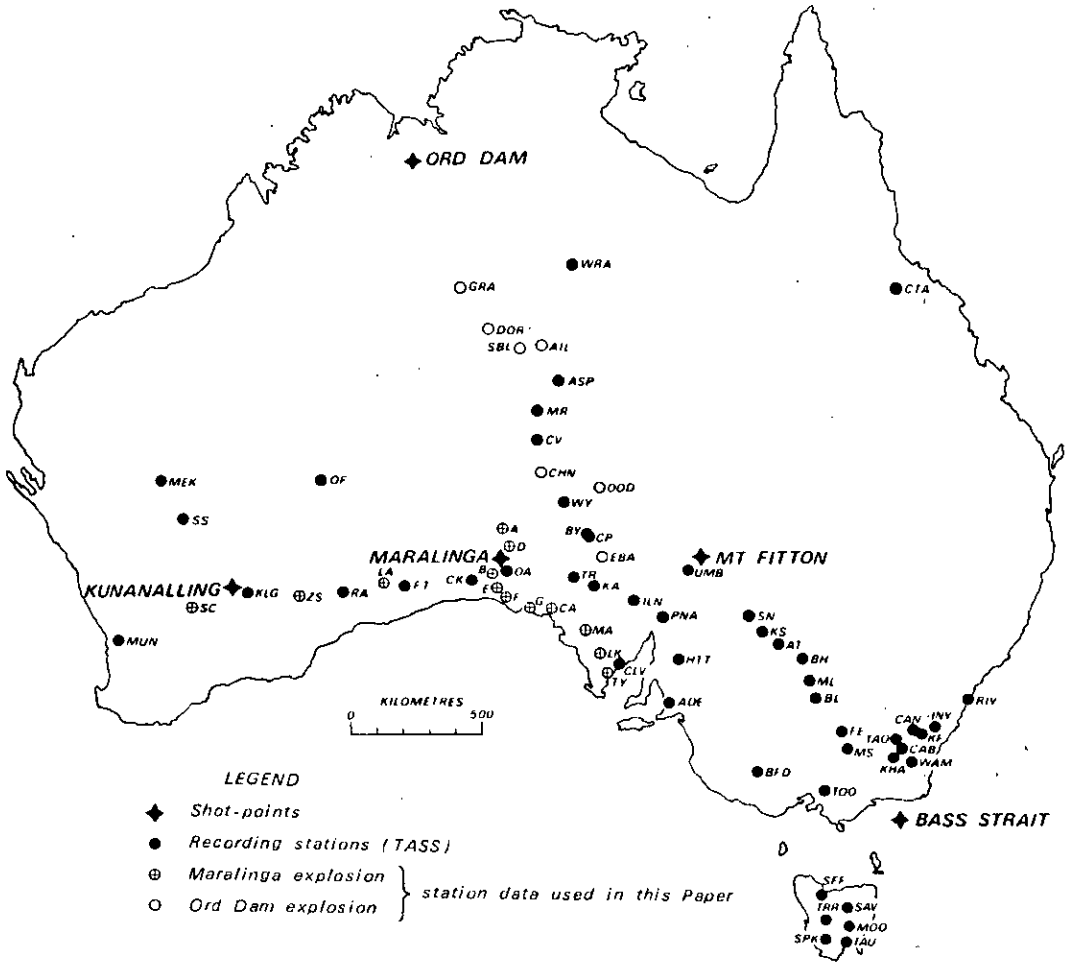

Fig. 1. TASS recording station locations and Maralinga and Ord Dam survey stations from which data has been used in this paper.

The *Premier Gold Mine at Kunanalling* is 40 km west of Kalgoorlie and 33 km north of Coolgardie; Western Mining Corp. indicated that there was little possibility of its ever becoming a viable gold mine again. The rocks in the area are composed of a metamorphosed shale, greywacke, and granite sequence alternating with a sequence of altered mafic and ultramafic extrusive igneous rocks (Kriewaldt, 1969). The Premier mine shaft used for the explosion was in sheared oxidized Archaean 'greenstone'. Eighty tonnes of Du Pont Nitramon was loaded into a drive off the bottom of the main shaft, which was 40 m deep. Four separate Cordtex lines were run through the explosive stack with AN60 gelignite primers attached at intervals. The drive was stemmed with broken dirt in bags to the bottom of the shaft and the firing lines were run to the surface. The explosive was detonated electrically, and the shot time recorded on a multi-channel recorder as at Mount Fitton.

The *Bass Strait shot* was similar in design to 10-tonne marine shots fired off the coast of Scotland by the Institute of Geological Sciences (Jacob & Willmore, 1972). Those were fired in an attempt to obtain teleseismic information out to angular distances of 90°, and further trial shots were recommended by a Working Group of the International Association of Seismology and Physics of the Earth's Interior (IASPEI) to provide a relatively cheap method of study of the Earth's deep mantle (Finlayson & Drummond, *op. cit.*).

A site for the shot was selected in Bass Strait where the sea bottom has a minimum

TABLE I
TASS Shot Parameters

	Mount Fitton	Kunanalling	Bass Strait
Latitude	30°00.4'S	30°40.5'	38°17.6'
Longitude	139°33.8'S	121°04.0'	148°48.6'
Date	25 Oct. 1972	25 Oct. 1972	19 Dec. 1972
Shot time (UT)	01h 05m 00.4s	04h 05m 01.23s	07h 50m 00.77s
Size (tonnes)	80	80	10
Explosive	Du Pont Nitramon WW	Du Pont Nitramon WW	RDX-TNT
Estimated magnitude m_b	3.7	3.1	3.8
Depth of water	—	—	250m

gradient at 250 m depth. An explosive consultant was engaged to design and fire the shot in co-operation with the Department of Supply explosives factory at St Marys, N.S.W. Ten tonnes of RDX-TNT in 35-kg cans was built into a steel cage and deployed from the oil rig supply vessel *Smit-Lloyd 33*. RDX-TNT is estimated to be 24 percent more powerful than ordinary TNT.

The charge was suspended 25 m above a 15 tonne concrete 'sinker' on the sea-bed by a steel rope connected to four mooring buoys located 18 m below the water surface. Four Cordtex lines were run from a 35-kg primer charge in the top of the main charge to a surface buoy. A detonator and primer were attached to the top of the Cordtex after the charge had been positioned, and the shot was detonated electrically with 2 km of firing line. Shortly before detonation, the charge seems to have settled on the sea bottom, possibly as a result of leaks in the main support buoys, and thus the ideal geometry for maximum generation of seismic energy was not achieved. The shot was positioned by a Shoran VHF network and timed by recording an impulse from the shot-firing mechanism together with VNG radio time signals and a crystal-clock time code on a multi-channel recorder.

The shot site was on the northern flank of the Gippsland Basin where 1 to 2 km of Ordovician to Miocene sediments overlie Cambrian or Precambrian metamorphic basement. The Upper Cretaceous to Miocene marine sediments contain oil source and reservoir rocks (Weeks & Hopkins, 1967; Underwood, 1969). The site lies near the edge of the continental shelf (which is usually taken as the 200 m isobath), and the sea bottom gradient was estimated to be 10°.

RECORDING STATIONS

The three shots were fired on two separate days, the two land shots on 25 October and the marine shot on 19 December. The temporary and permanent recording stations involved are plotted in Figure 1.

The permanent seismic observatory network recordings were nearly all obtained from short-period seismometers that use galvanometers and record on photographic paper. The temporary recording stations were nearly all short-period seismometers used in conjunction with a high-gain amplifier and slow-speed tape recorders. All stations recorded VNG radio time signals as their time reference standard. The survey was designed to obtain upper mantle arrivals out to distances greater than 1000 km, and no recordings were made at distances less than 200 km except where permanent stations happened to be within that radius.

The main temporary recording lines for the Mount Fitton and Kunanalling shots were across the Nullarbor Plain, from Mount Fitton to Alice Springs, and from Mount Fitton to the Snowy Mountains in southeast New South Wales. The main temporary recording line for the Bass Strait shot was from the Snowy Mountains to Mount Fitton. Finlayson & Drummond (*op. cit.*) list all the station positions and recorded data except those obtained along the Mount Fitton/Snowy Mountains line, which are being analysed separately by Australian National University staff.

NULLABOR REGION VELOCITIES AND UPPER MANTLE STRUCTURE

Most of the data were recorded in the range 200 to 1400 km and Figure 2 shows the travel times of the seismic arrivals plotted on a reduced scale against distance from shot to recorder. The data from the 1956 Maralinga atom bomb tests (Bolt *et al.*, 1958) are also plotted. A least-squares analysis of the data in the distance range 200-1400 km gives apparent P_n velocities and intercepts of 8.31 ± 0.01 km/s and 8.57 ± 0.17 s from the Mount Fitton shot, and 8.26 ± 0.02 km/s and 7.34 ± 0.25 s from the Kunanalling shot (Table

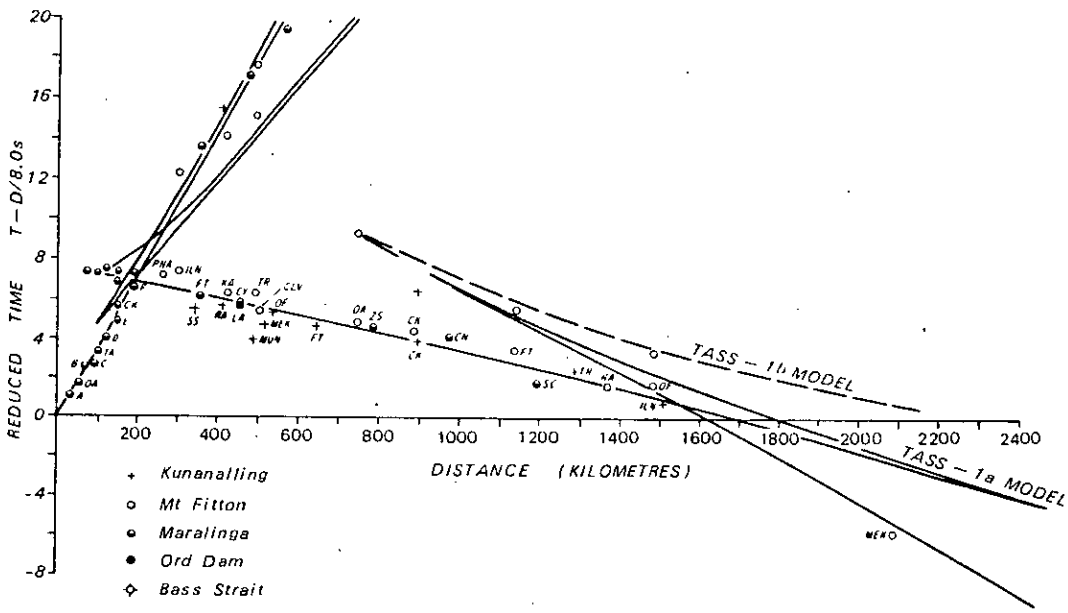

Fig. 2. Nullarbor line time-distance plot (times reduced by distance/8.0 km/s).

II). The Maralinga data towards the west give an apparent P_n velocity of 8.21 ± 0.01 km/s and intercept of 7.24 ± 0.06 s when the Southern Cross data are excluded. Southern Cross, together with other stations west of Kalgoorlie (MUN, MEK, and SS), appears to record arrivals earlier than stations on the Nullarbor line, and this may indicate a different crustal structure. The combined data from the Nullarbor stations give a least-squares apparent P_n velocity of 8.29 ± 0.02 km/s and intercept of 8.08 ± 0.02 s. The data from Coober Pedy (CY), Mount Brady (BY), Cleve (CLV), and Officer Basin (OF) also fit these values even though they are not on the direct recording line across the Nullarbor.

Various corrections for Earth curvature must be applied to the apparent velocities in order to obtain a value for the velocity in the refractor. The first correction takes into account the difference in arc lengths at the Earth's surface and at the refractor depth (Mereu, 1967); the second correction takes into account differences in the arc-chord path length, which become significant at distances greater than 600 km (Cull, 1973). These corrections reduce the apparent P_n velocity for the Nullarbor region from 8.29 km/s to 8.23 km/s (Table II). Mereu (*op. cit.*) also outlines the procedure for correcting depth estimates, and observes that corrections to refractor depths become important only at depths greater than 60 km and that, in practice, the apparent velocities may be used with uncorrected time/depth data to derive depths less than 60 km.

The data from the Mount Fitton, Kunanalling, and Maralinga shots along the east-west traverse across the Nullarbor have been treated as a reversed profile to obtain refractor depth estimates by the time/depth method (Hawkins, 1961). The TASS survey recorded very few crustal first arrivals and therefore the velocity model adopted for the crust must be obtained from other surveys. Bolt *et al.* (1958) give a crustal P_1 velocity of 6.03 ± 0.09 km/s from the Maralinga data and Doyle & Everingham (1964) derive a velocity of 6.30 ± 0.06 km/s for the region southeast of Maralinga. Hawkins *et al.* (1965) obtained basement velocities of 6.26 km/s on the continental shelf off South Australia, and Stewart (1972) has taken all these results into account in his derivation of a crustal model for use with the South Australian seismic recording network to locate local earthquakes. Stewart's 1971 (*b*) preferred model has a uniform crust with P velocity 6.25 ± 0.03 km/s overlying a mantle with apparent velocity 8.02 ± 0.03 km/s.

The most recent investigation of crustal velocity in the shield region is BMR's Geotraverse, which adjoins the western end of the TASS survey (Mathur, 1973). Just west of Kalgoorlie Mathur derives a P_1 velocity of 6.13± 0.01 km/s, a P_2 velocity of 6.74 km/s at 19.5 km depth, and an apparent P_n velocity of 8.29 ± 0.39 km/s at a depth of 34.0 km.

TABLE II
Least-Squares Velocities and Intercepts

Area	Apparent velocity km/s	Intercept s	No. of data	RMS residual s	Corrected velocity* km/s
P_n					
Mount Fitton west	8.31 ± 0.01	8.57 ± 0.17	9	0.24	
Kunanalling east	8.26 ± 0.02	7.34 ± 0.25	6	0.32	
Maralinga west	8.21 ± 0.01	7.24 ± 0.06	4	0.03	
Nullarbor combined	8.29 ± 0.02	8.08 ± 0.20	19	0.41	8.23
Mount Fitton north	8.24 ± 0.02	8.63 ± 0.32	5	0.14	
Ord Dam south	8.27 ± 0.01	8.80 ± 0.19	11	0.15	
Central Australia combined	8.26 ± 0.01	8.82 ± 0.16	16	0.16	8.18
Adelaide Geosyncline	8.04 ± 0.04	7.71 ± 0.28	9	0.28	7.98
Mount Fitton south and east	8.31 ± 0.04	9.29 ± 0.49	8	0.51	
Bass Strait north and west	8.20 ± 0.03	8.32 ± 0.36	6	0.35	
S_n					
TASS and Maralinga	4.78 ± 0.03	17.08 ± 1.04	15	1.64	4.75

* Corrected velocity = apparent velocity with Earth curvature corrections applied (see text).

Cleary (1973) has indicated that the data available in shield regions suggest a P_1 velocity of 6.2 km/s and a P_2 velocity greater than 6.5 km/s at 20 km depth, and these are the values adopted by Simpson (1973) for his modelling studies of the Ord explosion data along the Ord-Adelaide line. The crustal model adopted for the interpretation of the TASS Nullarbor data consists of a uniform layer with a P_1 velocity of 6.20 km/s and a thickness of 20 km overlying a lower crust with a P_2 velocity of 6.70 km/s.

Time depths were computed from arrivals from opposite directions for five Nullarbor stations and were used to derive delay times at a further eight sites. The resulting depths to the Moho refractor with a corrected P_n velocity of 8.23 ± 0.02 km/s are shown in Figure 3. The values show a general thinning of the crust from east to west: the depth to the refractor ranges between 41 and 49 km in the Adelaide Geosyncline region, decreases to 39-40 km under the eastern Nullarbor shield area, and further decreases to 34-35 km under the western Nullarbor. The crust and upper mantle section in the Adelaide Geosyncline are discussed later in this paper, and it is probable that a wedge of upper mantle material with velocity 7.96 km/s occurs in that region at a depth of 40 km.

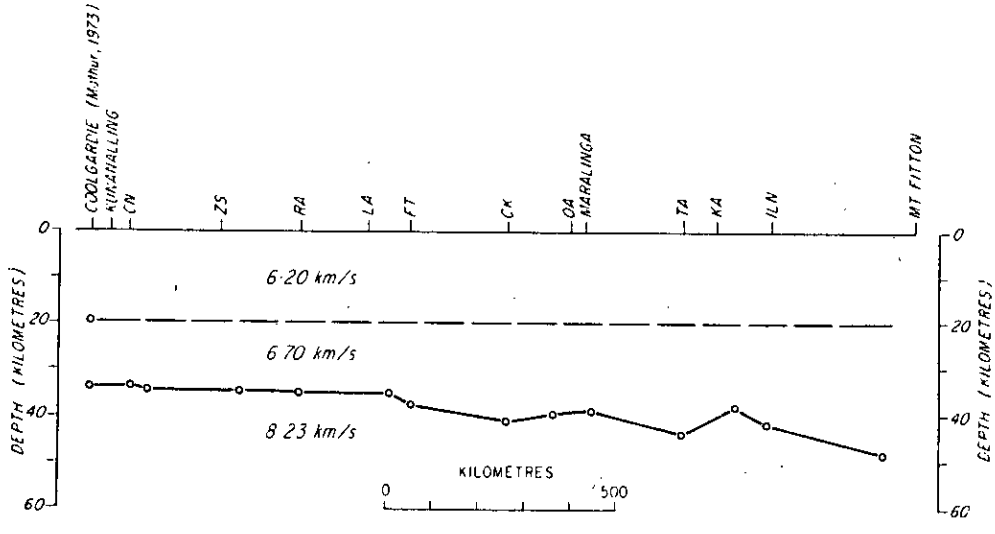

Fig. 3. TASS Nullarbor profile.

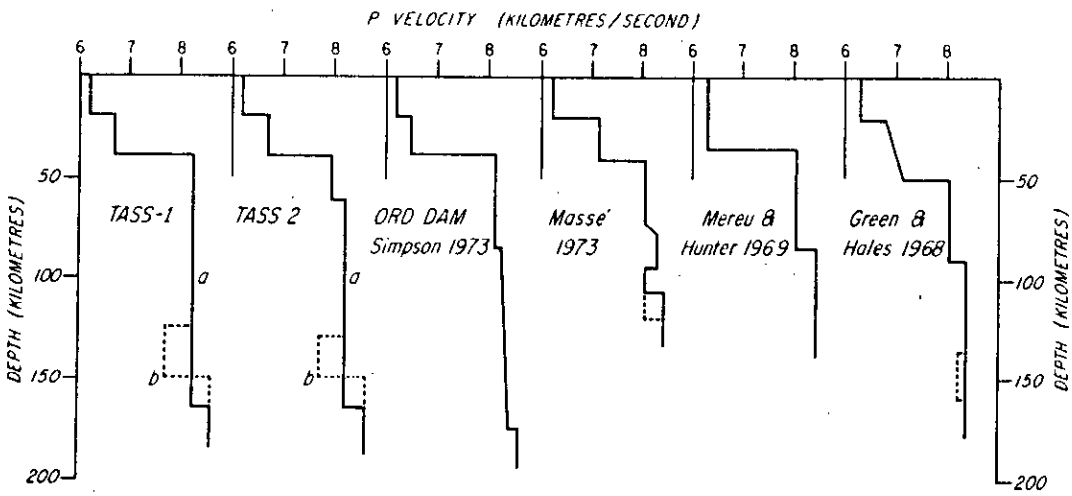

Fig. 4. Upper mantle P wave velocity models.

A spherically symmetric model of the crust and upper mantle structure in the Nullarbor region (Fig. 4, TASS-1a) was incorporated into a computer ray-tracing program (Cull, 1973). This model had a mantle structure similar to that of Simpson (1973) from the results of the Ord Dam explosion. The resultant fit of the data to the model travel-time curve (Fig. 2) was considered to be good along the section with apparent velocity 8.29 km/s.

The triplication in the travel time curve at about 1400 km results from the increase in apparent velocity to approximately 8.85 km/s within the upper mantle.

The possibility of there being a low-velocity zone within the upper mantle was considered, and the TASS-1b model (Fig. 4) and a number of variations were tried. Figure 5 illustrates the record sections for some of the recording stations across the Nullarbor; it is difficult to identify the retrograde cusp points with any certainty. Bearing in mind the amplitude variations expected at the cusp points, these records offer no convincing evidence for a low-velocity zone for P waves.

CENTRAL AUSTRALIA VELOCITIES AND UPPER MANTLE STRUCTURE

The seismic arrivals from the Mount Fitton shot recorded along the lines towards Alice Springs and Adelaide, together with those from Maralinga explosions towards Adelaide and the Ord Dam explosions southward across central Australia, are plotted in Figure 6. A least-squares analysis of the arrivals from the Maralinga explosion towards Adelaide gives an apparent P_n velocity of 8.05 ± 0.04 km/s and an intercept of 7.74 ± 9.99 s (Doyle & Everingham, 1964), and the results from the Mount Fitton shot in the Adelaide Geosyncline region seem to substantiate that this velocity is lower than that in the shield regions. There is a degree of scatter from the Mount Fitton shot not evident in the Maralinga data; the good first arrival at CLV seems particularly early.

However, at distances beyond 550 km towards Alice Springs the least-squares analysis gives an apparent velocity of 8.24 ± 0.02 km/s and intercept of 8.63 ± 0.32 s for P_n arrivals and the data, together with the Ord Dam data, can be treated as a reversed profile, as was done with the Nullarbor data.

The first interpretation model for the crust was taken to be the same as that for the Nullarbor line. The resulting Moho depths varied between 44 km and 48 km over the 2000 km profile. This was about 6-8 km deeper than the 8.23 km/s refractor under the Nullarbor Plain and was also thicker than the value of about 40 km determined from surface-wave dispersion studies (Thomas, 1969), so alternative models were tried.

The feature of the TASS and associated data which seems to indicate that the first model is too simple is that the first arrivals in the Adelaide Geosyncline region give an apparent velocity of 8.04 ± 0.04 km/s and an intercept of 7.71 ± 0.28 s (Table II). This velocity agrees with the upper mantle apparent velocity of 8.02 ± 0.03 km/s that Stewart (1972) used for his earthquake modelling studies. The data from the Maralinga and Mount Fitton shots are not along reversed profiles, so it

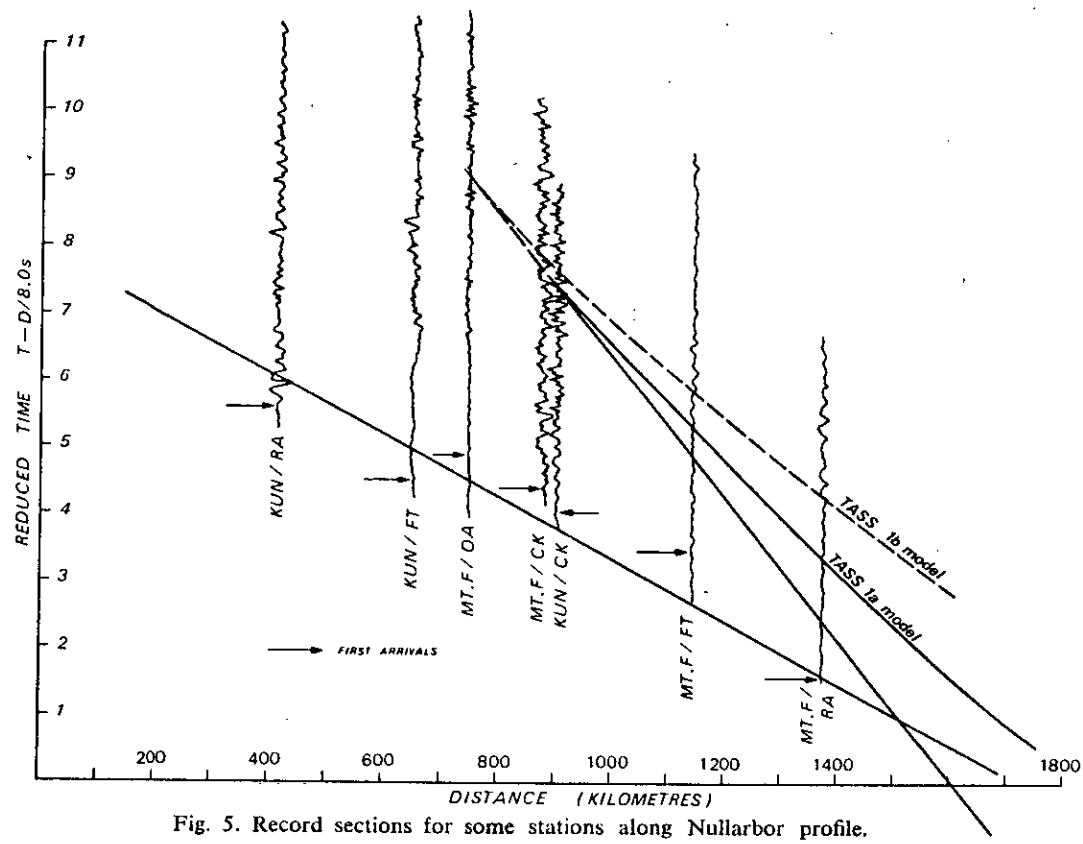

Fig. 5. Record sections for some stations along Nullarbor profile.

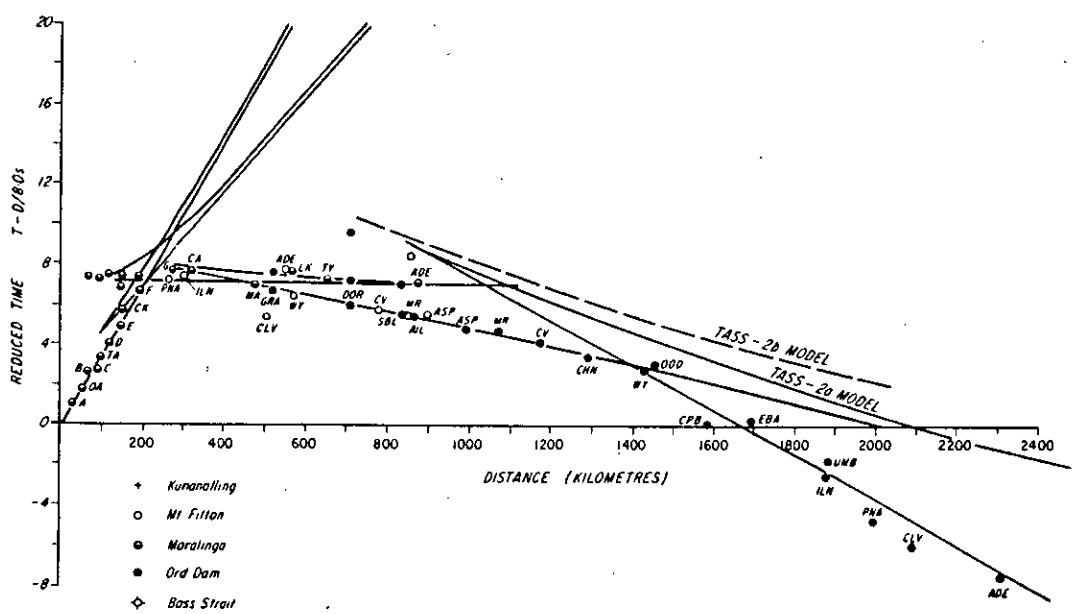

Fig. 6. Central Australian line time-distance plot (times reduced by distance/8.0 km/s).

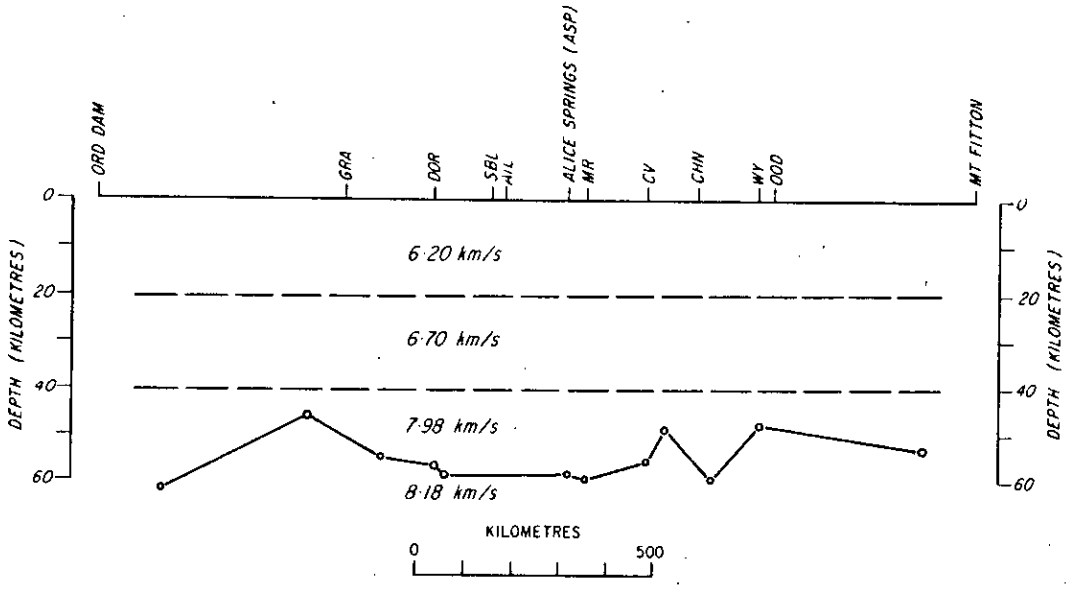

Fig. 7. Central Australian profile.

would be inappropriate to use them in a formal refraction interpretation; nor are there sufficient data for a time-term analysis. However, if all the data across central Australia including the Adelaide Geosyncline are combined, computer modelling of spherical layered Earth models shows that they are consistent with a Moho velocity of 7.96 km/s at 40 km depth and a further increase in velocity to 8.18 km/s at a depth of 61 km (Fig. 4, TASS-2a). The resultant travel time curve is plotted in Figure 6. The TASS data in the Adelaide Geosyncline itself, however, are also consistent with the models of White (1969) and Stewart (1972), which do not include the 8.18 km/s deeper horizon and may indicate that the geosyncline upper mantle structure differs in this respect from the areas to the west, north, and east.

The data from the 8.18 km/s refractor in central Australia can be treated as a reversed profile from the Ord Dam to Mount Fitton using the TASS-2a model for the crustal and Moho refractors with horizontal boundaries. The resultant profile is shown in Figure 7. The large variations in depth to the sub-Moho refractor correspond to comparatively small travel-time residuals which are amplified because of the small seismic velocity contrast across the boundary. These residuals could also be explained by smaller depth variations in one of the upper refracting boundaries. Thus those variations should not be taken as a definitive interpretation, though the average depth to the boundary is probably fairly accurate.

A low-velocity zone at a depth of 130 km was modelled also (TASS-2b), but as with the Nullarbor line there was not sufficient evidence in the record sections to define the retrograde part of the time/distance curve with any survey.

OBSERVATIONS IN SOUTH AUSTRALIA, VICTORIA, AND TASMANIA

The data recorded in Victoria, eastern South Australia, and Tasmania from the Bass Strait and Mount Fitton shots are plotted in Figure 8. There are not sufficient data to provide a thorough interpretation, but a number of features are evident. At distances in the range 200 to 1200 km the apparent velocity of approximately 8.25 km/s still appears. A least-squares analysis of data from TOO, BFD, and the eastern Adelaide network stations gives an apparent velocity of 8.31 ± 0.04 km/s and intercept of 9.29 ± 0.48 s from the Mount Fitton shot, and a velocity of 8.20 ± 0.03 km/s and intercept of 8.32 ± 0.36 s from the Bass Strait shot. The TASS-2a travel time curve has been superimposed on Figure 8 and it is seen that the data are consistent with that model. The data from a line farther north from Mount Fitton across New South Wales to the Snowy Mountains seismic recording network are being analysed by Australian National Uni-

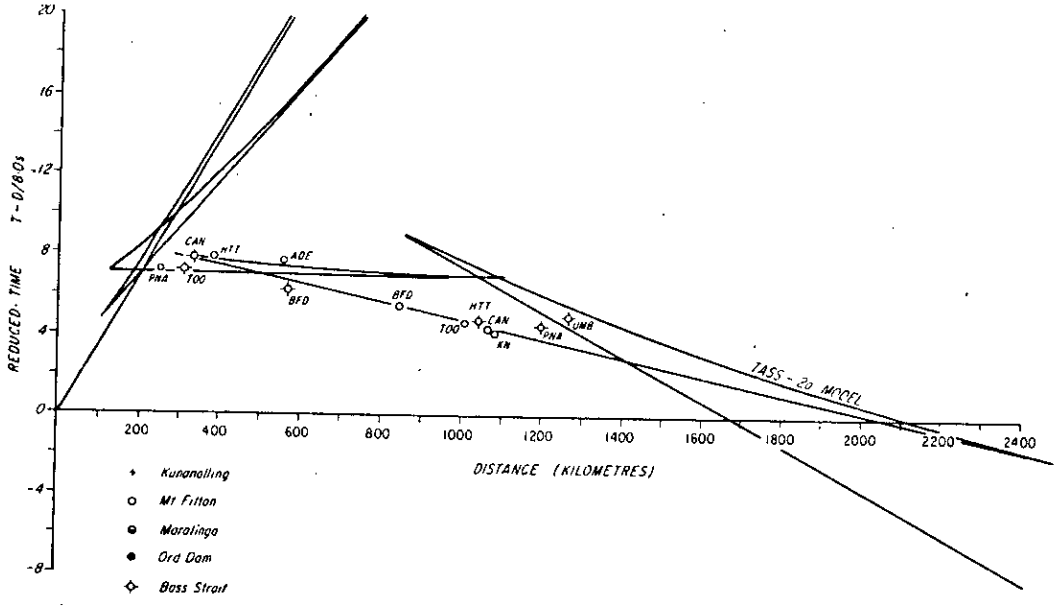

Fig. 8. South Australian-Victorian time-distance plot (times reduced by distance/8.0 km/s).

versity staff and should provide a more detailed interpretation. Further interpretation of the Bass Strait shot data together with other data in the region of the Tasman Geosyncline (Doyle *et al.*, 1959 Doyle *et al.*, 1966; Underwood, 1969) is also being undertaken.

S_n ARRIVALS

Not many shear wave arrivals were identified on the TASS records, but in central and western Australia the data are consistent with the Maralinga data. A least-squares analysis of S arrivals in the range 250 to 1400 km from the TASS and Maralinga data gives an apparent S_n velocity of 4.78 ± 0.03 km/s and an intercept of 17.08 ± 1.04 s (Table II). These are compatible with the velocity of 4.75 ± 0.07 km/s and intercept of 12.52 ± 2.29 s obtained by Denham *et al.* (1972) within the range 400 to 900 km from the Ord Dam explosions.

MAGNITUDES

Estimates of the magnitudes of the three explosions have been made from a number of permanent observatory records. The magnitude of a seismic event can be expressed in the form

$$m = \log (A/T) + A_2$$

where A is the ground amplitude in nanometres takes as the maximum amplitude of the initial P phase, T is the period in seconds, and A_2 is a function of distance and depth of source. The values of A_2 were taken from the curve derived by Everingham (1968) for m_b from Western Australian earthquakes. Five seismic stations were used to derive the value of m_b = 3.7 for the Mount Fitton shot, two for the value m_b = 3.1 for the Kunanalling shot, and four for the value m_b = 3.8 for the Bass Strait shot (Table I).

COMMENTS

In the Australian continent, the interpretations by Denham *et al.* (1972) and Simpson (1973) of long-range seismic refraction data were the first of their types to define sub-Moho velocity structures. In North America many such investigations have been undertaken using both chemical and nuclear explosion data (Green & Hales, 1968; Helmberger & Wiggins, 1971; Herrin, 1969; Masse *et al.*, 1972; Masse, 1973*a*; Mereu & Hunter, 1969). Some upper mantle P velocity profiles interpreted for North America are included in Figure 4.

The TASS-1a models (Table III) have features not previously recognized in the Australian continent. The refractor resulting in an apparent velocity of 8.26-8.29 km/s is recognized as the Moho under the shield areas of the Nullarbor Plain, but it dips to depths of roughly 60 km under central and eastern Australia, where a Moho refractor with apparent velocity of approximately 8.03 km/s is recognized at depths of roughly 40 km. It should be noted that reconnaissance deep seismic reflection work in the Broken Hill/Mildura region detected sub-Moho reflectors at two-way reflec-

TABLE III
TASS Computer Models

TASS-1a		TASS-1b		TASS-2a		TASS-2b	
depth, km	velocity km/s	depth	velocity	depth	velocity	depth	velocity
0	6.20	0	6.20	0	6.20	0	6.20
20	6.20	20	6.20	20	6.20	20	6.20
20	6.70	20	6.70	20	6.70	20	6.70
40	6.70	40	6.70	40	6.70	40	6.70
40	8.23	40	8.23	40	7.98	40	7.98
165	8.23	125	8.23	61	7.98	61	7.98
165	8.53	125	7.70	61	8.18	61	8.18
		150	7.70	165	8.18	130	8.18
		150	8.53	165	8.53	130	7.70
						150	7.70
						150	8.53

tion times of 14 to 15 s, and these have been interpreted as a horizon at a depth of about 50 km (Branson *et al.*, 1972). Similar two-tier increases in velocity at the Moho have been recognized under the Canadian shield (Gurbuz, 1970; Hall & Hajnal, 1973), where the Moho velocity of 7.90 km/s at 34 km gives way to a velocity of 8.48 km/s at 47 km.

It is also noted from the harmonic analysis of gravity anomalies along a number of profiles across Australia (P. Wellman, *pers. comm.*) that the power spectra reveal a distinct suggestion that the sources of most of the gravity anomalies are shallower than 60 km, which is approximately the depth to the sub-Moho refractor in the TASS-2a model.

Velocity distributions below 60 km are not well determined from TASS data, but inspection of subsequent seismic arrivals shows little evidence for a P-wave low-velocity zone similar to that indicated in the TASS-1b and 2b models at depths of roughly 130 km. However, data of better quality are required before the presence of such a zone can be disproved conclusively. Masse (1973*b*) has mentioned the possibility of such a low-velocity zone for the shield areas of Australia, but his velocity model is markedly different from the TASS models and the Ord model of Simpson (1973) and does not fit the observed data.

A number of points are raised by the wedging out of the 7.98 km/s sub-Moho layer from east to west. Associations can be made with the age of the upper crust, which is predominantly less than 500 m.y. in eastern Australia but increases to more than 3000 m.y. in the Archaean shield areas (Geological Society of Australia, 1971), and with heat flow, which decreases from east to west (Jaeger, 1970). If thinning of the sub-Moho layer with age is postulated, this implies a possible aging process associated with phase changes in the upper mantle. If this transformation is associated with energy release, it may account for gross features of heat flow across the continent.

Variations in the crustal and upper mantle velocities have been recognized as the source of P-wave travel-time residuals to Australian permanent seismic recording stations (Cleary, 1967). Negative residuals up to 1.5 s have been found in the shield areas and positive residuals up to 1.1 s in southeastern Australia. From the Canniken explosion Cleary *et al.* (1972) also found a residual difference of 1.3 s along their recording line from the Snowy Mountains to Maralinga. We estimate that the velocity variations in the upper mantle determined from the TASS results can only account for 0.5 s in the region down to 60 km; deeper regional velocity differences must account for the remaining travel-time residuals.

ACKNOWLEDGMENTS

We are grateful for the assistance received in firing the three TASS explosions from the Western and South Australian Departments of Mines, Esso Australia Pty Ltd, Smit-Lloyd (Australia) Pty Ltd, and the Department of Supply. We are also grateful to West Australian Petroleum Pty Ltd for donating the explosives for the land shots. We are indebted to Dr D. J. Sutton (University of Adelaide), Dr J. P. Webb (University of Queensland), Dr W. D. Parkinson (University of Tasmania), and Dr L. Drake (Riverview College Observatory) for making seismic records available, and to the Australian National University team, who recorded across New South Wales and whose results will be published elsewhere. This paper is published with the permission of the Director of the Bureau of Mineral Resources, Geology & Geophysics, Canberra.

REFERENCES

BOLT, B. A., DOYLE, H. A., & SUTTON, D. J., 1958: Seismic observations from the 1956 atomic explosions in Australia. *Geophys. J. R. astron. Soc., 1*, p. 135.

CLEARY, J. R., 1967: P times to Australian stations from nuclear explosions. *Bull. seism. Soc. Am., 57*, p. 773.

CLEARY, J. R., 1973: Australian crustal structure. *Proc. IUGG Congress, Moscow*, in *Tectonophysics, 20*, p. 241.

CLEARY, J. R., SIMPSON, D. W., & MUIRHEAD, K. J., 1972: Variations in Australian upper mantle structure from observations of the Canniken explosion. *Nature, 236*, p. 111.

COATS, R. P., & BLISSETT, A. H., 1971: Regional and economic geology of the Mount Painter Province. *Geol. Surv. S. Aust. Bull. 43*.

CULL, J. P., 1973: Seismic ray tracing in a spherical Earth using computer models. *Bur. Miner. Resour. Aust. Rec.* 1973/122 (unpubl.).

DENHAM, D., SIMPSON, D. W., GREGSON, P. J., & SUTTON, D. J., 1972: Travel times and amplitudes from explosions in northern Australia. *Geophys. J.R. astron. Soc., 28*, pp. 225-235.

DOYLE, H. A., & EVERINGHAM, I. B., 1964: Seismic velocities and crustal structure in southern Australia. *J. geol. Soc. Aust., 11*, p. 141.

DOYLE, H. A., EVERINGHAM, I. B., & HOGAN, T. K., 1959: Seismic recordings of large explosions in southeastern Australia. *Aust. J. Phys., 12*, p. 222.

DOYLE, H. A., UNDERWOOD, R., & POLAK, E. J., 1966: Seismic velocities from explosions off the central coast of New South Wales. *J. geol. Soc. Aust., 13*, p. 355.

EVERINGHAM, I. B., 1968: Mundaring Geophysical Observatory annual report 1966. *Bur. Miner. Resour. Aust. Rec.* 1968/97 (unpubl.).

FINLAYSON, D. M., & DRUMMOND, B. J., 1974: Trans-Australia seismic survey (TASS) 1972, operational report. *Bur. Miner. Resour. Aust. Rec.* 74/83 (unpubl.).

GEOLOGICAL SOCIETY OF AUSTRALIA, 1971: Tectonic map of Australia and New Guinea, 1:5 000 000. *Sydney, Geol. Soc. Aust.*

GREEN, R. W. E., & HALES, A. L., 1968—The travel times of P waves to 30° in the central United States and upper mantle structure. *Bull. seism. Soc. Am., 58*, pp. 267-289.

GURBUZ, B. M., 1970: A study of the Earth's crust and upper mantle using travel times and spectrum characteristics of body waves. *Bull. seism. Soc. Am., 60*, pp. 1921-1935.

HALL, D. H., & HAJNAL, Z., 1973: Deep seismic crustal studies in Manitoba. *Bull. seism. Soc. Am., 63(3)*, pp. 885-910.

HAWKINS, L. V., 1961: The reciprocal method of routine shallow seismic refraction investigations. *Geophysics., 26(6)*, pp. 806-819.

HAWKINS, L. V., HENNION, J. F., NAFE, J. E., & DOYLE, H. A., 1965: Marine seismic refraction studies on the continental margin to the south of Australia. *Deep Sea Res., 12*, pp. 479-495.

HELMBERGER, D., & WIGGINS, R. A., 1971: Upper mantle structure of mid-western United States. *J. geophys. Res., 76*, pp. 3229-3245.

HERRIN, E., 1969: Regional variations of P wave velocity in the upper mantle beneath North America. In *The Earth's Crust and Upper Mantle. Am. geophys. Un. Monogr. 13*, pp. 242-246.

JACOB, A. W. B., & WILLMORE, P. L., 1972: Teleseismic P waves from a 10 ton explosion. *Nature, 236*, p. 305.

JAEGER, J. C., 1970: Heat flow and radioactivity in Australia. *Earth planet. Sci. Lett., 8*, p. 285.

KRIEWALDT, M. J. B., 1969: Kalgoorlie, W.A.: 1:250 000 Geological Series. *Geol. Surv. W. Aust. explan. Notes* SH/51-9.

MASSE, R. P., 1973*a*: Compressional velocity distribution beneath central and eastern north America. *Bull. seism. Soc. Am., 63(3)*, pp. 911-935.

MASSE, R. P., 1973*b*: Upper mantle compressional velocity and continental drift rates. *Nature Phys. Sci., 245*, pp. 134-135.

MASSE, R. P., LANDISMAN, M., & JENKINS, J. B., 1972: An investigation of the upper mantle compressional velocity distribution beneath the Basin and Range Province. *Geophys. J.R. astron. Soc., 30*, pp. 19-36.

MATHUR, S. P., 1973: Crustal structure in southwestern Australia. *Bur. Miner. Resour. Aust. Rec.* 1973/112 (unpubl.).

MEREU, R. F., 1967: Curvature corrections to upper mantle seismic refraction surveys. *Earth planet. Sci. Lett., 3*, pp. 469-475.

MEREU, R. F., & HUNTER, J. A., 1969: Crustal and upper mantle structure under the Canadian Shield from Project Early Rise data. *Bull. seism. Soc. Am., 59*, pp. 147-165.

SIMPSON, D. W., 1973: P wave velocity structure of the upper mantle in the Australian region. Ph.D. Thesis, Australian National University, Canberra.

STEWART, I. C. F., 1972: Seismic interpretation of crustal structure in the Flinders-Mount Lofty Ranges and Gulf regions, South Australia. *J. geol. Soc. Aust., 19(3)*, pp. 351-362.

THOMAS, L., 1969: Rayleigh wave dispersion in Australia. *Bull. seism. Soc. Am., 59*, p. 167.

UNDERWOOD, R., 1969: A seismic refraction study of the crust and upper mantle in the vicinity of Bass Strait. *Aust. J. Phys., 22*, p. 573.

WEEKS, L. G., & HOPKINS, B. M., 1967: Geology and exploration of three Bass Strait basins, Australia. *Bull. Am. Ass. Petrol. Geol., 51,* pp. 742-760.

WHITE, R. E., 1969: Seismic phases recorded in South Australia and their relation to crustal structure. *Geophys. J.R. astron. Soc., 17(3),* pp. 249-261.

D. M. Finlayson,
J. P. Cull,
B. J. Drummond,
Bureau of Mineral Resources
Canberra, A.C.T.

Geophys. J. R. astr. Soc. (1977) 48, 509–519

A long-range seismic profile in South-eastern Australia

K. J. Muirhead and J. R. Cleary *Research School of Earth Sciences, Australian National University, Canberra, Australian Capital Territory, Australia*

D. M. Finlayson *Bureau of Mineral Resources, Canberra, Australian Capital Territory, Australia*

Received 1976 June 2

Summary. Nine portable seismic stations deployed across the Western Plains of New South Wales recorded signals in the distance range 250–1000 km from large timed explosions at both ends of the line. A velocity–depth model derived from the travel-time data has the following features: a two-layer crust with a thickness of 35 km; a sub-Moho velocity of 7.98 km/s; an abrupt increase to 8.36 km/s at 100 km depth; a further step to 8.72 km/s at 190 km depth, with a low-velocity channel immediately above the discontinuity. The model has several features in common with others derived from long-range profiles in Australia and elsewhere. The data, however, provide the first suggestion of a low *P*-velocity channel in Eastern Australia.

Introduction

In 1972 a series of long-range seismic experiments within Australia, collectively named TASS (Trans-Australia Seismic Survey), was organized by the Bureau of Mineral Resources; an analysis of TASS data obtained from BMR and University of Adelaide stations has been presented by Finlayson, Cull & Drummond (1974). As foreshadowed in that publication, we present here an analysis of data obtained from nine Australian National University portable stations deployed across the Western Plains region of New South Wales between the Mt Fitton and Bass Strait explosions of the TASS series, together with data from other stations in the region (Fig. 1). The Western Plains region is blanketed by Quaternary soils and alluvium. It is bounded in the east by the Southern Tablelands and by Palaeozoic granites of the Lachlan Mobile Zone, and in the west by the so-called Adelaide Geosyncline, of Precambrian age, which includes the Flinders and Mt Lofty ranges.

Details of the two explosions have been given by Finlayson *et al.* (1974). The portable stations consisted of Willmore Mark II seismometers recording on long-playing magnetic tape recorders of ANU design and construction (Muirhead & Simpson 1972). CAN, TAO, KHA, WAM, CBR, INV, JNL and WER to the east of the line are permanent stations of the ANU network; UMB, PNA, ILN, HTT, ADE and CLV are stations of the University of Adelaide network; BFD, TOO and KF are BMR stations.

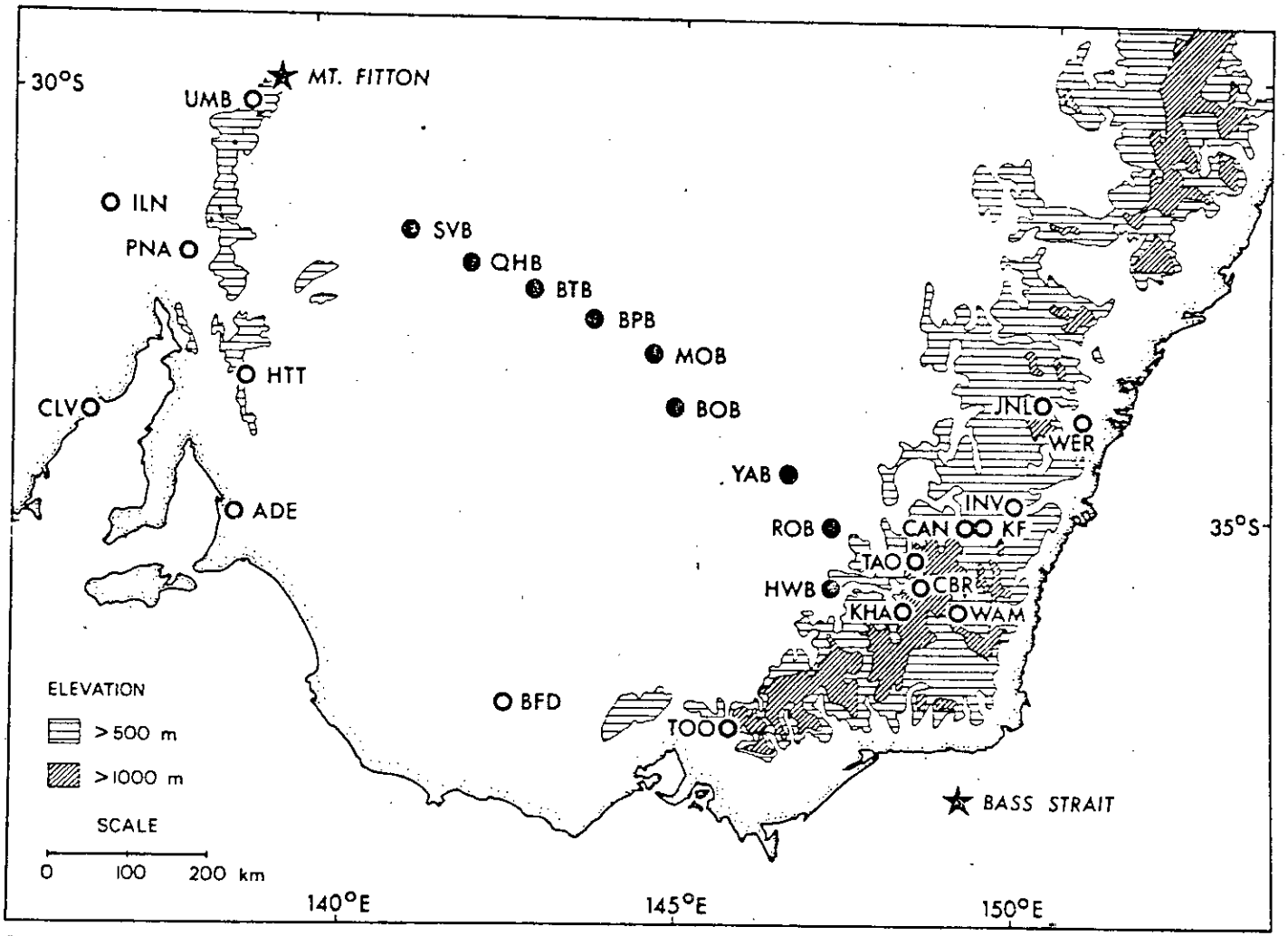

Figure 1. Map of South-eastern Australia, showing the two explosions (★), the portable stations (●), and other recording stations (○). The topography of the region is also shown.

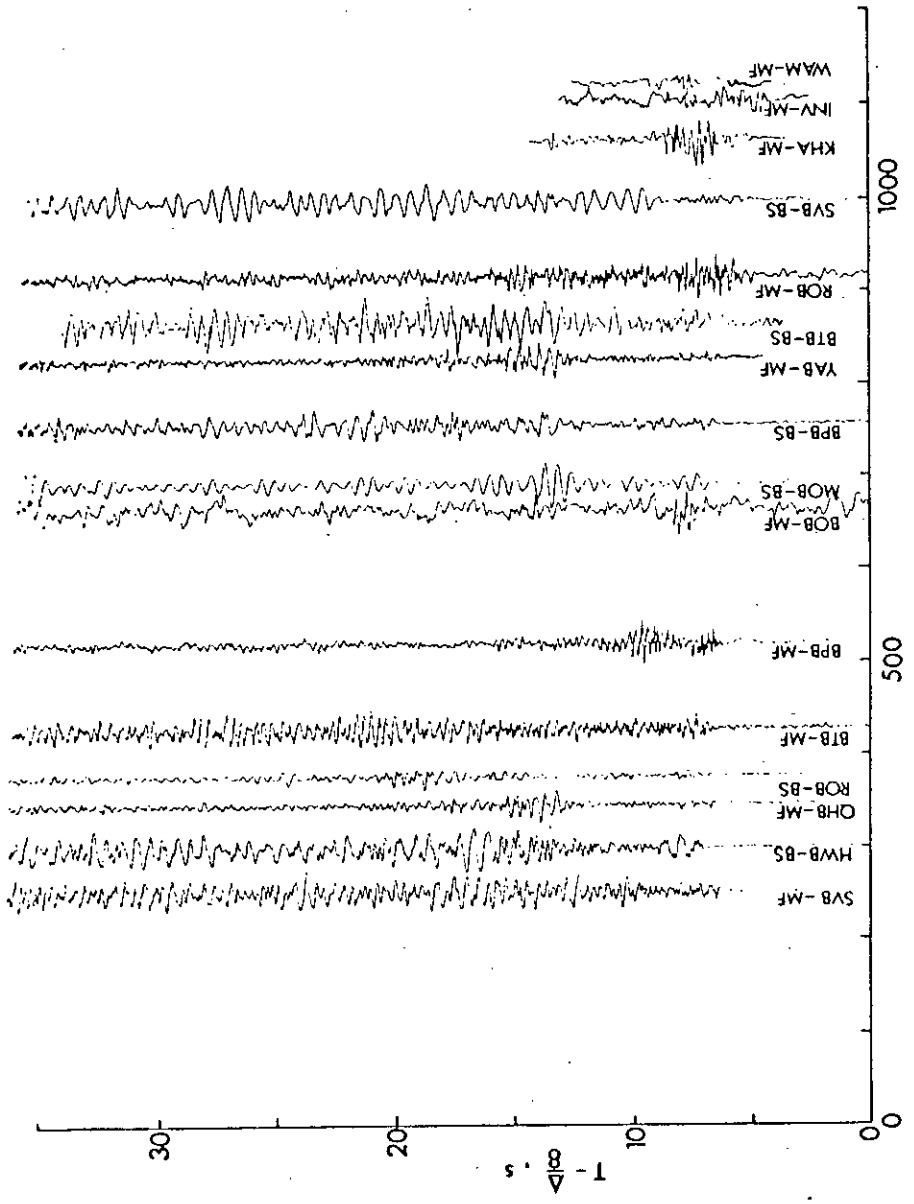

Figure 2. Record section of traces from the portable stations plus KHA, INV and WAM, on a reduced time scale. The suffixes MF, BS indicate whether the trace is from the Mt Fitton or Bass Strait explosion. Bass Strait times have been decreased by 0.8 s.

Data and results

The data recorded from both explosions by the portable stations, and by a few of the permanent stations at the end of the Mt Fitton line, have been digitized and played out on a time–distance plot with a reduction velocity of 8 km/s (Fig. 2). The amplitudes have been normalized to maximum trace amplitude. On this plot the times of the Bass Strait records have been reduced by 0.8 s so that their first arrivals line up with those from Mt Fitton. The Bass Strait shot is believed to have taken place on the sea bottom (Finlayson *et al.* 1974), so the larger delay times from that event are probably an effect of low-velocity sediments beneath the shot point (*cf.* Underwood 1969). The Bass Strait records are distinguished from those of Mt Fitton by the relative weakness of frequencies greater than about 2 Hz. Distances and first arrival times for all stations are listed in Table 1.

It can be seen from the figure and the table that the reduced first-arrival times from the portable stations are approximately constant out to a distance of about 800 km and then progressively decrease. The justification for combining the data from both explosions in the figure is that the two series of arrivals do not systematically depart from one another with distance, indicating that there are no systematic variations in structure along the traverse. (The arrivals of HWB-BS and WAM-MF are late with respect to the others; these and other 'anomalous' arrivals at some of the permanent stations will be examined in a later Section.) In the first five records, at distances between about 250 and 500 km, there are later arrivals which can be identified as the crustal phases P_1 and P_2. Beyond 500 km a series of later

Table 1. Data from Mt Fitton and Bass Strait explosions.

	Mt Fitton			Bass Strait		
	Δ (km)	t (s)	$t - \Delta/8$ (s)	Δ (km)	t (s)	$t - \Delta/8$ (s)
UMB*	49.3	8.2	2.0	1260.7	162.6	5.0
SVB*	254.5	38.2	6.4	998.4	130.8	6.0
PNA	258.8	39.6	7.2			
ILN	300.3	45.0	7.4			
QHB*	338.6	48.6	6.3			
HTT	384.4	56.0	7.9	1042.6	136.0	4.9
BTB*	423.9	59.7	6.7	835.5	113.3	6.9
CLV	501.2	68.2	5.5			
BPB*	513.0	70.4	6.3	753.3	101.1	6.9
ADE	555.9	77.2	7.7			
MOB*				681.8	92.4	7.2
BOB*	658.6	88.7	6.4			
YAB*	825.6	109.1	5.9			
BFD	841.8	110.8	5.5	565.9	77.0	6.3
ROB*	913.7	119.8	5.6	372.1	53.5	7.0
HWB*				298.1	45.0	7.7
TOO	1002.1	130.0	4.7	302.6	45.1	7.3
TAO	1025.9	133.4	5.2	301.2	45.9	8.3
KHA	1054.1	136.5	4.7	238.6	37.6	7.8
CBR	1056.5	137.1	5.0	264.8	41.3	8.2
CAN	1062.4	137.2	4.4	330.4	49.2	7.9
JNL	1075.2	139.0	4.6	507.7	70.7	7.3
KF	1083.8	139.7	4.2			
INV	1096.5	141.3	4.2	377.2	55.5	8.4
WAM	1106.7	143.3	5.0	233.7	36.9	7.7
WER				507.6	71.1	7.7
CTA	1288.9	164.0	2.9			

* Portable ANU stations.

arrivals apparently belong to triplication branches associated with the change in slope at 800 km. There is evidence of another branch of greater slope in the later arrivals beyond about 850 km. Between 600 and 900 km there is also a set of arrivals with reduced times of about 13 s. In addition, there are some apparently non-systematic arrivals which will be discussed later.

A time–distance curve has been fitted to the data by trial-and-error inversion of velocity–depth profiles. The simplest profile giving a reasonable fit is shown by the solid line in Fig. 3, and its corresponding time–distance curve is shown superimposed on the record section in Fig. 4. In this figure the WAM-MF record has been displaced downward by a further 0.8 s so that its first arrival corresponds to that of INV-MF at almost the same distance, in order to show the correspondence of later arrivals with those of nearby stations. Signal amplitudes have been used to establish the approximate positions of the cusps at the near ends of the retrograde branches.

The velocity–depth profile of Fig. 3 has been tabulated in Table 2. In the model, the two-layer crust has P_1 and P_2 velocities of 6.15 and 6.75 km/s, with Conrad and Moho discontinuities at depths of 20 and 35 km. Beneath the Moho, the (P_n) velocity is constant at 7.98 km/s down to 100 km, where it increases abruptly to 8.36 km/s. The later arrival data near the end of the record section have been fitted by another abrupt velocity change to 8.72 km/s at a depth of 190 km. In order to model adequately the triplication branch associated with this discontinuity, an 8.1 km/s low-velocity channel was inserted in the depth range 155–190 km.

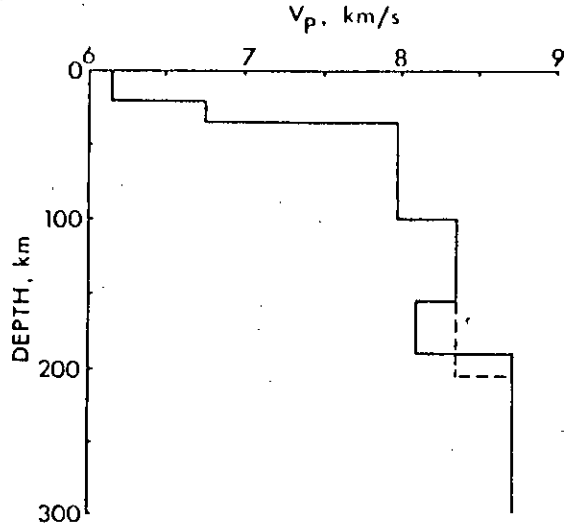

Figure 3. *P*-velocity model (solid line) from which the travel time curve shown in Figs 3 and 5 was derived. The dashed section of the model (no low-velocity channel) corresponds to the dashed travel-time curve in Fig. 5.

The later arrivals having a phase velocity of about 8 km/s in the 600–900 km range lie close to the dashed line in the figure, which corresponds to P_nP_n (i.e. with a single reflection at the surface). Similar arrivals were observed by Hales & Nation (1966), who identified them as $(P_mP)P_n$ and discussed the conditions necessary for the appearance of a phase of this type. Similar observations have been made in the US by Green & Hales (1968) and in Western Europe by Hirn *et al.* (1973).

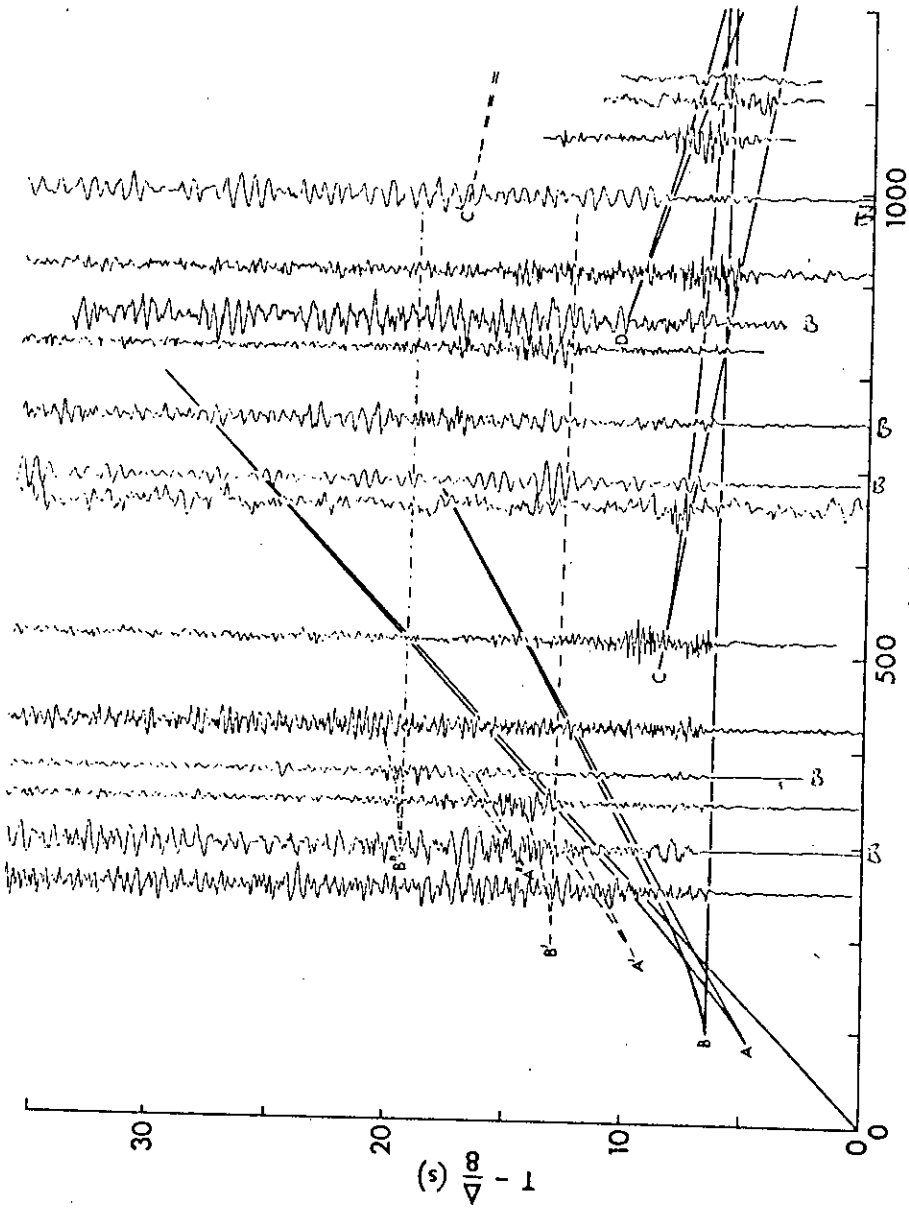

Figure 4. Record section of Fig. 2, with derived travel-time curve (solid line) superimposed. The time of the WAM trace has been reduced by a further 0.8 s (see text). Also shown are multiples of portions of the curve, corresponding to single reflections (-----) and double reflections (·····) at the surface.

Table 2. Earth models shown in Fig. 3.

(a) With low-velocity channel		(b) Without low-velocity channel	
Depth (km)	Velocity (km/s)	Depth (km)	Velocity (km/s)
0	6.15	0	6.15
20	6.15	20	6.15
20	6.75	20	6.75
35	6.75	35	6.75
35	7.98	35	7.98
100	7.98	100	7.98
100	8.36	100	8.36
155	8.36	205	8.36
155	8.10	205	8.72
190	8.10		
190	8.72		

As shown in the figure, some other arrivals in the records can be associated with multiples of the high-amplitude arrivals near the cusps marked A, B and C, corresponding to single reflections at the surface (A′, B′, C′) and perhaps double reflections (A″, B″) as well. The contribution to signal complexity of multiples of this kind seems to be insufficiently recognized.

DATA FROM OTHER STATIONS

To this point we have been concerned mainly with data from the ANU portable stations. In Fig. 5 the travel-time curve derived from these data is compared with arrivals from the other stations in the region. Once again the Bass Strait times have been reduced by 0.8 s.

It is apparent, first of all, that the Bass Strait times from the stations in the vicinity of the Snowy Mountains - Southern Tablelands region (WAM, KHA, CBR, TAO, CAN, INV – and also HWB) are on average about 1 s late with respect to the curve. The results of a number of seismic experiments in the southwest corner of Australia (Doyle, Everingham & Hogan 1959; Doyle, Underwood & Polak 1966; Underwood 1969 and a summary by Cleary 1973) indicate that the P_n velocity is about 7.9 km/s – slightly lower than that given here for the region to the west – and that the crustal thickness beneath the Snowy Mountains is about 42 km. The magnitude of the delays observed here is compatible with such a model. The delay at WER, on the other hand, is probably due to the sediments of the Sydney Basin (Doyle *et al.* 1966).

With the exception of WAM, the delays at these stations from the Mt Fitton explosion are much less marked, which suggests that the crust thins rapidly to the west of the tablelands. That this is an effect of isostasy is further suggested by the topography of the region, as shown in Fig. 1.

Stations UMB, PNA, ILN, HTT and ADE also have marked delays from Mt Fitton, which may be attributed to increased crustal thickness (~ 38 km) and low-velocity sediments in the Flinders–Mt Lofty ranges/Adelaide Geosyncline area (*cf.* Stewart, 1972). Of these stations UMB and HTT recorded first arrivals from Bass Strait, and only UMB has a significant delay, again suggesting an azimuthal effect.

Stations BFD (from both shots) and CLV (from Mt Fitton) are both early by about 0.5 s, which suggests that the crust is a few kilometres thinner beneath these regions than beneath the Western Plains.

At the extreme end of the range (1289 km) is an observation of the Mt Fitton explosion at CTA, Queensland, which has been included as an indication of the similarity of eastern Australian paths.

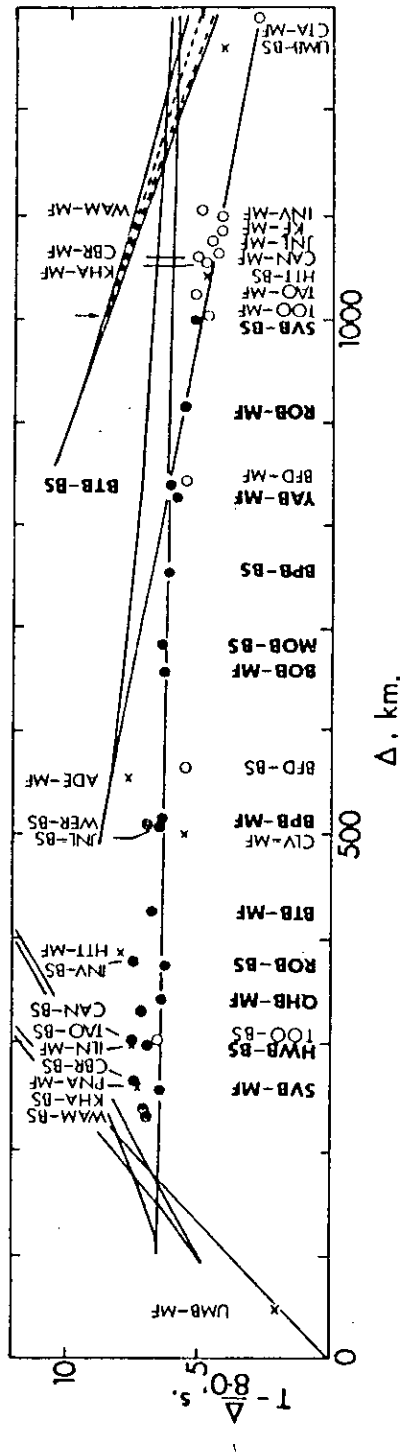

Figure 5. Comparison of the derived curve with travel times to portable stations (●), Adelaide network stations (X) and others (○). The station codes for the mobile stations are shown in bold-faced type. The dashed curve beyond 1000 km corresponds to the model with no low-velocity channel (*cf.* Fig. 3). The arrow marks the cusp on this curve.

OTHER POSSIBLE INTERPRETATIONS

From Fig. 5, it might be argued that it is possible to fit all the first-arrival data from the portable stations by a line corresponding to a velocity intermediate between the two first-arrival branches. We consider such an interpretation unlikely to be valid, for the following reasons:

Firstly, the residuals at the stations east and west of the traverse would then be positive at one end of the line and negative at the other. While we have argued above, on the basis of our interpretation, that there may be some azimuthal variation in the time terms at these stations, we consider that an *ad hoc* assumption of an azimuthal variation of up to 2 s in these terms would be difficult to defend.

Moreover, such an interpretation ignores the evidence from later arrivals of a triplication in the travel-time curve in this range. The amplitude of a reflection branch increases with decreasing distance as the critical distance is approached, and decreases rapidly at sub-critical distances (i.e. when the energy is no longer totally internally reflected). This is the type of behaviour observed in the vicinity of cusp C of our model (Fig. 4). No alternative interpretation could be found for these later arrivals.

A similar argument applies to the placement of cusp D, although here the character of the Mt Fitton record ROB-MF at about 900 km distance is different from the lower-frequency Bass Strait records BTB-BS and SVB-BS on either side. The presence or absence of a low-velocity channel above a depth of about 200 km depends critically upon the position of this cusp, and thus upon the interpretation of the later arrival at BTB-BS. We consider that the BTB-BS arrival is too strong to be omitted from the interpretation. Nevertheless, we have provided an alternative model in Table 2(b), shown dashed in Fig. 3, in which the low-velocity channel is absent. As shown by the dashed curve in Fig. 5, the triplication branch for this model extends back only to a distance of about 1000 km. It should be pointed out that the backward extension of the cusp in our preferred model could have been achieved equally well by means of a wider channel with less velocity contrast, or by a narrower, higher contrast channel (*cf.* Steinmetz, Hirn & Perrier 1974). Obviously, it would be desirable to test the interpretation with additional data from the same region; we are satisfied, however, that the present model is a reasonable interpretation of the data available to us at this time.

Discussion

Since the experiment was designed to study the upper mantle beneath New South Wales, no great precision is claimed for the crustal part of the model in Table 2 and Fig. 3. Nevertheless, the data do provide evidence for a two-layer crust, additional to that found previously and summarized by Cleary (1973). The study provides clear evidence that the crust beneath the Western Plains is several kilometres thinner than that of the tablelands to the east.

The P_n velocity of 7.98 km/s for the region confirms the east–west gradation of P_n noted by Cleary (1973), with velocities of 7.9 km/s to the east, 7.99–8.02 km/s beneath the Adelaide Geosyncline (Stewart 1972) and 8.05 km/s and higher to the west of the geosyncline (Doyle & Everingham, 1964; summary by Cleary 1973; Finlayson *et al.* 1974).

The abrupt increase in velocity from 7.98 to 8.36 km/s at 100 km depth is similar to, but slightly deeper than, that found in other regions. Green & Hales (1968) found a 7.9–8.3-km/s increase at 93 km depth for the Central US; Mereu & Hunter (1969) an 8.05–8.43-km/s increase at 84 km for the Canadian Shield; Hales, Helsley & Nation (1970) an 8.1–8.67-km/s increase at 57 km beneath the Gulf of Mexico; and Hirn *et al.* (1973) a more gradual change from 8.2 to 8.45 km/s at 80–90 km in France. It seems very likely that a velocity jump of this kind is universal.

The further increase to 8.72 km/s at 190 km depth is similar to an increase to about 8.8 km/s at 190 km found for the Gulf of Mexico by Hales *et al.* (1970), and to an increase to 8.74 km/s at 193 km beneath France by Steinmetz *et al.* (1974). The latter authors also found it necessary to include a low-velocity channel above this discontinuity, for reasons similar to the ones given in the preceding Section.

The model described here has some resemblance to those derived from other seismic experiments in Australia. Simpson's (1973) model for Central Australia has a P_n velocity of 8.1 km/s, with increases to 8.24 km/s at 85 km and to 8.53 km/s at 175 km, but with no low-velocity channel. Finlayson *et al.* (1974) have similar steps in their TASS-2a model (central Australian and South-Australian-Victorian data) but their TASS-1a model (Nullabor data) has no step between 40 and 165 km. They found 'no convincing evidence' for a low-velocity channel. It may be mentioned also that Goncz & Cleary (1976) found evidence of a low *S*-velocity channel centred at 130 km in Eastern Australia from Rayleigh wave group velocity data, although the validity of this interpretation has been questioned by Mills & Fitch (1976).

Acknowledgments

We are grateful for the advice and assistance of Professor Anton Hales and Dr Joseph Gettrust during the preparation and analysis of the data. One of us (DMF) publishes here with the permission of the Director of the Bureau of Mineral Resources.

References

Cleary, J., 1973. Australian crustal structure, *Tectonophysics*, 20, 241–248.

Doyle, H. A. & Everingham, I. B., 1964. Seismic velocities and crustal structure in southern Australia, *J. geol. Soc. Aust.*, 11, 141–150.

Doyle, H. A., Everingham, I. B. & Hogan, T. K., 1959. Seismic recordings of large explosions in south-eastern Australia, *Aust. J. Phys.*, 12, 222–230.

Doyle, H. A., Underwood, R. & Polak, E. J., 1966. Seismic velocities from explosions off the central coast of New South Wales, *J. geol. Soc. Aust.*, 13, 355–372.

Finlayson, D. M., Cull, J. P. & Drummond, B. J., 1974. Upper mantle structure from the Trans-Australia Seismic Survey (TASS) and other seismic refraction data, *J. geol. Soc. Aust.*, 21, 447–458.

Goncz, J. H. & Cleary, J. R., 1976. Variations in the structure of the upper mantle beneath Australia, from Rayleigh Wave observations, *Geophys. J. R. astr. Soc.*, 44, 507–516.

Green, R. W. E. & Hales, A. L., 1968. The travel times of *P*-waves to 30° in the central United States and upper mantle structure, *Bull. seism. Soc. Am.*, 58, 267–289.

Hales, A. L., Helsley, C. E. & Nation, J. B., 1970. *P* travel times for an oceanic path, *J. geophys. Res.*, 75, 7362–7381.

Hales, A. L. & Nation, J. B., 1966. Reflections at the M discontinuity and the origin of microseisms, in *The Earth beneath the continents*, p. 529–537, eds John S. Steinhart & T. Jefferson Smith, Am. geophys. Un., Washington, DC.

Hirn, A., Steinmetz, L., Kind, R. & Fuchs, K., 1973. Long range profiles in western Europe: II. Fine structure of the lower lithosphere in France (southern Bretagne), *Z. Geophys.*, 39, 363–384.

Mereu, R. F. & Hunter, J. A., 1969. Crustal and upper mantle structure under the Canadian Shield from Project Early Rise data, *Bull. seism. Soc. Am.*, 59, 147–165.

Mills, J. M. & Fitch, T. J., 1976. Thrust faulting and crust–upper mantle structure in east Australia, *Geophys. J. R. astr. Soc.*, 48, 351–384.

Muirhead, K. J. & Simpson, D. W., 1972. A three-quarter watt seismic station, *Bull. seism. Soc. Am.*, 62, 985–990.

Simpson, D. W., 1973. *P*-wave velocity structure of the upper mantle in the Australian region. *PhD thesis, Australian National University, Canberra.*

Steinmetz, L., Hirn, A. & Perrier, G., 1974. Réflexions sismiques à la base de l'asthénosphère, *Ann. Géophys.*, 30, 173–180.

Stewart, I. C. F., 1972. Seismic interpretation of crustal structure in the Flinders–Mt Lofty ranges and gulf regions, South Australia, *J. geol. Soc. Aust.*, 19, 351–362.

Underwood, R., 1969. A seismic refraction study of the crust and upper mantle in the vicinity of Bass Strait, *Aust. J. Phys.*, 22, 573–587.

FIRST ARRIVAL DATA FROM THE CARPENTARIA REGION UPPER MANTLE PROJECT (CRUMP)

By D. M. FINLAYSON

(With 8 Tables and 8 Text-Figures)

(*Received* 7 *November* 1967; *read in abstract at Canberra,* 23 *January* 1968)

ABSTRACT

Travel-time from explosions fired on the continental shelf round the Cape York Peninsula were recorded by a number of mobile seismic recording crews and seismic observatories. Least squares analysis of the results from various groups of shots indicated upper crustal velocities between 5·82 km/sec and 5·94 km/sec, lower crustal velocities between 6·62 km/sec and 6·83 km/sec, and upper mantle velocities between 7·84 km/sec and 8·09 km/sec. Subsequent time-term analysis of the results gave depths to the intermediate refractor of 10 km at the continental margins increasing to 25 km in the Gilbert River region of Cape York. The Mohorovičić "Discontinuity" (*M*) dips at an average of 3° from depths of 25 km at the edge of the continent to 45 km in Central Cape York and the regions northwest of Charters Towers.

1. INTRODUCTION

The Carpentaria Region Upper Mantle Project (CRUMP) was organised by the Bureau of Mineral Resources, Geology and Geophysics (B.M.R.) as a large scale seismic refraction survey in the Cape York Peninsula-Gulf of Carpentaria region. The field work was carried out during September and October 1966 by parties from a number of government and academic organisations who had gained experience from a similar experiment in the Bass Strait earlier in 1966. The Royal Australian Navy organised the detonation of the charges from H.M.A.S. *Kimbla,* a minesweeper which had previous experience of this type of work.

Crustal studies were carried out independently to the west and northeast of the survey area and it was hoped eventually to tie in these results. A number of exploration seismic and gravity surveys had been done in the region and some of those results have proved useful in interpreting the CRUMP results.

2. ORGANISATION

H.M.A.S. *Kimbla* detonated fourteen charges on the sea bed at predetermined positions on the continental shelf round Cape York Peninsula. The charges were made up to either one ton or half a ton and exploded in 10-13 fathoms (18-54 m) water. In order to make the best use of these explosions, the B.M.R. extended invitations to other government and academic bodies to contribute equipment and/or personnel for the duration of the experiment. Those who eventually participated in the field work were B.M.R., the Universities of Queensland, Sydney, and Melbourne and the Australian National University (A.N.U.), the Commonwealth Department of Works, the Geological Survey of Queensland and the University College of Townsville.

In all, seventeen mobile and seven stationary seismic recording crews were organised. Three of the mobile crews were organised by A.N.U. in the Northern Territory in the direction of their seismic array at Tennant Creek. Their results have been analysed elsewhere (R. Underwood [unpublished]). Five of the fixed recording sites were organised by the B.M.R. Port Moresby observatory staff in the Territory of Papua and New Guinea, but results have only been used from one of these stations in this analysis.

Each recording crew was equipped with short-period seismometers or exploration geophones matched to recorders running at speeds capable of resolving arrival times to better than 0·1 sec. Some form of timing was required on the records. Absolute time marks could be obtained from the VNG time signal transmission or relative time marks could be obtained from the ship's broadcast timing sequence used for each of the shots. There is already adequate literature on the type of

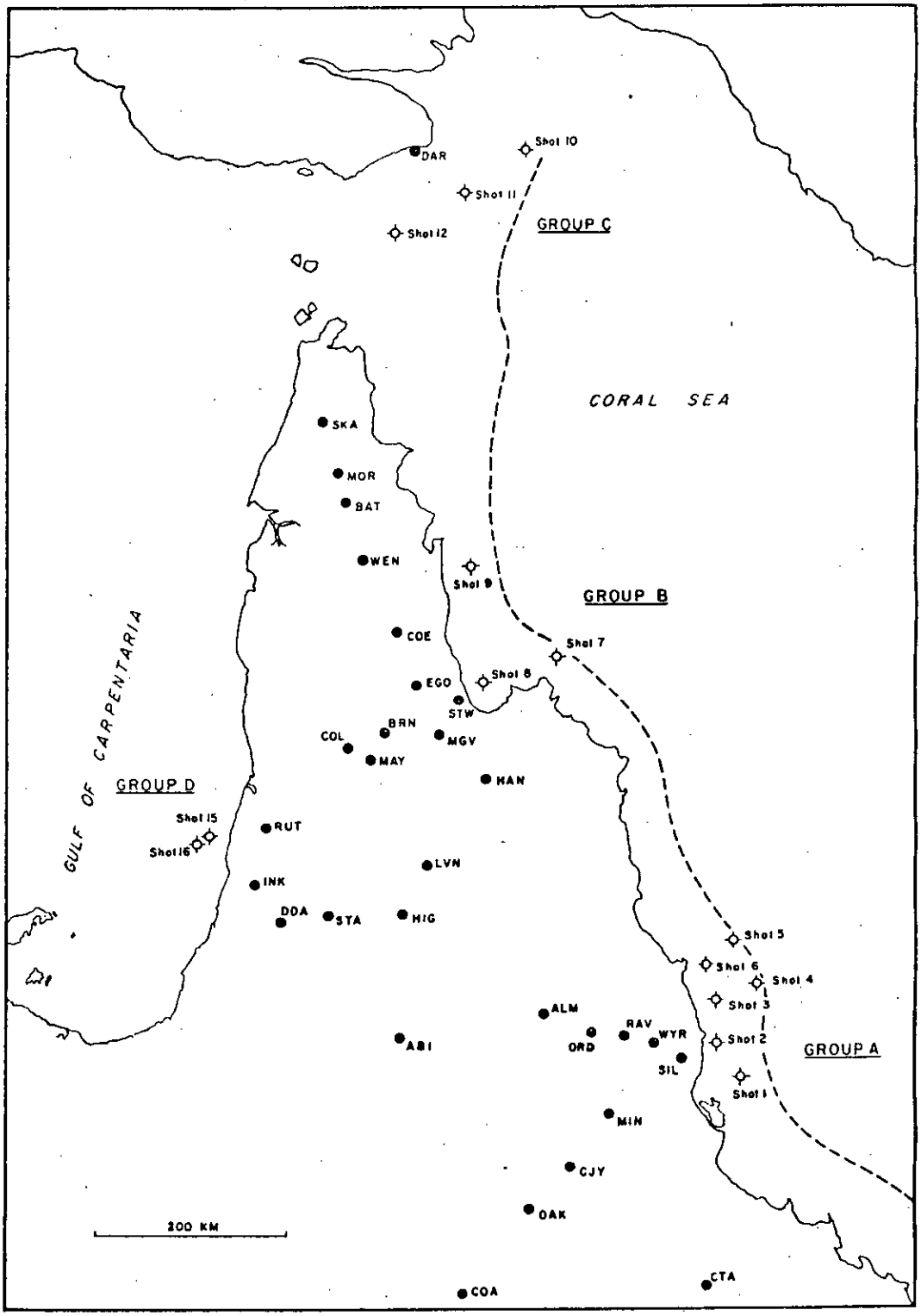

Fig. 1. Location of shot points and recording stations.

equipment and organisation required for projects such as CRUMP (Doyle, Everingham & Hogan, 1959; Doyle & Everingham, 1964; Doyle, Underwood & Polak, 1966; Steinhart & Smith, 1966; Finlayson, 1968).

The shot positions and the recording sites from which results have been used in this analysis are shown in Figure 1. It should be emphasised that the abbreviations allotted to the various recording sites do not necessarily correspond to any U.S. Coast and Geodetic Survey abbreviations and no confusion should arise since all the CRUMP stations are listed in Tables II-V. The shots were fired in four groups (A, B, C and D) with some of the recording sites common to more than one group. The positions of the recording sites were pinpointed on air photographs or detailed maps by the geophysicist at the site and the latitudes and longitudes subsequently computed from base maps. Most of the area had been recently surveyed for a B.M.R. helicopter gravity survey carried out during 1966. The ship's position was calculated by taking fixes on land marks or by sun shots (for Group D shots only). These position fixes were not noted or subjected to a close check and thus could be a source of error in the subsequent calculations.

Details of the shot positions and timings are given in Table I.

TABLE I

Shot Positions and Timing

Shot No.	Lat. S.	Long. E.	Date	Time of Detonation	Group	Size
1	18° 00′·0	146° 25′·0	21/9/66	06·50 33·16±0·020	A	1 ton
2	17° 42′·0	146° 12′·0	21/9/66	11·50 32·50±0·005	A	¼ ton
3	17° 15′·0	146° 03′·0	21/9/66	19·50 45·74±0·020	A	¼ ton
4	17° 02′·0	146° 18′·0	21/9/66	23·51 58·60±0·050	A	1 ton
5	16° 40′·0	146° 14′·0	22/9/66	07·50 09·50±0·005	A	1 ton
6	16° 53′·0	146° 02′·0	22/9/66	11·50 11·29±0·005	A	¼ ton
7	13° 59′·8	144° 35′·0	24/9/66	17·50 03·22±0·020	B	1 ton
8	14° 05′·0	143° 50′·0	25/9/66	06·50 22·57±0·020	B	¼ ton
9	13° 04′·4	143° 51′·0	25/9/66	16·50 08·85±0·020	B	1 ton
10	09° 10′·0	143° 54′·0	1/10/66	17·50 19·05±0·006	C	1 ton
11	09° 30′·6	143° 28′·3	2/10/66	22·50 17·88±0·006	C	1 ton
12	10° 00′·0	143° 04′·0	3/10/66	09·50 05·59±0·006	C	¼ ton
13			CANCELLED			
14			CANCELLED			
15	15° 33′·6	141° 07′·0	6/10/66	13·20 58·46±0·006	D	1 ton
16	15° 33′·8	141° 00′·5	6/10/66	17·20 34·32±0·006	D	1 ton

3. RESULTS

Only the first longitudinal (P) wave arrivals have been analysed in this paper. The picking of first arrivals from some of the records was necessarily a subjective procedure because the signals were very weakly recorded or the signal-to-noise ratio too low to give a definite arrival time. Arrivals that were "late" when plotted on the travel-time curve or were doubtful have been rejected and the remaining results have been given equal weight in the analysis. The distances between the various shots and recording sites were calculated on the C.S.I.R.O. CDC 3600 computer using programme EPICENT (DF).

Group A

The results from the Group A shots are presented in Table II. The travel-time plot of the results is given in Figure 2 where the time scale has been reduced by $\Delta/8$ (Δ = distance from shot to recorder in km). On consideration of the travel-time curve, a crustal model that splits the curve into three sections has been assumed for the purpose of interpretation. This implies that there are two layers in the crust above M. The selection of this particular model does not imply that the travel-time curve cannot be approximated by other models, but for a first analysis, it has been found suitable. Later on in this paper (Section 4), data from other geophysical surveys will be used to give information on a third surface layer.

For the purposes of identification, the longitudinal (P) waves with an apparent velocity of approximately 5·9 km/sec will be denoted as P_1 arrivals, waves having an apparent velocity of 6·5-7·0 km/sec will be denoted as P_2

TABLE II

Travel Times for P, Group A

Station	Lat. S	Long. E.	Shot	Distance km	Travel Time sec	Equation
Wyrema (WYR)	17° 36′·9	145° 43′·2	1	85·3	14·6	1, 2
			2	51·8	9·1	1
			3	53·5	9·5	1
			4	89·1	15·7	1, 2
			5	118·3	20·3	1, 2
			6	87·5	15·4	1, 2
Coalbrook (COA)	20° 13′·9	143° 24′·4	1	401·7	57·8	3
			2	406·2	57·8	3
			4	467·4	66·0	3
			5	494·7	69·3	3
Oak Park (OAK)	19° 17′·1	144° 10′·5	1	276·1	41·8	3
			2	276·6	41·9	3
			4	335·6	49·0	3
			5	362·5	52·7	3
Conjuboy (CJY)	18° 37′·5	144° 43′·6	1	191·6	30·27	2, 3
			2	186·5	30·70	2, 3
			4	242·6	37·40	3
			5	269·3	40·60	3
			6	237·3	36·42	3
Minnamoolka (MIN)	18° 11′·3	145° 05′·4	1	142·0	23·30	2
			2	129·4	21·74	2
			5	207·6	33·28	2, 3
			6	175·7	28·79	2, 3
Ravenshoe (RAV)	17° 38′·1	145° 24′·5	1	114·3	19·07	1, 2
			2	84·3	14·40	1, 2
			3	80·4	13·64	1, 2
			4	115·9	20·10	1, 2
			6	106·4	18·38	1, 2
Silkwood (SIL)	17° 45′·0	146° 00′·9	1	50·8	8·85	1
			2	20·4	3·70	1
			4	84·9	14·44	1
Ord (ORD)	17° 33′·7	144° 57′·8	3	120·5	20·40	2
			4	153·7	25·90	2
			5	167·5	27·50	2
Almaden (ALM)	17° 20′·4	144° 40′·4	1	198·9	31·41	2, 3
			2	167·0	27·49	2, 3
			5	182·1	29·67	2, 3
			6	153·3	25·39	2
Charters Towers (CTA)	20° 05′·3	146° 15′·0	3	314·7	46·4	3
			4	338·0	49·5	3
			5	378·5	54·9	3

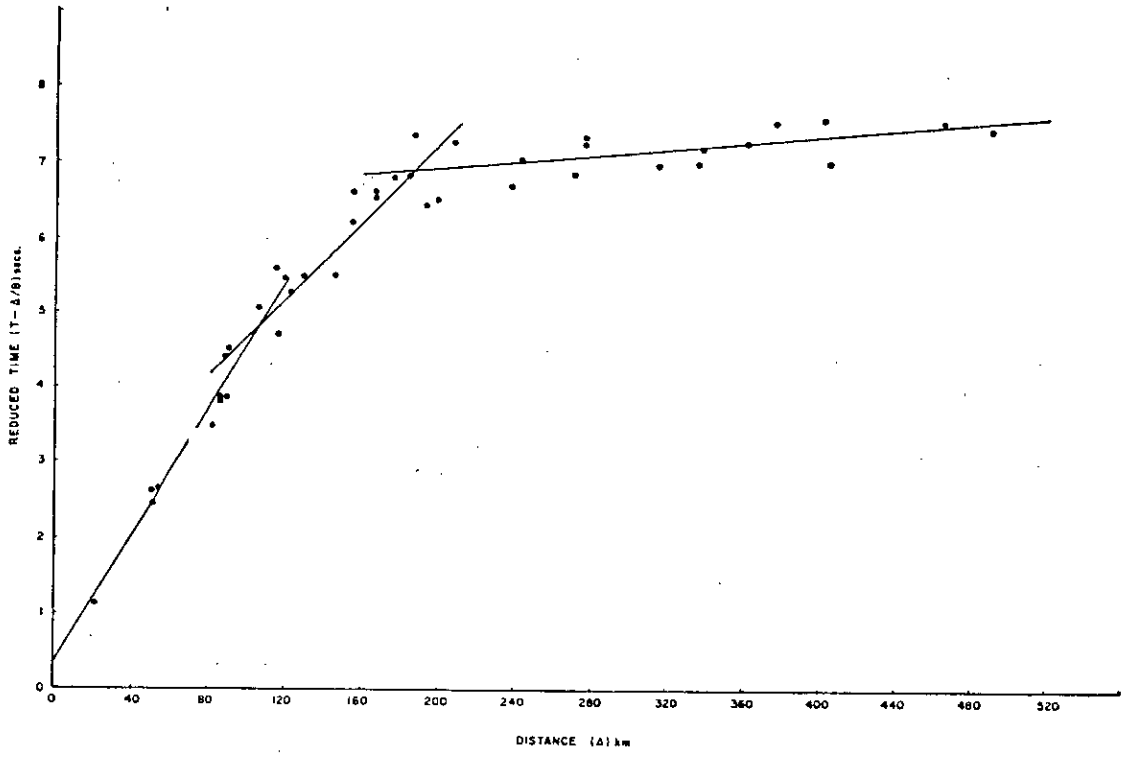

Fig. 2. Travel-time plot for Group A results.

arrivals, and those waves with an apparent velocity of approximately 8·0 km/sec will be denoted as P_n arrivals. The data in each section of the travel time plot have been analysed by the least squares method to give a linear expression for the travel time. The sections have been overlapped because of the difficulty in allotting datum points to a particular section in the region of the cross-over.

For Group A shots at distances less than 120 km the least squares analysis gives the P_1 travel time,

$$T = 0{\cdot}34 \pm 0{\cdot}21 + \Delta/5{\cdot}94 \pm 0{\cdot}08 \ldots 1$$
$$N = 14$$

where

T = travel time (secs)
Δ = distance along the surface between shot and recorder (km)
N = number of datum points

Least squares analysis of data lying between 80 and 210 km gives a travel time for P_2 arrivals,

$$T = 2{\cdot}08 \pm 0{\cdot}30 + \Delta/6{\cdot}62 \pm 0{\cdot}09 \ldots 2$$
$$N = 22$$

The P_n travel time is given by

$$T = 6{\cdot}42 \pm 0{\cdot}12 + \Delta/7{\cdot}84 \pm 0{\cdot}01 \ldots 3$$
$$N = 21$$

The data used in determining the various expressions are indicated in the last column of Table II.

If it is assumed that the crust is horizontally layered over the whole region and that there is a surface layer with mean velocity = 4·5 km/sec, then a formal solution to the expressions for the travel times (Eiby & Dibble, 1957), using the parameters in Equations 1, 2 and 3, gives depths to the refractors of 1 km, 12 km and 34 km.

Group B

The results from the Group B shots are shown in Table III and plotted in Figure 3.

The travel-time curve for the Group B results has been split into three sections like that for Group A. Because of the limited number of results at distances less than 120 km from the shot point, one Group D result has been

included in the data used to derive Equation 4 for P_1 arrivals:

$$T = 0{\cdot}24 \pm 0{\cdot}11 + \Delta/5{\cdot}82 \pm 0{\cdot}01 \ldots 4$$
$$N = 4$$

Analysis of the data between 80 and 210 km gives the travel time for P_g arrivals,

$$T = 2{\cdot}76 \pm 0{\cdot}51 + \Delta/6{\cdot}71 \pm 0{\cdot}13 \ldots 5$$
$$N = 10$$

50 and 210 km, the analysis gives the travel time for P_g arrivals:

$$T = 2{\cdot}69 \pm 0{\cdot}01 + \Delta/6{\cdot}72 \pm 0{\cdot}05 \ldots 7$$
$$N = 3$$

At distances greater than 160 km the least squares analysis gives the P_n travel time:

$$T = 6{\cdot}44 \pm 0{\cdot}24 + \Delta/8{\cdot}00 \pm 0{\cdot}09 \ldots 8$$
$$N = 12$$

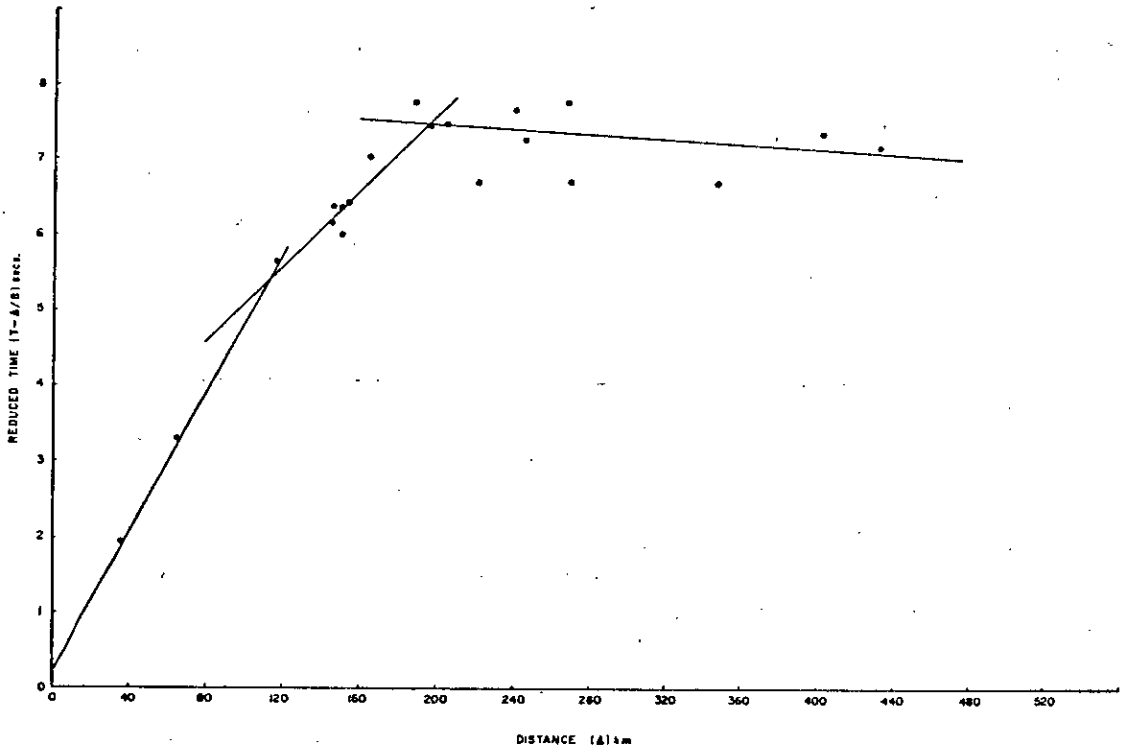

Fig. 3. Travel-time plot for Group B results.

At distances greater than 160 km, the analysis gives the P_n travel time:

$$T = 7{\cdot}70 \pm 0{\cdot}37 + \Delta/8{\cdot}09 \pm 0{\cdot}08 \ldots 6$$
$$N = 12$$

A formal solution to a horizontally layered crustal model using the parameters in Equations 4, 5 and 6 gives depths to the refractors of 1 km, 15 km and 39 km.

Group C

The results from the Group C shots detonated in Torres Strait are given in Table IV and plotted in Figure 4.

Because of the scarcity of data near the shot points, only two sections of the travel time can be defined. For the section between

Group D

The results from the Group D shots are listed in Table V and plotted in Figure 5. From the appearance of the travel-time curve it was obvious that the velocities and intercepts were going to be markedly different from those of Group A, B and C results. This led to a critical examination of the results for possible errors.

No proof of errors could be found but because it was felt that the calculated position of the ship might be in error, the Group D results have subsequently been given a much lower weighting in the interpretation of results.

At distances less than 120 km there was only one result and this has been included in Equation 4 with the Group B results.

TABLE III

Travel Times for P, Group B

Station	Lat. S	Long. E	Shot	Distance km	Travel Time sec	Equation
Highbury (HIG)	16° 25′·7	143° 08′·6	8	269·8	41·52	6
Strathleven (LVN)	15° 54′·2	143° 23′·1	7	247·0	38·20	5, 6
			8	206·9	33·40	6
Rutland Plains (RUT)	15° 38′·5	141° 48′·5	7	349·8	50·40	6
Coleman River (COL)	14° 49′·4	142° 30′·7	8	164·4	27·60	5, 6
			9	241·7	37·95	6
Strathmay (MAY)	14° 53′·0	142° 46′·1	8	145·0	24·49	5
Strathburn (BRN)	14° 28′·4	142° 49′·4	7	197·1	32·09	5, 6
			8	117·2	20·37	4, 5
			9	190·6	31·61	5, 6
Hann River (HAN)	15° 11′·3	143° 52′·4	7	152·4	25·48	5
Ebagoola (EGO)	14° 18′·5	143° 16′·3	7	145·8	24·41	5
			8	65·6	11·51	4
			9	150·3	24·76	5
Moreton (MOR)	12° 27′·1	142° 37′·7	7	272·3	40·7	6
			8	222·8	35·3	6
			9	149·4	25·0	5
Stewart River (STW)	14° 06′·8	143° 30′·0	8	36·2	6·45	4
Abingdon Downs (ABI)	17° 40′·7	143° 09′·5	7	434·9	61·63	6
			8	404·2	57·85	6

At distances between 80 and 210 km the least squares analysis gives the travel times,

$$T = 2{\cdot}85 \pm 1{\cdot}08 + \Delta/6{\cdot}83 \pm 0{\cdot}22 \quad \ldots 9$$
$$N = 5$$

At distances greater than 160 km the plot has been split into two sections depending on the location of the recording stations. The results from the southern stations at Highbury (HIG) and Staaten River (STA) give:

$$T = 7{\cdot}93 \pm 0{\cdot}25 + \Delta/8{\cdot}26 \pm 0{\cdot}08 \quad \ldots 10$$
$$N = 3$$

And the northern recording stations round Strathburn (BRN) give:

$$T = 7{\cdot}66 \pm 0{\cdot}56 + \Delta/8{\cdot}45 \pm 0{\cdot}05 \quad \ldots 11$$
$$N = 7$$

These velocities at distances greater than 160 km are higher than have been obtained from other CRUMP results and could be interpreted in terms of structural differences but until further work is carried out in the area they cannot be confirmed.

4. SURFACE GEOLOGICAL AND GEOPHYSICAL INFORMATION

Because of the design of CRUMP it was not possible to obtain very much geophysical information on any surface layers of rock that might lie above basement. This information is available in a number of reports from other geophysical and geological surveys done in the area (Robertson & Moss, 1959; B.M.R., 1965*a*; B.M.R., 1965*b*; Tectonic Map, 1960). The information in these reports has been summarised in the remainder of this section to give many of the h_1 data in Table VIII used subsequently in the derivation of depths to the Intermediate Refractor and Mohorovičić "Discontinuity" (see Section 5, Interpretation).

The recording sites to the southwest of Group A shots are nearly all situated on the tablelands, straddling the Great Dividing Range. Inland, surface rocks consist of Cainozoic volcanics (mainly basalt) and granites, and the coastal rocks consist mainly of lower Palaeozoic metamorphics (Tectonic Map, 1960). Therefore, for the majority of recording sites the depth to basement can be taken as zero but along the coast and under the Group A shot points basement rock might be expected at some small depth beneath the surface.

The sites for the Group B shots are situated in Princess Charlotte Bay where a considerable

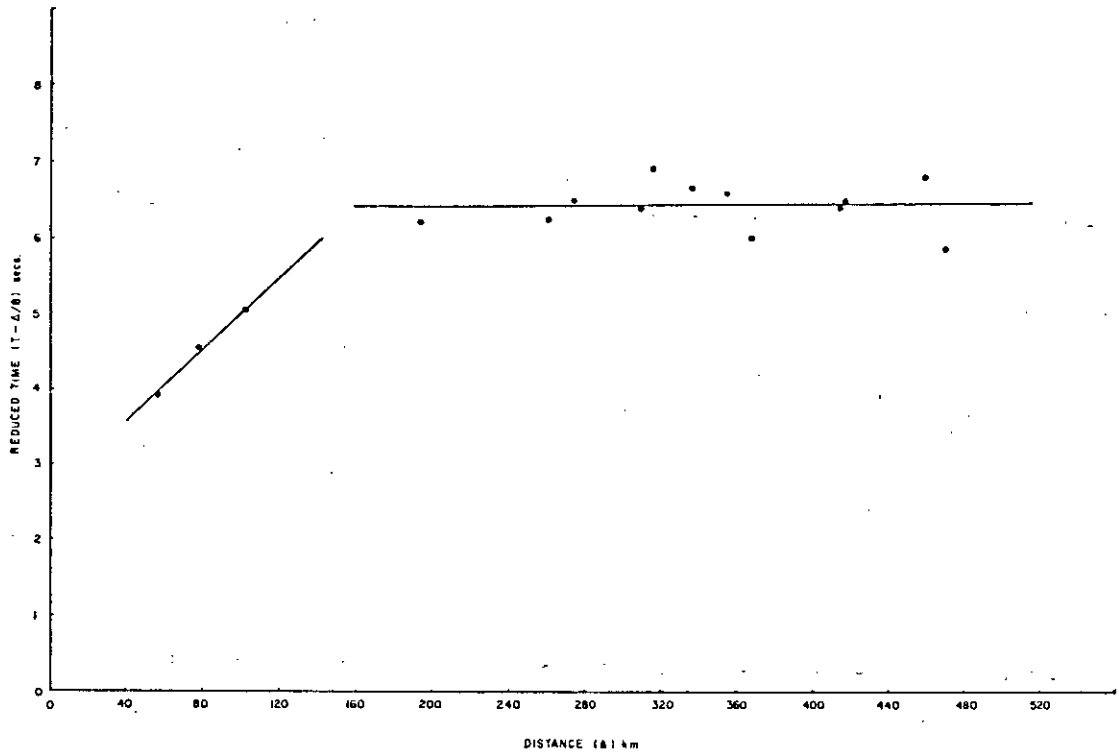

Fig. 4. Travel-time plot for Group C results.

TABLE IV

Travel Times for P, Group C

Station	Lat. S	Long. E	Shot	Distance km	Travel Time sec	Equation
Daru (DRU)	09° 05′·3	143° 12′·3	10	76·7	14·2	7
			11	54·9	10·8	7
			12	101·9	17·8	7
Moreton (MOR)	12° 27′·1	142° 37′·7	11	338·1	49·0	8
			12	275·3	40·9	8
Skardon River (SKA)	11° 38′·9	142° 27′·0	10	317·1	46·57	8
			11	261·6	38·98	8
			12	194·4	30·57	8
Batavia Downs (BAT)	12° 45′·8	142° 42′·6	11	369·3	52·50	8
			12	308·1	44·95	8
Wenlock Road (WEN)	13° 12′·5	142° 48′·2	10	462·8	64·93	8
			11	415·5	58·28	8
			12	356·0	51·08	8
Coen Airport (COE)	13° 45′·9	143° 07′·0	11	472·2	64·81	8
			12	416·5	58·55	8

depth of sediment is expected, as this area lies in the Laura Basin. Depth to basement under Shot 7 is estimated to be at 0·7 km and under Shots 8 and 9 at 1·5 km. The velocity at basement is approximately 5·7 km/sec. The recording sites for Group B shots were situated to the southwest and south of the shot points, again straddling the Great Dividing Range. Those stations on the ranges were normally sited on granites but farther west stations were situated on Mesozoic sediments which cover most of the central and western areas of the Cape York Peninsula. The depth to basement varies from about zero at Abingdon Downs (ABI) increasing in a northwesterly direction to about 0·9 km at Rutland Plains (RUT). The depth to basement at the Group D shots is estimated at 0·9 km. The velocity at basement is approximately 5·5 km/sec.

At the sites of Group C shots in Torres Strait the depth to basement is considerably greater than for any other shot or recording site. At Shot 10 the depth is 4·0 km, at Shot 11, 3·3 km and at Shot 12 it is 2·5 km. The Group C recording sites in northern Cape York Peninsula have a depth to basement varying between 0·5 km at Moreton (MOR) to zero at Coen Airport (COE). The velocity at basement varies between 5·1 and 6·0 km/sec.

5. INTERPRETATION

Because of the complex distribution of shots and recording sites, a method of interpretation must be used that is capable of handling all the data and arriving at a best-fit solution. Such a method was developed by Scheidegger & Willmore (1957) and elaborated by Willmore & Bancroft (1960) and involves the concept of "time terms" at the shot and recording sites. This method has been applied to a number of seismic refraction experiments in Britain (Agger & Carpenter, 1964), and America (Berry & West, 1966). The latter authors have given a lucid account of the theory of the method which will only be summarised in this paper. The application of both time-term analysis and conventional exploration type analysis to large-scale refraction experiments is given by Steinhart & Smith (1966).

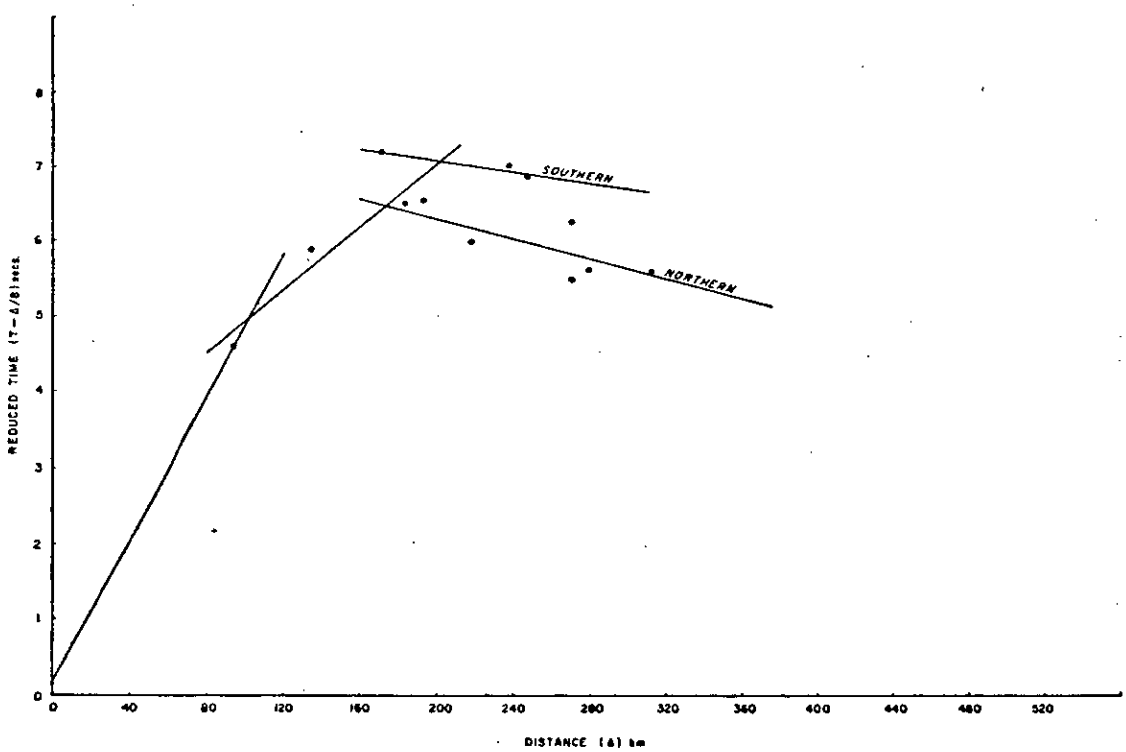

Fig. 5. Travel-time plot for Group D results.

TABLE V

Travel Times for P, Group D

Station	Lat. S	Long. E	Shot	Distance km	Travel Time sec	Equation
Inkerman (INK)	16° 17′·1	141° 26′·9	16	92·7	16·17	9
Highbury (HIG)	16° 25′·7	143° 08′·6	15	237·3	36·73	11
			16	247·8	37·91	11
Staaten River (STA)	16° 29′·2	142° 17′·7	16	171·5	28·7	9, 11
Dorunda (DDA)	16° 33′·3	141° 49′·8	15	134·0	22·70	9
Coleman River (COL)	14° 49′·4	142° 30′·7	16	181·1	29·1	9, 10
Strathmay (MAY)	14° 53′·0	142° 46′·1	15	192·7	30·64	9, 10
Strathburn (BRN)	14° 28′·4	142° 49′·4	15	219·5	33·40	10
Musgrave (MGV)	14° 47′·3	143° 30′·1	15	270·2	40·1	10
Ebagoola (EGO)	14° 18′·5	143° 16′·3	15	270·1	39·33	10
			16	280·3	40·73	10
Stewart River (STW)	14° 06′·8	143° 30′·0	16	312·6	44·71	10

The essence of time-term analysis is the solution of a set of equations of the form

$$T_{ij} = \Delta_{ij}/V + a_i + a_j \qquad \ldots 12$$

where

a_i and a_j = time terms, which characterise the shot and recording sites;
Δ_{ij} = distance along the surface between shot and recording sites;
V = velocity along the refractor;
T_{ij} = travel time.

The analysis may be applied to each section of the travel-time curve for the various groups of shots but in a number of cases the results from different groups can be combined provided there are common recording sites. If T_{ij} is the observed travel-time then the difference between the theoretical and observed travel-times, R_{ij}, is given by

$$T_{ij} - t_{ij} = R_{ij} \qquad \ldots 13$$

$$\text{therefore } R_{ij} = X_{ij} - a_i - a_j \qquad \ldots 14$$

$$\text{where } X_{ij} = T_{ij} - \Delta_{ij}/V \qquad \ldots 15$$

X_{ij} has been introduced because it contains two of the observable parameters T_{ij} and Δ_{ij}. If it is assumed that there are a total of N sites then a total of $N(N-1)$ equations of the form of Equation 14 may be expected if there are shots and recordings at each site. However, there will in general only be $N+1$ unknowns; the N time-terms and the refractor velocity. The criterion used for a best-fit solution is that the sum of the squares of the residuals should be minimised with respect to each time term and the velocity.

Ideally there will be $N(N-1)$ equations of the form 14 but in practice this is unlikely to be the case.

Take $\gamma_{ij} = 1$ if T_{ij} data exist
$= 0$ where it does not exist.
Hence $\gamma_{ii} = 0$

The sum of the squares of the residuals, I, is then given by

$$I = \sum_{i=1}^{N} \sum_{j=1}^{N} (X_{ij} - a_i - a_j)^2 \gamma_{ij}$$

and for this to be a minimum with respect to each time-term

$$dI/da_i = 0$$

This leads to a set of equations which are more easily expressed in matrix notation;

$$\left[c_{ij}\right]\left[a_j\right] = \left[\tilde{x}_i\right] \qquad \ldots 16$$

where

$$c_{ij} = \gamma_{ij},\ i \neq j$$

$$c_{ii} = \sum_{j=1}^{N} \gamma_{ij}$$

$$\bar{x}_i = \sum_{j=1}^{N} X_{ij}\, \gamma_{ij}$$

Hence

$$\left[a_j \right] = \left[c_{ij} \right]^{-1} \left[\bar{x}_i \right]$$

The matrix inversion was performed on the C.S.I.R.O. C.D.C. 3600 computer and the resultant time-terms are calculated using the velocities derived in Section 3 by the least-squares method.

based on other geophysical evidence such as that in Section 4.

The time terms at distances 0-120 km are determined uniquely using the velocity from Equation 1 and using the criterion postulated by the author that the time term at Ravenshoe (RAV) will be zero.

At distances between 80 and 210 km the velocity used is obtained from Equation 2 and the assumption used to determine the constant β is that the time terms are the same at the neighbouring sites of Silkwood (SIL) and

TABLE VI

Time Terms, Group A

Station	0 — 120 km		80 — 210 km		> 160 km	
	TT (sec) v = 5·94 km/sec	TT (sec) if γ = 0·00	TT (sec) v = 6·62 km/sec	TT (sec) if β = 1·87	TT (sec) v = 7·84 km/sec	TT (sec) if α = 3·70
S1	0·00−γ	0·00	2·03−β	0·16	6·32−α	2·62
S2	0·18−γ	0·18	2·57−β	0·70	6·38−α	2·68
S3	0·14−γ	0·14	2·09−β	0·22		
S4	0·35−γ	0·35	2·79−β	0·92	6·16−α	2·46
S5			2·40−β	0·53	6·27−α	2·57
S6	0·44−γ	0·44	2·72−β	0·85	5·97−α	2·27
ALM			−0·41+β	1·46	−0·08+α	3·62
MIN			−0·37+β	1·50	0·49+α	4·19
WYR	0·27+γ	0·27	−0·33+β	1·54		
RAV	+γ	0·00	−0·52+β	1·35		
CJY			−0·35+β	1·52	0·10+α	3·80
ORD			+β	1·87		
CTA					0·50+α	4·20
OAK					0·19+α	3·89
COA					+α	3·70
SIL	0·06+γ	0·06				

The time-terms can only be determined uniquely if there is a coincident shot and recorder site but this was never the case for any of the sets of CRUMP data. In one or two cases the neighbouring shot and recorder sites have been assumed to have the same time terms, otherwise an arbitrary constant is introduced, which is of opposite sign for the shot and recorder time terms, in order to keep the solution general until final assumptions are applied.

The time terms for the stations in the three sections of the Group A results are given in Table VI. α, β and γ are the arbitrary constants introduced into the general solution of the equations and are evaluated by considering possible structures at shot and recording sites

Shot 2. Thus an observation of Shot 4 at SIL can be used to determine β.

The velocity used to determine the time terms at distances greater than 160 km is obtained from Equation 3. The value of the constant cannot be determined uniquely so that it must be estimated from other geophysical evidence. Doyle, Underwood & Polak (1966) have suggested a structure of the continental shelf off New South Wales which might give an indication of the structure to be expected. The CRUMP results from Groups B and C shots give an approximate value of α = 3·70 and since the time terms are similar to those for Group A sites, the same value has been used in determining the Group A time terms uniquely.

The Groups B, C and D data have been analysed collectively but because of the uncertainty in the Group D results, the data have been weighted in favour of the Groups B and C results. The resultant time terms for the shot and recording sites are given in Table VII.

Because of lack of data there are no time terms for the section of the travel-time curve at distances less than 120 km. In the section between 80-210 km the Groups B and D results have been combined. The velocity used in determining the time terms was obtained from Equations 5 and 9.

The constant β has been evaluated by assuming that the time terms at the site of Shot 8 and at Hann River (HAN) are the same.

$$H = \sum_{j=1}^{n} h_j$$

$$= \sum_{j=1}^{n} \left[\left(a_j - \sum_{i=1}^{j-1} h_j / K(V_{j+1} V_i) \right) K(V_{j+1} V_j) \right]$$

where H = depth to the nth refractor
h_j = thickness of the jth layer
a_j = time term for the jth layer
V_j = velocity in the jth layer
$K(V_{j+1} V_j)$ = time-term conversion factor

$$= \frac{V_{j+1} V_j}{\left(V_{j+1}^2 - V_j^2 \right)^{\frac{1}{2}}}$$

TABLE VII

Time Terms Groups B, C and D

Station	80 — 210 km		> 160 km	
	TT (sec) v = 6·77 km/sec	TT (sec) if β = 1·94	TT (sec) v = 8·05 km/sec	TT (sec) if α = 3·50
S7	3·46−β	1·52	6·58−α	3·08
S8	3·39−β	1·45	6·76−α	3·26
S9	3·57−β	1·63	7·19−α	3·69
S10			7·08−α	3·58
S11			6·29−α	2·79
S12			6·46−α	2·96
S15	2·58−β	0·64	5·85−α	2·35
S16	2·29−β	0·35	5·88−α	2·38
HIG			1·31+α	4·81
MOR			0·53+α	4·03
MAY LVN	−0·37+β	1·57	0·89+α	4·39
COL	+β	1·94	0·64+α	4·14
ABI			0·96+α	4·46
BRN	−0·30+β	1·64	0·89+α	4·39
SKA			0·07+α	3·57
BAT			0·10+α	3·60
WEN			0·38+α	3·88
COE			0·13+α	3·63
EGO	−0·78+β	1·16	+α	3·50
DDA INK	0·27+β	2·21		

The analysis for Groups B, C and D results at distances greater than 160 km has been done in two steps, which favour the Groups B and C results. The analysis has first been carried out on the Groups B and C data; then the Group D data have been added and the analysis repeated so that the time terms from the first analysis remain unchanged.

Berry & West (1966) present a method for interpreting the time terms to give structure. Depths to various refractors are given by the expression:

For the purpose of interpreting CRUMP data the model shown in Figure 6 has been used.

In time-term analysis, such a model does not imply that this layering is uniform throughout the whole region covered by the survey but only that there is continuity of the refractors in the immediate vicinity of the shot and recording sites. Willmore & Bancroft (1960) have shown that there has to be considerable distortion of the refractors before the time-term analysis breaks down. The method of

TABLE VIII

Time Terms and Depths to the Various Refractors

Group A

Station	h_1 (km)	80 — 210 km		> 160 km		h_1+h_2 (km)	$h_1+h_2+h_3$ (km)
		TT (sec)	h_2 (km)	TT (sec)	h_3 (km)		
S1	0·0	0·16	2·2	2·62	29·5	2·2	31·7
S2	1·2	0·70	6·9	2·68	21·0	8·1	29·1
S3	0·9	0·22	0·9	2·52*	28·0	1·8	29·8
S4	2·4	0·92	7·2	2·46	15·2	9·6	24·8
S5	2·5*	0·53	1·6	2·57	24·0	4·1	28·1
S6	3·0	0·85	4·9	2·27	14·6	7·9	22·5
ALM	0·0*	1·46	19·7	3·62	18·1	19·7	37·8
MIN	0·0*	1·50	20·3	4·19	24·3	20·3	44·6
WYR	1·9	1·54	16·6	3·90*	21·4	18·5	39·9
RAV	0·0	1·35	18·3	3·90*	23·4	18·3	41·7
CJY	0·0*	1·52	20·6	3·80	19·1	20·6	39·7
ORD	0·0*	1·87	25·3	3·90*	13·9	25·3	39·2
CTA	0·0*	1·54*	20·8	4·20	23·7	20·8	44·5
OAK	0·0*	1·54*	20·8	3·89	19·9	20·8	40·7
COA	0·0*	1·54*	20·8	3·70	17·6	20·8	38·4

Groups B, C and D

Station	h_1 (km)	80 — 210 km		> 160 km		h_1+h_2 (km)	$h_1+h_2+h_3$ (km)
		TT (sec)	h_2 (km)	TT (sec)	h_3 (km)		
S7	0·7*	1·52	16·2	3·08	12·8	16·9	29·7
S8	1·5*	1·45	13·9	3·26	16·5	15·4	31·9
S9	1·5*	1·63	16·0	3·69	18·8	17·5	36·3
S10	4·0*	1·35*	8·0	3·58	23·5	12·0	35·5
S11	3·3*	1·35*	9·3	2·79	13·4	12·6	26·0
S12	2·5*	1·35*	10·9	2·96	15·0	13·4	28·4
S15	0·9*	0·64	5·7	2·35	18·6	6·6	25·2
S16	0·9*	0·35	2·3	2·38	24·1	3·2	27·3
HIG	0·6*	1·89*	20·7	4·81	28·0	21·3	49·3
MOR	0·5*	1·45*	15·9	4·03	25·5	16·4	41·9
LVN	0·6*	1·57	17·0	4·39	28·1	17·6	45·7
MAY	0·2*	1·57	17·8	4·39	27·8	18·0	45·8
COL	0·3*	1·94	21·9	4·14	18·5	22·2	40·7
ABI	0·0*	1·89*	21·9	4·46	23·1	21·9	45·0
BRN	0·0*	1·64	19·0	4·39	26·6	19·0	45·6
SKA	0·3*	1·45*	16·2	3·57	19·9	16·5	36·4
BAT	0·3*	1·45*	16·2	3·60	20·3	16·5	36·8
WEN	0·3*	1·45*	16·2	3·88	23·7	16·5	40·2
COE	0·0*	1·56*	18·0	3·63	18·6	18·0	36·6
EGO	0·0*	1·16	13·4	3·50	23·7	13·4	37·1
DDA	0·8*	2·21	24·1	3·87*	10·7	24·9	35·6
INK	0·8*	2·21	24·1	3·87*	10·7	24·9	35·6

* indicates values that have been approximated from other geophysical data.

calculating the depths implies that the velocity increases with depth, is constant in layers h_1, h_2 and h_3 and that there are no velocity reversals.

The thickness to the first refractor (h_1) has been interpreted from the results of other geophysical surveys presented in Section 4 of this paper. The average velocity in this layer (V_1) has been taken as 4·5 km/sec. The depths to the various refractors are given in Table VIII.

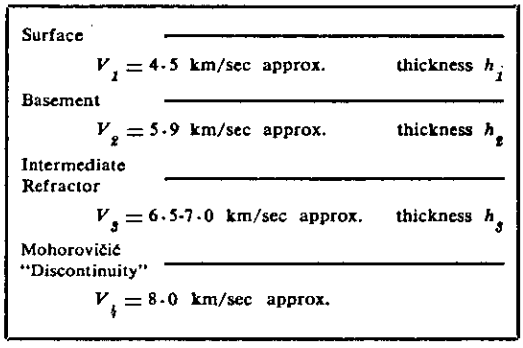

Fig. 6. Model used for the interpretation of CRUMP time terms.

The depths to the intermediate refractor and to M are illustrated in the contour maps in Figures 7 and 8.

On the western side of Cape York Peninsula the contours are influenced greatly by the values for the time terms at Shots 15 and 16 and are therefore not as reliable as those in other areas.

DISCUSSION

The refraction work carried out on CRUMP gives some indication of crustal structure in an area that has not been studied before. The distribution of shot and recorder sites does not enable detailed structure to be studied but a broad structure may be inferred. Crustal thickness appears to increase from a value of about 25 km on the continental shelf to about 40 km in the interior of the continent with some local values greater than 45 km. The thinning of the crust in the Gulf of Carpentaria suggested in Figures 7 and 8 will have to be confirmed by further work. Across Torres Strait there appears to be a thinning to values of about 28 km from values both to the north and south of 35 km.

Upper mantle velocities vary from 7·82 km/sec in southeast of the survey area to 8·00 km/sec in the northern region and 8·09 km/sec in the central region.

The crustal thickness over the area is greater than might have been expected from surface-wave dispersion studies carried out across the area (Bolt & Niazi, 1964) and the future results of refraction studies carried out by A.N.U. (R. Underwood [unpublished]) in the adjoining areas to the west will be of interest. Surface-wave dispersion analysis is currently being carried out at the University of Tasmania on results obtained from the outstations in Papua run by the geophysical observatory staff at Port Moresby (Brooks & Ripper, 1966). This analysis should provide structural information to the northeast of the CRUMP survey area.

The time-term method seems admirably suited to this type of seismic refraction survey and future work in the area might well be designed to extend the sets of data used in CRUMP by re-occupying a number of recording stations. Future work must also be designed so that there are coincident shot and recorder stations in order to eliminate all unknown factors inherent in time term analysis.

ACKNOWLEDGMENTS

The author would like to thank all the participants in CRUMP for their help and assistance in obtaining and preparing the results. In particular the author would like to thank the leaders of the various field parties, Dr J. P. Webb (University of Queensland), Mr C. Kerr Grant (University of Melbourne), Dr R. Underwood (Australian National University), Dr A. A. Day (University of Sydney), Mr D. F. Dyson (Commonwealth Central Testing Laboratory), Cdr Moorey who was the liaison officer for the R.A.N. at all stages of the project and Mr J. C. Dooley (B.M.R.) who directed the project and all the B.M.R. field parties.

This paper has been presented for publication with the permission of the Director of the Bureau of Mineral Resources, Geology and Geophysics.

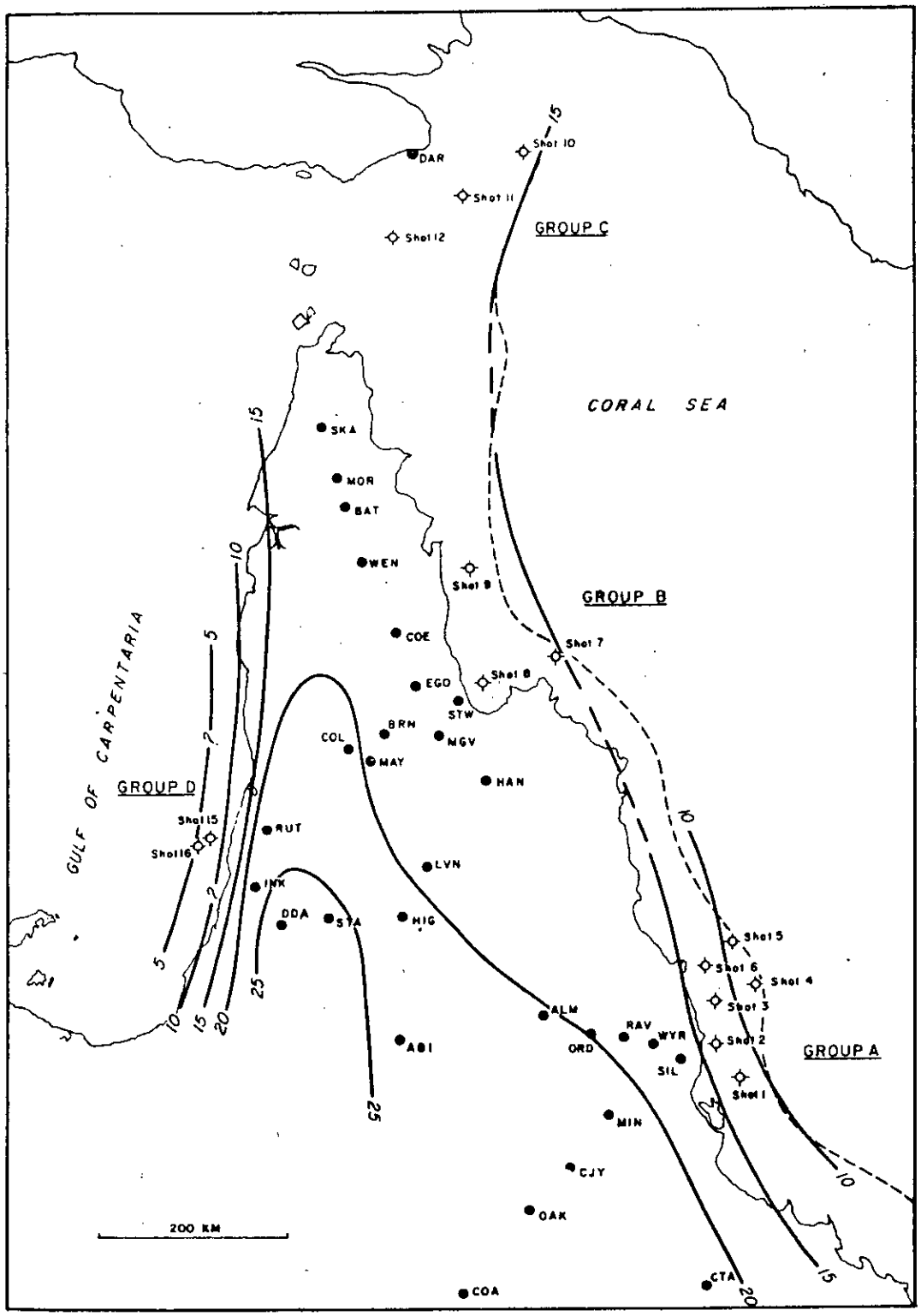

Fig. 7. Depth to intermediate refractor (km).

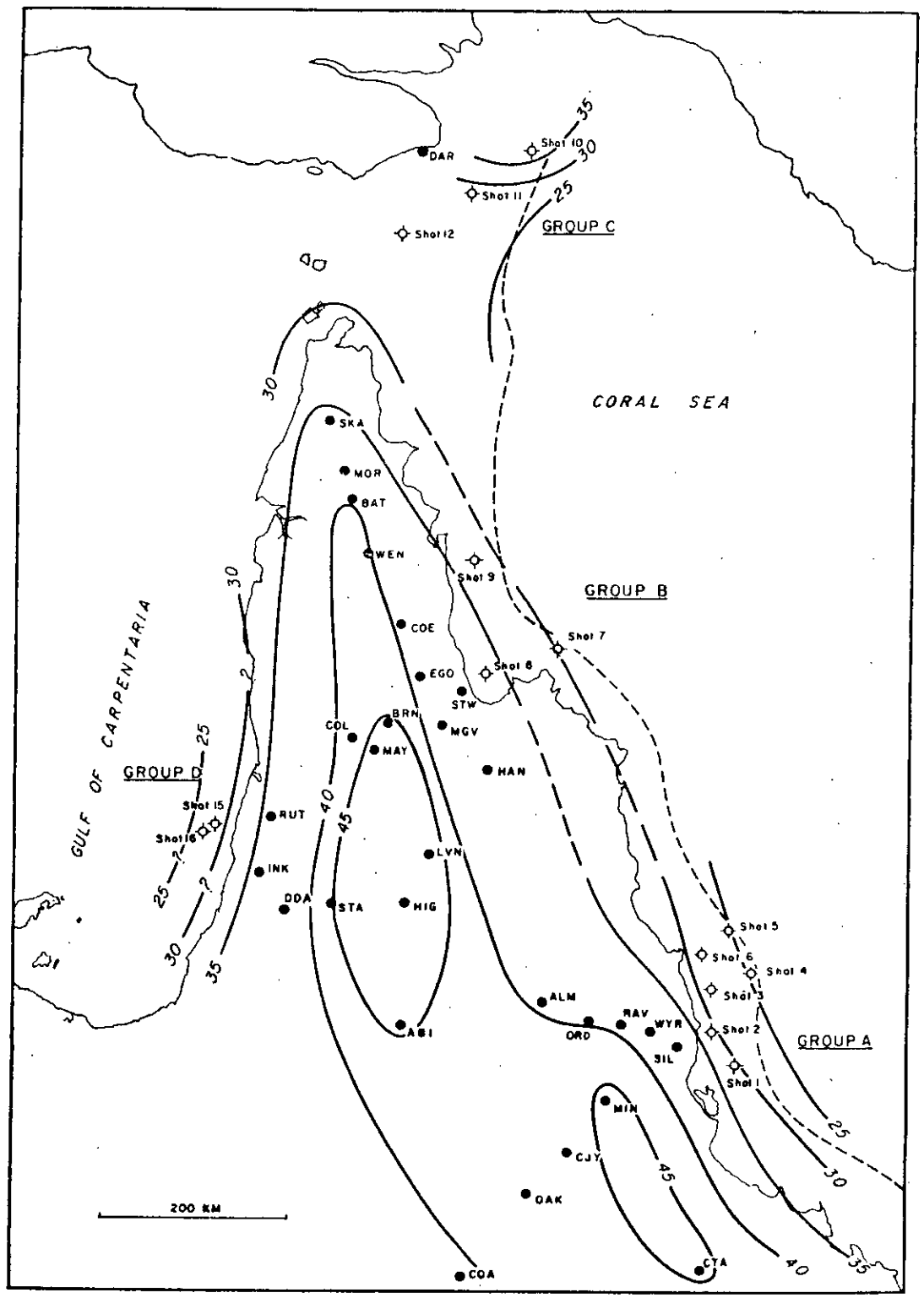

Fig. 8. Depth to Mohorovičić "Discontinuity" (km).

REFERENCES

AGGER, H. E., & CARPENTER, R. W., 1964: A crustal study in the vicinity of the Eskdalemuir seismological array station. *Geophys. J. R. astr. Soc., 9,* pp. 69-84.

BERRY, M. J., & WEST, G. F., 1966: An interpretation of the first arrival data of the Lake Superior experiment by the time term method. *Bull. seism. Soc. Am., 56,* pp. 141-171.

BOLT, B. A., & NIAZI, M., 1964: Dispersion of Rayleigh waves across Australia. *Geophys. J. R. astr. Soc., 9,* pp. 21-35.

BROOKS, J. A., & RIPPER, I. D., 1966: Proposed investigations of crustal structure in New Guinea. *Rec. Bur. Miner. Resour. Geol. Geophys. Aust.,* 1966/33.

BUREAU OF MINERAL RESOURCES, 1960: Tectonic Map of Australia. Dept natn. Dev., Canberra.

———, 1965*a*: Subsidised Oil Search Report No. 65/11019, Archer River.

———, 1965*b*: Subsidised Oil Search Report No. 65/4599. Torres Strait and Princess Charlotte Bay.

DOYLE, H. A., & EVERINGHAM, I. B., 1964: Seismic velocities and crustal structure in southern Australia. *J. geol. Soc. Aust., XI,* pp. 141-150.

———, ———, & HOGAN, T. K., 1959: Seismic recordings of large explosions in southeastern Australia. *Aust. J. Phys., 12,* pp. 222-230.

DOYLE, H. A., UNDERWOOD, R., & POLAK, E. J., 1966: Seismic velocities from explosions off the central coast of New South Wales. *J. geol. Soc. Aust., 13,* pp. 355-372.

EIBY, G. A., & DIBBLE, R. R., 1957: Crustal Study Project. *Geophys. Mem. N.Z., 5.*

FINLAYSON, D. M., 1968: Operational Report on the Carpentaria Region Upper Mantle Project (CRUMP). *Rec. Bur. Miner. Resour. Geol. Geophys. Aust.,* 1968/14.

ROBERTSON, C. S., & MOSS, F. J., 1959: Preliminary report on a seismic survey in the Carpentaria Basin, Queensland. July-December, 1958. *Rec. Bur. Miner. Resour. Geol. Geophys. Aust.,* 1959/4.

SCHEIDEGGER, A. E., & WILLMORE, P. L., 1957: Use of a least squares method for the interpretation of data from seismic surveys. *Geophysics, 22,* pp. 9-22.

STEINHART, J. S., & SMITH, T. J. (Eds.), 1966: The Earth beneath the Continents. *Geophys. Monogr., 10.*

WILLMORE, P. L., & BANCROFT, A. M., 1960: The time term approach to refraction seismology. *Geophys. J. R. astr. Soc., 3,* pp. 419-432.

D. M. Finlayson,
Bureau of Mineral Resources,
Geology & Geophysics,
P.O. Box 378,
Canberra City, A.C.T. 2601.

Reprinted from
BMR Journal of Australian Geology & Geophysics, 4, 1979, 243-252

Explosion seismic profiles, and implications for crustal evolution, in southeastern Australia

D. M. Finlayson, C. Prodehl[1], *& C. D. N. Collins*

The interpreted velocity-depth structure in the crust of the Lachlan Fold Belt in southeastern Australia indicates that velocity gradients, rather than discontinuous velocity changes, characterise the region. The velocity-depth morphology varies across the region. In the upper crust at depths less than 12 km, there is evidence in three areas for velocity decreases within a general velocity increase from about 5.6 km/s to 6.3 km/s. In the middle crust (depth range 16 km to about 35 km) a low velocity zone is interpreted within a general increase in velocity from 6.3 km/s to greater than 7 km/s; the prominence of the low velocity zone varies throughout the region. The upper mantle velocity is in the range 8.02 to 8.05 km/s; this velocity is reached at a depth slightly greater than 50 km under the highest topography in Australia, and at depths between 40 and 50 km elsewhere.

There are similarities between the velocity-depth structure in southeastern Australia and that in the Appalachian Orogen of North America. Geochemical mixing and/or compositional inhomogeneity is a likely reason for the velocity-depth structures, and such inhomogeneity is probably still influencing current moderate earthquake activity and continuing highland uplift. In pre-Ordovician times the region of the Lachlan Fold Belt probably consisted of continental crust which was submerged and thickened by episodic crustal development similar to the processes which resulted in the Appalachian Orogen.

Introduction

In the period 1976-78 the Bureau of Mineral Resources, Geology and Geophysics (BMR) made seismic recordings along four profiles radiating from the Dartmouth Dam construction site in southeastern Australia (Fig. 1). Finlayson & others (1979) have reviewed seismic crustal data from the area, presented an extensive bibliography, and have interpreted the 1976-77 data from one profile (Dartmouth-Marulan). They indicated that the crust in the Lachlan Fold Belt is neither uniform nor homogeneous; it is characterised by velocity transitions rather than discontinuities, it may contain one or more low velocity zones, and the crustal thickness exceeds 50 km in places. These results were significantly different from earlier, relatively simple, two-layer, crustal models.

This paper reports interpretations of recordings made during 1978 along three other profiles radiating from Dartmouth (Fig. 1), and supplements the earlier interpretation (Finlayson & others, 1979) along a fourth profile. Two of these 1978 profiles exceeded 400 km in length and were deployed to record upper mantle *P*-waves as first arrivals. This was not done satisfactorily during 1976-77, because the maximum recording distance (300 km) was too short to record first arrivals from the upper mantle through the unexpectedly thick crust. The profiles were chosen to try to determine the variation in velocity-depth structure along different azimuths from Dartmouth within the Lachlan Fold Belt, from which geological/geochemical differences may be inferred.

Geological setting

The geological development of the crust in the Lachlan Fold Belt of southeastern Australia is still the subject of debate. Discussion at a recent symposium on the Crust and Upper Mantle of South East Australia (CUMSEA) recognised that, although the oldest positively identified rocks are Ordovician, they must overlie older continental-style rocks. These are the source rocks for many granitoids which constitute about one quarter of the land surface (for recent references see Denham, 1979; Ferguson & others, 1979) (Fig. 1). White & Chappell (1977) have described a mechanism to derive granitoids from metasedimentary (S-type) and igneous (I-type) source rocks; both types imply sources of material at depths of 12-25 km and greater. White (1979) indicated that these sources are probably Precambrian and constituted the bulk of the crustal material at that time. However, they are now obscured by overlying Palaeozoic rocks.

A tectonic model for these features of the Lachlan Fold Belt may be evident at present-day lithospheric plate boundaries and passive continental margins. Dietz (1963) and Dewey & Bird (1970) have proposed models for continental evolution which involve multiple deformation episodes at continental margins. These models require a passive continental margin for the build-up of considerable sedimentary sequences out to 300-400 km from the shore, followed by dynamic crustal shortening accompanied by subduction of oceanic lithosphere. Finlayson & others (1979) have already pointed out that the thickness of the crust in the Lachlan Fold Belt favours subduction of oceanic lithosphere at a continental margin, rather than at the margin of another oceanic lithospheric plate as in some western Pacific-type models. Ferguson & others (1979) indicate that the Ordovician rocks of the Lachlan Fold Belt are compatible with a thickened, possibly continental, crust. Nicholls (1979) envisages a fault-bounded, post-orogenic, Basin-and-Range type province within a continental environment for the emplacement of Silurian volcanics near Dartmouth.

The geology of the Lachlan Fold Belt supports the concept of lateral inhomogeneity in the lower crust and upper mantle in the past. Beams (1979) has drawn attention to the considerable extent of the I-type Bega Batholith (Fig. 1), and concludes that at the time of emplacement there must have been large-scale lateral variations in the lower crust, involving hundreds of

1. Geophysikalisches Institut, Universitat, Hertzstr. 16, D7500 KARLSRUHE 21, Federal Republic of Germany.

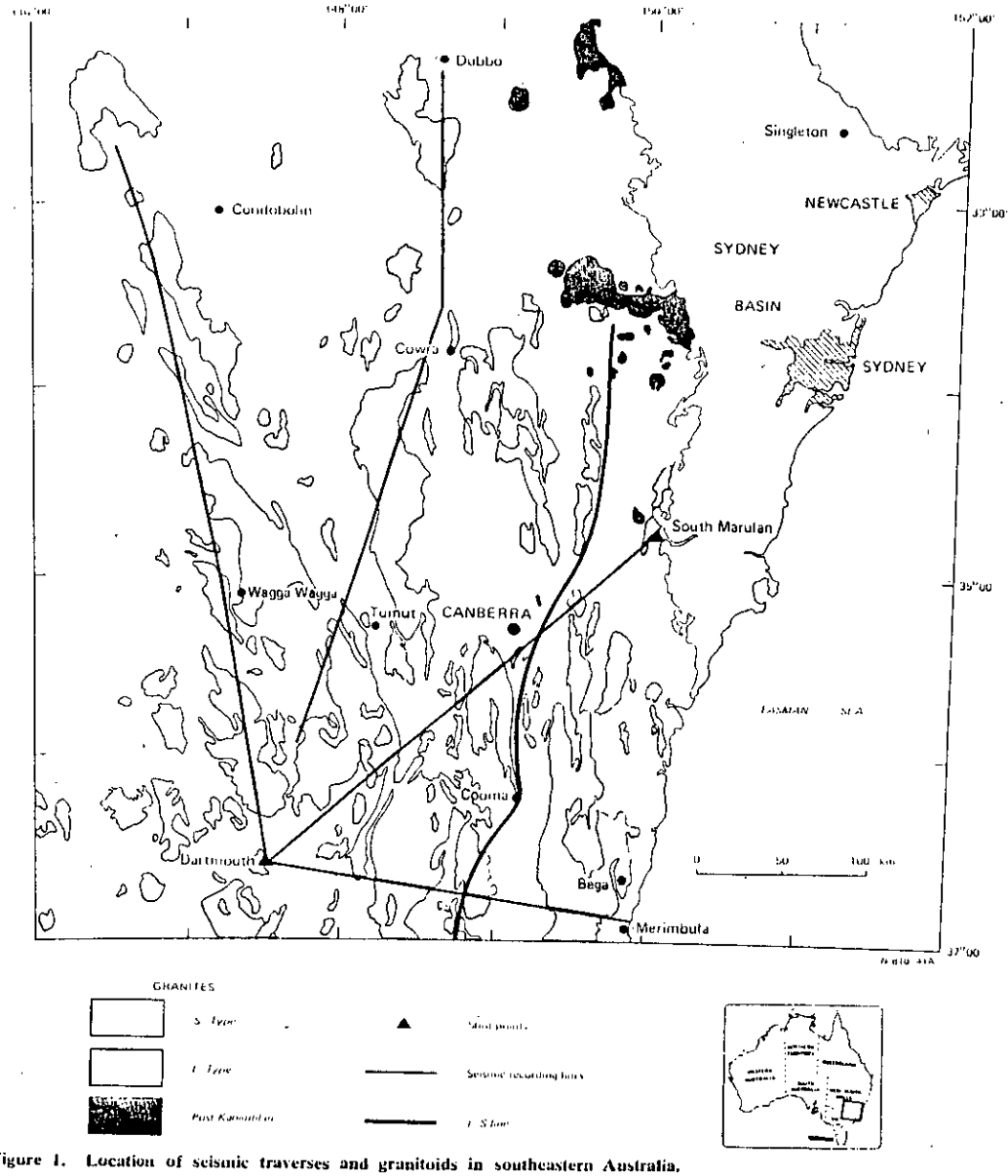

Figure 1. Location of seismic traverses and granitoids in southeastern Australia.

cubic kilometres of rock. The Bega Batholith is the major component of exposed I-type granite in southeastern Australia. The eastern limit of S-type granites has recently been re-defined by Flood & others (1979) (the I-S Line, Fig. 1), and this certainly marks a major crustal feature from Palaeozoic times. Wass (1979) has drawn attention to the inhomogeneities in the upper mantle which can be inferred from the geochemistry of Cainozoic alkali basalts in southeastern Australia. It is therefore not unreasonable to assume that inhomogeneities persist to the present day in both the crust and upper mantle as well as at the surface, and that detailed seismic investigations should be capable of identifying them.

Survey operations and data

At Dartmouth (Fig. 1), shots of between 1.5 and 16.0 tonnes of explosive were fired in granodiorite and Silurian volcanics to form the dam spillway and provide material for the rockfill dam. At Marulan, shots of between 2.0 and 4.0 tonnes of explosive were fired in Silurian limestone to provide material for cement manufacture. All shots were fired in shothole patterns, most with no delays in the firing line, but some with total delays of up to 50 ms. Shot timing tape recorders were installed at both shot sites for the duration of survey operations; the estimated error in shot timing is ± 10ms. Shot locations are known to within ± 50 m.

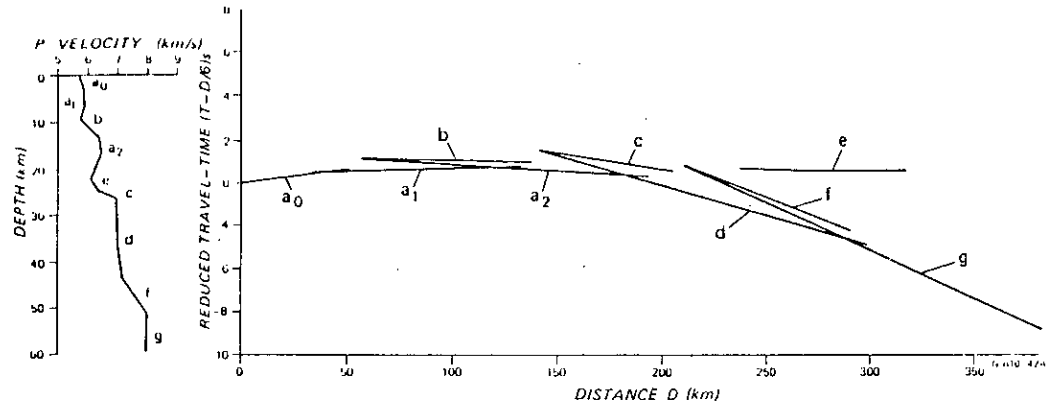

Figure 2. General features of travel-time curves identified in southeastern Australia. Letters indicate travel-time branches referred to in the text.

Recordings were made at sites 10-15 km apart along the lines shown in Figure 1. BMR-designed seismic tape recorders were usually deployed for about 1-2 weeks at each site. Seismometers were often placed on rock outcrop, but even where outcrop is not evident, the unconsolidated cover is generally not thick—usually a few metres at most.

The seismic tapes were played back. Seismic record sections were produced; these could be normalised to the maximum amplitude on each trace or for shot size, recorder gain or recorder distance. Digital filtering of the records was done using a number of bandpass filters. Those shown in Figures 3-7 were filtered using a 4 to 12 Hz bandpass.

Seismic record sections and interpretation

Of the four recording lines radiating from Dartmouth (Fig. 1), only that between Dartmouth and Marulan was reversed (Finlayson & others, 1979). This line has been included in the work presented here because further interpretation has been done on the data.

The general features of the seismic travel-time curves are contained in Figure 2. The seismic record sections interpreted in this paper are contained in Figures 3 to 7, together with the travel-time curves and synthetic seismograms for the preferred models.

In the directions of the four recording lines within 20 km of the Dartmouth shot source, the surface rocks consist of low-grade metamorphosed Ordovician sediments and Silurian volcanics, with granodiorite outcrops close to the damsite. Seismic records out to 50 km were interpreted using the Herglotz-Wiechert inversion of first arrival data (Bullen, 1963). This resulted in an average velocity-depth model near the source with an initial velocity of 5.67 km/s at the surface, increasing to 5.85 km/s at 2.2 km depth, and to 5.95 km/s at about 2.4 km depth. On the scale of the seismic work undertaken, this effectively represents the near-surface geology, but detailed work would have to be undertaken to determine a more precise model of all near-surface rock units. Laboratory tests on hand samples of the Silurian volcanics and granodiorites indicated P-wave velocities of between 4.83 and 5.71 km/s, the latter velocity being in the least weathered rock and agreeing substantially with the velocity observed in the field data.

The identification of distinct phases, apart from first arrivals, is not easy on the record sections from Dartmouth shots (Figs. 3-6). At distances less than 200 km, the record sections could perhaps be best characterised by their lack of strong subsequent arrivals.

Some generalisations can be made about the Dartmouth record sections; these are illustrated in Figure 2. This shows the seismic phases on the sections which have influenced the interpretation of velocity-depth functions. Phases a_0 and a_1 depict the arrival times of waves through the surface rocks and uppermost part of the crust, and generally have apparent velocities of up to 6.0 km/s. The a_2 phase usually has an apparent velocity greater than 6.2 km/s, which probably indicates higher grade metamorphic rocks within the upper crust. Finlayson & others (1979) have indicated the presence of such velocities in surface rocks near Canberra and Marulan. Phase b is not present on all record sections, but is interpreted on those toward Marulan and Merimbula as a reflected phase from the base of a low-velocity zone within the upper crust. Its presence is clearly evident only on some records, which indicates inhomogeneity in the upper crust.

Mid-crustal phases correspond to travel-time branches c, d and e in Figure 2. The d-phases have an apparent velocity between 6.9 and 7.4 km/s, and are interpreted as refracted arrivals from the lower crust. The reflection phases from the lower crust (c-phases) are only recorded over a short distance, indicating a velocity transition rather than a sharp boundary. The critically refracted arrivals from the lower crust are identified in the distance range 110-140 km. The e-phases depict a band of arrivals which is evident on all record sections, but perhaps more clearly on the Dartmouth-Marulan and Dartmouth-Condobolin sections. It has an apparent velocity of 6.0-6.3 km/s and is interpreted as energy returning from the base of a mid-crustal low-velocity zone (Finlayson & others, 1979).

The phases f and g (Fig. 2) are associated with the lower-crust/upper-mantle (Moho) boundary. In the observed data, the general lack of strong f-phases reflected from the Moho indicates that the boundary is transitional rather than sharp. The g-phases refracted through the upper mantle are evident on the record sections towards Dubbo and Condobolin as first arrivals

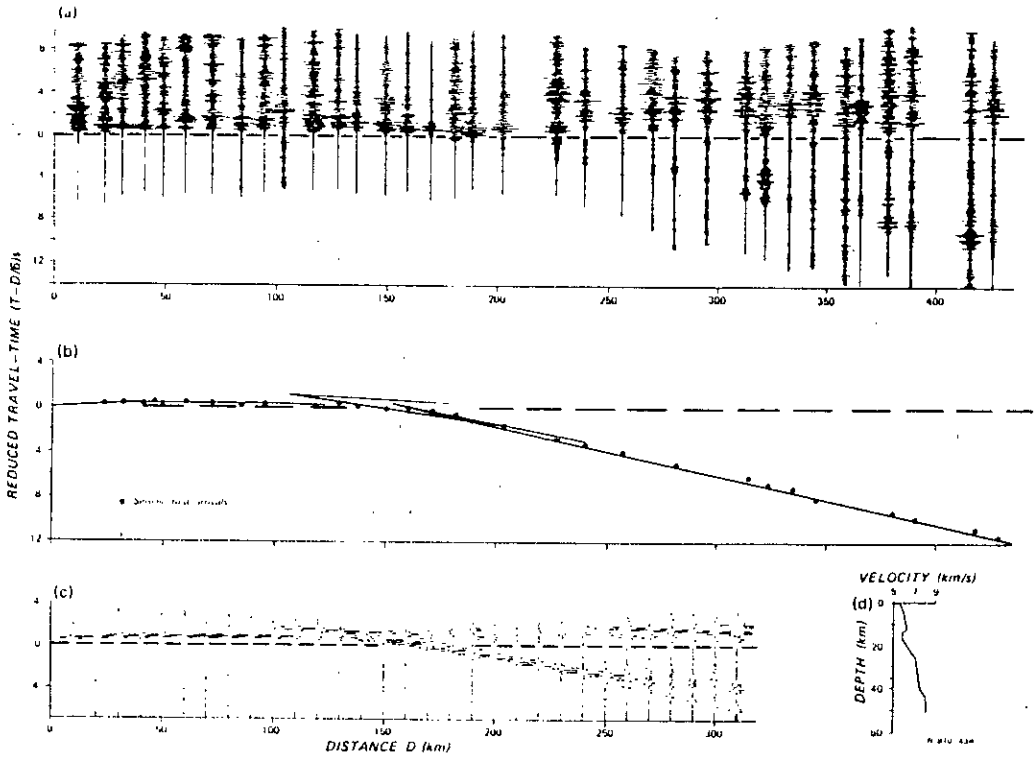

Figure 3. (a) Dartmouth to Condobolin seismic record section, (b) DCN-1 model travel-time curves and (c) synthetic seismograms, and (d) velocity-depth model DCN-1.

with an apparent velocity of 8.0-8.1 km/s. First arrivals at distances greater than about 150 km become earlier going from the Marulan to the Dubbo, and then to the Condobolin, lines. This decreasing travel-time pattern indicates a general thinning of the crust towards the west. It also gives a general indication that the critical point for lower crust and upper mantle arrivals must be at distances of 160-200 km.

The record section for the reverse profile from Marulan to Dartmouth (Fig. 7) can also be described in the general terms of the foregoing discussion. Details described later indicate some differences between this profile and the reverse profile from Dartmouth shots.

Interpretation methods

Only the profile towards Marulan has reverse data, therefore the interpretations along the other three lines were limited to features which could be identified from the Dartmouth shot source. Methods outlined by Giese (1976a, b) were used on the various seismic phases mentioned above to arrive at approximate velocity-depth models. These were then tested using various computer programs to calculate travel-time curves and to generate synthetic seismograms (Fuchs, 1968). Many models were tried in attempts to test the sensitivity of the procedure to changes in velocity-depth morphology. The velocity-depth functions finally determined for the four recording lines probably represent the simplest functions which adequately satisfy the observed data. Further recording using closer spaced stations and other shot points would be required to resolve finer detail. All velocities quoted have been corrected to a spherical earth model.

Dartmouth-Condobolin

On the record section towards Condobolin (Fig. 3) the a_0, a_1 and a_2 phases are evident out to distances of about 120 km. There is no convincing evidence for b-phases, and therefore no low-velocity layers are interpreted in the upper crust. Between 100 and 190 km there are events after the first arrivals which are interpreted as being from mid-crustal (c and d-phases) and Moho (f and g-phases) transitions. There are no markedly developed reflection phases from either transition, which is taken to indicate that there are no strong velocity gradients at either boundary. The e-phases are evident as arrivals in the distance range 200 to 430 km.

Figure 3 shows the preferred velocity-depth model (DCN-1) which has been used to illustrate features of the record section. No marked velocity gradients are interpreted. Model DCN-1 includes a decrease in velocity in the middle crust; this feature seems necessary to satisfy the travel-time separations of e and g-phases at distances beyond 200 km. The depth to the upper mantle velocity of 8.05 km/s is 42 km.

Dartmouth-Dubbo

No recordings were made on the line towards Dubbo within 80 km of Dartmouth. The records shown on the record section (Fig. 4) for this part of the line are taken from the Condobolin line. There are not great differences in travel-times within the upper crust in the

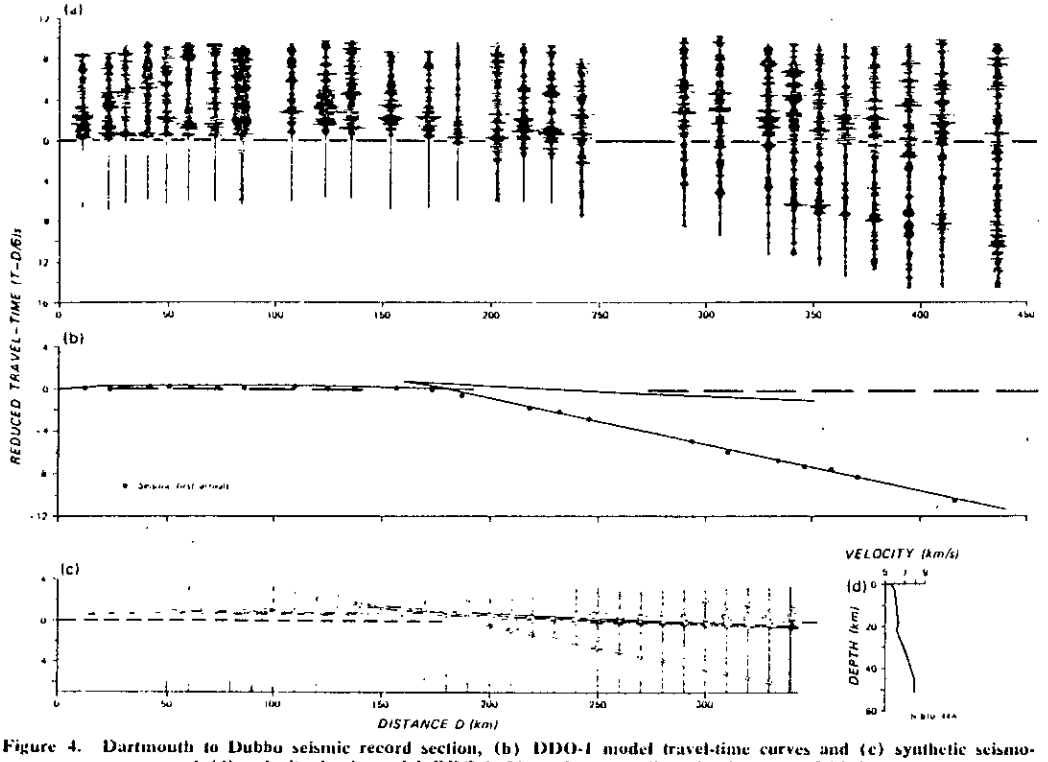

Figure 4. Dartmouth to Dubbo seismic record section, (b) DDO-1 model travel-time curves and (c) synthetic seismograms, and (d) velocity-depth model DDO-1. Note that recordings in the range 0-80 km are the same as those in Figure 3.

distance range 80-120 km. At greater distances seismic arrivals generally come in later than along the Condobolin line, indicating a thicker crust.

The c and d-phases from the mid-crust are not well developed, so that identification of any cusp points in the travel-time curves is difficult. Some later phases in the distance range 120 to 150 km are interpreted as critically refracted phases from the middle crust but, as on the Condobolin line, the limited distance over which they are seen indicates no marked velocity gradients.

The f and g-phases from the Moho transition are again only weakly developed, although first arrivals out to distances of over 400 km are evident. The pattern of e-phases is not as clear as on the Condobolin line. This is interpreted as indicating that any mid-crustal low-velocity zone is not a prominent feature.

Figure 4 shows the preferred model (DDO-1) whose travel-time curve and synthetic seismogram contain features evident on the record sections. The model contains a weak, low-velocity zone in the middle crust which serves to satisfy more closely the arrival times of weak e-phases beyond 200 km. An upper mantle velocity of 8.04 km/s at 44.5 km depth in DDO-1 satisfies the first arrival data beyond 200 km.

Dartmouth-Marulan

The seismic record section between Dartmouth and Marulan (Fig. 5) was examined to determine whether any improvements could be made to the velocity-depth model (DMA-1) of Finlayson & others (1979). In particular, some further recording have been made at the Marulan end of the line at distances beyond 190 km. These recordings served to reinforce the interpretation of a lower crustal apparent velocity of about 7.4 km/s (Fig. 5). Further modelling of the record section features produced a modification of the DMA-1 model. The preferred model (DMA-2) has the Moho at a depth of 50-51 km with an upper mantle velocity of 8.02 km/s.

Marulan-Dartmouth

The record section from Marulan towards Dartmouth is shown in Figure 6. Beyond 230 km the seismic records along the direct line were poor, but good recordings are available from the Dartmouth-Condobolin and Dartmouth-Dubbo lines in the vicinity of Dartmouth. These latter recordings have therefore been used in Figure 6. In the distance range 80 to 110 km there are a series of later arrivals which indicate some complexity in the upper and middle crust. Beyond 220 km the first arrivals are later than along the reversed line. It is possible that the g-phases are so weak that they cannot be identified within the seismic noise. However, if this is so, it indicates yet again a very weak velocity gradient at the Moho, and possibly a velocity decrease in the upper mantle. Figure 6 shows the velocity-depth model MDH-1 interpreted from the record section.

Dartmouth-Merimbula

The recording line from Dartmouth to Merimbula only extends 220 km from the shot source (Fig. 7), and

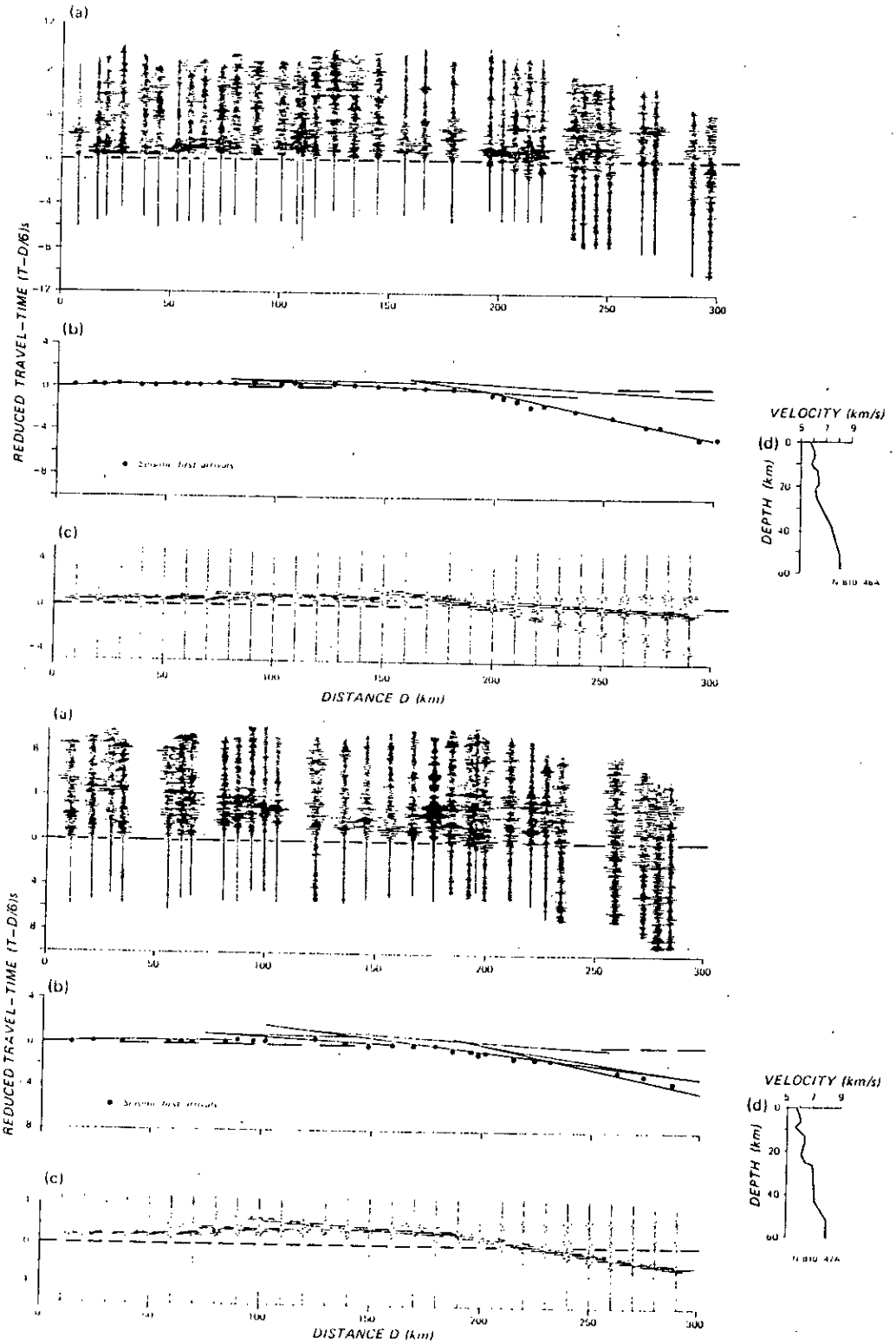
(a)
(b)
(c)
(d)
REDUCED TRAVEL-TIME (T-D/6)s
DISTANCE D (km)
VELOCITY (km/s)
DEPTH (km)
0
50
100
150
200
250
300
5
7
9
20
40
60

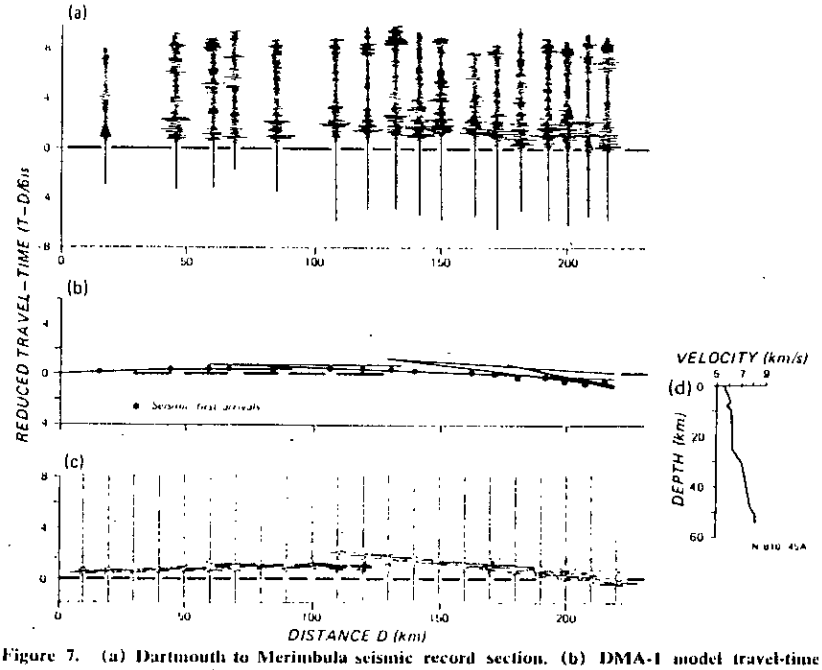

Figure 7. (a) Dartmouth to Merimbula seismic record section. (b) DMA-1 model travel-time curves and (c) synthetic seismograms, and (d) velocity depth model DMA-1.

therefore the detailed structure of the lower crust and upper mantle is not as well defined as along the other lines. In the distance range 50 to 90 km there is some evidence for subsequent arrivals within about 0.5 s of the first arrivals; these are interpeted as b-phases from a low-velocity layer in the upper crust.

Beyond 140 km there are phases which are interpreted as c and d-phases, and as f and g-phases, from the middle and lower crust respectively. Figure 7 shows the preferred velocity-depth model which displays travel-time and synthetic seismogram features close to those observed. Between 150 and 170 km there is a delay in first-arrival energy compared with the extrapolation of the travel-time curve at shorter distances. Synthetic seismograms and travel-time curves from model DMA-1 indicate that these phases are c and d-phases. The model DMA-1 also has a weak low-velocity zone in the middle crust, a Moho depth of 50 km, and an upper mantle velocity of 8.03 km/s.

Discussion

The interpretation of the seismic record sections radiating northward and eastward from Dartmouth indicates that the crustal structure is not simple. In the upper crust (at depths less than 12 km) there is evidence for velocity decreases within a general increase in velocity from about 5.6 km/s to 6.3 km/s. The diagnostic features of such velocity decreases occur on the record sections over a short distance range and the interpreted geological structures may extend over only a few tens of kilometres. Such structures could only be defined more accurately by further detailed seismic field work.

In the middle crust, the velocity transitions take the form of weak velocity gradients rather than sharp boundaries. Some features can be explained most simply by introducing a low-velocity zone in the middle crust, where velocities generally increase from about 6.3 km/s at about 16 km depth to greater than 7.0 km/s at depths of about 35 km. The low-velocity zone can be interpreted along all profiles, but is more prominent on the Dartmouth-Condobolin and Dartmouth-Marulan profiles. On the Dartmouth-Dubbo profile the low-velocity zone probably disappears, or is only very weakly developed.

The velocity-depth interpretation at the crust/mantle boundary indicates that the Moho is a velocity transition with a gradient of about 0.08-0.23 kms^{-1}/km extending over a depth of up to 10 km. The velocity in the upper mantle is in the range 8.02 to 8.05 km/s. The depth of these upper mantle velocities is greatest between Dartmouth and Marulan, i.e. under Australia's highest mountain range, and is shallower towards the east and west (Fig. 8).

Geological interpretation

The translation of the velocity-depth structures into geological terms is not an exact process. Black (1978) has made a study of the processes likely to influence the seismic parameters in crustal rocks based on results from USA. He has considered the inter-relation of seismic velocities and attenuation with temperature, effective pressure, bulk density, mean atomic weight and

Figure 5. (a) Dartmouth to Marulan seismic record section, (b) DMN-1 model travel-time curves and (c) synthetic seismograms, and (d) velocity depth model DMN-2.

Figure 6. (a) Marulan to Dartmouth seismic record section, (b) MDH-1 model travel-time curves and (c) synthetic seismograms, and (d) velocity depth model MDH-1.

fluid phases within crustal rocks. Some of his conclusions were that compositional changes with depth will overshadow pressure and temperature effects; that pressure and temperature effects cancel out in most areas of non-extreme heat flow on continents; the lack of velocity gradients in a crustal layer implies an isochemical composition; volatiles in the upper and middle crust result in low effective pressures; low-velocity layers in the Basin and Range Province of western USA are consistent with small amounts of melt in the crust; temperatures and velocities in continental crusts reach their equilibrium values within 200 m.y. of formation; and that velocity-depth structures in eastern and western USA represent different stages of the evolutionary process for continental crust.

A corollary to Black's conclusion that the lack of velocity gradients in a crustal layer implies an isochemical composition may be that velocity gradients, such as those found in southeastern Australia, are caused by compositional mixing. If this corollary is correct, the Moho under southeastern Australia can be interpreted as a zone of geochemical differentiation.

The velocity inversions interpreted in the Lachlan Fold Belt at the mid-crustal depths of 16 to 35 km are at the depths at which it is envisaged that Palaeozoic granitic partial melts were formed (Clemens & Wall, 1979). The seismicity of the Lachlan Fold Belt (Denham & others, 1979), although not manifest by large earthquakes, is persistent, and a testimony to present-day tectonic processes in southeastern Australia. All earthquakes are regarded as shallow (less than 30 km, with most being less than 20 km deep), i.e. above the depth of the mid-crustal velocity inversions as interpreted in this paper. The inversions may represent a depth at which plastic flow is more likely than brittle fracture. The Palaeozoic geochemical differentiation which occurred at such depth and resulted in the widespread emplacement of granitoids, may have resulted in a compositional anomaly, now seen as a velocity inversion. Wellman (1979) has reviewed the uplift of the southeastern Australian highlands, and concluded that the pattern is consistent with steady uplift over the last 90 m.y. He eliminates crustal shortening and arching of the crust as causal, and attributes it instead to a crustal underplating driving mechanism. It is hypothesised here that the mechanism may also be affected by intra-crustal inhomogeneities, as well as involving the lower crust-upper mantle boundary.

Tectonic comparisons

Prodehl (1977), among others, has made comparative studies of seismic crustal structures in a variety of tectonic provinces throughout the continents. Different seismic characteristics such as velocity gradients and their depth extent can be recognised in shield areas, old orogenic provinces, young orogenic provinces, mobile zones, and graben. The gradients and depths interpreted from the seismic record sections in southeastern Australia are similar to those observed in old orogenic provinces, such as the Appalachian Highlands of USA or the southern part of the Caledonide Province in southern Scotland. The Appalachian structures, in particular, contain features such as velocity transition zones and depths to the upper mantle which are similar to those in the Lachlan Fold Belt.

The seismic activity recorded in the Appalachian region is similar in style to that in southeastern Australia. Bollinger (1969) describes the central Appalachian region as having a moderate amount of low level activity. Bollinger (1970) has also examined the traveltimes from earthquakes within the Appalachian region and, using his simple model of a crust with average velocity 6.24 km/s overlying mantle with velocity 8.22 km/s, the average depth to the Moho is 43 km. This depth is likely to increase when a more detailed velocity structure is determined. Borcherdt & Roller (1966) determined velocities of 6.3 and 6.9 km/s under the Appalachian plateau with an upper mantle velocity of 8.0 km/s. Broad transition zones are interpreted from the record sections and the upper mantle is at a depth in excess of 50 km (Prodehl, 1976, 1977).

Dewey & Bird (1970) have described how they envisage the episodic development of Cordilleran-type mountain belts at continental margins, taking examples from their detailed studies of the Appalachian Orogen (Bird & Dewey, 1970). The essentials of the tectonic sequence include: the development of a passive continental margin on which large quantities of marine sediments are deposited out to a considerable distance offshore; an episode of active subduction of oceanic lithosphere beneath the continental margin; followed

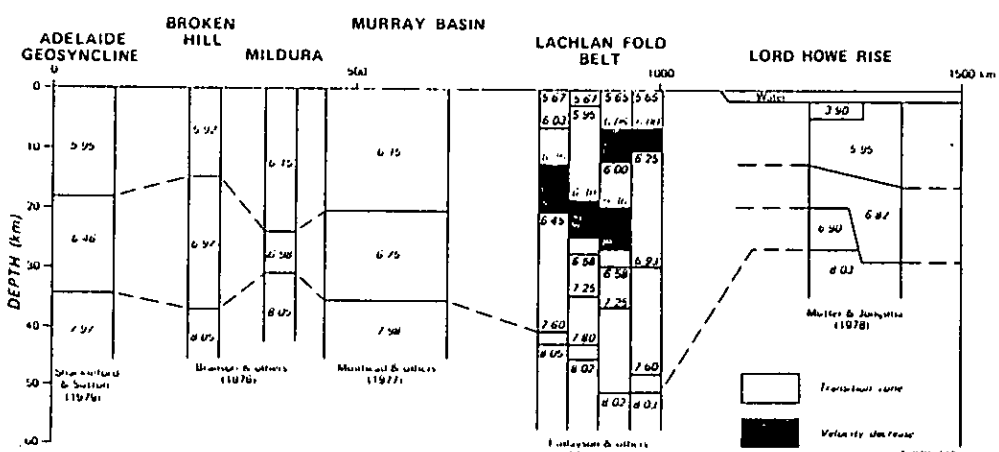

Figure 8. Reconstruction of crustal structure across the southeastern Australian margin without the Tasman Sea Basin. Branson & others (1976) upper mantle velocity is an assumed value.

by further development of another passive margin. The geological/geophysical record in southeastern Australia is compatible with such processes having occurred.

Finlayson & others (1979) have already drawn comparisons of the Palaeozoic evolution in southeastern Australia to the present-day activity along the Pacific coast of South America. The crustal thickness that can be achieved by this mechanism compares favourably with that in southeastern Australia and in the southern part of the Appalachian Highlands (Borcherdt & Roller, 1966).

In the Lachlan Fold Belt, therefore, it is considered that the seismic structure is similar to that of other Palaeozoic and older orogenic provinces which include a Cordilleran-type mountain belt within their geological development.

There are now interpretations of several seismic surveys which may be synthesised into a perspective of crustal structure across southeastern Australia. It is appropriate to include in this perspective the present-day marine area to the east of Australia. Shaw (1978) has described the location of the Lord Howe Rise adjacent to eastern Australia prior to the opening of the Tasman Sea. Jongsma & Mutter (1978) describe the nature of the continental breakup, which led to sea-floor spreading in the Tasman Sea during the period 60-80 m.y. B.P. They describe the asymmetric rifting of the southeastern Australian margin, which accounts for the sharp continental break off the present eastern Australian coast. Mutter & Jongsma (1978) describe further features of the Lord Howe Rise and have revised the crustal seismic interpretation of Shor & others (1971). This seismic profile was located on structures which were adjacent to the Tasman Fold Belt prior to the opening of the Tasman Sea. The revised model is included in Figure 8, which shows the variation in crustal structure across the region. The 500 km-wide Lord Howe Rise puts in perspective the 900 km-wide section of present-day continental eastern Australia.

Some idea of crustal thickness in the Murray Basin west of the profiles discussed in this paper is obtained from the interpretation of Muirhead & others (1977). Their seismic profiles extended out to 1200 km from large shots and the survey was primarily designed to obtain upper mantle information. Despite lack of detailed intra-crustal structure, a depth to the Moho of 35 km has been interpreted, a two-layer crust being modelled with a velocity of 6.15 km/s for the upper 20 km and 6.75 km/s being used for the velocity in the lower crust.

Near the western boundary of the Tasman Geosyncline, there are two deep seismic reflection surveys which give some indication of crustal structure near Broken Hill and Mildura (Branson & others, 1976). The interpretations are shown in Figure 8.

The thickest crustal section within the Tasman Geosyncline is under the region of highest topography traversed by the seismic lines interpreted in this paper. It is surmised that this region is the location of a pre-Ordovician subsided continental margin, upon which the present-day thick crustal sequence evolved.

Acknowledgements

The authors wish to thank the State Rivers and Water Supply Commission of Victoria and the Blue Circle (Southern) Cement Co. Ltd for their cooperation in providing data on quarry blasting. One of us (CP) wishes to thank the Bureau of Mineral Resources, Geology and Geophysics and the Australian Academy of Science for funding his visit to Canberra. The authors also wish to acknowledge the help provided by K. Fuchs, G. Müller and P. Giese in providing computer programs used in the interpretation. A. S. Murray provided assistance with computing problems in BMR, and R. Bates drew the diagrams for publication.

References

BEAMS, S. D., 1979—Geology and geochemistry of the Bega Batholith; *in* DENHAM, D. (Compiler), Crust and Upper Mantle of Southeast Australia. *Bureau of Mineral Resources, Australia—Record* **1979/2**, Abstract.

BIRD, J. M., & DEWEY, J. F., 1970—Lithosphere plate: continental margin tectonics and the evolution of the Appalachian Orogen. *Geological Society of America—Bulletin* **81**, 1031-60.

BLACK, P. R., 1978—Seismic and thermal constraints on the physical properties of the continental crust. Ph.D. Thesis, Purdue University, Indiana (unpublished).

BOLLINGER, G. A., 1969—Seismicity of the Central Appalachian States of Virginia, West Virginia and Maryland 1758 through 1968. *Bulletin of the Seismological Society of America*, **59**, 2103-12.

BOLLINGER, G. A., 1970—Travel-time study of six central Appalachian earthquakes. *Bulletin of the Seismological Society of America*, **60**, 629-38.

BORCHERDT, R. D., & ROLLER, J. C., 1966—A preliminary summary of a seismic refraction survey in the vicinity of the Cumberland Plateau observatory, Tennessee. *U.S. Geological Survey, Denver—Technical Letter, Crustal Studies*, **43**.

BRANSON, J. C., MOSS, F. J., & TAYLOR, F. J., 1976—Deep crustal reflection seismic test survey, Mildura, Victoria and Broken Hill, NSW, 1968. *Bureau of Mineral Resources, Australia*—Report **183**.

BULLEN, K. E., 1963—AN INTRODUCTION TO THE THEORY OF SEISMOLOGY. *Cambridge University Press.*

CLEMENS, J. D., & WALL, V. J., 1979—Crystallisation and origin of some "S-type" granitic magmas. *In* DENHAM, D. (Compiler), Crust and Upper Mantle of Southeast Australia, *Bureau of Mineral Resources, Australia*—Record **1979/2**, *Abstract.*

DENHAM, D., (Compiler), 1979—Crust and upper mantle of southeast Australia. *Bureau of Mineral Resources, Australia*—Record **1979/2**.

DENHAM, D., ALEXANDER, L. G., & WOROTNICKI, G., 1979—Stresses in the Australian crust from earthquakes and overcoring measurements. *BMR Journal of Australian Geology & Geophysics*, **4**, 289-94.

DEWEY, J. F., & BIRD, J. M., 1970—Mountain belts and the New Global Tectonics. *Journal of Geophysical Research*, **75**, 2625-47.

DIETZ, R. S., 1963—Collapsing continental rises: an actualistic concept of geosynclines and mountain building. *Journal of Geology*, **71**, 314-33.

FERGUSON, J., WYBORN L., & WYBORN, D., 1979—CUMSEA 1979 (Crust and Upper Mantle of Southeast Australia), Excursion Guide. *Bureau of Mineral Resources, Australia*—Record **1979/8**.

FINLAYSON, D. M., COLLINS, C. D. N., & DENHAM, D., 1979—Crustal structure under the Lachlan Fold Belt, southeastern Australia. *Physics of the Earth and Planetary Interiors*, in press.

FLOOD, R. H., SHAW, S. E., RILEY, G. H., 1979—S and I-type igneous activity in the northern part of Lachlan Fold Belt. *In* DENHAM, D. (Compiler), *Bureau of Mineral Resources, Australia*—Record **1979/2**, Abstract.

FUCHS, VON K., 1968—Das Reflexions- und Transmissionsvermögen eines geschichteten Mediums mit beliebiger Tiefen-Verteilung der elastichen Moduln unde der Dichte fur schragen Einfall ebener Wellen. *Zeitschrift für Geophysik*, **34**, 389-413.

GIESE, P., 1976a—Problems and tasks of data generalization. *In* GIESE, P., PRODEHL, C., & STEIN, A. (Editors). EXPLOSION SEISMOLOGY IN CENTRAL EUROPE, *Springer-Verlag, Berlin.*

GIESE, P., 1976b—Depth calculation. *In* GIESE, P., PRODEHL, C., & STEIN, A. (Editors), EXPLOSION SEISMOLOGY IN CENTRAL EUROPE, *Springer-Verlag, Berlin.*

JONGSMA, D., & MUTTER, J. C., 1978—Non-axial breaching of a rift valley: evidence from the Lord Howe Rise and the southeastern Australian margin. *Earth and Planetary Science Letters*, **39**, 226-34.

MUIRHEAD, K. J., CLEARY, J. R., & FINLAYSON, D. M., 1977—A long-range seismic profile in southeastern Australia. *Geophysical Journal of the Royal Astronomical Society*, **48**, 509-19.

MUTTER, J. C., & JONGSMA, D., 1978—The pattern of the pre-Tasman Sea rift system and the geometry of breakup. *Australian Society of Exploration Geophysicists Bulletin*, **9**, 70-75.

NICHOLLS, I. A., 1979—Sub-aluminous volcanic rocks of the Silurian and Devonian of eastern Victoria. Crust and Upper Mantle of Southeast Australia. *In* DENHAM, D. (Compiler), *Bureau of Mineral Resources, Australia* Record **1979/2**, Abstract.

PRODEHL, C., 1976—Comparison of seismic-refraction studies in central Europe and western United States. *In* GIESE, P., PRODEHL, C., & STEIN, A. (Editors), EXPLOSION SEISMOLOGY IN CENTRAL EUROPE *Springer-Verlag, Berlin.*

PRODEHL, C., 1977—The structure of the crust-mantle boundary beneath North America and Europe as derived from explosion seismology. *In* THE EARTH'S CRUST. *American Geophysical Union, Geophysical Monograph* **20**, 349-69.

SHACKLEFORD, P. R. J., & SUTTON, D. J., 1979—Crustal structure in South Australia using quarry blasts. *In* DENHAM, D. (Compiler), Crust and Upper Mantle of Southeast Australia, *Bureau of Mineral Resources, Australia—Record* **1979/2**, *Abstract.*

SHAW, R. D., 1978—Sea floor spreading in the Tasman Sea: a Lord Howe Rise—eastern Australian reconstruction. *Australian Society of Exploration Geophysicists Bulletin*, **9**, 75-81.

SHOR, G. C., KIRK, H. K., & MENARD, H. W., 1971—Crustal structure of the Melanesian area. *Journal of Geophysical Research*, **76**, 2562-86.

WASS, S. Y., 1979—Geochemical evidence for upper mantle inhomogeneity beneath south-eastern Australia. *In* DENHAM, D. (Compiler), Crust and Upper Mantle of Southeast Australia, *Bureau of Mineral Resources, Australia—Record* **1979/2**, Abstract.

WELLMAN, P., 1979—The timing of the late Mesozoic-Cainozoic uplift of the southeastern Australian highlands. *In* DENHAM, D. (Compiler), Crust and Upper Mantle of Southeast Australia, *Bureau of Mineral Resources, Australia—Record* **1979/2**, *Abstract.*

WHITE, A. J. R., 1979—An underplating model for formation of the lower crust. *In* DENHAM, D. (Compiler), Crust and Upper Mantle of Southeast Australia, *Bureau of Mineral Resources, Australia—Record* **1979/2**, *Abstract.*

WHITE, A. J. R., & CHAPPELL, B. W., 1977—Ultrametamorphism and granitoid genesis. *Tectonophysics*, **43**, 7-22.

Physics of the Earth and Planetary Interiors, 21 (1980) 321–342

CRUSTAL STRUCTURE UNDER THE LACHLAN FOLD BELT, SOUTHEASTERN AUSTRALIA

D.M. FINLAYSON, C.D.N. COLLINS and D. DENHAM

Bureau of Mineral Resources, Geology and Geophysics, Canberra, A.C.T. (Australia)

(Received February 5, 1979; revised and accepted June 15, 1979)

Finlayson, D.M., Collins, C.D.N. and Denham, D., 1980. Crustal structure under the Lachlan Fold Belt, southeastern Australia. Phys. Earth Planet. Inter., 21: 321–342.

Seismic investigations of the Earth's crust in the Lachlan Fold Belt of southeastern Australia, under the continent's highest mountain ranges, indicate a depth to the Moho of between 40 and 52 km, with P-wave velocities in the upper crust of 5.6–6.3 km s^{-1}, lower crustal velocities of 6.7–7.4 km s^{-1}, and upper mantle velocities of 8.0–8.1 km s^{-1}. Velocity changes within the crust and at the Moho boundary are transitional rather than discontinuous. A well-defined low-velocity layer in the crust, at a depth of about 15–20 km, is evident throughout the region, and localized low-velocity layers may be present in the upper crust at shallower depths. The thickness of the upper crust increases considerably (from 26 to 35 km) along a 300 km NE–SW traverse, with the greatest thickness occurring under the highest mountains. S-wave velocities are close to 3.65 km s^{-1} in the upper crust and 3.9 km s^{-1} in the lower crust. Many previous descriptions of the orogenic evolution of southeastern Australia invoke models analogous to the tectonic processes occurring in western Pacific island arcs. The very thick crustal section interpreted in the Lachlan Fold Belt indicates that such orogenic evolution was unlikely, and that an Andean-type model is probably more appropriate. Major granitic batholiths in the Lachlan Fold Belt have a P-wave velocity of about 5.9–6.0 km s^{-1}, compared with interspersed metamorphosed Palaeozoic sediments which have a velocity of about 6.25–6.5 km s^{-1}. There is evidence that the thickness of the batholiths ranges from 15 to 22 km.

1. Introduction

The Lachlan Fold Belt is that part of the Tasman Fold Belt in southeastern Australia bounded by, and underlying parts of, the Murray Basin, the Great Artesian Basin, the Sydney Basin, and the Otway/Gippsland Basins (Fig. 1). Most recent descriptions of the evolution of the Lachlan Belt during the Palaeozoic (from ~500–350 My B.P.) use the concepts associated with plate-tectonic models which have analogues in the present-day western Pacific margins (Scheibner, 1973, 1976; Vandenberg, 1976; Crook and Powell, 1976). The substrate of the Belt has been variously postulated as being continental crust (Rutland, 1973, 1976), substantially oceanic crust (Crook, 1974), or continental crust in the west and oceanic crust in the east (Scheibner, 1974). A comprehensive bibliography on the tectonic evolution of southeastern Australia is given by Crook and Powell (1976).

This paper reviews the seismic crustal models previously used for the southeastern Australia region and presents the results of recent seismic investigations of crustal structure along profiles within the Lachlan Fold Belt.

The problems associated with crustal structure interpretations are complex. Seismic models have usually assumed fairly homogeneous layering within the crust, which has been difficult to reconcile with geological evidence. Smithson and Brown (1977) attempted such a general reconciliation with seismic reflection and refraction data from the lower crust, and conclude that "With no speculative interpretation at all, these (seismic) reflections demonstrate the presence of numerous interfaces and much more complicated lower crustal structure than has previously

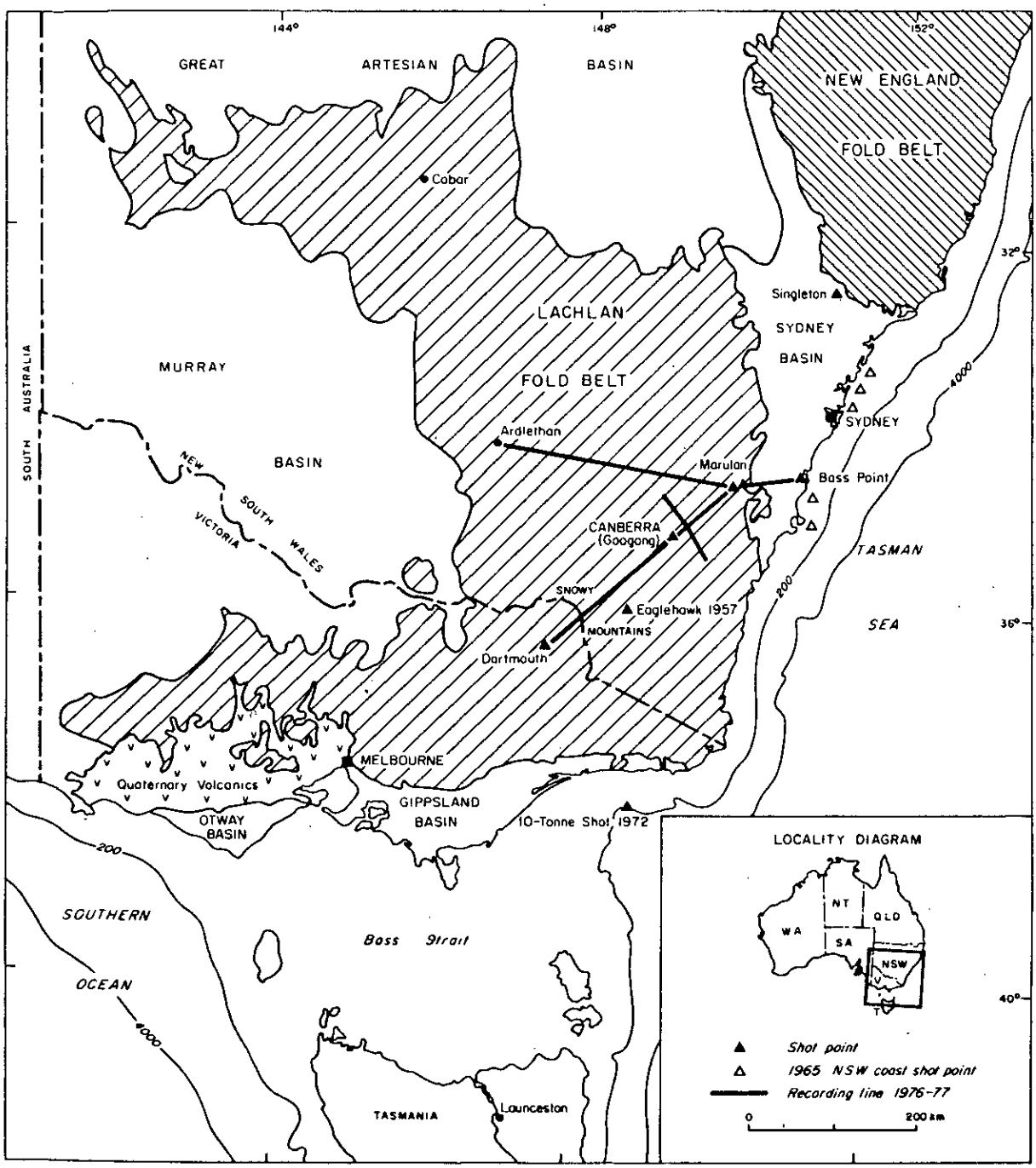

Fig. 1. Lachlan Fold Belt and surrounding geological provinces.

been supposed". It is now apparent that, although layered models are useful for some purposes, a heterogeneous crust must be expected, with seismic models providing only some of the constraints on our knowledge of crustal structure.

2. Previous seismic models for southeastern Australia

There are a few previous explosion seismic investigations in southeastern Australia which provide information on the structure of the crust. Doyle et al. (1959) used three large-quarry blast sources at Eaglehawk (Fig. 1) in the Snowy Mountains; these were recorded at a number of stations in the direction of Sydney and also at two stations in Victoria. At distances up to 160 km towards Sydney seismic first arrivals gave a consistent velocity of 6.04 km s^{-1}, which was taken as the direct P-wave through crustal rock.

Good first arrivals beyond 170 km were recorded at two stations in Victoria and two in New South Wales at Marulan and Berrima (Fig. 2). The apparent velocity between the latter two stations was 8.2–8.3 km s^{-1}, but because of the paucity of data this velocity can only be regarded as a preliminary indication. An indefinite first arrival at Warragamba in the Sydney Basin, classified as eP, had a large travel-time residual from both the crustal and upper mantle groups of arrivals and was discarded from calculations. No consistent evidence was seen for further layering above the Mohorovičić discontinuity.

Doyle et al. (1966) interpreted seismic observations made during 1965, when five shots were fired at sea off Sydney (Fig. 2) and recorded at stations in the direction of the Snowy Mountains, with many stations in common with those used in the Eaglehawk survey. They reported that 22 first arrivals between 25 and 230 km lay on a least-squares straight line with a travel-time (T) in seconds given by:

$$T = 1.8\ (\pm 0.024) + D/6.52\ (\pm 0.036)$$

where D = distance (km), while at distances between 203 and 385 km the first arrivals gave a travel-time of:

$$T = 5.2\ (\pm 0.026) + D/7.58\ (\pm 0.017).$$

The apparent velocities of 6.52 and 7.58 km s^{-1} were noted as being in marked contrast to the values derived from previous studies in the vicinity. The 6.52 km s^{-1} velocity was taken as the first definitive evidence of an "intermediate layer" within the Earth's crust in Australia. The data were then combined with the previously rejected indefinite first arrival at Warragamba from the Eaglehawk survey to interpret a Conrad discontinuity extending from the Sydney Basin to the Snowy Mountains, ranging in depth from ~7 to 21 km. The Moho was interpreted as having a depth ranging from ~25 km under the Sydney Basin to ~42 km under the Snowy Mountains, with an upper mantle velocity of 7.86 km s^{-1}. In the light of more recent observations, however, it is evident that there are shortcomings in this interpretation. The shots fired in 1965 were all fired offshore in about 70 m of water above sediments of the Sydney Basin. The data which define the 6.52 km s^{-1} apparent velocity are predominantly from stations which lie within 160 km of the shots, mainly where the seismic travel path is either entirely or predominantly under the Sydney Basin.

Collins (1978) has interpreted the crustal structure under the Permo-Triassic Bowen Basin in Queensland, which may be connected with the Sydney Basin under cover rocks. A basement velocity of 6.39 km s^{-1} was found there. If this velocity is used as an indicator of that under the Sydney Basin, dips of only 1–2° are necessary to account for the apparent velocity of 6.52 km s^{-1} found by Doyle et al. (1966). Geological and geophysical data indicate that such dips are likely. Hence the evidence for an intermediate layer and a Conrad discontinuity from this survey can also readily be interpreted in terms of the structure of the Sydney Basin. However, the idea of an intermediate layer and Conrad discontinuity has permeated throughout all subsequent interpretations of crustal structure in southeast Australia, and the 1965 survey has been quoted as the best evidence. Underwood (1969) mentions the possible existence of a Conrad discontinuity beneath northern Tasmania in his interpretation of explosions in the Bass Strait. Cleary (1973) envisaged the Conrad discontinuity occurring in all parts of Australia at an average depth of about 20 km and a lower crustal velocity of 6.5–6.7 km s^{-1}. The possible existence of the Conrad discontinuity was mentioned by Dooley (1971) and McElhinny (1973) in their summaries of geophysical

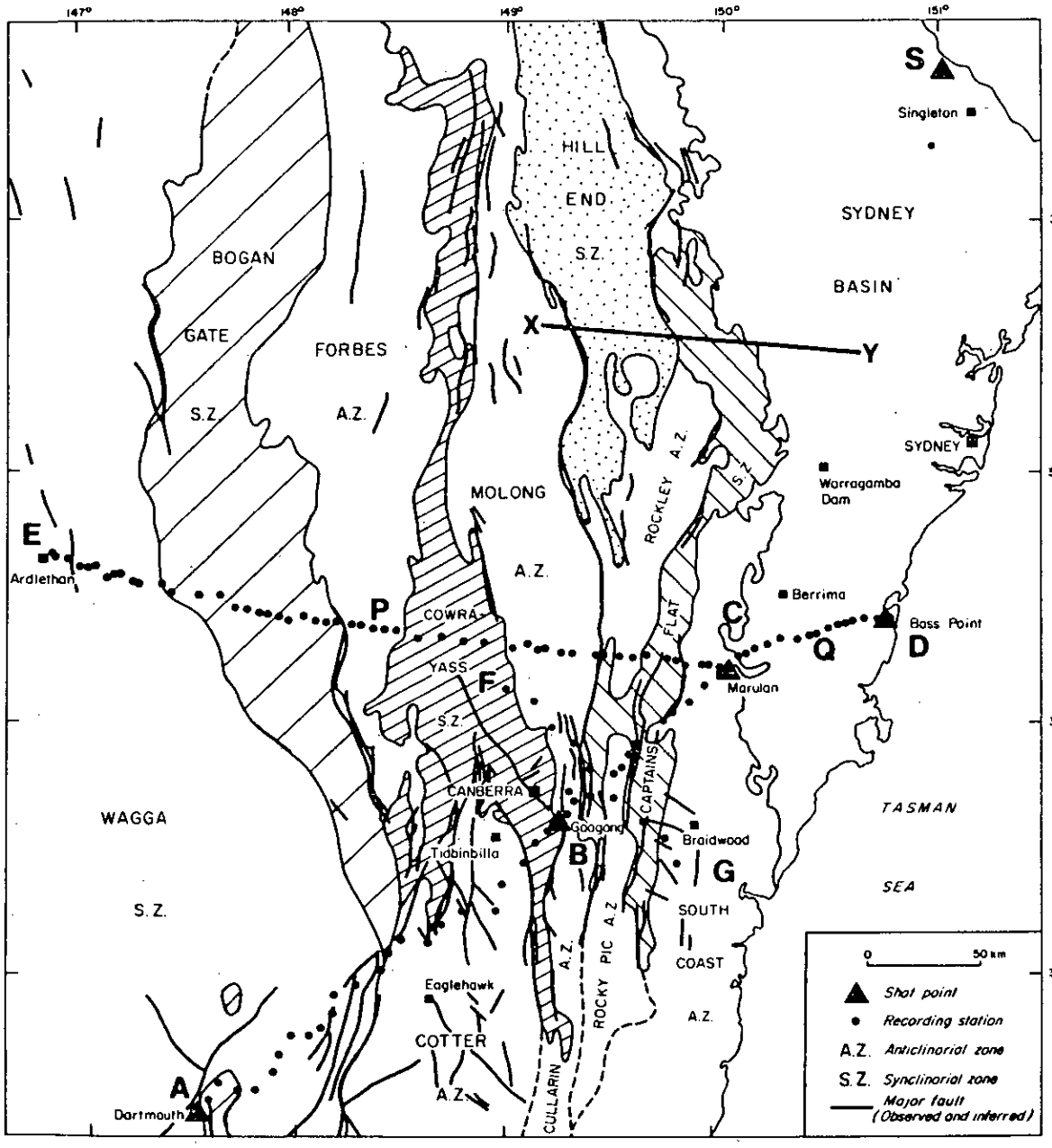

Fig. 2. Orogenic provinces of the Lachlan Fold Belt (Scheibner, 1973), seismic shot points, recording traverses and major geological faults.

investigations of crustal structure in Australia. In interpreting the upper mantle structure across Victoria and southern N.S.W., Muirhead et al. (1977) used a two-layer crustal model, which included a Conrad discontinuity at 20 km where the velocity increased from 6.15 to 6.75 km s^{-1}.

The crustal structure of the southeastern Lachlan Fold Belt was further investigated by seismic refrac-

tion methods in 1966 (Underwood, 1969; Johnson, 1973). The crustal interpretation was inconclusive in terms of structure above the Moho because, in most cases, the shots were too far from the recording stations to record reliable crustal data. Seven shots were fired in eastern Bass Strait and recorded at stations in a line towards the Snowy Mountains. All arrivals out to 140 km were complicated by the Gippsland Basin structure, where the depth to magnetic basement exceeds 5 km in places. Underwood (1969) interpreted a crust with velocity 5.9 km s^{-1} overlying an upper mantle with a true velocity of 7.86 km s^{-1}. Depth to the Moho was interpreted as being 25 km under western Bass Strait and 37 km under the Snowy Mountains. Johnson (1973), in his interpretation, used a mean crustal velocity of 6.0 km s^{-1} overlying an upper mantle with velocity of 8.0 km s^{-1}. The interpreted depths to Moho ranged from ~20 km under the eastern Bass Strait to ~45 km under the Snowy Mountains.

Muirhead et al. (1977) reported the results of a seismic investigation of upper mantle structure across the southern Lachlan Fold Belt. Recordings were made out to distances of 1200 km of a 10-tonne shot fired in eastern Bass Strait and an 80-tonne shot fired in the northern Flinders Ranges in South Australia. The interpreted upper mantle P-wave structure included a velocity of 7.98 km s^{-1} at depths between 35 and 100 km; 8.36 km s^{-1} between 100 and 155 km; 8.10 km s^{-1} between 155 and 190 km; and 8.72 km s^{-1} at greater depth.

To date, most interpretations of seismic data in southeastern Australia have used only the kinematic information from the records. However, the dynamic characteristics of seismic record sections obtained in many parts of the world contain valuable information on crustal structure, and have resulted in a questioning of many of the early simplistic ideas of crustal structure. Mueller and Landisman (1966), among others, have emphasised that many significant arrivals evident in seismic wave trains can be interpreted in terms of seismic velocity gradients and structural boundaries. Doyle et al. (1959) described pronounced arrivals about 1 s after the initial arrival at a distance of 47 km from the Eaglehawk shots, which Mueller and Landisman (1966) interpret, with data from other parts of the world, as indicating a low-velocity zone at a depth of ~6–10 km.

The complexity of the crustal structure has been further highlighted by the detail evident in deep seismic sounding records of vertical incident waves

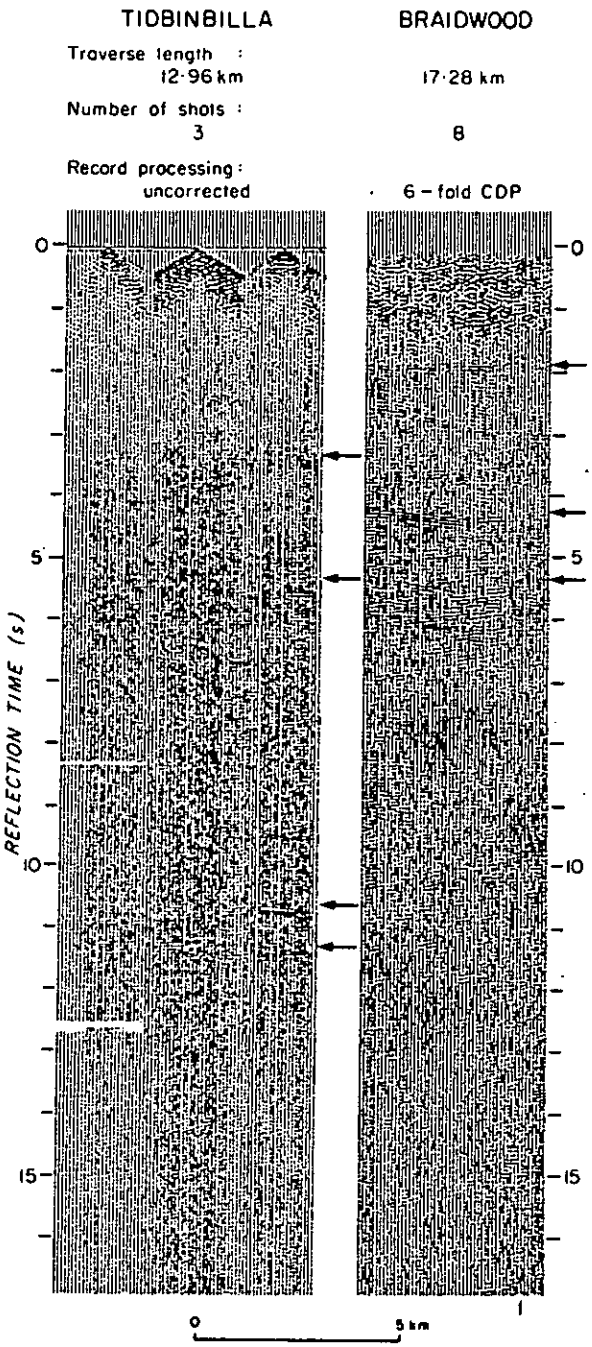

Fig. 3. Vertical seismic sounding records from Tidbinbilla and Braidwood. Arrows indicate interpreted reflecting horizons.

(Mueller and Landisman, 1966). Oliver et al. (1976) have described a number of profiles in continental north America where vertical reflection data show detailed crustal layering in some areas and few seismic reflecting horizons in adjacent areas. Smithson and Brown (1977) have used such evidence, together with geological and geochemical data, to propose a continental crustal model consisting largely of metamorphic rocks.

Vertical reflection data are available from some isolated points in Australia. Branson et al. (1976) have interpreted the intra-crustal reflection data in the Broken Hill and Mildura areas of western N.S.W., where well-defined horizons were recorded with two-way reflection times of up to 15 s. Adjacent to the A–C traverse described later in this paper (Fig. 2), are two deep seismic sounding sites at Braidwood and Tidbinbilla (Taylor et al., 1972). Record sections at these two sites are shown in Fig. 3.

At Tidbinbilla, the reflections at 3.4, 5.4, 10.7 and 11.4 s were interpreted as indicating interfaces at 9.5, 15.5, 33.0 and 35.3 km depth respectively. At Braidwood, reflections at 1.9, 4.2 and 5.4 s were interpreted as interfaces at 5.0, 12.0 and 15.6 km. The reflection times are converted to depths using Cleary's (1973) crustal velocities. Work in other parts of the world indicates that it is unlikely that the intra-crustal reflecting horizons are continuous over the large distances covered in seismic refraction surveys, although they may be evident as wide-angle reflections on some records from long profiles if common depth-point recording is achieved.

3. Fieldwork in 1976 and 1977

Routine quarry blasts in southeastern Australia were used as seismic sources for fieldwork conducted by the Bureau of Mineral Resources, Geology and Geophysics (BMR) during 1976 and 1977. Recording sites were located at 7–10 km intervals along two profiles, one between the South Marulan limestone quarry and the Dartmouth Dam construction site, and the other running west from three road-metal quarries near Bass Point, through South Marulan limestone quarry to Ardlethan (Fig. 2). Additional seismic sources were situated at four open-cut coal mines near Singleton in the northern Sydney Basin and at the Googong Dam construction site near Canberra. Coal mining shots were typically 20–30 tonnes, with shot-pattern delays of up to 250 ms; other shots were typically less than 5 tonnes with delays of less than 100 ms. Shot-position uncertainties were less than 100 m and shot-timing uncertainties were estimated at less than 50 ms.

Recordings were made at 112 sites along the two profiles; an additional site near Singleton was used solely to time the coal mining shots. Seismic tape recording systems were deployed for about 7 days at each site to enable data from all necessary quarry sites to be obtained. Each system recorded two gain levels from a vertical component short-period seismometer and amplifier, an internal crystal-controlled clock signal, and the Australian radio time signal (VNG). Recording site positional uncertainties were less than 100 m, and timing uncertainties were typically less than 20 ms. Details of survey operations have been described by Collins (1976) and Finlayson (1977).

4. Seismic record sections

Seismic tapes from all recording stations were played back in analogue form. The amplitudes of playback recordings were adjusted so that the surface wave amplitudes on all records were approximately constant. Instrumental recording noise was substantially reduced by subtracting low-gain from high-gain recorded signals and filtering through a bandpass filter set between 1 Hz and 8 Hz (amplitude 3 dB down at cutoff frequency; roll-off 24 dB octave^{-1}). Seismic record sections were produced photographically for all traverses shown in Fig. 2; these are contained in Figs. 4–8. Elevation corrections have been applied to travel-times to reduce them to a mean 600 m datum level. The seismic record sections have their travel-times reduced by distance/6.0. At distances beyond 200 km, seismic energy from first arrivals was generally much attenuated. In many instances energy could be detected in the unfiltered or enlarged records which is not readily apparent on the smaller reproductions. In Figs. 4–8, dots have been used to indicate onset times which can confidently be identified on the original records.

Giese (1976a) has discussed the many aspects of

correlating seismic phases across record sections produced from crustal seismic investigations. Precise phase correlation is usually possible only where recordings are made at station spacings less than the wavelength of the seismic waves (about 1 km). In the present surveys with station spacings of about 10 km, group correlation, characterised by amplitude signatures, was used to identify seismic phases. In a few cases phase correlation was possible on impulsive first arrivals.

4.1. Dartmouth–Marulan

The general features of the record sections along the line A–B–C (Fig. 2) between Dartmouth and Marulan are evident in Figs. 4a and 4b. The records from Dartmouth shots are characterised by clear first arrival onsets along the complete recording line, thus defining the progressive branches of the travel-time curve; there is a general lack of pronounced subsequent phases. This lack of well-developed retrograde branches to the travel-time curves probably indicates velocity gradients rather than discontinuities. The correlations used in the interpretation are shown in Fig. 4a, together with the associated apparent velocities.

Some velocities from these and other traverses, were determined by least-squares methods (standard errors are quoted for such velocities). Where insuffi-

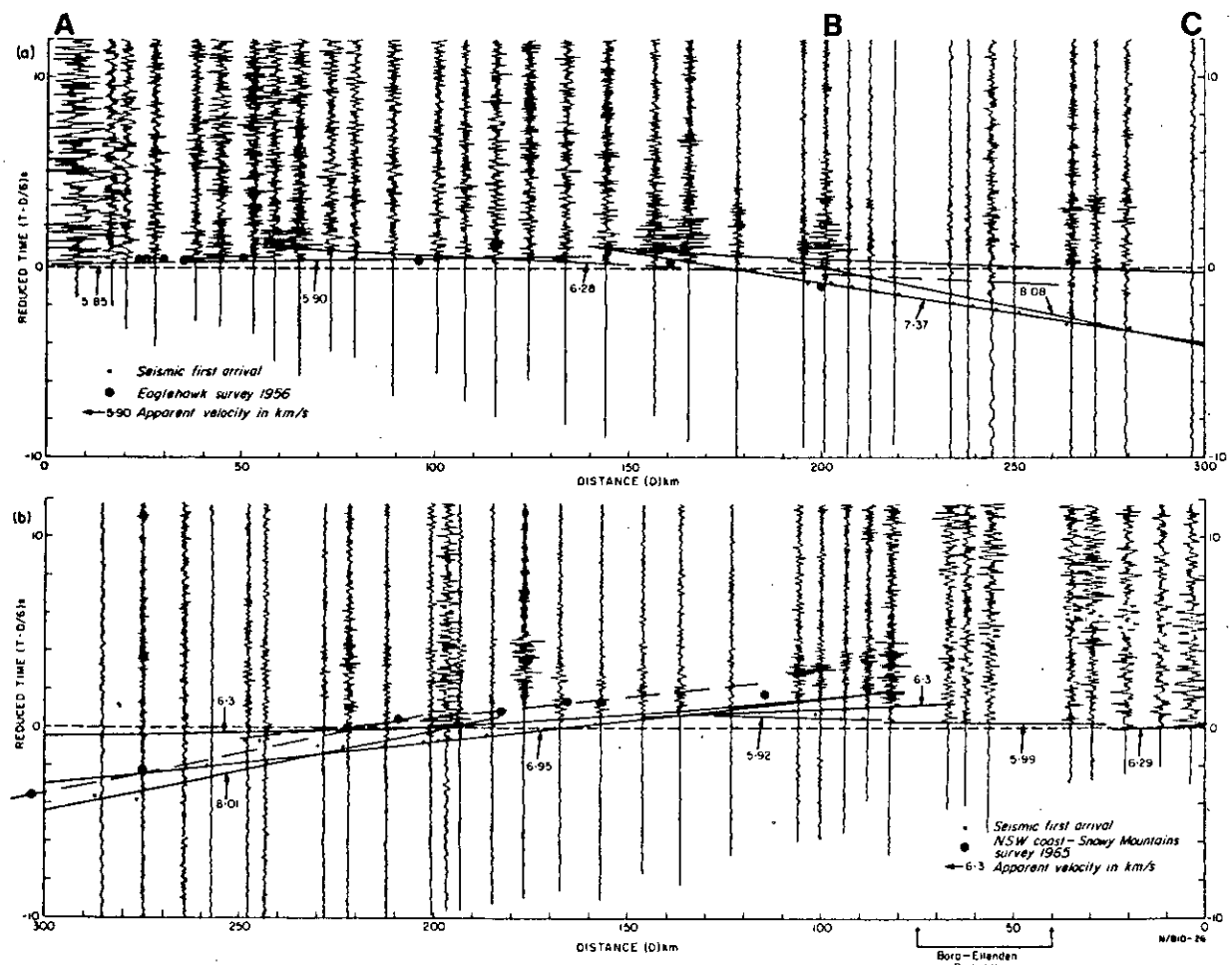

Fig. 4. Seismic record sections along recording line A–B–C from (a) Dartmouth shots and (b) Marulan shots. Dots indicate seismic first arrivals which can confidently be identified on enlarged records. 1956 Eaglehawk seismic first arrivals are shown in (a) and 1965 N.S.W. coast first arrivals in (b).

cient data were available to justify least-squares methods, graphical methods have been used. Upper and middle crustal P-wave velocities of 5.85, 5.90 ± 0.03, and 6.28 km s^{-1} are evident, and beyond 170 km a lower crustal phase with an apparent velocity of 7.37 ± 0.07 km s^{-1} is clearly evident from first arrivals. This phase has not been identified previously in southeastern Australia and its presence as a first arrival out to 280 km necessitates a review of previously interpreted upper mantle data. Beyond 140 km a retrograde travel-time branch is identified with an asymptotic velocity of 6.28 km s^{-1}, but offset by about 0.7 s from the progressive branch with that velocity. No phases with apparent velocities approaching 8 km s^{-1} are seen as first arrivals at distances less than 280 km, but large-amplitude wide-angle reflections from the Moho can be identified near the critical distance at about 200 km.

Weak S-phase arrivals were clearly evident on some of the records (not all shown in Fig. 4a); these arrivals fit two straight lines. From 0 to 145 km the S-wave apparent velocity is 3.62 ± 0.05 km s^{-1}, with an intercept of 0.47 ± 0.27 s; from 155 to 245 km the apparent velocity is 3.90 ± 0.04 km s^{-1}, with an intercept of 4.37 ± 0.51 s. There is a 1 s discontinuity in the two lines at about 150 km which is associated with the mid-crustal low-velocity layer (see Section 5).

The record section from Marulan shots (Fig. 4b) along the same line displays some different characteristics from the Dartmouth section. Progressive segments of the travel-time curve have been identified with apparent P-phase velocities of 6.29, 5.99 ± 0.06 and 6.95 ± 0.07 km s^{-1}. The correlation of the 6.95 km s^{-1} arrivals beyond 220 km is tenuous. There is some evidence for weak first arrivals with an apparent velocity near 8 km s^{-1} from 240 to 190 km, and as with the Dartmouth recordings, there are strong arrivals interpreted as wide-angle reflections from the Moho at about 200 km. Subsequent arrivals indicate a retrograde travel-time branch with an asymptotic velocity of about 6.3 km s^{-1}, converging with the 6.95 km s^{-1} progressive branch at about 80 km. There is no evidence for a 6.3 km s^{-1} layer in the first arrivals, but strong subsequent arrivals between 60 and 100 km indicate a progressive travel-time branch with that velocity. The retrograde branch is offset from this progressive branch by about 0.8 s.

As with the Dartmouth shot recordings, weak S-phase arrivals were recorded from Marulan shots and these arrivals fit two straight lines. From 0 to 100 km the apparent S-wave velocity is 3.71 ± 0.03 km s^{-1} with an intercept time of 0.79 ± 0.16 s; from 100 to 280 km the apparent velocity is 3.76 ± 0.04 km s^{-1} and the intercept is 3.05 ± 0.53 s. There is an offset in the data of about 2 s at 100 km.

4.2. Googong Dam

The Googong Dam seismic source provides further upper-crustal information along line A–B–C. Figure 5a shows the record sections both towards Dartmouth and towards Marulan. Progressive P-phase travel-time branches with apparent velocities of 6.30, 6.15 and 6.38 km s^{-1} are identified towards the SW, and with apparent velocities of 6.57 and 6.01 km s^{-1} towards the NE. S-waves out to 100 km towards the NE, and out to 190 km towards the SW, had apparent velocities of about 3.60 km s^{-1}.

4.3. Singleton

A record section along the line A–B–C, compiled from shots fired in the Singleton area, is presented in Fig. 6. Clear weak first arrivals (indicated by dots in Fig. 6) are evident on some of the records in the distance range 270–510 km, with an apparent velocity of 8.01 ± 0.06 km s^{-1}. Also plotted in Fig. 6 are some first arrivals from the 1965 New South Wales seismic survey reported by Doyle et al. (1966). Their data are plotted with the origin in common with our data; but the geographic location of their traverse is displaced from our traverse, A–B–C.

Data from only the two southernmost shots (Fig. 2) recorded at stations roughly along line A–B–C are plotted to minimise the effects of Sydney Basin structures. These 1965 arrivals at distances less than 270 km have an apparent velocity of ~7 km s^{-1} corresponding to the 6.95 km s^{-1} and 7.37 km s^{-1} observed on the Dartmouth–Marulan line; those at greater distances have an apparent velocity of about 8 km s^{-1}, in close agreement with the 8.01 km s^{-1} determined from the Singleton shots, but with an intercept ~2.5 s greater. The value of the upper mantle apparent velocity from north to south has therefore been taken as 8.01 km s^{-1} for the purposes

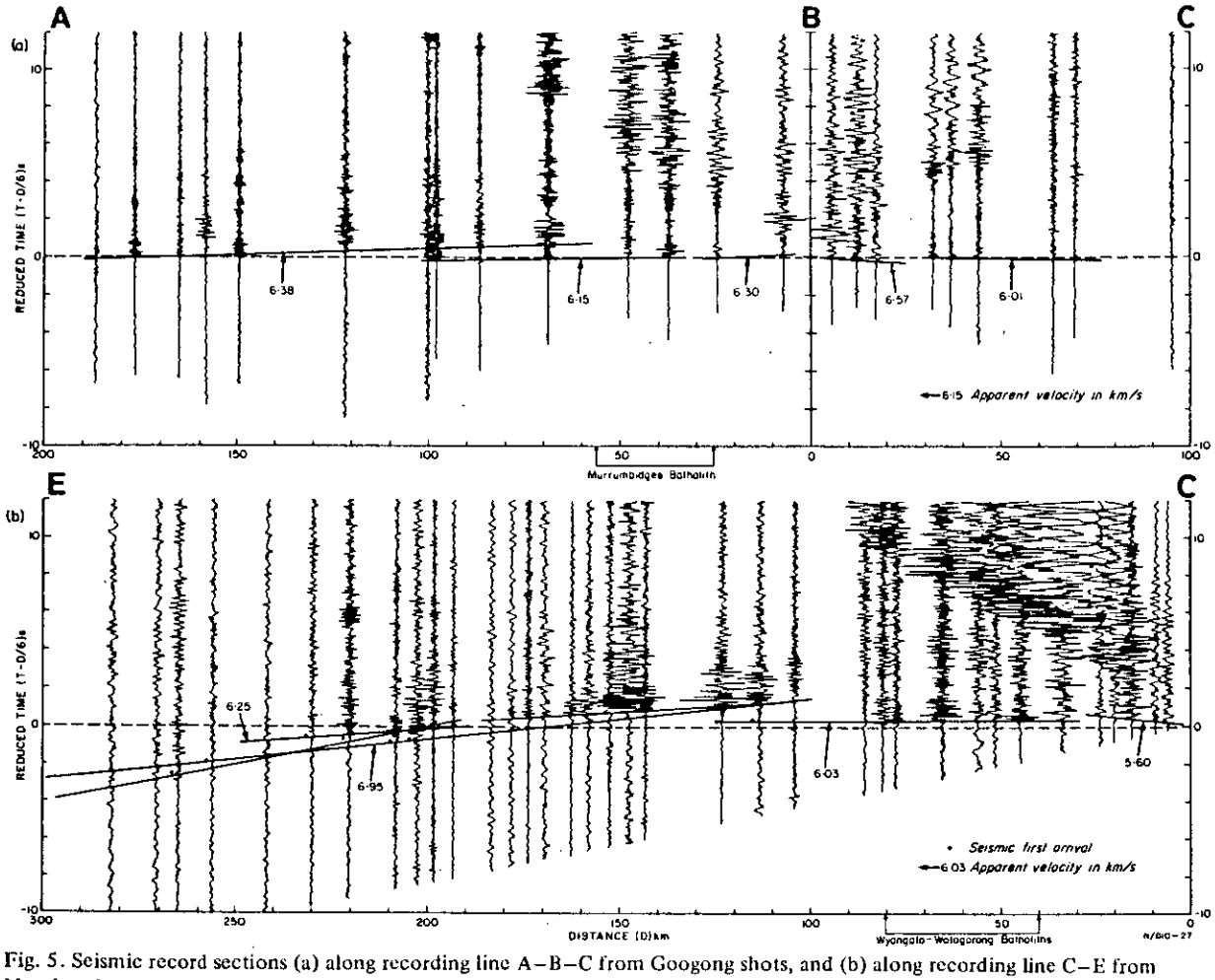

Fig. 5. Seismic record sections (a) along recording line A–B–C from Googong shots, and (b) along recording line C–E from Marulan shots.

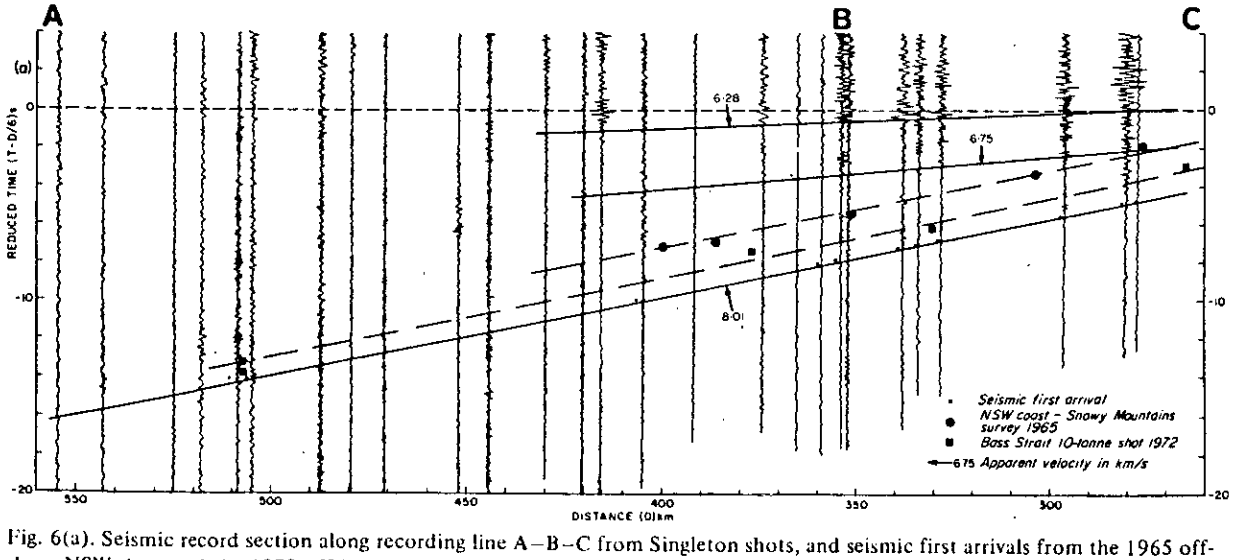

Fig. 6(a). Seismic record section along recording line A–B–C from Singleton shots, and seismic first arrivals from the 1965 offshore NSW shots and the 1972 offshore Bass Strait shot.

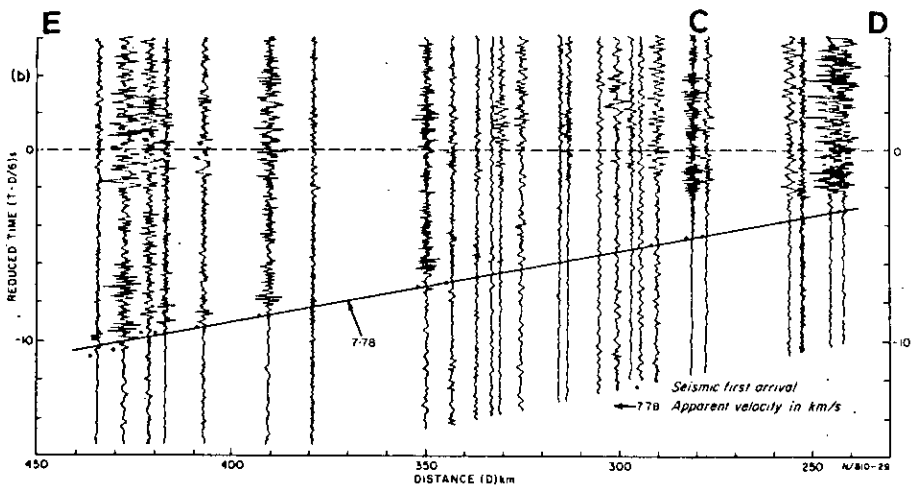

Fig. 6(b). Seismic record section along recording line D–C–E from Singleton shots.

of interpretation. Also evident in Fig. 6a are clear subsequent arrivals with apparent asymptotic velocities of 6.75 and 6.28 km s^{-1}, interpreted as wide-angle reflections from intra-crustal boundaries.

Other upper mantle data from explosion seismic work near the line A–B–C is available, from the 1972 10 tonne shot fired in the Bass Strait (Finlayson et al., 1974; Muirhead et al., 1977). The first-arrival data from that shot (Fig. 6a) indicate an apparent velocity of 8.08 ± 0.09 km s^{-1}, and this S–N velocity has been adopted for the interpretation presented in this paper.

4.4. East–west traverses

Record sections from the line D–C–E (Fig. 2) have been assembled for shot sources at Marulan, Singleton and Bass Point (Figs. 5b, 6b, 7). Along the line C–E (Fig. 5b) progressive travel-time branches are evident from first arrivals with apparent velocities of 5.60, 6.03 ± 0.04 and 6.25 km s^{-1}. Prominent subsequent arrivals in the 100–170 km range have been interpreted as near critical reflections from a lower crustal 6.95 km s^{-1} layer, although a progressive branch with this apparent velocity is only poorly identified. This velocity is adopted from the data available from Marulan shots along line A–B–C.

The record sections along the line C–D from sources at Marulan and Bass Point are shown in

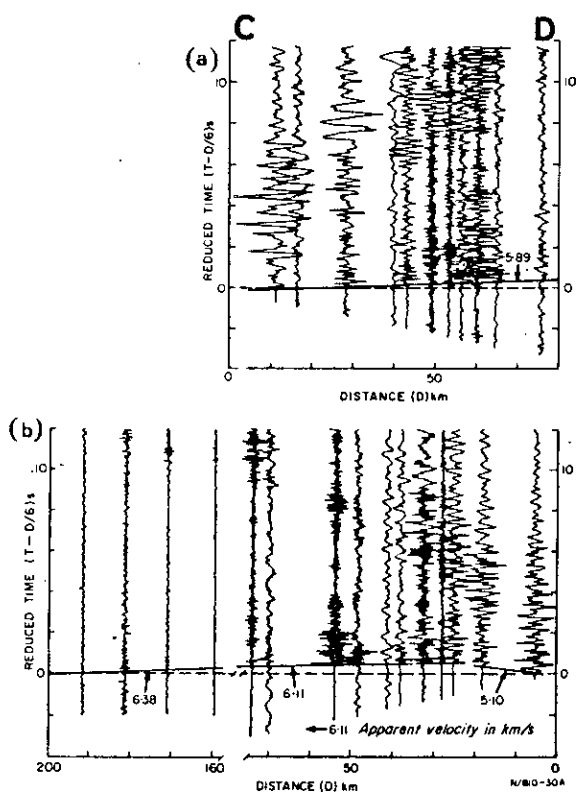

Fig. 7. Seismic record sections along recording line C–D from (a) Marulan shots and (b) Bass Point shots.

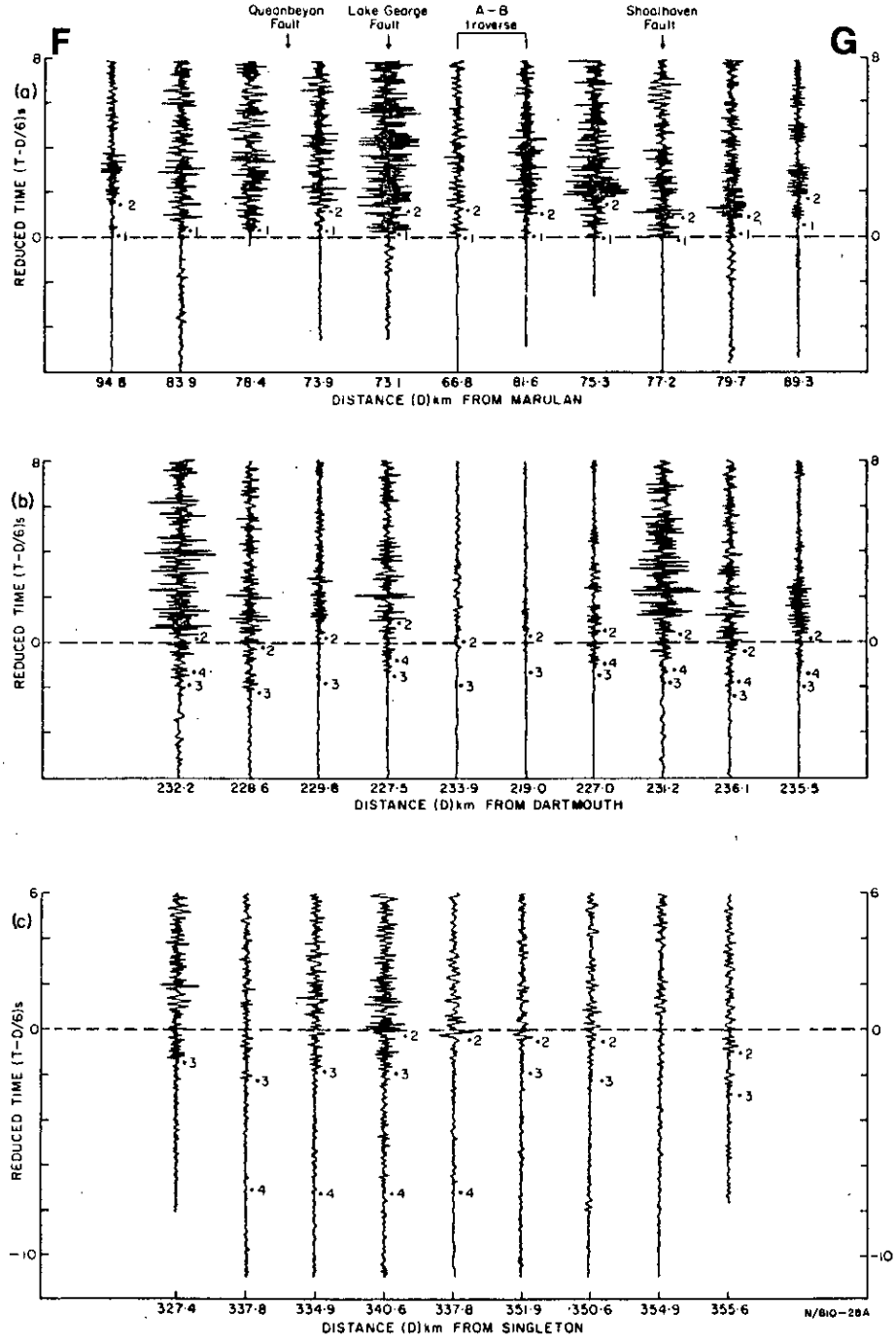

Fig. 8. Seismic recordings made along cross traverse F–G from (a) Marulan shots, (b) Dartmouth shots and (c) Singleton shots. Numbers indicate events which are correlated with phases identified on the seismic record sections along traverse A–B–C: (1) 5.99 km s^{-1} phases, (2) 6.28 km s^{-1} phases, (3) 6.75 and 7.37 km s^{-1} phases and (4) 8.01 km s^{-1} phases.

Fig. 7. Progressive travel-time branches are evident from first arrival data with apparent velocities 5.10, 6.11, and 6.38 km s^{-1} from Bass Point shots, and 5.89 km s^{-1} from Marulan shots. None of the subsequent P-phase arrivals can be correlated with any confidence. Marulan and Bass Point shot sources also produced prominent S-phases along the recording line D–C–E, stronger than along the line A–B–C, possibly a result of the shot-firing patterns at the quarry sources (Figs. 5b, 6). At distances of <100 km west of the Marulan shot source, S-phases are produced with an apparent velocity of 3.65 ± 0.02 km s^{-1} and a time-axis intercept of 0.61 ± 0.10 s. In the range 100–270 km the S-phase apparent velocity was 3.87 ± 0.03 km s^{-1}, with an intercept of 4.31 ± 0.35 km s^{-1}. There is a prominent offset of about 2.00 s in these two sets of data at about 100 km (not shown on Fig. 5b).

At distances of between 165 and 270 km from Marulan there is evidence for S-phases with a velocity of 4.48 ± 0.18 km s^{-1} and intercept of 8.79 ± 1.94 s, although these arrivals are not well recorded. East of Marulan, S-phases are recorded with an apparent velocity of 3.66 ± 0.15 km s^{-1} and zero intercept. The Bass Point shot source gives S-phases with an apparent velocity of 3.20 ± 0.06 km s^{-1} and intercept of 0.30 ± 0.10 s at distances less than 33 km (probably associated with the Sydney Basin sediments and the 5.1 km s^{-1} P-wave velocity), and a velocity and intercept of 3.63 ± 0.04 km s^{-1} and 0.79 ± 0.31 s respectively at greater distances.

Shots from the Singleton area recorded along the line D–C–E in the range 240–440 km are shown in Fig. 6b. Clear first arrivals identified on the original records are indicated by black dots. The fan shooting geometry from Singleton along this line precludes any realistic assessment of velocities, but an apparent velocity of 7.78 ± 0.08 km s^{-1} was observed at distances between 240 and 440 km. For the purposes of interpretation the velocities determined from Singleton shots along line A–B–C have been used. The first arrivals are taken as being from the upper mantle with an apparent velocity of 8.01 km s^{-1}; their amplitudes are small up to a distance of ~350 km, but their character changes beyond that to more pronounced events. Strong wide-angle reflections are evident at stations east of Marulan in the distance range 240–250 km, and may indicate a different character to the Moho boundary under the Sydney Basin. Subsequent arrivals at distances beyond 270 km are not well correlated across the record section. Tenuous correlations have been made to the intra-crustal boundaries taken from line A–B–C recordings with apparent velocities of 6.28 and 6.75 km s^{-1} (Fig. 6a).

The cross-spread of recording stations F–G (Fig. 2) provided valuable confirmation of the lateral continuity of refractors identified from the other recording lines. Figures 8a, b and c show the recordings made along line F–G from seismic sources at Marulan (range 66–95 km), Dartmouth (range 219–237 km) and Singleton (range 327–356 km). The recordings from Marulan shots show correlation of events with the 5.99, 5.92, 6.30 and 6.95 km s^{-1} apparent velocities identified along line A–B–C. The recordings from Dartmouth shots strongly confirm the 7.37 and 6.28 km s^{-1} apparent velocities in Fig. 4, and tentatively show a correlation of upper-mantle arrivals about 1 s after the prominent first arrivals. Singleton shot recordings confirm the lateral extent of the 8.01 km s^{-1} boundary and show strong correlations with the 6.75 and 6.28 km s^{-1} apparent velocity boundaries identified along line A–B–C.

Throughout the survey area as a whole, upper-mantle arrivals are not clearly evident as first arrivals at distances less than ~280 km. There is a lack of wide-angle Moho reflections over an extended distance range as are seen in many parts of the world (e.g. Giese et al., 1976). This suggests that the Moho boundary in southeastern Australia is complex, rather than a simple first-order discontinuity. Unambiguous S-wave arrivals from the upper mantle are not seen on any traverse.

5. Velocity–depth models

Giese (1976b) has described the many steps which should be taken to determine a velocity–depth model from explosion seismic data. Inversion of travel-time curves by the Wiechert–Herglotz method requires a high degree of confidence in the identification of all progressive and retrograde branches of the travel-time curves, a confidence which is rarely achieved in practice. The approach adopted in this interpretation has been to derive approximate velocity–depth models from the kinematic data, and test these

models using the dynamic characteristics of the record sections in conjunction with synthetic seismogram computer programs.

The method adopted for the determination of approximate velocity–depth models is that of Pavlenkova (1973) which is similar to that of Puzyrev et al. (1963). Reduced travel-time values were computed for identified significant arrivals using reduction velocities close to the apparent velocities. These values were plotted in a section at a point half way between the shot and recording station and thus reduced time sections were constructed along the profiles. Puzyrev et al. (1963) have shown that the error in boundary-depth determination is minimised

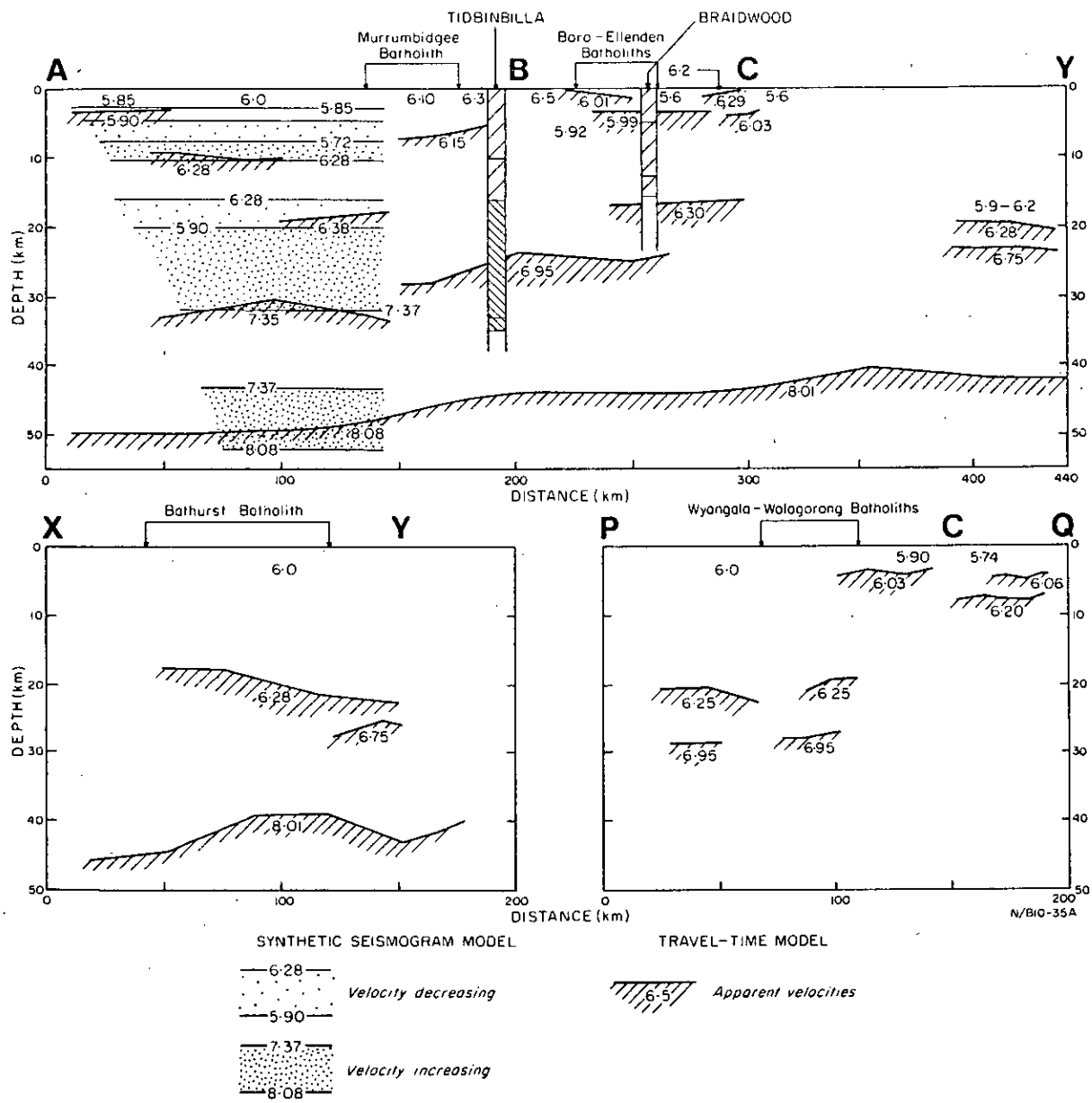

Fig. 9. Crustal profiles along traverses A–B–C, X–Y and P–C–Q (located in Fig. 2), together with Dartmouth crustal model derived from synthetic seismic models, and interpreted sections from seismic vertical soundings.

with respect to boundary-inclination uncertainties at the mid point, and minimised with respect to refractor velocity uncertainties near the critical point. Angles of inclination of up to 15° have a negligible effect on the boundary depth determined at the midpoint.

Velocity–depth models for computer investigations were obtained from these reduced travel-time sections using the approximating methods of Pavlenkova (1973), Puzyrev et al. (1963), Bram and Giese (1968), and Hinz et al. (1976). Models were constructed along profiles between Dartmouth and Marulan, between Murrumburrah and Fitzroy Falls, and between Spring Hill and Wilberforce (Fig. 9 profiles A–C, P–Q, and X–Y respectively). The depths of reflection horizons at Tidbinbilla and Braidwood (Fig. 3) from seismic vertical sounding are also shown on Fig. 9 (using the velocity–depth function from Fig. 13). It seems probably that the horizon identified at 33–36 km under Tidbinbilla is a lower crustal horizon and not the Moho as was originally thought (Taylor et al., 1972).

The dynamic characteristics of the record sections were modelled by computer using the reflectivity method developed by Fuchs (1968, 1970). The method was used by Braile and Smith (1975) to demonstrate the nature of the velocity gradients, layering in transition layers, and discontinuities. The characteristics of the record sections along the recording line between Dartmouth and Marulan were the principal targets for synthetic seismogram modelling. In particular the nature of the transitions in the approximate velocity intervals 5.9–6.3 km s^{-1}, 6.3–7.3 km s^{-1}, and 7.3–8.1 km s^{-1}, were investigated in detail.

The velocity structure in the top 15 km of crust was determined from the Dartmouth, Marulan, and Googong record sections out to distances of about 150 km. The velocity generally changes from 5.6–5.85 km s^{-1} near the surface to 5.90–6.03 km s^{-1}, and at greater depth to about 6.25–6.28 km s^{-1}. However, at Marulan and Googong the apparent velocities at distances less than 30 km have been measured in the range 6.29–6.57 km s^{-1}, indicating that velocities in the near surface Ordovician–Silurian rocks are in excess of those in near-surface granitic bodies. Hence the velocity models determined from the Dartmouth and Marulan near-surface data may well be only an indication of the velocity structure near those shot sources; under the intervening traverse, near-surface velocity structures are likely to vary considerably.

On the Dartmouth record section (Fig. 4a) large amplitude events are seen within 1 s of the first arrivals at distances of 58–65 km, and similar events are evident on the Marulan section (Fig. 4b) at about 82 km. Doyle et al. (1959) indentified similar amplitude changes on recordings from the Eaglehawk shots at Cooma (47 km), which were interpreted by Mueller and Landisman (1966) as indicative of a low-velocity layer in the upper crust. We concur with this view, but propose that such velocity inversions probably suggest local upper-crustal inhomogeneities rather than an extended uniform feature. The limited extent of the larger amplitudes near the critical point for the transition between the velocities 5.90 and 6.28 km s^{-1} in Fig. 4a (in the distance range 58–65 km), indicates a velocity gradient rather than a first-order discontinuity (Braile and Smith, 1975). The preferred velocity–depth model (Model 5) for the upper crust is shown in Fig. 10 together with other models and synthetic record sections.

The transition from 6.28 to 7.37 km s^{-1} in the Dartmouth record section (Fig. 4a) occurs in first arrivals at 178 km, and critical reflections are identified between 140 and 170 km. This record section also has supercritical reflections, with an apparent asymptotic velocity of 6.28 km s^{-1} out to 280 km, which are displaced from the first-arrival travel-time branch with this velocity, indicating a low-velocity layer. The limited range within which the critical reflections appear can be modelled using a velocity gradient in the depth range 18–36 km of 0.08–0.11 km s^{-1} km^{-1}. The preferred model (Model 4) is shown in Fig. 11, together with the synthetic seismograms for trial models.

The Marulan record section (Fig. 4b) differs from that of Dartmouth shots in some respects. The apparent velocity in the lower crust is about 6.95 km s^{-1}, and prominent critical-point reflections near 160 km, evident from Dartmouth shots, are absent. However they probably correspond to prominent arrivals 2–3 s after the first arrivals in the range 80–110 km from Marulan towards the southwest and to those in the range 110–160 km from Marulan towards the west. These correlations are supported by the offsets observed in the S-wave plots which occur at 100 and 150 km respectively.

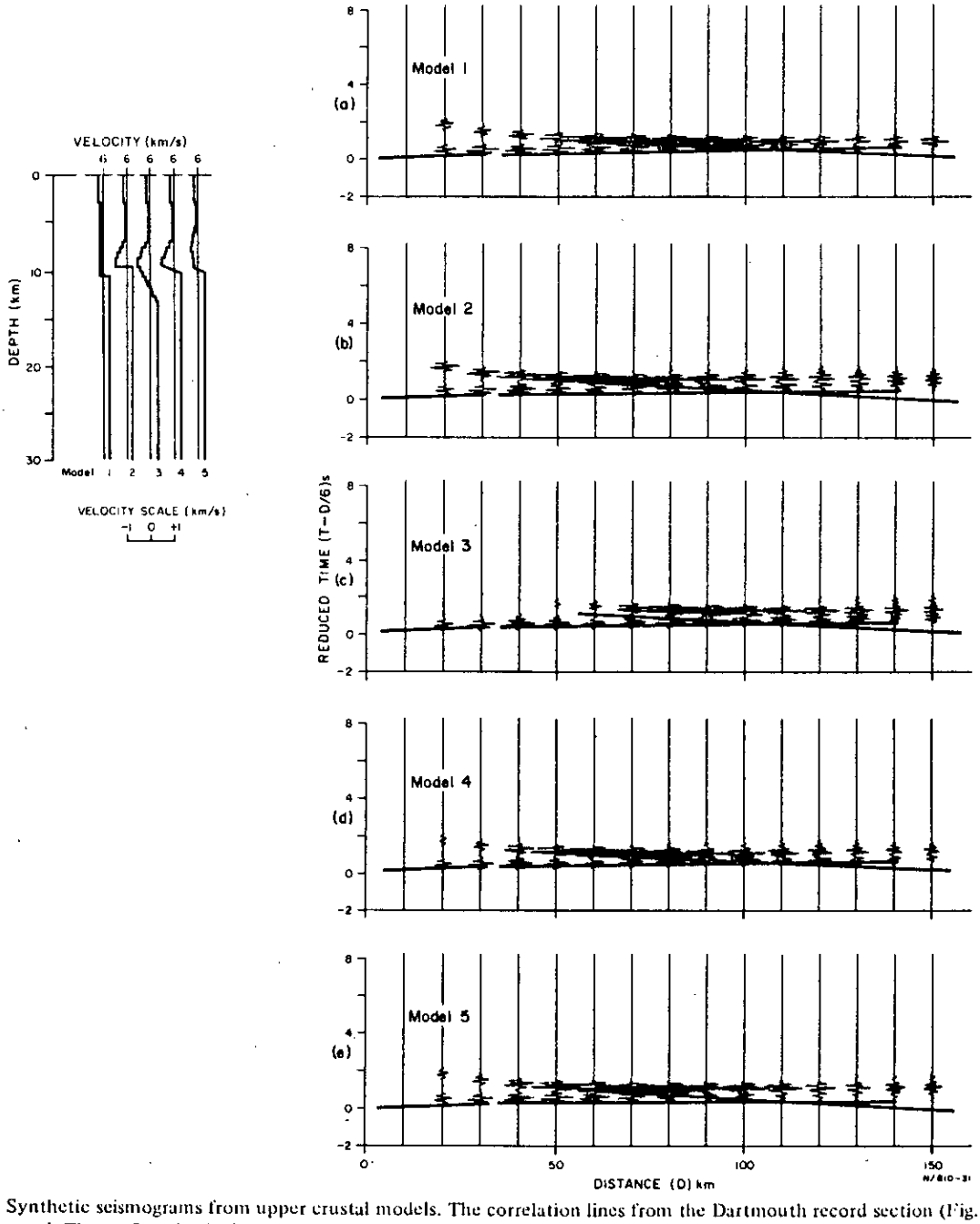

Fig. 10. Synthetic seismograms from upper crustal models. The correlation lines from the Dartmouth record section (Fig. 4a) are superimposed. The preferred velocity profile is Model 5.

We therefore assume that the S-waves with velocities of 3.76–3.90 km s^{-1} from Dartmouth and Marulan sources traverse the lower crust with P-wave velocities of 6.95–7.35 km s^{-1} (Fig. 9). On a gross scale both the P- and S-waves indicate a mid-crustal transition with a dip of 3–3.5° from Marulan to Dartmouth, and with the top of the lower crust (P-wave velocity about 7.15 km $^{-1}$ at ~35 km under Dart-

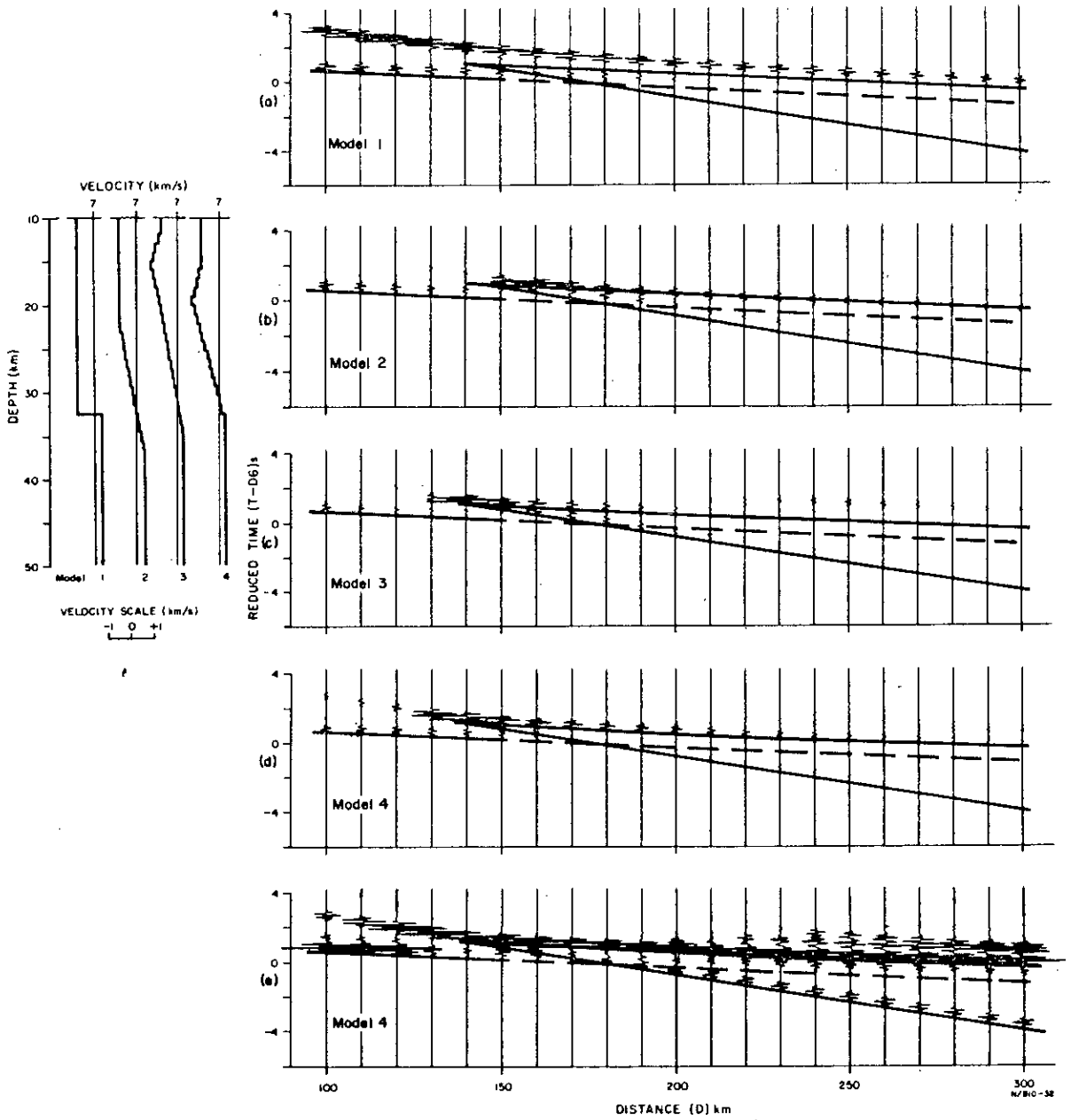

Fig. 11. Synthetic seismograms for mid-crustal models. The correlation lines from the Dartmouth record section (Fig. 4a) are superimposed. The preferred mid-crustal velocity profile is Model 4. The seismogram from Model 4 is also shown with each trace having equal maximum amplitude to demonstrate the initial onsets of phases (e).

mouth and ~26 km under Marulan.

The pronounced phases within 3 s of the first arrivals at distances of ~200 km on Dartmouth and Marulan record sections (Figs. 4a, 4b) are interpreted as critical reflections from the Moho. The limited range over which reflections are evident indicates that the change from lower crustal velocities of 6.95–7.37 km s^{-1} to upper mantle velocities of about 8.0–8.1

km s^{-1} is in the form of a gradient in the depth interval 43–52 km, and not a first-order discontinuity as in often depicted. First arrivals between Marulan and Dartmouth from Singleton shots (Fig. 6a) indicate very weak energy in the upper mantle arrivals. This has been modelled by not incorporating any velocity increase below the Moho transition; it is even possible that a slight decrease may apply. The preferred model

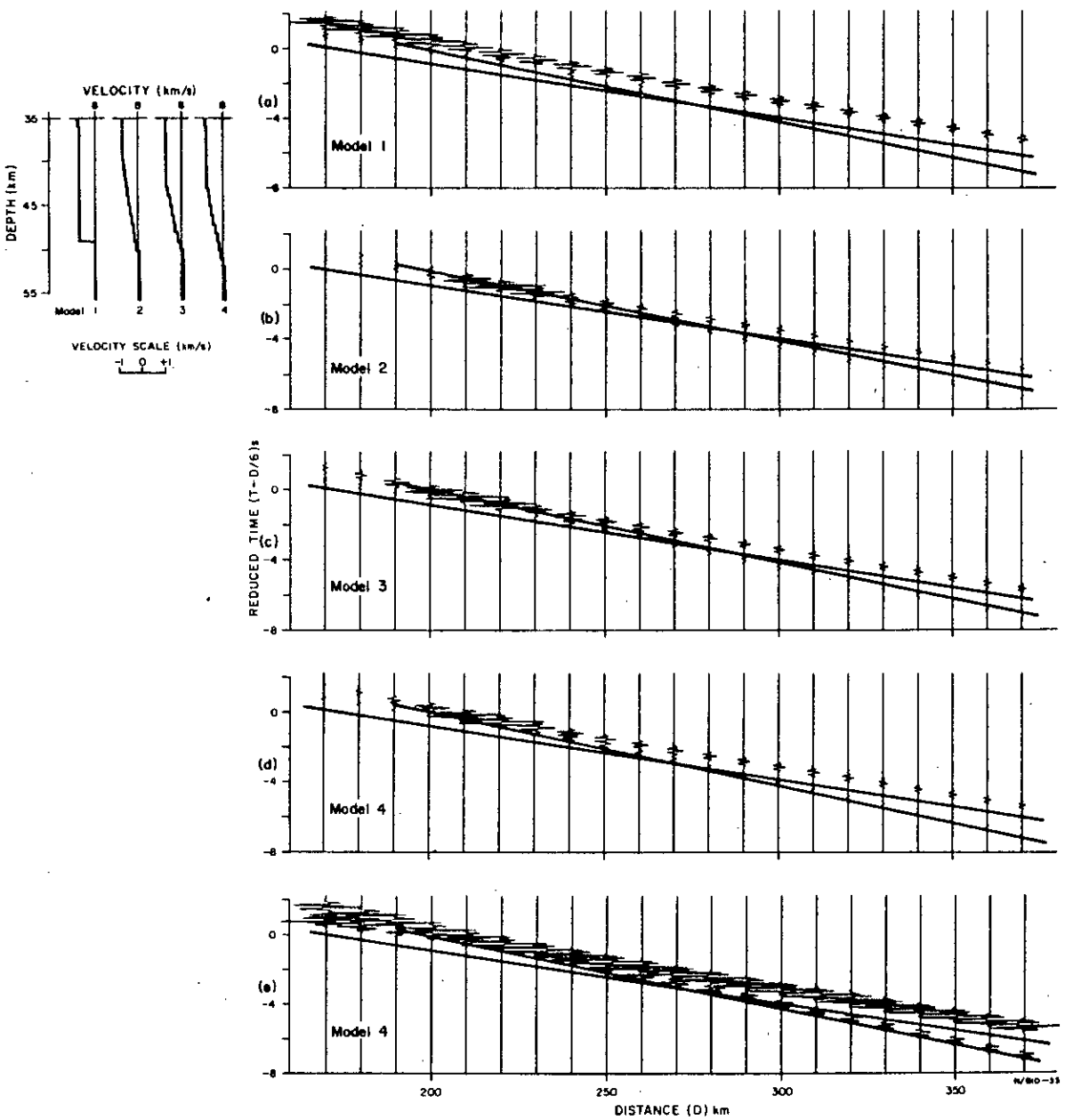

Fig. 12. Synthetic seismograms for the Moho boundary. The correlation lines from the Dartmouth record section (Fig. 4a) are superimposed. The preferred Moho velocity profile is Model 4. The seismogram from Model 4 is also shown with each trace having equal maximum amplitude to demonstrate the initial onset of phases (e).

and synthetic seismograms for the Moho transition are shown with other trial models in Fig. 12.

The preferred crustal velocity–depth model for the Dartmouth–Marulan line is shown in Fig. 13, combining the features from Figs. 10, 11 and 12.

As stated earlier the structure in the upper crust varies and there are significant differences in the velocity–depth profiles. Furthermore, although the main low-velocity layer is present throughout the survey area, its depth varies considerably (see above), and realistic models can be devised where the depth to the velocity minimum differs by as much as 5 km. However, one feature that appears common is the velocity gradient in the lower crust, in the 20–35 km depth range. All models tested that fit the observations have a gradient of close to 0.1 kms^{-1} km^{-1}.

The record section of Singleton shots (Fig. 6a) also contains seismic first arrivals from the 1965 N.S.W. coast survey (Doyle et al., 1966) and for the 1972

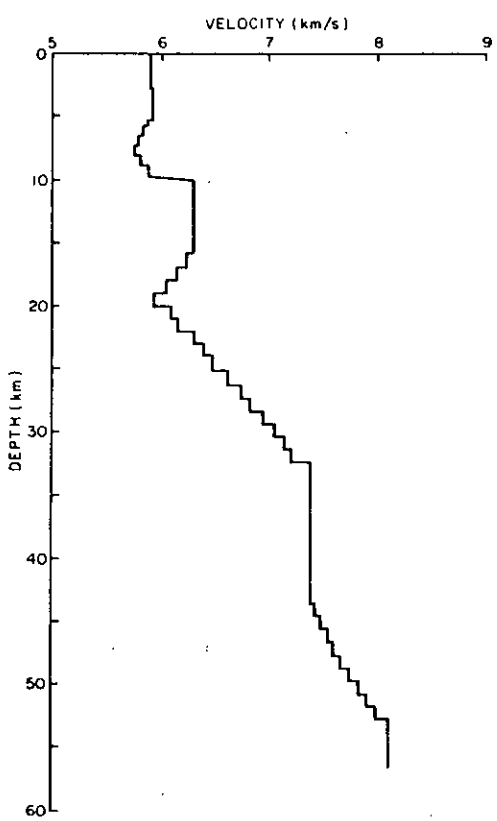

Fig. 13. Preferred seismic velocity model for the Earth's crust derived from Dartmouth–Marulan recordings.

Bass Strait shot (Muirhead et al., 1977), recorded 260–560 km at stations in the vicinity of the Dartmouth–Marulan line. The apparent velocities from these shots are those used in the interpretation presented here, but the intercepts from the two marine shot sources and the Singleton source differ from that of the preferred crustal model for the Dartmouth–Marulan line.

There are two major opposing effects which control the intercept time using these marine shots, the crustal thickness and the thickness of low-velocity sediment under the source. Crustal thickness at the continental margin is undoubtedly less than that under the Dartmouth–Marulan line, which should result in early first arrivals. However, a large, low-velocity sediment thickness will delay arrivals; this may result in the net intercept time being greater. This is the case for the N.S.W. coast shots, where first arrivals are about 0.9 s later than the preferred model arrivals; the net effect on the Bass Strait source is travel-times which are about 0.5 s early. The first arrivals from the Singleton sources (Fig. 6a) are between 1.4 and 1.5 s earlier than the preferred model, indicating a crustal thickness under the Sydney Basin of 34–36 km, not inconsistent with Collins' (1978) crustal thickness of about 36 km under the central Bowen Basin in Queensland, which is thought to be continuous with the Sydney Basin under Quaternary cover rocks.

Using the preferred velocity–depth model along the Dartmouth–Marulan recording line and the travel-times from the Bass Strait 10-tonne shot (Muirhead et al., 1977) to sites near Canberra, a depth of 34–36 km to the Moho transition is calculated under the southeast Australian coast.

6. Discussion

The prominent features of the Earth's crust in the eastern Lachlan Fold Belt determined from the seismic work are: (1) a depth to the Moho of between 45 and 52 km, (2) an inhomogeneous crust, and (3) velocity changes occurring as transitions rather than "discontinuities". These features can be compared with similar features in other areas of the world to determine the likely regime for crustal evolution in southeastern Australia.

Mueller (1973) has assembled crustal information from worldwide sources, and other regional summaries of crustal structure have been published as part of the Upper Mantle Project. A crustal thickness of about 50 km has been determined by seismic methods in the Plains–Rocky Mountains Front area of western Canada, the Prairies–Sierra Nevada, Montana and Lake Superior regions of the USA, southern USSR in Asia, north of the Black Sea under the Ukrainian Shield, the European Alps, and in the Peru–Chile coastal area of South America (Meyer et al., 1976). In all areas there is a juxtaposition of a mobile belt and an older continental craton; in some areas major earthquakes indicate that crustal shortening and/or subduction processes are currently active.

Notably absent from the areas of thick crust mentioned above are any island-arc areas on the western Pacific margin. Detailed investigations of seismic structure have been conducted in Japan (Miyamura and Uyeda, 1972), in the New Britain/New Ireland area (Finlayson and Cull, 1973), and in eastern Papua (Finlayson et al., 1977). In these areas depths to Moho rarely exceed 40 km and more typically are 30–36 km. Recent models of crustal evolution in eastern Australia (Crook and Powell, 1976) have invoked a western Pacific island-arc-type model. This model conflicts with the crustal thicknesses determined by the current seismic work, which are much greater than those measured in simple island-arc areas. It seems that a more appropriate present-day analogue would be an Andean-type model, in which the crustal thickness is much greater than that encountered in a simple island-arc regime.

The intra-crustal velocity structure is consistent with other areas of thick continental crust without current major tectonic activity. In Canada, The Plains area of Alberta consists of a thick wedge of Phanerozoic sediments overlying Precambrian basement; further west the Rocky Mountains chain consists of Palaeozoic and Mesozoic sediments thrust over Precambrian basement, exposed portions of which show massif-type structures resulting from uplift. Chandra and Cumming (1972), and Mereu et al. (1977), among others, have shown the complexity of the seismic structure across the Rocky Mountains Front. Although there are differences between the interpretations of these authors, there is general agreement that a velocity of about 6.5 km s^{-1} is evident in the upper crust, with a velocity greater than 7 km s^{-1} in the lower crust. Mereu et al. (1977) have interpreted the dynamic characteristics of the seismic waves using synthetic seismograms, and concluded, as we do for southeastern Australia, that velocity gradients characterise the intra-crustal velocity structure, and that the Moho also is a transition zone. A pronounced transition was also found at a depth of about 63 km under the Rocky Mountains Front, where the upper mantle velocity increases to about 8.5 km s^{-1}. This may correspond to the velocity of 8.63 km s^{-1} found by Muirhead et al. (1977) at 100 km depth under southeastern Australia. Mereu et al. (1977) also conclude that there are lateral intra-crustal density (and presumably velocity) variations, but little relief on the Moho transition.

The low-velocity zones (LVZ's) in the upper and middle crust of the Lachlan Fold Belt indicate lateral, as well as vertical, inhomogeneities within the crust. Recordings within 30 km of shots indicate velocity contrasts up to 0.5 km s^{-1} between surface granitic and metamorphic rocks, and it is not difficult to envisage such local variations within the upper crust. It is also probable that differing metamorphic grades create similar velocity differentials in the lower crust.

The Lachlan Fold Belt contains some major geological features which might be expected to show up in the seismic data. Our interpretation shows that crustal thickness decreases by some 7 km from the area of highest topography in the south towards the Sydney Basin margin in the north. The crust under the central Sydney Basin is probably about 34–37 km, much thinner than under the Lachlan Belt. About the same crustal thickness has been interpreted under the Bass Strait–Victoria coast.

The seismic recording traverse F–G (Fig. 2) intersects three major N–S trending fault zones, which can be traced for distances in excess of 100 km. Such major faults probably penetrate to considerable depth, and may extend to the lower crust. The ranges of seismic arrival times from phases with apparent velocities of 5.99, 6.28, 7.37 and 8.01 km s^{-1} (Fig. 8) are 0.3, 0.5, 0.7 and 0.2 s respectively, if the extreme maxima and minima are ignored as being possibly caused by poor recording or other instrumental effects. These ranges in travel-time represent depth variations of about 2.7, 5.4, 3.9 and 1.1 km respectively, distributed along a traverse which is about 100

km long. However, the depth changes are not correlated with the fault locations, whose positions are shown in Fig. 8. There is some evidence that the 7.37 km s^{-1} phases are later in the centre of the traverse than at the outer extremities (Fig. 8b), indicating a shallowing of this lower crustal transition layer away from the principal recording line A–B.

Southwest of the Googong shot source (Fig. 2) a major granitic batholith crops out in the range 25–60 km (the Murrumbidgee Batholith). It is bounded by two major N–S trending faults (the Murrumbidgee and Cotter Faults). The seismic record section from Googong in a southwesterly direction (Fig. 5a) displays features which are interpreted as indicating a granitic body with a P-velocity of 6.15 km s^{-1} overlying and surrounded by metamorphosed Ordovician and Silurian rocks with a P-velocity of 6.38 km s^{-1}. Such velocities and higher are evident as direct phases in the Ordovician rocks northeast of Googong. Model calculations indicate a depth to the base of the batholith of about 15–17 km.

The seismic recording line A–B (Fig. 2) crosses the major Long Plains Fault system in a zone 80–120 km from Dartmouth. At stations which would record seismic rays bottoming under the fault system there are some effects which may be attributable to this major fault. On the record section from Dartmouth shots (Fig. 4a) the 6.28 km s^{-1} events may have two small offsets (~0.1–0.2 s) which could be a result of a downthrow on the NE side. If the upper crustal rock has a velocity of 5.9 km s^{-1} the size of this downthrow would be about 1.7–3.4 km in granitic rock.

The recording line B–C (Fig. 2) crosses the Boro-Ellenden Granite batholiths 40–75 km from the Marulan source. Seismic phases bottoming under these batholiths (80–150 km from Marulan) display many of the same characteristics (Fig. 4b) as those bottoming under the Murrumbidgee Batholith. The prominent second arrival about 0.9 s after the first arrival at a distance of 82 km from Marulan is interpreted as resulting from a batholithic structure, similar to arrivals about 69 km southwest of Googong. A velocity of 5.99 km s^{-1} is regarded as the velocity in the granite, and the 6.3 km s^{-1} velocity as that in metamorphosed Ordovician sediments. Model calculations indicate a depth of the batholith of about 16–19 km.

Along the recording line C–E (Fig. 2), west of the Marulan seismic source, the Wyangala-Wologorong batholiths crop out in the distance range 40–80 km. Seismic rays bottoming under the batholiths will be recorded in the range 80–160 km, which, as described earlier in this interpretation, is also the range in which low-velocity zone phenomena are evident in the S-phases. The 6.03 km s^{-1} velocity arrivals are interpreted as being the direct P-phases through the granitic rocks at the 6.25 km s^{-1} arrivals as through older metamorphosed sediments and other upper crustal rocks. Model calculations indicate the depth to the base of the batholith as being in the range 20–25 km.

This interpretation of the 6.0/6.3 km s^{-1} velocity contrast as the base of granitic batholiths may be extended to the section along profile X–Y (Figs. 2, 9). It is inferred that the 6.28 km s^{-1} horizon is the base of the Bathurst Granite. The evidence in the amplitude data from Dartmouth seismic source described earlier in this paper suggests that there is a low-velocity zone at the base of these granitic batholiths above the higher velocity zone of about 6.3 km s^{-1} in the middle crustal rocks.

The recording line C–D (Fig. 2) traverses the southern boundary of the Sydney Basin and seismic recordings are reversed from the shot points at Marulan and Bass Point (Fig. 7). The apparent velocities of 5.89 and 6.11 km s^{-1} can be used in a simple model of the Basin with Permo-Triassic sediments overlying a dipping basement. If the velocity in the sediments is assumed to be 3.65 km s^{-1}, as determined from Sydney Basin borehole data (Mayne et al., 1974), a basement dip of about 0.8° is estimated with a depth at Bass Point on the N.S.W. coast of about 1.4 km, and zero at Marulan.

Acknowledgements

The authors wish to thank the many private companies and government instrumentalities involved with shot firing for their cooperation and assistance. We also wish to acknowledge the assistance with field work by other BMR staff, in particular the major contribution of J. Williams in maintaining and servicing field recording equipment. The cooperation of land owners in allowing access to recording sites is also appreciated.

Professor K. Fuchs provided a copy of his synthetic seismogram program REFLEX, and his contribution to the overall BMR seismic investigation of crustal structure is gratefully acknowledged.

This paper is published with the permission of the Director of the Bureau of Mineral Resources, Geology and Geophysics, Canberra.

References

Braile, L.W. and Smith, R.B., 1975. Guide to the interpretation of crustal refraction profiles. Geophys. J.R. Astron. Soc., 40: 145–176.

Bram, K. and Giese, P., 1968. Die Geschwindigkeitsverteilung der P – Welle in der Erdkruste im Raum Augsburg (Sud-Deutschland) – Ergebnisse and Vergleich zweier seismischer Messungen. Z. Geophys., 34: 611–626.

Branson, J.C., Moss, F.J. and Taylor, F.J., 1976. Deep crustal reflection seismic test survey, Mildura, Victoria and Broken Hill, N.S.W., 1968. Bur. Mineral. Resour. Aust. Rep. 183.

Chandra, N.N. and Cumming, G.L., 1972. Seismic refraction studies in western Canada. Can. J. Earth Sci., 9: 1099–1109.

Cleary, J.R., 1973. Australian crustal structure. Tectonophysics, 20: 241–248.

Collins, C.D.N., 1976. Seismic investigations of crustal structure in southeast Australia, March–May 1976: operational report. Bur. Mineral. Resour. Aust. Rec., 1976/103.

Collins, C.D.N., 1978. Crustal structure of the central Bowen Basin, Queensland. BMR J. Aust. Geol. Geophys., 3(3): 203–209.

Crook, K.A.W., 1974. Kratonization of West Pacific-type geosynclines. J. Geol., 82: 24–36.

Crook, K.A.W. and Powell, C.McA., 1976. The evolution of the southeastern part of the Tasman Geosyncline. 25th Int. Geol. Congr., Excursion Guide No. 17A.

Dooley, J.C., 1971. Seismological studies of the upper mantle in the Australian region. In: Proc. 2nd Symp. Upper Mantle Project, Hyderabad 1970, Geophys. Res. Board Nat. Geophys. Res. Inst., Hyderabad, pp. 113–146.

Doyle, H.A., Everingham, I.B. and Hogan, T.K., 1959. Seismic recordings of large explosions in southeastern Australia. Aust. J. Phys., 12: 222–230.

Doyle, H.A., Underwood, R. and Polak, E.J., 1966. Seismic velocities from explosions off the central coast of New South Wales. J. Geol. Soc. Aust., 13: 355–372.

Finlayson, D.M., 1977. Seismic investigations of crustal structure in southeastern Australia, November 1976–March 1977 (MARDAR survey): operational report. Bur. Mineral. Resour, Aust. Rec. 1977/62.

Finlayson, D.M. and Cull, J.P., 1973. Time-term analysis of New Britain – New Ireland island arc structures. Geophys. J.R. Astron. Soc., 33: 265–280.

Finlayson, D.M., Cull, J.P. and Drummond, B.J., 1974. Upper mantle structure from the trans-Australia seismic refraction data. J. Geol. Soc. Aust., 21: 447–458.

Finlayson, D.M., Drummond, B.J., Collins, C.D.N. and Connelly, J.B., 1977. Crustal structures in the region of the Papuan Ultramafic Belt. Phys. Earth. Planet Inter., 14: 13–29.

Fuchs, K., 1968. Das Reflexions–Transmissionsvermögen eines geschichteten Mediums mit beliebiger Tiefen-Verteilung der elastischen Moduln und der Dichte für schrägen Einfall ebener Wellen. Z. Geophys., 34: 389–413.

Fuchs, K., 1970. On the determination of velocity depth distributions of elastic waves from the dynamic characteristics of the reflected wave field. Z. Geophys., 36: 531–548.

Giese, P., 1976a. General remarks on travel time data and principles of correlation. In: P. Giese, C. Prodehl and A. Stein (Editors), Explosion Seismology in Central Europe. Springer-Verlag, Berlin, pp. 130–145.

Giese, P., 1976b. Depth calculation. In: P. Giese, C. Prodehl and A. Stein (Editors), Explosion Seismology in Central Europe. Springer-Verlag, Berlin, pp. 146–161.

Giese, P., Prodehl, C. and Stein, A., 1976. Explosion Seismology in Central Europe. Springer-Verlag, Berlin, 429 pp.

Hinz, E., Kaminski, W. and Stein, A., 1976. Results of a seismic refraction profile from Hoher Meissner to the North German Plain. In: P. Giese, C. Prodehl and A. Stein (Editors), Explosion Seismology in Central Europe. Springer-Verlag, Berlin, pp. 257–267.

Johnson, B.D., 1973. A time term analysis of the data obtained during the Bass Strait Upper Mantle Project (Operation BUMP). Bull. Aust. Soc. Explor. Geophys., 4: 15–20.

Mayne, S.J., Nicholas, E., Bigg-Wither, A.L., Rasidi, J.S. and Raine, M.J., 1974. Geology of the Sydney Basin – a Review. Bur. Mineral. Res. Bull. 149.

McElhinny, M.W., 1973. Earth sciences and the Australian continent. Nature (London) 246: 264–268.

Mereu, R.F., Majumdar, S.C. and White, R.E. 1977. The structure of the crust and upper mantle under the highest ranges of the Canadian Rockies from a seismic refraction survey. Can. J. Earth Sci., 14: 196–208.

Meyer, R.P., Mooney, W.D., Hales, A.L., Helsley, C.E., Woollard, G.P., Hussong, D.M., Kroenke, L.W. and Ramirez, J.E., 1976. Project Narino III: refraction observation across a leading edge, Malfelo Island to the Columbian Cordillera occidental. In: G.H. Sutton, M.H. Manghnani and R. Moberly (Editors). The Geophysics of the Pacific Ocean Basin and its Margins, The Woollard Volume. Am. Geophys. Union Mongr., 19: 105–132.

Miyamura, S. and Uyeda, S., (Eds.) 1972. The crust and upper mantle of the Japanese area. Part I, Geophysics. Earthquake Research Institute, University of Tokyo, 119 pp.

Mueller, S., (Ed.), 1973. The structure of the Earth's crust based on seismic data. Tectonophysics, 20: 1–391.

Mueller, S. and Landisman, M., 1966. Seismic studies of the Earth's crust in continents. I : Evidence for a low-velocity

zone in the upper part of the lithosphere. Geophys. J.R. Astron. Soc., 10: 525–538.

Muirhead, K.J., Cleary, J.R. and Finlayson, D.M., 1977. A long-range seismic profile in south-eastern Australia. Geophys. J.R. Astron. Soc. 48: 509–519.

Oliver, J., Dobrin, M., Kaufman, D., Meyer, R. and Phinney, R., 1976. Continuous seismic reflection profiling of the deep basement, Hardeman County, Texas. Geol. Soc. Am. Bull., 87: 1537–1546.

Pavlenkova, N.I., 1973. Interpretation of refracted waves by the reduced travel time curve method. Phys. Solid Earth, 8: 544–550.

Puzyrev, N.N., Krylov, S.V., Potapyev, S.V. and Treskova, Yu.A., 1963. Seismic soundings by refracted waves for regional geological investigations. In: J.C. Dooley, Translation of papers on seismic reflection and refraction methods by N.N. Puzyrev and others. Bur. Mineral. Resour. Aust. Rec. 1974/8.

Rutland, R.W.R., 1973. Tectonic evolution of the continental crust of Australia. In: D.H. Tarling and S.K. Runcorn (Editors), Continental Drift, Sea Floor Spreading and Plate Tectonics: Implications to the Earth Sciences. Academic Press, London, pp. 1003–1025.

Rutland, R.W.R., 1976. Orogenic evolution of Australia. Earth Sci. Rev., 12: 161–196.

Scheibner, E., 1973. A plate tectonic model of the Palaeozoic tectonic history of New South Wales. J. Geol. Soc. Aust., 20: 405–426.

Scheibner, E., 1974. Correlation problems in the Tasman Fold Belt. In: A.K. Denmead, G.W. Tweedale and A.F. Wilson (Eds.), The Tasman Geosyncline. Geol. Soc. Aust., pp. 65–98.

Scheibner, E., 1976. Tasman Fold Belt system in New South Wales. Geol. Surv. N.S.W. Rep. GS 1976/195.

Smithson, S.B. and Brown, S.K., 1977. A model for lower continental crust. Earth Planet. Sci. Lett., 35: 134–144.

Taylor. F.J., Moss, F.J. and Branson, J.C., 1972. Deep crustal reflection seismic test survey, Tidbinbilla A.C.T. and Braidwood N.S.W., 1969. Bur. Mineral. Resour. Aust., Rec. 1972/126.

Underwood, R., 1969. A seismic refraction study of the crust and upper mantle in the vicinity of Bass Strait. Aust. J. Phys., 22: 573–587.

Vandenberg, A.H.M., 1976. The Tasman Fold Belt in Victoria. Geol. Surv. Victoria Rep., 1976/3.

Journal of the Geological Society of Australia (1981), 28, 177-190

Crustal structure under the Sydney Basin and Lachlan Fold Belt, determined from explosion seismic studies

D. M. Finlayson & H. M. McCracken

B.M.R., P.O. Box 378, Canberra City, A.C.T. 2601.

ABSTRACT

The Lachlan Fold Belt has the velocity-depth structure of continental crust, with a thickness exceeding 50 km under the region of highest topography in Australia, and in the range 41–44 km under the central Fold Belt and Sydney Basin. There is no evidence of high upper crustal velocities normally associated with marginal or back-arc basin crustal rocks. The velocities in the lower crust are consistent with an overall increase in metamorphic grade and/or mafic mineral content with depth. Continuing tectonic development throughout the region and the negligible seismicity at depths greater than 30 km indicate that the lower crust is undergoing ductile deformation.

The upper crustal velocities below the Sydney Basin are in the range 5.75–5.9 km/s to about 8 km, increasing to 6.35–6.5 km/s at about 15–17 km depth, where there is a high-velocity (7.0 km/s) zone for about 9 km evident in results from one direction. The lower crust is characterised by a velocity gradient from about 6.7 km/s at 25 km, to 7.7 km/s at 40–42 km, and a transition to an upper mantle velocity of 8.03–8.12 km/s at 41.5–43.5 km depth.

Across the central Lachlan Fold Belt, velocities generally increase from 5.6 km/s at the surface to 6.0 km/s at 14.5 km depth, with a higher-velocity zone (5.95 km/s) in the depth range 2.5–7.0 km. In the lower crust, velocities increase from 6.3 km/s at 16 km depth to 7.2 km/s at 40 km depth, then increase to 7.95 km/s at 43 km. A steeper gradient is evident at 26.5–28 km depth, where the velocity is about 6.6–6.8 km/s. Under part of the area an upper mantle low-velocity zone in the depth range 50–64 km is interpreted from strong events recorded at distances greater than 320 km.

There is no substantial difference in the Moho depth across the boundary between the Sydney Basin and the Lachlan Fold Belt, consistent with the Basin overlying part of the Fold Belt. Pre-Ordovician rocks within the crust suggest fragmented continental-type crust existed E of the Precambrian craton and that these contribute to the thick crustal section in SE Australia.

INTRODUCTION

Since 1976 the Bureau of Mineral Resources, Geology & Geophysics (BMR) has been using explosion seismic methods to determine the gross crustal structure of the Lachlan Fold Belt (Finlayson et al., 1979, 1980). Some data from these investigations were obtained using explosions detonated in open-cut mines near the northern margins of the Sydney Basin. The sesimic ray paths from these shots travelled under the Sydney Basin for distances as large as 200 km and consequently were influenced by structures in and underlying the basin sediments.

During November-December 1978, the BMR conducted seismic investigations within the Sydney Basin, so that additional detailed knowledge of Basin crustal structures could be interpreted; some of the results are presented in this paper. Figure 1 shows the location of seismic sources and recording stations. In addition, some recordings were obtained during 1978 to distances greater than 300 km W of a shot source at the South Marulan limestone quarry. This enabled the velocity/depth structures in that part of the Lachlan Fold Belt to be determined more accurately than those presented by Finlayson et al. (1980).

GEOLOGY

The Sydney Basin developed as a structural basin between the Lachlan Fold Belt and the New England Fold Belt in the late Carboniferous to the Triassic, and is the southern part of the larger, elongate Sydney-Bowen Basin which extends N to Queensland. The Basin (Fig. 2) is bounded to the NE by the Hunter-Mooki Thrust, to the NW by the Mount Coricudgy Anticline, to the E by the continental

MS received 1 October 1980; revised MS received 19 December 1980.

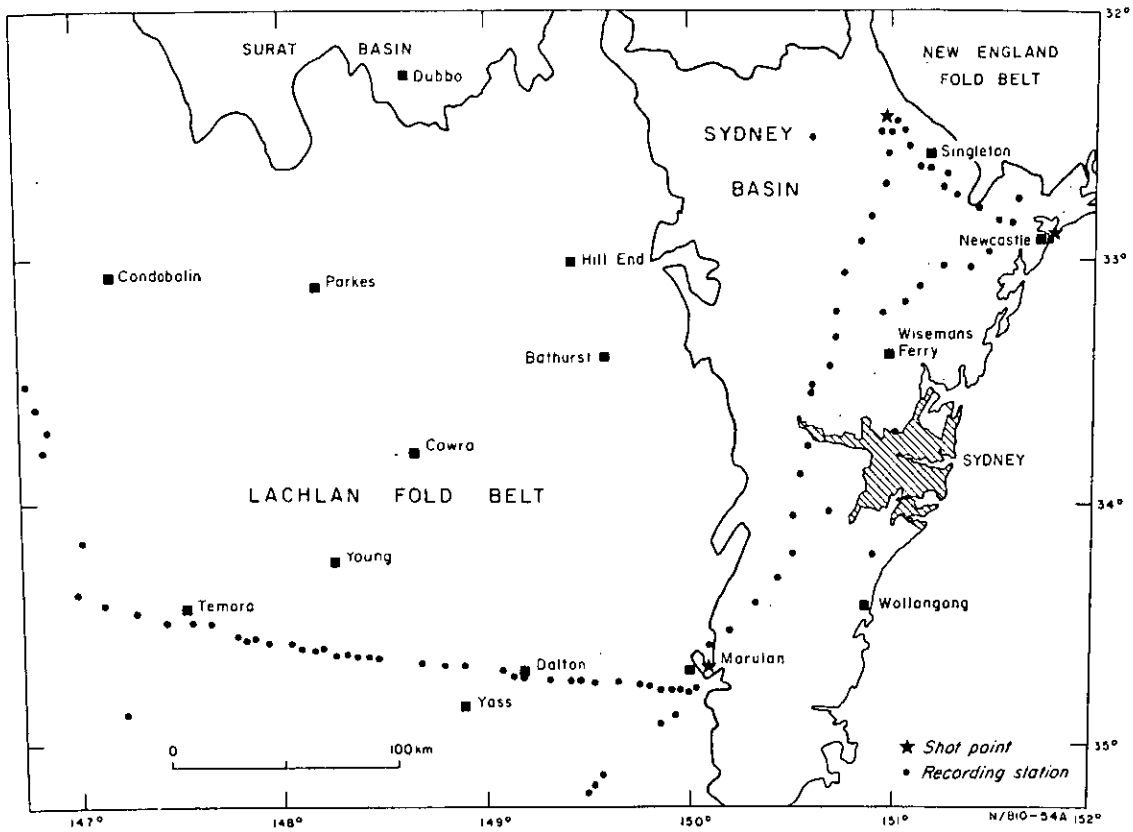

Fig. 1. Shot point and recording station locations.

shelf, and to the W by a depositional/erosional margin with the Lachlan Fold Belt (Mayne et al., 1974; Passmore, 1979; Branagan et al., 1979).

According to Branagan et al. (1979), towards the end of the Carboniferous a back-arc basin developed between the New England Orogenic Zone and the Lachlan Fold Belt, which by this time was part of the stable continental craton. However, this interpretation is difficult to reconcile with other statements (Passmore, 1979) that Lachlan Fold Belt rocks underlie parts of the basin. From the late Carboniferous to the Early Permian, sediments were transported into the basin from the Lachlan Fold Belt. In the Early Permian, subduction further to the E, associated with the New England Orogenic Zone, ceased. The Hunter Orogeny in the mid-Permian caused uplift and deformation in the New England Fold Belt, and the Hunter-Mooki Thrust developed from folding and thrust faulting along its western edge.

Overthrusting of the New England Fold Belt against the older Lachlan Fold Belt produced downwarping at the site of the back-arc basin and a rapidly subsiding trough developed, which remained active until the end of the Permian (Branagan et al., 1979). Late Permian sediments from the New England Fold Belt were rapidly deposited in the narrow elongate trough that is now the Sydney Basin. The final development of the Basin was the formation of an intracratonic basin between the two stable fold belts at the end of the Permian. Deposition of sediments into the Basin from the New England Fold Belt declined during the Triassic.

There are many centres of post-depositional igneous activity, some of which are sites for quarrying shots, which can be used for seismic work. Dating of these intrusions indicates periods of activity in the Triassic, Jurassic-Cretaceous, Middle Eocene-Middle Oligocene, and Miocene.

Along the NE margin of the Basin, Devonian sediments occur beneath the Carboniferous. Towards the S there are few Carboniferous sediments, and the Permo-Triassic sequence rests directly on Lower Palaeozoic Lachlan Fold Belt basement.

Mayne et al. (1974) reported the results of airborne magnetic survey work in the Basin. Magnetic basement coincides in the S with the unconformity between the Lachlan Fold Belt and the Permian sediments, and, in the N with the top of Lower Permian volcanics. Well-log data also provide information on the thickness of Basin sediments (Mayne et al., 1974; Passmore, 1979).

The sediment thickness exceeds 3.5 km in only a few areas. One of these is crossed by the seismic traverse from Singleton to Marulan (Fig. 1). More typically, sediment thickness is about 1.5–1.8 km in the Singleton area and about 2.5–3.0 km towards the southern end of the line, before shallowing rapidly to

zero at the boundary with exposed Lachlan Fold Belt rocks. Between Newcastle and Singleton the thickness of Basin sediments decreases from about 2.5 km to 1.5 km, and under the recording line between Newcastle and Wisemans Ferry the thickness is about 2.5 km.

SEISMIC SURVEY OPERATIONS

Details of the 1978 field work have been reported by Finlayson (1979). The location of shots and recording stations from both this and earlier survey sites used in the interpretation are shown in Figure 1. Commercial quarry blasts were used as seismic sources; these were located at the South Marulan limestone quarry, open-cut coal mines in the Singleton area, and underwater blasts in Newcastle Harbour associated with deepening of the shipping channel. Shot sizes at South Marulan were 1-4 t, at Singleton up to 50t, and at Newcastle less than 1t. Shot monitoring recorders were maintained at all shot sources; the estimated error in shot timing is ± 10 ms and in shot location is ± 50 m horizontally.

Recording stations were set out across the central Sydney Basin to investigate deep crustal structure between shot sources at South Marulan and Singleton. The recording sites, between Singleton and Newcastle, and between Newcastle and Wisemans Ferry, were positioned to investigate upper crustal structure under the northern margin of the Sydney Basin. Digital seismic record sections were producted from the frequency modulated field tape recordings, and these were commonly normalised to the maximum amplitude on each trace, and bandpass filtered to eliminate unwanted noise.

VELOCITIES WITHIN THE SYDNEY BASIN

Branagan et al. (1979) summarised the structures within the sedimentary sequence of the Sydney Basin (Fig. 2). Little information on such structure is available from the present survey data, but such information is required for the interpretation of deeper velocity structures. As the data obtained from the seismic work reported in this paper are not confined to any one structural unit, they can be used to cal-

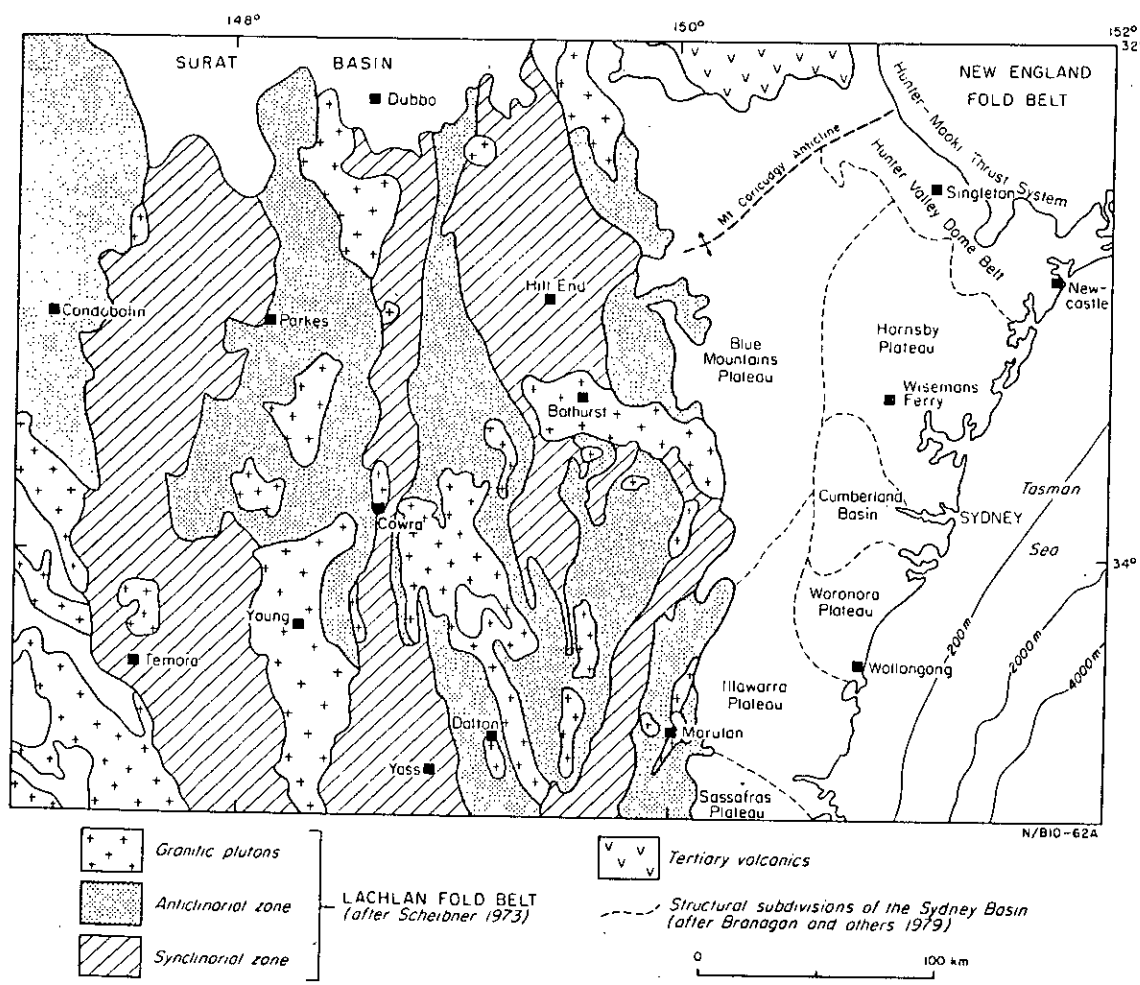

Fig. 2. Simplified geology of the Sydney Basin and northern Lachlan Fold Belt.

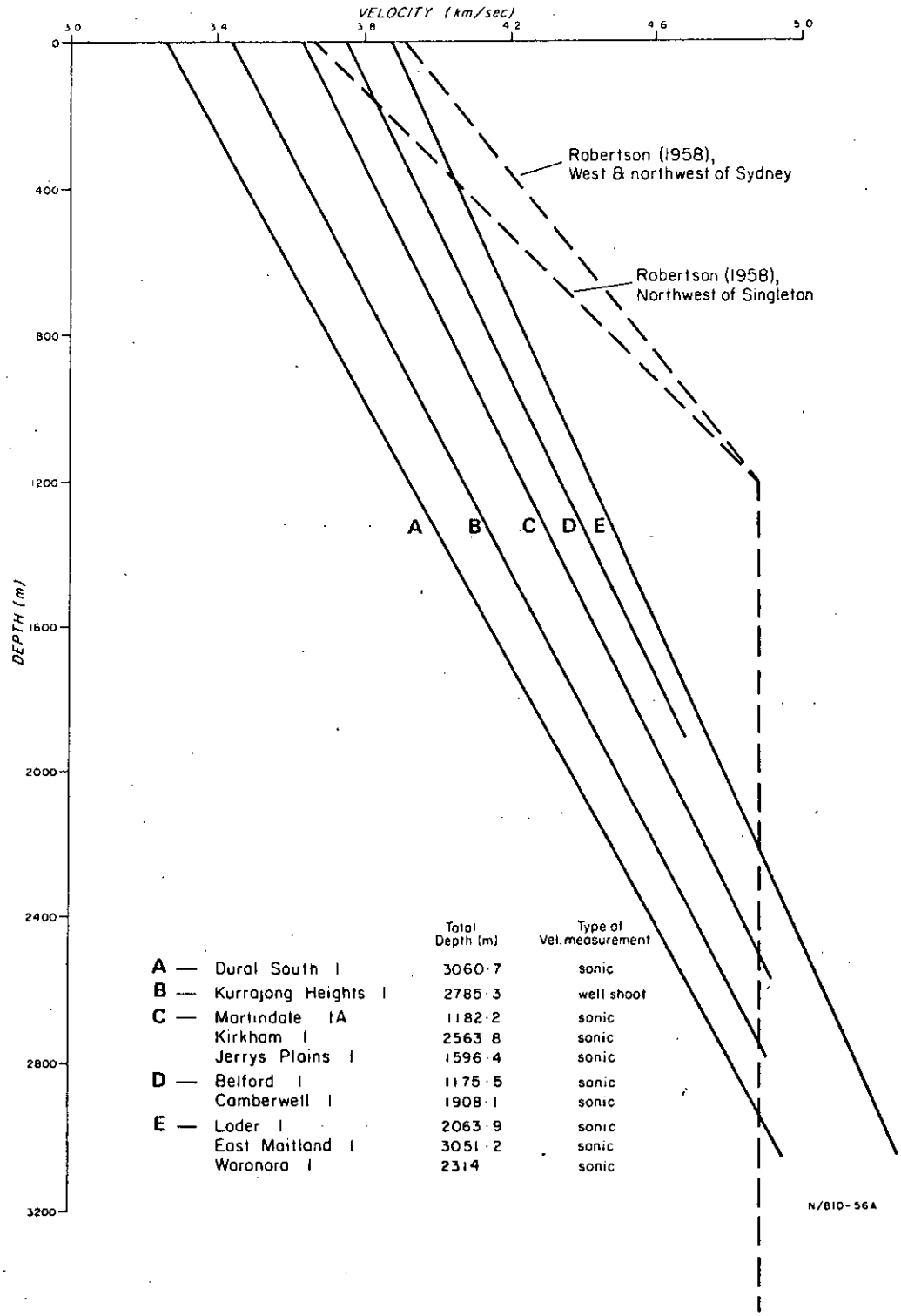

Fig. 3. Velocities determined from well logs (after Mayne et al., 1974) and seismic surveys (Robertson, 1958) in the Sydney Basin.

TABLE 1. Basement velocities beneath the Sydney Basin

Shot location	Direction	P-wave velocity	Distance range of 1st arrivals
Marulan	N	5.89 km/s	0–50 km
Newcastle	NW	5.82 km/s	20–50 km
Newcastle	SW	5.83 km/s	20–85 km
Singleton	SE	5.55 km/s	15–40 km
Singleton	S	5.70 km/s	15–50 km

culate only average velocities that apply to a combination of several units.

Mayne et al. (1974) reported the results of velocity determinations from well logs within the Basin, and indicated that a linear increase in velocity with depth applied throughout the Basin (Fig. 3). Results were typically within the range 3.6–3.9 km/s at the surface to 4.6–4.8 km/s at 2 km depth, but included velocities as low as 3.25 km/s at the surface and 4.35 km/s at 2 km depth in two holes. Shots recorded from the Singleton coal mines and Newcastle harbour, at distance less than 20 km, yielded velocities of 4.45 km/s in the Newcastle area and 4.34 km/s near Singleton.

Seismic reflection work (Robertson, 1958) in three areas between 19 and 50 km W and NW of Sydney indicated velocities of 3.9 km/s at sea level, increasing to 4.88 km/s at 1.2 km depth, and only a very slight increase at greater depth. About 6 km NW of Singleton, velocities of 3.65 km/s were determined at sea level, increasing to 4.88 km/s at 1.2 km, with no increase at greater depth. These velocities are higher than the sonic well-log velocities discussed earlier (Fig. 3). The seismic velocity determinations give a much coarser picture of real velocity structure, and their interpretation may involve simplifying assumptions that result in higher average velocities being estimated. Anisotropy within the sedimentary sequences may also contribute to the velocity differences.

Doyle et al. (1966) reported a velocity of 4.5 km/s from shots fired offshore and recorded in Sydney, but used a velocity of 4.9 km/s in their crustal interpretations, taking this value to be more representative of the average velocity in the sedimentary column. The minimum shot-to-station distance was 22.7 km; it is therefore unlikely that ray paths were confined solely to the sedimentary section. The velocity of 4.5 km/s probably represents a maximum velocity in the sediments.

In summary, the best determined estimates of P-wave velocities in the Sydney Basin sediments range from 3.6–3.9 km/s at the surface to 4.35–4.8 km/s at depths of 2 km and greater.

BASEMENT VELOCITIES

Values for the P-wave velocity in the basement rocks under the Sydney Basin are available from recordings made near shot sources in the present survey, and from a number of previous investigations. Bolt (1962) determined a velocity of 5.88 ± 0.14 km/s and a travel-time curve intercept of 0.97 ± 0.18 s from recordings of quarry blasts in the western suburbs of Sydney. This was taken to be the velocity in the basement rocks. Using a value of 3.5 km/s for sediments, he estimated their average thickness to be 2.4 km in the central-southern part of the Basin. A higher assumed sediment velocity would increase this value for Basin sediment thickness; e.g. a value of 4.3 km/s results in a thickness of 3.1 km, in good agreement with the average seismic reflection value of 3.0 km reported by Mayne et al. (1974) for the depth of the Lower Permian Pebbly Beach Formation.

Finlayson et al. (1980) have calculated reversed basement velocities of 5.89 and 6.11 km/s for the southern part of the Sydney Basin; using a sedimentary velocity of 3.65 m/s they estimated the thickness of Permo-Triassic sediments to be 1.4 km at the coast, thinning to zero near Marulan. They also derived a value of 5.60 km/s for the near-surface velocity to the W of Marulan. Doyle et al. (1966) gave a tentative value of 6.0 km/s for the apparent velocity under the Basin sediments, determined from shots detonated off the coast near Sydney and recorded at stations within the Basin.

The velocities measured from seismic first-arrival data during the 1978 survey work are listed in Table 1. Using a simple model of basin sediments overlying basement with an average velocity of 5.75 km/s, the intercept times from travel-time plots in the Singleton-Newcastle area yield depths to basement of about 2.1 km near Singleton and about 3.5 km near Newcastle. Seismic reflection work (Mayne et al., 1974) has indicated that the depths to the Lower Permian Rutherford Formation, near the base of the Basin sediments in these areas, are 1.8–2.1 km and 3.6–3.8 km, respectively.

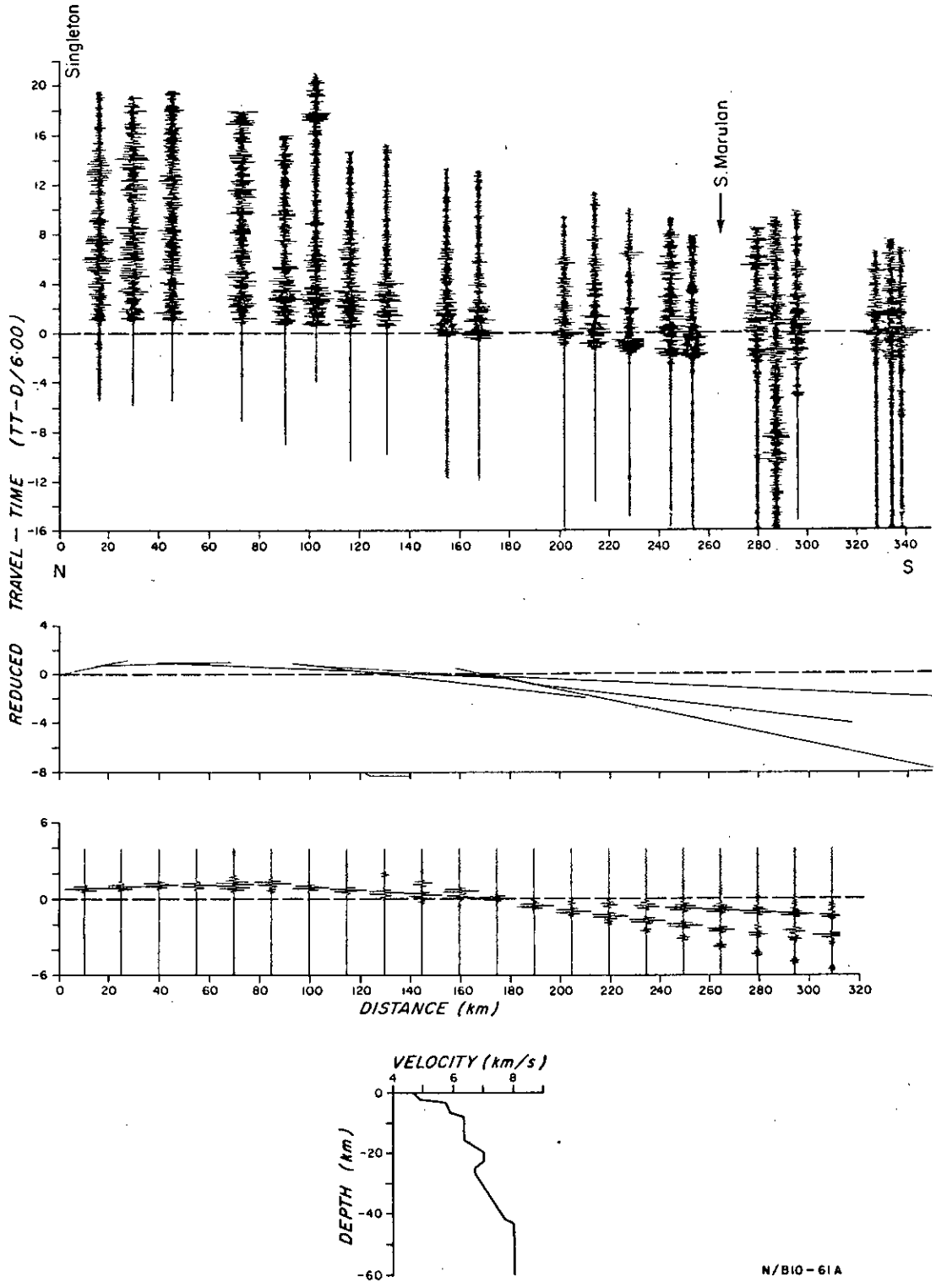

Fig. 4. Seismic record section and preferred model of travel-times and signal amplitudes along the traverse between Singleton and Marulan.

VELOCITY-DEPTH MODELS BENEATH THE SYDNEY BASIN

The principal recording traverse across the Sydney Basin used to determine the velocity/depth structure beneath the Basin lay between shot sources at the South Marulan limestone quarry and the open-cut coal mines near Singleton (Fig. 1). The seismic record sections for shot sources at each end of the line are shown in Figures 4 and 5.

The N-to-S record section has recordings from Singleton area shots out to a distance of about 340 km. Recordings S of Marulan, beyond 270 km, were obtained during 1976 (Finlayson et al., 1980) and are used to assist with the identification of upper mantle seismic phases. In the distance range 0–220 km, no prominent phases other than the initial onsets can be correlated between adjacent traces. This indicates a lack of strong intra-crustal and Moho velocity contrasts that would produce pronounced subcritical reflections. Beyond 220 km a prominent phase occurs after the weak first arrivals. This phase has an apparent velocity of about 6.5 km/s, and its presence

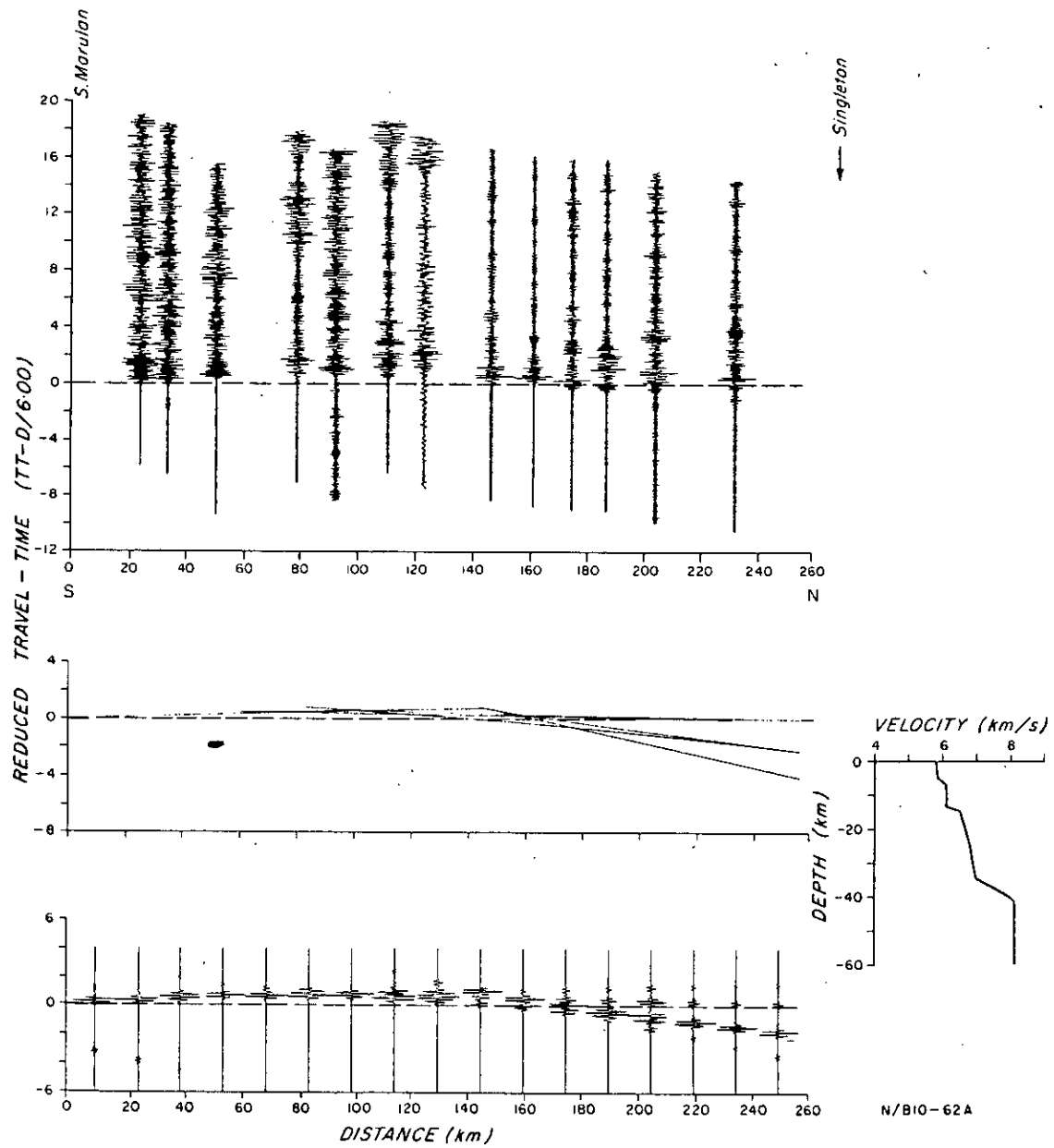

Fig. 5. Seismic record section and preferred model of travel-times and signal amplitudes along the traverse between Marulan and Singleton.

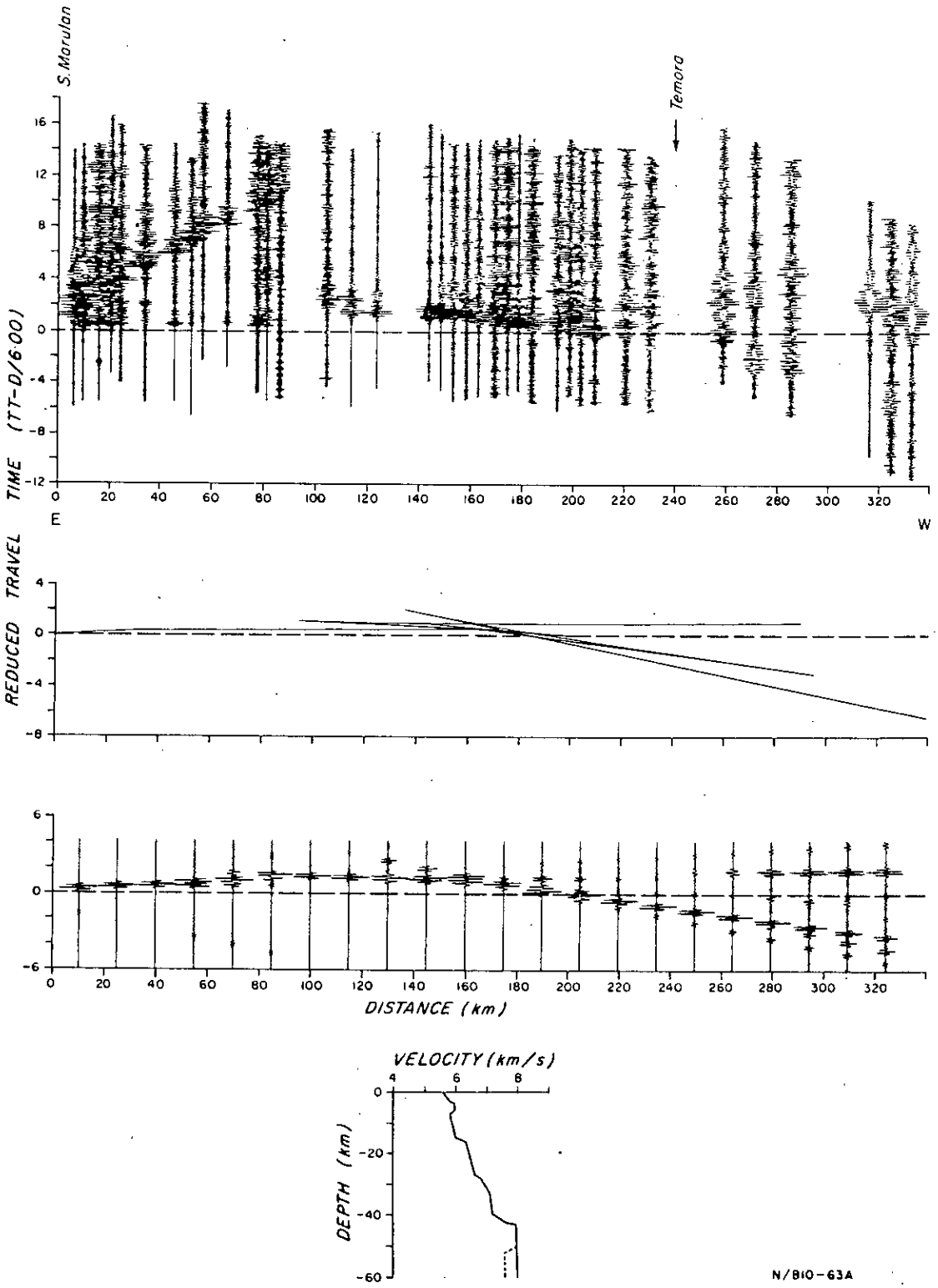

Fig. 6. Seismic record section and preferred model of travel-times and signal amplitudes along the traverse westward from Marulan. The low velocity section in the mantle model is for paths from the Singleton shotpoint.

indicates that there must be mid-crustal structures to sustain the return of seismic energy to the surface.

The interpretation of the record section reconciles both the travel-time and phase amplitude data. Velocity/depth models were first derived using seismic ray-tracing models to satisfy the travel-time information, and then tested against synthetic seisograms generated by the reflectivity method (Fuchs, 1968). The models are applicable along the cone of emergence of the rays from the shots, and the upper and middle crustal structures near the shot source dominate the velocity/depth model near the surface. Some models that satisfy the travel-time criteria have been discarded, because they do not satisfy amplitude criteria.

The preferred velocity/depth model for the N-to-S record section (Fig. 4) incorporates the values estimated earlier in this paper for the basin sediment and basement velocity structure. Below the basin sediment/basement contact, the velocity increases from 5.75 km/s to 5.9 km/s at 6.5 km depth, below which there are two prominent features in the upper crust. The first is an increase in velocity from 5.9 to 6.35 km/s in the depth range 6.5 to 8.0 km. The second is a higher-velocity zone in the depth range 16 to 25 km, where the maximum velocity is 7.0 km/s before decreasing to 6.7 km/s in the middle crust (depth 25 km). In the lower crust the velocity increases to about 7.7 km/s at 42 km, and an upper mantle velocity of 8.03 km/s is reached at 43.5 km depth. The travel-time curves and synthetic seismograms for this preferred model are shown in Figure 4.

The S-to-N record section across the Sydney Basin is shown in Figure 5. Recording were made only out to distances of 230 km; consequently the interpretation of the upper mantle velocity and structure is less well founded than for the reverse traverse. The poor recordings beyond 230 km may be a function of the shot-source parameters, but could also result from the complexity of structure beneath the Sydney Basin. Cerveny (1979) has emphasised the importance of curvature on refractor interfaces in determining the amount of seismic energy returned to the surface, and it is likely that curvature affects recordings in south-eastern Australia.

The interpretation methods used were the same as those for the N-to-S traverse. The preferred velocity/depth model is shown in Figure 5. Surface velocities of 5.8 km/s increase to 6.1 km/s at 7 km depth; the velocity increases further to 6.5 km/s at 15 km depth, below which a gradient to a velocity of 7.0 km/s at 34.5 km is interpreted. An upper mantle velocity of 8.12 km/s is reached at 4.15 km depth. The travel-time curves and synthetic seismograms for this model are shown in Figure 5.

VELOCITY/DEPTH MODELS ACROSS THE LACHLAN FOLD BELT

Data from the shot source at South Marulan limestone quarry recorded at stations towards the W are shown in Figure 6. Some of the data were recorded during 1976 and reported by Finlayson et al. (1980). Additional data beyond 250 km were recorded at the western end of the traverse during 1978, and an improved interpretation can now be made. The same interpretation methods were used along this traverse as were used for the Sydney Basin traverses.

The preferred velocity/depth model for the traverse is shown in Figure 6. A general velocity increase from 5.6 km/s at the surface to 6.0 km/s at 14.5 km depth is evident, with the inclusion of a higher-velocity section (about 5.95 km/s) in the depth range 2.5 to 7.0 km. At greater depth the velocity increases from 6.3 km/ at 16 km, to 7.2 km/s at a depth of 40 km, and then increases to an upper mantle velocity of 7.95 km/s at 43 km depth. A higher velocity gradient is in evidence at a depth of 26.5–28 km; this is required to explain high-amplitude events with an apparent velocity of about 6.6–6.8 km/s at distances beyond 140 km from the shot-point.

Finlayson et al. (1980) drew attention to strong-amplitude first arrivals recorded at distances greater than 320 km along the line W of Marulan from shot sources near Singleton. Their apparent velocity was taken as 7.78 km/. A record section for these observations has been assembled in Figure 7 and interpreted, neglecting the azimuth variation to the different stations. There is possibly more than one event in the first 2–3 seconds of the wave train, and this is interpreted as indicating structure below the transition to upper mantle velocities. The velocity/depth model dotted in Figure 6 indicates one possible structure that could account for the observed amplitudes, viz. a velocity decrease below the Moho from 7.85 km/s in the depth range 50 to 64 km.

Cerveny (1979) has drawn attention to the influence of lateral inhomogeneities on the amplitudes of upper mantle arrivals. The prominent arrivals in Figure 7 are all at distances greater than 320 km, at which distance the seismic amplitudes could be modified by structure at and beyond the western boundary of the Sydney Basin. However, the apparent velocities of the prominent arrivals, and the distance range in which they are recorded, indicate that the structures causing them are probably below the Moho transition, and the velocity/depth structure in Figure 6 is the preferred interpretation. This upper mantle

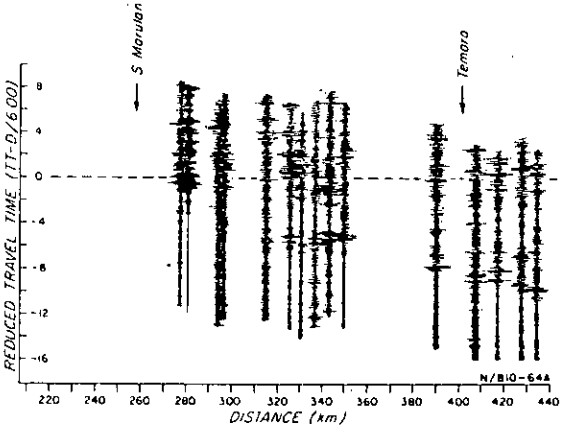

Fig. 7. Seismic record section of shots fired near Singleton, recorded along the traverse westward from Marulan.

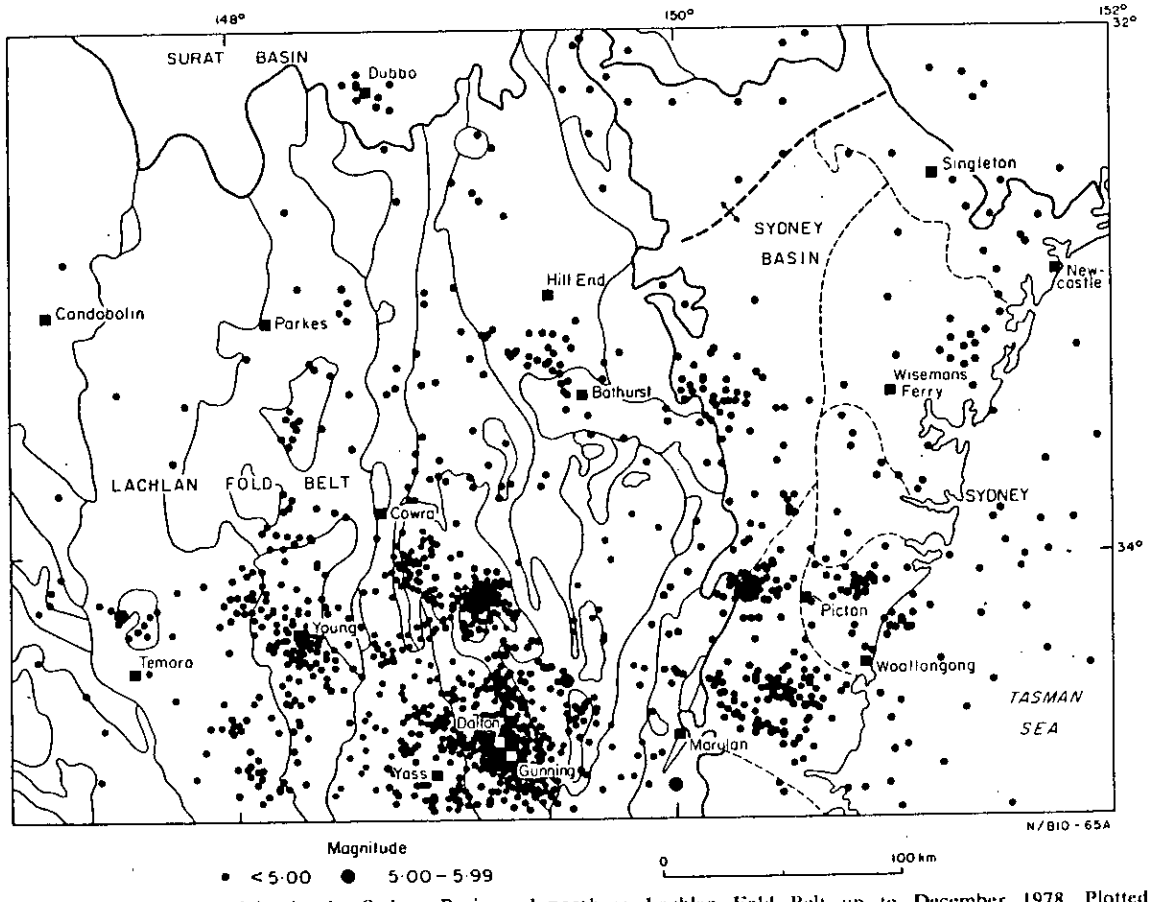

Fig. 8. Earthquake activity in the Sydney Basin and northern Lachlan Fold Belt up to December 1978. Plotted earthquakes have all been recorded by three or more recording stations.

structure differs from the others interpreted for this area, and we believe it is evidence for lateral heterogeneity in the upper mantle. Fuchs (1979) has summarised the evidence for such structure in the subcrustal lithosphere from other continents, and concluded that such lateral heterogeneity is not confined to the crust above.

CRUSTAL DYNAMICS

The Sydney Basin and the adjacent region of the Lachlan Fold Belt are still being deformed. The seismicity of the area has been described by a number of authors (Cleary, 1967; Doyle et al., 1968; Mills & Fitch, 1977; Everingham & Smith, 1979). Figure 8 gives an indication of the principal centres of activity. All earthquakes are within the crust, and 85% are in the upper 20 km (Fig. 9).

Cleary (1967) associated the seismicity in the Dalton-Gunning area with the margins of granitoid batholiths, and indicated that movement is probably taking place along old high-angle faults as a result of nearly horizontal compressive forces. Doyle et al. (1968) drew attention to the activity along the western edge of the Sydney Basin, and along the western edge of the Cumberland Sub-Basin in the central part of the Sydney Basin. They associated the

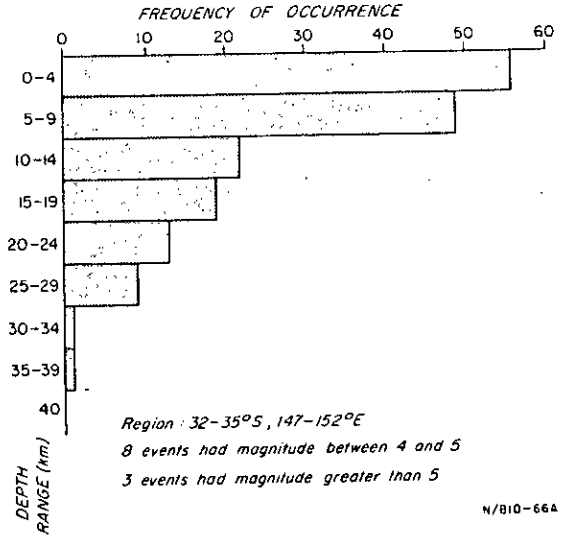

Fig. 9. Depth distribution of earthquakes in the Sydney Basin and northern Lachlan Fold Belt. Only those earthquakes recorded by five or more stations have been used.

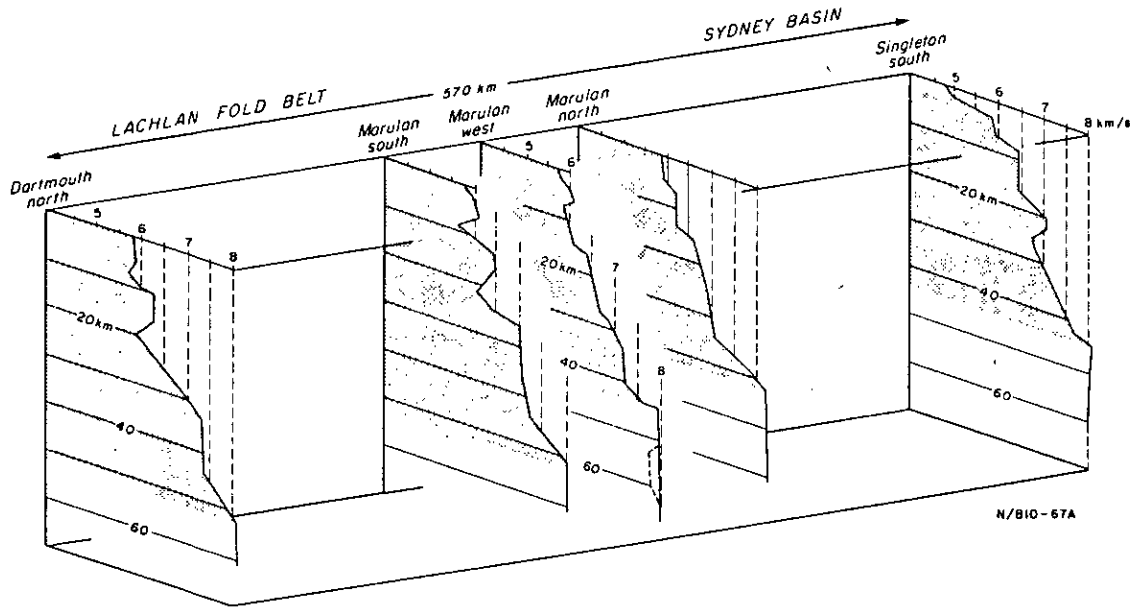

Fig. 10. Velocity/depth profiles along the Lachlan Fold Belt and Sydney Basin. Profiles from Marulan S and Dartmouth N are taken from Finlayson et al. (1980).

activity with long established fault systems and with possible Basin subsidence.

Mills & Fitch (1977) investigated the Picton earthquake (Fig. 8) of 9 March 1973 (m_b = 5.5, h ~ 20 km) in considerable detail, and concluded that the focal mechanism was consistent with thrust faulting due to E-W compression. The aftershock sequence indicated a steeply dipping fault in the depth range 8 to 24 km, with a lateral extent of about 8 km. The minimum stress drop was 1 bar and the minimum slip was estimated as 2 cm.

Denham et al. (1979) have summarised the results of *in situ* stress measurements in the Lachlan Fold Belt, and indicate that different directions of principal stress are measured in different areas. Denham (1980) has also summarised the evidence for compressive stress from earthquake data. A simple plate-tectonic model applying to a rigid lithosphere does not fit the observations. The maximum stress axis in the W of the Belt is E-W, and near the E coast it is predominantly N-S. Denham (1980) concluded that the crust under both the Lachlan Fold Belt and the Sydney Basin is reacting to compressive stresses. The velocity/depth profiles across the Basin and Fold Belt (Fig. 10) indicate no great difference in depth to the Moho transition across the boundary between the two geological provinces, consistent with the concept that Fold Belt rocks underlie the Basin sediments. It therefore follows that, in the absence of any evidence of present-day shear or tensional tectonic regimes, comprehensive stresses should be transmitted throughout the region.

Vertical movements are also much in evidence in the region. Wellman (1979) has indicated that uplift of the SE Australian highlands has probably been continuous for the last 90 m.y., and may be connected with rifting of the continent and the opening of the Tasman Sea 80–60 m.y. ago. In the northern Lachlan Fold Belt the uplift has been about 0.6 km. Wellman (pers. comm.) has also indicated that, in the same region, significant systematic differences are detected between horizontal geodetic survey measurements made during the last century and repeat measurements made in recent years.

Figure 10 also shows the velocity/depth profiles from further S in the Lachlan Fold Belt (Finlayson et al. 1979, 1980). The thicker crust (up to 52 km) coincides with the highest mountains in Australia. It should be noted that, although there is earthquake activity in the area of thick crust, the major activity is to the N, in the Dalton-Gunning-Sydney Basin region, where crustal thicknesses of 41–44 km are measured.

Therefore at least the upper 20 km of crust in the survey area is actively responding to tectonic processes at the present time. The widespread nature of the earthquake activity indicates that these processes must involve the lower crust and upper mantle as well. It seems unlikely that any of the early Palaeozoic crust has remained undeformed. The current stress patterns suggest that such deformation will be non-uniform throughout the region.

DISCUSSION

The velocity/depth models derived from the Sydney Basin and the Lachlan Fold Belt are illlustrated in Figure 10. All models are characterised by velocity gradients; some have high-velocity features within the general velocity increases, and there is a velocity gradient in the lower crust leading to upper mantle velocities at depths of 41–44 m, which is up

to 10 km less than the Moho depths farther S under the Fold Belt (Finlayson et al., 1980).

Various models for the evolution of eastern Australia have been reviewed by Packham & Leitch (1974). Many incorporate the concepts of plate tectonics. Some models include the idea of dense simatic crust having a high average crustal velocity (about 7.0 km/s) at depths of less than 10 km. No such high velocities were measured in the upper crust in southeastern Australia and consequently there is no evidence in the seismic data for remnants of inter-arc or marginal basins. The seismic evidence is consistent with the crust under the Sydney Basin being broadly similar to that under the Lachlan Fold Belt, and consistent with the Basin being underlain by Fold Belt rocks.

As mentioned earlier, the difference in the depth to the Moho transition across the boundary between the central Sydney Basin and the Lachlan Fold Belt is small. This agrees with the gravity interpretation of Wellman (1976), who investigated the relation between free-air anomalies and elevation averaged over a 1° x 1° grid, assuming that the crust is in isostatic equilibrium. The simplifying assumption in the gravity model of a sharp density contrast at the Moho results in a depth value to the upper mantle that is on average about 5 km thinner than that obtained from the seismic work.

Green (1977) has summarised the features of sedimentary basin development and indicated that features in the sedimentary sequence are a good indication of the tectonic activity in the underlying crust. Therefore, the geological record of the Sydney Basin summarised by Branagan et al. (1979) is an indication of the nature of the continental margin since the middle to late Palaeozoic. Green (1977) has shown that sedimentary basins are formed in the rifts, interior basins, and shelves of continental structures, and that, although certain guiding principles govern their development, the resulting basins may differ considerably from one region to another. The present seismic work complements the geological evidence, and indicates that the Syndy Basin formed on the margin of the Lachlan Fold Belt, which was of continental-type structure at the time of basin formation.

Bott (1976) and McKenzie (1978) have also studied models for the formation of sedimentary basins within continents, and both incorporate a mechanism of lithospheric thinning due to deeper asthenospheric processes. Bott considered the crust as consisting of a brittle upper layer overlying a ductile lower layer, within which lateral flow is possible. The earthquake activity indicative of brittle fracture in the northern Lachlan Fold Belt-Sydney Basin region is negligible at depths greater than 30 km, 85% of seismicity being in the upper 20 km. Bott's lower crustal ductile zone corresponds with the zone of crustal velocity generally increasing from about 6.5 km/s, in the velocity/depth models for southeastern Australia (Fig. 10).

The present seismic data and those from previous surveys in the region (Finlayson et al., 1979; 1980) are in accord with the findings of Smithson et al. (1977) that the continental crust is heterogeneous, both vertically and laterally. Smithson et al. (1977) showed that there is probably a crude layering related to metamorphic grade and composition: intermediate igneous composition at the surface, felsic migmatite in the middle crust, and more mafic rocks in the lower crust. However, because of granitic and mafic intrusions, any simple layering may be grossly distorted and velocity reversals are likely.

Mueller (1977) showed that the seismic evidence in Europe is in accord with the idea of metamorphic 'fronts' within the continental crust along the lines of the finding of Smithson et al. (1977). He interpreted the zones of lower velocity as zones of possible weakness, thus supporting the idea of 'flake' tectonics in which crustal material can be sheared at three levels; the first at the top of metamorphic basement, the second near the lower boundary of upper crustal low-velocity zones, and the third deep in the lower crust. He interpreted the low-velocity zones in the upper crust as being caused by quasi-continuous laccolithic zones consisting of numerous intrusions.

The crustal velocity/depth models in southeastern Australia show their most obvious differences in the upper 20 km, which is the depth range within which the extensive granitic magmas of the region have been formed (Clemens & Wall, 1979; Crook, 1980a). Together with the current earthquake activity in this depth range and stress and strain data, the evidence support the possibility of 'flake' tectonics, and suggests that the upper crust, although its deformation is driven by processes in the lower crust and lithosphere, may be mechanically decoupled from the lower crust.

The origin of the lower crust is still subject to debate. Gass & Wright (1980) have briefly outlined some current ideas on the nature of the continental crust and pointed out that investigators are divided into the 'accretionists' and the 'reworkers'. In southeastern Australia, Crook (1980*a*, *b*) represents the 'accretionist' case for an early Palaeozoic region, 1300 km long (including the Lord Howe Rise) by 600 km wide, of fore-arc development on the eastern margin of the Precambrian continent, based on surface geological evidence.

Finlayson et al. (1979, 1980) have indicated that the depth to the Moho transition in southeastern Australia is greater than that in island-arc regions in Melanesia. Even in Japan, which is considered to be a typical island arc, the crustal structure indicates that some areas of southwestern Honshu contain fragments of early continental crust that have drifted to their present position (Mashizume & Matsui, 1979; Mashizume, Ito & Yoshii, in prep.).

Wyborn & Chappell (1979) and Fagan (1979) have shown that the source-rock geochemistry for the S-type granites in SE Australia is imcompatible with the geochemistry of Ordovician or younger sediments, and I. S. Williams (pers. comm., 1980) has identified Precambrian zircon in some of the granitic rocks. Such data support the case proposed by the 'reworkers' for alteration or development of pre-existing continental margin or quasi-continental structures. Such quasi-continental structures exist at

present on the Lord Howe Rise (2000 x 350 km), and in the western Pacific on the Ontong Java Plateau (1600 x 800 km) where a crustal thickness of 35–40 km has been interpreted by Furumoto et al. (1973).

As Gass & Wright (1980) have re-emphasised, the crust and lithosphere cannot be treated separately when discussing crustal evolution, and the fragmentation of the Precambrian continental or subcontinental margin of eastern Australia, before subduction activity of the type described by Crook (1980*a*, *b*), cannot yet be discounted.

ACKNOWLEDGMENTS

The authors acknowledge the contributions of C. D. N. Collins, J. Williams, and D. Pownall towards the 1978 field work. The assistance of Blue Circle Southern Cement Co. Pty. Ltd, Costain (Aust.) Pty Ltd, Hebden Mining Co., Clutha Developments Pty Ltd, and Westham Dredging Co. Pty Ltd in providing assistance and shot-firing details is gratefully acknowledged. The seismicity data and map were provided by staff of the Observatories Group, BMR. This paper is published with the permission of the Director, BMR.

REFERENCES

Bolt, B. A., 1962: A seismic experiment using quarry blasts near Sydney. *Aust. J. Phys., 15*, 293-300.

Bott, M. H. P., 1976: Formation of sedimentary basins of graben type by extension of the continental crust. *Tectonophysics, 36*, 77-86.

Branagan, D., Herbert, C. & Langford-Smith, T., 1979: *An outline of the geology and geomorphology of the Sydney Basin*. Science Press, Sydney.

Cerveny, V., 1979: Ray theoretical seismograms for laterally inhomogeneous structures. *J. Geophys., 46*, 335-42.

Cleary, J. R., 1967: The seismicity of the Gunning and surrounding areas, 1958-1961. *J. geol. Soc. Aust., 14*, 23-9.

Clemens, J. D. & Wall, V. J., 1979: Crystallisation and origin of some S-type granitic magmas; *in* Denham, D. (ed.) Crust and upper mantle of southeast Australia. *Rec. Bur. Miner. Resour. Geol. Geophys., Aust., 1979/2*, 10-12.

Crook, K. A. W., 1980*a*. Fore-arc evolution and continental growth: a general model. *J. Struct. Geol., 2*, in press.

Crook, K. A. W., 1980*b*: Fore-arc evolution in the Tasman Geosyncline: the origin of the southeast Australian continental crust. *J. geol. Soc. Aust., 28*, 215-32.

Denham, D., 1980: The 1961 Robertson earthquake —more evidence for compressive stress in southeast Australia. *BMR J. Aust. Geol. Geophys., 5*, 153-6.

Denham, D., Alexander, L. G. & Worotnicki, G., 1979: Stresses in the Australian crust; evidence from earthquakes and in situ stress measurements. *BMR J. Aust. Geol. Geophys., 4*, 289-95.

Doyle, H. A., Underwood, R. & Polak, E. J., 1966: Seismic velocities from explosions off the central coast of New South Wales. *J. geol. Soc. Aust., 13*, 355-72.

Doyle, H. A., Cleary, J. R. & Gray, N. M., 1968: The seismicity of the Sydney Basin. *J. geol. Soc. Aust., 15*, 175-81.

Everingham, I. B. & Smith, R. S., 1979: Implications of fault-plane solutions for Australian earthquakes on 4 July 1977, 6 May 1978, and 25 November 1978. *BMR J. Aust. Geol. Geophys., 4*, 297-301.

Fagan, R. K., 1979: S-type granite genesis and emplacement in N-E Victoria and its implications; *in* Denham, D. (ed.) Crust and upper mantle of southeast Australia. *Rec. Bur. Miner. Resour. Geol. Geophys. Aust., 1979/2*, 29-30.

Finlayson, D. M., 1979: 1978 BMR seismic crustal investigations in southeast Australia: operational report for the DART 78 and MANESI surveys. *Rec. Bur. Miner. Resour. Geol. Geophys. Aust., 1979/92*.

Finlayson, D. M., Prodehl, C. & Collins, C. D. N., 1979: Explosion seismic profiles, and implications for crustal evolution, in southeastern Australia. *BMR J. Aust. Geol. Geophys., 4*, 243-52.

Finlayson, D. M., Collins, C. D. N. & Denham, D., 1980: Crustal structure under the Lachlan Fold Belt, southeastern Australia. *Phys. Earth planet. Int.*, 21, 321-42.

Fuchs, K., 1968: Das Reflexions—und Transmissionsvermögen eines geschichteten Mediums mit beliebiger Tiefen-Verteilung der elastischen Moduln und der Dichte für schrägen Einfall ebener wellen. *J. Geophys., 34*, 389-413.

Fuchs, K., 1979: Structure, physical properties and lateral heterogeneities of the subcrustal lithosphere from long-range deep seismic sounding observations on continents. *Tectonophysics, 56*, 1-15.

Furumoto, A. S., Wiebenga, W. A., Webb, J. P. & Sutton, G. H., 1973: Crustal structure of the Hawaiian Archipelago, northern Melansia, and the central Pacific Basin by seismic refraction methods. *Tectonophysics, 20*, 153-64.

Gass, I. G. & Wright, J. B., 1980: Continents old and new. *Nature, 284*, 217-8.

Green, A. R., 1977: The evolution of the earth's crust and sedimentary basin development; *in* Heacock, J. G. (ed.) The Earth's crust. *Am. Geophys. Un., Geophys. Mono. 20*, 1-17.

Mashizume, M. & Matsui, Y., 1979: Crustal structure of southwestern Honshu, Japan, derived from explosion seismic waves. *Geophys. J. R. astro. Soc., 58*, 181-99.

Mayne, E. J., Nicholas, E., Bigg-Wither, A. L., Rasidi, J. S. & Raine, M. J., 1974: Geology of the Sydney Basin, —a review. *Bull. Bur. Miner. Resour. Geol. Geophys. Aust., 149*.

McKenzie, D., 1978: Some remarks on the development of sedimentary basins. *Earth planet. Sci. Lett., 40*, 25-32.

Mills, J. M, & Fitch, T. J., 1977: Thrust faulting and crust—upper mantle structure in east Australia. *Geophys. J. R. astro. Soc., 48*, 351-84.

Mueller, S., 1977: A new model of the continental crust; *in* Heacock, J. G. (ed.) The Earth's crust *Am. Geophys Un, Geophys. Mono. 20*, 289-317.

Packham, G. H. & Leitch, E. C., 1974: The role of plate tectonic theory in the interpretation of the Tasman Orogenic Zone; *in* Denmead, A. K., Tweedale, A. W. & Wilson, A. F. (eds) *The Tasman Geosyncline*, Queensland Div. Geol. Soc. Aust., Brisbane.

PASSMORE, V. L., 1979: Sydney Basin explanatory notes and stratigraphic columns. *Rec. Bur. Miner. Resour. Geol. Geophys. Aust., 1979/58.*

ROBERTSON, C. S., 1958: Final report on a seismic reflection survey in the Sydney Basin. *Rec. Bur. Miner. Resour. Geol. Geophys. Aust., 1958/48.*

SMITHSON, S. B., SHINE, P. N. & BROWN, S. K. 1977: Seismic velocity, reflections, and structure of the crystalline crust; *in* Heacock, J. G. (ed.) The Earth's crust. *Am. Geophys. Un., Geophys. mono 20,* 254-70.

WELLMAN, P., 1976: Regional variation of gravity and isostatic equilibrium of the Australian crust. *BMR J. Aust. Geol. Geophys., 1,* 297-302.

WELLMAN, P., 1979: On the Cainozoic uplift of the southern Australian highland. *J. geol. Soc. Aust., 26,* 1-10.

WYBORN, L. A. I. & CHAPPELL, B. W., 1979: Geochemical evidence for the existence of a pre-Ordovician sedimentary layer in south-eastern Australia; *in* Denham, D. (ed.) Crust and Upper Mantle of Southeast Australia. *Rec. Bur. Miner. Resour. Geol. Geophys. Aust., 1979/2,* 104.

Reprinted from
BMR Journal of Australian Geology & Geophysics, 6, 1981, 245-252

Reconnaissance of upper crustal seismic velocities in the Tennant Creek Block, Northern Territory

D. M. Finlayson

Upper crustal seismic investigations of the Tennant Creek Block indicate that the Warramunga Group rocks have P-wave velocities of 5.22-5.55 km/s (average 5.42 km/s) and S-wave velocities of 3.26-3.41 km/s (average 3.34 km/s). The P-wave velocity beneath these surface rocks is 6.06 km/s. A simple layered model for the thickness of the Warramunga Group gives values of about 2.6 km near Nobles Nob mine, thinning to about 1.2 km near Warrego mine. South of the Warramunga Group rocks, granitic rocks have an estimated upper value for the P-wave velocity of 5.69 km/s. Underneath, the P-wave velocity of 6.06 km/s is the same as that further north, under the Warramunga Group rocks, but the depth to this velocity is as much as 0.7 km less. The corresponding S-wave velocity is 3.53-3.59 km/s. An intracrustal S-wave velocity of 3.86 km/s is observed from the Warrego shot.

The nature of the change between the surface and 'basement' rocks is likely to be complex, resulting in a velocity transition zone rather than a simple boundary. The estimated depths to 'basement' are, therefore, minimum estimates. Because of the expected increase in the seismic velocity of the rocks when subjected to overburden pressures equivalent to depths of 2-3 km, there is little evidence from the present work that the 'basement' is compositionally or lithologically different from the surface rocks. At recording distances beyond 50 km there is evidence in the record sections that both P and S-wave energy is being returned from deeper intracrustal refractors/reflectors.

Introduction

During July-August 1979, reconnaissance seismic refraction work was undertaken in areas of Proterozoic outcrop near Tennant Creek, Northern Territory, to investigate near-surface structures. The work was part of a project to investigate the use of seismic methods to determine geological structures in areas where younger cover rocks prevent direct examination of rocks of potential economic importance.

Geology

The Tennant Creek area lies within the North Australian Craton and is entirely underlain by Precambrian basement (Plumb, 1979). The craton has been relatively stable for over 1700 m.y., but much of the Precambrian geology is obscured by Palaeozoic cover. Areas where basement crops out are referred to as 'inliers' because they are considered to be merely the exposed parts of much larger features. The seismic survey was conducted entirely within the Tennant Creek Block which is the central part of the Tennant Creek Inlier.

In the northern part of the North Australian Craton, basement rocks of the Archaean Rum Jungle and Nanambu Complexes (older than 2500 m.y.) are exposed, but the full extent of Archaean basement is not known. Plumb (1979) speculates that it could underlie the whole craton.

In the Tennant Creek Inlier, pelitic gneisses were metamorphosed at 1920 ± 10 m.y. (Black, 1977) and these possibly form basement to the Warramunga Group sedimentary and volcanic rocks, considered to be older than 1800 m.y. (Early Proterozoic). The granites intruding the Warramunga Group have ages of about 1500-1700 m.y. Tucker & others (1979) indicated that the Warramunga Group and associated plutonic rocks underlie much of the Georgina Basin east of Tennant Creek. Gravity trends suggest that inliers within a radius of 400 km of Tennant Creek may belong to a single orogenic belt. The fundamental basement fracture patterns of the North Australian Craton are considered to have been established no later than the end of the Early Proterozoic.

The principal seismic traverse described in this paper (Fig. 1) lies wholly on rocks of the Warramunga Group, a geosynclinal sequence of Proterozoic interbedded sedimentary and volcanic lenses, considered to be no more than 3 km thick (Dodson & Gardener, 1978), although a composite section of all individual units gives a total thickness of 6 km.

The sedimentary sequence of the Warramunga Group consists of siltstone, greywacke, shale, sandstone, and conglomerate. There are two main volcanic sequences: the Warrego Volcanics crop out near Warrego Mine (Fig. 1) and consist of rhyolite, ignimbrite, ashstone, and tuff, but also include siltstone, greywacke, and shale; the Gecko Volcanics, which crop out to the east of recording station number 14 (Fig. 1), consist of tuff, quartz and quartz-feldspar porphyry, and greywacke.

Three phases of folding are recognised in the Warramunga Group, and faults are common throughout the region. The major faults trend northwest. However, several northerly trending strike-slip and oblique-slip faults are also recognised.

Granitic rocks intrude the Warramunga Group (Fig. 1). Outcrops range from isolated tors to low weathered hills. However, most of the plutons are covered by superficial deposits. The Warramunga Seismic Array (WRA) (King & others, 1973) is located on granitic rocks, 20-25 km south of Nobles Nob mine (Fig. 1). No tectonic activity has been observed in Cainozoic cover rocks and no local seismicity has been recorded by WRA. Regional compressive horizontal stresses of 11-25 MPa have been measured at Warrego Mine (Worotnicki & Denham, 1976) and the direction of principal stress is approximately east-west.

Seismic field investigations

The locations of seismic stations that recorded data used in this interpretation are shown in Figure 1. The principal recording line was between the Warrego and Nobles Nob mines, and a routine mining blast at each

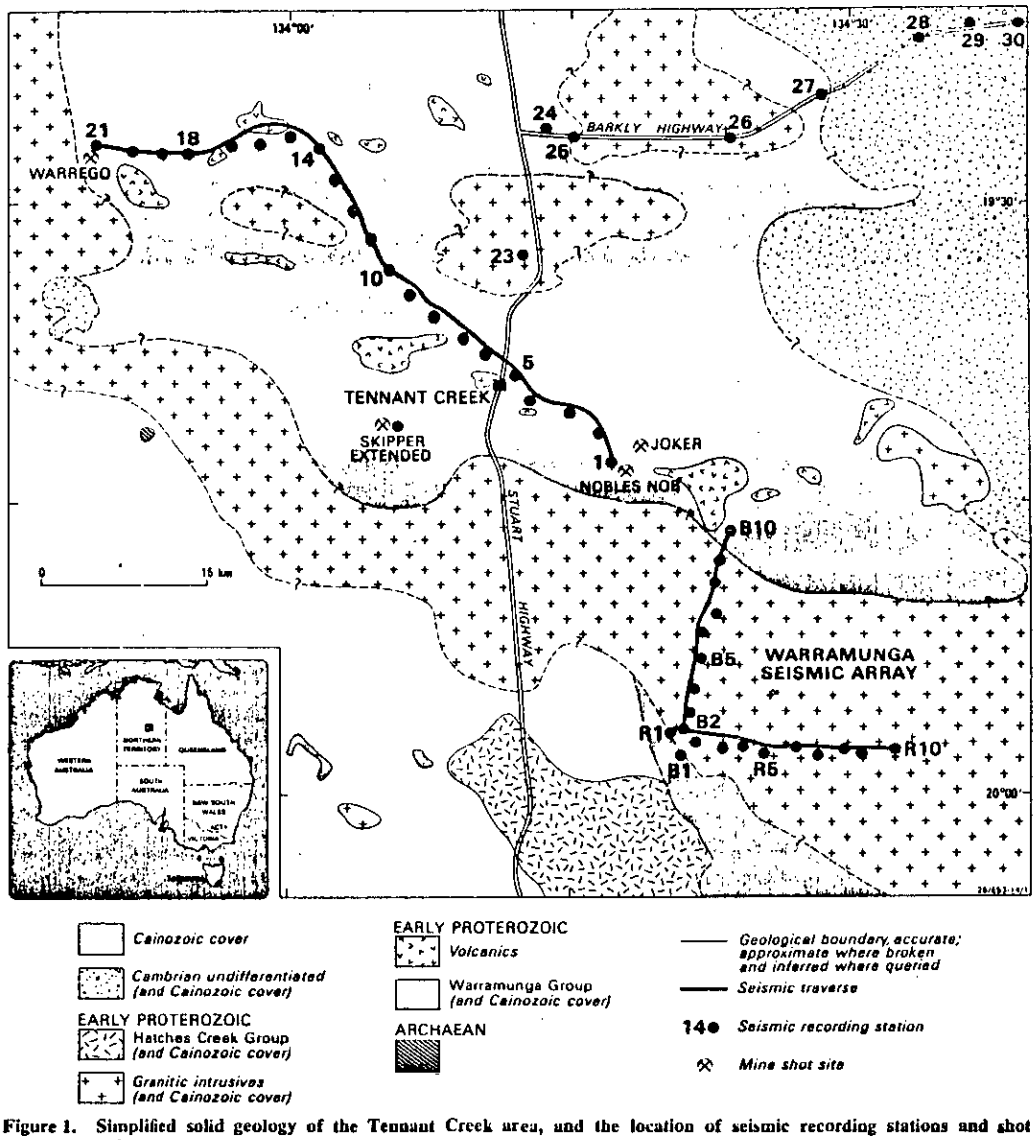

Figure 1. Simplified solid geology of the Tennant Creek area, and the location of seismic recording stations and shot points.

Location	*Date*	*Size* *l*	*Latitude (S)* *deg.* *min.*	*Longitude (E)* *deg.* *min.*	*Depth* *m*	*Shot time (U.T.)* *h.* *min.* *s.*
Warrego	17/7/79	0.7	19 26.68	133 49.20	643	06 42 38.81
Nobles Nob	19/7/79	4.5	19 43.00	134 17.50	20	02 29 42.65
Skipper	9/8/79	5.0	19 40.66	134 05.50	40	06 45 00.93

Table 1. Shot information.

mine was used as the seismic source. Another shot was fired in an abandoned gold mine (Skipper Extended), and recorded at a number of stations along a line approximately at right angles to the principal line. Shot parameters are contained in Table 1.

Recordings were made on portable seismic tape-recording systems (Finlayson & Collins, 1980). Data were subsequently digitised and displayed as seismic record sections (Figs. 2, 3, 4). The shots were also recorded at WRA, and these record sections are shown in Figures 3, 4 and 5.

Previous interpretations

Previous investigations of seismic structures in the Tennant Creek area (Underwood & others, 1968) were connected principally with determining near-surface travel-time corrections for WRA. Underwood (1967) interpreted recordings of a shot fired at the Joker Mine

near Nobles Nob (Fig. 1) (Underwood & others, 1968). However, this survey was essentially a single-ended refraction experiment, in which it was not possible to determine model parameters uniquely, and a simple inclined-plane model of the refractor geometry under WRA was adopted. The model was an upper layer with P-wave velocity 5.42 km/s overlying rock with velocity 6.10 km/s. The refractor was 0.99 km deep at Joker Mine, dipping at 5.3° in the direction 205.5°, resulting in a depth of about 3.6 km near the apex of the array.

Geological factors indicate that the shape of granitic plutons is unlikely to be simple. Pitcher (1979) indicated that granite batholiths result from multiple episodes of magmatic activity rather than a single massive episode, and are emplaced along pre-existing lines of weakness, which extend deep into the crust, perhaps following volcanic activity in the same area. Magma may be emplaced in the form of cauldrons or diapirs, depending on the mechanical properties of the near-surface crustal rocks. Plutons may be from 4 km to 10 km thick, but the floor of the batholith may be indistinguishable from the country rock in terms of its physical parameters. Bott & Smithson (1967) concluded that a combination of stoping and intrusion provided the most satisfactory explanation for gravity anomalies associated with granites.

Cleary & others (1968) considered Underwood's (1967) interpretation with respect to travel-time residuals and slowness measurements at WRA using earthquakes in different azimuths. They indicated that the major features of the residuals and slowness data could be explained by a structure increasing in depth towards the southwest, probably a series of monoclinal folds with a northwest strike. At three seismometer positions near the apex of the WRA array, the travel-time residuals for teleseismic events from the southwest were anomalously early. Cleary & others (1968) suggested this was probably caused by Proterozoic rocks of the Hatches Creek and Warramunga Groups less than a kilometre to the southwest. However, they also indicated that not all features of the slowness data can be reconciled with near-surface geology alone, and deeper structures must contribute to the travel-time variations.

Recordings

The Nobles Nob records (Fig. 2) contain no strong events following the first break that can be correlated with neighbouring traces. Consequently, significant events that can be interpreted in terms of structure are restricted to the first arrival data.

The character of the recordings of the Warrego shot (Fig. 3), detonated 643 m below the ground surface, changes beyond 22 km. In the range 26-36 km from the shot, weak first arrivals are followed within 0.3 s by another event lasting about 1-1.5 s and, later, by strong S-waves.

Recordings of the Skipper Extended shot (Fig. 4), made along the Barkly Highway, are similar in character to the Nobles Nob records: apart from the initial arrivals, there are no phases that can be correlated to adjacent traces.

A striking feature of the recordings made at WRA is the pronounced S-wave events. Such events were recorded at stations sited on Warramunga Group rocks from the Warrego shot, but only poorly at sites to the north and northeast of the Nobles Nob and Skipper Extended shots. Part of the character difference of the records can be attributed to the lower frequency response of the WRA instruments.

Seismic velocities and interpretation

The correlation of seismic events used to estimate velocities is indicated in Figures 2-5, together with their apparent velocities. At distances less than 20 km from the shots, the velocities within the exposed Warramunga Group can be measured. The P-wave velocity is 5.22-5.55 km/s, with an average of 5.42 km/s. The S-wave velocities are 3.26-3.41 km/s, with an average of 3.34 km/s.

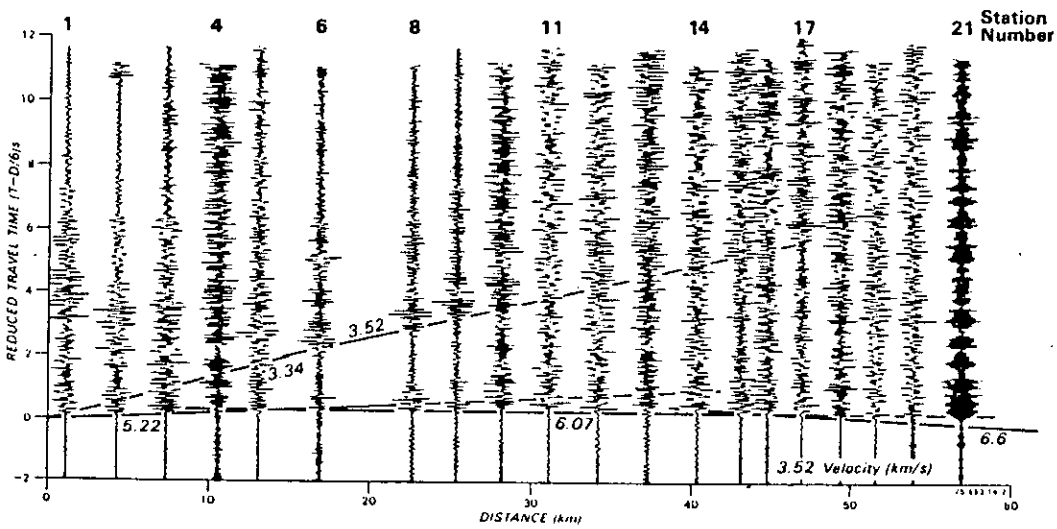

Figure 2. Seismic record section for the Nobles Nob mine shot recorded towards Warrego mine.
The records are normalised so that the maximum signal amplitude is the same on each recording, and band-pass filtered in the range 4-20 Hz.

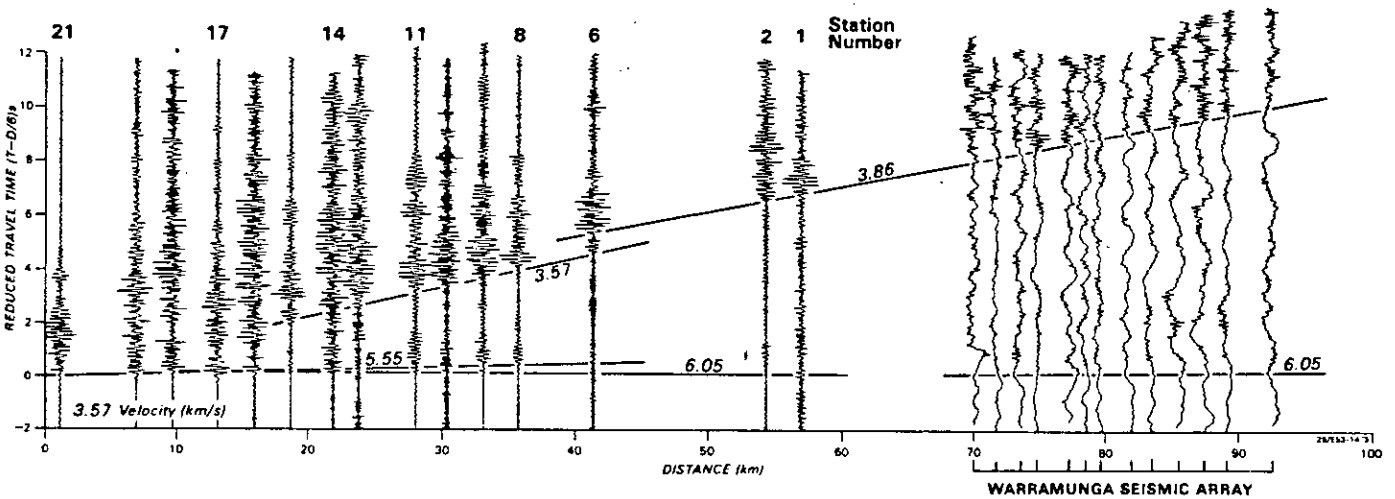

Figure 3. Seismic record section for the Warrego mine shot, recorded towards Nobles Nob mine and to the Warramunga Seismic Array. Normalising and filtering as in Figure 2; array records are unfiltered.

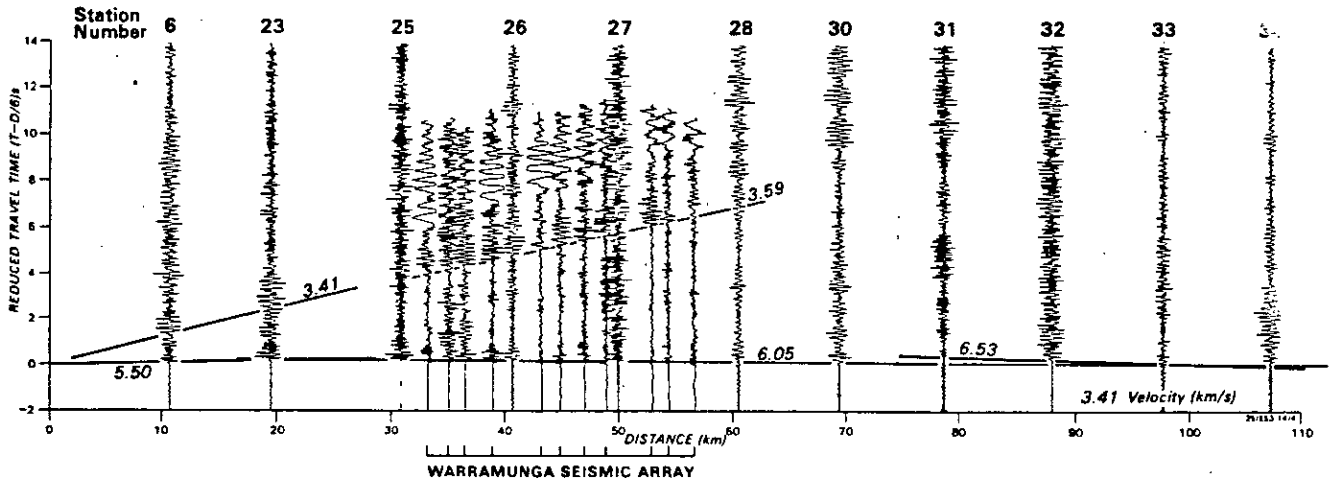

Figure 4. Seismic record section for the Skipper Extended mine shot, recorded along the Barkly Highway towards Mount Isa, and to the Warramunga Seismic Array. Normalising and filtering as in Figure 2; array records are unfiltered.

Velocities beneath the exposed Warramunga Group were estimated from the reversed seismic traverse between Nobles Nob and Warrego, and from the Skipper Extended shot recorded towards the northeast. The apparent velocities from these sources are 6.07, 6.05, and 6.05 km/s, respectively.

Using a simple refraction model in which rocks with a velocity of 6.06 km/s are overlain by Warramunga Group rocks with a velocity of 5.42 km/s, the depths to the refractor from Nobles Nob, Skipper Extended, and Warrego shots are 2.6, 1.9, and 1.2 km, respectively. The shallowing at the Warrego end of the traverse is in accord with the high apparent velocity of 6.6 km/s measured beyond 44 km from the Nobles Nob shot (Fig. 2). This high apparent velocity can also be explained by the fact that, at recording station number 14 (Fig. 1), the traverse changes direction from northwest to west, and seismic waves, instead of passing wholly under the Warramunga Group, must pass under granites exposed at the surface. The presence of structure can also be interpreted from the pronounced change in character of Warrego shot recordings beyond 22 km.

Of the recordings made at the WRA seismic array, none can be said unequivocally to represent seismic rays travelling solely within granitic rocks. At distances of less than 20 km from the Nobles Nob shot (Fig. 5), a velocity of 5.69 km/s has been estimated from those five recording sites located on granite.

The range of granite surface velocities can vary considerably. Bandu Rao Naik & others (1980) have investigated surface velocities in some southern Indian granites, and concluded that a weathered layer exists that is up to 40 m thick and has a P-wave velocity of 1.6-2.8 km/s. This overlies granite which has a velocity of 4.0-6.0 km/s (average 4.6 km/s). In SE Australia, Taylor & others (1972) determined the thickness of surface weathering in the Braidwood Granite to be 25 m (average velocity 0.85 km/s); the underlying bedrock velocity was 5.5 km/s. These results from India and SE Australia, although being greatly influenced by climatic conditions in the regions, illustrate the range of surface effects in weathered granitic terrains. The value of 5.69 km/s estimated for the granites south of Tennant Creek is taken to be the upper limit of the near-surface P-wave velocity.

Beyond 20 km from the shot source, the apparent P-wave velocity recorded at WRA from the Nobles Nob shots is 6.12 km/s, and from the Skipper Extended and Warrego shots 6.05 km/s. The arrivals from the Skipper Extended shot are clearly recorded earlier at the WRA array than at sites to the northeast (Fig. 4). Using a simple model of the granitic rocks overlying a higher velocity refractor, 5.96 km/s over 6.12 km/s, the depths to that refractor are estimated to be at 2.1, 1.2, and 1.2 km, respectively, from the Nobles Nob, Skipper Exended, and Warrego shots. These depths can be compared with the values of 2.6, 1.9, and 1.2 km, respectively, obtained from these shots for the depth to the basement velocity under the Warramunga Group derived earlier. First arrivals at WRA from the Warrego shot also arrive about 0.1 s earlier than arrivals from the Skipper Extended shot at the same recording distances along the Barkly Highway, supporting the general observation of shallower depth to the basement velocity south of the exposed Warramunga Group. It is possible that a higher velocity branch of the travel-time curve is being observed beyond 75 km from the Skipper Extended shot (Fig. 4), but good first arrivals still correlate with the 6.05 km/s travel-time branch observed at shorter distance.

The S-waves recorded at the WRA array (Figs 3-5) indicate velocities of 3.26 km/s from poor data at shot distances less than 20 km, and, at larger distances, velocities of 3.53 and 3.59 km/s are measured from the Nobles Nob and Skipper Extended shot, respectively. The average S-wave velocity in the basement rocks is taken to be 3.56 km/s. The 3.86 km/s events at distances beyond 50 km from the Warrego shot (Fig. 3) are interpreted as being from an intracrustal horizon, perhaps 9 km deep.

Comment

The nature of the basement rocks with a velocity of about 6.06 km/s is not known. The seismic record sections (Figs. 2-5) do not display any clear diagnostic

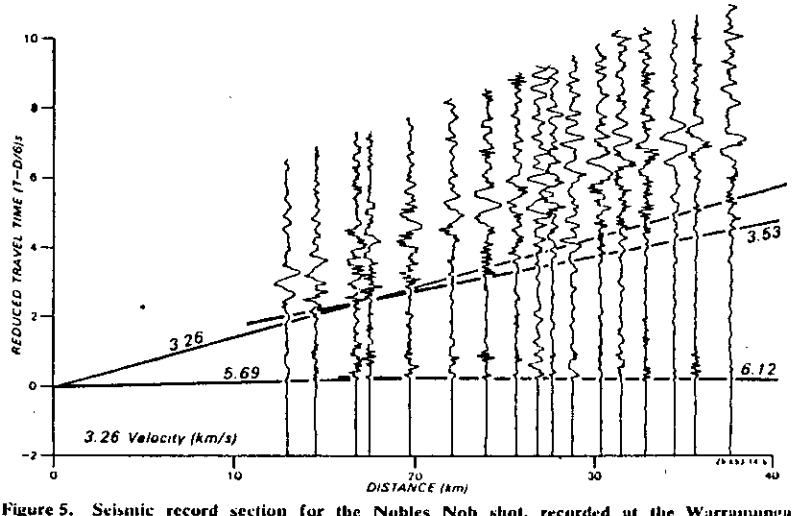

Figure 5. Seismic record section for the Nobles Nob shot, recorded at the Warramunga Seismic Array; no filtering.

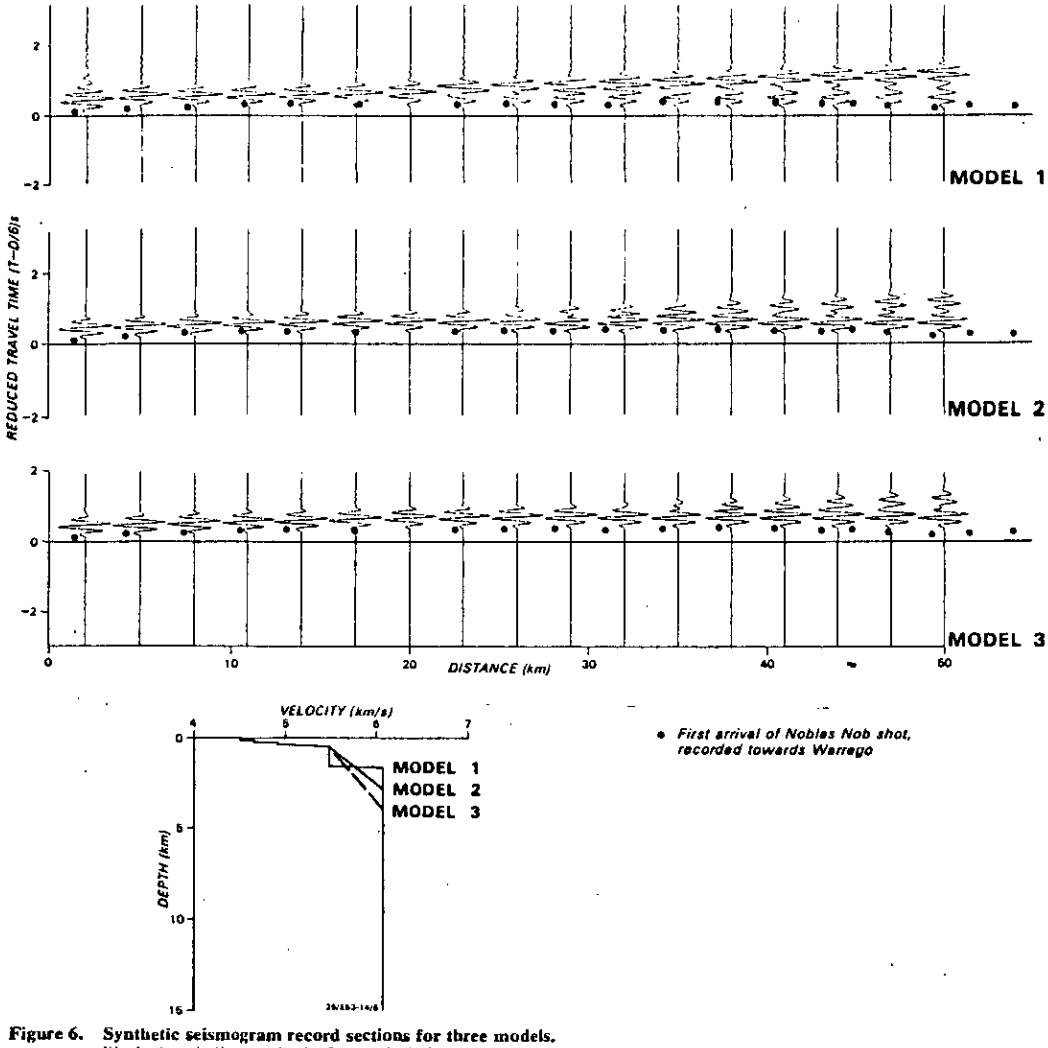

Figure 6. Synthetic seismogram record sections for three models.
Black dots indicate seismic first arrival times of the Nobles Nob mine shot recorded towards Warrego mine. Model 1 produces large-amplitude wide-angle reflections after the first arrivals at distances of 30-50 km, which are not observed in the recorded data.

reflection and refraction events characteristic of simple transitions. Figure 6 indicates the sort of subcritical and supercritical reflections to be expected from various types of velocity transition; these record sections were derived from a synthetic seismogram computer program (Fuchs, 1968). Once a velocity transition zone is introduced, the depth to the basement velocity must be greater than that arrived at using simple refraction models. Green & Steinhart (1962) and Berry (1971), among others, have demonstrated the variety of models that can satisfy first-arrival seismic data. The basement depths derived earlier are, therefore, minimum estimates, but are consistent with a shallowing of basement under the granitic rocks to the south and west of the Warramunga Group.

The interpretation of the velocity changes with depth in terms of changes in rock type must be regarded as speculative without other geological/geophysical information. There are substantial changes in the seismic velocity of rocks as overburden pressure increases, especially at pressures of up 1 kbar (within the uppermost 3 km), where pore collapse is considered to be a major factor. Bott (1971, p. 65) illustrated the change in P-wave velocity of a granite from about 5.1 km/s to 6.1 km/s in laboratory experiments at pressures up to 1 kbar.

The transition to the basement velocity illustrated in Figure 6 is consistent with expected changes in velocity with overburden pressure. Thus, although a 'basement' rock type is assumed in the foregoing interpretation, it is by no means necessary in order to satisfy the seismic data. The granite and Warramunga Group (surface rocks) may well both have a velocity of 6.06 km/s at depth. Only further, more detailed, seismic field and laboratory studies can resolve this problem.

Despite these complications on the nature of the transition to basement velocities, the seismic method is still useful in determining the structure wihin areas of complex geology. Smithson & others (1977) highlighted the use of reflection methods to determine structure within the upper crust in areas of Precambrian outcrop. However, other, less expensive, geophysical methods may also yield useful information, depending on the detail required.

Acknowledgements

The author wishes to thank Clive Collins, John Williams, David Pownall, and Howard Hughes, who were also in the BMR field recording party, and Heather McCracken, who assisted with the preparation of seismic record sections. Staff from the Australian National University under the leadership of Doug Christie and Ken Muirhead provided field recordings from temporary stations and the Warramunga Seismic Array. The assistance of staff at the Australian Development Ltd mine at Nobles Nob (manager, Graham Reveleigh) and at the Peko-Wallsend Operations Ltd Warrego Mine (production manager, Roland Lee) is gratefully acknowledged, as is .that from the Northern Territory Geological Survey (resident geologist, John Howard) and Mines Department (explosives inspector, Peter Sciberras), and the staff of the Tennant Creek Battery. I am grateful to D. Denham and R. Underwood for comments on the manuscript.

References

Bandu Rao Naik, S., Nand Kumar, G., & Vijaya Raghava, M. S., 1980—The correlation refraction method as applied to weathered zone studies in a granite terrain. *Geophysical Prospecting*, 28, 18-29.

Berry, M. J., 1971—Depth uncertainties from seismic first-arrival refraction studies. *Journal of Geophysical Research*, 76, 6464-8.

Black, L. P., 1977—A Rb-Sr geochronological study in the Proterozoic Tennant Creek Block, central Australia. *BMR Journal of Australian Geology & Geophysics*, 2, 111-22.

Bott, M. H. P., & Smithson, S. B., 1967—Gravity investigations of subsurface shape and mass distributions of granite batholiths. *Bulletin of the Geological Society of America*, 78, 859-78.

Bott, M. H. P., 1971—THE INTERIOR OF THE EARTH. *Edward Arnold, London.*

Cleary, J. R., Wright, C., & Muirehead, K. J., 1968—The effects of local structure upon measurements of the travel time gradient at the Warramunga Seismic Array. *Geophysical Journal of the Royal Astronomical Society*, 16, 21-9.

Dodson, R. G., & Gardener, J. E. F., 1978—Tennant Creek, Northern Territory—1:250 000 Geological Series. *Bureau of Mineral Resources, Australia, Explanatory Notes* SE/53-14.

Finlayson, D. M., & Collins, C. D. N., 1980—A brief description of BMR portable seismic tape recording systems. *Bulletin of the Australian Society of Exploration Geophysicists*, 11, 75-7.

Fuchs, K., 1968—Das Reflexions—und Transmissions vermögen eines geschichteten Mediums mit beliebiger Tiefen—Verteilung der elastischen Modul und der Dichte für schrägen Einfall ebener Wellen. *Zeitschrift für Geophysik*, 34, 389-413.

Green, R., & Steinhart, J. S., 1962—On crustal structure deduced from seismic time-distance curves. *New Zealand Journal of Geology & Geophysics*, 5, 579-91.

King, D. W., Mereu, R. F., & Muirhead, K. J., 1973—The measurement of apparent velocity and azimuth using adaptive processing techniques on data from the Warramunga Seismic Array. *Geophysical Journal of the Royal Astronomical Society*, 35, 137-67.

Pitcher, W. S., 1979—The nature, ascent and emplacement of granitic magmas. *Journal of the Geological Society, London*, 136, 672-62.

Plumb, K. A., 1979—Structure and tectonic style of the Precambrian shields and platforms of northern Australia. *Tectonophysics*, 58, 291-325.

Smithson, S. B., Shive, P. N., & Brown, S. K., 1977—Seismic reflections from Precambrian crust. *Earth & Planetary Science Letters*, 37, 333-8.

Taylor, F. J., Moss, F. J., & Branson, J. C., 1972—Deep crustal reflection seismic test, Tidbinbilla, A. C. T., and Braidwood, N.S.W., 1967. *Bureau of Mineral Resources, Australia, Record* 1972/126 (unpublished).

Tucker, D. H., Wyatt, B. W., Druce, E. C., Mathur, S. P., & Harrison, P. L., 1979—The upper crustal geology of the Georgina Basin region. *BMR Journal of Australian Geology & Geophysics*, 4, 209-26.

Underwood, R., 1967—The seismic network and its applications. *Ph.D. Thesis, Australian National University* (unpublished).

Underwood, R., Elliston, J., & Matthews, K. E., 1968—Shooting for deep refraction experiments. *Geophysics*, 33, 135-6.

Worotnicki, G., & Denham, D., 1976—The state of stress in the upper part of the Earth's crust in Australia according to measurements in mines and tunnels and from seismic observations. *In* Investigation of stress in rock. *Institution of Engineers, Australia, National Conference Publications* 76/4, 74-82.

JOURNAL OF GEOPHYSICAL RESEARCH, VOL. 87, NO. B13, PAGES 10,569-10,578, DECEMBER 10, 1982

SEISMIC CRUSTAL STRUCTURE OF THE PROTEROZOIC NORTH AUSTRALIAN CRATON BETWEEN TENNANT CREEK AND MOUNT ISA

D. M. Finlayson

Bureau of Mineral Resources, Geology and Geophysics, Canberra City, ACT 2601, Australia

Abstract. Seismic recording along a 600-km traverse across the southern part of the North Australian craton indicates that lateral velocity variations exist in the middle/lower crust. Taken together with other data from the Craton, there is evidence for midcrustal velocities increasing from east to west and from south to north. These trends could result from a greater proportion of high-velocity granulites being emplaced at higher levels in the crust. Between Tennant Creek and Mount Isa the velocity structures near the surface are compatible with an assemblage of younger and older metamorphic rocks intruded by granites. Near-surface (0-5 km) P wave velocities on the Tennant Creek Inlier increase from 5.47 km/s at the surface to about 6.2 km/s at 6-km depth and correspond with low-grade metamorphics of the Warramunga Group interspersed with weathered granites overlying amphibolite facies rocks of older metamorphic domains. In the Mount Isa Geosyncline, velocities of 6.03-6.15 km/s correspond to the Leichhart Metamorphics interspersed with granites. In the middle crust, P wave velocities of 6.85 km/s occur at a depth of 26 km near Tennant Creek, whereas such velocities are not evident until depths of about 37 km near Mount Isa. There is therefore a trend for midcrust velocities to increase from east to west. The lower crust is characterized by velocities of 7.3-7.5 km/s, and the upper mantle velocities of 8.16-8.20 km/s are reached at depths of 51-54 km. Exposed granulite facies rocks in central Australia are low in heat-producing elements and are compatible with the low surface heat flow generally measured in Precambrian Australia. These data taken together with laboratory velocity measurements on worldwide samples reported elsewhere indicate that middle to lower crustal rocks could be an assemblage of granulite facies rocks varying from pyroxene granulite in the middle crust, through hornblende granulite, to garnet granulite in the lower crust.

Introduction

The geophysical differences under Precambrian and Phanerozoic Australia have long been recognized. Cleary [1973] summarized the early seismic information on crustal structure; Goncz and Cleary [1976] have highlighted the surface wave dispersion differences; Cleary et al. [1972] determined the teleseismic travel time differences; Lilley et al. [1981] have described the differences in electrical conductivities; and the depth extent of the geophysical differences has been discussed by Finlayson [1982]. However, despite these recognized differences, little has been done to examine in detail the comparative geophysical differences in the crust of the major cratonic subdivisions of Australia.

Hence in 1976 the Bureau of Mineral Resources, Geology and Geophysics (BMR), accelerated a program of seismic investigations aimed at examining major crustal features throughout continental Australia. As part of this program, BMR undertook three explosion seismic investigations within the Proterozoic North Australian Craton during 1979 [Collins, 1981]. The first was within the McArthur Basin [Collins, 1982] (Figure 1), the second was an investigation of upper crustal structure within the Tennant Creek Inlier [Finlayson, 1981], and the third was a seismic investigation along a line between Tennant Creek and Mount Isa. The latter survey is the principal subject of this paper and was conducted in cooperation with the Australian National University (ANU).

Paper number 2B1013

Geological and Geophysical Summaries

The tectonic setting of the Proterozoic North Australian Craton has been described by Plumb [1979a, b]. The craton includes the cratonized domains of the early Proterozoic North Australian Orogenic Province and the overlying platform covers and has been stable for over 1700 m.y. It is bounded on the south and east by the cratonized elements of the Central Australian Orogenic Province, which includes the Arunta Complex and the Mount Isa Geosyncline (Figure 1). In the north there are elements of the Archaean West Australia Orogenic Province (Rum Jungle and Nanambu Complexes) underlying the North Australian Orogenic Province, but the full extent of the Archaean basement is unknown; Archaean rocks have been identified in the Tennant Creek area. The Mount Isa Geosyncline contains mid-Proterozoic sedimentary rocks deposited on the early Proterozoic basement and then intensely deformed, metamorphosed, and intruded by granites. In much of the region there are overlying late Proterozoic and Paleozoic platform covers as well as younger Mesozoic-Cainozoic platform cover rocks. Basement outcrops are referred to as 'inliers' because they represent the exposed parts of much larger features.

Tucker et al. [1979] have analyzed the gravity and total magnetic intensity patterns between the Tennant Creek Inlier and the Mount Isa Geosyncline. Basement rocks along this line are hidden by the cover rocks of the Georgina Basin. The basement rocks are considered to be subsurface extensions of the Tennant Creek Inlier, the Arunta Inlier, and the Mount Isa Geosyncline and to consist predominantly of metamorphic rocks and granites. The gravity models used in the analysis included a Moho at 33-35-km depth. Shirley [1979] also has analyzed the gravity field in northeast

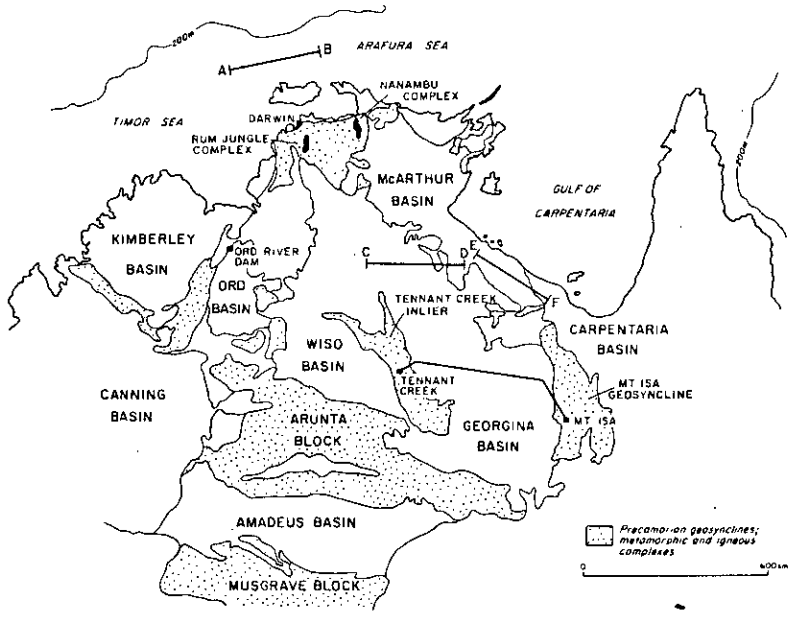

Fig. 1. Principal geological provinces of the North Australian Craton and central Australia and locations of seismic crustal investigations: A-B, West Arafura Sea investigation [Rynn and Reid, 1982]; C-D and E-F, McArthur Basin seismic crustal investigation [Collins, 1982].

Australia, including the Mount Isa Geosyncline, and indicated a 'thinner than normal' crust for the geosyncline (38-40 km). Dooley [1979] reviewed the gravity and seismic data in northeast Australia, including the analyses of Shirley [1979] and Wellman [1976], and indicated Moho depths of 35-40 km under the Mount Isa Geosyncline and adjacent Georgina Basin.

The seismic crustal structure of the North Australian Craton had received little attention prior to 1979. Some seismic studies had been undertaken in connection with ANU lithospheric studies under northern Australia and, in particular, studies of structures under the Warramunga Seismic Array near Tennant Creek (Figure 2). Hales and Rynn [1978] reported the results of explosion seismic work conducted along a 1150 km line from the Arafura Sea to Tennant Creek. Their Model-AS indicated a velocity of 5.97 km/s to about 13-km depth, 6.51 km/s in the interval 13-41-km depth, 8.19 km/s below the Moho to 76-km depth, and 8.40 km at greater depths.

Denham et al. [1972] reported the interpretation of recordings from two large explosions at the Ord River Dam site (Figure 1). However, very little information on crustal structure was derived from that survey. Based on the data from these explosions, Simpson [1973] proposed a two-layer model for the crust with a velocity of 6.2 km/s in the upper 20 km and 6.5 km/s in the lower crust to 39-km depth. Below the Moho a velocity of 8.10 km/s was interpreted to 85-km depth and a velocity gradient from 8.24 to 8.38 km/s in the depth range 85 to 175 km.

In neither the Hales and Rynn [1978] nor the Simpson [1973] models was there any substantial information on the structure of the crust above the Moho. Cleary et al. [1968] indicated possible structures within the crust which might account for slowness values recorded at the Warramunga Seismic Array, but no definitive model was proposed. Underwood [1967] reported some reconnaissance explosion seismic work conducted near the array but there were insufficient data to interpret a seismic model of the crust.

Crustal Surveys, McArthur Basin and Tennant Creek Inlier

The two other seismic crustal investigations conducted during 1979 by BMR within the North Australian Craton were aimed at determining the structure of the McArthur Basin and the Tennant Creek Inlier (Figure 1).

In the McArthur Basin, seismic recording was conducted along two 300-km traverses (Figure 1), C-D and E-F), each with five large refraction shots together with vertical reflection recordings at some shot points [Collins, 1982]. Platform cover rocks obscure basement on both traverses. The results from this survey are discussed later in this paper.

The upper crust of the Tennant Creek Inlier was investigated by explosion seismic methods out to distances of 100 km [Finlayson, 1981] (Figure 2). Near-surface Warramunga Group rocks, consisting of interbedded Proterozoic sedimentary and volcanic lenses, were found to have a P wave velocity of 5.22-5.55 km/s (average 5.42 km/s) and an S wave

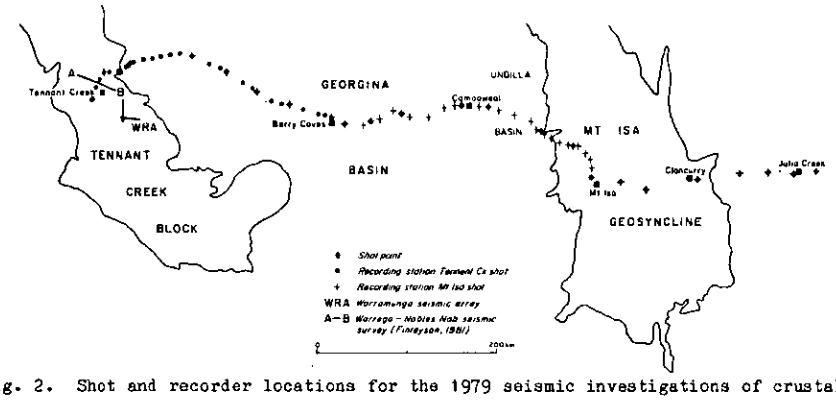

Fig. 2. Shot and recorder locations for the 1979 seismic investigations of crustal structure between Tennant Creek and Mount Isa.

velocity in the range 3.26-3.41 km/s (average 3.34 km/s). The P wave velocity at depths greater than 2.6 km was 6.06 km/s. This latter velocity was also determined through surface granites which had an upper value for their P wave velocity of 5.69 km/s and an S wave velocity of 3.26 km/s. The S wave velocity at depths greater than 2-3 km was in the range 3.53-3.59 km/s, and a velocity of 3.86 km/s was interpreted for the middle crust. There was no indication whether all these velocity changes represent compositional or lithological changes in the rock type or were dominated by the large changes in velocity which result from pore collapse as overburden preasure increases at depth in near-surface rocks. The increased temperature at 3-km depth (about 100°C) causes only a minor decrease in P wave velocity of less than 0.04 km/s in granites and less than 0.02 km/s in granulite and amphibolite rocks [Kern, 1978]. The seismic horizons were considered to be transitional rather than sharp boundaries.

Seismic Survey, Tennant Creek - Mount Isa

Two shots were used to obtain seismic data between Tennant Creek and Mount Isa, a distance of about 600 km. The information on the shots is contained in Table 1.

The Mount Isa shot comprised 18 rows of shot holes with 25-ms delays between each row. Charge per row varied between 250 and 4460 kg. The shot was fired to break siltstone used as backfill in the underground operations of the Mount Isa Mines. The Skipper shot near Tennant Creek was fired in an old gold mine 40 m deep. The charge was specially prepared for the seimic survey in a small alcove off a drive extending 40 m from the bottom of the vertical access shaft. The charge was stemmed and fired instantaneously.

The recorder deployment is shown in Figure 2. Within 100 km of the shots, recorders were placed at 10-km spacing, and between 100 and 300 km, stations were about 20-km apart. At greater distances the station spacing was 40-50 km. BMR deployed 21 FM tape recording systems [Finlayson and Collins, 1980]; ANU deployed 13 direct-record tape recorders [Muirhead and Simpson, 1972] between the two shots and another seven recorders to the east of Mount Isa. Digital seismic records were obtained from both BMR and ANU field tapes using playback equipment in Canberra. All recording systems and shot point recorders used the Australian radio time signal VNG as a common timing standard.

Maximum timing uncertainties of 0.02 s are estimated for BMR recording systems; maximum station position uncertainties of 100 m are estimated; BMR systems used Willmore Mk 2 and 3 seismometers with a free period of 0.7 s and amplifiers with a flat response in the range 0.01-20 Hz.

Earthquake Recording

During the period of recording for the Tennant Creek shot, an earthquake occurred in the New Britain area of Papua New Guinea. This provided an opportunity to assess the relative uniformity of crustal structure west of Barry Caves (Figure 2) using P waves emerging at angles of incidence of 30° to 35° [Pho and Behe, 1972]. The earthquake data have been taken from the U.S. Geological Survey Preliminary Determination of Epicenter bulletins (Table 2) and may

TABLE 1. Shot Information

Shot	Date, 1979	Latitude, S	Longitude, E	Elevation, m	Size, t	Time, UT
Mount Isa	July 26	20°42.40'	139°28.27'	360	40	0159:50.41
Skipper	Aug 9	19°40.66'	134°05.50'	320	5	0645:00.93

The size of the shot is given as tonnes

TABLE 2. New Britain earthquake data, August 9, 1979

Latitude, S	Longitude, E	Depth, km	Time, UT	Magnitude M_b.
05°11.7'	152°07.1'	45	0636:05.6	5.0

subsequently be modified in the Bulletins of the International Seismological Centre. However, the preliminary data serve the purpose of illustrating relative structural changes between the various recording sites.

Figure 3 shows the seismic record section. The travel time has been reduced by a factor (distance/10.8). A prominent second phase is evident 2-4 s after the initial onsets; this phase has an apparent velocity of about 11.7 km/s. Both the initial and second phases are consistently recorded along the 300-km recording line. Hales et al. [1980] have proposed a velocity distribution within the mantle which accommodates many phases observed over the recording distance range 2000-2500 km. It is probable that the initial and second phases observed on the western end of the Tennant Creek-Mount Isa line were from structure in the depth range 400-700 km.

Simpson et al. [1974] examined the travel time curve branches from the Papua New Guinea region using the Warramunga Seismic Array (WRA) in the distance range of the present survey data (20.8°-22.7°). The initial and second phases correspond with the C_3 and D phases, respectively, from the SMAK-1 velocity-depth model of Simpson et al. [1974] with slownesses of 10.5-10.0 s/deg and 9.9-9.2 s/deg. The C_3 phases result from an increase in velocity gradient in the depth range 500-520 km and the D phases from a velocity discontinuity at a depth of 680 km.

Apart from arrivals at distances of 2372 and 2383 km which are about 0.25 s early, the initial onsets display little deviation from a travel time branch with an equation travel time = 66.06 ± 0.52 + distance/(10.84 ± 0.02) s. The residual is 0.048 s. The character of the traces for the initial onsets of the two exceptions mentioned above is disturbed. The early arrivals could result from a velocity variation along the ray path. However, subsequent arrivals correlate well with neighboring traces, and therefore the travel time anomalies in these two initial onsets are attributed to local disturbance at this stage. The earthquake recordings therefore seem to indicate a uniform average velocity structure within the crust and upper mantle under the western 300 km of survey line, supporting the use later in this paper of layered models in the interpretation of structure.

Tennant Creek Shot Record Section and Modeling

The seismic record section from the Tennant Creek shot is shown in Figure 4 together with the travel time curves and synthetic seismograms for the preferred interpretation model (TCMI-2). For display purposes in this paper the BMR recordings were all filtered in the band pass 6-15 Hz and normalized so that the traces had equal maximum amplitude. The first arrivals are indicated on these traces where onsets are not clear at the scale presented. In all cases, examination of traces with a larger time scale or with different filter settings enabled first arrivals to be determined within ± 0.02 s. At the

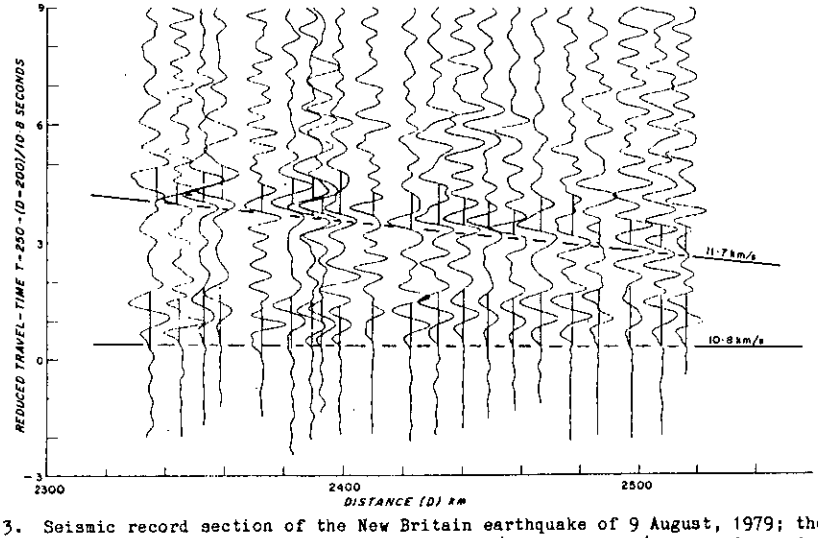

Fig. 3. Seismic record section of the New Britain earthquake of 9 August, 1979; the two principal phases with apparent velocities of 10.8 km/s and 11.7 km/s are indicated.

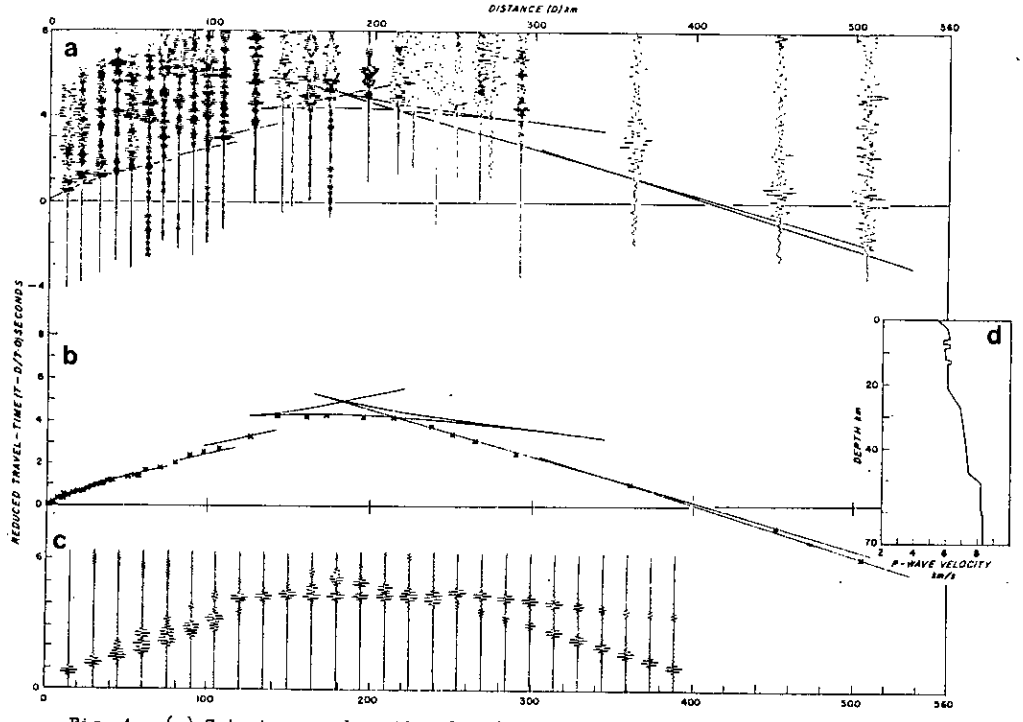

Fig. 4. (a) Seismic record section for the Tennant Creek shot recorded toward Mount Isa. (b) Preferred travel time curve and clearly identified first arrival data. (c) Synthetic record section for the velocity-depth model TCMI-2. (d) Preferred velocity-depth model TCMI-2.

shorter distances, low-gain recordings have been used in compiling the record sections, the high-gain traces having impulsive onsets and trace amplitudes which extended beyond the dynamic range of the high-gain recording channel.

The travel time curve (Figure 4b) for the Tennant Creek shot includes first arrivals from the Warrego shot [Finlayson, 1981] at distances less than 50 km. These have been used to define the near-surface velocity structure on the Tennant Creek Inlier. Offsets in the travel time curve have been interpreted at distances of about 75, 120, and 140 km. These have been taken to indicate velocity structure in the upper 20 km of the earth's crust. These travel time offsets have, in all cases, been identified from high-gain recordings not displayed in Figure 4 because of saturation of the amplifiers by later, large-amplitude events. Paleozoic sedimentary cover on this western part of the survey line is comparatively uniformly distributed and estimated to be less than 0.3 km thick [Tucker et al. 1979], thus not contributing significantly to any non-uniformity in travel time delays.

The record sections and first arrival data from the Tennant Creek shot give some indication of significant correlations which can be used as a basis for modeling studies. For distances less than 70 km a velocity model has been adopted based on the interpretation of all refraction data from the Tennant Creek Inlier, including those interpreted by Finlayson [1981]. The model includes P wave velocities increasing from 5.47 km/s at the surface to 6.06 km at 2.8-km depth and increasing further to 6.20 km/s at 6-km depth. Out to distances of 140 km, two offset segments of the travel time curve have been identified with apparent velocities of 6.2-6.3 km/s.

Beyond 140 km an apparent velocity of 6.8-6.9 km/s is interpreted from first arrival data to a distance of 210 km (Figure 4). At greater distances an apparent velocity of 8.2-8.3 km/s is evident in the first arrival data.

Typically, for both the Tennant Creek and the Mount Isa shots, the velocity error is less than 0.03 km/s when regression analysis is applied to linear segments of arrivals defining the travel time curve. Root-mean-square residuals are typically less than 0.1 s.

Significant later arrivals are difficult to identify. The apparent lack of correlation between neighboring traces in Figure 4 indicates that scattering processes in the upper crust contribute to significant energy variations in the seismic coda. However, beyond 100 km from the shot point a correlation of large-amplitude events can be seen which corresponds to events coming as first arrivals in the range 140-210 km with an apparent velocity of about 6.8-6.9 km/s. This

TABLE 3. Velocity-Depth Models TCMI-2 (Tennant Creek) and TCMI-3 (Mount Isa)

TCMI-2		TCMI-3	
Depth, km	P Wave Velocity, km/s	Depth, km	P Wave Velocity, km/s
0.0	5.47	0.0	6.03
2.8	6.06	3.3	6.15
6.0	6.20	4.1	5.90
6.2	5.75	5.3	5.95
7.2	5.77	6.3	6.20
7.4	6.21	8.1	6.25
8.5	6.23	8.5	6.00
8.7	5.90	9.9	6.01
12.0	5.92	11.0	6.25
12.3	6.25	14.7	6.35
13.3	6.27	15.0	6.25
13.5	6.05	25.0	6.30
21.0	6.07	32.0	6.45
27.0	6.85	40.0	7.40
40.0	7.30	48.0	7.45
47.5	7.40	55.0	8.23
50.5	8.16	70.0	8.29
58.0	8.18		
61.0	8.29		
70.0	8.31		

series of arrivals can be seen as subsequent events beyond 210 km from the shot point. At distances between 210 and 300 km the first arrivals with an apparent velocity of 8.2-8.3 km/s are weak. However, at distances greater than 350 km the onsets have significant energy, and a prominent event arriving about 1 s after the first arrival is indicative of a velocity increase within the upper mantle.

Using the characteristics of the travel times and the record section described above, velocity-depth models of crustal structure were developed iteratively. No shots were fired between the principal shots at Tennant Creek and Mount Isa; thus simple one dimensional velocity-depth models had to be used. Initially, a ray tracing program was used to generate travel time plots which could be compared with observed events. Once a matching model was achieved, the amplitude characteristics of record sections were used to refine the model using a reflectivity synthetic seismogram program [Fuchs, 1968]. The preferred model together with the travel time curves and synthetic traces are shown in Figure 4. All modeling included earth curvature corrections. A Ricker wavelet synthetic source function was used with a 7-Hz center frequency; no absorption (Q) operators were included in the modeling.

The preferred model (TCMI-2) is not unique but serves to indicate the general character of the velocity-depth profile for the earth's crust. The velocity structure in the upper 6 km has been derived from the seismic refraction work on the Tennant Creek Inlier [Finlayson, 1981]. Below 6 km the upper crust to 20-km depth is characterized by three velocity inversions. The minimum velocity in these velocity inversions cannot be estimated from the data. Only the time delay and the length of segments evident in the travel time data provide constraints on the velocity models. At depths greater than 20 km the crust is characterized by a series of velocity gradients until the upper mantle, velocity of 8.16 km/s is reached at 50.5-km depth. Below the Moho there is a velocity gradient in the upper mantle, with velocities increasing to 8.29 km/s in the depth range 58-61 km and a velocity of 8.31 km/s is reached at 70 km depth (Figure 4). Table 3 contains details of the preferred velocity-depth models.

Mount Isa Shot Record Section and Modeling

Near-surface low-velocity cover rocks are comparatively evenly distributed along the seismic line between Tennant Creek and Mount Isa except at distances in the range 75-170 km from Mount Isa, where the Adelaidean and underlying Carpentarian sediments of the Undilla Basin (Figure 2) have a significant effect on travel time delays at the recording sites. Robertson [1963] gave some indication of the velocities to be expected within the sedimentary sequence. The effects of near-surface limestones with a velocity of about 5.2 km/s complicate the travel time corrections. However, Robertson eventually used an average velocity of 3.96 km/s to calculate depths down to 2.4 km. Northwest of the Undilla Basin, in the western McArthur Basin, Collins [1982] has interpreted 4 km of Proterozoic Roper Group sediments or their equivalents with a velocity of 4.62 km/s. Tucker et al. [1979] attribute a broad gravity low in the Undilla Basin to a maximum of 5 km of Adelaidean sediments underlain by up to 8 km of Carpentarian rocks. The travel times in the range 75-170 km from the Mount Isa shot have been adjusted by 0.2-0.5 s to compensate for low-velocity cover rocks.

The seismic record section for the Mount Isa shot is shown in Figure 5 together with the preferred velocity-depth model (TCMI-3), the associated travel time curves, and synthetic seismograms. As with the Tennant Creek shot, the recordings have been band-pass-filtered in the range 6-15 Hz and normalized so that all BMR traces have the same maximum amplitude.

The first arrivals at distances less than 60 km have an apparent velocity of greater than 6 km/s, indicating high velocities within the metamorphic rocks of the Mount Isa Geosyncline. An offset in the first arrival data is evident at about 65 km from the shot point, and an apparent velocity of 6.2-6.3 km/s is observed out to 110 km. The character of the initial onsets changes in the distance range 120-160 km from strong initial onsets to more emergent arrivals, but the apparent velocity remains at 6.2-6.4 km/s. The onset times can still be clearly identified on enlarged records, and these are plotted in Figure 5b.

Beyond 160 km from the shot the initial onsets are emergent, and there is no evidence for apparent velocities less than 7.4 km/s. At distances greater than 240 km the apparent velocity of the first arrivals is 8.2- 8.3 km/s. There are no recordings at distances beyond 305 km except those at the Warramunga Seismic Array (WRA) at distances of about 541 km.

As with the Tennant Creek shot interpretation, seismic ray-tracing models were formed initially to fit the travel time data, and these models were

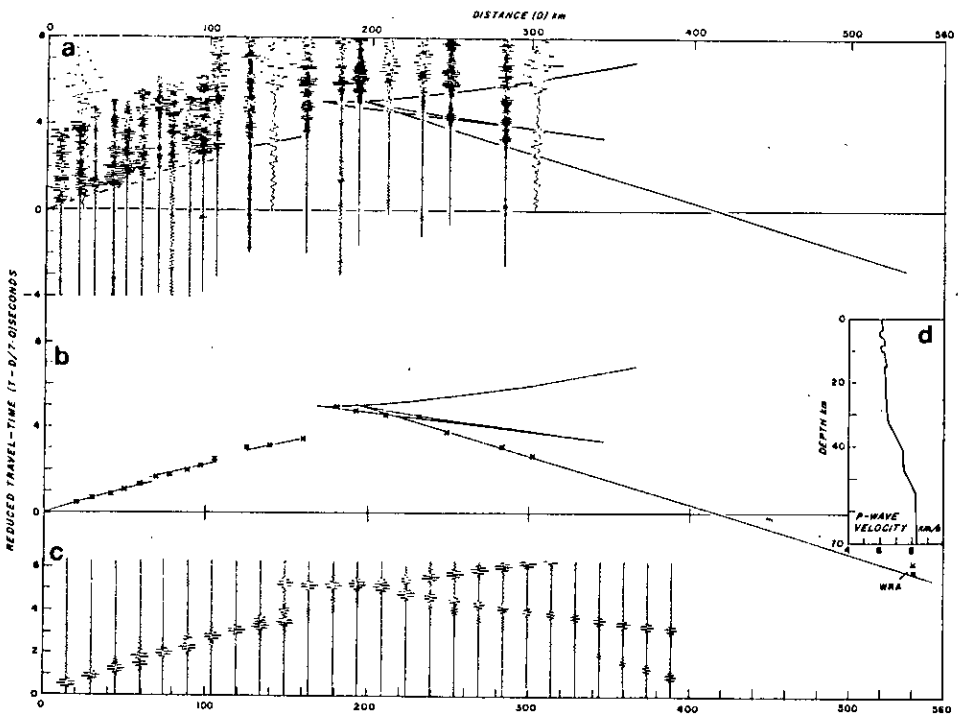

Fig. 5. (a) Seismic record section for the Mount Isa shot recorded toward Tennant Creek. (b) Preferred travel time curve and clearly identified first arrival data. (c) Synthetic record section for the velocity-depth model TCMI-3. (d) Preferred velocity-depth model TCMI-3.

then further constrained using a synthetic seismogram program to model amplitudes. The resulting preferred velocity-depth model (Figure 5) indicates some complexity of structure within the upper 20 km of crust. Three velocity reversals are apparent in this region, with the velocity generally increasing from 6.03 km/s at the surface to a maximum of 6.35 km/s at 14.7-km depth. In the model the minimum velocity in the low-velocity zones is 5.90 km/s. Details of the velocity/depth model TCMI-3 are contained in Table 3.

Interpretation and Discussion

The use of seismic interpretation methods which make a priori assumptions that the geology is near-horizontally stratified requires discussion. Certainly the surface geology at Mount Isa cannot be described as flat lying. However, analysis of the regional gravity field between Tennant Creek and Mount Isa does not indicate any abrupt lateral changes in crustal density which cannot be satisfied in terms of near surface geology. Wellman [1976] indicated that there is no appreciable difference between adjacent exposed and covered basement in mean density, density variability, or history of formation. As mentioned earlier, Tucker et al. [1979] attribute the comparatively minor gravity features between Tennant Creek and Mount Isa to geological variations in the upper 10 km of crust. Dooley [1979] does not peceive any abrupt density variations in the crust based on gravity interpretations. Hence, in the upper 10 km of crust, the derived seismic models must be regarded as having little wide-scale geological application. However, at greater depths some form of gross horizontal metamorphic/geochemical stratification seems to be justified and appropriate for the bulk crustal structure derived from the long-range seismic profiles.

The velocity-depth profiles from the Tennant Creek and Mount Isa shots are illustrated in Figure 6 along with profiles from other areas of the North Australian Craton.

There are significant differences between the profiles determined from the Tennant Creek and Mount Isa shots. At depths less than 20 km both profiles indicate interspersed high- and low-velocity zones. The near-surface velocities at Tennant Creek are less than those at Mount Isa to depths of about 5 km. In the depth range 25-35 km the P wave velocity near Tennant Creek is greater (6.85-7.3 km/s) than that near Mount Isa (6.3-6.4 km/s).

This latter feature of the velocity-depth profiles is essentially defined by the presence of prominent intracrustal arrivals in the distance range 125-300 km on the Tennant Creek record section (Figure 4a) and the lack of corresponding arrivals on the Mount Isa record section (Figure 5a) until greater distances. The cusp points of

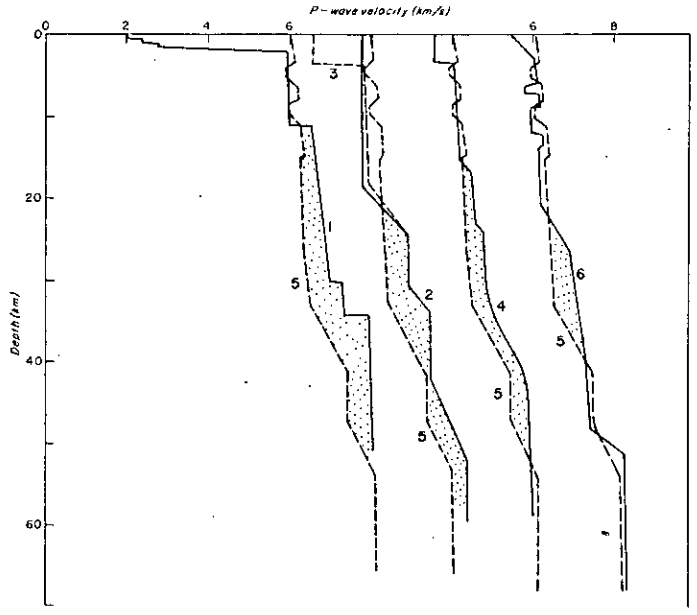

Fig. 6. Seismic P wave velocity-depth profiles from the Proterozoic North Australian Craton: 1, West Arafura Sea [Rynn and Reid, 1983]; 2 and 3, west McArthur Basin [Collins, 1982]; 4, east McArthur Basin [Collins, 1982]; 5, North Australian Craton model TCMI-3 (Mount Isa shot); 6, North Australian Craton model TCMI-2 (Tennant Creek shot). Stippled areas indicate velocity differences in the middle to lower crust fromthe TCMI-3 model.

the travel time curves can be identified on the record sections and modeled using ray tracing and synthetic seismogram programs, the slowness in velocity models closely controlling the extent and amplitude of arrivals. The difference in depth to the velocity of 6.85 km/s of about 10 km in Figures 4d and 5d is therefore considered significant.

Further north on the North Australian Craton, Collins [1982] has interpreted the results of seismic refraction/reflection work in the McArthur Basin (Figure 1). The velocity/ depth profiles from the two survey lines are shown in Figure 6. Comparisons with the present survey data indicate that P wave velocities between Tennant Creek and Mount Isa are greater in the upper crust but that velocities in the lower crust are significantly less. Velocities of about 7.5 km/s occur at depths of 34 km under the West McArthur Basin, whereas such a velocity is not reached until 42 to 50-km depth between Tennant Creek and Mount Isa. Under the East McArthur Basin, P wave velocities are significantly greater in the depth range 15-25 km and also in the range 38-50 km than under the eastern part of the Tennant Creek-Mount Isa line. In the McArthur Basin profiles there is also a trend, evident in the present data, for lower crustal velocities to be greater under the western line than under the eastern line.

Farther north again under the West Arafura Sea the P wave velocities are greater in the upper crust (10-25 km), and the transition to an upper mantle velocity occurs at 32-34 km [Rynn and Reid, 1983].

Hence there appears to be a progressive increase in crustal velocities from the southern part of the North Australian Craton to the northern part. In particular, there are higher velocities at depths greater than 30 km in the north than in the south. There also appear to be higher deep crustal velocities under the central part of the craton than under the eastern part.

Smithson [1978] has outlined the constraints on crustal composition provided by (1) surface exposures, (2) tectonically exposed deep crust, (3) xenoliths, and (4) laboratory experiments on the physical properties of rocks. In Precambrian provinces he indicates the upper crust with P wave velocities of 6.0-6.3 km/s corresponds to granodiorite, being an assemblage of intermediate supracrustal rocks and granitic intrusives. Velocity inversions in the middle crust can be associated with migmatites depending on the overlying sequences. For the lower crust he draws attention to the Ivrea zone in Europe, which contains interlayered mafic and granitic rocks with an overall intermediate composition. Xenoliths from the Precambrian United States indicate a lower crust with a composition more felsic than gabbro with corresponding seismic velocities of 6.5-6.8 km/s.

In Australia, Moore and Goode [1978] have described the granulite facies rocks from the Precambrian Musgrave Block of central Australia (Figure 1), part of the Musgrave-Fraser orogenic subprovince of Rutland [1976]. These rocks are characterized by layered quartz-feldspathic gneisses which could have been formed from

metasedimentary rocks dehydrated in multiple metamorphic episodes or from anhydrous metavolcanic or metasedimentary sequences undergoing a single metamorphic episode. These granulites are considered to have been formed in the lower crust at depths of 30 to 35 km with temperatures of 680° to 800°C and pressures of 6 to 8 kbar. Their felsic nature is contrary to the notion of a gabbroic lower crust but is in agreement with the model of Smithson and Brown [1977] for a heterogeneous mixture of lithologies in the lower crust.

The various early Proterozoic domains of the North Australian Orogenic Province constitute the basement to the North Australian Craton [Plumb, 1979b], and outcropping rocks from these domains have similar ages, rock types, and tectonic styles. Older and younger domains can be identified, metamorphism reaching a higher grade in the older domains. Younger domain rocks at Tennant Creek and Mount Isa are designated greenschist facies or lower, with some amphibolite facies rocks. Pelitic gneisses, metamorphosed to amphibolite facies, underlie the low-grade Warramunga Group rocks near Tennant Creek. At Mount Isa the Kalkadoon granite and Leichhardt metamorphics are interpreted as being underlain by an older orogenic domain.

The velocities encountered in the upper 20 km (5.75-6.35 km/s) are compatible with an assemblage of younger and older domain metamorphics intruded by granites. The velocity reversals probably result from the deformations and intrusions in the basement rocks compatible with the tectonic style described by Plumb [1979b].

Lambert [1971] indicated that anhydrous granulite facies rocks depleted in radioactive heat-producing elements satisfied the below-average heat flow in western and central Australia, basic granulites having too high a velocity to satisfy the available observed seismic velocity data. Smithson and Brown [1977] reiterate these findings in examples from the Precambrian of the United States with supporting evidence from deep vertical seismic soundings. They argue that the nature of these reflections from the lower crust indicates that multiple contrasting rock types must be present, similar to granulite terrains exposed at the surface. Granulites are preferred to amphibolites because of their much smaller proportion of heat-producing elements and because amphibolites have too high a velocity to be a major component of the lower crust. Smithson and Brown [1977] indicate that the lower crust must be distinctly less mafic (less dense) than gabbro where velocities are less than 7 km/s on average. Between Tennant Creek and Mount Isa, however, the velocity is 7.3-7.45 km/s.

Christensen and Fountain [1975] evaluated the velocities of granulite facies rocks using laboratory experiments and demonstrated that such rocks satisfy observed velocities for both P and S waves and therefore must be likely candidates as major constituents in the lower crust. P wave velocities in laboratory samples at appropriate pressures were in the range 6.39-7.49 km/s. Such a range of velocities can be satisfied by a wide range of mineral assemblages; the addition of S wave velocity data is required to provide tighter constraints. P wave velocity gradients in the lower crust also provide a constraint on composition; Christensen and Fountain [1975] indicate that changes in mineralogy can satisfy the gradient data, with or without a change in chemistry. They prefer metamorphic assemblages as a model for the lower crust because igneous rocks are less stable at lower crustal temperatures and pressures.

Manghnani et al. [1974] have considered the possibility of granulite facies rocks at the crust-mantle boundary. They indicate that garnet granulites are compatible with lower crustal velocities of 7.1-7.8 km/s.

The principal differences in crustal structure within the North Australian Craton are in the depth range 25-40 km, where the proportion of rocks with velocities in the range 6.9-7.5 km/s increases from east to west and also from south to north. Finlayson [1982] and Cull et al. [1981a,b] indicate that there are no high electrical conductivity layers within the lower crust in Precambrian central and northern Australia. This is in accord with the proposition that the water content in the lower crust is negligible and consequently granulite facies rather than amphibolite facies rocks are the major constituent.

Using the data of Christensen and Fountain [1975] the P wave velocities generally increase systematically with increasing pyroxene, amphibole, and garnet, the relative proportions of these minerals being important in determining the average velocity. Within the pyroxene and hornblende-granulite subfacies the ratio of hornblende to pyroxene is important, the greater the proportion of pyroxene, the higher the velocity in rocks with equivalent percentages of mafic mineral. Thus in the depth range 25-40 km, within the North Australian Craton, an increasing proportion of pyroxene, hornblende, and garnet within granulite facies rocks can satisfy the increasing proportion of rocks with bulk velocities in the range 6.9-7.5 km from east to west and from south to north.

Acknowledgments. The author wishes to thank all those who took part in the field work, including Clive Collins, John Williams, and Howard Hughes, who were also in the BMR field recording party; the Australian National University recording party under the leadership of Doug Christie and Ken Muirhead; and John Howard and Peter Sciberras from the Northern Territory Department of Mines. The cooperation of Mount Isa Mines Ltd, in particular, the assistance of Peter Stoker, Chief Geologist, in enabling us to record the KSOC quarry blast is greatly appreciated. This paper is published with the permission of the Director of the Bureau of Mineral Resources, Geology and Geophysics, Canberra.

References

Christensen, N. I., and D. M. Fountain, Constitution of the lower continental crust based on experimental studies of seismic velocities in granulite, Geol. Soc. Am. Bull., 86, 227-236, 1975.

Cleary, J. R., Australian crustal structure, Tectonophysics, 20, 241-248, 1973.

Cleary, J. R., C. Wright, and K. J. Muirhead,

The effects of local structure upon measurements of the travel time gradient at the Warramunga Seismic Array, Geophys. J. R. Astron. Soc., 16, 21-29, 1968.

Cleary, J. R., D. W. Simpson, and K. J. Muirhead, Variations in Australian upper mantle structure from observations of the Cannikin explosion, Nature, 236, 111-112, 1972.

Collins, C. D. N., Crustal seismic investigations in northern Australia, 1979: Operation report, Rec. 1981/2 Bur. of Miner. Resour., Canberra, Australia, 1981.

Collins, C. D. N., Crustal structure of the southern McArthur Basin from deep seismic sounding, submitted to BMR J. of Aust. Geol. Geophys., 1982.

Cull, J. P., A. G. Spence, K. A. Plumb, J. A. Major, and D. W. Kerr - The 1978 McArthur Basin magnetotelluric survey, Rec. 1981/1, Bur. of Miner. Resour., Canberra, Australia, 1981a.

Cull, J. P., A. G. Spence, and K. A. Plumb, The 1979 McArthur Basin magnetotelluric survey, Rec. 1981/64, Bur. of Miner. Resour., Canberra, Australia, 1981b.

Denham, D., D. W. Simpson, P. J. Gregson, and D. J. Sutton. Travel times and amplitudes from explosions in northern Australia, Geophys. J. R. Astron. Soc., 28, 225-235, 1972.

Dooley, J. C., A review of crustal structure in northeastern Australia, in The Geology and Geophysics of Northeastern Australia, edited by P. J. Stephenson and R. A. Henderson, Geological Society of Australia (Queensland Division), Brisbane, 27-45, 1979.

Finlayson, D. M., Reconnaissance of upper crustal seismic velocities within the Tennant Creek Block. BMR, J. Aust. Geol. Geophys., 6, 245-252, 1981.

Finlayson, D. M., Geophysical differences in the lithosphere between Phanerozoic and Precambrian Australia, Tectonophysics, 84, 287-312, 1982.

Finlayson, D. M., and C. D. N. Collins, A brief description of BMR portable seismic tape recording systems, Aust. Soc. Explor. Geophys. Bull., 11, 75-77, 1980.

Fuchs, K., Das Reflexions - und Trasmissions vermogen eines geschichteten Mediums mit beliebiger Tiefen - Verteilung der elastischen Modul und der Dichte fur schragen Einfall ebener Wellen, Z. Geophys., 34, 389-413, 1968.

Goncz, J. H., J. R. Cleary - Variations in the structure of the upper mantle beneath Australia from Rayleigh wave observations, Geophys. J. R. Astron. Soc., 44, 507,516, 1976.

Hales, A. L., and J. M. W. Rynn, - A long-range, controlled source seismic profile in northern Australia, Geophys. J. R. Astron. Soc., 55, 633-644, 1978.

Hales, A. L., K. J. Muirhead, and J. M. W. Rynn, A compressional velocity distribution for the upper mantle, Tectonophysics, 63, 309-348, 1980.

Kern, H., - The effect of high temperature and high confining pressure on compressional wave velocities in quartz-bearing and quartz-free igneous and metamorphic rocks, Tectonophysics, 44, 185-203, 1978.

Lambert, I. B., - The composition and evolution of the deep continental crust, Geol. Soc. Aust. Spec. Publ., 3, 419-428, 1971.

Lilley, F. E. M., D. V. Woods, and M. N. Sloane, Electrical conductivity profiles and implications for the absence or presence of partial melting beneath central and southeast Australia, Phys. Earth Planet. Inter., 25, 419-428, 1981.

Manghnani, M. H., R. Ramananantoandro, and S. P. Clark, Compressional and shear wave velocities in granulite facies rocks and eclogites to 10 kbar, J. Geophys. Res., 79, 5427-5446, 1974.

Moore, A. C., and D. T. Goode, Petrography and origin of granulite-facies rocks in the western Musgrave Block, Central Australia, J. Geol. Soc. Aust., 25, 341-358, 1978.

Muirhead, K. J., and D. W. Simpson, A three-quarter watt seismic station, Bull. Seismol. Soc. Am., 62, 985-990, 1972.

Pho, H., and L. Behe, Extended distances and angles of incidence of P-waves, Bull. Seismol. Soc. Am., 62, 885-902, 1972.

Plumb, K. A. - The tectonic evolution of Australia, Earth Sci. Rev., 14, 205-249, 1979a.

Plumb, K. A. - Structure and tectonic style of the Precambrian shields and platforms of northern Australia, Tectonophysics, 58, 291-325, 1979b.

Robertson, C. S. - Undilla Basin seismic survey, Queensland, 1961, Rec. 1963/63, Bur. of Miner. Resour., Canberra, Australia, 1963.

Rutland, R. W. R. - Orogenic evolution of Australia, Earth Sci. Rev., 12, 161-196, 1976.

Rynn, J. M. W., I. D. Reid, - Crustal structure of the western Arafura Sea from ocean bottom seismograph data, J. Geol. Soc Aust., in press, 1983.

Shirley, J. E. - Crustal structure of north Queensland from gravity anomalies, BMR J. Aust. Geol. Geophys., 4, 309-321, 1979.

Simpson, D. W., P-wave velocity structure of the upper mantle in the Australian region, Ph.D. thesis, Australian National University, Canberra, 1973.

Simpson, D. W., R. D. Mereu and D. W. King. An array study of P-wave velocities in the upper mantle transition zone beneath northeastern Australia, Bull. Seismol. Soc. Am., 64, 1757-1788, 1974.

Smithson, S. B., Modeling continental crust: Structural and chemical constraints, Geophys. Res. Lett., 5, 749-752, 1978.

Smithson, S. B., and S. K. Brown, A model for the lower continental crust. Earth Planet. Sci. Lett., 35, 134-144, 1977.

Tucker, D. H., B. W. Wyatt, E. C. Druce, S. P. Mathur, and P. L. Harrison. The upper crustal geology of the Georgina Basin region, BMR J. Aust. Geol. Geophys., 4, 209-226, 1979.

Underwood, R., The seismic network and its applications, Ph.D. thesis, Australian Natl. Univ., Canberra, 1967.

Wellman, P., Regional variation of gravity, and isostatic equilibrium of the Australian crust, BMR J. Aust. Geol. Geophys., 1, 297-302, 1976.

(Received February 26, 1982;
revised June 11, 1982;
accepted July 8, 1982.)

THE AUSTRALIAN CONTINENTAL CRUST : EXPLOSION SEISMIC STUDIES IN ARCHAEAN, PROTEROZOIC, AND PALAEOZOIC PROVINCES

D.M. Finlayson

Bureau of Mineral Resources, Geology and Geophysics,
P.O. Box 378, Canberra City, 2601, Australia.

Explosion seismic studies of the crust in continental Australia since 1976 have benefited from improvements in recording and interpretation methods. Investigations of crustal structure have been undertaken in widely separated geological provinces, and this paper reviews three such investigations; the first from the Palaeozoic Lachlan Fold Belt in southeastern Australia, the second from the Lower/Middle Proterozoic McArthur Basin - Mt Isa Block - Tennant Creek Block of northern Australia, and the third from the Archaean Pilbara - Yilgarn Blocks of northwestern Australia.

The Lachlan Fold Belt is characterised seismically by inhomogeneities in the upper and middle crust which probably extend to the lower crust as well. Seismic velocity - depth models incorporate velocity gradients rather than sharp velocity boundaries, and include velocity decreases in the upper and middle crust. The Belt includes the highest mountain ranges in Australia and it is under these that the greatest crustal thickness is measured (about 50 km); the upper mantle velocity is in the range 8.02 - 8.05 km/s.

In northern Australia much of the Proterozoic craton is obscured by younger cover rocks. Preliminary seismic results of crustal structure are available from the McArthur Basin, from the Tennant Creek Block, and from the Mount Isa Block separated from Tennant Creek by the Georgina Basin. Earlier work (Hales & Rynn, 1978) indicated a crustal thickness of 40 - 45 km and an average crustal velocity of 6.49 - 6.56 km/s on the continental shelf to the north of Australia. Reconnaissance data from a 1972 Ord Dam explosion indicated that a crustal thickness of about 27 km may be expected in the Georgina Basin - Mount Isa region.

In northwestern Australia explosion seismic investigations have been undertaken across the Archaean Pilbara and northern Yilgarn Blocks and the

intervening Proterozoic Hamersley Basin and Capricorn Orogenic Belt. The results to date (Drummond, 1979) indicate that the Pilbara Block, which contains the oldest known rocks in Australia, may be modelled with an upper crust having a velocity of 6.0 km/s overlying a lower crust at about 13 km, which has velocities transitional between 6.4 km/s and the upper mantle velocity of 8.2 - 8.5 km/s. The crustal thickness is in the range 28 - 33 km. South of the Pilbara Block the crust thickens under the region of the Capricorn Orogenic Belt, and the Moho is at a depth of about 52 km under the northern edge of the Yilgarn Block. More studies of these general features will be required to determine detailed intra-crustal structure.

Revista Brasileira de Geociências 12(1-3): 132-134, Mar.-Set., 1982 - São Paulo

VELOCITY DIFFERENCES IN THE MIDDLE-LOWER CRUST ACROSS THE PROTEROZOIC NORTH AUSTRALIAN CRATON

D. M. FINLAYSON*

ABSTRACT Seismic refraction surveys conducted in two onshore and one offshore areas of the Proterozoic North Australian Craton indicate complex P-wave velocity variations in the upper 20 km of crust compatible with an assemblage of younger and older metamorphic rocks intruded by granites which are overlain by a 2 km thick sedimentary sequence offshore. In the middle-lower crust between 20 and 50 km depth there appears to be an increase in P-wave velocity from east to west and from south to north. These trends can be interpreted as indicating a greater proportion of high-velocity granulites being emplaced at higher levels in the crust.

INTRODUCTION Detailed seismic refraction surveys have been conducted at three locations on the North Australian Craton. The first was conducted offshore during 1976 in the Western Arafura Sea by the Australian National University (ANU) and Woods Hole Oceanographic Institute/Indonesian Geological Institute (Rynn and Reid, 1982). The second was conducted in the McArthur Basin during 1979 by the Bureau of Mineral Resources, Geology & Geophysics (BMR) (Collins, 1982), and the third was also conducted by BMR and ANU during 1979 between the Tennant Creek Inlier and the Mt Isa Geosyncline across the cover rocks of the Georgina Basin (Finlayson, 1982) (Fig. 1). These three surveys provided data for the interpretation of velocity-depth models to depth of about 60 km for comparative studies.

TECTONIC SETTING Plumb (1979*a*, *b*) has described the tectonic evolution of the North Australian Craton. The Craton includes domains of the early Proterozoic North Australian Orogenic Province and overlying platform covers, and has been stable since 1,700 Ma B.P. It is bounded to the south and east by the cratonised elements of the Central Australian Orogenic Province which includes the Arunta Complex, and the Mt Isa Geosyncline. In the north, elements of the Archaean West Australian Orogenic Province underlie the North Australian Craton. Archaean rocks have been identified near Tennant Creek but the full extent of Archaean basement is unknown (Black, 1981).

Proterozoic and Palaeozoic platform covers as well as Mesozoic-Cenozoic platform cover rocks overlie much of the region. Consequently outcrops are referred to as inliers

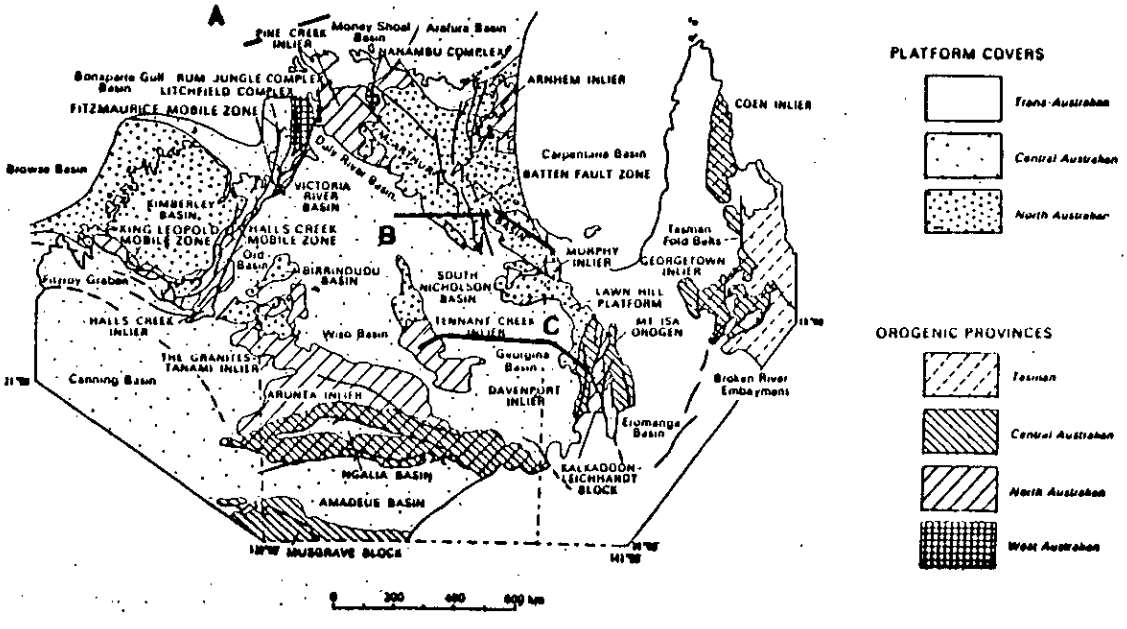

Figure 1 – Principal tectonic elements of the North Australian Craton and its margins (Plumb, 1979b) together with seismic refraction traverses: A – west Arafura Sea; B – McArthur Basin; C – Tennant Creek Inlier to Mount Isa Geosyncline

* Bureau of Mineral Resources, Geology & Geophysics, P.O. Box 378, Canberra City, ACT 2601, Australia

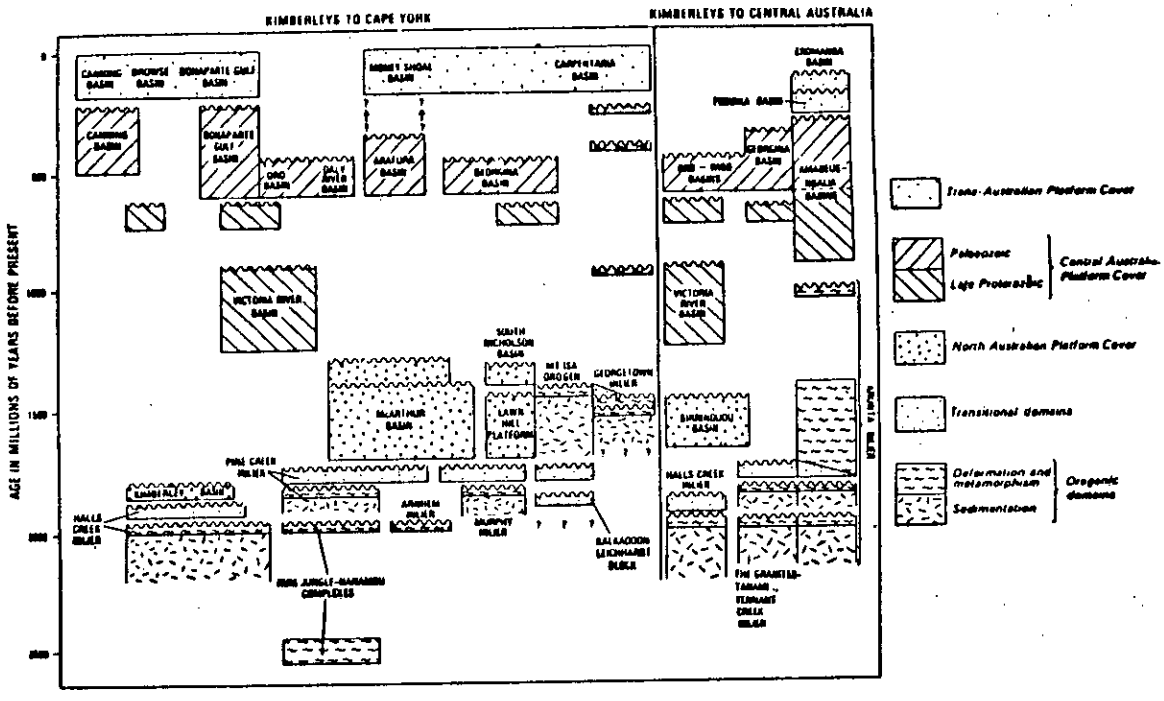

Figure 2 — Diagrammatic relationship of the tectonic units of the North Australian Craton and its margins (Plumb, 1979b)

because they represent the exposed parts of much larger features.

The Mt Isa Geosyncline contains mid-Proterozoic sedimentary rocks deposited on the early Proterozoic basement and then intensely deformed, metamorphosed and intruded by granites.

The Proterozoic McArthur Basin consists mainly of relatively undeformed shallow water sediments which are part of the North Australian Platform Cover. The basement comprises transitional domains of the North Australian Orogenic Province. The McArthur Basin succession is up to 12 km thick. The fault-bounded Batten Trough which is about 50-60 km wide extends N-S along the axis of the basin.

The Arafura Shelf north of the Australian coast is regarded as part of the North Australian Craton. Near-horizontal Mesozoic and Cenozoic marine sediments overlie lower Mesozoic rocks and Cambrian/Precambrian basement (Jongsma, 1974).

The overall relationship of tectonic units within the North Australian Craton is shown in Fig. 2 compiled by Plumb (1979*b*).

SEISMIC SURVEYS In the western Arafura Sea 71 shots fired along a 280 km traverse were recorded on two ocean bottom seismometer systems at distances out to 300 km (Rynn and Reid, 1982). The resultant velocity-depth model comprises a 2 km thick sedimentary sequence overlying basement with a velocity of 6.0 km/s. At 11 km depth the velocity increases to 6.5 km/s and continues to increase along a velocity gradient to 7.0 km/s at 30 km depth where there is a step-wise increase to 7.3 km/s. A further increase in velocity is interpreted to 8.0 km/s at the Moho depth of 34 km.

The McArthur Basin seismic data were derived from two 300 km long seismic refraction traverses with seismic reflection probes at six locations (Collins, 1982). The Tawallah, McArthur and Roper Group rocks of the McArthur Basin succession, deposited in the period 1,750-1,300 Ma B.P. are overlain, in places, by Cenozoic, Mesozoic and Cambrian sediments 100-200 m thick. The P-wave velocities in the basin sediments vary from 3.58-4.62 km/s for the Roper Group to 5.44-5.9 km/s for the Tawallah Group. The thickness of basin sediments varies from 4.2 km in the west to 2.7 km in the east. The basement velocities are characterised by broad gradient zones. On the western traverse the velocity increases from 5.9 to 6.9 km/s in the depth range 12 to 26 km, from 6.9 to 7.5 km/s between 31 and 35 km, and from 7.5 to 8.4 km/s between 43 and 53 km. On the eastern traverse the basement velocity of 6.04 km/s increases to 6.47 km/s in the depth range 15 to 16.5 km, increases from 6.5 to 6.8 km/s in the range 21 to 24 km and increases further to 7.5 km/s at 40 km depth. An upper mantle velocity of 7.9 km/s is reached at 44 km depth and continues to increase below this depth.

The seismic data between the Tennant Creek Inlier and the Mt Isa Geosyncline were recorded along a 600 km reverse refraction line with additional detailed near-surface data near Tennant Creek (Finlayson, 1982). These latter data indicated P-wave velocities of 5.47-6.2 km/s and correspond to low grade metamorphics of the Warramunga Group interspersed with weathered granites overlying amphibolite facies rocks of older metamorphic domains. At Mt Isa P-wave velocities of 6.03 to 6.15 km/s correspond to the

Leichhart Metamorphics interspersed with granites. In the middle crust, velocities of 6.85 km/s occur at depth of 26 km near Tennant Creek but not until a depth of 37 km near Mt Isa. The lower crust is characterised by velocities of 7.3 to 7.5 km/s and upper mantle velocities of 8.16-8.20 km/s are reached at 51-54 km depth.

DISCUSSION Fig. 3 illustrates the velocity structures from the three surveys on the North Australian Craton and also data from other relevant surveys. One of Drummond's typical (1982) velocity models from the Archaean Pilbara Craton is superimposed on the model for the west Arafura Sea. Although the velocities in the upper 11 km of the crust differ, the middle-lower crustal velocities are similar and upper mantle velocities are evident at depths of 28-35 km where there is a pronounced velocity increase from lower crustal velocities of less than 7.0 km/s. Onshore from the west Arafura Sea traverse lie the Archaean Litchfield, Rum Jungle and Nanambu Complexes (Fig. 1) and it seems likely that the crust offshore is also Archaean. The seismic data would certainly support such a proposal.

A comparison of velocities in the middle-lower crust of the McArthur Basin (Fig. 3) reveals very few significant differences. However the data do fit in with a trend of higher velocities below 20 km depth in the west (Finlayson, 1982). The velocities in the middle crust under the Tennant Creek Inlier do appear to be significantly greater than those under the Mt Isa Geosyncline.

Hence, although sampled in only three areas, the North Australian Craton is not uniform in its crustal velocities. The velocity structure in the north is more akin to that of the Archaean Pilbara Craton in north-western Australia. The velocities at middle-lower crustal levels appear to be lower under the Mt Isa Geosyncline than farther to the north and west suggesting that there may be a correlation with age since final cratonisation.

As indicated by Finlayson (1982), exposed granulite facies rocks in central Australia are low in heat producing elements and are compatible with the low surface heat flow generally measured in Precambrian Australia. (Lambert, 1971). Laboratory measurements made on world-wide samples (Manghnani *et al.*, 1974; Christensen and Fountain, 1975) indicate that mid-lower crustal rocks could be an assemblage of granulite facies rocks varying from pyroxene granulite in the middle crust, through hornblende granulite, to garnet granulite in the lower crust. The velocity trends in the North Australian Craton could result from a greater proportion of high velocity granulites being emplaced at higher levels in the crust.

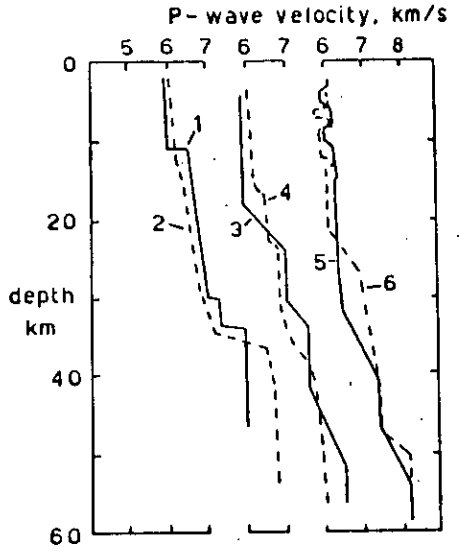

Figure 3 – P-wave velocities in the crust and upper mantle of northern Australia: 1 – west Arafura Sea; 2 – Pilbara Craton (Drummond, 1982); 3 – west McArthur Basin (Collins, 1982); 4 – east McArthur Basin (Collins, 1982); 5 – Mount Isa (Finlayson, 1982); 6 – Tennant Creek (Finlayson, 1982)

Acknowledgements This paper is published with the permission of the Director, Bureau of Mineral Resources, Geology & Geophysics, Canberra.

REFERENCES

BLACK, L.P. – 1981 – Age of the Warramunga Group, Tennant Creek Block, Northern Territory. *BMR Journal of Australian Geology & Geophysics* 6: 253-258.

CHRISTENSEN, N.I. and FOUNTAIN, D.M. – 1975 – Constitution of the lower Continental crust based on experimental studies of seismic velocities in granulite. *Geological Society of America Bulletin* 86:227-236.

COLLINS, C.D.N. – 1982 – Crustal structure of the southern McArthur Basin from deep seismic sounding. *BMR Journal of Australian Geology & Geophysics* (in prep.).

DRUMMOND, B.J. – 1982 – Crustal evolution in northwest Australia: evidence from seismic refraction data. PhD Thesis, Australian National University, Canberra.

FINLAYSON, D.M. – Seismic crustal structure of the Proterozoic North Australian Craton between Tennant Creek and Mount Isa. *Journal of Geophysical Research* (in press).

JONGSMA, D. – 1974 – Marine geology of the Arafura Sea. Bureau of Mineral Resources, Geology & Geophysics Bulletin 147.

LAMBERT, I.B. – 1971 – The composition and evolution of the deep continental crust. *Geological Society of Australia* No. 3: 419-428.

MANGHNANI, M.H., RAMANANANTOANDRO, R. and CLARK, S.P. – 1974 – Compressional and shear wave velocities in granulite facies rocks and eclogites to 10 kbar. *Journal of Geophysical Research* 79: 5427-5446.

PLUMB, K.A. – 1979*a* – The tectonic evolution of Australia. *Earth Science Reviews* 14: 205-249.

PLUMB, K.A. – 1979*b* – Structure and tectonic style of the Precambrian shields and platforms of northern Australia. *Tectonophysics* 58: 291-325.

RYNN, J.M.W. and REID, I.D. – Crustal structure of the western Arafura Sea from ocean bottom seismograph data. *Journal of the Geological Society of Australia* (in press).

Recebido em 15 de agosto de 1982

Tectonophysics, 101 (1984) TEC00817 [NC]
Elsevier Science Publishers B.V., Amsterdam – Printed in The Netherlands

P-WAVE VELOCITY FEATURES OF THE LITHOSPHERE UNDER THE EROMANGA BASIN, EASTERN AUSTRALIA, INCLUDING A PROMINENT MID-CRUSTAL (CONRAD?) DISCONTINUITY

D.M. FINLAYSON, C.D.N. COLLINS and J. LOCK

Bureau of Mineral Resources, Geology and Geophysics, P.O. Box 378, Canberra City, ACT 2601 (Australia)

(Received February 23, 1983; revised version accepted July 11, 1983)

ABSTRACT

Finlayson, D.M., Collins, C.D.N. and Lock, J., 1984. P-wave velocity features of the lithosphere under the Eromanga basin, eastern Australia, including a prominent mid-crustal (Conrad?) discontinuity. *Tectonophysics*, 101: ●●●–●●●.

The crustal structure of the central Eromanga Basin in the northern part of the Australian Tasman Geosyncline, revealed by coincident seismic reflection and refraction shooting, contrasts with some neighbouring regions of the continent. The depth to the crust–mantle boundary (Moho) of 36–41 km is much less than that under the North Australian Craton to the northwest (50–55 km) and the Lachlan Fold Belt to the southeast (43–51 km) but is similar to that under the Drummond and Bowen Basins to the east.

The seismic velocity boundaries within the crust are sharp compared with the transitional nature of the boundaries under the North Australian and Lachlan provinces. In particular, there is a sharp velocity increase at mid-crustal depths (21–24 km) which has not been observed with such clarity elsewhere in Australia (the Conrad discontinuity?).

In the lower crust, the many discontinuous sub-horizontal reflections are in marked contrast to lack of reflecting horizons in the upper crust, further emphasising the differences between the upper and lower crust. The crust–mantle boundary (Moho) is characterised by an increase in velocity from 7.1–7.7 km/s to a value of 8.15 + 0.04 km/s. The depth to the Moho under the Canaway Ridge, a prominent basement high, is shallower by about 5 km than the regional Moho depth: there is also no mid-crustal horizon under the Canaway Ridge but there is a very sharp velocity increase at the Moho depth of 34 km. The Ridge could be interpreted as a horst structure extending to at least Moho depths but it could also have a different intra-crustal structure from the surrounding area.

The sub-crustal lithosphere has features which have been interpreted, from limited data, as being caused by a velocity gradient at 56–57 km depth with a low velocity zone above it.

Because of the contrasting crustal thicknesses and velocity gradients, the lithosphere of the central Eromanga Basin cannot be considered as an extension of the exposed Lachlan Fold Belt or the North Australian Craton. The lack of seismic reflections from the upper crust indicates no coherent accoustic impedance pattern at wavelengths greater than 100 m, consistent with an upper crustal basement of tightly folded meta-sedimentary and meta-volcanic rocks. The crustal structure is consistent with a pericratonic or arc/back-arc basin being cratonised in an episode of convergent tectonics in the Early Palaeozoic. The seismic reflections from the lower crust indicate that it could have developed in a different tectonic environment.

0040-1951/83/$03.00

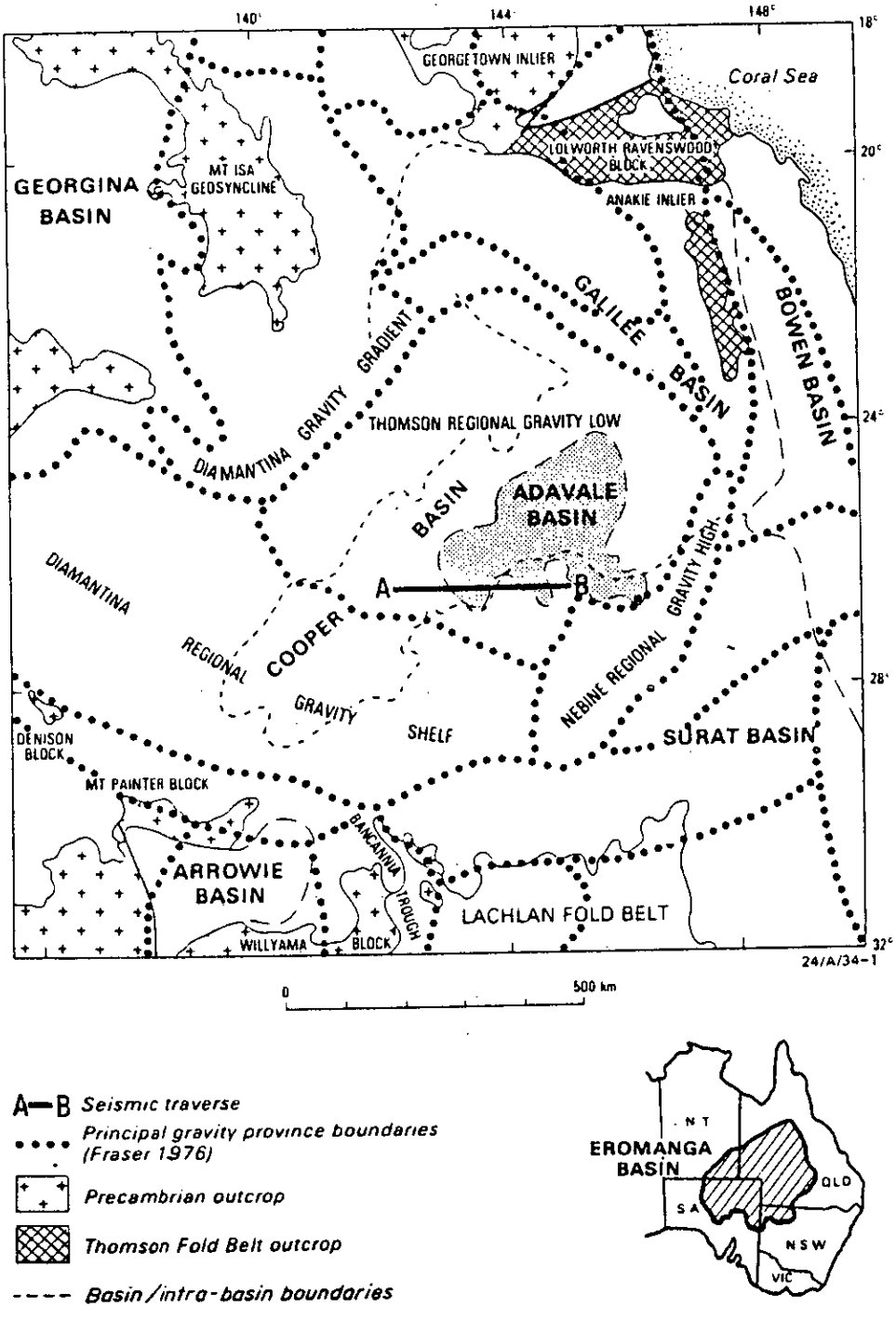

Fig. 1. Gravity province boundaries of the Eromanga Basin and neighbouring regions together with simplified geological province boundaries and the 1980 seismic traverse location.

INTRODUCTION

The Mesozoic Eromanga Basin in eastern Australia conceals a number of mid-Palaeozoic infra-basins which overlie the basement rocks of the Early Palaeozoic Thomson Fold Belt. This fold belt is a province within the Phanerozoic Tasman Geosyncline of eastern Australia and has been described by a number of authors (Kirkegaard, 1974; Murray and Kirkegaard, 1978). It falls within the proposed Barcoo Basin of Harrington (1974). The fold belt is concealed by overlying sedimentary basins and is therefore better defined by the gravity expression. Wellman (1976) recognised many of its features in his discussions of gravity trends and the growth of the Australian continent. Fraser (1976) has outlined the gravity boundaries for the region and these, together with the structural features of the Thomson Fold Belt, are shown in Fig. 1, adapted from Murray & Kirkegaard (1978). The tectonic development of the basins in the region has been described by Veevers (1980). This took place at the eastern (Pacific) margin of Precambrian Australian largely in the period 550–250 m.y. B.P.

During 1980–1982 the region was the target for geophysical studies designed to determine a better understanding of basin structure. These studies included coincident, detailed seismic refraction and reflection shooting along major traverses to enable structures down to depths of about 80 km to be investigated.

FIELD SURVEY AND DATA PROCESSING

The seismic recordings interpreted in this paper are from a 300 km east–west traverse centrally placed across the Thomson Fold Belt between Cheepie and Terebooka Bore (Fig. 2). The basement fold belt rocks are concealed in places by about 2 km of Jurassic–Cretaceous Eromanga Basin sequence overlying 0.4 km of Permian–Triassic rocks of the northeastern Cooper Basin or up to 3 km of Devonian rocks of the Warrabin and Quilpie Troughs, structural remnants of the Adadale Basin (Pinchin and Senior, 1982). Basement rocks of the Thomson Fold Belt from drillholes have Cambrian–Ordovician ages (Rumph, 1978).

Seismic reflection records are available along 270 km of the 300 km refraction traverse described in this paper (Pinchin and Senior, 1982; Wake-Dyster and Pinchin, 1981). In addition, 37.5 and 75 km-long seismic refraction traverses were shot along the same 270 km (Fig. 2). These data have been interpreted in terms of basin and basement velocity structure to depths of about 10 km (Lock et al., 1983).

Spence and Finlayson (1983) have interpreted magnetotelluric data along the central portion of the traverse in terms of basement morphology and the conductivity structure of the lithosphere. They found that magnetotelluric data were characterised by the similarity of orthogonal components, indicating that simple one-dimensional models were appropriate for the region.

Figure 3 illustrates the simplified basin structure derived from seismic reflection

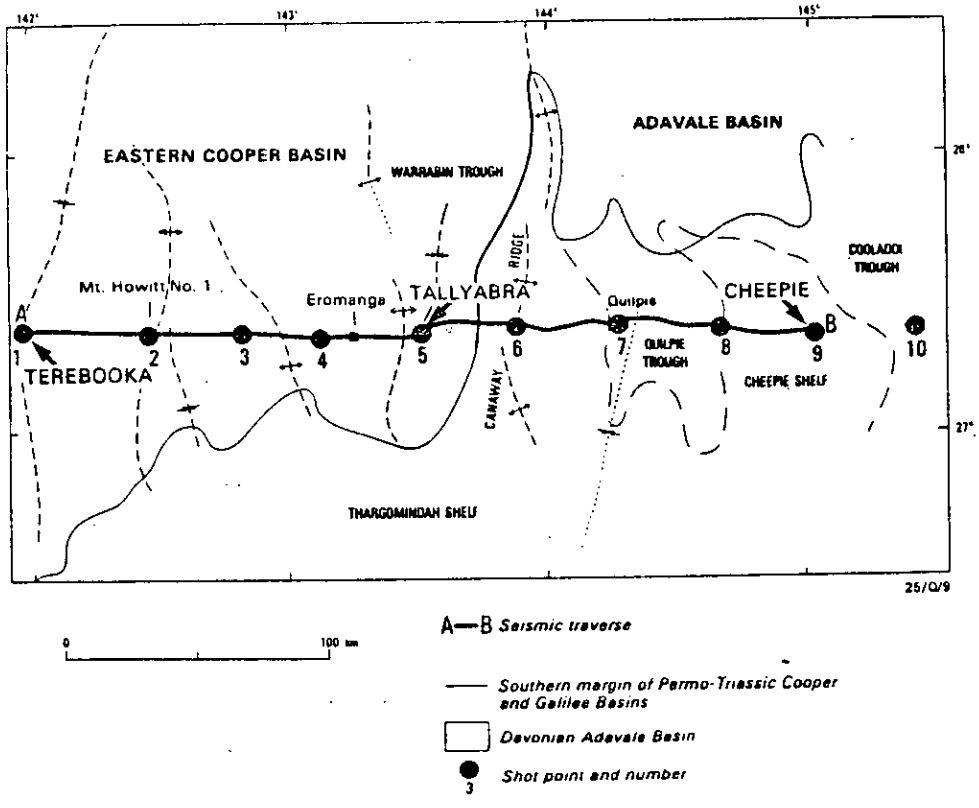

Fig. 2. Seismic traverse and shot point locations in the central Eromanga Basin.

profiling. The Warrabin Trough, Canaway Ridge and the Quilpie Trough are the major north-south trending structures intersected by the seismic traverse. Otherwise the traverse is characterised by comparatively flat-lying basin sediments overlying basement.

The locations of seismic refraction shot points 1–10 are indicated in Fig. 2. The data interpreted in this paper are derived from large shots fired at shot point 1, Terebooka (0.75 and 2.0 tonnes), shot point 5, Tallyabra (2 × 0.75 tonnes) and shot point 9, Cheepie (0.75 and 2.0 tonnes). Thus a reversed data set was achieved along the length of the 300 km traverse and also separately along the eastern and western halves. The shot points 2–4, 6–8 and 10 were used for short-line refraction shooting with shot sizes of 200–400 kg and recording distances of 37.5 and 75 km.

The shots were fired in shot-hole patterns drilled to at least 40 km depth, each hole being loaded with 0.1–0.2 t of explosive. The shots were fired electrically. Recorders were deployed at 7.5 km intervals along the 300 km traverse. Twenty-one sets of automatic, 4-channel, tape recording equipment were used (Finlayson and

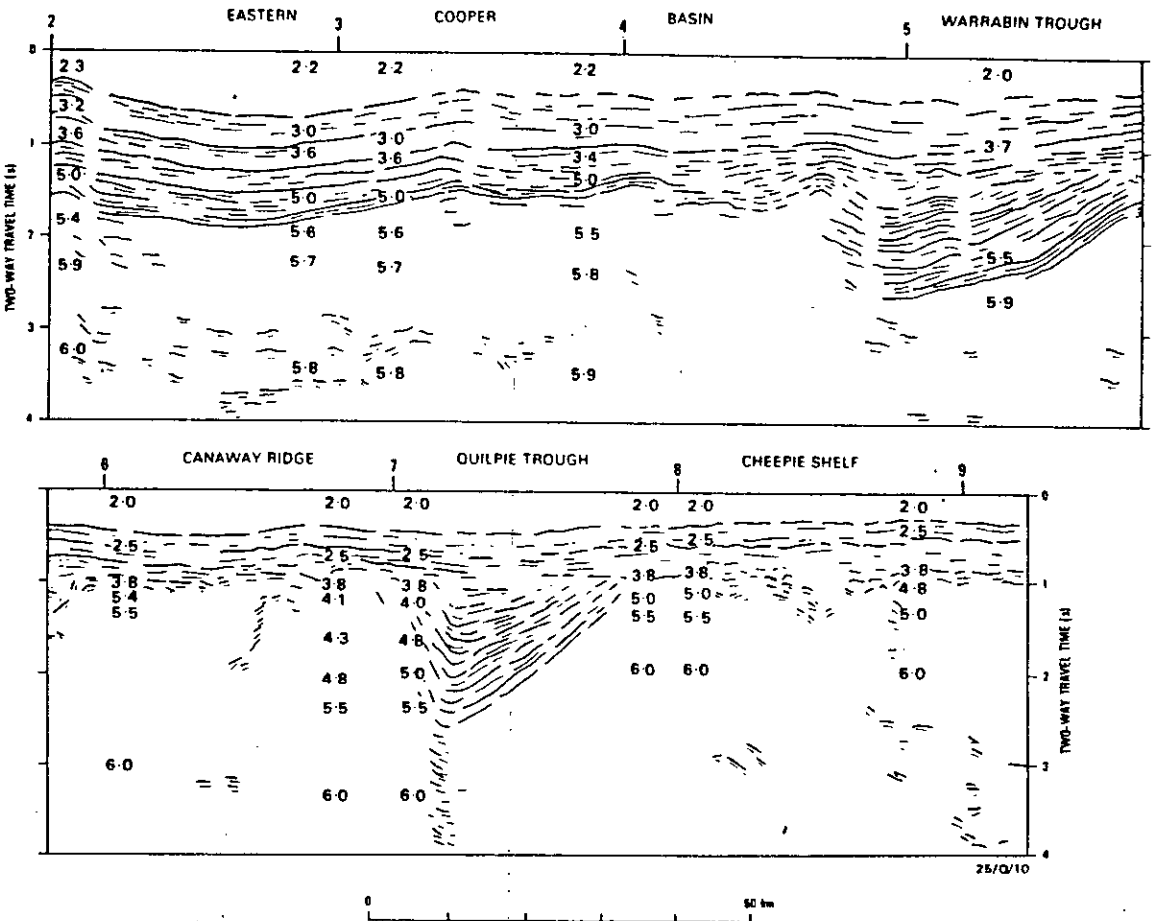

Fig. 3. Schematic seismic record section derived from the vertical seismic reflection profiling between shots 2 and 9 (see Fig. 2) (after Wake-Dyster and Pinchin, 1981). Velocities are indicated in km/s (from Lock et al., 1983 and Collins and Lock, 1983).

Collins, 1980). Each set recorded frequency modulated high and low gain seismic channels from a vertical seismometer, a digital clock signal and the Australian standard radio time signal (VNG) broadcast by Telecom Australia.

The positions of shot and recorder sites in the central 150 km of the traverse were tied to the surveyed lines used for coincident reflection seismic shooting. Consequently, relative distances between their positions are known to within a few metres. The shot and recorder station locations at the extremities of the traverse were tied to known survey lines using aerial photography and shot-station distances are estimated to have uncertainties of less than 50 m.

The seismic data were digitised and plotted as record sections using programs incorporating provisions for normalising shot weight, distance and recorder gain, and various filter settings. The record sections in this paper are mostly from low-gain channels filtered digitally within the bandpass 4–16 Hz.

SHALLOW SEISMIC VELOCITIES

The seismic P-wave velocity structure at depths less than 8 km has been interpreted from 37.5 and 75.0 km detailed seismic refraction traverses. The velocities are indicated under the appropriate shot points in Fig. 3. Velocities from shot points 2–4 were derived by Lock et al. (1983) and those from shot points 6–9 were derived by Collins and Lock (1983). The velocities in the Warrabin Trough are approximate values used to estimate the relative delays in travel-times. These velocities were derived from travel-time modelling studies of both refraction and reflection data, and also refracted arrivals multiply reflected at the surface.

Generally, within the sedimentary sequence at depths less than 2.4 km (about 1.75 s two-way-time), velocities increase from 2.0–2.3 km/s at the surface to 5.0 km/s. In the Devonian infra-basins (Warrabin and Quilpie troughs) the velocities reach 5.5 km/s. Within basement the P-wave velocity generally increases from about 5.4 km/s to about 5.7–6.0 km/s within an interval of about 2.3 km and does not exceed 5.8–6.1 km/s at depth.

SEISMIC RECORD SECTIONS AND VELOCITY MODELS

One crucial step in the interpretation of crustal structure from the seismic record sections is that of identifying the significant seismic phases to be interpreted. Giese (1976), among others, has discussed the problems associated with the identification, especially when the phases are not first arrivals but are part of a complex wave-train. Much of the complexity in the wave-train can be attributed to scattering from local inhomogeneities. Giese (1976) suggests seismic phases may be correlated across the record section when, (a) amplitudes of the events being correlated exceed those of background noise, (b) the apparent velocity must show values within a possible and reasonable range, and (c) the travel-time branches are of some length. On any record section the reflected phases from a particular horizon generally have larger ampli-

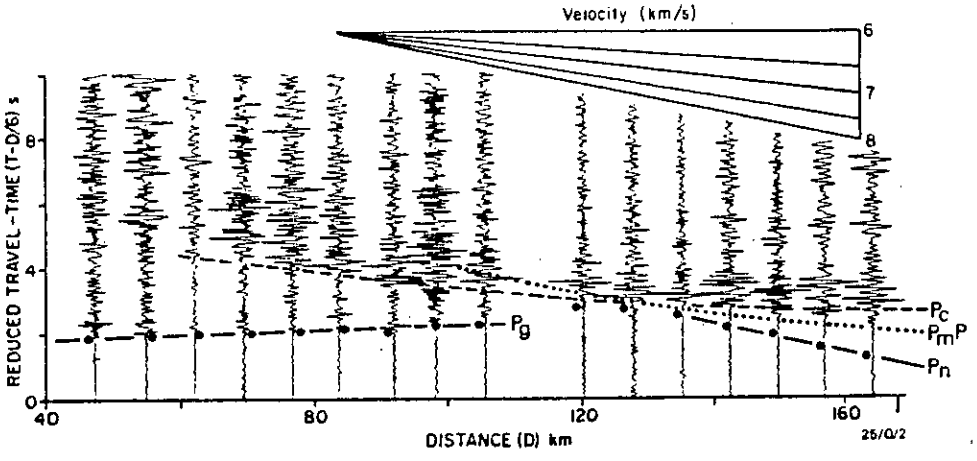

Fig. 4. Seismic record section from shots fired at Terebooka and recorded in the distance range 40–170 km, illustrating the principal seismic phases used in the interpretation (see text). The seismic traces are normalised to have equal maximum amplitude and are filtered in the bandpass 4–16 Hz. All traces are from low-gain channels. Dots indicate first arrivals clearly seen on high-gain recordings.

tudes than the refracted phases beyond the critical distance. Hence within the coda of seismic recordings those phases which are more readily apparent are often reflections from intra-crustal horizons or from the crust–mantle boundary.

These principles were used in the identification of significant phases on the Eromanga Basin record sections. Figure 4 illustrates the principal phases used to interpret the velocity/depth functions; this record section is part of the section from the Terebooka shots recorded eastward towards Cheepie. It should be emphasised that the record section in Fig. 4, like the others in this paper, is compiled mostly from low-gain recordings because the large amplitude phases tended to overmodulate the high-gain recordings. The traces in Fig. 4 have been normalised to have equal maximum amplitude. The high-gain records give reliable onset times for first arrival phases, the majority of which can be timed with an uncertainty of less than 0.05 s and frequently with uncertainties of less than 0.02 s. These first arrivals are marked on Fig. 4 as a dot beside each seismic trace.

On Fig. 4 the first arrivals at distances less than 100 km are identified with P-waves refracted within the basement under the Eromanga Basin and infra-basins. On the high-gain records these phases are impulsive and are commonly labelled Pg events (Giese, 1976). Beyond 100 km the first onsets become emergent and are not clearly impulsive again until distances beyond 120 km where clear first arrivals on high-gain records are identified with P-waves refracted within the upper mantle (Pn). Data recorded out to 300 km indicate these events have an apparent velocity of about 8.14 km/s.

In Fig. 4, super-critical reflections are identified from two horizons, one from a

mid-crustal horizon (Pc) and another from the crust–mantle boundary (PmP). The travel-time branch for the latter phases should be asymptotic to that for the Pn phases near the critical distance which must therefore be at 100–120 km. There are prominent events identified on the records 1.0–2.5 s after the Pg phases in the distance range 60–100 km. The apparent velocity of these events is about 6 km/s beyond 150 km and is about 7 km/s between 60 and 80 km. The prominence of these phases lends support to the argument for the existence of a pronounced mid-crustal horizon. These phases have here been labelled Pc, although sometimes such a nomenclature is used only for horizons in the upper crustal basement.

The Pg and Pn refracted phases and the Pc and PmP reflected phases are the principal phases used in the interpretation of the long-line seismic data from the Eromanga Basin. Although all these phase cannot always be seen in the record sections illustrated in this paper, it must be emphasised that alternative presentations from high-gain records with different normalizing and filtering factors have also been used in arriving at the prefered phase correlations for subsequent modelling studies.

TEREBOOKA TO CHEEPIE

Figure 5a shows the complete record section from shots fired at Terebooka and recorded eastward to Cheepie. The traces are all low gain records at 72 dB gain setting and filtered in the bandpass 4–16 Hz. Trace amplitudes have been normalized for distance (D) using a factor 1/D.

Strong first arrivals form a forward travel-time branch between 10 and 120 km (Fig. 5, *A–B*). Linear regression of the time–distance data give an apparent velocity, intercept and RMS residual travel-time of 5.82 ± 0.03 km/s, 1.63 ± 0.07 s and 0.09 s respectively. This apparent velocity is taken to be that of the Pg phase within the Thomson Fold Belt below basin cover rocks.

In the distance range 60–120 km there are strong later arrivals 1–3 s after the first arrivals and these are interpreted as being Pc phase reflections from a mid-crustal horizon. A forward travel-time branch is evident from below this horizon in the range 60–210 km with an apparent velocity of about 6.9 km/s (Fig. 5, *C–D*). Beyond 120 km there is another series of prominent arrivals with an apparent velocity of about 6 km/s (Fig. 5, *M–N*). These are interpreted as being either wide-angle reflections from-the mid-crustal horizon or as channel waves within the upper crust.

Beyond 125 km prominent first arrivals on the high-gain were recorded out to a distance of about 300 km, the limit of the traverse (Fig. 5, *E–F*). These are interpreted as upper mantle arrivals (Pn). When all arrivals are fitted to a least squares straight line, the apparent velocity, intercept and RMS residual are 8.16 ± 0.06 km/s, 8.49 ± 0.20 s and 0.22 s respectively. If the data recorded in the Warrabin Trough (139–162 km) and the Quilpie Trough (215–245 km) are adjusted

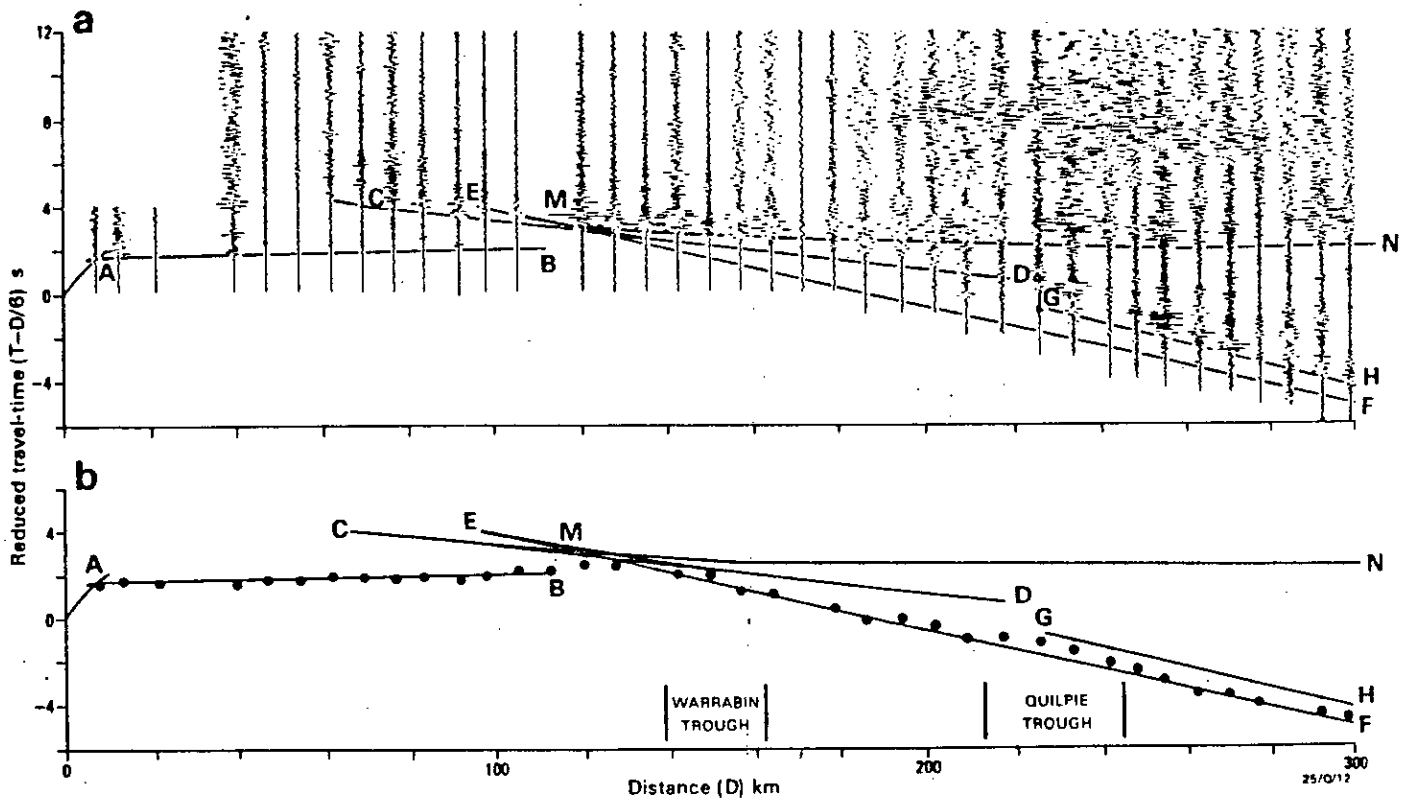

Fig. 5. a. Seismic record section for shots at Terebooka (shot point 1) recorded eastwards towards Cheepie. The trace amplitudes are normalized for (1/distance). b. First-arrival data and travel-time curve derived from the prefered velocity/depth model (a) shown in Fig. 6 and tabulated in Table I.

because of delays introduced by thick basin sediments, the apparent velocity, intercept and residual are 8.14 ± 0.04 km/s, 8.31 ± 0.12 s and 0.12 s respectively. If the velocity represents the upper mantle velocity and a spherical Earth correction is applied (Mereu, 1967), the upper mantle velocity reduces to 8.10 km/s.

Beyond 220 km prominent subsequent arrivals occur up to 1.5 s after the Pn first arrivals (Fig. 5, *G–H*). These are interpreted as being reflections from a sub-Moho horizon. Their apparent velocity is about 8.5 km/s but this is not well controlled.

These features of the seismic record section were modelled by iterative ray tracing using a computer program which assumes horizontal layering. The preferred model is listed in Table I and illustrated in Fig. 6a.

The character and relative amplitudes of the events must also be considered when refining the preferred model. Amplitude features were modelled using the REFLEX program described by Fuchs (1968) and the synthetic seismograms for two important examples of velocity/depth features are shown in Fig. 7. To establish strong reflections at mid-crustal levels and the forward travel-time branch *C–D* a step increase in velocity is interpreted at 26 km depth. This is illustrated in Fig. 7a where

TABLE I

P-wave velocity/depth models for profiles (a) Terebooka to Cheepie, (b) Tallyabra to Terebooka, (c) Cheepie to Terebooka, and (d) Tallyabra to Cheepie. A spherical Earth correction has been applied.

(a)		(b)		(c)		(d)	
depth (km)	velocity (km/s)	depth (km)	velocity (km/s)	depth (km)	velocity (km/s)	depth km)	velocity (km/s)
0.0	2.20	0.0	2.00	0.0	2.00	0.0	2.00
0.6	2.50	0.5	2.30	0.5	2.60	0.6	2.60
2.7	3.90	2.1	3.70	1.4	3.70	2.4	4.20
2.8	5.35	2.2	5.00	1.5	5.40	2.5	5.10
3.5	5.85	3.5	5.40	5.0	5.90	5.5	5.90
7.0	5.90	7.0	5.75	11.5	6.10	9.5	6.10
8.0	5.70	8.5	5.77	12.6	5.90	10.0	5.60
17.0	5.72	8.6	5.60	21.5	5.95	24.0	6.40
24.0	6.30	13.0	5.62	21.6	6.40	34.0	6.90
24.1	6.90	22.5	6.30	28.0	6.50	34.1	7.70
28.0	6.91	22.6	6.70	30.0	6.65	35.0	7.72
30.0	7.04	30.0	7.10	37.5	7.10	37.7	7.20
36.0	7.70	36.0	7.70	41.0	8.15	39.5	7.21
36.4	8.15	36.4	8.15	50.0	8.20	40.0	8.15
45.0	8.17	45.0	8.20	51.0	7.70	50.0	8.20
46.0	7.85			56.0	7.75		
55.0	7.90			57.0	8.35		
56.0	8.35			80.0	8.37		
80.0	8.37						

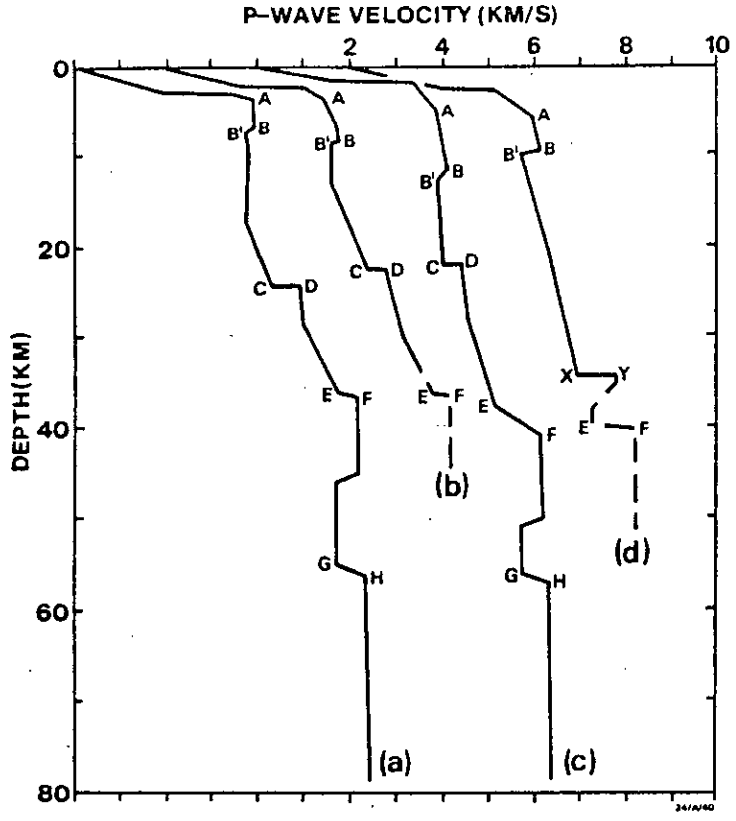

Fig. 6. Velocity/depth models derived from (a) Terebooka shots recorded towards Cheepie, (b) Tallyabra shots recorded towards Terebooka, (c) Cheepie shots recorded towards Terebooka, (d) Tallyabra shots recorded towards Cheepie.

synthetic seismic records show the combined effect of large amplitude Pc and PmP phases in the distance range 110–160 km. The Pc phases are evident at reduced amplitude back to the cusp point *C* at about 60 km.

The lower crustal velocity increases with depth until 36 km. There the Moho is represented by a strong velocity gradient and the upper mantle velocity of 8.15 km/s is reached at 36.4 km depth. Below the Moho an increase in velocity from 7.75 to 8.35 km/s is interpreted at 56 km depth below a low velocity zone to account for the travel-time branch *G–H* (Fig. 5). This latter feature was modelled using synthetics and is illustrated in Fig. 7b. There is no control on the minimum velocity and depth extent in the low-velocity zone, but a time delay between the Pn phases and the sub-Moho reflections must be introduced and 7.75 km/s perhaps represents the least velocity likely in the upper mantle.

CHEEPLE TO TEREBOOKA

The record section for shots fired at Cheepie recorded towards Terebooka is shown in Fig. 8a. As in Fig. 5a, mostly low-gain records were used to compile the record section so that the character of the large amplitude later arrivals can be illustrated. Filtering and distance normalizing are the same as in Fig. 5. The first arrivals determined from the high gain records are indicated in Fig. 8b.

The travel-time branch *A–B* (Fig. 8) results from Pg refracted waves in the basement Thomson Fold Belt rocks with an apparent velocity, intercept and RMS residual of 5.95 ± 0.02 km/s, 1.28 ± 0.04 s and 0.06 s respectively when the arrivals from the Quilpie Trough area are corrected for basin morphology. The character of the first arrivals changes at about 95 km from impulsive to emergent arrivals and the *A–B* branch terminates at about 120 km. Strong subsequent arrivals in the distance range 70–120 km (near *C*, Fig. 8) are interpreted as Pc reflections from a mid-crustal horizon. The forward branch *C–D* (Fig. 8) is evident out to about 210 km.

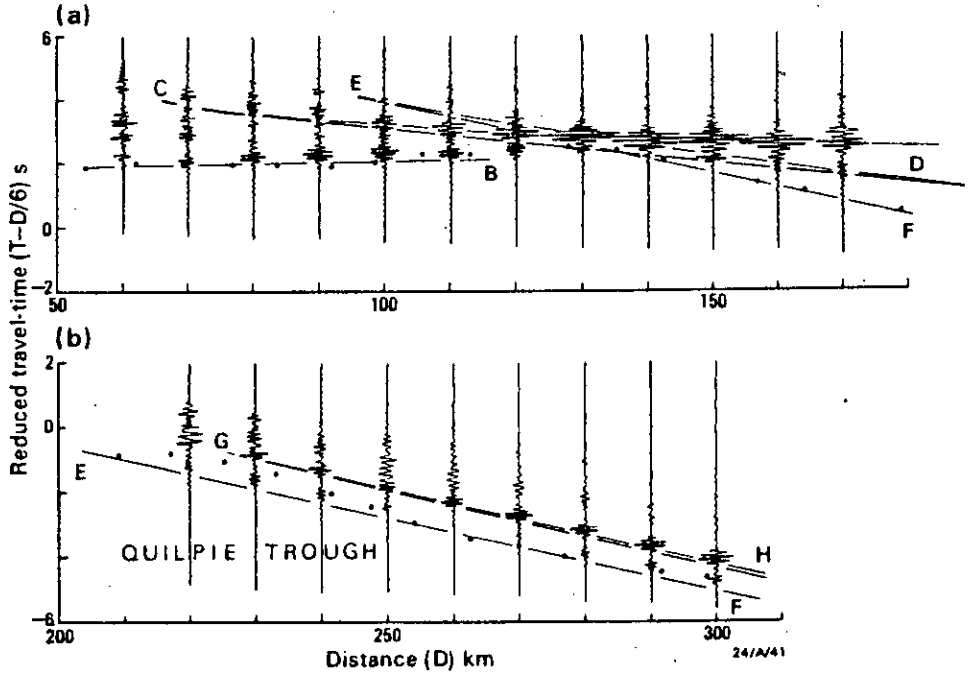

Fig. 7. Representative synthetic record sections illustrating velocity/depth features: (a) the upper/middle crust velocity distribution from a Terebooka shot recorded towards Cheepie; (b) the sub-Moho velocity distribution from a Terebooka shot recorded towards Cheepie. The observed first arrivals are indicated by dots. The travel-time curves are from the models in Table 1. Letters indicate the travel-time branches in Fig. 5.

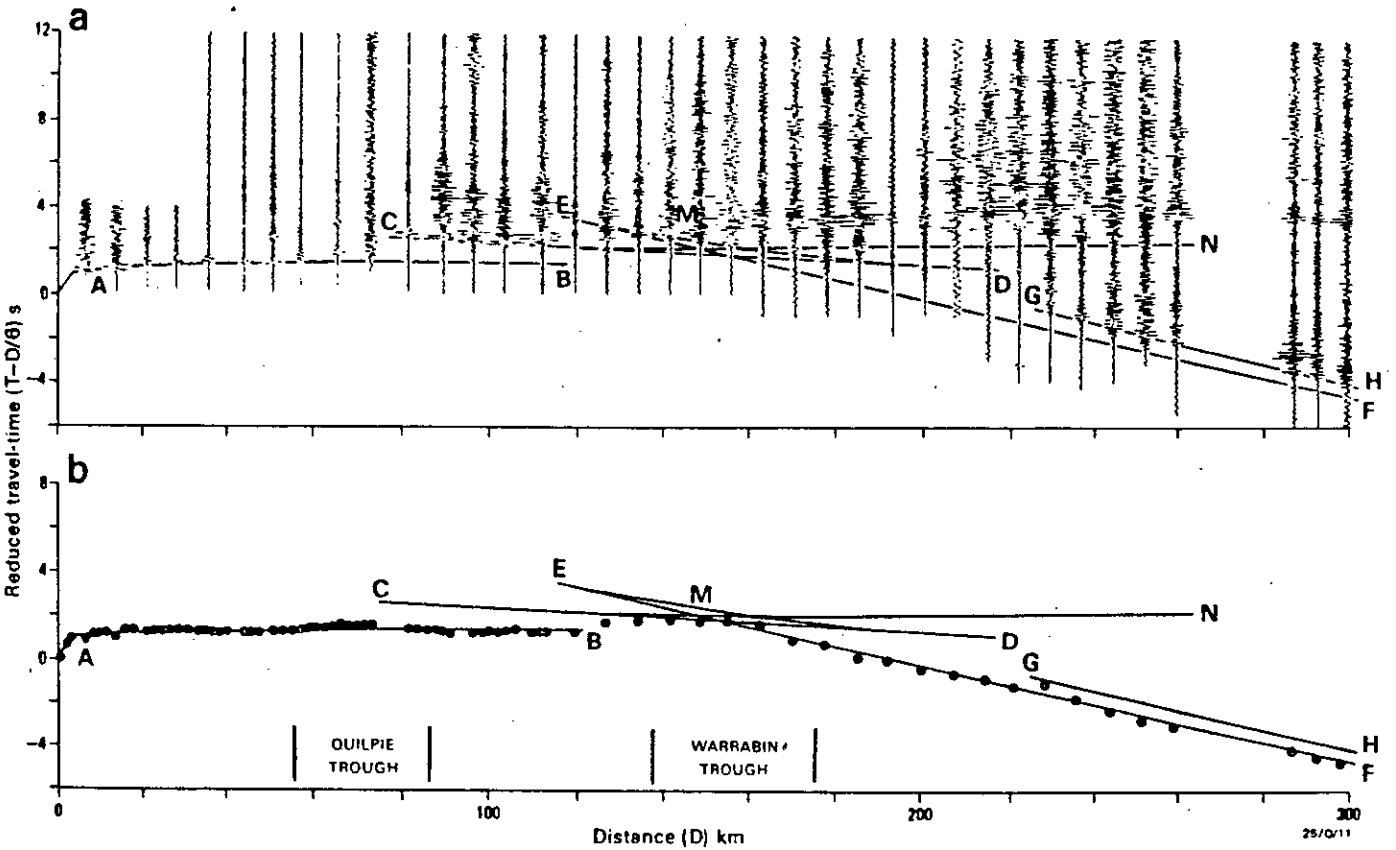

Fig. 8. a. Seismic record section for the shots at Cheepie (shot point 9) recorded westward towards Terebooka. The trace amplitudes are normalized for (1/distance). b. First arrival data and travel time curve derived from the prefered velocity/depth model (c) in Fig. 6 and tabulated in Table I.

The PmP reflection phase from the crust/mantle boundaries is evident at distances of 130–160 km and the cusp point for super-critical reflections must be about 120 km.

Upper mantle Pn refractions occur along the travel-time branch E–F (Fig. 8). They have an apparent velocity, intercept and RMS residual of 8.25 ± 0.04 km/s, 8.97 ± 0.15 s and 0.11 s respectively. After a spherical Earth correction is applied the velocity reduces to 8.20 km/s. When these data are combined with the reverse data from Terebooka shots the upper mantle velocity, with a spherical Earth correction applied, is determined as 8.15 ± 0.04 km/s, there being a small dip on the Moho from west to east.

Subsequent arrivals at distances greater than 220 km indicate that there is evidence for a travel-time branch G–H (Fig. 8) resulting from a phase reflected from

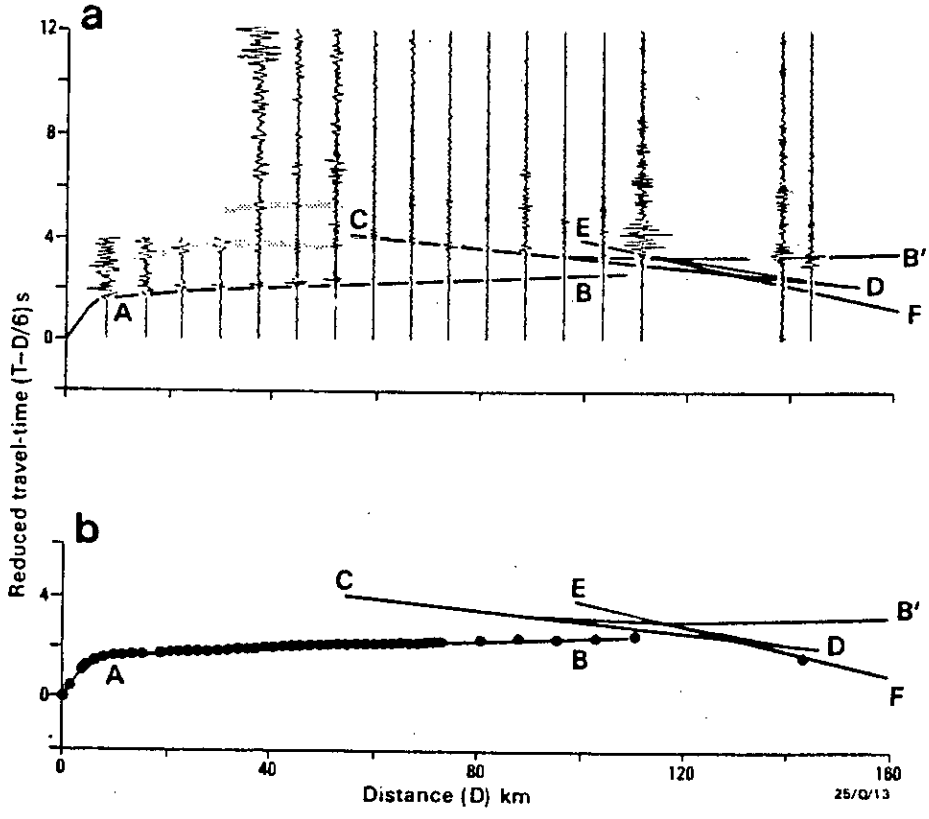

Fig. 9. a. Seismic record section for shots at Tallyabra (shot point 5) recorded westward towards Terebooka. Shaded areas indicate multipli-reflected/refracted arrivals from within the sediment–basement boundary region (after Lock, et al., 1982). The trace amplitudes are normalized for (1/distance). b. first-arrival data and travel-time curve derived from prefered velocity/depth model (b) in Fig. 6 and tabulated in Table I.

a sub-Moho horizon. As with the same phase recorded from the Terebooka shots, the amplitude of the arrivals and the distance range over which it is recorded lends support to the preferred interpretation that a strong velocity increase is present at sub-Moho depths. The only way that this can be modelled without unreasonably high upper mantle velocities being used is to incorporate a low-velocity zone.

The preferred velocity/depth model was derived by modelling both the travel-time and amplitude data from the record section. The principal features of the synthetic seismograms are similar to those from the reversed profile which are illustrated in Figs. 7a and b. The preferred velocity/depth model from the Cheepie shots is illustrated in Fig. 6 (model c) and listed in Table I.

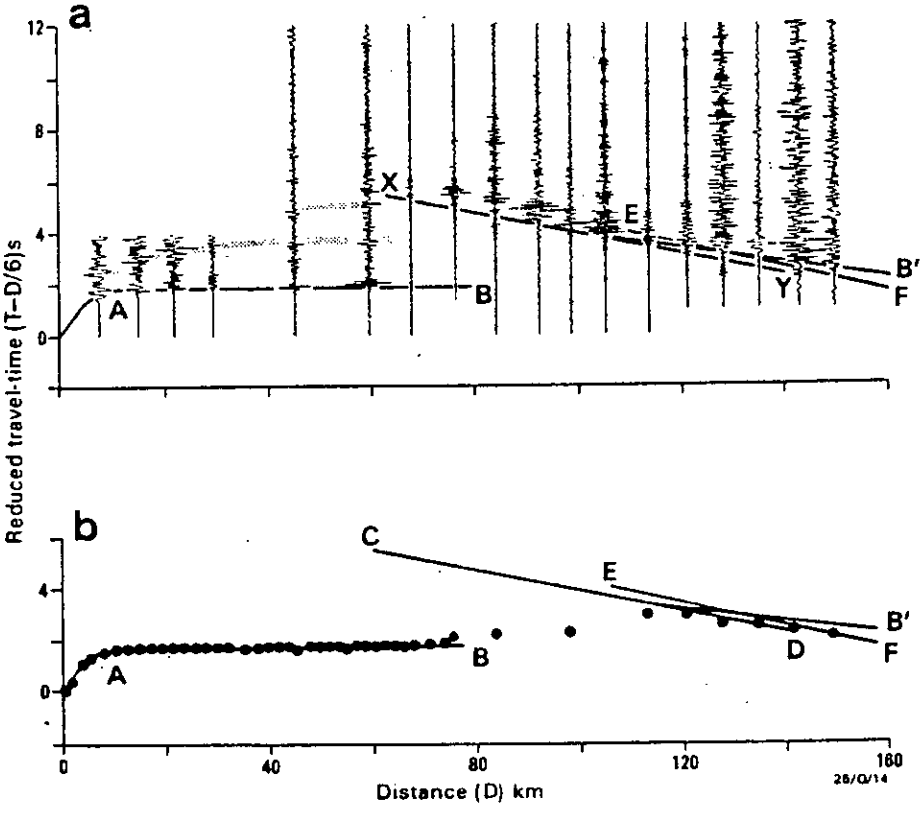

Fig. 10. a. Seismic record sections for shots at Tallyabra (shot point 5) recorded eastward towards Cheepie. Shaded areas indicate multiple-reflected/refracted arrivals from within the sediment–basement boundary region (after Lock et al., 1982). The trace amplitudes are normalized for (1/distance). b. First-arrival data and travel-time curve derived from the prefered velocity/depth model (d) in Fig. 6 and tabulated in Table I.

TALLYABRA TO TEREBOOKA

Shots were fired at the centre point of the 300 km traverse (Tallyabra) to enable mid-crustal structure to be interpreted from reversed seismic refraction profiles. The seismic record section from Tallyabra to Terebooka, is shown in Fig. 9a together with the travel-time curve for the prefered velocity/depth model. The trace normalizing and filtering in Fig. 9a are the same as for Figs. 5a and 8a.

The principal features of the record which control the velocity/depth model are as follows. Strong Pg first arrivals are evident on travel time branch $A-B$ (Fig. 9); these extend out to a distance of about 100 km. A Pc travel-time branch $C-D$ (Fig. 9) is also prominent on the record section. The method of deriving the velocity structure was the same as for previous traverses. The prefered velocity/depth model is shown in Fig. 6 (model b) and listed in Table I. The model for the lower crust is taken from that derived from the shots at Terebooka. The large amplitude event at 110 km is interpreted as being a PmP reflection near the cusp point with Pn phases.

The shaded regions in Fig. 9a at distances less than 50 km indicate some of the arrivals which are interpreted by Lock et al (1983) as multiple underside reflections of the Pg phase from the surface. These have assisted considerably in constraining the velocity models at depths less than 8 km.

TALLYABRA TO CHEEPIE

The seismic record section from Tallyabra to Cheepie is shown in Fig. 10a. The trace normalization and filtering are the same as those for Figs. 5a, 8a and 9a. There are major differences between this record section and the sections from other shots, namely the prominent arrivals along travel time branch $X-Y$ (Fig. 10) and the lack

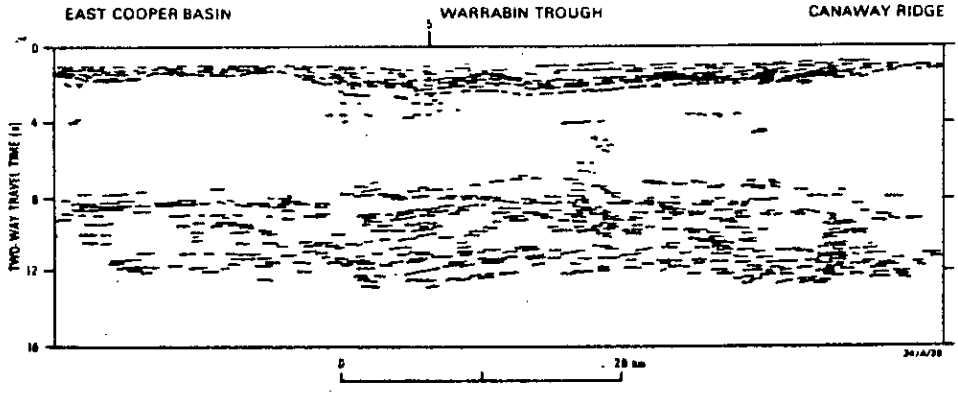

Fig. 11. Schematic deep vertical seismic reflection profiling record from the central part of the $A-B$ traverse near Tallyabra (after Mathur, 1983a, b).

of a travel-time branch with an apparent velocity of about 6.65–6.9 km/s. In Fig. 10 the $X-Y$ travel-time branch has a poorly determined apparent velocity of about 7.7 km/s at point X and the events are interpreted as being super-critical reflections from a deeper, lower-crustal horizon. It is therefore evident that the mid-crustal structure east of Tallyabra is markedly different from that to the west. The method of deriving the velocity structure was the same as for previous traverses. A prefered velocity/depth model derived from the record section is shown in Fig. 6 (model d) and listed in Table I.

The $X-Y$ branch of the travel-time curve (Fig. 10) is interpreted as being from a prominent horizon in the lower crust at 34 km depth. The possibility of the arrivals being from a rapidly shallowing mid-crustal horizon was considered. The $X-Y$ branch persists over a distance of at least 80 km. If a velocity ratio of 6.3/6.9 is assumed in the middle crust, a shallowing of over 8 km is required, assuming the events are reflections from a shallowing horizon. The magnetotelluric results of Spence and Finalyson (1983) and the seismic reflection data of Mathur (1983a) do not substantiate a major shallowing feature over any great distance, in the upper/middle crust. Also the gravity difference between the Warrabin Warrabin Trough and the Canaway Ridge is about 150 $\mu m/m^2$ and this is accounted for by the basin structure in the upper 10 km of crust. Hence a major shallowing feature at mid-crustal depths is inconsistent with the observed gravity field (Antiloff, pers. commun.).

The prefered interpretation is that the Canaway Ridge is tectonically different from the surrounding region, that no major mid-crustal horizon exists under it at a depth of about 22–24 km, but that the major ($X-Y$) reflections come from a deeper horizon. Prominent reflections with an apparent velocity of about 6.3 km/s from the reverse profile from Cheepie towards Terebooka cut out at about 120 km, consistent with the disappearance of the mid-crustal horizon under the Canaway Ridge. The prefered velocity/depth model shown in Fig. 6 (model d) and listed in Table I has a prominent horizon at 34 km depth. This horizon is difficult to distinguish from the crust–mantle boundary because PmP reflections from a Moho at the same depth as that in Fig. 6 model c would have large amplitudes virtually coincident with the $X-Y$ travel-time branch. The travel-time curve from the prefered model is shown in Fig. 10b. It seems probable that events on the $X-Y$ travel-time branch are PmP phases and therefore the crust/mantle boundary under the Canaway Bridge is shallower than that under the surrounding region.

SEISMIC REFLECTION PROFILING

Six-fold CDP continuous seismic reflection profiling, with recording times to 20 s, was conducted along a line coincident with the refraction line east of shot point 2 (Fig. 2). This was part of 1400 km of continuous seismic reflection profiling conducted by BMR in the central Eromanga Basin in the period 1980–1982. Mathur

(1983a) has interpreted part of this data and Fig. 11 is a simplified line diagram of the essential features of the record section between shot points 2 and 5 (Fig. 2).

Four zones have been described by Mathur (1983a). The uppermost zone is that from 0 to 2 s two-way-time (TWT) and is identified with the sedimentary sequences shown in Fig. 3. The zone between 2 and 8 s TWT is largely devoid of reflections and includes rocks of the Thomson Fold Belt. In the zone between about 8 and 12.5 s two-way reflection time there are discontinuous sub-horizontal reflections (Mathur, 1983a). This zone is in marked contrast to the almost reflection-free zone in the upper crust. King and Falvey (1977) reported a more limited burst of energy at 11–12 s two-way reflection time from a region farther north in the Eromanga Basin but the areal extent of their survey was not as extensive as the BMR work. However, the lower depth limit of their reflections (about 12 s) is in broad agreement with the B.M.R. profiling data. Below 12.5 s TWT there are very few reflections. This zone corresponds to the upper mantle.

TECTONIC SETTING OF THE CENTRAL EROMANGA BASIN

The Palaeozoic tectonic models envisaged for the survey region vary. Kirkegaard (1974) sees the development of the Thompson Fold Belt underlying the Eromanga Basin being associated with a continental margin which graded to an oceanic crust at its eastern limit, the deepest Cambrian sediments being deposited in a deep marine environment. Cook (1982) also indicates the edge of the Late Cambrian (510–520 m.y.B.P.) continental margin as being west of the seismic survey area. Harrington (1974, 1983) envisages the region of the survey being part of a small ocean basin or back-arc marginal sea (Barcoo Marginal Sea) analogous to the Sea of Japan. Henderson (1980) has suggested that Precambrian rocks form the basement under the whole of the Eromonaga Basin to as far east as the Bowen Basin (Fig. 1), based on the possibility that cratonised Proterozoic crust may be identified in the Lolworth–Ravenswood Block. Such crust, however, could also be interpreted as Precambrian cratonic fragments rifted from the Palaeozoic continental margin (Harrington, 1974).

Doutch and Nicholas (1978) have outlined the development of the Phanerozoic sedimentary basins of Australia. The region of the seismic interpretation is described in terms of internal (intracratonic) basins which developed at the end of orogenic transformation of the region into a craton. Veevers et al. (1982) envisage a convergent plate margin in the region during the early Palaeozoic and the region being cratonised through marginal sea opening and filling behind an island arc. The basement rocks found in drillholes in the region of the seismic work are phillite, schist, basalt, granite, mica quartz, hornblende granodiorite, slate, siltstone, shale, basaltic andesite, and greywacke (Rumph, 1978). Hence Veevers et al. (1982) see the region as being part of a pericratonic basin whose development began with partial continental breakup around 570 m.y.B.P. and included the Amadeus Basin region in

central Australia and island arc convergent tectonics in the east.

At the elevations flown by the MAGSAT satellite the Eromanga Basin stands out as being a distinct negative anomaly contrasting with the positive anomalies identified with the adjacent Precambrian areas (Frey, 1982). In the north, outcrops of the Thomson Fold Belt rocks occur in the Early Palaeozoic Lolworth–Ravenswood Block and the Anakie Inlier; the Precambrian Georgetown Inlier is to the north of these outcrops. In the west, the Precambrian rocks of the Mount Isa Geosyncline are partly concealed under the Georgina Basin but the limits of the Geosyncline are well defined by the Diamantina Gravity Gradient and the Winton–Machattie Magnetic Lineament as described by Rumph (1978). To the south, Precambrian rocks crop out in the Adelaide Geosyncline and on the flanks of the Bancannia Trough.

The southeast–east boundary of the Thomson Fold Belt is taken by Murray and Kirkegaard (1978) to be the gravity boundary defined by Wellman (1976) where the north-northwest trends of the Lachlan Fold Belt contrast with the northeast trends of the Thomson Fold Belt. This corresponds with the Nebine Arc of Harrington (1974, 1983) and the Nebine Regional Gravity High of Fraser (1976) which is a continuation southwestward of the Anakie Regional Gravity Ridge.

Thus, prior to this seismic survey , there are quite a few geological as well as geophysical indications that the central Eromanga Basin crustal structure contrasted with its surrounding tectonic provinces.

SEISMIC FEATURES OF THE LITHOSPHERE

The upper crust

The sedimentary sequence down to depths at which velocities of 5.0–5.5 km/s are reached is thicker under the western end of the line (in excess of 2.1 km) than under the eastern shelf and ridge areas (1.5–1.8 km). In the Warrabin and Quilpie Troughs up to 3.8 km of Devonian sediments underlie the Eromanga sequence (Pinchin and Senior, 1982). Beneath the sedimentary sequence basement rocks in Mt. Howitt No. 1 well and GSQ Eromanga No. 1 well on the western side of the Canaway Ridge penetrated Ordovician shales and low grade metamorphic sandstones/shales at 2.1 and 1.2 km depth respectively. Murray and Kirkegaard (1978) consider that terrigenous clastics which have been metamorphosed to slate, phyllite, quartzite and schist form the basement under most of the region and that they are most probably of Cambrian and Ordovician age. From the seismic refraction work basement velocities increase to about 5.8–5.9 km/s in the west and to 6.1 km/s in the east before decreasing to a value taken to be not less than 5.7 km/s at depths of greater than 8 km.

There are a number of explanations for such decreases in velocity. Christensen (1979) has listed (1) high temperature gradients, (2) quartz alpha–beta transition, (3) increased fluid pressure in rock pores (4) low-velocity granite plutons, (5) partially

molten rocks, and (6) extensive hydration (serpentinisation), as possible causes of low velocity zones. Because of the widespread occurence of crustal low-velocity zones kern (1979, 1982) considers the alpha–beta quartz solid–solid phase transition to be the likely cause of velocity decreases in the crust. The Sass and Lachenbruch (1979) geotherm for the region indicates temperature of 500°C may be reached at depths as shallow as 15 km and consequently decreases of up to 0.4 km/s can be expected in quartzites, granulites and granites. Christensen (1979) has commented that, even allowing for the effect of pressure on velocities, crustal velocity inversions produced, in part, by high temperatures are likely to be common within the crust.

The lack of seismic reflectors within the upper crustal basement could imply a plutonic origin, however, Spence and Finlayson (1983) have argued against this interpretation based on magnetotelluric data from along the seismic traverse. It is therefore likely that the upper crust is composed of highly deformed rocks which do not present any acoustic impedence contrasts across sub-horizontal surfaces amenable to detection by vertical seismic sounding at wavelength greater than 100 m but whose velocity/depth distribution is being influenced by temperature gradients. The resistivity values interpreted by Spence and Finlayson (1983) are consistent with the basement being predominantly tightly folded, meta-sedimentary and meta-volcanic rocks.

THE MIDDLE-LOWER CRUST

At depths of 21–24 km there is a prominent increase in P-wave velocity which results in wide-angle reflections on all record sections except that eastward from Tallyabra. The wide-angle reflections from the mid-crustal horizon are a feature of the record sections which has not been conspicuous in other regions of Australia except, to a lesser degree, under the Pilbara craton (Drummond, 1981). The velocities in the lower crust below the mid-crustal horizon are in the range 6.4–7.7 km/s with the velocity at the western end of the line interpreted as being about 0.5 km/s greater than at similar depths to the east under the Cheepie Shelf area. The most distinguishing feature of the lower crust with respect to the upper crust is the numerous sub-horizontal reflections from within the lower crust on seismic reflection profiling records.

The interpreted depth of the mid-crustal horizon is a function of the velocity in the over-lying crust. The velocity in the sediments and upper crustal basement is well determined from seismic refraction and reflection profiling. However, the minimum velocity in the low-velocity region (Fig. 6, *B'C*) is not known with any certainly. A conservative estimate has been made that the velocity will not be less than 0.2 km/s lower than the basement velocity. This estimate is based on likely geothermal gradients the likely bulk compositions in the upper crust. The velocity increase at the mid-crustal horizon controls the cusp point *C* in the record sections so there are some limits to the likely velocity distributions within the low velocity region. The

prefered model contains one simple distribution which adequately satisfies the observed data. The distribution also satisfies the reflection profiling data where the lower-crustal reflections start at about 8 s TWT. However, even within these constraints the mid-crustal horizon can be modelled almost anywhere in the depth range 20–25 km.

The P-wave velocities in the lower crust are difficult to interpret in terms of rock type. Green and Lambert (1965) have pointed out that such velocities can be reached by rocks of granitic composition metamorphosed to granulite facies. For higher velocities some increase in mafic content is necessary under anhydrous conditions (Drummond, 1982). Drummond has argued that basic rocks have velocities which would be much higher than the observed 6.3–7.7 km/s and also the velocities in acid rocks would be much too low at lower crustal depths. Hence at intermediate composition is implied (Green, 1970). Green and Lambert (1965) have pointed out that increasing garnet content in anhydrous rocks of granitic metamorphosed to eclogite facies increases velocities to those typically observed in the lower crust. However under hydrous conditions, amphibolite facies rocks also could be have similar velocities. Hence, under the Eromanga Basin, the competing effects of increasing mafic content and higher metamorphic grade are not resolved.

The nature of the multiple discontinuous reflection horizons in the lower crust suggests a mechanism of formation akin to magma intrusion/underplating or the influence of metamorphic "fronts". However, it is difficult to resolve these mechanisms without geological control from, say, xenoliths brought to the surface in later episodes of volcanism.

THE CRUST–MANTLE BOUNDARY AND UPPER MANTLE

The Moho is taken to be the depth at which a velocity of 8.15 km/s is reached. Wide angle reflections are less prominent than those from the mid-crustal horizon, indicating that the velocity gradient is less at the Moho; a gradient over a depth range of 1–4 km is interpreted. The depth of the Moho is 36 km deep in the west and 41 km deep in the east. The accuracy with which the depth to the crust–mantle boundary can be determined is dependent on the velocity distribution in the crustal and this is not uniquely determined. Bessonova et al. (1974), Orcutt et al. (1980) and others have discussed the problems of placing bounds on the velocity/depth estimates from travel-time data. However, the formal bounds so obtained are often so wide that it is difficult to use the information in any form of geological/tectonic interpretation. Some estimate of the precision of the calculated depths to the crust–mantle boundary in the Eromanga Basin can be gauged from the standard deviation (SD) values of the Pn velocity and intercept, 0.11–0.12 km/s and 0.12–01.15 s respectively. Using an average crustal velocity to a depth of 38.5 km, the depth uncertainty is about 2km at the two SD level.

As mentioned earlier the crust–mantle boundary under the Canaway Ridge is

different from that under the surrounding region. The boundary there seems to be much sharper and at a depth of about 34 km, i.e. 4–5 km shallower than the average for the region. The shallowing of the Moho under the Canaway Ridge is in agreement with the shallowing of upper crustal seismic and magnetotelluric features and the Ridge could therefore be interpreted as a major horst structure extending at least to Moho depths. The different intra-crustal velocity structure from the surrounding region could also indicate development in a different tectonic episode.

There are few reflecting horizons evident at greater than 12.5 s TWT on the seismic reflection profiling records (Fig. 11). Thus the principal seismic feature of the upper mantle is the velocity increase at depths of 56–57 km below a low-velocity zone. This seems to indicate that there are broad-scale velocity features in the upper mantle which do not have related short wavelength impedance contrasts detectable by reflection methods.

DISCUSSION

The lithospheric structure of the Eromanga Basin determined from the seismic work highlights the contrast between the region and its surrounding tectonic provinces. The upper mantle velocity immediately below the crust–mantle boundary under the Eromange Basin is 8.15 ± 0.04 km/s. Under the North Australian Craton, northwest of the present survey area, Finlayson (1982) interpreted upper mantle velocities between Tennant Creek and Mount Isa of 8.16–8.23 km/s at 50–55 km depth increasing to 8.29 km/s at 61 km depth. The upper mantle velocity under the central Eromanga Basin is therefore slightly lower but the depths to this velocity are, on average 14 km shallower than under the North Australian Craton.

Southeast of the survey area, under the Lachlan Fold Belt, the crustal thickness is about 43 km and the upper mantle velocity is in the range 7.95–8.05 km/s (Finlayson et al., 1979; Finlayson and McCracken, 1981). Farther south the crustal thickness increases to over 50 km. Thus the crustal thickness under the Lachlan Fold Belt is, on average, at least 5 km thicker than under the central Eromanga Basin.

To the east of the present survey area Collins (1978), Leven (1980) and Cull and Riesz (1972) have interpreted seismic refraction data to obtain crustal models. Under the Drummond Basin just to the west of the Anakie regional gravity ridge (Fig. 1), Cull & Riesz (1972) recorded very limited refraction and reflection data and interpreted a crustal thickness of between 33 and 40 km using velocities of 6.01, 6.75 and 8.00 km/s for the upper crust, lower crust and upper mantle respectively.

More detailed, reversed, refraction data have been interpreted by Collins (1978) along the axis of the Bowen Basin (Fig. 1). He interpreted a Moho depth ranging from 35 km in the north to 37 km in the south of the Basin using a crustal velocity model of 4.00–5.53 km/s for the sedimentary sequence overlying an upper crust with velocity of 6.39 km/s and a lower crust with velocity of 7.07 km/s. The upper mantle velocity was interpreted as 8.10 ± 0.11 km/s.

In the southern part of the Bowen Basin Leven (1980) derived his CQEW model. The weak refracted arrivals from the Moho at 32 km are designated Pn(1) by Leven and the much stronger arrivals 1–2 s later from the 42–48 km zone recorded at distances beyond 220 km are designated Pn(2) (Leven, 1980; Fig 3.11). However, the data were recorded on cross-strike, unreversed, profiles and therefore the crustal thickness of 35–34 km obtained by Collins (1978) seems better controlled. The Pn(2) arrivals detected by Leven have characteristics similar to the *G–H* arrivals recorded in the Eromanga Basin and a similar interpretation is prefered. Thus there does not appear to be any great difference in crustal thickness or upper mantle velocity between the Eromanga Basin region and the tectonic provinces to the east of it.

Within the crust there are also seismic features which contrast the Eromanga region with surrounding provinces. The mid-crustal horizon is not a conspicuous feature in the crust of the North Australian Craton, Lachlan Fold Belt or Bowen Basin although there are less prominent velocity increases at mid-crustal depths (Finlayson, 1982; Finlayson McCrackan, 1981; Collins, 1978). Seismic reflection profiling, too, contrasts the Eromanga crust with other regions. Pinchin (1980), Collins (1983) and Mathur (1983b) have shown that there are many significant reflecting horizons in the upper-crustal basement of the Lachlan Fold Belt, McArthur Basin region of the North Australian Craton, the Drummond and Georgina Basins and the Denison Trough. Hence the conspicuous lack of horizons between 2 and 8 s TWT on Eromanga profiling records is a noteable feature.

Beneath the crust–mantle boundary the velocity structure under the Eromanga Basin requiring a velocity increase at depths less than 80 km is not unusual in continental Australia. Leven (1980), Finlayson and McCracken (1981), and Finlayson (1982) and Drummond (1983) have all interpreted sub-crustal velocity increases. Velocity reductions in the upper mantle are also interpreted for the lithosphere under parts of Europe (Fuchs, 1979). However in Australia the data are too sparse to draw any general conclusions about upper mantle structure.

ACKNOWLEDGEMENTS

The author wishes to acknowledge the major contribution to this investigation by the B.M.R. field seismic crew and by Chris Rochford in particular. Surendra Mathur is thanked for discussions on his unpublished interpretations. This paper is published with the permission of the Director, Bureau of Mineral Resources, Geology and Geophysics, Canberra.

REFERENCES

Bessonova, E.N., Fishman, V.M., Ryaboyi, V.Z. and Sitnikova, G.A., 1974. The tau method for inversion of travel times. I. Deep seismic sounding data. Geophys. J.R. Astron. Soc., 36: 377–398.

Christensen, N.I., 1979. Compressional wave velocities in rocks at high temperatures and pressures, critical thermal gradients, and crustal low velocity zones. J. Geophys. Res., 84: 6849–6859.

Collins, C.D.N., 1978. Crustal structure of the central Bowen Basin, Queensland. Bur. Miner. Res., J. Aust. Geol. Geophys., 3: 203–209.

Collins, C.D.N., 1983. Crustal structure of the southern McArthur Basin from deep seismic sounding. Bur. Miner. Resour. J. Aust. Geol. Geophys., 8,19–34.

Collins, C.D.N. and Lock, J., 1983. A seismic refraction study of the Quilpie Trough and adjacent basement highs, Eromanga Basin, Queensland, Australia. Tectonophysics, *100, in press.*

Cook, P.J., 1982. The Cambrian palaeogeography of Australia and opportunities for petroleum exploration. Aust. Pet. Explor. Assoc. J., 22 (1): 42–64.

Cull, J.P. and Riesz, E.J., 1972. Deep crustal seismic reflection/refraction survey between Clermont and Charters Towers, Queensland 1971. Bur. Miner. Resour. Aust., Rec. 1972/97.

Doutch, H.F. and Nicholas, E., 1978. The Phanerozoic sedimentary basins of Australia and their tectonic implications. Tectonophysics, 48: 365–388.

Drummond, B.J., 1981. Crustal structure of the Precambrian terrains of northwest Australia from seismic refraction data. Bur. Miner. Resour., J. Aust. Geol. Geophys., 6: 123–135.

Drummond, B.J., 1982. Seismic constraints on the chemical composition of the Pilbara Craton, northwest Australia. Proc. Int. Symp. on Archaean and Early Proterozoic Evolution and Metallogenesis, Salvador, Brazil, September 1982.

Drummond, B.J., 1983. Detailed seismic velocity/depth models of the upper lithosphere of the Pilbara Craton, northwest Australia. Bur. Miner. Resour., J. Aust. Geol. Geophys., 8, 35–51.

Finlayson, D.M., 1982. Seismic crustal structure of the Proterozoic North Australian Craton between Tennant Creek and Mount Isa. J. Geophys. Res., 87: 10569–10578.

Finlayson, D.M. and Collins, C.D.N., 1980. A brief description of BMR portable seismic tape recording systems. Aust. Soc. Explor. Geophys., Bull, 11: 75–77.

Finlayson, D.M. and McCracken, H.M., 1981. Crustal structure under the Sydney Basin and Lachlan Fold Belt determined from explosion seismic studies. J. geol. Soc. Aust., 28: 177–190.

Finlayson, D.M., Prodehl, C. and Collins, C.D.N., 1979. Explosion seismic profiles and implications for crustal evolution in southeastern Australia. Bur. Miner. Resour., J. Aust. Geol. Geophys., 4: 243–25.

Fraser, A., 1976. Gravity provinces and their nomenclature. Bur. Miner. Resour., J. Aust. Geol. Geophys., 1: 351–352.

Frey, H., 1982. MAGSAT scaler anomaly distribution: the global perspective. Geophys. Res. Lett., 9: 277–280.

Fuchs, K., 1968. Das Reflexions- und Transmissions Vermögen eines geschichteten Mediums mit beliebiger Tiefen: Verteilung der elastischen Modul and der Dichte für schrägen Einfall ebener Wellen. Z. Geophys., 34: 389–413.

Fuchs, K., 1979. Structure, physical properties and lateral heterogeneities of the subcrustal lithosphere from long-range deep seismic sounding observations on continents. Tectonophysics, 56: 1–15.

Giese, P., 1976. General remarks on travel-time data and principles of correlation. In: (P. Giese, C. Prodehl and A. Stein (Editors), Explosion Seismology in Central Europe. Springer, Berlin–Heidelberg, pp, 130–136.

Green, T.H., 1970. High pressure experimental studies on the mineralogical constitution of the lower crust. Phys. Earth Planet. Inter., 3: 441–450.

Green, D.H. and Lambert, I.B., 1965. Experimental crystallisation of anhydrous granite at high pressures and temperatures. J. Geophys. Res., 70: 5259–5268.

Harrington, H.J., 1974. The Tasman Geosyncline in Australia. In: A.K. Denmead, G.W. Tweedale and A.F. Wilson (Editors), The Tasman Geosyncline, Geological Society of Australia (Qld. Div.), pp. 383–407.

Harrington, H.J., 1983. ACORP and testing the "rift" hypothesis of the origin of the main interior basin systems. In: F.J. Moss and B.R. Golby, (Editors), ACORP Workshop, May 1982, Summaries of Papers. Bur. Miner. Resour. Aust., Rec., in prep.

Henderson, R.A., 1980. Structural outline and summary geological history for northeastern Australia. In: R.A. Henderson and P.J. Stevenson (Editors), The Geology and Geophysics of Northeastern Australia. Geological Society of Australia (Qld. Div.), pp. 1–26.

Kern, H., 1979. Effect of high-low quartz transition on compressional and shear wave velocities in rocks under high pressure. Phys. Chem. Miner., 4: 161–172.

Kern, H., 1982. Elastic-wave velocity in crustal and mantle rocks at high-low quartz transition and of dehydration reactions. Phys. Earth Planet. Inter, 29: 12–23.

King, D. and Falvey, M., 1977. A seismic survey in the Cooper Basin in Queensland. Aust. Pet. Explor. Assoc. J., 17(1), 78–84.

Kirkegaard, A.G., 1974. Structural elements of the northern part of the Tasman Geosyncline. In: A.K. Denmead, G.W. Tweedale A.F. Wilson (Editors), The Tasman Geosyncline. Geological Society of Australia (Qld. Div.), pp. 383–407.

Leven, J.H., 1980. The application of synthetic seismograms to the interpretation of crustal and upper mantle structure. PhD Thesis, Australian National University, Canberra.

Lock, J., Collins, C.D.N. and Finlayson, D.M., 1983. Basement structure and velocities under the central Eromanga Basin from seismic refraction studies. In: P.S. Moore (Editors), Eromanga Basin Symposium Papers, Adelaide Nov 1982. Geol. Soc. Aust., Spec. Publ.

Mathur, S.P., 1983a. Deep reflection studies in the central Eromanga Basin. Tectonophysics, 100, in press.

Mathur, S.P., 1983b. Deep reflection probes in eastern Australia reveal differences in the nature of the crust. First Break, Europ. Assoc. Explor. Geophys., 1(7), 9–16.

McMechan, G.A., 1982. Low-velocity zone reflections observed in geometrical shadows of refraction profiles. Geophys. J.R. Astron. Soc., 71: 261–268.

Mereu, R.F., 1967. Curvature corrections to upper mantle seismic refraction surveys. Earth Planet. Sci. Lett., 3: 469–475.

Murray, C.G. and Kirkegaard, A.G., 1978. The Thomson orogen of the Tasman orogenic zone. Tectonophysics, 48: 299–325.

Orcutt, J.A., McKenzie, K. and McClain, J., 1980. The role of X(p) constraints in linear, extremal inversion of explosion profile data. Bull. Seismol. Soc. Am., 70: 2103–2116.

Pinchin, J., 1980. Intracrustal seismic reflections from the Lachlan Fold Belt near Canberra. Bur. Miner. Resour. J. Aust. Geol. Geophys., 5: 305–309.

Pinchin, J. and Senior, B.R., 1982. The Warrabin Trough, western Adavale Basin. J. Geol. Soc. Aust., 29: 413–424.

Rumph, B., 1978. Regional gravity and magnetic data of the central Eromanga Basin area: implications on crustal structure, regional geology and tectonic history. MSc Thesis, Univ. of Sydney.

Sass, J.H. and Lachenburch, A.H., 1979. Thermal regime of the Australian continental crust. In: M.W. McElhinny (Editor), The Earth, its Origin, Structure and Evolution, Academic Press, London, pp. 301–351.

Spence, A.G. and Finlayson, D.M., 1983. The resistivity structure of the crust and upper mantle in the central Eromanga Basin, Queensland, using magnetotelluric techniques. J. Geol. Soc. Aust., 30, 1–16.

Veevers, J.J., 1980. Basins of the Australian craton and margin. In: A.W. Bally, P.L. Bender, T.R. McGetchin and R.I. Walcott (Editors), Dynamics of Plate Interiors. Am. Geophys. Union, Geodyn. Ser., 1: pp. 73–80.

Veevers, J.J., Jones, J.G. and Powell, C, McA., 1982. Tectonic framework of Australia's sedimentary basins. Aust. Pet. Explor. Assoc. J., 22(1), 283–300.

Wake-Dyster, K.D. and Pinchin, J., 1981. Central Eromanga Basin seismic Survey, Queensland 1980. Bur. Miner. Resour. Aust., Rec. 1982/22.

Wellman, P., 1976. Gravity trends and the growth of Australia: a tentative correlation. J. Geol. Soc. Aust., 23: 11–14.

Journal of the Geological Society of Australia (1983), 30, 1-16

The resistivity structure of the crust and upper mantle in the central Eromanga Basin, Queensland, using magnetotelluric techniques

A. G. Spence & D. M. Finlayson

Bureau of Mineral Resources, Geology & Geophysics, P.O. Box 378, Canberra City, A.C.T. 2601.

ABSTRACT

Magnetotelluric data from the central Eromanga Basin indicate that one-dimensional resistivity models are appropriate for the region. The uppermost Jurassic-Cretaceous Eromanga Basin sequence contains flowing aquifers and has an average section resistivity in the range 1 to 7 ohm m with a mean of 4 ohm m. This overlies the older sedimentary sequences of the Cooper (Permo-Triassic) and Adavale (Devonian) Basins with resistivities in the range 10 to 400 ohm m, which present good resistivity contrasts for determining sub-surface morphology at the base of the Eromanga sequence. The depth extent of the older sequences is not well resolved because of the overlying highly conductive layers, but it appears to be greater than that determined from seismic reflection data in the Coonavalla Syncline and Warrabin Trough.

Basement rocks of the Thomson Fold Belt have resistivities in the range 750 to 3800 ohm m with an average of 1300 ohm m. This resistivity is evident to depths of 40–60 km, and consequently represents the conductivity of the Earth's crust in the region. No highly conductive layers were detected within this crustal sequence. In the depth range 60 to 150 km, resistivities decrease to less than 5 ohm m. Such resistivities at 150 km depth are in broad agreement with data obtained from magnetometer array studies in southeastern Australia, which are explained by other authors in terms of a 5% partial basalt melt.

KEY WORDS: Magnetotelluric data, crust, upper mantle, Eromanga Basin, Queensland, resistivity, conductivity, aquifers.

INTRODUCTION

In 1980 the Bureau of Mineral Resources, Geology & Geophysics (BMR) undertook a multidisciplinary geophysical survey to examine the regional structure of the central Eromanga Basin in Queensland and the underlying Cooper, Adavale and Galilee Basins (Harrison et al., 1980). As part of this program, magnetotelluric (MT) techniques were employed to examine the conductivity of the Earth's crust and upper mantle. Recordings were made at 12 sites in the central part of a 300 km seismic reflection/refraction traverse, which was surveyed to determine the deep structure of the crust. A 150 km profile in the centre of this traverse was investigated by 6-fold continuous seismic reflection profiling to determine detail within the sedimentary sequence and the underlying crust (Fig. 1).

Vozoff (1972) has described in some detail the techniques for applying the MT method to sedimentary basins and deeper structures. Electromagnetic disturbances generated in the Earth's upper atmosphere penetrate the Earth, resulting in telluric currents within the Earth's strata. These currents, in turn, perturb the electric (E) and magnetic (H) components of incoming electromagnetic field measured at the Earth's surface.

The depth of penetration of electromagnetic disturbances is inversely related to the rock conductivity. In a uniformly conducting Earth, the depth at which the amplitude of the disturbance has fallen off to 1/e (e = exponential constant) of its surface value is called the skin depth (δ) and is approximately given by the function:

$$\delta \sim \tfrac{1}{2}(\rho/f)^{\frac{1}{2}} \text{ km}$$

where f = frequency of oscillation (Hz)
ρ = resistivity (ohm-m) = 1/conductivity (siemens/m)

Thus by measuring both the H and E fields over a range of frequencies, the conductivity structure within the Earth can be established using the inversion techniques described by Vozoff & Jupp (1975), Jupp & Vozoff (1975), Hermance (1973), and Vozoff (1972). The electrical conductivities of rocks are strongly influenced by ionic transport, fluid content and temperature; hence all these factors must be taken into account in the interpretation of models resulting

MS. received 4 May 1982; revised MS. received 25 June 1982.

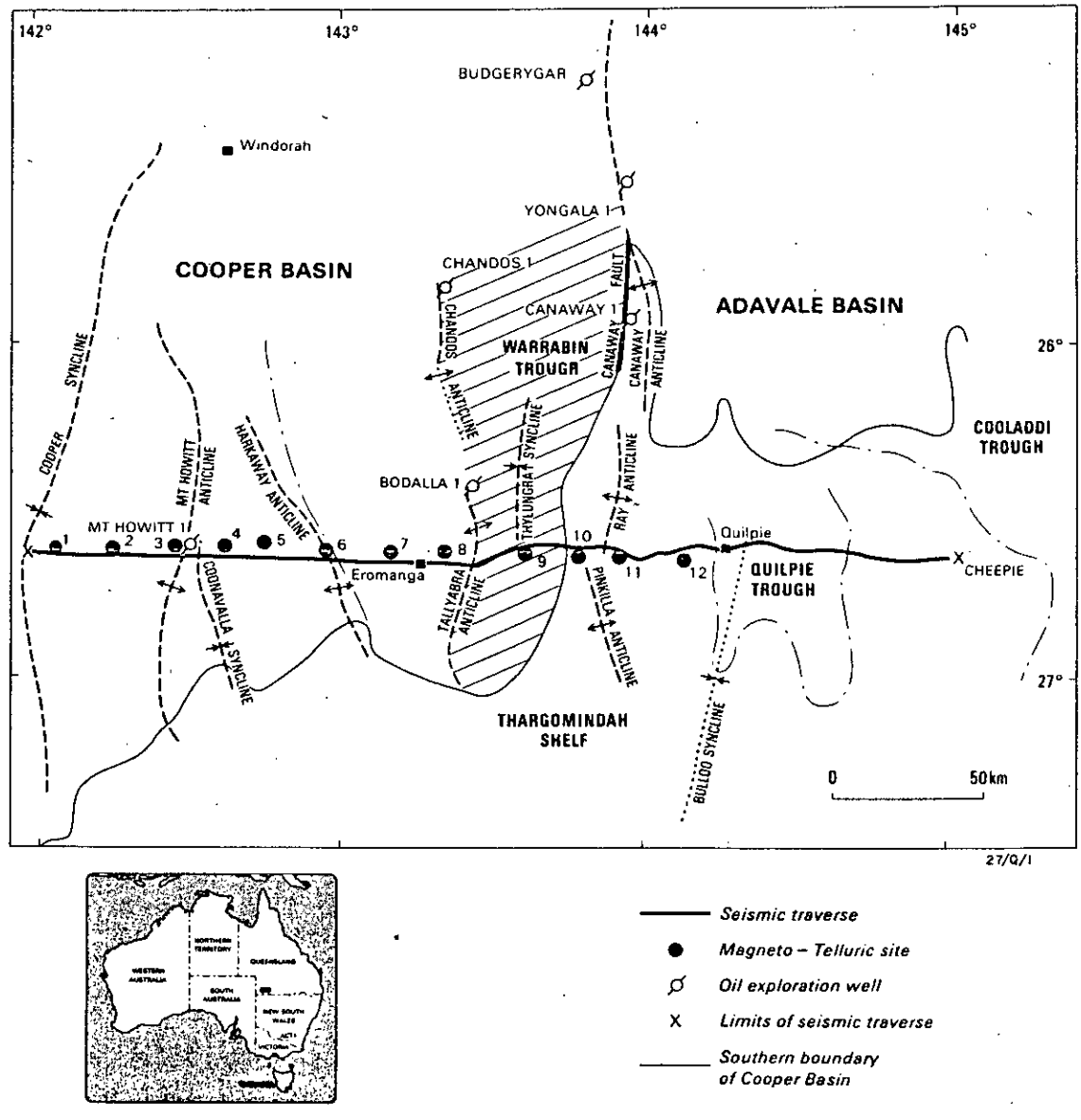

Fig. 1. Simplified basin structure and magnetotelluric site locations in the central Eromanga Basin.

from the data inversion process. Other geophysical constraints from well log data, geological models and seismic information should be applied where appropriate.

GENERAL GEOLOGY OF THE CENTRAL EROMANGA BASIN

The geology of the sedimentary sequences within and underlying the Eromanga Basin has been described by Senior et al. (1978), Senior & Habermehl (1980), Ingram (1971), Rumph (1978), and Pinchin & Senior (1982). The simplified geological structure is illustrated in Figure 1.

The Eromanga Basin is a large sedimentary basin within the Great Artesian (hydrological) Basin. In the area of study it overlies and entirely conceals two older basins, the Adavale Basin and the Cooper Basin. The Basin was formed in Jurassic to Cretaceous time and forms a flat-lying blanket of sediments over the whole of the region. Within the Eromanga succession the Jurassic sequence is 500 to 1200 m thick, and consists mainly of continental deposits of quartzose arenite interbedded with carbonaceous siltstone and mudstone. The Cretaceous sequence is 500 to 1800 m thick in the central Eromanga region; the thickest accumulations are thought to be in the Cooper Syncline (Fig. 1). A marine environment per-

sisted throughout most of the Lower Cretaceous period. However, in the Middle to Upper Cretaceous the Winton Formation (generally the thickest unit) was formed during a return to continental conditions, and the weathered surface of this formation now forms the surface cover over a large part of the region. The remaining cover consists of Tertiary remains on the structurally high areas and Quaternary alluvium in the synclinal areas.

Sediments of the Permo-Triassic Cooper Basin immediately underlie the Eromanga sequence, except on the shelf-areas to the south and east. East of the Canaway Ridge, Permian sediments extend for a short distance in places and Triassic sediments are continuous; in this region the Permo-Triassic sequence is known as the Galilee Basin sequence. West of the Canaway Ridge, along the line of the MT sites, Cooper Basin sediments extend westward from site 8 as a thin layer, gradually thickening towards the Cooper Syncline (Pinchin & Senior, 1982). At Mt Howitt No. 1 well the total thickness of Cooper Basin sediments is 500 m. The Permian sequence was laid down in fluviatile, lacustrine and deltaic environments, which later resulted in thick coal measures. The early Triassic was a period of fluviatile and lacustrine sedimentation, and some of the coarse-grained Triassic sandstones have good porosity and permeability; however, the Nappamerri Formation contains tight sandstones, shales, siltstones and minor coal, and forms the cap-rock for gas fields in the South Australian part of the Cooper Basin.

Mid-Devonian to Lower Carboniferous sediments are contained in the concealed north-trending Warrabin Trough (Fig. 1) and may extend farther north and west (Pinchin & Senior, 1982). The sequence can be correlated with the sediments of the Adavale Basin, a subsurface Devonian-Carboniferous basin to the east of the Canaway Ridge. Pinchin (pers. comm.) has recently indicated that the Adavale Basin is now considered to contain only Devonian sediments, and in this paper the validity of the statement is assumed. In Late Carboniferous times epeirogenic movements resulted in uplift and erosion along the Canaway Ridge and downwarping of the Warrabin Trough, which has thus been preserved, in the same way as the Adavale Basin and its associated troughs, as a structural remnant of a once continuous area of shelf-facies deposition between the Australian Craton and the Tasman Syncline (Ingram, 1971).

The Adavale Basin sediments are considered prospective for hydrocarbons on the basis of the gas find in the Log Creek Formation at Gilmore No. 1 well (Senior et al., 1978, table B6). A number of exploration wells penetrated Adavale Basin sediments within the Warrabin Trough, including Chandos No. 1, Chandos South No. 1, and Cumbroo and Bodalla No. 1. However, tests on cores from these wells did not provide sufficient encouragement for further exploration (Fig. 1).

SEDIMENTARY STRUCTURE

The structure of the sedimentary sequences in the region has a dominantly northerly trend and is characterised by broad, generally low-amplitude folds and linear faults. The combination of faulting and draping of the overlying sediments, with differential compaction, is probably due mainly to basement block-faulting. Fault movements have been accommodated in the sediments by monclinal flexure or by faults that reach the surface.

The major deformation of the Eromanga sequence took place in Early Tertiary time, when, following a period of intense weathering, fluvial deposits accumulated in slowly subsiding synclines. A second phase involving generally gentle warping, occurred in Mid to Late Tertiary time.

The principal structures of the sedimentary sequence along the geophysical traverse described in this paper are, from west to east, as follows (Fig. 1):

Cooper Syncline, the axis of which coincides with the present position of Cooper Creek; it contains the maximum thickness of Eromanga and Cooper Basin sediments.

Mt Howitt Anticline, a broad, closed structure approximately 140 km long and 50 km wide, which is slightly asymmetrical with a steeper eastern flank.

Coonavalla Syncline, a gently plunging feature to the east of the Mt Howitt Anticline.

Harkaway Anticline, a N-W trending feature about 90 km long. Dips are very low, but indicate it is slightly asymmetrical with a steeper eastern flank.

Tallyabra Anticline, possibly resulting from the same fault system as the Chandos Anticline farther to the north.

Thylungra Syncline, gravity and seismic work indicating a considerable thickness of sediment in this area, which probably corresponds to the deepest part of the underlying Warrabin Trough.

Canaway Ridge, a subsurface feature, represented at the surface by the Ray-Pinkilla Anticline near the MT traverse, and forming the divide between the Warrabin Trough and the Adavale Basin.

Thargomindah Shelf, a broad basement feature mainly to the south of the survey region, but with an extension via the Canaway Ridge along the eastern margin of the region.

HYDROGEOLOGY

The central Eromanga Basin forms part of the Great Artesian Basin (Habermehl, 1980), which is a multi-layered, confined aquifer system in which the aquifers occur in continental quartzose sandstones of Triassic, Jurassic and Cretaceous age. The aquifer flow direction is mainly towards the west and SW in this section of the basin. This flow direction, combined with the predominantly northerly structural trend, has led Senior & Habermehl (1980) to postulate that hydrocarbons could have accumulated in stagnation zones formed where aquifers have been partially blocked by fault movement. They noted that relatively small fault displacements would be sufficient to cause this and, using LANDSAT-enhanced surface-fault data, pointed out many locations in the central Eromanga Basin where such conditions occur.

BASEMENT GEOLOGY

Lower Palaeozoic rocks of the Thomson Fold Belt form a basement to the sedimentary basins of the

central Eromanga region. A Cambrian transgression occurred to the east of the Precambrian Australian craton. Cambrian lithologies have been identified in many wells to the SW and west of the present survey region (Rumph, 1978), over 1600 m of section being penetrated in at least one well. Lower-Middle Ordovician sedimentation is evident in cores from wells in the Cooper Basin area to the SW of the survey area. The Late Cambrian-Ordovician Delamerian Orogeny in southeastern Australia resulted in Ordovician ages being overprinted on the earlier Palaeozoic sediments, isotopic ages of 430–480 Ma being measured (Rumph, 1978). Basaltic and metamorphic rocks in the basement of wells drilled in the Adavale Basin to the NE of the survey area indicate ages of 417–480 Ma (Ordovician-Silurian). Drillcore data from throughout the region define a northeasterly trend for the early phase of the Thomson Fold Belt (Plumb, 1979).

PRE-SURVEY MODELLING

To estimate the responsiveness of the MT method to variations in resistivity and thickness of layers of interest, forward modelling was carried out using data from the Mt Howitt No. 1 (Delhi-Santos, 1966) and Bodalla No. 1 (Buchan, 1968) exploration wells (Fig. 1). These wells were drilled to depths of 2.4 km and 2.6 km, respectively—comparatively shallow depths in terms of conventional MT sounding frequencies. Unless there were major contrasts in layer resistivities, little resolution could be expected to these depths. Resistivities and corresponding thicknesses were extracted from the electric well-log data to form a one-dimensional model to put into the modelling program.

The Mt Howitt No. 1 well, drilled on the Mt Howitt Anticline, intersected approximately 500 m of Cooper Basin sediments. In the input MT model, the Cooper Basin sedimentary layer was varied successively in resistivity and thickness by factors of 0.5 to 2.0. This produced a variation in MT response of only about 1%–2%.

The Bodalla No. 1 well, sited near the Tallyabra Anticline, intersected Eromanga, Cooper and Adavale Basin sediments; the Adavale Basin sediments are about 700 m thick. The object of the modelling in this case was to determine the MT response of the Adavale sequence. The MT forward modelling program was run first with, and then without, the Adavale Basin sequence in the input model. The presence of the Adavale Basin sediments also produced only about 1%–2% change in the MT response.

The outcome of the modelling, therefore, is not very encouraging, as far as direct detectability of the Cooper and Adavale sediments are concerned. However, as discussed in the next section, MT work in the South Australia extension of the Cooper Basin (Moore et al., 1977) has shown that MT methods can detect the base of the Cretaceous sequence and large-scale conductive features in the upper mantle, and give some indication of pre-Permian sediments and basement structure.

CONDUCTIVITY STRUCTURE

Grant & West (1965), among others, draw attention to the fact that, in the absence of semimetallic minerals, the electrical conductivity of rocks is largely controlled by moisture content, even in the tightest igneous and metamorphic rocks. In sedimentary basins, therefore, the permeability and porosity of the sequences and the conductivity of the contained fluids largely determine the apparent resistivities measured by the magnetotelluric method. Sedimentary rocks and unconsolidated material are distinctly more conductive than igneous rocks. The conductivity of metamorphic rocks is variable, because they have a wide variety of porosities. Coupled with the increase in temperature with depth, these factors indicate that great care is required in any geological interpretation of conductivity structures.

A number of previous surveys provide information on the conductivity structures in the Central Eromanga Basin. Whiteley & Pollard (1971) reported early resistivity and magnetotelluric work at Windorah (Fig. 1) near the present survey areas. The resistivity data indicated an 11-ohm m surface layer 5 m thick, overlying a 67-m thick layer of resistivity 55 ohm m, interpreted as brackish groundwater. Beneath this was a 82 m thick saline layer (1.5 ohm m), and a 1.22-km thick layer of resistivity 2.6 ohm m, overlying an 8-ohm m layer 3 km thick. Based on borehole data, the 8 ohm m layer was interpreted as being an aquifer sequence in the basal Winton/Mackunda Formations. The MT data extended the depth of the interpretation to indicate a very resistive (10 k ohm m) layer 90 km thick under the 8-ohm m layer. This is interpreted as being crustal and upper mantle rocks, and below this the resistivity decreases considerably to 20 ohm m.

Middleton (1979) reported the results of deep electrical sounding near Chandos No. 1 petroleum exploration well (Fig. 1) north of the present magnetotelluric sites. This interpretation indicated a 20 m thick surface layer with resistivity 74 ohm m overlying a 1000 m section with resistivity 4.4 ohm m; at greater depths the resistivity exceeded 10 ohm m. Also a deep sounding near Budgerygar No. 1 well, about 90 km NE of Chandos No. 1, indicated a low-resistivity layer extending from 330 to 1400 m depth.

Moore et al. (1977) reported the results of magnetotelluric sounding at 5 sites in the northern Cooper Basin (250–300 km SW of the present survey area) which underlies the Eromanga Basin. Their pre-survey modelling, based on the electrical logs from 16 exploration wells, indicated that the Eromanga sequence (about 1.5 km thick) had resistivities of 1.8–3.4 ohm m, overlying the Permo-Triassic Cooper Basin sediments with resistivities of 13–73 ohm m. It was considered that the magnetotelluric method could be applied to mapping the Eromanga sequence, but could not provide detailed information within the Cooper Basin sediments. However, the method should respond to the conductivity contrast between pre-Permian sediments and basement rocks of the Thomson Fold Belt.

The results from the 5 northern Cooper Basin sites substantiated the modelling data. Resistivities between 0.9 and 5.9 ohm m were interpreted to depths of

1.4–1.5 km, where there is a marked resistivity increase corresponding to the Lower Cretaceous Transition Beds. Pre-Permian resistivities were interpreted as having significantly greater resistivities than the Permo-Triassic sequence, but were variable and did not present a good contrast with resistive basement.

On a larger scale, Woods & Lilley (1980) have reported on telluric currents channelled through the Eromanga Basin, based on the analyses of magnetometer array data. Current flow is concentrated in a model basin structure, with a maximum thickness of 5 km and a resistivity of 2.86 ohm m overlying a basement with resistivity of 500 ohm m. These authors also commented that this basin structure alone was insufficient to account for the observed data, and that additional conductors must exist within or beneath the basin, causing current concentrations.

MAGNETOTELLURIC (MT) RECORDING SYSTEM AND FIELD WORK

Cull et al. (1981) have described the BMR recording, data acquisition and processing system, and only a brief outline is given here.

Three magnetic (H) components of the Earth's magnetic field are measured using Geotronics induction coil magnetometers. Field strengths in the picotesla (pT) range are detected and routed to amplifiers with extremely low noise characteristics. Two horizontal components of the electric field (E) are detected using two sets of electrodes set out in an orthogonal arrangement. The separation of the electrodes on each set is 600 m; contact with the ground is achieved using cadmium rods inserted in a cadmium chloride solution in a porous pot, which is in contact with moist earth. Voltages across the electrodes are in the range 10–100 mV.

The utility of a magnetotelluric recording system in remote areas depends largely on its ability to handle large quantities of data and its capacity to process the data on-site to the stage at which judgements can be made about data quality and possible interpretations.

The BMR MT system (Fig. 2) used on this survey comprised a standard computer-based data-acquisition system to record and analyse the three magnetic and two electric field components. Data were recorded on a 10-Megabyte capacity disc memory and later transferred to a 9-track digital tape. Data were recorded in seven frequency bands as follows:

Band 1	0.001–0.012	Hz
2	0.01 –0.033	Hz
3	0.03 –0.12	Hz
4	0.10 –0.55	Hz
5	0.5 –2.5	Hz
6	2.5 –12.5	Hz
7	10.0 –40.0	Hz

In the higher frequency bands, data sets were collected in a few minutes; some data sets in the low-frequency bands took over a day to record. Usually several data sets were recorded in each frequency band to ensure good signal-to-noise ratios.

Data recorded in the time domain were transformed to the frequency domain for processing. The transfer functions of the various amplifiers and filters

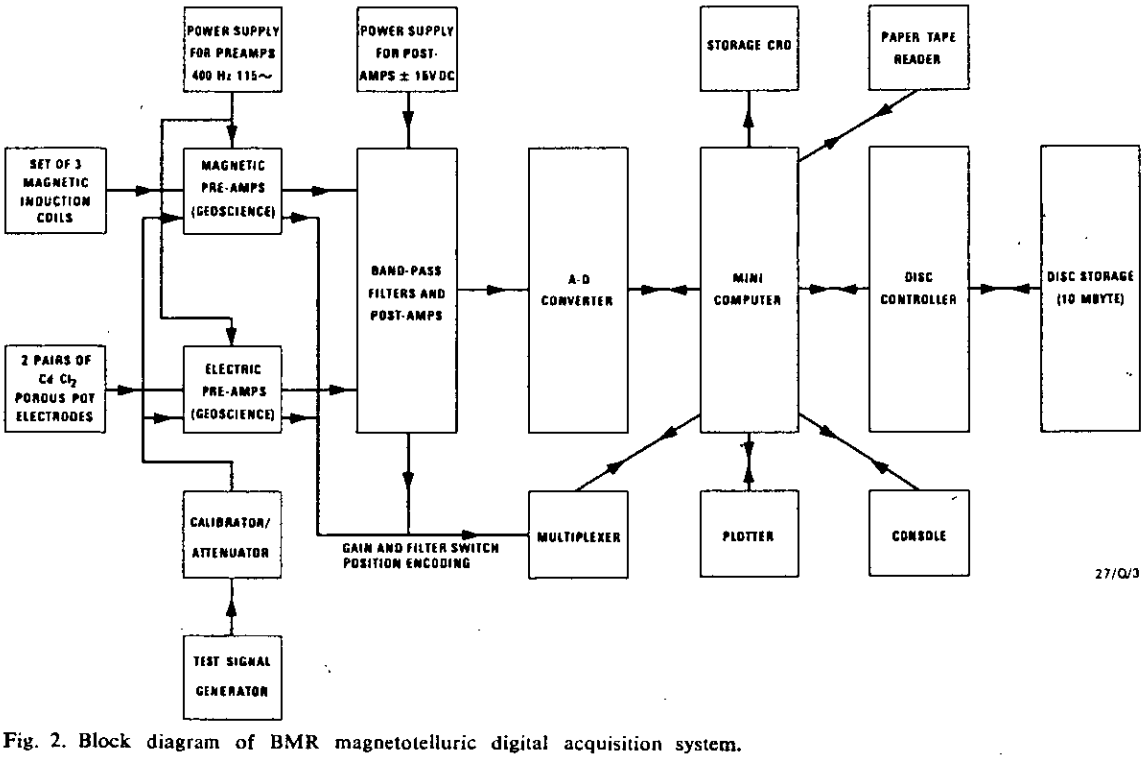

Fig. 2. Block diagram of BMR magnetotelluric digital acquisition system.

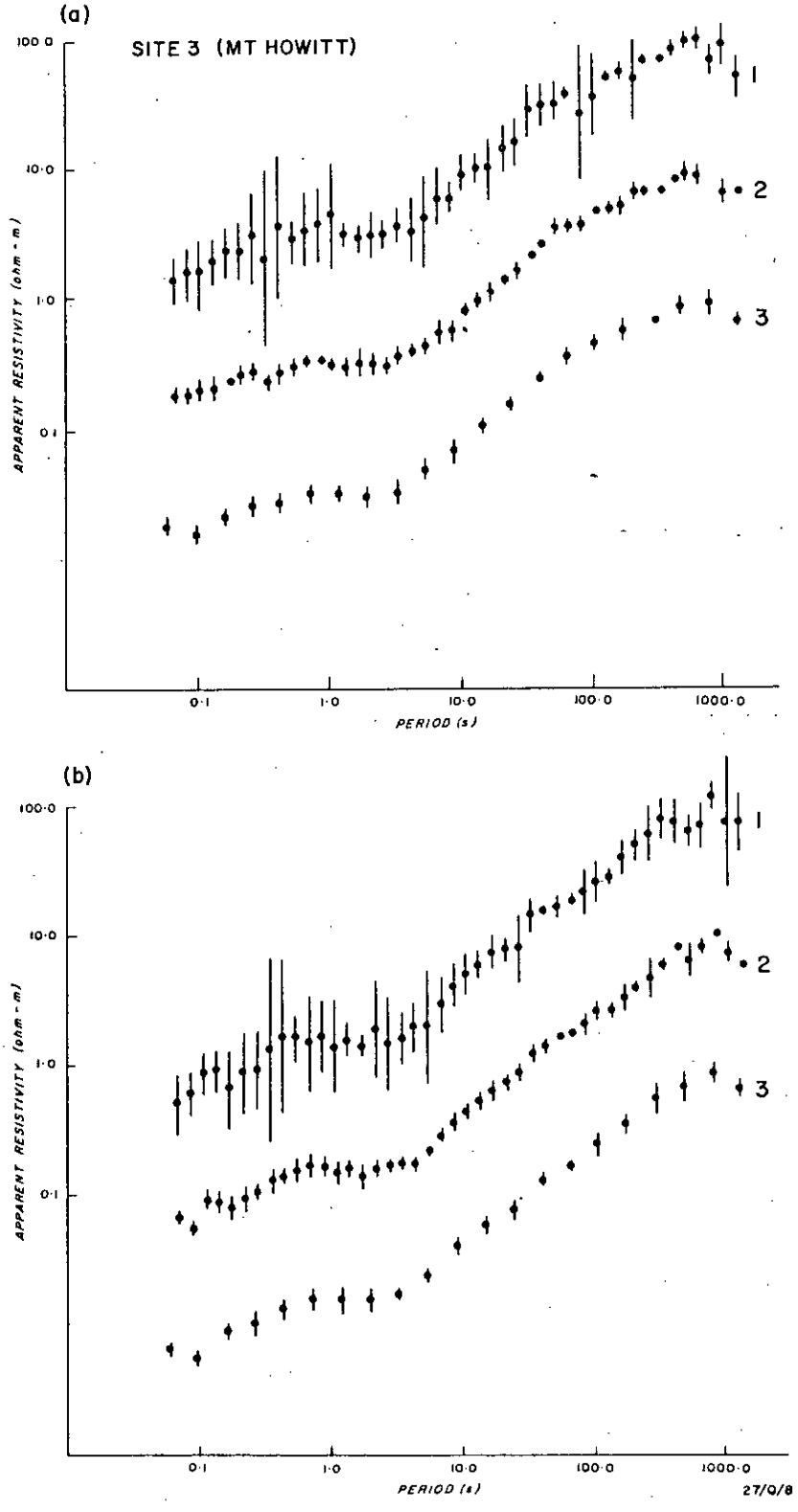
(a)
SITE 3 (MT HOWITT)
100·0
10·0
1·0
0·1
APPARENT RESISTIVITY (ohm - m)
1
2
3
0·1
1·0
10·0
100·0
1000·0
PERIOD (s)
(b)
100·0
10·0
1·0
0·1
APPARENT RESISTIVITY (ohm - m)
1
2
3
0·1
1·0
10·0
100·0
1000·0
PERIOD (s)
27/9/8

were calculated prior to recording and used to reduce data to a common base. The usual output from the initial processing consisted of plots of the rotated-tensor apparent resistivities and phases versus frequency for each orthogonal component, together with tensor-rotation angles.

In September-October 1980, 12 MT sites were occupied along an E-W line at latitude 26°37'S between longitudes 142° and 144°10'E. The site spacing was 15–20 km (Fig. 1) and the locations are listed in Table 1.

TABLE 1. Site localities.

Site No.	Latitude (S) deg.	min.	sec.	Longitude (E) deg.	min.	sec.
1	26	37	33	142	02	50
2		37	25		15	30
3		37	09		27	38
4		36	31		37	00
5		35	53		44	10
6		36	12		57	56
7		37	20	143	11	10
8		37	23		20	32
9		37	23		36	37
10		37	34		47	06
11		37	15		55	23
12		37	55	144	08	04

Apparent resistivity data were obtained from all sites, but unfortunately an equipment failure caused the loss of phase data from sites 7–10, inclusive.

DATA ANALYSIS AND MODELLING

All field data were first screened to remove those that were unacceptable in terms of coherency (self-consistency between E and H components) or skewness (indicating complicated three-dimensional structures) at the frequencies involved (Vozoff, 1972; Moore, 1977). The data were then rotated mathematically to compile apparent resistivity and phase plots for the electric components perpendicular (E_{perp}) and parallel (E_{par}) to the strike by minimising the diagonal elements in the impedance matrix (Vozoff, 1972). The screened and rotated data were then combined into a number of bands (normally 45 or 21) of equal logarithmic width on the period axis; a single average value was then specified for all apparent resistivity and phase data within each band. These screened, rotated and averaged data from each site provided the basic input data for subsequent interpretations. The improvement to the apparent resistivity data from site 3 (Mt Howitt) is illustrated in Figure 3. Signal period, rather than frequency (1/period) has been used in data presentation.

Pseudosections along the line of 12 sites were constructed for the E_{perp} and E_{par} components, to obtain some indication of structural uniformity under the Eromanga Basin. The apparent resistivities at various periods are plotted under each site location and contoured (Fig. 4). A comparison of the two pseudosections highlights the similarity in their main features, which we interpret as indicating that there is no pronounced strike direction and that the one-dimensional modelling of conductivity structures is appropriate. The pseudosections generally can be divided into three period zones. At periods less than 10 s there is a zone of low apparent resistivity (less than 4 ohm m). At periods in the range 10–700 s the apparent resistivity increases from 4 to 40 ohm m, and at greater periods under some sites the apparent resistivity begins to decrease, indicative of conductive zones within the upper mantle. Some anisotropy is evident in the top and bottom zones at the eastern end of the traverse, possibly caused by Canaway Ridge structures.

One-dimensional modelling of structures at each site was conducted using the inversion scheme described by Jupp & Vozoff (1975). The inversions require starting models to be set up based on well log and other geological information. Data from the Mt Howitt No. 1 well (Site 3) were used to construct a starting model at that site (Fig. 5). Intracrustal and upper mantle conductivity estimates were derived from the character of inflexions on the apparent resistivity curves. Inversions were conducted separately on two resistivity amplitude and two phase data sets from each site, where available.

Not all data sets for any one site could be completely reconciled with a single one-dimensional model. However, the basic characteristics of the models that fitted the observations at any one site were similar. The four models derived at the Mt Howitt site (Site 3) are illustrated in Figure 5. A geological section of the drillhole is also shown. Low resistivities are associated with the Cretaceous Winton, Mackunda, Allura Mudstone, Toolebuc and Wallumbilla Formations, with an increase in resistivity corresponding with the Jurrasic Horray, Westbourne, Adori, Birkhead and Hutton Sandstone Formations. A further increase in conductivity is evident at the base of the Permo-Triassic Nappermerri, Gidgealpa and Merrimelia Formations, which overlie Ordovician basement at a depth of 2.3 km.

At greater depths, the general character of the conductivity structure is apparent from the inversion process. The final models from the inversion are dependent on the starting models; conductivity structure should not be considered solely in terms of formation depths because, within the crust and upper mantle, temperature as well as fluid content and composition plays an important role in determining the conductivity. At sites where all four data sets are available (2 for apparent resistivity amplitude and 2 for phase) there is a highly resistive layer from the basement contact down to depths greater than 20 km (Fig. 5). Below this there is evidence of resistivity decreasing until at a depth of about 120 km, where the resistivity is very low (of the order of 1 ohm m).

Fig. 3. Magnetotelluric site 3 (Mt Howitt) apparent resistivity rotated, screened and averaged data for (a) E perpendicular-to-strike (E_{perp}) and (b) E parallel-to-strike (E_{par}) components. Data set 1 is basic data arranged into 44 bands; set 2 is rotated and screened data averaged into 44 bands; set 3 is data rotated and screened data averaged into 21 bands. Apparent resistivity scale refers to data set 1.

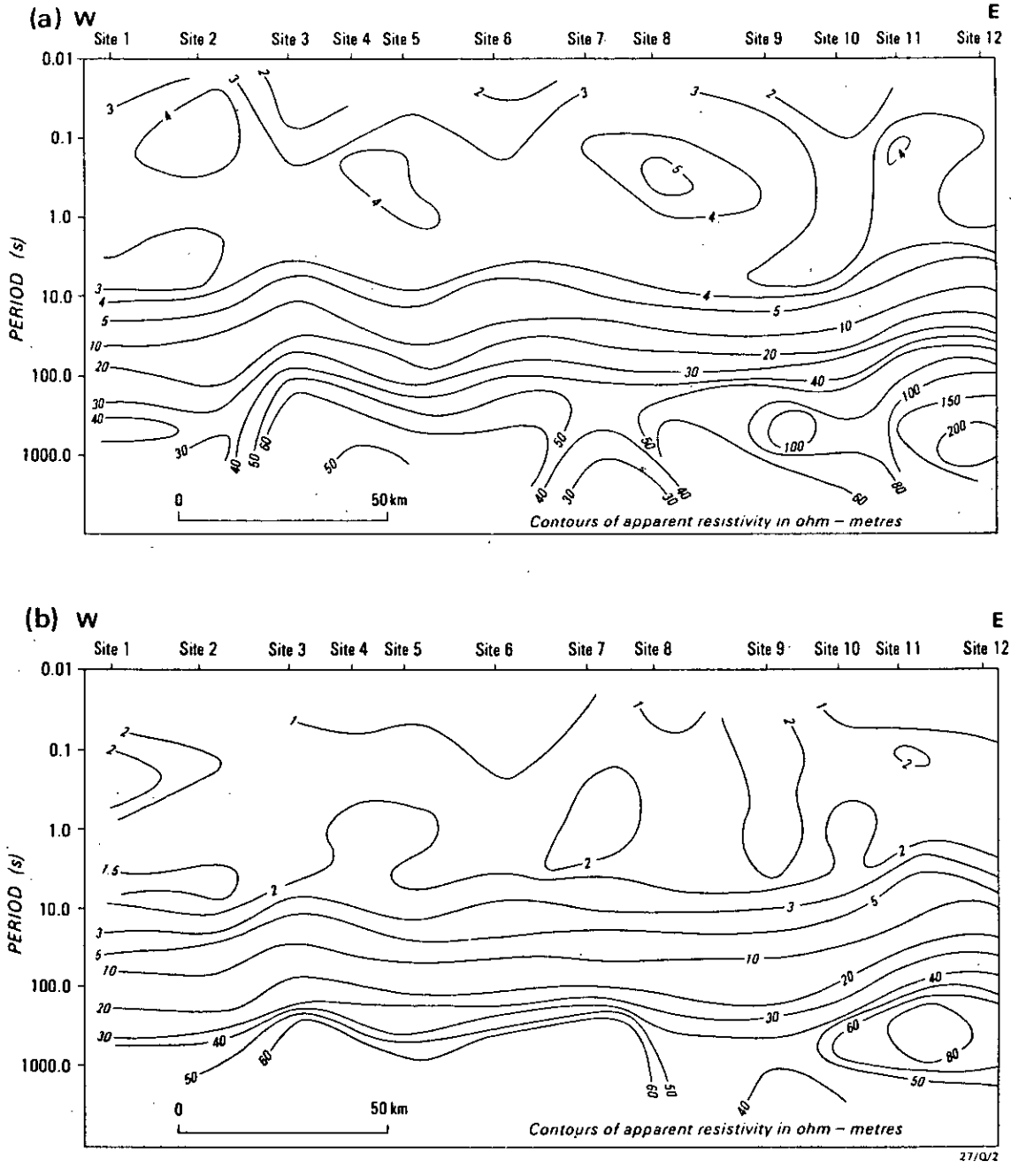

Fig. 4. Pseudo-section of apparent resistivity amplitude along the magnetotelluric traverse for (a) E perpendicular-to-strike and (b) E parallel-to-strike components.

Model paramenters (resistivities and depths) are termed sensitive if moderate changes in them produce moderate or large changes in the calculated response (apparent resistivity or phase versus frequency) and insensitive if large changes in them produce little change in the calculated response. Some measure of the sensitivity of model parameters is obtained from the sensitivity matrix produced by the inversion process (Jupp & Vozoff, 1975). The sensitive and insensitive parameters of the Mt Howitt (Site 3) final models are indicated in Fig. 5. As might be expected, the final solutions are clearly more sensitive to the conductive layers and their depth than to the resistive features of models. For sites 1, 2, 3, 4, 5, 6, 11

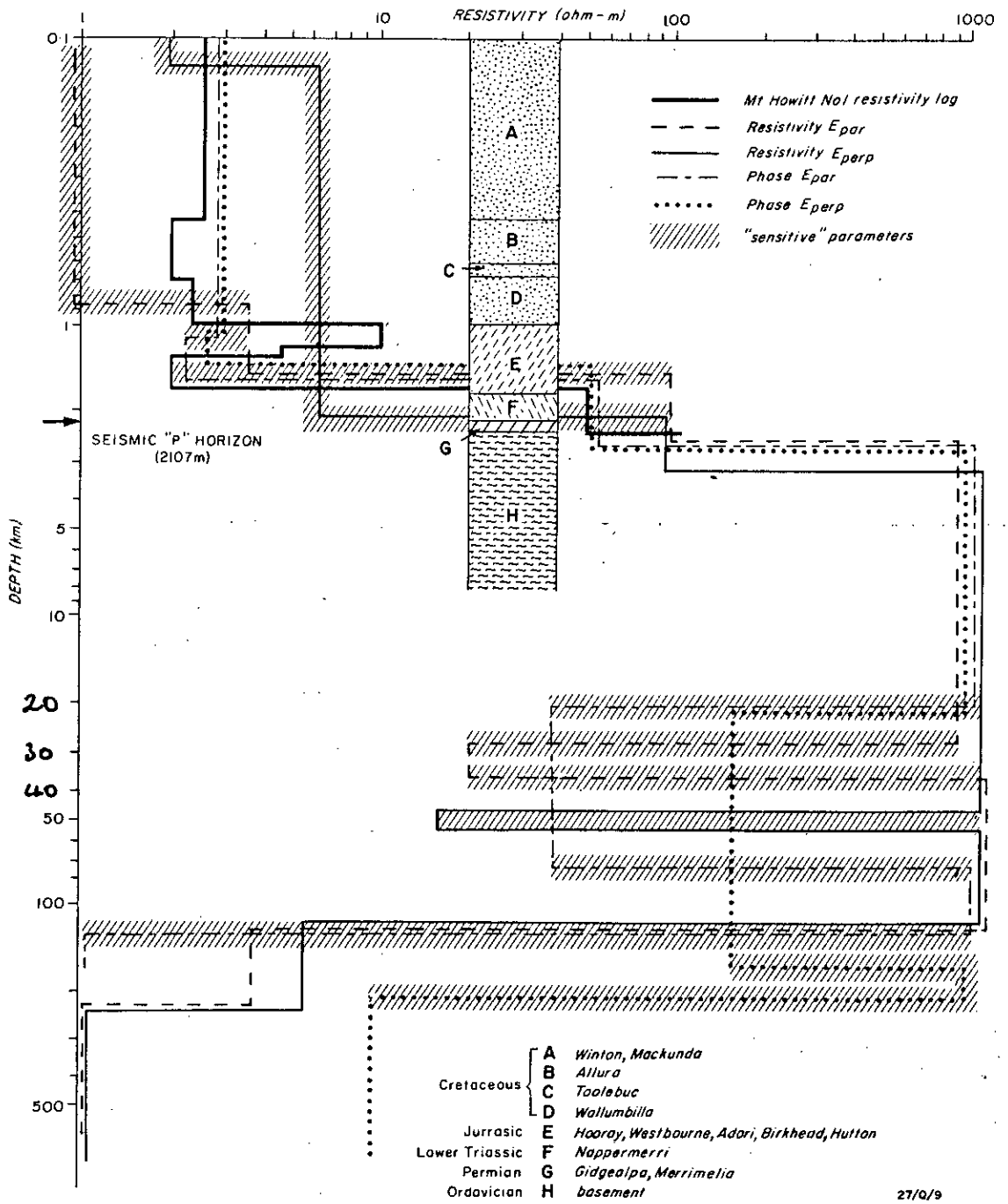

Fig. 5. Site 3 (Mt Howitt) resistivity/depth models derived from one-dimensional inversion of the apparent resistivity and phase components (E_{par} and E_{perp}). Also indicated are the 'sensitive' values of resistivity and depth that produce large changes in the fit of models to the observed data if changed. The Mt Howitt No. 1 exploration well lithology and resistivity log are also shown.

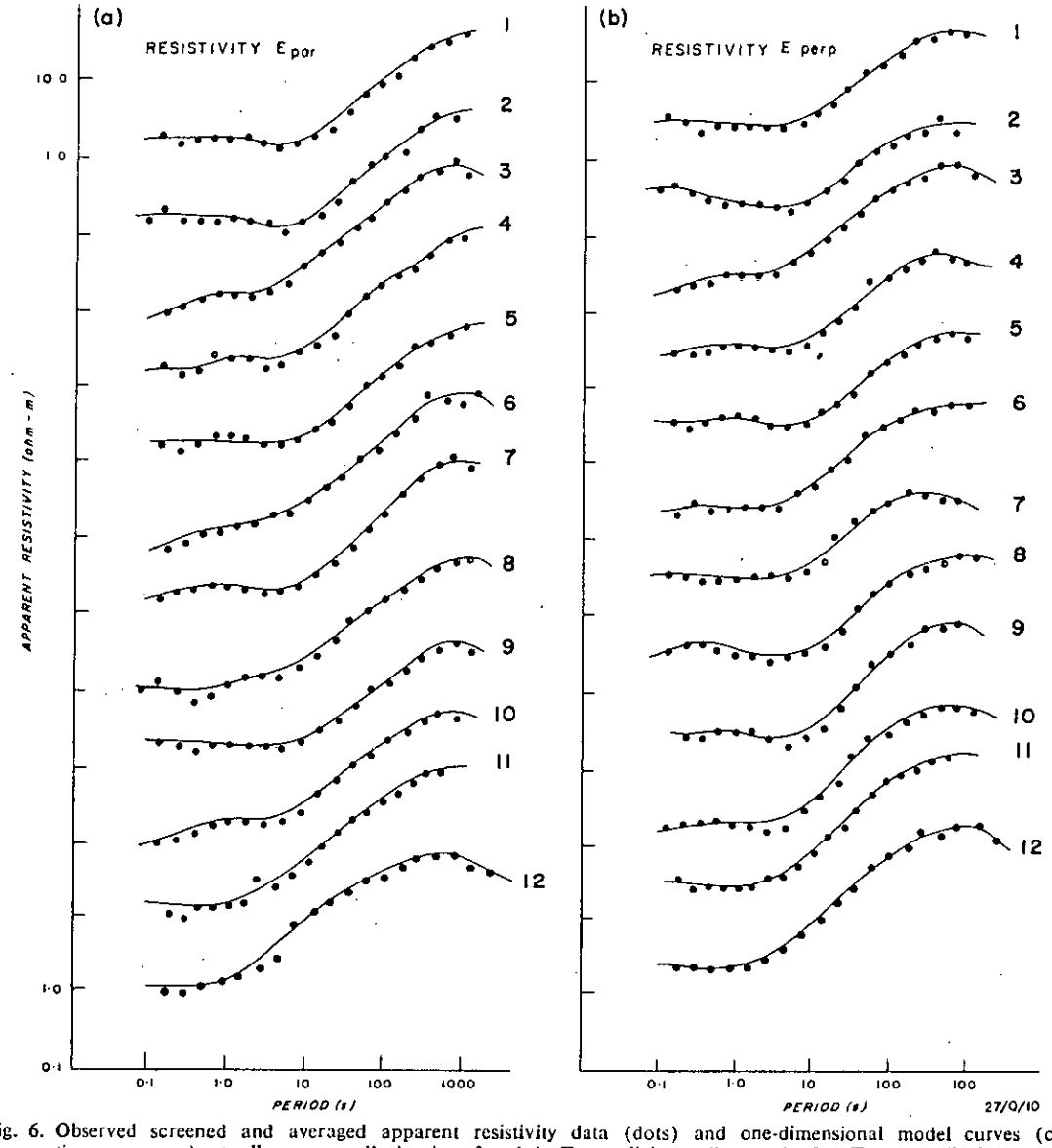

Fig. 6. Observed screened and averaged apparent resistivity data (dots) and one-dimensional model curves (continuous curves) at all magnetotelluric sites for (a) E parallel-to-strike, and (b) E perpendicular-to-strike components.

and 12 separate one-dimensional inversions were produced from the resistivity and phase data. For sites 7, 8, 9 and 10 inversions were produced from resistivity data alone.

The resulting fit of the models to the screened and averaged input data are shown in Figures 6 and 7. The resistivity models derived for all sites from the E_{par} and E_{perp} components of apparent resistivity amplitude have been combined into resistivity profiles shown in Figures 8a and 8b. In these profiles an average resistivity within the near-surface Eromanga sequence has been used to obtain a broad regional picture of the deeper resistivity features. The average resistivity was calculated using the expression:

$$\bar{\rho} = \frac{\Sigma\, m_i}{\Sigma \left(\frac{m_i}{\rho_i}\right)}$$

where $\bar{\rho}$ = average resistivity of the sequence
m_i = thickness of the i th layer
ρ_i = resistivity of the i th layer

The one-dimensional results were subsequently used to formulate input models for a two-dimensional linear inversion procedure developed by Jupp & Vozoff (1977). However, the one-dimensional models were not greatly changed and the preferred interpretation is based on the one-dimensional results.

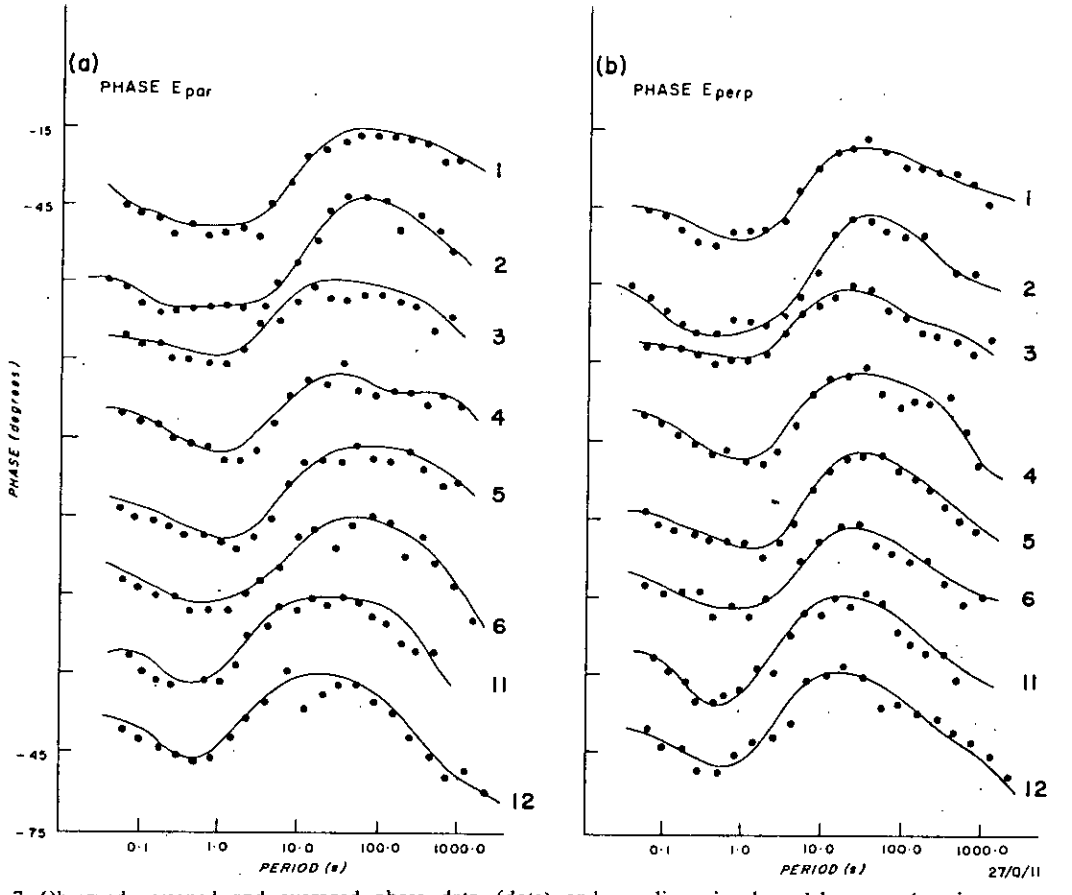

Fig. 7. Observed screened and averaged phase data (dots) and one-dimensional model curves (continuous curves) at 8 magnetotelluric sites for (a) E parallel-to-strike, and (b) E perpendicular-to-strike components. No phase data were obtained from sites 7 to 10, inclusive.

INTERPRETATION ABOVE BASEMENT

The uppermost zones of consistently low average resistivities in Figures 8a and 8b (generally less than 5 ohm m) corresponds to the sediments of the Jurrassic-Cretaceous Eromanga Basin sequence. The low average resistivities reflect high average porosity and saturation levels. In the survey area the water-table, which is taken to mark the upper boundary of the saturated zone, generally occurs at depths of less than 20 m. The base of the sequence of low-resistivity sediment lies at an average depth of 2 km and contains depressions corresponding to the Cooper Syncline, Coonavalla Syncline and Warrabin Trough, and at its eastern end there is an uplift to within 0.5 km of the surface over the Canaway Ridge (Fig. 8a).

Another feature of this upper zone is the occurrence at some sites of average resistivities that are anomalously lower than the mean for that zone. This occurs at sites 2, 6, 7 on the E_{par} component, and at site 8 on the E_{perp} component (Figs 8a, 8b). The mean resistivity, parallel to strike, for all 12 sites is 3.1 ± 0.8 ohm m.

The general conductivity trends in rocks have been discussed earlier in this paper. In the central Eromanga Basin the sediments are part of a large flowing artesian basin and there is a considerable thickness of these sediments under each site. Keller (1971) indicated that the resistivity in near-surface rocks is almost totally due to three factors, namely: (1) the water content of the rock, (2) the conductivity of the water, and (3) the way the water is distributed in the rock. In partially-saturated sediments, the influence of the water-content factor is orders of magnitude greater than those due to the other two. However, when this factor can exert no further effect, owing to the fully-saturated state of the sediments, variation in the conductivity of the water itself becomes the main source of resistivity variation. This is expected to be the situation in the central Eromanga Basin, where we consider the porosity and saturation level to be nearly uniform from site to site along the magnetotelluric traverses.

The conductivity of the groundwater is controlled by the concentration of dissolved salts and the cation-exchange capacity of the host rock. Both these processes are temperature and time dependent. Local vertical movement along faults of hot groundwater from great depths can increase near-surface tempera-

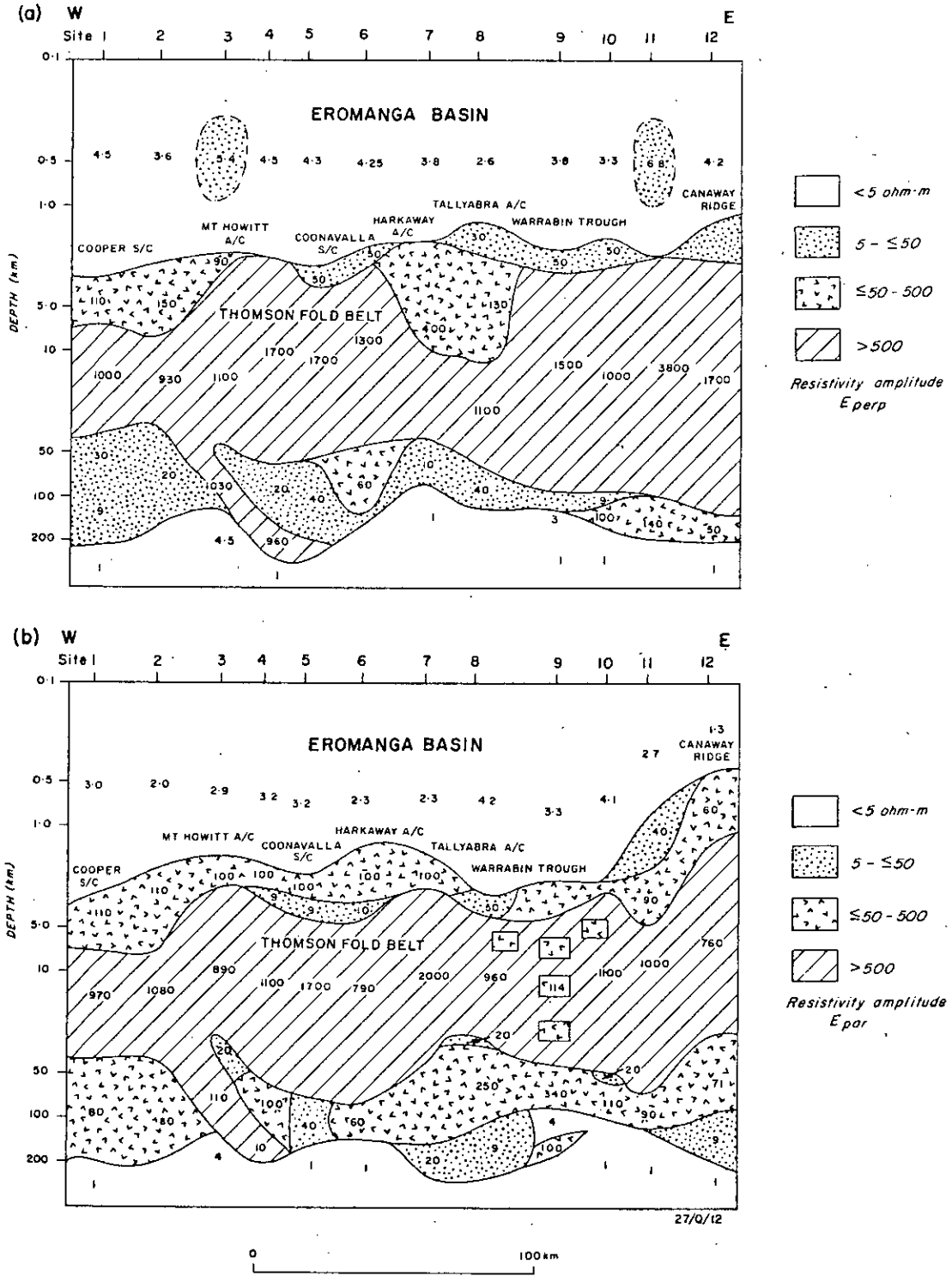

Fig. 8. Resistivity/depth sections along the magnetotelluric traverse derived from (a) E perpendicular-to-strike, and (b) E parallel-to-strike components of apparent resistivity by one-dimensional modelling.

tures. Polak & Ramsay (1977) explained anomalously high temperatures along the northern part of the Canaway Fault by upward migration of groundwater in the fracture zone adjacent to the fault. Faulting may also cause increased salinity, due to long periods of chemical interaction between water and rock.

As mentioned in the earlier section on hydrogeology, Senior & Habermehl (1980) have shown that comparatively small fault-displacements can obstruct several aquifers and cause stagnation zones. These displacements (approx. 50 m) are more likely to produce an effective seal of disconnected aquifers than larger movements, which would probably result in a broad fracture zone, permitting substantial leakage.

The significantly low average resistivity values in the near-surface zones at Sites 2, 6, 7 and 8 could be due to local increases in porosity or to increased salinity resulting from long periods of stagnation. Senior & Habermehl (1980) associated such stagnation zones with hydrocarbon entrapment.

The zone immediately underlying the uppermost low-resistivity sediments has resistivities in the range 5 to 500 ohm m, which are hereinafter referred to as intermediate resistivities (Figs 8a, 8b); it lies immediately under low-resistivity rocks and is consequently not well resolved. Drillhole data indicate porosities in the range 4% and 10%, the average conductivity of the water being the same as that in the overlying sequences. At the eastern end of the magnetotelluric traverses (Fig. 1) the Canaway Ridge structure is evident as a shallowing of this zone in the E_{par} section (Fig. 8a). There is also evidence for this zone within the Cooper Syncline, the Coonavalla Syncline, the Warrabin Trough, and a feature on the western flank of the Canaway Ridge.

Figures 8a and 8b indicate that below Sites 1 and 2 in the Cooper Syncline are probably 4–5 km of isotropic sediment with resistivity in the range 95 to 150 ohm m. Within the Warrabin Trough under sites 7, 8 and 9, the upper few kilometres of this zone of intermediate-resistivity rocks appear anisotropic. The underlying isotropic rocks with resistivities in the range 5 to 500 ohm m have an ill-defined base, but probably are at least 10 km thick. In the Coonavalla Syncline the intermediate resistivity zone appears to be 2–3 km thick and anisotropic. On the E_{par} resistivity section (Fig. 8b) is a layer of fairly uniform resistivity (95–110 ohm m) extending from the Cooper Syncline to under Site 7. The Permo-Triassic Cooper sequence is known to extend into the region, and although variations in this Cooper sequence could barely be detected in pre-survey modelling, it is quite probable that some associated feature, such as steep dips or folding with an axis along strike, is producing an MT response.

SEISMIC DATA COMPARISON

Wake-Dyster & Pinchin (1981) have described the seismic reflection profiling conducted by BMR during 1980 in the Central Eromanga Basin. The magnetotelluric Sites 3 to 11, inclusive, lie along Traverse 1 of this survey. The uppermost 4 seconds of two-way reflection record section are shown in Figure 9, together with the locations of magnetotelluric sites and one-dimensional interpretation above basement from the E_{par} component.

As described earlier, the Mt Howitt No. 1 well-log data have been used as a basis for models of the sedimentary sequence. The depth to the top of the Permian is 2.1 km; this horizon is detected as a strong reflector (P-horizon) west of Site 8. It is recognised in the magnetotelluric data as the resistivity contact between the Eromanga sequence and the higher resistivity Permo-Triassic sequence (Fig. 9).

Beneath the P-horizon west of Site 8 few clear seismic horizons are recognised. The magnetotelluric data do, however, indicate a thicker sedimentary section, and its extent is indicated in Figure 9. As mentioned earlier, part of the section may correspond to the eastward extension of the Cooper Basin sequence. The deeper part of this section is speculatively interpreted by us as a Devonian sequence, possibly the equivalent of the Adavale Basin sediments in the Warrabin Trough, but separated from them by the Harkaway Anticline.

East of Site 8 are the structures of the Warrabin Trough described by Pinchin & Senior (1982) based on the seismic data. The low-resistivity Eromanga Basin sequence here overlies Devonian Adavale Basin sediments (Fig. 9) which are interpreted as being of intermediate resistivity. Its thickness is estimated at 3 km from the seismic data. The magnetotelluric data indicate a greater thickness of intermediate-resistivity rocks, but the interpretation of their depth extent is weakened by the lack of phase data at sites 7 to 10, inclusive.

Data from Sites 11 and 12 are strongly influenced by the Canaway Ridge, which is regarded by Pinchin & Senior (1982) as a fault-bounded basement horst. There does appear to be some evidence of intermediate-resistivity rocks under these sites.

DEEP CRUSTAL AND UPPER MANTLE INTERPRETATIONS

Below the hydrocarbon-prospective sequences, the basement rocks at Mt Howitt No. 1 well are Ordovician shales. Along the Canaway Ridge, exploration well information indicates granodiorite basement in Budgerygar No. 1, schist and basalt in Yongala No. 1, and phyllite in Canaway No. 1 (Pinchin & Senior, 1982). These rocks are taken by us to be representative of the underlying Thomson Fold Belt. They are characterised in the magnetotelluric data by resistivities in excess of 500 ohm m and generally in the range 900–2000 ohm m.

The Fold Belt rocks are generally isotropic and free of large lateral resistive discontinuities, except below Sites 8 and 9, where Warrabin Trough sediments are present to considerable depth. The Belt has little major structural deformation, and the pseudo-sections suggest it consists of low-amplitude folds of long wavelength. The upper surface of the Fold Belt rocks marks the basement of the hydrocarbon-prospective sequence in this region and occurs at an average depth of 3–4 km.

The lower boundary of this resistive zone is a 'sensitive' parameter in the magnetotelluric modelling and generally occurs at 40–60 km depth. This highly

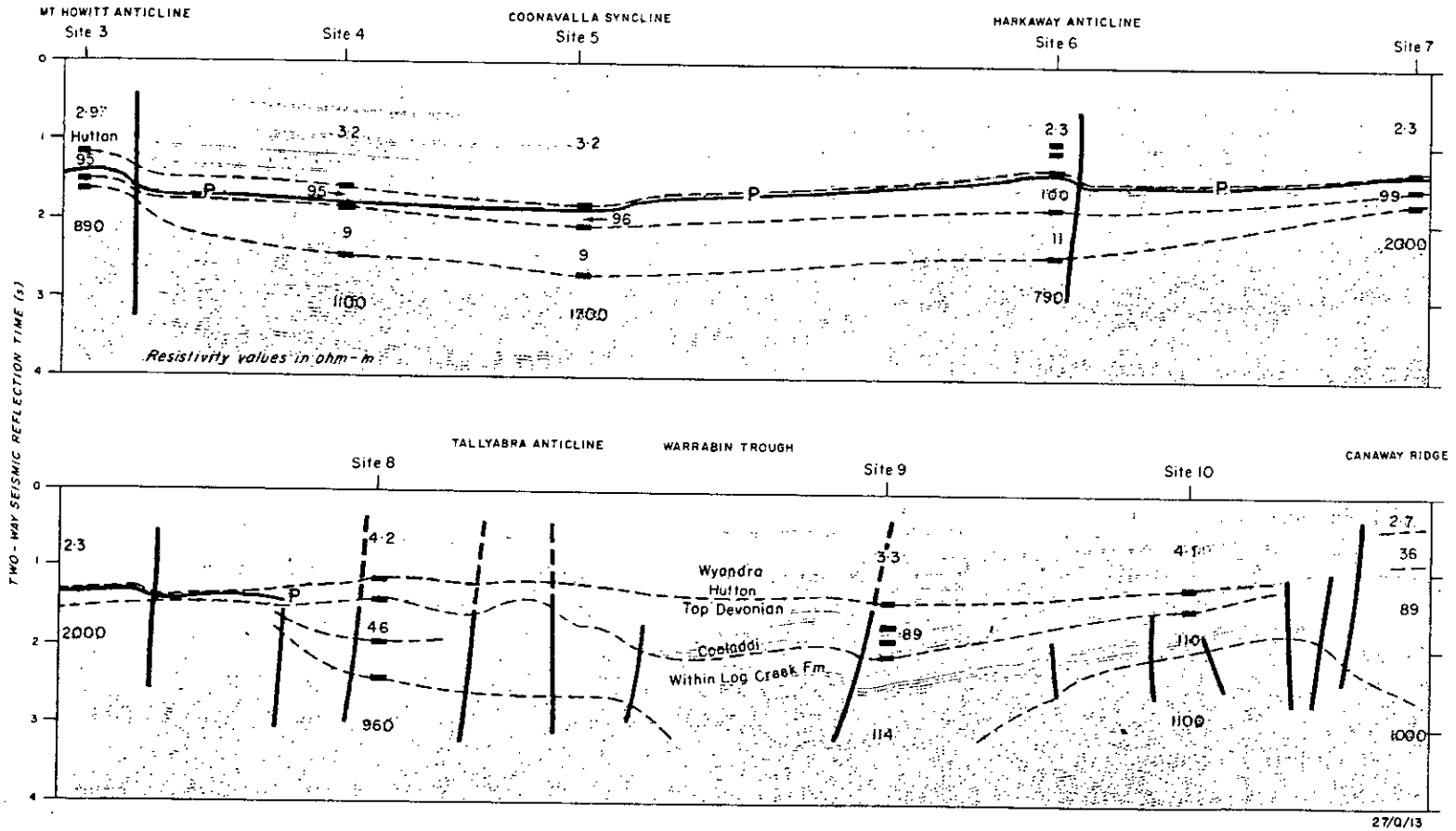

Fig. 9. Seismic reflection record section between magnetotelluric sites 3 and 11, together with one-dimensional resistivity interpretations. The seismic 'P' horizon is indicated on the western part of the traverse. Seismic section derived from Wake-Dyster & Pinchin (1981).

resistive zone, therefore, corresponds to most of the Earth's crust in the region. The strike obtained from the rotation angle information is 17–75°, which agrees with the compilation of Rumph (1978) who indicated that Thomson Fold Belt rocks underlie most of the central Eromanga Basin, consisting mainly of metamorphic rocks displaying a strong northeasterly trend.

There is no evidence in the data for highly conductive regions within this zone as have been inferred elsewhere. Resistivities of about 5 ohm m at 20 km depth have been inferred under the Basin and Range Province (Lienert & Bennett, 1977), and of about 13 ohm m at 28 km depth under the Colorado Plateau (Pedersen & Hermance, 1981) in western USA. Resistivities of 10–20 ohm m have been inferred at depths of 25 km in southern Africa (Van Zijl, 1977).

At depths in excess of 60 km there is a general trend toward lower resistivities, the transition from 1000 ohm m to about 1 ohm m occurring in the depth range 60 to 150 km. Moore et al. (1977) indicated a similar general decrease in resistivity at about 90 km depth in the southern Cooper Basin, and in the Murray Basin of southeastern Australia, Vozoff et al. (1975) interpreted a decrease in conductivity at about 100 km depth. It is probably simplistic to interpret the model resistivity layering in terms of geological layering, because of the considerable effects of temperature (partial melting) at such depths. Lilley et al. (1981) discussed the minimum depths to various resistivity levels within the upper mantle, and indicated that in southeastern Australia the minimum depth to 100 ohm m is about 120 km, and to 1 ohm m is about 230 km. The equivalent depths in central Australia are about 200 km and 450 km, respectively. The indications from the Eromanga Basin data are that resistivities in the range 1 to 10 ohm m are reached at depths less than 150 km, and therefore broadly agree with data from southeastern Australia. Lilley et al. (1981) indicated that a zone of 5% partial basalt melt at depths of about 150 km satisfies the conductivity structures for southeastern Australia.

COMMENT

The relatively small departures from one-dimensional structures along the greater part of the magnetotelluric traverse have allowed simple layered models to be used as a basis for interpretation. Porstendorfer (1975) estimated that in situations where a conductor overlies a resistive substratum, which is the case in the Central Eromanga Basin, the calculated depths are likely to have an error of about 10%.

No attempt has been made to interpret the stratigraphy within the Eromanga Basin sequence, because with a site separation of about 20 km and skin depths at the higher frequencies of less than 0.2 km, correlating between sites is speculative.

Below the low-resistivity, near-surface Eromanga Basin sequence there are indications that the sedimentary sequence is thicker than that indicated from the seismic data. The basement morphology from the magnetotelluric data highlights the long-wavelength features of the Thomson Fold Belt.

ACKNOWLEDGMENTS

The authors acknowledge the considerable contribution of Dr J. P. Cull to the BMR magnetotelluric interpretation program and his comments on our interpretation. D. Denham and F. J. Moss critically reviewed the manuscript. This paper is published with the permission of the Director, Bureau of Mineral Resources, Geology & Geophysics, Canberra.

REFERENCES

BUCHAN, S. H., 1968: *Bodalla No. 1 well completion report.* BP Petroleum Development Australia Pty Ltd *(unpubl.)*.

CULL, J. P., SPENCE, A. G., MAJOR, J. A., KERR, D. W. & PLUMB, K. A., 1981: The 1978 McArthur Basin magnetotelluric survey. *Aust., Bur. Miner. Resour., Geol. Geophys., Rec., 1981/1.*

DELHI-SANTOS, 1966: *Mt Howitt No. 1 well completion report, ATP 66 and 67P, Qld (unpubl.).*

GRANT, F. S. & WEST, G. F., 1965: *Interpretation theory in applied geophysics.* McGraw-Hill, New York.

HABERMEHL, M. A., 1980: The Great Artesian Basin, Australia. *BMR J. Aust. Geol. Geophys., 5,* 9-38.

HARRISON, P. L., MATHUR, S. P., MOSS, F. J., PINCHIN, J. & SENIOR, B. R., 1980: Central Eromanga Basin, program proposals, 1980-1982. *Aust., Bur. Miner. Resour., Geol. Geophys., Rec., 1980/32.*

HERMANCE, J. F., 1973: Processing of magnetotelluric data. *Phys. Earth Planet. Inter., 7,* 349-64.

INGRAM, J. A., 1971: *Explanatory notes, Eromanga, Queensland 1:250 000 geological map SG 54-12.* Bur. Miner. Resour., Geol. Geophys.

JUPP, D. L. B. & VOZOFF, K., 1975: Stable iterative methods for the inversion of geophysical data. *R. Astron. Soc., Geophys. J., 42,* 957-76.

JUPP, D. L. B. & VOZOFF, K., 1977: Two-dimensional magnetotelluric inversion. *R. Astron. Soc., Geophys. J., 50,* 333-52.

KELLER, G. V., 1971: Electrical characteristics of the Earth's crust; *in* Wait, J. R. (ed.) *Electromagnetic probing in geophysics.* The Golem Press, Boulder, Colorado, 13-76.

LILLEY, F. E. M., WOODS, D. V. & SLOANE, M. N., 1980: Electrical conductivity profiles and implications for the absence or presence of partial melting beneath central and southeast Australia. *Phys. Earth Planet. Inter., 25,* 419-28.

LIENERT, B. R. & BENNETT, D. J., 1977: High electrical conductivities in the lower crust of the northwestern Basin and Range: an application of inverse theory to a controlled source deep-magnetic-sounding experiment; *in* Heacock, J. G. (ed.) The Earth's crust. *Am. Geophys. Union, Geophys. Mongr., 20,* 531-52.

MIDDLETON, M. F., 1979: Correlation between well-log and surface resistivity measurements—a case study in the Eromanga Basin, Queensland. *Aust. Assoc. Explor. Geophys., Bull., 10,* 176-8.

MOORE, R. F., 1977: Screening and averaging magnetotelluric data prior to one-dimensional inversion. *Aust., Bur. Miner. Resour., Geol. Geophys., Rec., 1977/8.*

MOORE, R. F., KERR, D. W., VOZOFF, K. & JUPP, D. L. B., 1977: Southern Cooper Basin magnetotelluric survey, South Australia, 1974. *Aust., Bur. Miner. Resour., Geol. Geophys., Rec. 1977/41.*

PEDERSEN, J. & HERMANCE, J. F., 1981: Deep electrical structure of the Colorado Plateau as determined from magnetotelluric measurements. *J. Geophys. Res., 86,* 1849-57.

PINCHIN, J. & SENIOR, B. R., 1982: The Warrabin Trough, western Adavale Basin, Queensland. *Geol. Soc. Aust., J., 29,* 413-24.

PLUMB, K. A., 1979: The tectonic evolution of Australia. *Earth-Sci. Rev., 14,* 205-49.

POLAK, E. J. & RAMSAY, D. C., 1977: Canaway Ridge, Queensland, geophysical survey 1973. *Aust., Bur. Miner. Resour., Geol. Geophys., Rec., 1977/29.*

PORSTENDORFER, G., 1975: *Principles of magneto-telluric prospecting. Geo-publication Associates, Series 1, No. 5.* Gebrunder Borntraeger, Berlin-West & Stuttgart.

RUMPH, R., 1978: Regional gravity and magnetic data of the Central Eromanga Basin area: implications on the crustal structure, regional geology and tectonic history. M.Sc. thesis, Univ. Sydney (*unpubl.*).

SENIOR, B. R., MOND, A. & HARRISON, P. L., 1978: Geology of the Eromanga Basin. *Aust., Bur. Miner. Resour., Geol. Geophys., Bull., 167.*

SENIOR, B. R. & HABERMEHL, M. A., 1980: Structure, hydrodynamics and hydrocarbon potential, central Eromanga Basin, Queensland, Australia. *BMR J. Aust. Geol. Geophys., 5,* 47-55.

VAN ZIJL, J. S. V., 1977: Electrical studies of the deep crust in various tectonic provinces of southern Africa; *in* Heacock, J. E. (ed.) The Earth's crust. *Ann. Geophys. Union, Geophys. Mongr., 20,* 470-500.

VOZOFF, K., 1972: The magnetotelluric method in the exploration of sedimentary basins. *Geophysics, 37,* 98-141.

VOZOFF, K. & JUPP, D. L. B., 1975: Joint inversion of geophysical data. *R. Astron. Soc., Geophys., J., 42,* 977-91.

VOZOFF, K., KERR, D. W., MOORE, R. F., JUPP, D. L. B. & LEWIS, R. J. G., 1975: Murray Basin magnetotelluric study. *Geol. Soc. Aust., J., 22,* 361-75.

WAKE-DYSTER, K. D. & PINCHIN, J., 1981: Central Eromanga Basin seismic survey, Queensland, 1980: operational report. *Aust., Bur. Miner. Resour., Geol. Geophys., Rec., 1981/22.*

WHITELEY, R. J. & POLLARD, P. C., 1971: A combined deep resistivity and magnetotelluric sounding in the Eromanga Basin, Queensland. *Search, 2,* 103-5.

WOODS, D. V. & LILLEY, F. E. M., 1980: Anomalous geomagnetic variations in the concentration of the telluric currents in south-west Queensland, Australia. *R. Astron. Soc., Geophys. J., 62,* 675-89.

THE MID-CRUSTAL HORIZON UNDER THE EROMANGA BASIN, EASTERN AUSTRALIA.

D.M. FINLAYSON

Bureau of Mineral Resources, Geology & Geophysics, Canberra, Australia.

ABSTRACT

Long-line explosion seismic recordings indicate that a major mid-crustal P-wave velocity increase exists under the Eromanga Basin which contrasts the crust of this region from its neighbouring tectonic provinces. The velocity increase is shown to be a regional feature and to correspond to the upper boundary of a zone of discontinuous seismic reflections characteristic of the lower crust. The velocity increase of 0.35-0.6 km/s occurs over a small depth range at an average depth of 24 km. This velocity gradient produces conspicuous wide-angle reflections at distances greater than 60 km from the shot point. The seismic data present the clearest evidence to date of the existence of a major mid-crustal horizon in continental Australia, a feature not prominent in other cratonic provinces which have been investigated in detail. The velocity in the lower crust below the horizon is 6.7-7.0 km/s. The horizon represents a boundary between the upper and lower crust which could imply a different tectonic history for these two zones.

INTRODUCTION

On a world scalar anomaly map of Magsat data, the Eromanga Basin in eastern Australia stands out as a prominent magnetic anomaly low (Frey, 1982) which contrasts with its neighbouring tectonic provinces. A large proportion of the Earth's crust must be involved in producing this anomaly.

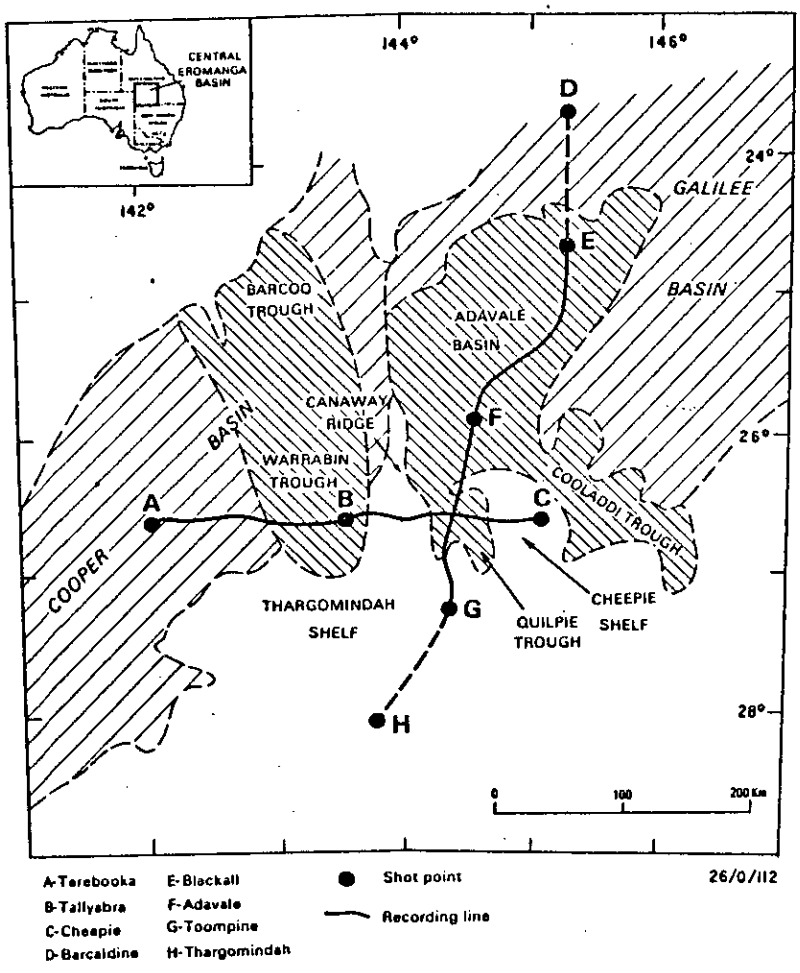

1. General geology of the central Eromanga Basin and the location of long-line seismic refraction profiles. Eromanga Basin sediments overlie the whole of the region.

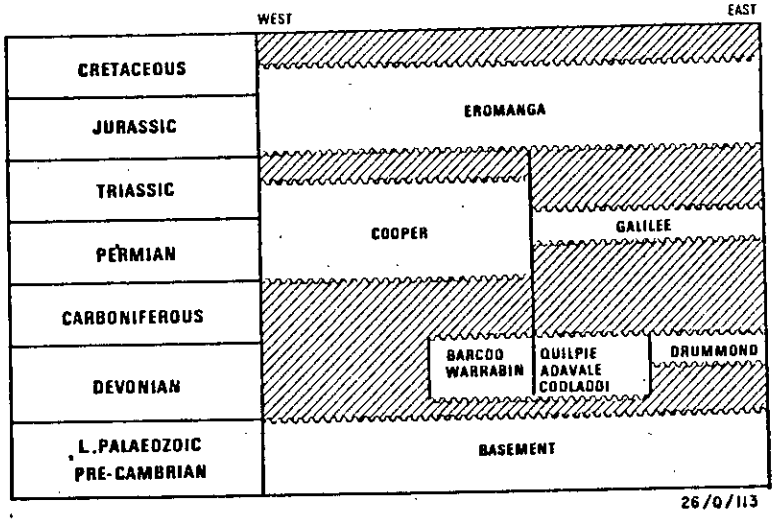

2. The Eromanga Basin and infra-basins.

Using a magnetite Curie point of 670 degrees C and the Sass & Lachenbruch (1979) geotherms for central and eastern Australia, a Curie point depth of 35-40 km is appropriate for the Eromanga Basin and surrounding region. Thus we have at least one geophysical parameter which strongly suggests that the Earth's crust under Eromanga Basin is significantly different from that of surrounding regions of continental Australia.

In 1980 the Bureau of Mineral Resources, Geology & Geophysics (BMR) conducted a long-line seismic refraction survey and coincident vertical seismic profiling to 20s in the central Eromanga Basin region (Fig. 1). Finlayson et al (1983, in press) have already reported some results from the refraction work along the 300 km east-west traverse and summarised the major geological features of the region. Mathur (1983, this volume) has highlighted the significant features of the deep vertical profiling records. A major feature of the velocity/depth distribution from the east-west data is the prominent mid-crustal horizon at a depth of 21-24 km where the P-wave velocity increases by up to 0.6 km/s in a depth range of less than 0.5 km. This is interpreted from large-amplitude wide-angle reflection phases beyond the critical distance.

During 1981 BMR conducted further long-line seismic refraction recording on a north-south azimuth traversing the Adavale Basin, Quilpie Trough and Thargomindah Shelf (Fig. 1). Figure 2 is a simplified stratigraphic diagram of the Eromanga Basin and its underlying basins. This paper presents interpretations of data from this traverse and provides further evidence for a mid-crustal seismic horizon as a general feature of the crust under the Eromonaga Basin and discusses its significance for theories on the tectonic evolution of the region.

THE MIDDLE CRUST

Seismic models of the Earth's continental crust have long recognised the necessity of including some form of increase in the P-wave seismic velocity with depth in order to satisfy observed data (e.g. see Bott,

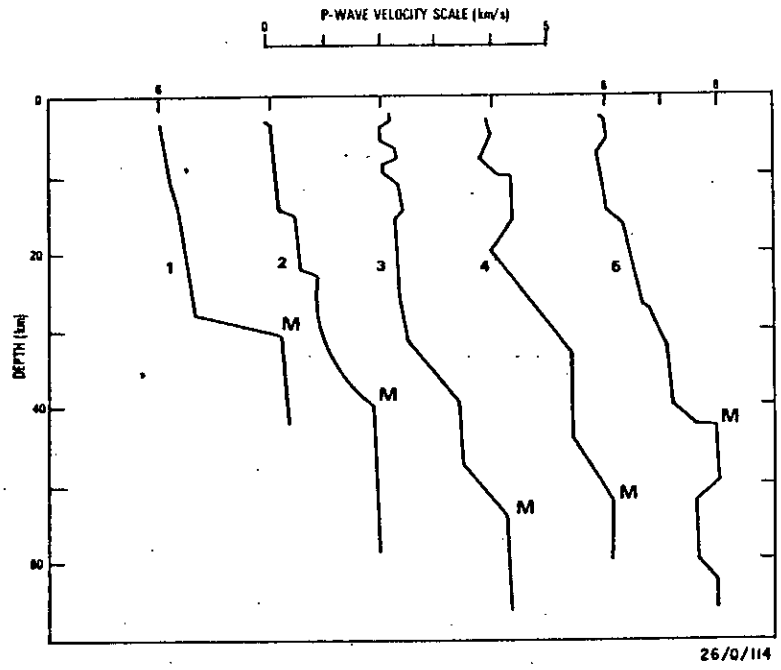

3. Velocity/depth profiles from other regions of continental Australia. 1) Pilbara Block (Drummond, 1983), 2) McArthur Basin, North Australian Craton (Collins, 1983); 3) Tennant Creek, North Australian Craton (Finlayson, 1982); 4) southern Lachlan Fold Belt (Finlayson et al, 1979); 5) northern Lachlan Fold Belt (Finlayson & McCracken, 1981).

1971). Such models often include the concept of upper and lower crustal layers separated by a Conrad discontinuity at which the velocity increased.

Explosion seismic work during 1950-1970 indicated that such simple models were not appropriate and more complex velocity/depth distributions were required to satisfy the observed data (for reviews see Closs, 1969; Sollogub, 1969; Kosminskaya et al 1969; Healy and Warren, 1969). The concept of a single mid-crustal discontinuity changed to one of many possible velocity gradients in the crust. At the extreme there were places where no layering within the crust was evident and continuous velocity increases with depth were enough to satisfy data. Mueller & Landisman (1966) pointed out that low velocity zones were likely in the crust at depths less than 20 km. In fact, these authors included observations from southeastern Australia by Doyle et al (1959) to substantiate their interpretations. Mueller & Landisman (1966) also used statistical evidence from deep vertical soundings by Liebscher (1962) to illustrate further evidence for horizons throughout the crust, including a Conrad discontinuity at 7s two-way reflection time i.e. at about 21 km depth. However, the widespread existence of a Conrad discontinuity throughout all continents was rightly questioned.

In Austrtalia recent detailed investigations of continental structure resulted in more complex crustal features being recognised. Figure 3 illustrates examples of velocity/depth models from the Phanerozoic Lachlan Fold Belt in southeast Australia (Finlayson et al, 1979; Finlayson & McCracken, 1981), Proterozoic North Australian Craton (Collins, 1983; Finlayson, 1982) and Archaean Pilbara Craton (Drummond, 1983). All models are characterised by velocity gradients rather than 'discontinuities' at mid-crustal depths (Finlayson, 1979). Thus in regions of exposed basement geology throughout Australia there does not appear to be a major mid-crustal horizon.

In recent years the tectonic significance of mid-crustal seismic horizons has changed also. The models of continental crustal structure have long been constrained by the geochemistry of rocks comprising the continental lithosphere

(see for example McLennan & Taylor, 1982: Ringwood, 1982). However, the introduction of long, deep-seismic, reflection profiles in continental USA has highlighted the possibility of large scale decollement and mylonite horizons in the middle crust many hundreds of kilometers in extent resulting from horizontal tectonic movements (see for example Smithson et al 1980; Cook et al, 1979; Harris & Bayer, 1979). Hence continental mid-crustal horizons may not only be interpreted in terms of compositional or metamorphic horizons resulting from vertical geochemical differentiation but also in terms of large scale extension and shortening of the lithosphere.

SEISMIC REFRACTION PROFILES

The locations of seismic refraction profiles used in this paper are shown in Figure 1. The east-west traverse extends from the Cooper Basin across the Warrabin Trough, Canaway Ridge, Quilpie Trough and Cheepie Shelf. The north-south traverse extends along the axis of the Adavale Basin and Quilpie Trough on to the Thargomindah Shelf.In this paper only the recorded seismic data out to distances of 150 km will be discussed. Hence the east-west line will be considered as two reversed, 150 km traverses A-B and B-C, and the central part of the north-south line will be considered as two reversed, 150 km traverses E-F and F-G. A full description of survey operations has been written by Lock (1983).

The shots for the interpretation in this paper were, respectively, 0.7t and 0.9t on the east-west and north-south lines. DuPont Anzite Blue explosive was placed at 40 m depth in drillhole patterns, usually 100 kg of explosive per hole. The shots were fired electrically and timed with respect to the Telecom Australia radio time signal broadcast by VNG. Seismic recordings were made at 7.5 km intervals on BMR automatic seismic tape recording systems, 21 of which were used on this survey. These systems record both a high and a low-gain vertical seismic channel (24 dB separation, frequency modulated),

a programmable crystal clock time-code and the VNG radio time signal to ensure a common time source for all data (Finlayson & Collins, 1980).

SEISMIC RECORD SECTIONS

Seismic recordings were digitized using the playback system described by Liu & Seers (1982). The seismic record sections produced from the data for this paper all have the traces nomalized to the maximum amplitude on each individual trace and all have been filtered in the bandpass 2-15 Hz. In many cases the low-gain seismic channel displayed the character of the seismic phases better than the high-gain channel because of overmodulation of the large amplitude phases on the high-gain channel. Consequently the majority of traces displayed on the record sections are from the low-gain channel. The high-gain channel has however been used to determine the arrival times of the various phases, often with an error of less than 0.05s; these are indicated by dots on the record sections.

The diagnostic features of a major velocity boundary at mid-crustal depths have been outlined by Bott (1971) and Braile & Smith (1975). These are principally the large amplitudes expected for super-critically reflected energy from the boundary, the apparent velocities of the refracted and reflected phases from within the upper crust and the identification of refracted phases from the lower crust.

TRAVERSE A-B-C (EAST-WEST)

Data from the traverse A-B-C have already been described by Finlayson et al (1983; in press); only the essential features of the mid-crustal horizon will be described here. Figures 4 a,b,c and d show the seismic record sections along the two halves of the traverse in the distance range 40 to 160 km. They clearly illustrate seismic phases interpreted as traversing the upper and middle crust. The series of first arrivals out to distances of about 100 km (labelled p-q) are usually implusive and have an

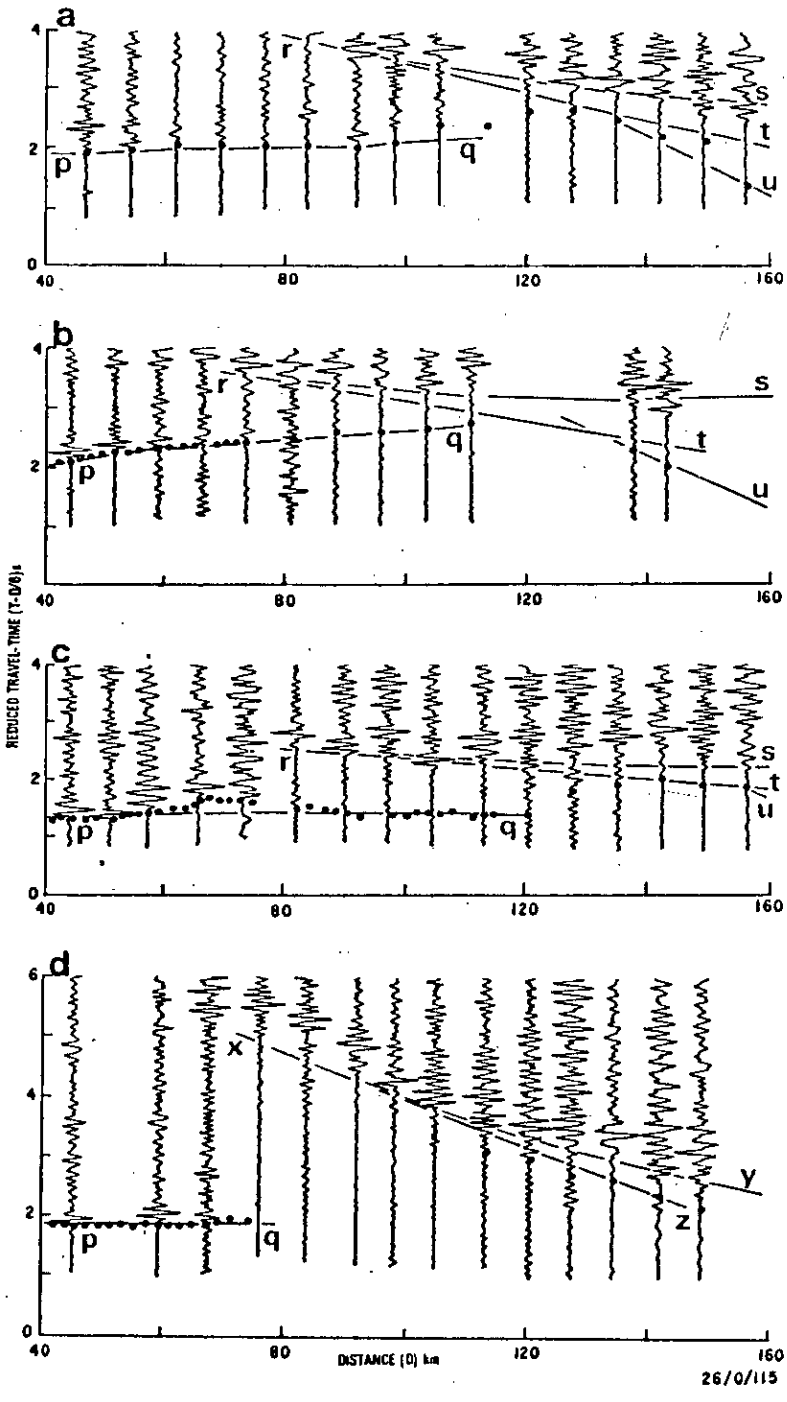

4. Seismic record sections from the east-west traverse A-B-C. a) Shots at A recorded to B; b) shot at B recorded to A; c) shots at C recorded to B; d) shot at B recorded to C. Seismic traces have been normalised to equal maximum amplitude and filtered in the bandpass 2-15 Hz. Dots indicate first arrivals confidently read from high-gain records (not all shown). The various seismic phases are described in the text.

apparent velocity of less than 6.1 km/s. They are identified with P-waves traversing the upper crustal basement beneath the sedimentary sequence.

The other significant phases displayed in the record sections are the events labelled r-s. In Figures 4 a,b and c they are evident at distances greater than 60 km. Near point 'r' the apparent velocity is greater than 6.5 km/s and near point 's' it approaches that of the upper crustal basement i.e. about 6.1 km/s. The low apparent velocity of the critically refracted events 'r-t' precludes their being upper mantle arrivals. These large amplitude events are interpreted as being wide-angle reflections from a prominent mid-crustal velocity increase. In Figure 4d the events labelled x-y have a much higher apparent velocity than events r-s and Finlayson et al (1983, in press) have indicated that they result from a shallower crust/mantle boundary under the Canaway Ridge where the crustal velocity/depth distribution is significantly different from the surrounding region.

TRAVERSE E-F-G (NORTH-SOUTH)

The traverse E-F-G was designed to extend the regional coverage of crustal investigations to ensure that features found on the east-west traverse were not isolated features. Figures 5 a,b,c and d show the seismic record sections in the distance range 40 to 160 km from the central part of the north-south traverse. Traverse E-F (Figs 5 a,b) is centrally placed in the Adavale Basin. The features seen on the east-west traverse are again evident on this north-south traverse. Arrivals p-q have apparent velocities of less than 6.1 km/s and arrivals r-s have a similar character to wide-angle reflections from the mid-crustal horizon on the east-west traverse. This interpretation is therefore attached to the r-s events on the north-south traverse.

Traverse F-G (Figs 5 c,d) crosses from the Adavale Basin and Quilpie Trough onto the Thargonindah Shelf. The difference in thickness of low-velocity basin sediments under shot points F and G is an obvious feature of the record sections, the first arrivals at distances out to 60 km being

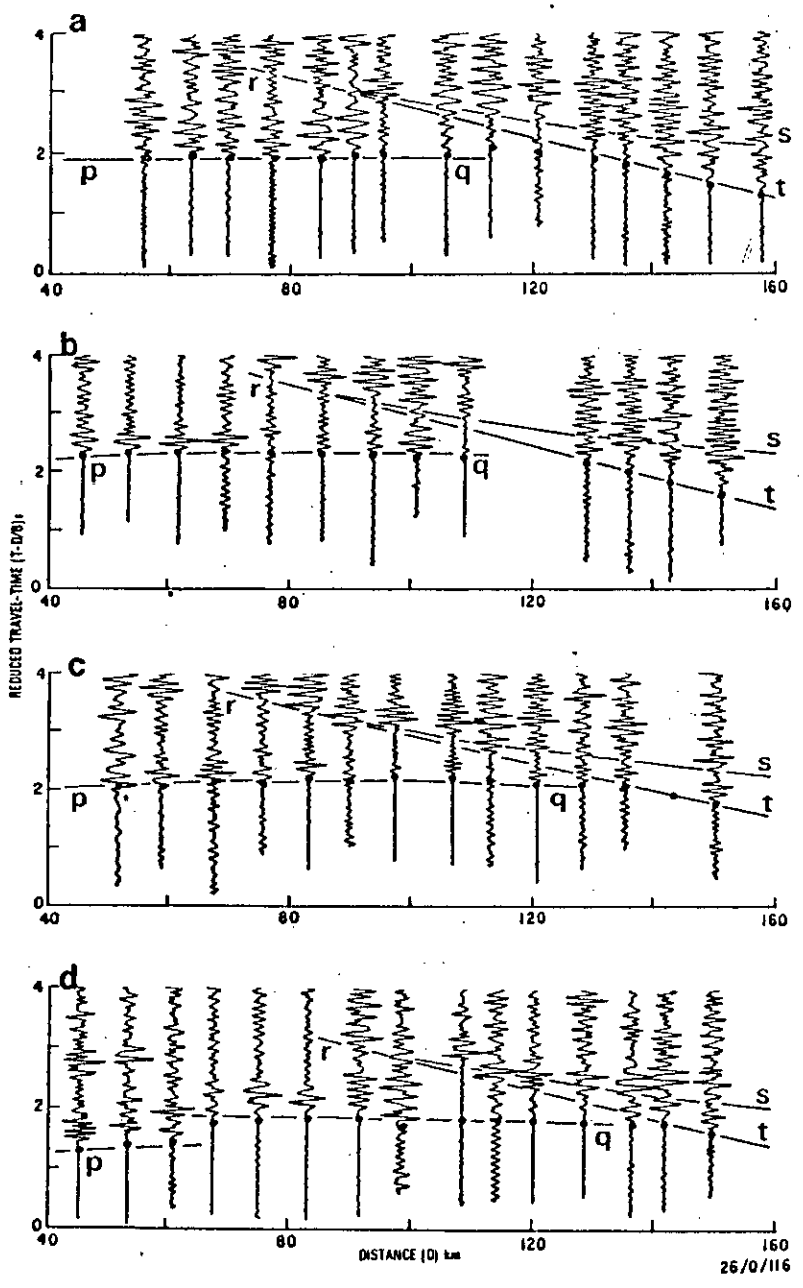

5. Seismic record sections from the north-south traverse E-F-G. a) Shots at E recorded to F; b) shot at F recorded to E; c) shot at F recorded to G; d) shots at G recorded to F. Trace display and annotation the same as in Figure 4.

0.8-0.9s earlier from shot point G. However this difference between the thickness of basin and shelf sediments can be taken into account in any interpretation. The principal feature of the record sections beyond 40 km is still the series of wide-angle reflections from a horizon in the middle crust.

VELOCITY/DEPTH MODELS

Finlayson et al (1983, in press) have derived velocity/depth models for the traverse A-B-C. The travel-time curves for these models are superimposed on the record sections in Figures 4 a,b,c, and d. The models themselves are shown in Figure 6. The interpretation of the record sections from the north-south traverse D-E-F was conducted in a manner similar to that for the east-west traverse. The travel-time curves from the preferred models are superimposed on Figures 5 a,b,c and d. These models are also shown in Figure 6.

One feature of the models different for the north-south line compared with those for the east-west line is the lack of a reduction in velocity in the upper crust at depths of 5-12 km. The models shown in Figure 6 indicate that there is no decrease in velocity in the approximate depth range 12-22 km and it is possible that the sharp velocity reduction on the models from the east-west line should not be taken as a significant feature. Certainly, if the velocity reduction in Fig. 6 model 3 was reduced, the depth to the mid-crustal horizon would increase and be more in accord with the average depth of 24 km for this horizon.

VERTICAL SEISMIC REFLECTION PROFILING

As mentioned in the introduction, extensive seismic reflection work was also conducted in the central Eromanga Basin. Approximately 1500 km of 6 fold CDP shooting was recorded to 20s two-way reflection time. Mathur (1983, this volume) has described some of the deep reflection recording results from the central part of the east-west traverse A-B-C. Below the sedimentary

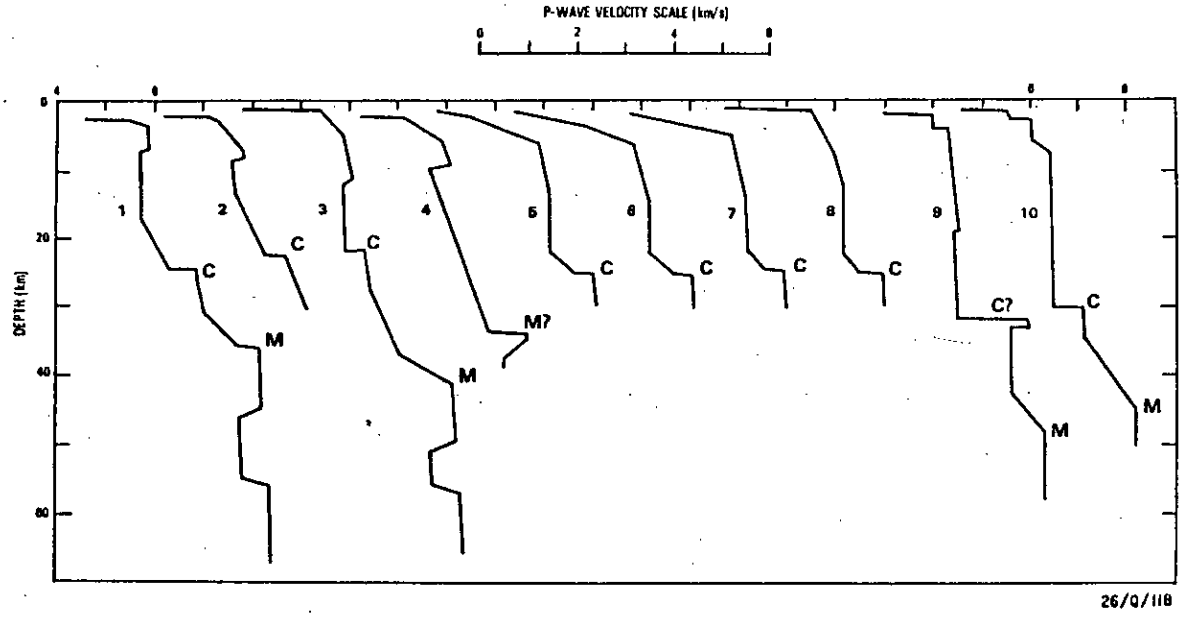

6. Velocity/depth models for the central Eromanga Basin and Bowen Basin. 1) Shot point A towards the east; 2) B west; 3) C west; 4) B east; 5) E south; 6) F north; 7) F south; 8) G north; 9) Bowen Basin CQEW model (Leven, 1980); 10) Bowen Basin model 3 (Collins,1980).

sequence there is a zone of very few reflections until a two-way reflection time of about 8 s is reached. Between 8 and 12.5 s there is a broad zone of numerous short, discontinuous reflection events which model studies (Fuchs,1969) have shown can be produced by laminae of alternating high and low velocity the layer thicknesses being less than the seismic wavelength of about 100 m. The mid-crustal horizon interpreted from the long-line refraction work described in this paper corresponds with the start of the prominent reflection events in the middle crust.

Under the north-south traverse D-E-F the same zonation can be applied to the reflection events. The zone of reflection events is in the two-way-time interval 8-14 s (Mathur, pers. comm.). The velocity/depth models in Figure 6 are compatible with the vertical reflections at 9 s.
of the Adavale Basin.

DISCUSSION

The seismic record sections in Figures 4 and 5 present the clearest evidence to date of the existance of a major mid-crustal velocity increase in continental Australia. The data from both east-west and north-south traverses show that this feature is not an isolated structure but is general throughout the central Eromanga Basin. The only exceptional structure is that under the Canaway Ridge from shot point B shooting eastwards which results from a different tectonic environment under the Ridge.
The mid-crustal horizon does, however, generally seem to be present under both basin and shelf areas. The velocity increase at this horizon is interpreted as being in the range 0.35 to 0.6 km/s and its depth being in the range 21 to 25 km, however the average depth is about 24 km.

In Figure 7 the refraction and reflection information have been combined to produce a schematic representation of the Earth's crust in the central Eromanga Basin. The deep velocity structure has been taken from the interpretation of Finlayson (1983, in press). It includes a crust/

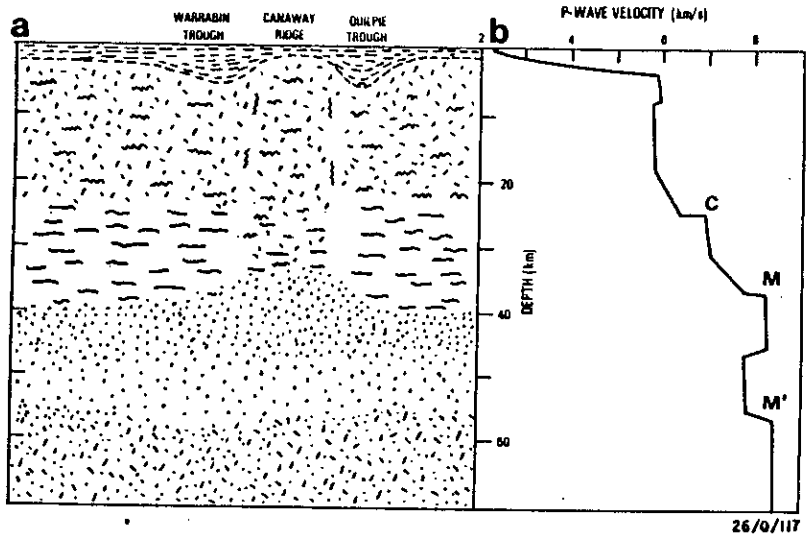

7. Schematic lithospheric section for the central Eromanga Basin region, a) derived from the character of the vertical seismic reflections (Mathur, this volume), and b) velocity/depth profile from shots at A (Fig. 1) recorded eastward. Deep reflection data (greater than 4 s two-way-time) are not available east of the Canaway Ridge, therefore the nature of the reflection horizons there is only diagramatic. In a), symbols in the depth range 0-5 km represent Devonian and younger sediments; 5-24 km — highly deformed metasediments/metavolcanics of the Thomson Fold Belt and other late Proterozoic-early Palaeozoic rocks; 24-40 km -- lower crustal rocks with increasing average velocity and layered, possibly by metamorphic fronts, underplating or magma intrusion; 40-70 km -- amorphous upper mantle rocks with broadly varying velocity with depth, including a low velocity zone.

mantle boundary at a depth of 36-41 km with a velocity in the upper mantle of 8.15 km/s. Deeper within the upper mantle at a depth of 56-57 km there is another seismic horizon where the velocity increases to 8.35 km/s. A low velocity zone is interpreted above this horizon. The vertical reflections apparent in the lower crust cut out at the crust/mantle boundary and within the upper mantle there are no further reflections (Mathur, this volume).

The tectonic significance of the mid-crustal horizon in the Eromanga Basin is difficult to determine. Such prominent horizons are by no means always recorded in continental regions. In some areas of Europe particular horizons evident on reflection records are associated with 'discontinuities' e.g. the Conrad and Subconrad discontinuities of Dohr & Meissner (1975), and not with broad zones of reflections.

Under the Columbia Plateau and Basin and Range Provinces of western USA Prodehl (1970, 1977) identified his 'b' and 'a-b' events on long-line refraction profiles with retrograde branches of the travel-time curve originating at fairly strong velocity increases at mid-crustal depths. However the events are not ubiquitous. Prodehl (1970) for example, interpreted a distinct lower crustal layer with the velocity increasing from 6.4-6.6 km/s to 7.0 km/s under the northern Basin and Range Province but not in the southern part. Braile (1977) and Muller & Mueller (1979) have shown how in another parts of the Basin and Range Province (eastern) there is a thin crust (30 km) with the lower crustal velocity only reaching 6.4-6.6 km/s and the dominent mid-crustal reflections come from a velocity increase at about 10-12 km depth, below a low velocity zone.

Thus the long-line refraction data alone can be interpreted in many ways. However, combined with the vertical reflection profiling data there seems to be a major difference in the geological character of the upper and lower crustal zones of the central Eromanga Basin, the upper crust under the

sediments being effectively 'transparent' and the lower crust displaying effectively a multiple series of short reflecting horizons.

Some measure of credibility must therefore be accorded to a number of tectonic models mentioned below. Mueller (1977) has taken characteristics such as those found under the Eromanga Basin into account in his generalised model of the continental crust, emphasizing the diversity of possible tectonic situations which can arise. In this model the lower crust with velocities of about 7 km/s is composed of mafic metamorphic rocks with, perhaps, migmatitic rocks overlying amphibolite facies rocks contributing towards the rapid velocity increase at mid-crustal depths.

The different character in the vertical reflection records from the upper and lower crust leads to speculation that tectonic episodes in these two crustal regions were different. The upper crust could be uniformly plutonic so that no seismic reflectors arise, or else it could be highly folded and faulted thus precluding the return of coherent seismic energy.This latter interpretation is preferred based on the comparatively low resistivities of the crust (Spence & Finlayson,1982). The lower crustal reflection character could result from metamorphic 'fronts' (Mueller, 1977) during some tectonic episode which may or may not be contemporaneous with upper crustal tectonism. Rutland (1982), for instance, has argued in favour of the separate development of the upper and lower crust in continental Australia. Much of the upper crustal rock in eastern Australia is envisaged as being reworked older continental material with platformal cover. The lower crustal rocks are considered to be from a different chelogenic cycle (global thermal cycle of the order of 1000 Ma) and this may result in a different seismic reflection character as well as causing a velocity unconformity corresponding to the mid-crustal horizon (Conrad discontinuity).

Other mechanisms which may cause the lower crustal 'laminated' seismic

character include the introduction of basaltic melt fractions or some form of underplating by differentiated upper mantle components either at the time of cratonisation or later. Ewart et al (1980) and Wass & Hollis (1983) have proposed such underplating for crustal thickening under eastern Australia. Similar episodes could arise during the cratonisation of back-arc or pericratonic basins to cause the laminated structure under the Eromanga Basin.

The structure under the Canaway Ridge (Fig. 6 profile 4) is enigmatic at this stage. Finlayson et al (1983) have compared the velocity structure with that of Leven's (1980) CQEW model from the Bowen Basin (Fig. 6 profile 9). However, this latter model, derived from seismic profiles recorded cross-strike, differs from the longer reversed profiles of Collins (1980) along the axis of the Bowen Basin (Fig. 6 profile 10). Collins interprets a lower L-crustal horizon at slightly shallower depths than Leven's 'Moho' suggesting that they may be the same feature. The true Moho may well be at 44-48 km depth where both authors agree that velocities in excess of 8.2 km/s are reached below similar velocity gradients. Thus under the Canaway Ridge there is undoubtedly a strong velocity feature at 34 km depth, but there is still some doubt about whether it should be identified with the Moho.

ACKNOWLEDGEMENTS

The author would like to acknowledge the help and assistance with the long-line seismic refraction survey work by many people, in particular by Clive Collins, Jo Lock, Chris Rochford, Jim Whatman, John Williams and Jane Rogers. The field work was greatly assisted by help from the BMR seismic reflection crew under the leadership of John Moss, John Pinchin and Owen Dixon(Geological Survey of Queensland). This paper is published with the permission of the Director, Bureau of Mineral Resources, Geology & Geophysics, Canberra.

REFERENCES

Bott, M.H.P., 1971. The Interior of the Earth. Edward Arnold, London, 28-70.

Braile, L.W. & Smith, R.B., 1975. Guide to the interpretation of crustal refraction profiles. Geophys. J. R. Astr. Soc., 40, 145-176.

Braile, L.W., 1977. Interpretation of crustal velocity gradients and Q structure using amplitude-corrected seismic refraction profiles. In; The Earth's Crust (ed J.G. Heacock), Am. Geophys. Un., Geophys. Mono 20, 427-439.

Closs, H., 1969. Explosion seismic studies in western Europe. In; The Earth's Crust and Upper Mantle (ed. P.J. Hart), Am. Geophys, Un., Geophys. Mono 13, 178-188.

Collins,C.D.N.,1980. Crustal structure of the central Bowen Basin from deep seismic sounding. MSc Thesis, University of Queensland, Brisbane.

Collins, C.D.N., 1983. Crustal structure of the southern McArthur Basin from deep seismic sounding. BMR J. Aust. Geol. Geophys., 8, in press.

Cook, F.A., Albaugh, D.S., Brown, L.D., Kaufman, S., Oliver, J., & Hatcher, R.D., 1979. Thin-skinned tectonics in the crystalline southern Appalachians; COCORP seismic-reflection profiling of the Blue Ridge and Piedmont. Geology, 7, 563-567.

Dohr, G.P. & Meissner, R., 1975. Deep crustal reflections in Europe. Geophysics, 40, 25-39.

Doyle, H.A., Everingham, I.B. & Hogan, T.K., 1959. Seismic recordings of large explosions in southeastern Australia. Aust. J. Phys., 12, 222-230.

Drummond, B.J., 1983. Detailed seismic velocity/depth models of the upper lithosphere of the Pilbara Craton, northwest Australia. BMR J. Aust. Geol. Geophys., 8, in press.

Ewart,A., Baxter,K. & Ross, J.A.,1980. The petrology and petrogenesis of the Tertiary anorogenic mafic lavas of southern and central Queensland,

Australia - Possible implications for crustal thickening. Contrib. Mineral. Petrol., 75, 129-152.

Finlayson, D.M., 1979. The Australian continental crust: explosion seismic studies in Archaean, Proterozoic and Palaeozoic provinces. IASPEI Programs and Abstracts, IUGG XVII General Assembly, Canberra, 84-85.

Finlayson, D.M., 1982. Seismic crustal structure of the Proterozoic North Australian Craton between Tennant Creek and Mount Isa. J. Geophys. Res., 87, 10569-10578.

Finlayson, D.M., & Collins, C.D.N., 1980. A brief description of BMR portable seismic tape recording systems. Aust. Soc. Expl. Geophys. Bull., 11, 75-77.

Finlayson, D.M. & McCracken, H.M., 1981. Crustal structure under the Sydney Basin and Lachlan Fold Belt, determined from explosion seismic studies. J. Geol. Soc. Aust., 28, 177-190.

Finlayson, D.M., Prodehl, C. & Collins, C.D.N., 1979. Explosion seismic profiles and their implications for crustal evolution in southeastern Australia. BMR J. Aust. Geol. Geophys., 4, 234-252.

Finlayson, D.M., Collins, C.D.N. & Lock, J., 1983. P-wave velocity features of the lithosphere under the Eromanga Basin, eastern Australia, including a prominant mid-crustal (Conrad?) discontinuity. Tectonophysics (in press).

Frey, H., 1982. MAGSAT scalar anomaly distribution: the global perspective. Geophys. Res. Lett., 9, 277-280.

Fuchs,K.,1969. On the properties of deep crustal reflectors. Zeitschrift fur Geophys., 35, 133-149.

Harris, L.D. & Bayer, K.C., 1979. Sequential development of the Appalochian orogen above a master decollement - A hypothesis. Geology, 7, 568-572.

Healy, J.H. & Warren, D.H., 1969. Explosion seismic studies in North America. In, The Earth's Crust and Upper Mantle (ed. P.J. Hart), Am. Geophys. Un., Geophys. Mono. 13, 208-220.

Kosminskaya, I.P., Belyaevsky, N.A. & Volvovsky, I.S., 1969. Explosion seismology in the USSR. In, The Earth's Crust and Upper Mantle (ed. P.J. Hart), Am. Geophys. Un., Geophys. Mono. 13, 195-208.

Leven, J.H.,1980. Application of synthetic seismograms to the interpretation of crustal and upper mantle structure. PhD Thesis, Australian National University, Canberra.

Liebscher, H.J., 1962. Reflexionshorizonte der tieferen Erdkruste im Bayerischen Alpenvorland, abgeleitet aus Ergebnissen der Reflexionsseismik. Z. Geophys., 28, 162.

Liu, Y.S.B. & Seers, K.J., 1982. A plackback system for portable seismic recorders. Bull. Aust. Soc. Expl. Geophys., 13, 77-81.

Lock, J., 1983. Central Eromanga Basin seismic refraction surveys 1980, 1981; operations report. Bur. Miner. Resour. Aust., Record in press.

Mathur, S.P., 1983. Preliminary deep crustal reflection results from the central Eromanga Basin, Australia. Tectonophysics (this volume).

McLennan, S.M. & Taylor, S.R., 1982. Geochemical constraints on the growth of the continental crust. J. Geol., 90, 347-361.

Mueller, S. & Landisman, M., 1966. Seismic studies of the Earth's crust in continents. Geophys. J.R. astr. Soc., 10, 525-538.

Mueller, S., 1977. A new model of the continental crust. In; The Earth's Crust (ed. J.G. Heacock), Am. Geophys. Un., Geophys. Mono. 20, 289-317.

Muller,G. & Mueller,S.,1979. Travel-time and amplitude interpretation of crustal phases on the refraction profile Delta-W, Utah. Bull. Seis. Soc. Amer., 69, 1121-1132.

Prodehl, C., 1970. Seismic refraction study of crustal structure in the western United States. Geol. Soc. Am. Bull., 81, 2629-2646.

Prodehl, C., 1977. The structure of the crust-mantle boundary beneath North America and Europe as derived from explosion seismology. In; The Earth's Crust (ed. J.G. Heacock), Am. Geopnys. Un., Geophys. Mono. 20, 349-369.

Ringwood, A.E., 1982. Phase transformations and differentiation in subducted lithosphere: implications for mantle dynamics, basalt petrogenesis and crustal evolution. J. Geol., 90, 611-643.

Rutland, R.W.R., 1982. On the growth and evolution of continental crust: a comparative tectonic approach. J. Proc. Roy. Soc. NSW, 115, 33-60.

Sass, J.H. & Lachenbruch, A.H., 1979. Thermal regime of the Australian continental crust. In; The Earth, its Origin, Structure and Evolution (ed. M.W. McElhinny), Academic Press, 301-351.

Smithson, S.B., Brewer, J.A., Kaufman, S., Oliver, J.E. & Zawislak, R.L., 1980. Complex Archean lower crustal structure revealed by COCORP crustal refelction profiling in the Wind River Range, Wyoming. Earth Planet. Sc. Lett., 46, 295-305.

Sollogub, V.B., 1969. Seismic crustal studies in southeastern Europe. In; The Earth's Crust and Upper Mantle (ed. P.J. Hart), Am. Geophys Un., Geophys. Mono. 13, 189-195.

Spence, A.G. & Finlayson, D.M.,1982. The resistivity structure of the crust and upper mantle in the central Eromanga Basin, Queensland, using magnetotelluric techniques. J. Geol. Soc. Aust., in press.

Wass,S.Y. & Hollis, J.D., 1983. Crustal growth in southeastern Australia - Evidence from lower crustal eclogitic and granulitic xenoliths. J. Metamor. Geol., in press.

SEISMIC FEATURES OF THE LITHOSPHERE UNDER THE CENTRAL EROMANGA BASIN -- A CONTRAST WITH ADJACENT TECTONIC PROVINCES.

D.M.Finlayson & S.P.Mathur

Bureau of Mineral Resources, Geology & Geophysics, Canberra.

MAGSAT observations at heights of 400 to 450 km and regional gravity anomalies serve to distinguish the Eromanga Basin region from its neighbouring tectonic provinces. Seismic refraction and coincident seismic reflection profiling data from a 300 km traverse across the central part of the Basin quantify some of the features which contrast this region with the North Australian Craton to the northwest, the Lachlan Fold Belt to the southeast and the Anakie Inlier to the northeast.

Seismic refraction record sections indicate strong seismic velocity gradients at basement depths (about 2 km) and at a mid-crustal horizon (a Conrad discontinuity?), and lesser velocity gradients at the crust/mantle boundary (Moho) and in the sub-crustal lithosphere.

The P-wave velocity in the basement increases from 5.0-5.4 km/s at about 2 km depth to about 5.9 km/s at 5-7 km, and at greater depths does not exceed 6.1 km/s. Velocity decreases are evident at depths below about 9 km and these are interpreted in terms of the alpha-beta quartz transition at high temperatures (Kern, 1982).

Strong super-critical reflections evident as second arrivals at distances less than 100 km are interpreted as coming from a prominent velocity gradient at depths of 19-26 km. This mid-crustal horizon is in contrast to mid-crustal features from some other geological provinces of Australia. In other continents it has been referred to as the Conrad discontinuity.

The Moho deepens from about 36 km in the west to about 41 km in the east with the sub-crustal lithosphere having a velocity of 8.15+0.04 km/s. Energy returning after the first arrivals beyond 220 km indicates that there is a velocity gradient at depths of about 55-60 km, possibly with a low-velocity zone above it.

The seismic reflection section along the western half of the traverse can be divided into four 2-way reflection-time zones based on the character of events. Between 0 and 2 s there are fairly uniform, coherent and continuous events which correlate with the Late Palaeozoic and Mesozoic sediments. The zone from 2 to 7 s is relatively free of primary reflections although a few multiples of the stronger sedimentary reflections exist. The absence of reflections in this zone suggests that the upper crust (6-20 km) is seismically homogeneous and may represent crystalline igneous rocks or highly deformed metasedimentary/metavolconic rocks. Relatively low resistivity values for basement rocks favour the latter rock type. Without any recognizable reflections or diffraction patterns in this zone, it is difficult to say whether faulting observed in the sediments extends deep into the crust.

The zone from 7 to 13 s shows numerous short, discontinuous reflection events with variable amplitude and varying, sometimes cross-cutting, dips. Model studies made elsewhere suggest that such events can be produced by laminae of alternating high and low velocity, the layer thicknesses being less than the seismic wavelengths (about 100 m). The reflection-free zone below 13 s corresponds to the upper mantle, which therefore seems to be free of acoustic impedence contrasts. The lower crust with velocities of 6.3-7.0 km/s and numerous reflection segments could consist of finely interlayered rocks of intermediate composition.

The Moho under the Canaway Ridge is at a depth of about 34 km and is characterised by a sharp velocity increase. There does not appear to be a mid-crustal velocity discontinuity under the Ridge. Thus the Ridge could be a major horst at least to the depth of the Moho but it also has an intra-crustal structure different from the surrounding region. No deep reflection data is available yet from the Ridge area.

The crustal thickness of the region is less than that of the North Australian Craton (50-55 km) (Finlayson, 1982) and of the Lachlan Fold

Belt (43-50 km) (Finlayson & McCracken, 1981) but is similar to that interpreted for the Drummond (Cull & Riesz, 1972) and Bowen Basins to the east (Collins, 1978; Leven, 1980). The distinct velocity gradients of the lithosphere under the central Eromanga Basin are in in contrast to the gradational velocity increases interpreted for the North Australian and Lachlan provinces. The reflection characteristics of the deep crust in the Eromanga region are significantly different from those of the North Australian Craton, the Lachlan Fold Belt and the Anakie Inlier.

The crustal structure is consistent with a pericratonic or arc/backarc basin being cratonised in an episode of convergent tectonics in the Late Proterozoic - Early Palaeozoic. The contrast in seismic reflection characteristics of the upper and lower crusts could indicate that the latter developed in a different tectonic environment.

REFERENCES

COLLINS,C.D.N.,1978 - Crustal structure of the central Bowen Basin, Queensland. BMR J. Aust. Geol. Geophys., 3, 203-209.

CULL,J.P., & RIESZ,E.J.,1972 - Deep crustal seismic reflection/refraction survey between Clermont and Charters Towers, Queensland 1971. Bur. Miner. Resour. Aust., Record 1972/97.

FINLAYSON,D.M.,1982 - Seismic crustal structure of the Proterozoic North Australian Craton between Tennant Creek and Mount Isa. J. Geophys. Res., in press.

FINLAYSON,D.M., & McCracken,H.M.,1981 - Crustal structure under the Sydney Basin and Lachlan Fold Belt determined from explosion seismic studies. J. Geol. Soc. Aust., 28, 177-190.

KERN,H.,1982 - Elastic-wave velocity in crustal and mantle rocks at high pressure and temperature: the role of the high-low quartz transition and of dehydration reactions. Phys. Earth Planet. Int., 29, 12-23.

LEVEN,J.H.,1980 - The application af synthetic seismograms to the interpretation of crustal and upper mantle structure. PhD Thesis, Australian National University, Canberra.

MATHUR,S. ,1983 - Deep reflection studies in the central Eromanga Basin. Tectonophysics, in prep.

Basement structure and velocities under the central Eromanga Basin from seismic refraction studies.

J. Lock, C.D.N. Collins & D.M. Finlayson

Bureau of Mineral Resources, Geology & Geophysics, P.O. Box 378, Canberra, City, A.C.T. 2601.

ABSTRACT

Seismic refraction recordings along a line extending from Mt Howitt 1 to Eromanga, over Eromanga and Cooper Basin sediments, revealed two intra-basement refractors not recorded by co-incident reflection profiling. These refractors were recorded at 3.5 and 5.0 km depth between the basal unconformity at 2.4 km depth and a low velocity zone at about 8.5 km depth. Faulting within the basin sediments extends into basement to at least 5.5 km, with increasing displacement with depth, causing lateral variation of structure and velocity. P-wave velocities increase gradationally with depth and average values along the traverse are 2.2 km s-1 at the surface to 5.0 km s-1 at the basal unconformity; below that, the velocity increases to 6.0 km s-1 above a low velocity zone. A sequemce of up to five multiples can be observed from 10 km beyond the shot, to at least 40 km and possibly 50 km. Travel-time characteristics indicate that they are waves refracted within basement and multiply reflected at the surface. Travel-time modelling of the first arrivals, multiple arrivals, and two way reflection times provide a tight constraint on the velocity and structure to a depth of about 5.5 km.

INTRODUCTION

In 1980, the Bureau of Mineral Resources, Geology and Geophysics (BMR) conducted seismic refraction surveys in the central Eromanga Basin as part of large scale multidisciplinary study to investigate structure, stratigraphy, geological evolution and petroleum potential of the area (Pinchin & Senior, 1982). The program for the central Eromanga Basin Project its objectives, and previous geological and geophysical investigations are outlined by Harrison et al. (1980). The planned geophysical program and its objectives are discussed in more detail by Moss (1980) and Pinchin (1980).

One of the objectives of the seismic refraction program was to determine seismic velocities within the Eromanga basin, the infra-basins and the basement, which, combined with the vertical reflection data could be used to interpret geological structure and rock type. There are few vertical reflections recorded from within the basement down to 8 seconds two-way vertical reflection time. The refraction program was designed to define the velocity structure to any sub-basement horizons or within any hidden basins. This detailed upper crustal velocity information would also be used to interpret vertical reflection and refraction data from the deep crust and upper mantle and to determine travel-time residuals.

Two reversed end-to-end 37.5 km traverses were recorded from 200 kg shots fired at Mt Howitt 1, Little Wonder Mine, and near Eromanga township (Eromanga) (Fig. 1). These two traverses were combined to give one reversed 75 km line by firing 400 kg at Mt Howitt 1 and Eromanga. Recordings were made at 21 stations deployed at 1.875 km intervals between adjacent shot locations. Details of survey design and field operations have been described by Lock (1983). In this paper the data are interpreted in terms of basin and basement velocity structure to depths of 8.5 km.

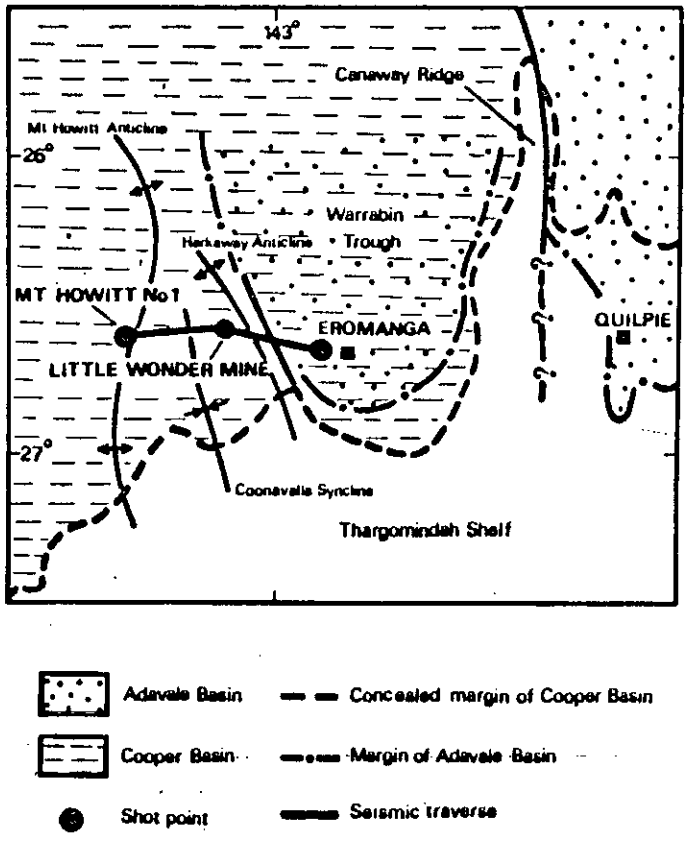

Fig. 1. Seismic traverse and shot point locations central Eromanga Basin.

GEOLOGY AND STRUCTURE

In the survey area the Early Jurassic to Late Cretaceous Eromanga Basin sequence is concealed by Tertiary and Quaternary sediments. The Permian to Triassic north-eastern Cooper Basin unconformably underlies the Eromanga Basin. The Cooper Basin is thicker at the western end of the seismic traverse where it is drilled in Mt. Howitt 1. It thins eastward and wedges out east of Eromanga and west of the Canaway Ridge. The detailed geology and structure of the basins have been inferred from well completion reports and previous seismic data. The combined average thickness of the Eromanga and Cooper Basins is 2.4 km. Eromanga Basin stratigraphy and structure are discussed in detail by Senior et al. (1978) and that of the Cooper Basin by Senior (1975) and Battersby (1976).

Mt Howitt in tightly folded Ordovician shales and meta-sediments of the Thompson Fold Belt (Murray & Kirkgaard,1978: Rumph, 1978) which forms the basement to this part of the Cooper Basin.

The vertical reflection section recorded along the refraction traverse (Wake-Dyster & Pinchin, 1981) shows that the sediments are generally flat-lying but, in places, are gently displaced by three faults which extend from basement through the basal sediments of the Cooper Basin. Younger sediments of the Cooper Basin and the Eromanga Basin are draped over the faults which do not have surface expression. The most westerly fault is associated with the Mt Howitt Anticline and the most easterly, with the Harkaway Anticline (Fig. 1). The Coonovalla Syncline lies between these anticlines. The adjoining geological provinces and tectonic setting are described in more detail by Finlayson et al. (1983).

FIRST-ARRIVAL DATA

Figure 2(a) shows the seismic refraction record section from Mt Howitt 1 to Eromanga and Figure 3(a) shows the reverse section. No strong wide angle reflection branches are observed at short distances; therefore the velocity

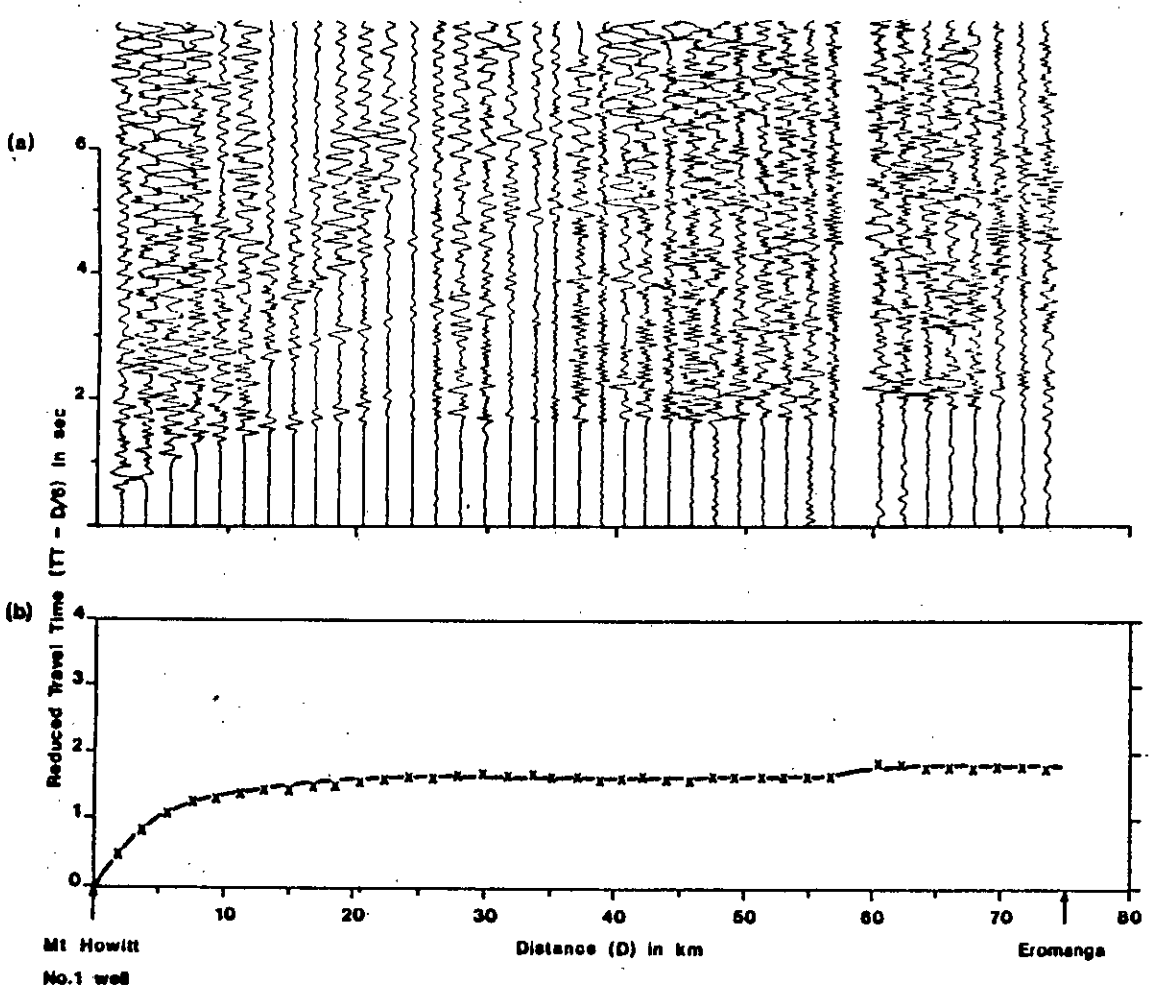

Fig. 2. (a) Seismic record section for shots at Mt Howitt 1 recorded eastwards to Eromanga. Trace amplitudes are adjusted to constant gain, digitally band-pass filtered (2-15 Hz), and an adjustment proportional to distance-1 made to account for geometrical spreading. (b) Comparison of first-arrival data (X) and travel-time curve derived from the preferred velocity/depth model shown in Figure 4.

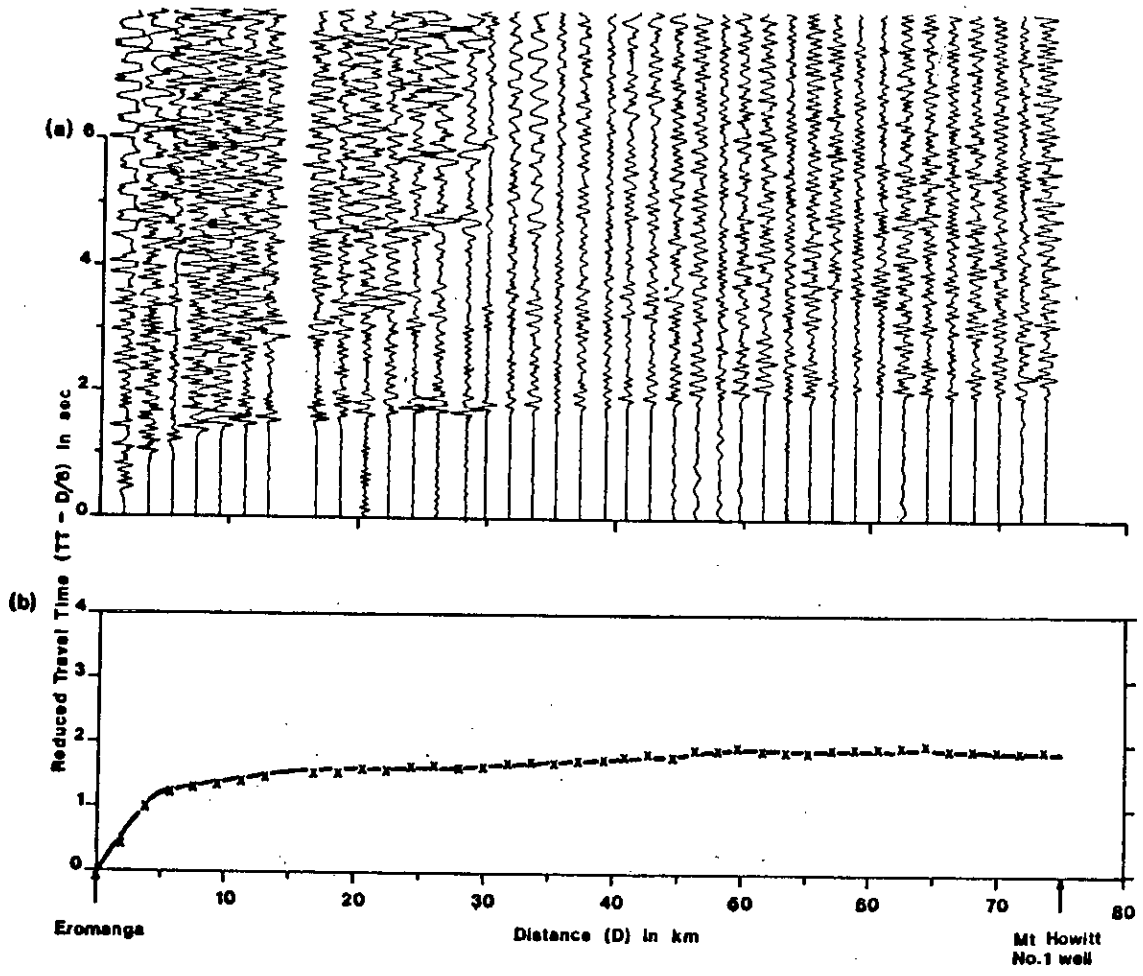

Fig. 3. (a) Seismic record section for shots at Eromanga recorded westwards to Mt Howitt 1. Trace amplitudes are adjusted to constant gain, digitally band-pass filered (2-15 Hz), and an adjustment proportional to distance-1 made to account for geometrical spreading. (b) Comparison of first-arrival data (X) and travel-time curve derived from the preferred velocity/depth model shown in Figure 4.

of the Eromanga and Cooper Basin sequences is interpreted as increasing continuously with depth. Arrivals between about 8 and 18 km distance have a lower apparent velocity than those recorded at greater distances. Data recorded on a reversed overlapping traverse extending east and west shows that the clear impulsive first arrivals out to 75 km shown in Figures 2(a) and 3(a) extend out to about 100 km. Beyond this, the waveform changes and the first arrivals become emergent (Finlayson et al., 1983).

Because the Permian-Cretaceous strata are generally flat lying and the structure is relatively simple (Wake-Dyster & Pinchin, 1981), preliminary models were developed from the first-arrival data assuming flat layering. Table 1 lists and Figure 4(a) shows, the model derived from shots at Mt Howitt 1, Little Wonder Mine and Eromanga. In each model the velocity increases with depth and there are no first-order velocity discontinuities within either the basin strata or Ordovician basement. At Mt Howitt 1 (Table 1(a), Figure 4(a)) the surface velocity of 2.3 km s-1 increases through the sedimentary sequence to 3.2 km s -1 at 800 m, 3.6 km s-1 at 1.2 km and 5.0 km s-1 at the 2.4 km deep basement unconformity. Between 2.4 km and 3.5 km depth the velocity increases relatively rapidly from 5.0 to 5.6 km s-1. Between 3.5 and 5.0 km depth the velocity increases from 5.6 5.9 km s-1. .As the velocity gradient below 3.5 km decreases, the zone between the basement unconformity at 2.4 km and 3.5 km depth may, perhaps, represent the vertical extent of the Ordovician shales and meta-sediments. The reflectivity method for modelling synthetic seismograms (Fuchs, 1968 (transl. Collins, 1979)), which assumes planar layers, demonstrated that if the velocity decreases from about 5.9 km s-1 to 5.6 km s-1, amplitudes of first arrivals decay beyond 100 km distance; as was observed by Finlayson et al., 1983. As there are no other constraints on velocity in this low velocity zone, 5.6 km s-1 is only an estimate of the true velocity. Comparison of the velocity/depth profiles at each shot point shows that while the velocity of the refractors varies little across the traverse, depths vary up to 500 m.

Table 1. P wave seismic velocity models for depths less than 10 km for (a) Mt Howitt 1 shooting east, (b) Little Wonder Mine shooting west, (c) Little Wonder Mine shooting east, (d) Eromanga shooting shooting west.

(a)		(b)		(c)		(d)	
Depth	Velocity	Depth	Velocity	Depth	Velocity	Depth	Velocity
km	km s-1	km	km s-1	km	km s-1	km	km s-1
0.0	2.3	0.0	2.2	0.0	2.2	0.0	2.2
0.8	3.2	1.2	3.0	1.1	3.0	1.1	3.0
1.2	3.6	1.5	3.6	1.4	3.6	1.3	3.4
2.4	5.0	2.5	5.0	2.4	5.0	2.4	5.0
3.5	5.6	3.5	5.6	3.5	5.6	3.5	5.5
5.0	5.9	4.5	5.7	4.5	5.7	5.0	5.8
8.0	6.0	8.0	5.8	8.0	5.8	8.0	5.9
8.5	5.6	8.5	5.6	8.5	5.6	8.5	5.6

Refractors in the Eromanga Basin correlate with the Toolebuc Formation, the Wyandra Sandstone member at the top of the Cadna-Owie Formation, and also with the unconformity at the base of the Cooper Basin in Mt Howitt 1, at the western end of the line. These prominent horizons can be identified on the vertical record section (Wake-Dyster & Pinchin, 1981) and are reflectors 2, 3, and 7 of Pinchin & Senior (1982). These time horizons were used to extrapolate between the velocity/depth profiles at Mt Howitt 1, Little Wonder Mine and Eromanga thus enabling the development of a continuous velocity/depth model along the traverse which incorporated basin structure. The lithological units which give rise to vertical reflections must be thin, as the abrupt increases in velocity seen at these horizons the Mt Howitt 1 sonic log (Wake-Dyster & Pinchin, 1981) would otherwise produce wide-angle reflections which are not observed in the refraction data.

In order to precisely model the first arrival times at distances beyond 20 km, it is necessary to invoke basement structure. Extension of faults identified on the seismic reflection secton into basement and increasing the displacement on the faults with depth accomplishes this. Waves which propagate into the basement and arrive at the surface at distances greater than 30 km, have long path lengths and travel-times within the basement. As a result, arrivals beyond 30 km are quiet sensitive to small changes in basement velocity gradient. This accounts for the small variations in velocity along the second basement refractor (Table 1, Fig. 4(b)). Departures of the observations from the travel-times calculated for a flat-layered model are satisfied by varying the thickness and velocity gradient of the layers within the Eromanga and Cooper Basins and basement along the traverse. Figures 2(b) and 3(b) show first-arrival times compared with travel-times using the preferred velocity/depth model. The preferred model is further constrained by ensuring that the two-way vertical reflection times to the three reflecting horizons calculated from this model are in good agreement with the times shown on the vertical reflection section.

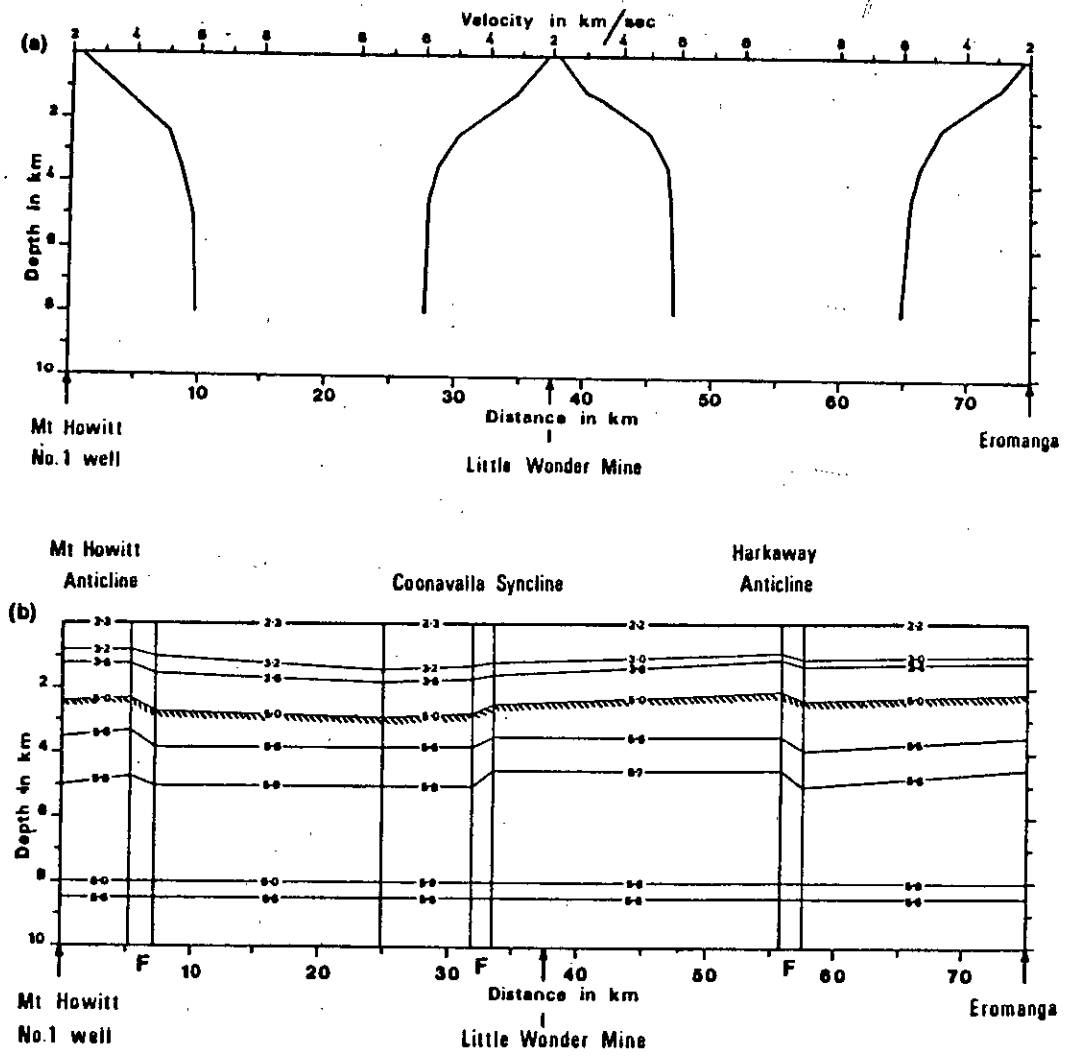

Fig. 4. (a) 1-D velocity/depth models derived from shots at Mt. Howitt 1, Little Wonder Mine and Eromanga using first arrival data.
(b) Preferred 2-D velocity/depth model between Mt. Howitt 1 and Eromanga.

SECONDARY-ARRIVAL DATA

A feature of seismic refraction data in this region is a sequence of clear later arrivals which, in general, consist of a wavelet of the same shape as the primary wave but often larger amplitude. There are at least three such arrivals on any record section. These later arrivals are observed beyond 10 km to at least 40 km and possibly 50 km. Unambiguous identification of the secondary arrivals is difficult at larger distances. The dominent frequency in the initial and secondary arrivals is 5 Hz. Application of a 3 to 7Hz band-pass filter removes the higher frequencies and accentuates five secondary arrivals in the record section from Mt Howitt 1 to Eromanga (Fig. 5). King & Falvey (1977) also recognised these multiples in refraction data recorded in the Cooper Basin in the vicinity of Thunda 1 to the northeast of this survey. These multiples are relatively rare but have also been reported by McMechan & Mooney (1980) in the Imperial Valley, California.

Multiples with purely reflected paths are characterised by travel-time curves which are concave upwards (Fig. 6(a)). The observations have travel-time curves which are concave downwards and are therefore refracted rays which are multiply reflected at the free surface (Fig. 6(b)). Meissner (1965), in a study of multiple events from flat layers in which the velocity increases with depth, showed five multiples with observable amplitudes were possible. He noted several features of this type of multiple, which can be seen in Figure 5. Multiple travel-time curves diverge slowly with time, and energy shifts progressively to larger distances as the number of multiples increases. He suggested that the amplitude along one multiple event depended on velocity in the region through which the ray travelled, local differences in the depth of the weathering layerand changes in the surface reflection coefficient. This probably explains the much lower amplitude of multiple 1 near 35 km (Fig. 5).

The conditions necessary for the existence of these multiples are, a high velocity gradient in the sedimentary sequences and a relatively high velocity

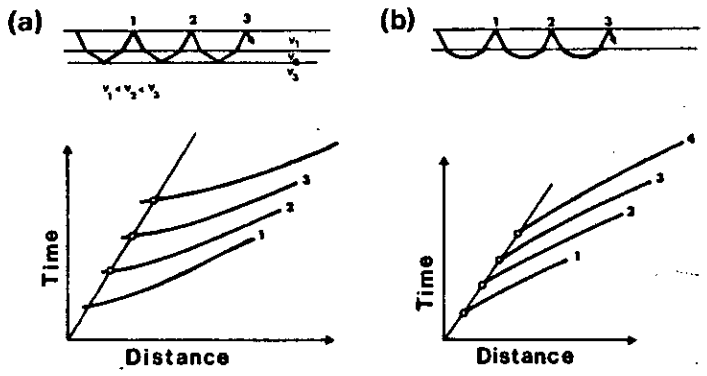

Fig. 5. Seismic record section for shots at Mt Howitt 1 resorded eastwards to Eromanga. Trace amplitudes are adjusted as in Figure 2(a) and digitally band-pass filtered (3 to 7 Hz). Travel-times derived from the preferred model for refracted arrivals multiply reflected at the surface are superimposed on the observed secondary arrivals. Numbers 0 to 5 indicate the number of timesthe arrival has been reflected at the surface.

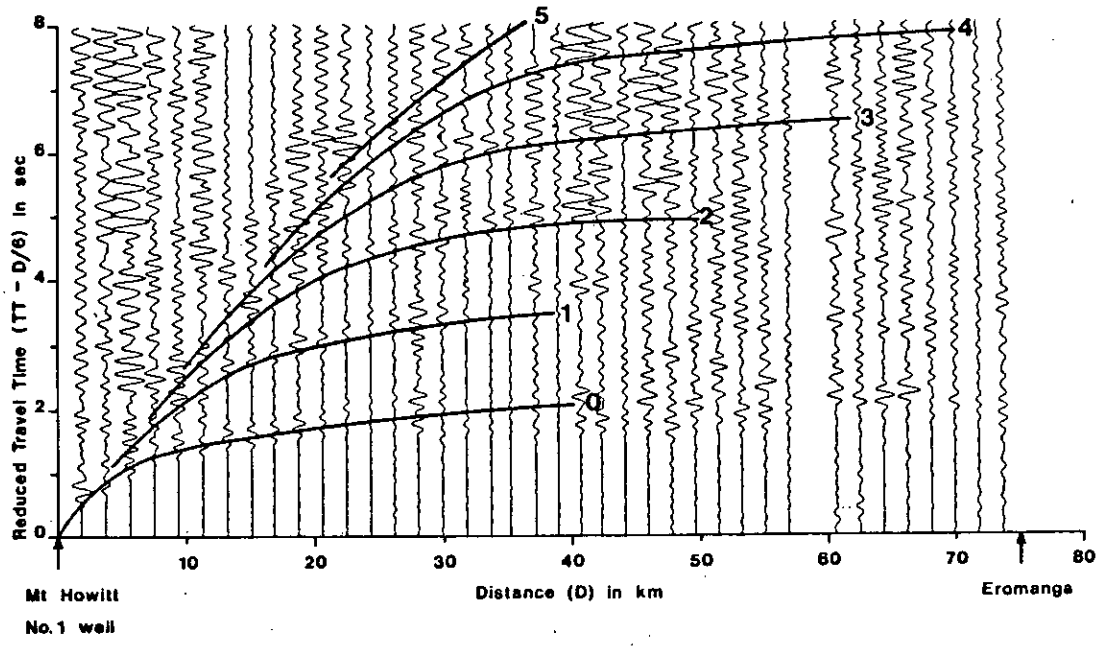

Fig. 6. Schematic ray paths and travel times for multiply reflected waves: (a) multiply reflected arrivals, (b) reflected-refracted arrivals (after Meissner, 1965).

gradient in the zone where the multiples turn (ie are refracted). This ensures relatively energetic propagation of the multiples to extended distances (McMechan & Mooney, 1980). A further requirement is a low surface velocity so that the energy returns to the surface at near vertical incidence. All three conditions are met by the preferred model (Fig. 4(b)) and ray tracing through the preferred model comfirmed that the energy is returned to the surface near vertical incidence.

Travel-times for rays refracted in the layer below the basins at 2.4 to 3.5 km depth and reflected at the free surface, were calculated using the preferred model. These times are shown on Figure 5 for five multiples. Curve 0 represents the primary wave, and curves 1, 2, 3 , 4 and 5 are those multiples which have been reflected at the surface one, two, three, four and five times respectively. These travel-times are in good agreement with the observations indicating that the preferred model is well constrained to at least 3.5 km depth (the base of the Ordovician ?).

CONCLUSIONS

Refractors in the Eromanga Basin correlate with the Toolebuc Formation, the Wyandra Sandstone Member of the Cadna-Owie Formation and also with the Cooper Basin Permian-Ordovician basement unconformity. There are two refractors at 3.5 and 5.0 km, recorded between the unconformity and a low velocity zone at about 8.5 km. The uppermost basement refractor between 2.4 and 3.5 km depth may indicate the vertical extent of the Ordovician shales and metasediments. Faulting within the basin sediments extends downward to at least 5.5 km, with increasing displacement at depth (up to 500 m) causing lateral variation in structure and velocity. The angle of faulting cannot be resolved and is assumed to be vertical.

When structure is taken into account, velocity models developed assuming flat layering where structure is simple give a good fit to the first arrival data, and two-way travel-times to identified reflecting horizons. The

secondary arrivals observed in the refraction record sections are multiples refracted within the basement and multiply reflected at the surface. The preferred velocity model for the traverse has velocity gradients which return the rays to the surface sufficiently focussed, and at near vertical incidence, to give multiples with observable amplitudes fot up to five surface reflections. The accordance of the multiple travel-times, first-arrival times and two-way reflection times with the observations, indicates that the model is well constrained to 5.5 km depth.

ACKNOWLEDGEMENTS

We wish to acknowledge the contribution of Chris Rochford, and the BMR seismic crew, to the field program. Dr B.J. Drummond critically reviewed the manuscript and his comments are gratefully acknowledged. This paper is published with the permission of the Director, Bureau of Mineral Resources, Geology and Geophysics.

REFERENCES

BATTERSBY, D.G., 1976: Cooper Basin gas and oil fields; in Leslie, R.B., Evans, H.J. & Knight, C.L. (eds) Economic geology of Australia and Papua New Guinea-3. Petoleum. Australas. Inst. Min. Metall., Monogr., 7, 321-69.

COLLINS, C.D.N., 1979: Adaptation of the synthetic seismogram program "REFLEX" to the CSIRO CYBER 76 computer. Aust., Bur. Miner. Resour., Geol. Geophys., Rec., 1979/7.

FINLAYSON, D.M., COLLINS, C.D.N. & LOCK J., 1983: P-wave velocity features of the lithosphere under the Eromanga Basin, eastern Australia, including a prominent mid-crustal (Conrad?) discontinuity. Tectonophysics, (in press).

FUCHS, K., 1968: Das Reflexions- und Transmissionsvermogen eines geschichteten Mediums mit beliebiger Tiefen-Verteilung der elastischen Moduln und der Dichte fur schragen Einfall ebener Wellen. Zeitschrift fur Geophysik, 34, 389-413.

HARRISON, P.L., MATHUR, S.P., MOSS, F.J., PINCHIN, J. & SENIOR, B.R., 1980: Central Eromanga Basin Program proposals, 1980-1982. Aust., Bur. Miner. Resour., Geol, Geophys., Rec., 1980/32.

KING, D. & FALVEY, M., 1977: A seismic survey in the Cooper Basin in Queensland., APEA J., 17(1), 78-84.

LOCK, J., 1983: Central Eromanga Basin seismic refraction surveys, 1980, 1981; Operations Report. Aust., Bur. Miner. Resour., Geol. Geophys., Record., (in prep.).

McMECHAN, G.A. & MOONEY, W.D., 1980: Assymptotic ray theory and synthetic seismograms for laterally varying structures: theory and application to the Imperial Valley, California. Seism. Soc. Am., Bull., 70, 2021-35.

MEISSNER, R., 1965: Multiple events in refractions shooting. Geophys. Prospect., 13, 617-58.

MOSS, F.J., (coordinator), 1980: Central Eromanga Basin Project, progress report, January-June 1980. Aust., Bur. Miner. Resour., Geol. Geophys., Rec., 1980/60.

MURRAY, C.G. & KIRKEGAARD, A.G., 1978: The Thomson Orogen of the Tasman Orogenic Zone. Tectonophysics, 48, 299-325.

PINCHIN, J., 1980: Central Eromanga Basin seismic survey, Qld, 1980-preview report. Aust,. Bur. Miner. Resour., Geol. Geophys., Rec., 1980/77.

PINCHIN, J. & SENIOR, B.R., 1982: The Warrabin Trough, western Adavale Basin, Queensland. Geol. Soc. Aust. J., 29, 413-44.

RUMPH, B., 1978: Regional gravity and magnetic data of the central Eromanga Basin area: implications in crustal structure, regional geology and tectonic history. M.Sc. Thesis, Univ. Sydney (unpubl.)

SENIOR, B.R., 1975: Notes on the Cooper Basin in Queensland. Qld. Gov. Min. J., 76, 260-5.

SENIOR, B.R.,MOND, A. & HARRISON, P.L., 1978: Geology of the Eromanga Basin. Aust., Bur. Miner. Resour., Geol. Geophys., Bull., 167.

WAKE-DYSTER, K.D. & PINCHIN, J., 1981: Central Eromanga Basin seismic survey Queensland 1980. Aust., Bur. Miner. Resour., Geol. Geophys., Rec., 1982/22.

Tectonophysics, 84 (1982) 287–312
Elsevier Scientific Publishing Company, Amsterdam—Printed in The Netherlands

GEOPHYSICAL DIFFERENCES IN THE LITHOSPHERE BETWEEN PHANEROZOIC AND PRECAMBRIAN AUSTRALIA

D.M. FINLAYSON

Bureau of Mineral Resources, Geology and Geophysics, P.O. Box 378, Canberra City, A.C.T., 2601 (Australia)

(Received July 14, 1981; revised version accepted October 7, 1981)

ABSTRACT

Finlayson, D.M., 1982. Geophysical differences in the lithosphere between Phanerozoic and Precambrian Australia. *Tectonophysics*, 84: 287–312

Cannikin atomic bomb recordings indicate that there are differences in travel-times from the Aleutian Islands test site to Phanerozoic and Precambrian provinces in Australia of up to 1.1 s. Explosion seismic studies in central and southeastern Australia enable travel-time corrections for crustal and upper mantle structure to be made to recordings of such teleseismic events. Structure in the upper 60 km can account for, at most, about 0.2 s of the residual difference, but attempts to constrain the remaining residual time to the region above the Lehmann discontinuity at about 200 km depth are difficult to reconcile with explosion seismic models. Regional differences in seismic velocity structure between Phanerozoic and Precambrian Australia therefore appear to exist at depths greater than 200 km.

Electrical conductivities within the mantle have been investigated using two methods. Long-period electromagnetic depth sounding using magnetometer arrays demonstrates that conductivities increase at about 200 km under Phanerozoic Australia but not until about 500 km depth under Precambrian Australia. Shorter period magnetotelluric measurements can only resolve shallower structures; these too indicate a similar trend but with sub-crustal conductivities increasing at less than 100 km under Phanerozoic Australia. Magma at these depths and shallower may be the source for Cainozoic volcanism in eastern Australia. Under Precambrian central and northern Australia magnetotelluric investigations indicate that pronounced conductivity increases do not occur until depths of 150–200 km are reached.

Oceanic magnetic observations indicate that the Australian lithospheric plate as a whole is separating from Antarctica at a rate of about 7 cm/yr. The seismic and conductivity structures under the continental region of this plate indicate that lateral inhomogeneities possibly extend to depths as great as 500 km and are probably caused by the passage of eastern Australia over a hot spot. Hawaiian studies indicate that hot spots are not local features but result from large scale disturbances in the mantle. Conductivity increases commencing in the depth range 100–250 km may give an indication of uppermost zones within which the Palaeozoic lithosphere has been substantially modified resulting in elevated surface heat flow, volcanism and seismic travel-time anomalies.

INTRODUCTION

The concept of the lithosphere being the outer part of the solid Earth has come into being along with the other concepts of plate tectonics developed principally from the structure under the oceans (Le Pichon et al., 1973). The lithosphere is usually envisaged as that outer part of Earth which translates away from mid-ocean ridges, separated from the Earth's deep interior by an asthenosphere which cannot sustain substantial shear stresses for long periods. The continents translate with the lithospheric plates, and it is therefore implied that there is an asthenospheric boundary under the continents which may be evident in the lateral variation of geophysical parameters at various depths.

This paper reviews some geophysical data which has contributed to our understanding of the sub-crustal structure in southeastern and central Australia, and compares the structural differences between southeastern Australia and the older Precambrian craton from the surface downwards to examine the depths at which lateral inhomogeneities have been resolved. The boundary between the lithosphere and the asthenosphere, if such a boundary exists at a uniform depth under continents, may show up as the common depth for various geophysical features.

GEOLOGY AND GEOCHEMISTRY

The geological structural framework of continental Australia considered in this paper is shown in Fig. 1 (adapted from Derrick, 1979); Plumb (1979) has described the major crustal subdivisions. The eastern limit of Precambrian Australia is indicated in Fig. 1. The Tennant Creek Block and the platform cover in the Wiso and Georgina Basins form part of Plumb's North Australian Craton which has been a relatively stable crustal block for 1700 m.y. The mid-Proterozoic Mount Isa orogen developed upon a reworked basement of the North Australian Craton.

The Arunta and Musgrave Blocks formed part of large orogenic provinces in central Australia active from 2300–1950 m.y. onwards and have long records of repeated mobilisation. These blocks and the intervening basins were progressively cratonised in the period 1400–900 m.y. and now constitute the Central Australian Mobile Belts (Plumb, 1979). Isotopic dates of greater than 2300 m.y. have been determined within the Gawler Craton, and rocks of the Broken Hill Block date from 2300–1950 m.y. The main Adelaidean succession of the Adelaide Fold Belt was deposited from 900 m.y. to the Early Cambrian (about 510 m.y.). Plumb (1979) speculates that the widely scattered occurrences of Archaean rocks suggest that much of Precambrian Australia is underlain by Archaean continental crust.

Crook (1980a, b) has presented evidence for the Palaeozoic evolution of the continental crust in eastern Australia, using a model incorporating fore-arc extension in an island arc situation to transform areas of oceanic crust into cratonic continental crust. In eastern Australia this continental growth extends for 1000 km from the

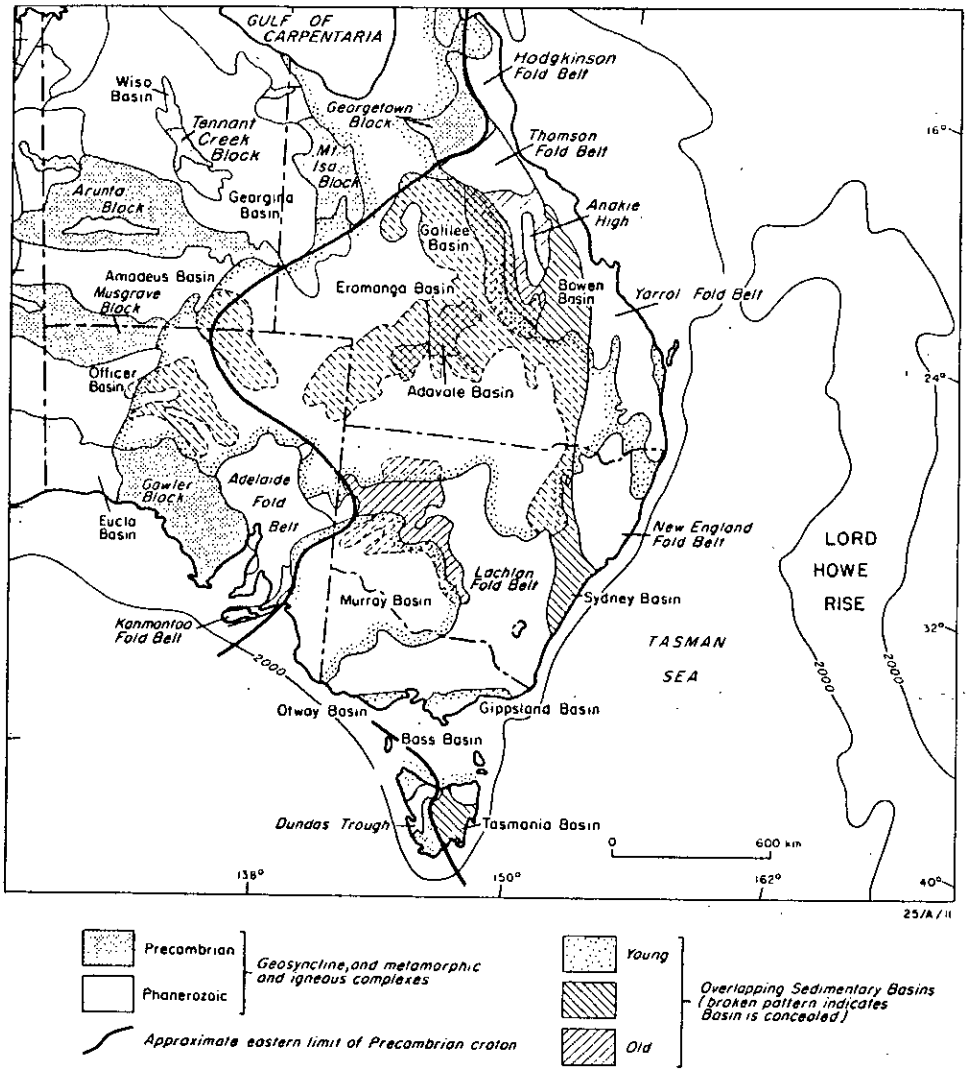

Fig. 1. Principal geological provinces of eastern and central Australia, (adapted from Derrick, 1979), the approximate eastern limit to the Precambrian based on surface geology, and the simplified bathymetry illustrating the Tasman Sea basin and the quasi-continental Lord Howe Rise.

eastern limits of the Precambrian craton, and, if the formation of the 300 km wide Lord Howe Rise is included, a total of 1300 km of new continental crust must have been added during the Palaeozoic (Fig. 1).

This process of continental accretion outlined above is in broad agreement with the concepts of Taylor (1979), who proposed that the origin of most post-Archaean upper crustal rocks demands at least two stages of chemical fractionation: (1)

fractionation from the mantle; and (2) intra-crustal melting and fractionation to provide upper crustal material of predominantly granodioritic composition, either or both stages occurring episodically throughout geological time.

Such a continental accretion process, if applied to southeastern Australia, would require the subduction of material equivalent to 4–6 times the thickness of oceanic crust and therefore the total width of subducted oceanic crust must have been 5200–7800 km, i.e. about the width of the present-day Atlantic Ocean. If the rates of plate motion were similar to those in the Atlantic, the accretion process would have taken about 260–340 m.y. If, as suggested below, only two-thirds of continental material accreted in this way, the process would have taken about 173–226 m.y.

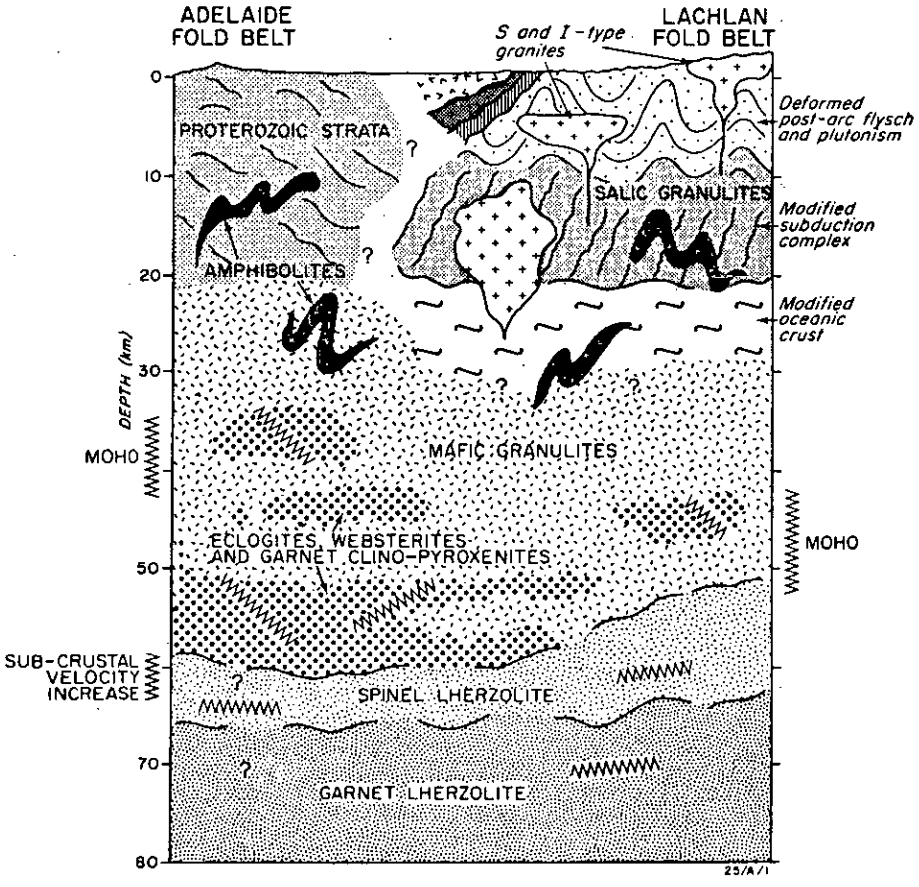

Fig. 2. Simplified geological section of the upper lithosphere in southeastern Australia (adapted from Ferguson et al. 1979, and Crook, 1980a). The mineralogy is based on the analysis of kimberlitic nodules which contain crust–mantle inclusions. The Moho boundaries are derived from the seismic refraction interpretations of Finlayson et al. (1979, 1980) (Lachlan Fold Belt) and Shackleford (1978) (Adelaide Fold Belt).

One enigmatic aspect of geology in southeastern Australia is revealed by geochemical analysis of S-type granites (Compston and Chappell, 1979). The geochemistry and source rock age of these granites is incompatible with surrounding Palaeozoic rock sources, but compatible with Precambrian continental material. Compston and Chappell (1979) estimate that the age of the lower crust in southeastern Australia is probably late–middle Precambrian (1.1 B.y.) rather than Palaeozoic, thus severely weakening an argument for a totally oceanic Precambrian regime. Crook (1980a) estimates that about a third of the continental crust of southeastern Australia is recycled from older continental material.

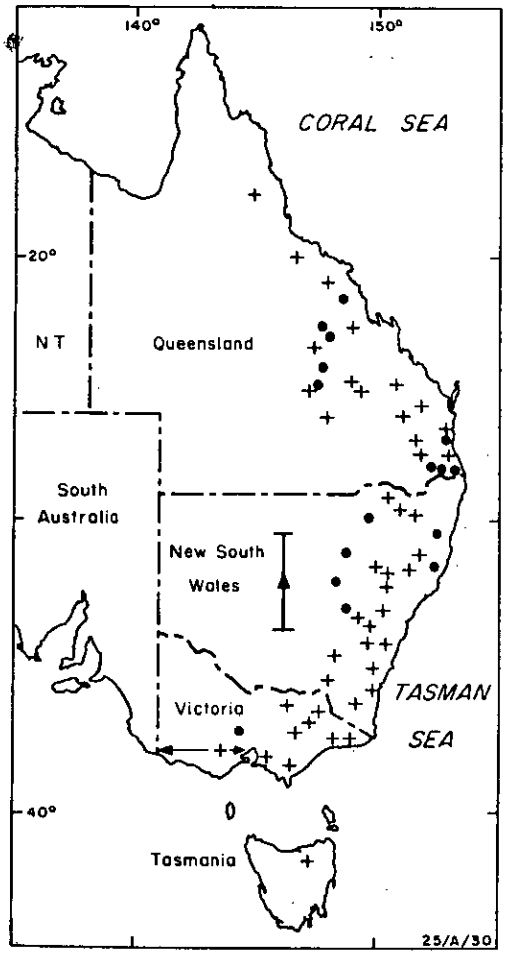

Fig. 3. Dated Cainozoic volcanic provinces in eastern Australia (from Wellman and McDougall, 1974a; Sutherland, 1981). Central volcano provinces are indicated by dots, lava field provinces by crosses, and a leucite lava province by a triangle. All except the latter province are restricted to the near-highland regions.

Ferguson and others (1979) have described the composition of the lower crust and upper mantle in southeastern Australia (Fig. 2) using samples from kimberlites. The intrusion of the kimberlites has been dated isotopically from Permian to Late Jurassic and the maximum depth estimates for material recovered from the intrusions is about 70 km. The samples include granulite-facies rocks of a basaltic lower crust consistent with the velocity gradients described later in this paper and thus, at the time of intrusion (late Palaeozoic–early Mesozoic), a lower crust of considerable thickness was present.

The continental character of southeastern Australia was largely established by the Silurian (Crook, 1980a), but eastern Australia has since been subject to Cainozoic volcanism (Wellman and McDougall, 1974a; Sutherland, 1981) the most recent of which occurred less than 2000 years ago (Fig. 3). Wellman and McDougall (1974a) attribute major activity to the northward drift of continental Australia over a fixed hot spot at a rate of 66 mm/yr. Sutherland (1981) extended this model and associated centres of thermo-tectonic activity with trails extending from the Coral Sea to Tasmania. Wellman (1979a) has described current uplift in the southeastern Australian highlands starting 90 m.y. ago. Ewart et al. (1980) and Wellman (1979b) have proposed models for underplating of the crust based, respectively, on petrological interpretations on megacrysts and the isostatic compensation of topography. Cainozoic volcanism appears to have modified the earlier eastern Australian Palaeozoic lithosphere but not necessarily grossly changed its structure, as is apparent in western U.S.A. where there is substantial evidence for major tectonic activity.

SEISMIC INTERPRETATIONS

The travel-times, amplitudes, and dispersion characteristics of the various body and surface waves generated by earthquakes and artificial sources place the best available controls on our knowledge of the Earth's fine structure and regional variations. There is still no general agreement about how seismic variations relate to rheology, the essential physical property required to define the lithosphere. However, making the assumption that continental Australia is drifting as part of a single lithospheric plate, we can investigate the possibility of there being seismic velocity features at a common depth under the whole continent which could be interpreted as a lithospheric boundary.

The velocity/depth structure of the crust in Phanerozoic southeastern Australia has been investigated by explosion seismology; the locations of some of the more recent surveys are shown in Fig. 4 (Finlayson et al., 1979, 1980; Finlayson and McCracken, 1981). The P-wave velocity–depth structure under the region of highest topography in Australia, which is within the Lachlan Fold Belt, and under the Sydney Basin, is shown in Fig. 5.

The P-wave velocity in basement rocks of the upper crust generally increases from

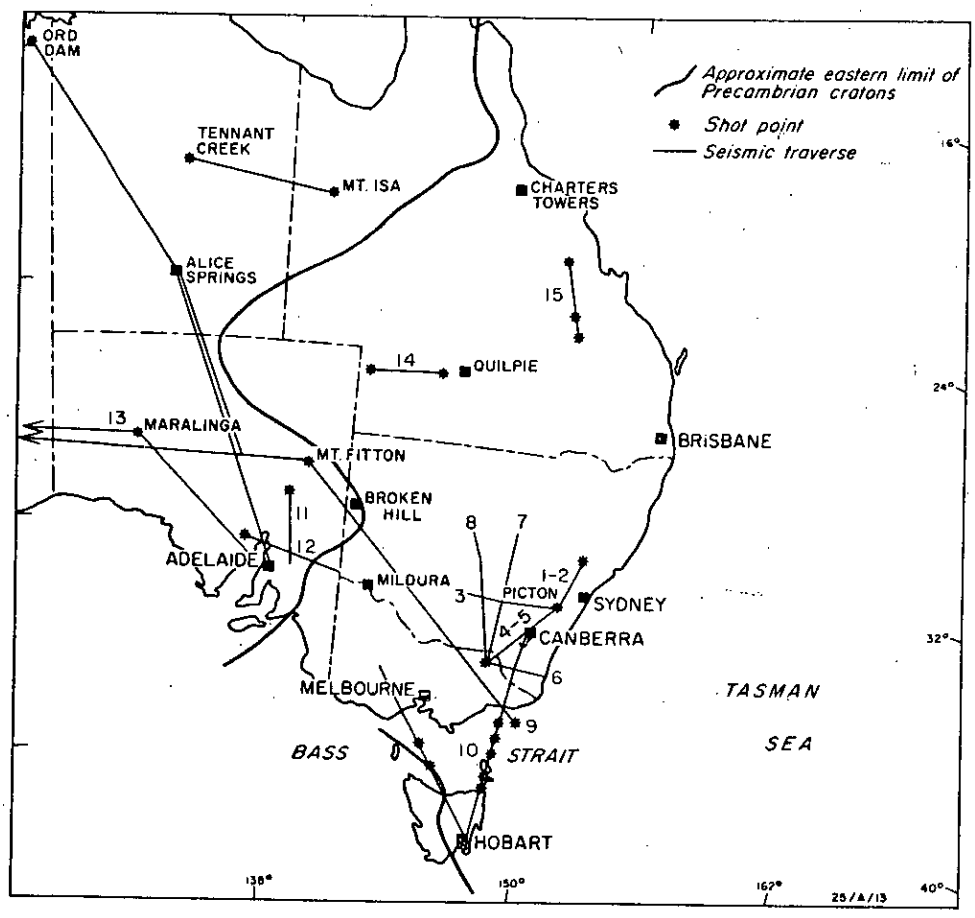

Fig. 4. Location of selected seismic investigations of the crust and upper mantle in eastern and central Australia. *1*, *2* = reversed profile Marulan to Singleton; *3* = Marulan–Ardlethan; *4*, *5* = reversed profile Dartmouth–Marulan; *6* = Dartmouth–Merimbula; *7* = Dartmouth–Dubbo; *8* = Dartmouth–Condobolin; *9* = Bass Strait 10 tonne shot; *10* = Bass Strait Upper Mantle Project; *11* = Leigh Creek profile; *12* = Iron Knob profile; *13* = Maralinga atomic test site; *14* = Eromanga Basin; *15* = Bowen Basin.

about 5.6 km/s near the surface to about 6.3 km/s at depths of 10–15 km; velocity decreases and inhomogeneities within the upper crust are evident. Within the Sydney Basin sediments (Fig. 1), velocities range from 3.6–3.9 km/s at the surface to 4.35–4.8 km/s at 2 km depth and greater. The basement velocity beneath the sediments is 5.75–5.9 km/s, increasing to 6.36–6.5 km/s at about 15–17 km depth. These velocities are consistent with the idea that Lachlan Fold Belt rocks underlie the Basin (Finlayson and McCracken, 1981). In agreement with geology, the seismic data present a picture of a laterally and vertically inhomogeneous upper crust.

It is to this upper crustal region that earthquake activity in southeastern Australia is largely confined, 85% of earthquakes occurring in the upper 20 km (Finlayson and

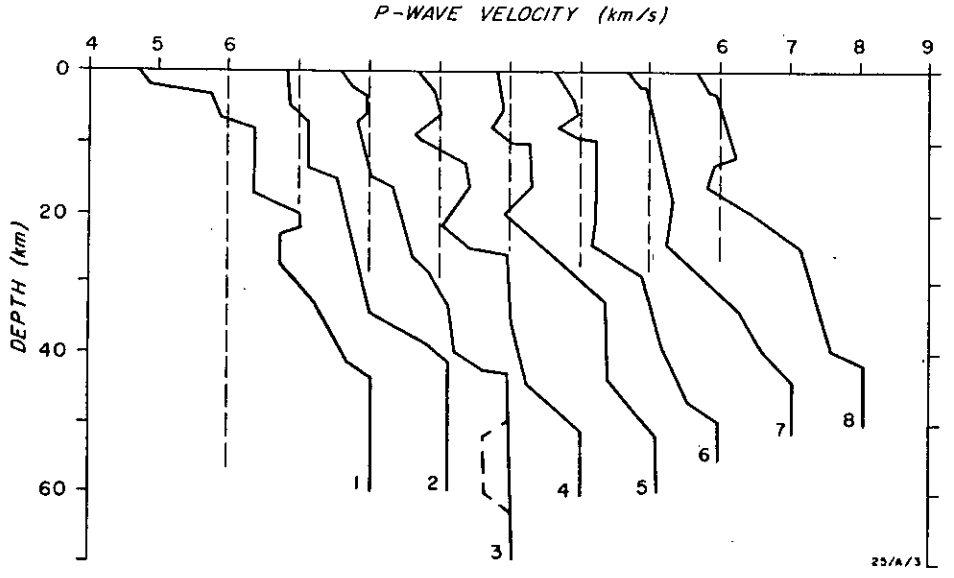

Fig. 5. P-wave velocity/depth profiles from the Lachlan Fold Belt and Sydney Basin in southeastern Australia (adapted from Finlayson et al. 1979, 1980, and Finlayson and McCracken, 1981). Profile locations are indicated by numbers in Fig. 4.

McCracken, 1981). Activity is attributed to compressive stresses (Denham, 1980) affecting pre-existing joints, fractures, and faults in the inhomogeneous upper 20 km where brittle-elastic rock characteristics are evident at confining pressures of 5 kb (500 MPa) or less. At greater depths, the lithosphere behaves as an elastic-plastic medium, responding elastically to seismic waves and plastically to long-term stress evident from Cainozoic regional uplift of between 0.6–1.3 km over the last 90 m.y. in the highlands of southeastern Australia (Wellman, 1979a, b).

The earthquake activity in southeastern Australia may be compared to that over another hot spot, Hawaii. There, the localised activity described by Crosson and Koyanagi (1979) is in marked contrast to the widespread activity in southeastern Australia (Denham, 1980). In the oceanic lithosphere the crustal thickness is about 13 km with quite pronounced low velocity layers produced by volcanic activity. Earthquakes are in the depth range 0–35 km. Detrick and Crough (1978) have described a lithosphere thinning model to account for structural features in the Hawaiian region and this will be discussed later in this paper.

In the middle and lower crust of the Lachlan Fold Belt the P-wave velocity increases from about 6.3–6.5 km/s to greater than 7 km/s, and there is evidence for velocity decreases within the middle crust. The Moho is characterised by a velocity gradient rather than a sharp velocity discontinuity. This is in accord with the geochemical evidence presented earlier (Ferguson et al., 1979) for a gradual geo-

chemical differentiation in the lower crust and upper mantle rather than a single major boundary at the Moho.

The upper mantle velocity is in the range 7.95–8.12 km/s, and there is evidence that the lithosphere beneath the crust under the northern Fold Belt has a velocity decrease in depth range 50–60 km (profile 3, Fig. 5). The depth at which upper mantle velocities are reached varies from over 50 km under the highest topography, to 41–44 km under the northern Lachlan Fold Belt and the Sydney Basin.

In the western region of Phanerozoic southeastern Australia there is only limited seismic crustal information. In the Broken Hill–Mildura region (Fig. 4) deep vertical seismic sounding has been interpreted by Branson et al. (1976). Using assumed crustal velocities, well-recorded events at 8.6, 10.1, and 14.7 sec two-way reflection time near Mildura were identified with intra-crustal, Moho, and sub-Moho boundaries at 24.5, 30.3, and 48.8 km depth. A diagrammatic summary of the crustal information across the southern Tasman Geosyncline is given in Fig. 6, together with models for Precambrian provinces further northwest.

The structure of the sub-crustal lithosphere under southeastern Australia is derived from only one explosion seismic study (Finlayson et al., 1974; Muirhead et al., 1977). Recordings were made in the distance range 250–1100 km from shots fired at the two ends of the recording line, in the northern Adelaide Geosyncline (Mount Fitton) and in Bass Strait (Fig. 4). The survey gives no information on the structure of the crust; an assumed model for crustal velocities is used to determine the lithospheric velocity/depth model shown in Fig. 7 (Muirhead et al., 1977). These authors drew attention to the larger travel-times to stations under the Snowy Mountains than to sites in the central Tasman Geosyncline (differences of about 0.5 s). They also drew attention to an adjustment to records of the Bass Strait shot of 0.8 s because of about 4.5 km of Gippsland Basin sediments with velocities in the range 2.5–3.4 km/s underlying the shot.

The models presented by Muirhead et al. (1977) must be regarded as simplified, and further data would undoubtedly alter them. Alternative models may even be derived from the existing data using prominent later events in the distance range 600–1000 km. The later arrivals from the Bass Strait shot in particular suggest that, rather then being multiply reflected phases as originally interpreted, they may represent near-critically reflected phases from the sub-crustal lithosphere. An alternative model for structure at depths greater than 150 km includes a low velocity zone (Fig. 7) with the velocity being reduced from 8.36 to 8.10 km/s in the depth interval 155–190 km. Thus the velocity/depth structure in the transition from a velocity of 8.36 km/s to 8.72 km/s in the depth range 190–205 km may differ from that shown in Fig. 7. However, the evidence that a transition exists in that approximate depth range still stands.

Surface-wave dispersion studies also contribute to our knowledge of the sub-crustal lithosphere. Goncz et al. (1975) and Goncz and Cleary (1976) have derived general dispersion characteristics for two-station paths which lie wholly within Precambrian

or Phanerozoic provinces. Their preferred general model, E1, for eastern Australia is shown in Fig. 7; the two-station paths traversed both the eastern highland areas and the western areas of the Tasman Geosyncline.

Mills and Fitch (1977) have interpreted the surface-wave dispersion data from the March 1973 Picton earthquake, recorded along particular paths northward under the eastern highlands at Charters Towers and eastward under the Tasman Geosyncline at Adelaide (locations shown in Fig. 4). Their S-wave velocity/depth models allowed by the data do not include pronounced low-velocity zones or high-velocity lids in the sub-crustal lithosphere. One of their models is shown in Fig. 7. The authors indicate that the general model, E1, of Goncz and Cleary (1976) with a high-velocity lid of 4.6–4.7 km/s above 90 km (Fig. 7) is not acceptable along the particular paths analysed; they also indicate that, although low-contrast low-velocity zones can be reconciled with their data, pronounced zones cannot. Although there are differences between the models produced by various authors, they give an indication of the range of velocities required by the surface-wave data. As indicated later in this paper, this range cannot be reconciled with the teleseismic data from earthquakes in the Fijian region, analysed by Frohlich and Barazangi (1980). Models by Mills and Fitch (1977), however, contain an S-wave velocity increase from about 4.3 to 4.6 km/s in the depth range 180–220 km, in moderate agreement with the Goncz and Cleary (1976) E1-model increase at 171 km. The shear-wave data also substantiate the presence of a discontinuity at about 200 km depth determined from P-wave data.

The seismic velocity/depth structure under the Precambrian Adelaide Geosyncline to the west of the Tasman Geosyncline has been determined from both explosion and earthquake seismic investigations (Shackleford, 1978; Shackleford and Sutton, 1979). P-wave velocities in the Adelaide Geosyncline sediments are in the range 3.59–5.18 km/s, with an average of 4.8 km/s; sediment thickness varies from 1 to 5 km. Upper crustal velocities range from 5.70–5.88 km/s near the surface to 6.3 km/s at depth, with an average of 5.95 km/s. A mid-crustal velocity of 6.42 km/s is reached at about 18 ± 5 km depth; the average P-wave velocity in the lower crust is 6.46 km/s. An upper mantle velocity of 7.97 km/s is reached at a depth of 38.5 ± 5 km depth (Fig. 6).

The seismic velocity/depth structure in the upper mantle under Precambrian central Australia has been determined from explosion seismic work by Denham et al. (1972), Simpson (1973), Finlayson et al. (1974), and Finlayson (1979). The traverse locations are shown in Fig. 4 and the simplified interpretations are shown in Fig. 7. The most striking difference between the Precambrian and Phanerozoic provinces is the higher upper mantle velocities at shallower depth under Precambrian Australia. Simpson (1973) interpreted a sharp increase in velocity from 8.38 km/s to 8.53 km/s at 175 km depth, and Finlayson et al. (1974) interpreted a velocity increase from 8.18–8.23 km/s to 8.53 km/s at 165 km for their TASS 1a and 2a models. The latter two models indicate possible differences in upper mantle structure within Precambrian Australia. Under northern Australia, Hales et al.

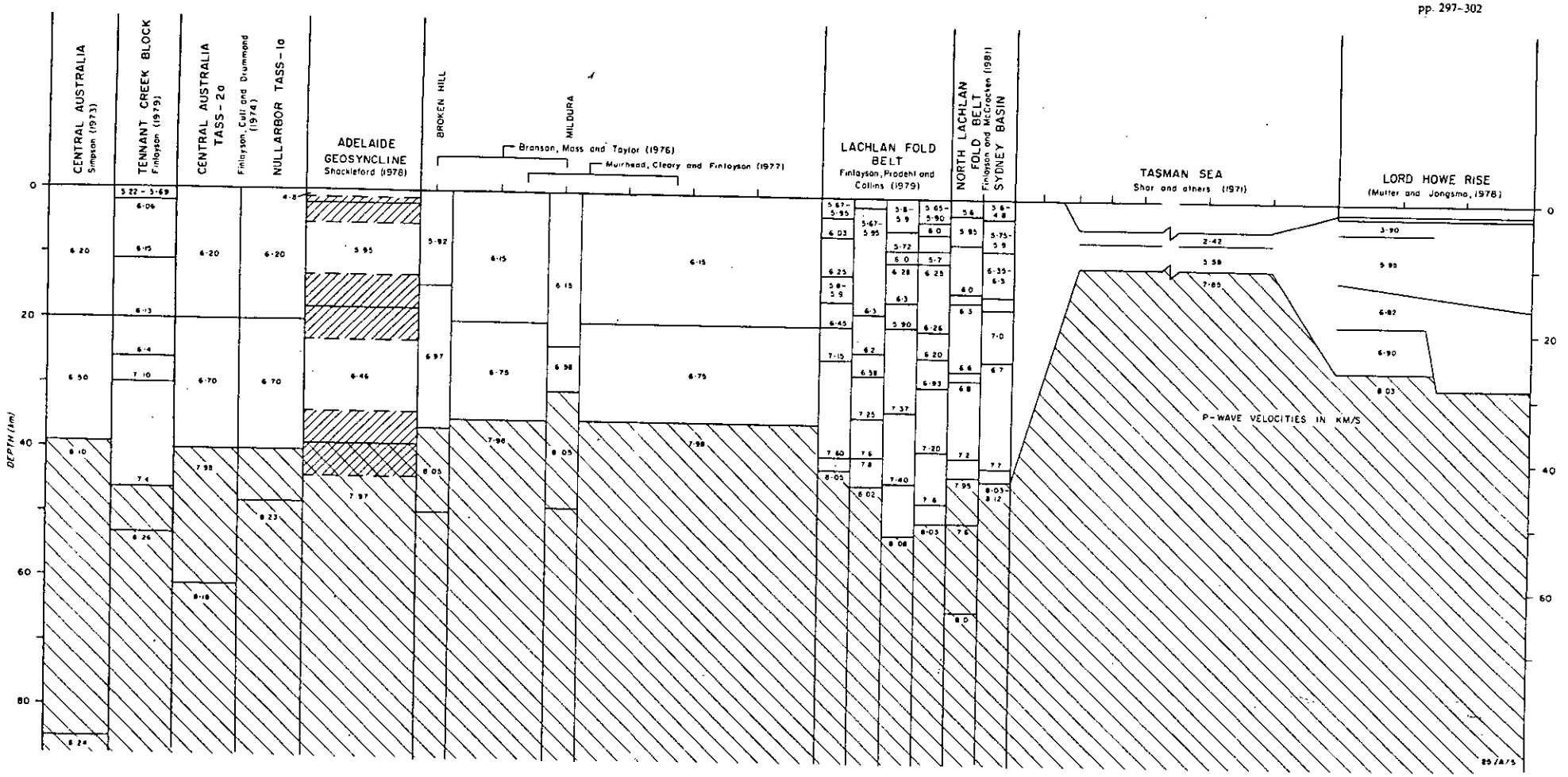

Fig. 6. Diagramatic section of the upper lithosphere from the Australian Precambrian craton, across Phanerozoic southeastern Australia to the Lord Howe Rise.

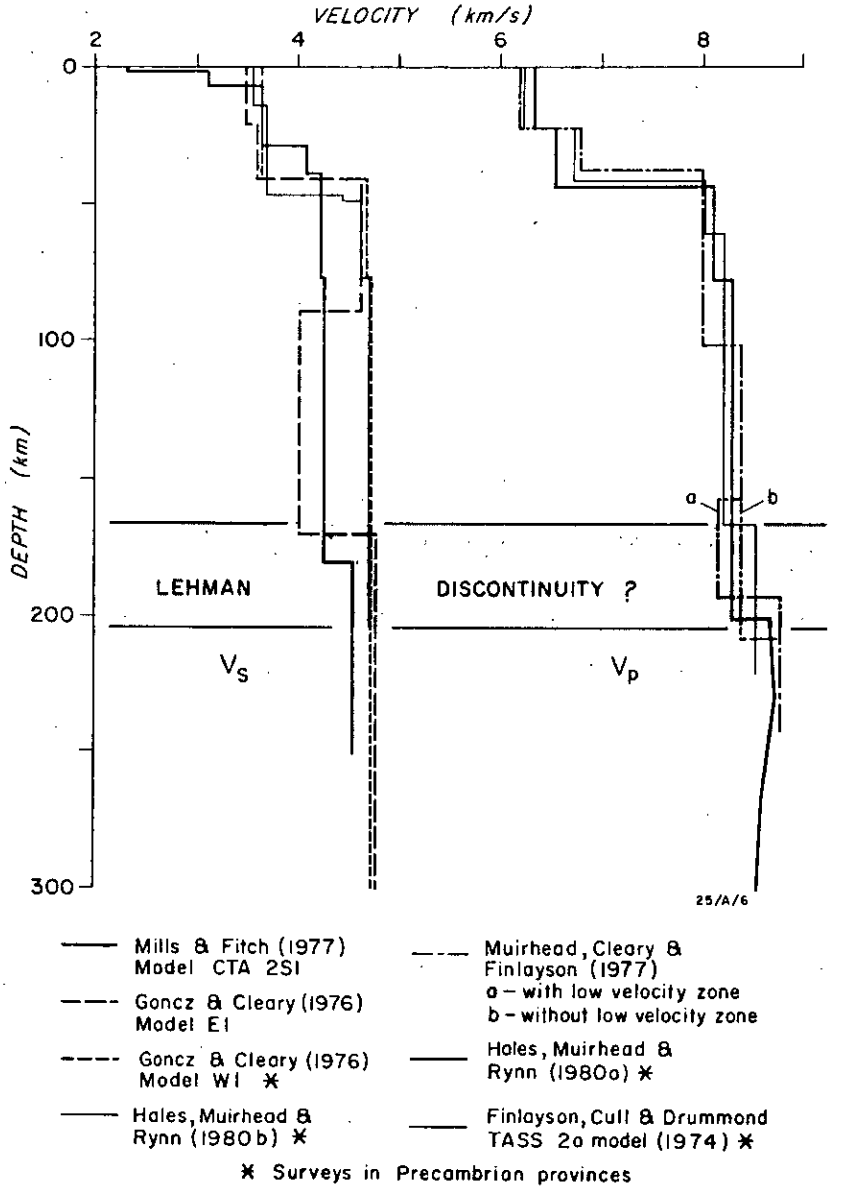

Fig. 7. Seismic velocity/depth distributions for the subcrustal lithosphere in southeastern Australia and the Precambrian craton. All V_p models and the Hales et al. (1980b) model are derived from controlled source seismic studies. A speculative Lehman Discontinuity is indicated.

(1980a) interpreted a P-wave velocity increase from 8.24 km/s to 8.62 km/s at 200 km depth (Fig. 7). Hales et al (1980b) also showed that there was an S-wave velocity increase at 76 km depth from 4.60 km/s to 4.72 km/s (Fig. 7). At depths greater than 45 km, their model is substantially the same as the model of Goncz and Cleary (1976).

Thus, there are explosion and earthquake seismic data relevant to the structure to depths of at least 200 km from both Precambrian central Australia and Phanerozoic southeastern Australia. Models for both provinces require the velocity to increase in the 165–205 km depth range. Is this velocity feature the base of the lithosphere? Anderson (1979) has presented data supporting the concept of a world-wide Lehmann discontinuity at about 220 km depth, with all strong lateral variations occurring above this depth under both continents and oceans.

In Australia there is little difficulty in demonstrating regional differences down to 200 km. Goncz and Cleary (1976, fig. 2) have shown convincingly the difference in surface-wave dispersion characteristics between eastern Australia and shield regions to the west. Cleary et al. (1972) have demonstrated the differences in teleseismic

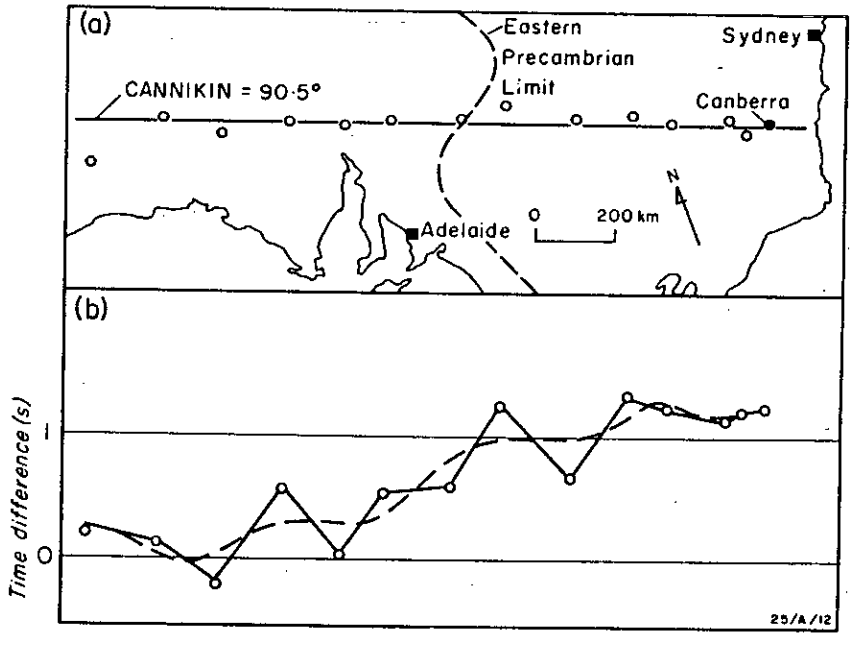

Fig. 8. a. Location of stations in southeastern Australia recording the Canniken atomic explosion in the Aleution Islands (after Cleary et al., 1972). The line through the stations is at an angular distance of 90.5° from the explosion site. The eastern limit of Precambrian craton is indicated by dashed line.
b. Relative residual travel-time differences between stations using the Herrin (1968) travel-time tables for P phases. An arbitrary residual zero point has been taken on the Precambrian craton. Open circle represents observed difference; dashed line is the smoothed three station running average.

travel-time residuals for recording stations sited across the southern Tasman Geosyncline and on to Precambrian shield areas further west. Their recordings of the Cannikin atomic bomb test at angular distances of about 90° indicate residual differences between sites in the eastern highlands and sites on the Precambrian craton of about 1.1 s (Fig. 8) with the earlier arrivals being recorded in the Precambrian regions. These data agree with studies of P-wave residuals from deep earthquake sources (Sengupta and Julian, 1976). Angles of incidence of P-waves from the Cannikin shot under the recording stations are 14–15°; consequently, the travel-time differences due to structure in the upper 60 km can be estimated from known crustal structure to be, at most, about 0.20 s after allowance is made for low velocity cover rocks. A substantial proportion of the residuals must be attributed to structures deeper than 60 km.

If the remaining residual time differences are distributed in the depth range 60–200 km, estimates can be made of the seismic velocities to be expected in the Precambrian regions, using as a starting point the model for southeastern Australia produced by Muirhead et al. (1977). Any reasonable distribution of the residual times within this depth interval produces average velocities in the range 8.65–8.70 km/s, which are unacceptably high when compared to a value of about 8.3 km/s measured by Finlayson et al. (1974) and Simpson (1973) in the Precambrian of western and central Australia. This discrepancy may be attributed either to deficiencies in the velocity/depth models determined from the explosion seismic studies, or to the teleseismic travel-time anomalies at depths greater than 200 km. By considering only the explosion seismic data, the uncertainties associated with earthquake positioning and timing are eliminated. Generally, the quality of the explosion seismic data considered in this paper is good. However, the interpretation of the data in terms of velocity/depth profiles must include the ambiguities associated with the inversion of geophysical data. The models derived for central and southeastern Australia must be regarded as preferred general models, but any differences from these general models must be constrained by the integrated P-wave travel times satisfying the data.

There is evidence that the model for southeastern Australia of Muirhead et al. (1977) may require modification in the Adelaide Fold Belt and eastern Lachlan Fold Belt. Their fig. 5 shows delayed first arrivals at distances less than 600 km, at which P-waves do not penetrate deeply within the upper mantle. The diversity of crustal and upper mantle structures that can account for delays at such distances is illustrated in Fig. 4 by the Lachlan Fold Belt models.

At greater distances the apparent velocities measured by Muirhead et al. (1977) can be regarded as the average velocities at the deepest point of penetration of the rays. Attributing teleseismic traveltime residuals to the interval above 200 km depth results in average velocities which are not observed. A distribution of the residuals within a greater depth range (60–500 km) produces average velocities which are more in accord with observed data. There is therefore some doubt whether regional

seismic velocity variations in continental Australia can be limited to the upper 200 km without involving low velocity zones in southeastern Australia of a magnitude not evident in the explosion seismic data.

There are not many explosion seismic surveys which probe to depths greater than 200 km. Given and Helmberger (1980) compare the structures of northwestern Eurasia with those of western U.S.A. and conclude that there is no distinguishable difference below 250 km. Hales et al. (1980a) have, however, demonstrated that, when comprehensive data are available, there is considerable structure to depths of at least 700 km; Hales (1981) questions whether there is yet any indication of a base to the lithosphere beneath continental platforms and shield regions.

Hales (1981, fig. 11) also shows a range of velocity models in the upper 200 km which satisfy data from northern Australia; these illustrate that more detailed work needs to be undertaken to determine the fine structure in different tectonic provinces. Yegorkin and Pavlenkova (1981) and Vinnik and Ryaboy (1981) have reported interpretations of long-range explosion seismic profiles in western, central, and southern USSR. These illustrate the differences in velocity/depth structure which can occur. In particular, low-velocity zones were interpreted in the upper mantle beneath the east European platform from explosion seismic data, and converted waves from transitions deeper than 200 km illustrate the differences from average Earth models that can occur.

ELECTROMAGNETIC SOUNDING

Constraints on the structure of the sub-crustal lithosphere can also be made using its electrical properties. Electrical conductivities in rock are strongly dependent on ionic transport, and this is greatly influenced by temperature (other major controlling factors being water and mineral content). Tozer (1979) has reviewed the interpretation of electromagnetic depth sounding experiments and indicated that, although upper mantle conductivities have been commonly connected with the behaviour of olivine under various conditions of temperature and impurity, this does not exclude a great many other compositional and physical correlations. He has pointed out that it may well be the anomalous aspects of lithospheric structure confined to comparatively small regions that control measured conductivities, and not the bulk composition, which merely adds a resistive component. In particular, chemical variations and fluid content can drastically alter conductivities on a local scale.

Tozer (1979) argues that, at the microscopic level, conductivity may be closely related to viscosity. This may be of greater significance when considering lithospheric processes than the more common interpretation linking conductivity to temperature. Conductivity anomalies may therefore be interpreted not only in terms of heat-flow anomalies but as zones of possible convection and other transport phenomena.

In southeastern and central Australia there have been a number of magnetotelluric and magnetic variation studies which have been interpreted in terms of the electrical conductivity structure within the Earth. Tammemagi and Lilley (1971) reported data from four sites across the eastern highlands, and indicated that, at depths of 100–300 km, conductivities decreased westward across the Tasman Geosyncline.

Bennett and Lilley (1973) and Lilley et al. (1981a, b) have reported the results of geomagnetic spatial gradient experiments in southeastern and central Australia. The method is only sensitive to conductivity structures at depths greater than 200 km. Lilley et al. (1981b) indicate that, on a regional scale, there is a major conductivity increase at about 200 km depth in southeastern Australia, but that such a conductivity increase is not observed until about 500 km depth in central Australia (Fig. 9). The case for regional variations in the physical properties below continental Australia at depths greater than 200 km is therefore strengthened.

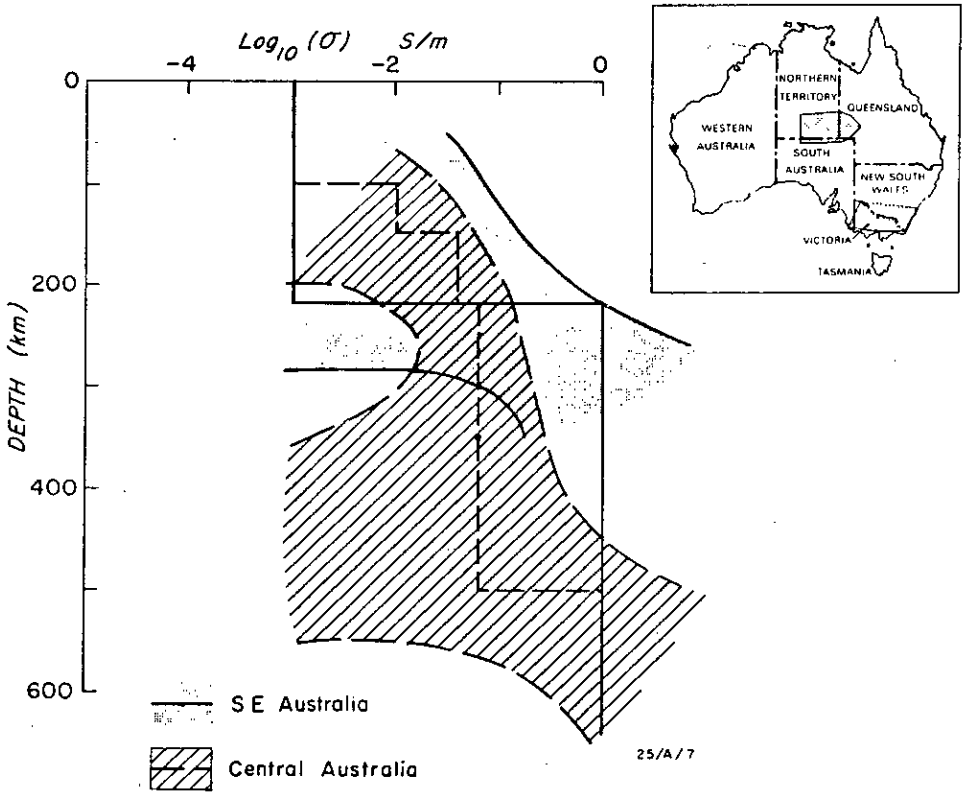

Fig. 9. Conductivity model ranges for the mantle under southeastern and central Australia (after Lilley et al., 1981b). The logarithm of the conductivity (σ) is represented. The solid and dashed lines represent the preferred models for Phanerozoic and Precambrian Australia respectively; the shaded and hachured areas represent the limits of models which fit the data.

Magnetotelluric investigations can be interpreted in terms of conductivities at depths less than 200 km. In the western Tasman Geosyncline relatively high conductivities in the range 10^{-1} to $2 \cdot 10^{-2}$ S/m have been interpreted by Vozoff et al. (1975) at depths of about 100 km. For the Precambrian Officer Basin (Fig. 1) Jupp et al. (1979) have drawn attention to the greater depth (200–250 km) at which high conductivity layers are reached in the mantle compared with the western Tasman Geosyncline.

Cull and Spence (pers. commun., 1981) report conductivity increasing at depths of about 150 km under the Precambrian North Australian Craton, and at depths less than 100 km under the Phanerozoic Eromanga Basin (Fig. 1).

The conductivity increase at about 200 km in southeastern Australia can be interpreted in terms of elevated temperature and partial melting (Lilley et al., 1981b) or in terms of viscous flow (Tozer, 1979). Both interpretations embrace the idea of dynamic processes operating in the mantle. For shallower depths, Van Zijl (1977) has interpreted conductivity increases in the lower crust in southern Africa in terms of hydration of lower crustal rocks and possibly serpentinised mantle material, i.e., in terms of anomalous zones as suggested by Tozer (1979). Olhoeft (1981) has drawn attention to the importance of free water in lower crustal and upper mantle rocks, and the magnetotelluric results in eastern Australia may reflect this effect.

It is possible that at greater depth the conductivity increase under southeastern Australia may be part of an anomalous zone of mobile material associated with eastern highland uplift. However, the direct evidence from Cainozoic volcanism in southeastern Australia indicates magmatic activity at depths of about 70 km, with intrusions having taken place along pre-existing fissures (Emerson and Wass, 1980). The generation depth for Permian–Late Jurassic kimberlitic material analysed by Ferguson et al. (1979) is generally in the range 60–70 km, with material from one site estimated to have come from about 125 km depth. Any direct connection between volcanic intrusive activity and possible deeper mobile material is conjectural.

Thermal models of the lithosphere can be constructed by making assumptions about the distribution of heat sources in the Earth's crust and about the conductivity of the various rock types. However, it is important to include the role of convection as well as conduction in any models of heat flow. Because convection is a more efficient means of heat transfer and because it requires assumptions about magmatic and hydrologic processes within the Earth, it is difficult to quantify in any heat-flow model. Little control is therefore achieved from heat-flow data on lithospheric structure because of the ambiguities surrounding the interpretation of source regions.

DISCUSSION

Regional variations of the seismic and electrical conductivity structure within the crust and upper mantle of central and southeastern Australia extend deeper than 200

km. Thus, although there is a major seismic velocity feature at 165–205 km depth under continental Australia that may correspond to the Lehmann discontinuity of Anderson (1979), regional differences in continental structure extend to greater depths.

Frohlich and Baranzangi (1980) have examined teleseismic events from the Fijian region recorded at stations in eastern and central Australia. Using the differences between P and S-wave residuals for both direct and core-reflected phases, Frohlich and Barazangi highlighted the considerable differences between the Precambrian and Phanerozoic provinces, and attributed these differences principally to S-wave velocity variations in the upper part of the mantle. They were unable to quantify the depth range within which the variations occur; however, they did comment that, if the variations were restricted to the upper 200 km, S-wave velocity differences of about 8% would be required. The observed data of Mills and Fitch (1977) and Goncz and Cleary (1976) do not support such a large velocity difference.

On the basis of isostatic compensation and compositional differences in the upper mantle under the Australian region, Dooley (1977) has expressed doubts that an asthenosphere can exist under the shield regions at depths less than 200 km, implying that deeper processes must be involved and that there are differences between sub-continental and sub-oceanic mantle to depths of "several hundreds of kilometres".

Interpretation of the difference in electrical conductivity between the Precambrian and Phanerozoic provinces in terms of either viscosity or temperature indicates a shallower, active tectonic environment within the sub-crustal lithosphere under eastern Australia than under the remainder of the continent. Source material for volcanism in eastern Australia may well be in anomalous conductivity zones at depths of less than 100 km (Emerson and Wass, 1980). Wellman and McDougall (1974a, b) attribute the southward aging of basaltic volcanics in eastern Australia to the northward movement of Australia over a hot spot during the last 60 m.y.

In an oceanic environment Detrick and Crough (1978) use a lithospheric thinning model to account for the geophysical features of an oceanic plate passing over a hot spot, namely Hawaii. They take the lithospheric boundary to be an isotherm near the solidus, and this boundary moves upwards as the lithosphere translates over the hot spot. Magma convection as well as conduction must occur to an account for the formation and subsidence of the Hawaiian swell. However, in highlighting the implications of their model, they emphasize the wavelength of the feature (1000–1400 km) which supports the view that hot spots are not just local features but are caused by mantle processes on a massive scale.

The problem of defining a lower lithospheric boundary for continental Australia from the available geophysical data is not yet resolved. In eastern Australia Cainozoic volcanism and uplift, and magnetotelluric data suggest that mobile zones may exist at depths shallower than 100 km. Under Precambrian Australia such zones are at greater depths.

ACKNOWLEDGEMENTS

The author acknowledges the considerable contributions of many colleagues to the seismic investigations of the crust and upper mantle in Australia. Useful comments by Peter Wellman and David Denham greatly assisted in preparing the manuscript. This paper is published with the approval of the Director, Bureau of Mineral Resources, Geology and Geology and Geophysics, Canberra.

REFERENCES

Anderson, D.L., 1979. The deep structure of continents. J. Geophys. Res., 84: 7555–7561.

Bennett, D.J. and Lilley, F.E.M., 1973. Electrical conductivity structure in the south-east Australian region. Geophys. J. R. Astron. Soc., 37: 191–206.

Branson, J.C., Moss, F.J. and Taylor, F.J., 1976. Deep crustal reflection seismic test survey, Mildura, Victoria and Broken Hill, N.S.W. 1968. Aust. Bur. Miner. Resour., Geol. Geophys., Rep. 193.

Cleary, J.R., Simpson, D.W., Muirhead, K.J., 1972. Variations in Australian upper mantle structure from observations of the Cannikin explosion. Nature, 236: 111–112

Compston, W. and Chappell, B.W., 1979. Sr-isotope evolution of granitoid source rocks. In: M.W. McElhinny (Editor), The Earth: Its Origin, Structure and Evolution, Academic Press, London–New York–San Francisco.

Crook, K.A.W., 1980a. Fore-arc evolution in the Tasman Geosyncline: the origin of the southeast Australian continental crust. J. Geol. Soc. Aust., 27: 215–232.

Crook, K.A.W., 1980b. Fore-arc evolution and continental growth: a general model. J. Struct. Geol., 2: 289–305.

Crosson, R.S. and Koyangi, R.Y., 1979. Seismic velocity structure below the island of Hawaii from local earthquake data. J. Geophys. Res., 84: 2331–2342.

Denham, D., 1980. The Robertson earthquake-more evidence for compressive stress in southeast Australia. Bur. Miner. Resour., J. Aust. Geol. Geophys., 5: 153–156.

Denham, D., Simpson, D.W., Gregson, P.J. and Sutton, D.J., 1972. Travel times and amplitudes from explosions in northern Australia. Geophys. J. R. Astron. Soc., 28: 225–235.

Derrick, G.M., 1979. General geology (of Australia). BMR Earth Science Atlas of Australia.

Detrick, R.S. and Crough, S.T., 1978. Island subsidence, hot spots, and lithospheric thinning. J. Geophys. Res., 83: 1236–1244.

Dooley, J.C., 1977. Implications of Australian seismic and gravity measurements for the structure and composition of the upper mantle. Bur. Miner. Resour., J. Aust. Geol. Geophys., 2: 1–5.

Emerson, D.W. and Wass, S.Y., 1980. Diatreme characteristics—evidence from the Mogo Hill intrusion Sydney Basin. Bull. Aust. Soc. Explor. Geophys., 11: 121–133.

Ewart, A., Baxter, K. and Ross, J.A., 1980. The petrology and petrogenesis of the Tertiary anorogenic mafic lavas of southern and central Queensland, Australia—possible implications for crustal thickening. Contrib. Mineral. Petrol., 75: 129–152.

Ferguson, J., Arculus, R.J. and Joyce, J., 1979. Kimberlite and kimberlitic intrusives of southeastern Australia: a review. Bur. Miner. Resour., Aust. Geol. Geophys., 4: 227–241.

Finlayson, D.M., 1979. The Australian continental crust: explosion seismic studies in Archaean, Proterozoic and Palaeozoic provinces. Abstr. Int. Assoc. Seismol. Phys. Earth's Inter., Canberra, Aust., pp. 84–85.

Finlayson, D.M. and McCracken, H.M., 1981. Explosion seismic studies of the crustal structure under the Sydney Basin and northern Lachlan Fold Belt. J. Geol. Soc. Aust., 28: 117–190.

Finlayson, D.M., Cull, J.P. and Drummond, B.J., 1974. Upper mantle structure from the Trans-Australia Seismic Refraction data. J. Geol. Soc. Aust., 21: 447–458.

Finlayson, D.M., Prodehl, C. and Collins, C.D.N., 1979. Explosion seismic profiles, and the implications for crustal evolution in southeastern Australia. Bur. Miner. Resour., J. Aust. Geol. Geophys., 4: 243–252.

Finlayson, D.M., Collins, C.D.N. and Denham, D., 1980. Crustal structure under the Lachlan Fold Belt, southeastern Australia. Phys. Earth Planet. Inter., 21: 321–342.

Frohlich, C. and Barazangi, M., 1980. A regional study of mantle velocity variations beneath eastern Australia and the southwestern Pacific using short-period recordings of P, S, PcP, ScP and ScS waves produced by Tongan deep earthquakes. Phys. Earth Planet. Inter., 21: 1–14.

Given, J.W. and Helmberger, D.V., 1980. Upper mantle structure of northwestern Eurasia. J. Geophys. Res., 85: 7183–7194.

Gonez, J.H. and Cleary, J.R., 1976. Variations in the structure of the upper mantle beneath Australia from Rayleigh wave observations. Geophys. J. R. Astron. Soc., 44: 507–516.

Gonez, J.H, Hales, A.L. and Muirhead, K.J., 1975. Analysis to extended periods of Rayleigh and Love wave dispersion across Australia, Geophys. J. R. Astron. Soc., 41: 81–105.

Hales, A.L., 1981. The upper mantle velocity distribution. Phys. Earth Planet. Inter., 25 1–11.

Hales, A.L., Muirhead, K.J. and Rynn, J.M.W., 1980a. A compressional velocity distribution for the upper mantle. Tectonophysics, 63: 309–348.

Hales, A.L., Muirhead, K.J. and Rynn, J.M.W., 1980b. Crust and upper mantle shear velocities from controlled sources. Geophys. J. Royal Astron. Soc., 63: 659–670.

Jupp, D.L.B., Kerr, D., Lemaire, H., Milton, B.E., Moore, R.F., Nelson, R. and Vozoff, K., 1979. Joint magnetotelluric-DC resistivity survey, eastern Officer Basin. Bull. Aust. Soc. Explor. Geophys., 10: 209–212.

Le Pichon, X., Francheteau, J. and Bonnin, J., 1973. Plate Tectonics. Develop. Geotectonics, 6. Elsevier, Amsterdam, 300 pp.

Lilley, F.E.M., Woods, D.V. and Sloane, M.N., 1981a. Electrical conductivity from Australian magnetometer arrays using spatial gradient data. Phys. Earth Planet. Inter., 25: 202–209.

Lilley, F.E.M., Woods, D.V.; Sloane, M.N., 1981b. Electrical conductivity profiles and implications for the absence or presence of partial melting beneath central and south-east Australia. Phys. Earth Planet. Inter., 25: 419–428.

Mills, J.M. and Fitch, T.J., 1977. Thrust faulting and crust–upper mantle structure in east Australia. Geophys. J. R. Astron. Soc., 48: 351–384.

Muirhead, K.J., Cleary, J.R. and Finlayson, D.M., 1977. A long-range seismic profile in south-eastern Australia. Geophys. J. R. Astron. Soc., 48: 509–519.

Mutter, J.C. and Jongsma, D., 1978. The pattern of the pre-Tasman Sea rift system and the geometry of breakup. Aust. Soc. Explor. Geophys. Bull., 9: 70–75.

Olhoeft, G.R., 1981. Electrical properties of granite with implications for the lower crust. J. Geophys. Res., 86: 931–936.

Plumb, K.A., 1979. The tectonic evolution of Australia. Earth-Sci. Rev., 14: 205–249.

Sengupta, M.K. and Julian, B.R., 1976. P-wave travel times from deep earthquakes. Bull. Seismol. Soc. Am., 66: 1555–1579.

Shackleford, P.R.J., 1978. The determination of crustal structure in the Adelaide Geosyncline using quarry blasts as seismic sources. M.Sc. Thesis, Department of Physics, University of Adelaide.

Shackleford, P.R.H. and Sutton, D.J., 1979. Crustal structure in South Australia using quarry blasts. In: D. Denham (Editor), Crust and Upper Mantle of Southeast Australia. Aust. Bur. Miner. Resour., Rec. 1979/2.

Shor, G.G., Kirk, H.K. and Menard, G.L., 1971. Crustal structure of the Melanesian area. J. Geophys. Res., 76: 2562–2586.

Simpson, D.W., 1973. P-wave velocity structure of the upper mantle in the Australian region. Ph.D. Thesis, Australian National University.

Sutherland, F.L., 1981. Migration in relation to possible tectonic and regional controls in eastern Australian volcanism. J. Volcanol. Geotherm. Res., 9: 181–213.

Tammemagi, H.Y. and Lilley, F.E.M., 1971. Magnetotelluric studies across the Tasman Geosyncline, Australia. Geophys. J. R. Astron. Soc., 22: 505–516.

Taylor, S.R., 1979. Chemical composition and evolution of the continental crust: the rare earth element evidence. In: M.W. McElhinney (Editor), The Earth: Its Origin, Structure, and Evolution. Academic Press, London–New York–San Francisco.

Tozer, D.C., 1979. The interpretation of upper mantle electrical conductivities. Tectonophysics, 56: 147–164.

Van Zijl, J.S.V., 1977. Electrical studies of the deep crust in various tectonic provinces of southern Africa. In: J.G. Heacock (Editor), The Earth's Crust. Geophys. Monogr., Am. Geophys. Union, 20: 470–500.

Vinnik, L.P. and Ryaboy, V.Z., 1981. Deep structure of the east European platform according to seismic data. Phys. Earth Planet. Inter., 25: 27–37.

Vozoff, K., Kerr, D., Moore, R.F., Jupp, D.L.B., and Lewis, R.J.G., 1975. Murray Basin magnetotelluric study. J. Geol. Soc. Aust., 22: 361–375.

Wellman, P., 1979a. On the Cainozoic uplift of the southeastern Australian highland. J. Geol. Soc. Aust., 26: 1–9.

Wellman, P., 1979b. On the isostatic compensation of Australian topography. Bur. Miner. Res., J. Aust. Geol. Geophys., 4: 373–382.

Wellman, P. and McDougall, I., 1974a. Cainozoic igneous activity in eastern Australia. Tectonophysics, 23: 49–65.

Wellman, P. and McDougall, I., 1974b. Potassium-argon ages on the Cainozoic volcanic rocks of New South Wales. J. Geol. Soc. Aust., 21: 247–272.

Yegorkin, A.V. and Pavlenkova, N.I., 1981. Studies of mantle structure of USSR territory on long-range seismic profiles. Phys. Earth Planet. Inter., 25: 11–26.

SEISMIC REFRACTION AND REFLECTION FEATURES OF THE LITHOSPHERE IN NORTHERN AND EASTERN AUSTRALIA, AND CONTINENTAL GROWTH

D.M. Finlayson & S.P. Mathur

Bureau of Mineral Resources, Geology & Geophysics,
P.O. Box 378, Canberra City - ACT 2601, Australia.

ABSTRACT. Seismic refraction and reflection data from a transect of the lithosphere across Proterozoic and Phanerozoic eastern Australia indicate that the depth to the upper mantle under outcropping igneous, metamorphic and fold belt provinces is 10-15 km greater than that under the intra-cratonic basins. This is probably a result of crustal underplating during episodes of high thermal flux from the mantle. Under the larger basins the upper crustal basement is mostly transparent to vertical seismic waves (i.e. there are few reflecting horizons) whereas the lower crust displays multiple reflecting horizons: the velocity boundary at mid-crustal depths is a prominent feature, seen also under intra-cratonic basins on other continents. The different character of reflecting horizons in the upper and lower crust suggests separate tectonic histories.

Under outcropping igneous, metamorphic and fold belt provinces their complex tectonic history is displayed in the multiplicity of both upper and lower crustal velocity/depth distributions. In the lower crust the velocity changes are transitional rather than sharp: seismic reflecting horizons are shorter and more varied under the Proterozoic than under the Phanerozoic

provinces, consistent with the relative youth of the latter.

In the sub-crustal lithosphere there are few, if any, seismic reflecting horizons but there are velocity changes with depth which indicate geochemical zonation. The upper mantle velocity under the Proterozoic crust is about 8.15 km/s on average and about 8.06 km/s under Phanerozoic Australia. A velocity increase to about 8.3 km/s is interpreted at its shallowest (55 km) under the central Eromanga Basin. There is no obvious difference between upper mantle velocities measured north-south from those measured east-west under the North Australian Craton.

The crustal growth patterns indicated by the seismic data, together with xenolith studies, suggest that the Phanerozoic development of eastern Australia was propagated by episodes of high geothermal flux from the mantle rifting and underplating/intruding a pre-existing crust. The development of the major basins on the eastern margin of the Precambrian craton probably has analogues in central/western European basin development.

Key words: Australian lithosphere, deep seismic, refraction and reflection.

INTRODUCTION

The structure under the Eromanga Basin in eastern Australia provides an important link when comparing lithospheric structure under the Proterozoic provinces of northern Australia with that under the outcropping Palaeozoic provinces of the eastern Australian seaboard. The Mesozoic Eromanga Basin is the largest intra-cratonic basin in Australia (Fig. 1) and it conceals a number of infra-basins dating back to at least the Devonian. The sedimentary sequences have been targets for oil and gas exploration and the subject of much lithological discussion (Moore & Mount,1982). However, the deep lithospheric structure of the Eromanga Basin is important in assessing

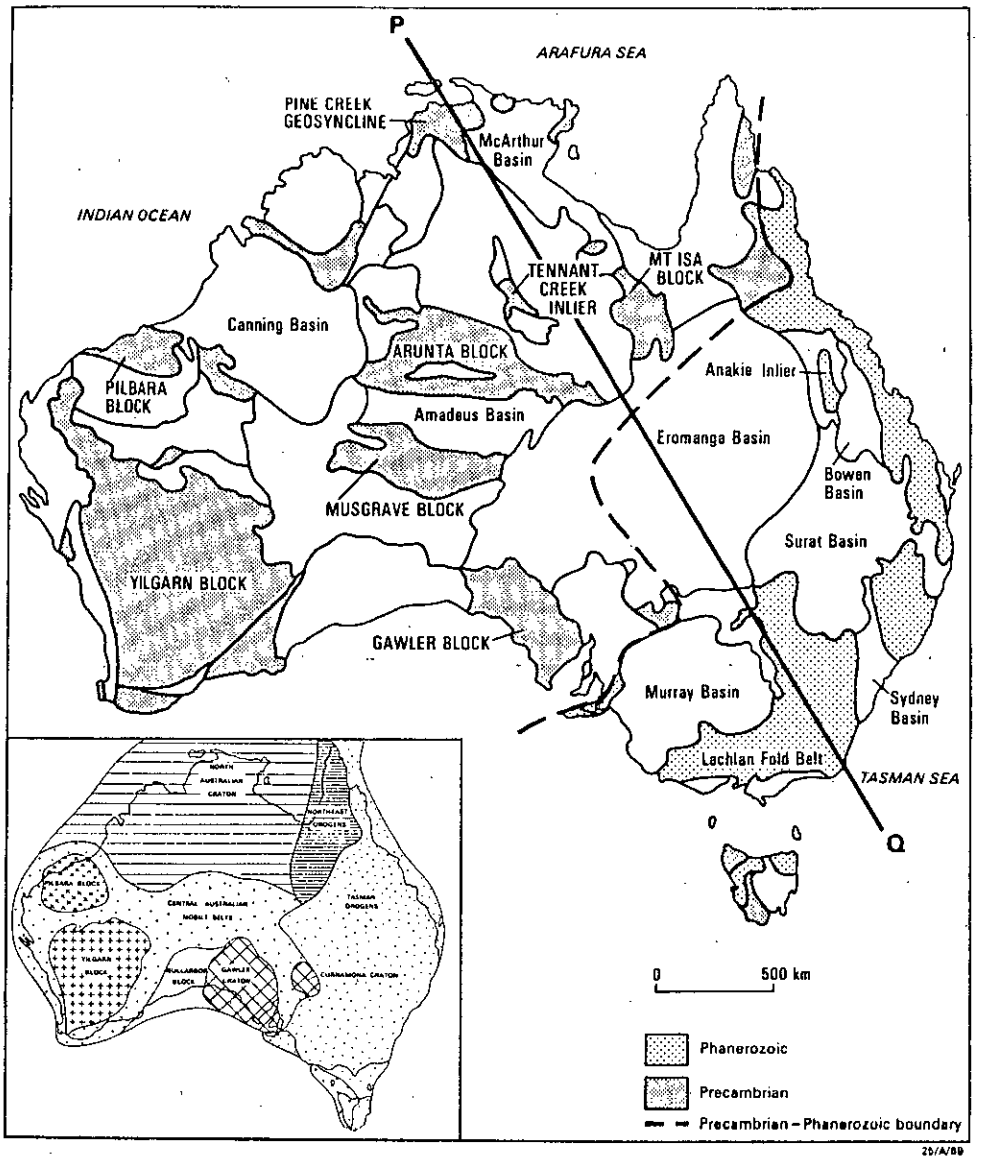

1. Simplified geology of continental Australian. Shaded areas indicate outcropping igneous, metemorphic and geosynclinal provinces. Inset: major crustal subdivisions (from Plumb, 1979a). P-Q is the location of the transect depicted in Figures 3 & 8.

models for the tectonic development of the region and this was largely unknown until 1980-82 when a series of deep seismic reflection and refraction surveys was conducted in the central part of the Basin.

Some results from these surveys are presented in this paper together with results from other seismic surveys in northern and eastern Australia to provide a 3500 km transect of upper lithospheric structure across continental Australia from the Arafura Sea to the Lachlan Fold Belt (Fig. 1).

PRECAMBRIAN GEOLOGY

An understanding of the evolution and composition of the Australian continental lithosphere is more easily attainable than elsewhere since cratonisation has progressed from west to east throughout geological time with comparatively few episodes of major reworking of earlier cratonic provinces (Plumb,1979a). Thus the Pilbara and Yilgarn cratons in western Australia have remained comparatively undisturbed since 2.3 b.y.B.P. and the North Australian Craton and Northeast Orogens, incorporating the Tennant Creek Block, the Mount Isa Geosyncline and the McArthur Basin (Fig. 1) have been largely stable since 1.4 b.y.B.P. The Mount Isa Geosyncline contains mid-Proterozoic sedimentary rocks deposited on early Proterozoic basement (1780 m.y.B.P.) and then intensely deformed, metamorphosed and intruded by granites with final cratonisation about 1490-1460 m.y.B.P.

Elsewhere in northern Australia basement outcrops are often referred to as 'inliers' because they are considered to be the exposed parts of much larger features. In the Tennant Creek Inlier pelitic gneisses were metamorphosed at 1920 m.y.B.P. (Black,1977) and these form basement to the Warramunga Group of sedimentary and volcanic rocks (older than 1800 m.y. B.P.) which were intruded by granites in the period 1500-1700 m.y.B.P. Farther north Archaean rocks of the Pine Creek Geosyncline crop out

(older than 2500 m.y.B.P.) but the full extent of Archaean basement is not known under cover rocks. The McArthur Basin is a mid-Proterozoic basin consisting of relatively undeformed, mainly shallow marine sediments which are part of the North Australian Platform Cover (Plumb,1979b); the McArthur Basin succession was deposited about 1700-1400 m.y.B.P.

The offshore areas of northern Australia are regarded as a continuation of the Australian continental lithosphere (Curray et al.,1977). The early Cambrian-mid Ordovician Arafura Basin probably has a Precambrian basement. The Money Shoal well located on the seismic line shown in Fig. 2 bottomed at about 3 km depth in basement regarded as late Proterozoic-early Cambrian.

PHANEROZOIC GEOLOGY

Veevers et al.(1982) indicate that the development of Phanerozoic eastern Australia began with breakup of the central Australian Precambrian craton around 570 m.y.B.P. Doutch & Nicholas(1978) regard the Eromanga Basin and infra-basins as being "younger internal (intracratonic) basins" overlying the Tasman Fold Belt System. Murray & Kirkegaard(1978) suggest that the central Eromanga Basin region was the site of a marginal sea between the Precambrian craton and a Cambro-Ordovician volcanic island arc, but this was deformed and metamorphosed by about 480 m.y.B.P. Cook(1982) considers that the late Cambrian (510 m.y.B.P.) continental shelf was to the west of the Eromanga seismic traverses shown in Fig. 2. Harrington (1974) envisages the central Eromanga region being part of a small ocean basin or back-arc marginal sea (Barcoo Marginal Sea) analogous to the Sea of Japan with cratonic fragments rifted from the Precambrian craton lying to the east.

Infra-basins of the Jurassic-Cretaceous Eromanga sequence include the Cambro-Ordovician Warburton Basin, the Devonian Adavale, the Devonian-

Carboniferous Drummond Basins, and the Permo-Triassic Cooper and Galilee Basins (Doutch & Nicholas,1978). MAGSAT data highlight the contrast between the negative magnetic anomaly over the Eromanga Basin and the positive anomalies identified with adjacent Precambrian areas (Frey, 1982).

The tectonic development of southeast Australia has been the subject of a substantial number of interpretations. There are essentially two interpretational models; one implies that the Lachlan Fold Belt evolved largely in a western Pacific-type continental-margin environment with island arcs and back-arc basins (Scheibner,1973; Crook,1980; Crook & Powell,1976), and the second model implies development on reworked Precambrian continental crust (Compston & Chappell,1979; White et al., 1976), a model which is gaining increasing support as better dating methods are developed.

Crawford(1983) has put forward a tentative model reconciling aspects of both models. He indicates that three widely separate, narrow elongate belts of Cambrian greenstones provide substantial evidence for the western Pacific-type model. Crook(1980) describes ten 'arc' terrains in the southern Tasman Geosyncline and several features formed by crustal extension. He indicates that the Tasman Geosyncline was possibly initiated as early as 750-800 m.y.B.P. with subsequent development analogous to that currently existing between Vietnam and the Marianas Trench in the Pacific. Crook(1980) envisages that subduction had largely ceased in southeast Australia by the late Ordovician(about 460 m.y.B.P.) but there was a period of mid-Silurian crustal extension and sediment filling during the Silurian and Devonian.

However, lower and middle Palaeozoic granitoids constitute about 25% by area of the Lachlan Fold Belt and these have been divided into I-type granites, derived largely from mafic-intermediate sources which have not been through a weathering cycle, and S-type granites which are derived from a metasedimentary source. Compston & Chappell(1979)

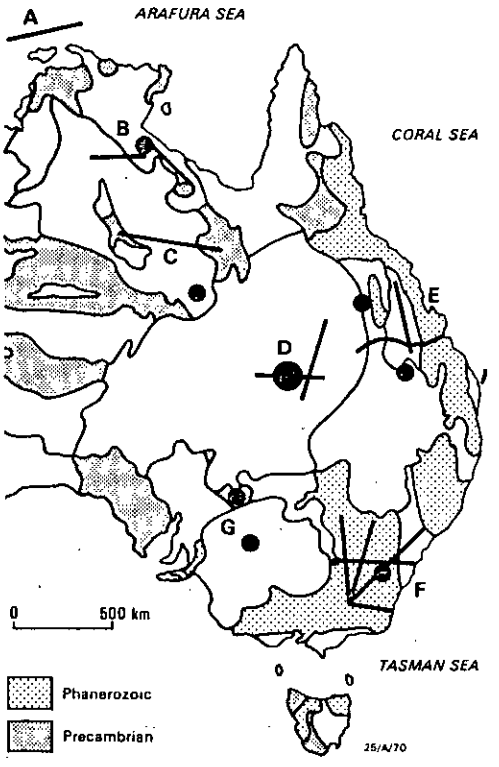

2. Location of seismic refraction (lines) and reflection (dots) traverses in eastern Australia. A, western Arafura Sea; B, McArthur Basin; C, Tennant Creek to Mount Isa and southern Georgina Basin; D, central Eromanga Basin; E, Bowen Basin and eastern Drummond Basin; F, Lachlan Fold Belt; G, Murray Basin and Broken Hill Block.

in the Eromanga Basin, the traverse lengths at sites considered in this paper were generally less than 20 kilometers; however this was usually sufficient to gauge the style of reflecting horizons. In the Eromanga Basin deep reflection profiling was continuous on thirteen traverses totalling 1400 km in length.

Western Arafura Sea

The marine profile in the western Arafura Sea (Fig. 2), with recordings out to 300 km, has been interpreted by Rynn & Reid(1983). They interpret a sedimentary layer 2 km thick with velocities in the range 2.00-5.28 km/s. The upper crustal basement has a velocity of 5.97 km/s extending to 11 km depth where an increase in velocity to 6.52 km/s is interpreted. In the lower crust a velocity gradient was evident with the velocity increasing from 6.52 to 7.0 km/s in the depth range 17 to 30 km. A higher velocity (7.33 km/s) is interpreted in the depth range 30 to 34 km at which an upper mantle velocity of 8.0 km/s is reached (Fig. 3).

From recordings made of the marine shots at land stations out to distances of over 1000 km towards the Tennant Creek Block, Hales & Rynn (1978) interpreted an upper mantle velocity of 8.18 km/s between 45 and 76 km depth and below this a velocity of 8.38 km/s (after spherical earth corrections have been made). This lithospheric model applies almost wholly to the velocity structure under the Archaean Pine Creek Geosyncline. Hales, Muirhead & Rynn(1980) have determined deeper structure under the region using earthquake sources north of Australia. Major velocity discontinuities were interpreted at depth of 75, 200, 325, 411, 512, 610, 630, 645 and 722 km, with the possibility of a low velocity zone between 200 and 325 km. Leven(1980) has refined this model, the main modifications being the interpretation of velocity gradients in the ranges 190-210 km, 320-330 km, 610-645 km and 700-750 km rather than discontinuities and a prominent

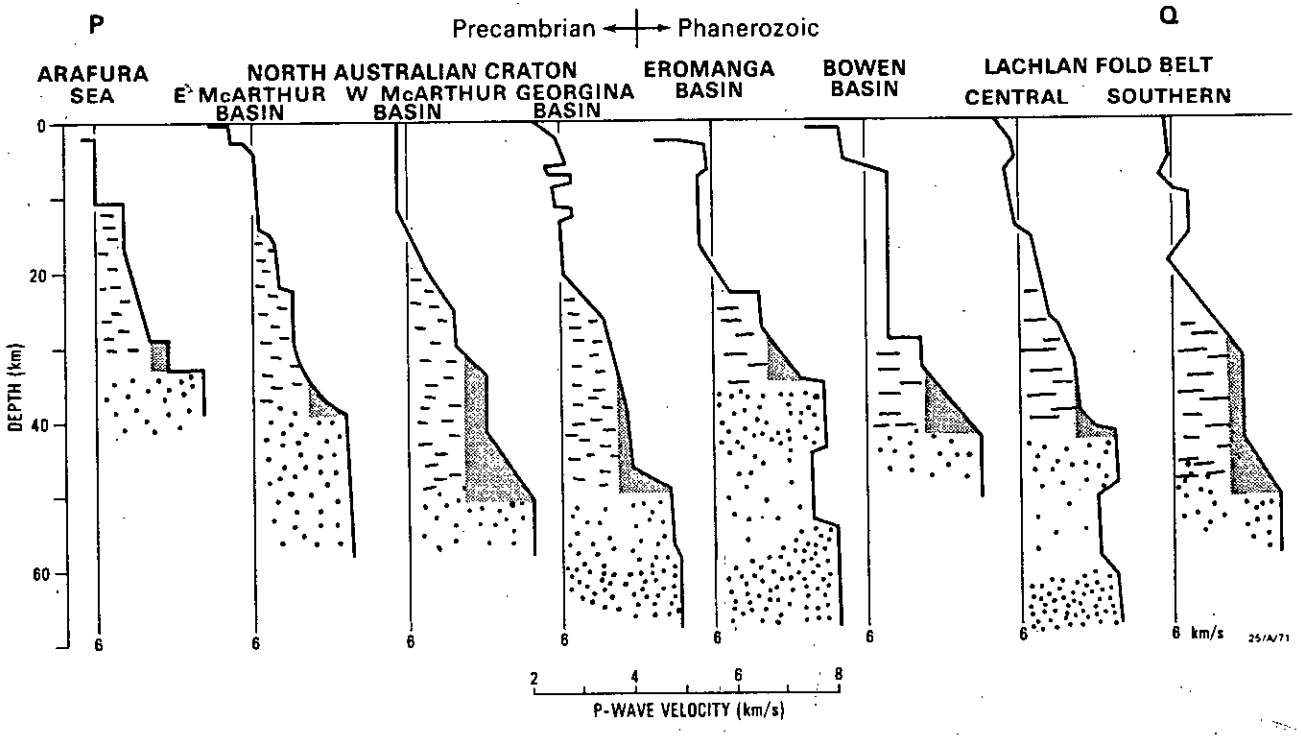

3. Representative velocity/depth distributions along a lithospheric transect between the Arafura Sea and the Lachlan Fold Belt. In the lower crust the dashed lines indicate short and long vertical seismic reflection horizons and the shaded areas indicate the extent of velocities over 7 km/s. In the upper mantle screening density indicates velocity zonation, with higher velocities indicated by a denser screen.

decrease in velocity between 220 and 225 km.

McArthur Basin

Two seismic refraction traverses were shot in the McArthur Basin region of northern Australia (Fig. 2). The western traverse is almost wholly across the central part of the North Australian Craton; the eastern traverse is across the region of exposed McArthur Basin sequence and is probably more representative of the McArthur Basin province as a whole (Collins, 1983). Vertical seismic reflection recording was conducted at seven sites on the refraction traverses.

Under the eastern traverse the McArthur Basin sequence is about 3.3 km thick (velocity range 3.5-5.57 km/s). A basement velocity of 5.99-6.04 km/s increases to 6.47 km/s at 16 km depth and to 6.8 km/s at 23 km. An upper mantle velocity of 7.9 km/s is reached at 44 km depth. Under the western traverse Precambrian McArthur Basin sediments up to 9 km thick (velocity 4.1-5.9 km/s) overly basement with a velocity of 5.9-6.0 km/s. Velocity increases to 6.42 km/s are interpreted at 21 km and from 6.94 to 7.53 km/s in the depth range 26 to 43 km. A poorly determined upper mantle velocity of 8.47 km/s is interpreted at 53 km, 9 km deeper than the Moho depth under the eastern traverse (Fig. 3). There are no outstanding velocity discontinuities within the crust below basement and the crust/mantle boundary is interpreted as gradational (Collins, 1983).

Hence the depth to the crust/mantle boundary under the McArthur Basin (44 km) is close to the Hales & Rynn (1978) value for the Pine Creek Geosyncline (45 km). However towards the central part of the North Australian Craton the Moho depth increases to about 53 km.

Mathur (1983a) and Collins (1983) have described the character of vertical seismic reflections from the two traverses. In the upper

crust (less than 7 s two-way reflection time) there are notable differences between the eastern and western traverses. The eastern traverse displays reflecting bands within the upper crustal basement suggesting strongly layered basement rocks (Fig. 4). The western traverse displays no reflections in the upper crust, emphasising the difference between the upper crustal tectonics under the two traverses.

At two-way reflecting times greater than 7 s the characteristics of the reflecting horizons are similar under both traverses, namely short (up to 1 km long) weak segments dispersed evenly to the limit of recording, 16 s. The reflections tend to increase in strength, continuity and coherency with depth.

Tennant Creek - Mount Isa, Georgina Basin

Between Tennant Creek and Mount Isa, on the North Australian Craton (Fig. 1), seismic recordings have been made at distances up to 600 km from explosive sources (Finlayson, 1982a). Basement outcrop occurs at Tennant Creek and Mount Isa but the intervening basement is largely hidden by up to 10 km of late Proterozoic-Palaeozoic sediments in the Georgina Basin. The basement rocks are however considered to be subsurface extensions of the Tennant Creek Inlier, the Arunta Inlier and the Mount Isa Geosyncline.

Near Tennant Creek, Finlayson(1981,1982a) interpreted the seismic refraction data in terms of near-surface (less than 6 km) velocities of 5.47-6.2 km/s in the Warramunga Group low-grade metamorphics and weathered granites overlying amphibolite facies rocks of older metamorphic domains with velocities greater than 6.2 km/s. These latter rocks are possibly interspersed with lower velocity rocks (5.75-5.9 km/s). In the Mount Isa Geosyncline the upper crustal velocities of 6.03-6.15 km/s correspond to the Leichhardt Metamorphics interspersed with granites.

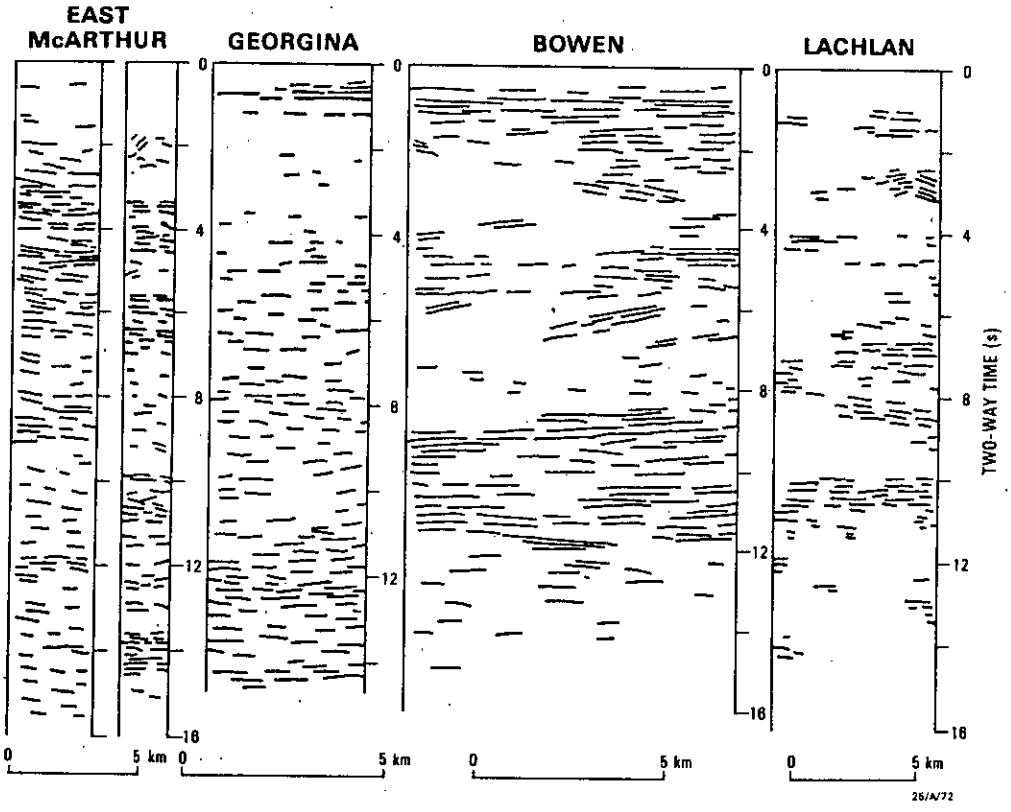

4. Sketch of vertical reflection horizons evident on seismic profiling records from the east McArthur Basin, the Georgina Basin, the Bowen Basin (Dennison Trough), and the Lachlan Fold Belt (Gundary Plains).

In the middle crust velocity gradients are evident with velocities reaching 6.85 km/s at 26 km depth near Tennant Creek and 37 km near Mount Isa. The lower crust is characterised by velocities of 7.3-7.5 km/s and the upper mantle velocity of 8.16-8.20 km/s is reached at depths of 51-54 km (Fig. 3). The Moho depth and upper mantle velocity are in accord with data from the western traverse in the McArthur Basin. The upper mantle velocity range straddles the value determined by Hales & Rynn (1978) on their north-south traverse(8.18 km/s). At a depth of 76 km they interpreted a further increase in velocity to 8.38 km/s; this can be compared with the velocity increase to 8.29 km/s interpreted by Finlayson (1982a) at 61 km depth from Tennant Creek data, increasing to 8.31 km/s at 70 km.

There is no seismic reflection profiling near the Tennant Creek-Mount Isa traverse but farther south in the Georgina Basin Mathur (1983a) has described profiling on the eastern edge of the Precambrian craton (Fig. 4). The character of the reflections is similar to that under the western McArthur Basin, namely, a general lack of reflections in the upper crustal basement to two-way reflection times of 4-5 s with short, discontinuous, reflection segments in the lower crust showing increasing strength, continuity and coherency with depth.

Eromanga Basin

Deep seismic refraction and reflection data from the Eromanga Basin (Fig. 2) have been interpreted by Finlayson et al. (1983), Finlayson (1983), Mathur (1983a, b). These data complement a large amount of upper crustal information available from the exploration industry (Armstrong and Barr, 1982) and from government research organisations (Moss & Wake-Dyster, 1983). In the region, 1400 km of continuous deep seismic profiling was conducted to 20 s two-way reflection time and, additionally,

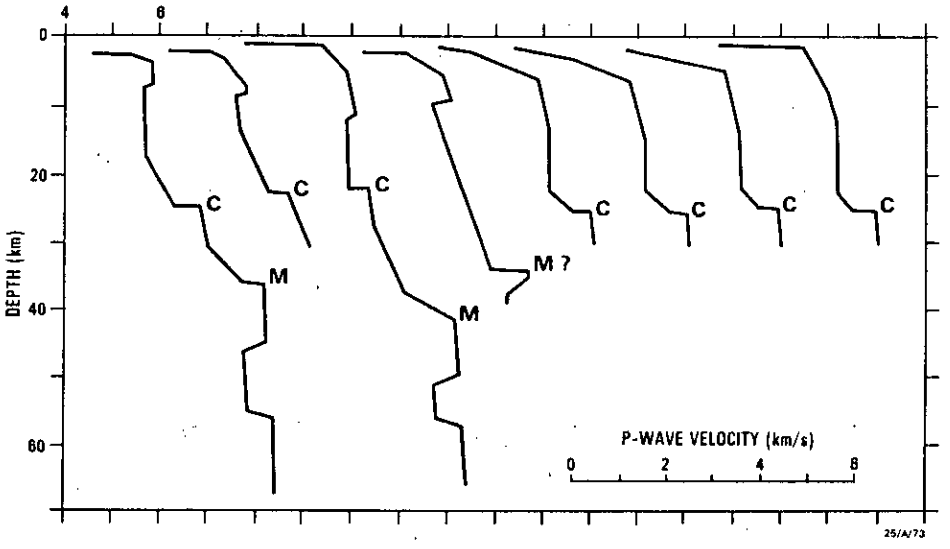

5. Velocity/depth distributions from the central Eromanga Basin. C indicates mid-crustal velocity horizon and M indicates the crust/mantle boundary.

shallow seismic refraction investigations were conducted to determine detailed velocity structure at depths less than 10 km (Lock et al., 1983; Collins & Lock, 1983).

The seismic refraction data recorded at distances out to 400 km revealed comparatively simple velocity/depth models for the region (Fig. 5). The upper crust is characterised by velocities of 2.0-5.5 km/s in the Eromanga Basin sequence and infra-basins grading to 5.6-6.0 km/s in basement rocks. A velocity reduction is possible at depths of about 8-12 km to values not less than 5.7 km/s. However the prominent feature in the record sections is evidence of a pronounced velocity increase at mid-crustal depths of 21-24 km (Finlayson et al., 1983; Finlayson, 1983). A similar feature is evident under intra-cratonic basins elsewhere, e.g. the Mississippi Embayment (Mooney et al.,1983).

In the lower crust the velocity increases to values of about 7.7 km/s and the crust/mantle boundary is defined over a 4 km depth range with an upper mantle velocity of 8.15 km/s being reached at depths of 36-41 km. There is evidence of a further increase in velocity in the sub-crustal lithosphere to a value of 8.35 km/s at 56-57 km with a low velocity zone above this depth.

The deep seismic reflection data from the upper crust of the region are characterised by the general lack of reflections below the sedimentary section (Mathur, 1983a, b) (Fig. 6). However between 8 and 13 s two-way reflection time there are a significant number of reflections which are generally coherent over horizontal distances of about 3 km. This reflection zone is a prominent feature of the record section. At two-way times greater than 13 s there are no prominent reflections. The onset of the reflection zone at 7 s corresponds to the prominent mid-crustal velocity increase and the lower limit at 13 s corresponds with the crust/mantle boundary.

In the Murray Basin (Figs. 1 & 2) between the Precambrian craton and

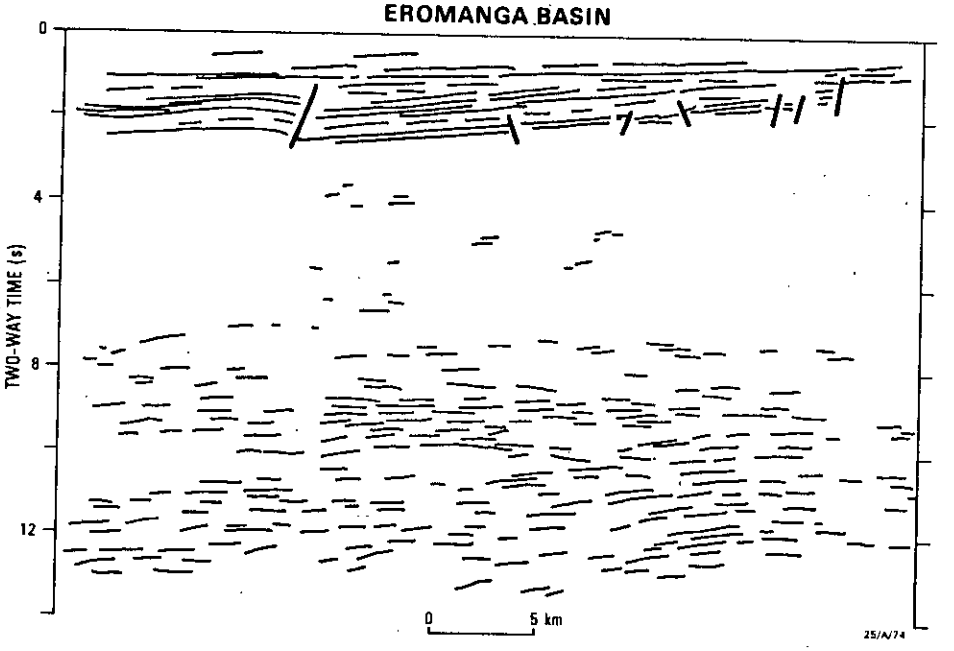

6. Sketch of vertical reflection horizons from the Warrabin Trough region of the central Eromanga Basin.

the Lachlan Fold Belt, Branson et al. (1976) have reported the results of split-spread recordings from the deep crust and upper mantle. These results, too, clearly indicate reflection segments between 8 and 12 s, i.e. in the lower crust, with very few reflections from the upper crustal basement (Fig. 7). In this case the data were recorded on low sensitivity analogue equipment. On the neighbouring Precambrian craton near Broken Hill similar recording techniques produced a record section with only a few reflections notable for their lack of strength, continuity and coherence.

Bowen-Drummond Basins

Collins (1978) and Leven (1980) have reported the results of seismic refraction surveys along and across the Bowen Basin respectively (Fig. 2). Along the Basin axis reversed seismic data were interpreted in terms of a sedimentary section about 6 km thick on average with velocities between 4 and 5.53 km/s, an upper and middle crust with a velocity of 6.39 km/s. There is a prominent increase in velocity in the lower crust to 7.07 km/s at 31 km depth and a velocity gradient to the crust/mantle boundary at 44 km depth, with an upper mantle velocity of 8.10km/s (Fig. 3). Leven's (1980) model differs slightly; a velocity gradient of 6.3 to 6.49km/s is interpreted between 4 and 32 km depth, with a prominent increase in velocity at the deeper level interpreted as the crust/mantle boundary. However it is more likely to be equivalent to Collins' lower crustal horizon and Leven's Moho is probably at 48 km where he interprets an upper mantle velocity of 8.3 km/s. The Collins' Moho depth and velocity is thought to be more reliably determined, being interpreted from reversed data along strike.

Deep seismic reflection data are available from the Denison Trough part of the Bowen Basin and from the Drummond Basin flank of the Anakie

basement high (Fig. 2). The Bowen Basin record sections below the sedimentary section indicate strong reflection bands at 4-5 s and 8-12 s (Fig. 4). The strength, coherence and continuity of the reflecting segments are prominent. The reflection zone in the lower crust is similar in character to that from the Eromanga Basin. The Drummond Basin record section, below the sedimentary/volcanic sequence at 4 s, is characterised by uniformly short, poor reflections to the recording limit of 16 s, leading Mathur (1983a) to suggest that the crust is Precambrian, a suggestion supported by some tectonic models for the origin of the Anakie Inlier.

Lachlan Fold Belt

Seismic refraction surveys have been conducted in the outcropping areas of the Lachlan Fold Belt with recording distances in excess of 400 km (Finlayson et al., 1979; Finlayson et al., 1980; Finlayson & McCracken, 1981), (Fig. 2).

Velocity gradients rather than velocity discontinuities characterise the structure of the Lachlan Fold Belt (Fig. 3). At depths less than 12 km there is evidence for velocity decreases within a general velocity increase from about 5.6 km/s to 6.3 km/s. In the middle crust (16-35 km) the velocity increases from 6.3 to greater than 7.0 km/s with some evidence again for velocity decreases. The prominence of the low velocity zones varies throughout the region. Such zones may be interpreted in terms of rock composition or of physical processes such as temperature effects and seismic scattering. Detailed studies have not yet been conducted in Australia. The upper mantle velocity of 8.02-8.05 km/s is reached at a depth greater than 50 km under the highest topography but is reached at 43-50 km towards the north of the Belt. There is some evidence for structure in the sub-crustal lithosphere; a low-velocity zone is interpreted in the depth

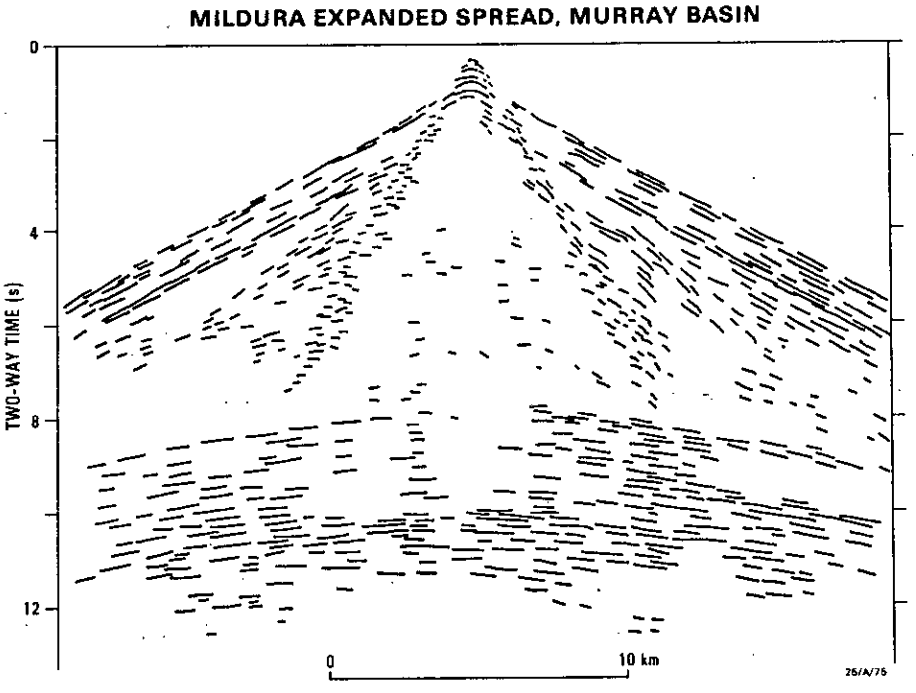

7. Sketch of reflection horizons recorded in a split-spread layout at Mildura, Murray Basin.

range 50-64 km with a strong velocity gradient below it (Fig. 3).

Along a traverse from the Lachlan Fold Belt to the Precambrian craton across the Murray Basin (Fig. 1) Muirhead, Cleary & Finlayson (1977) interpreted an upper mantle velocity of 7.98 km/s at 35 km depth, with subsequent velocity increases at 100 km (to 8.36 km/s) and at 205 km (to 8.72 km/s). If a low velocity zone is interpreted above this latter velocity increase, its depth reduces to 190 km depth.

Seismic reflection profiling in the eastern Lachlan Fold Belt has been described by Pinchin (1980) and Mathur (1983a). At the Gundary Plains site (Fig. 2) reflections at two-way times of less than 2 s are attributed to Palaeozoic sediments and intersecting events at about 3 s to complex basement structure in the neighbourhood of the site. There are however also prominent bands of reflections at 7-9s and 10-11 s which are seen on all profiles, indicating a layered structure in the middle-lower crust at depths of about 20-33 km. These bands fit into the zone of general velocity increase from 6.3 to 7.0 km/s interpreted from refraction data in the depth range 16-35 km. At two-way times greater than 11 s, reflections become less coherent and at times greater than 13 s they cut out altogether. There are no prominent reflecting horizons which might correspond to the crust/mantle boundary estimated to be at about 50km depth by Finlayson et al. (1979), with a velocity gradient in the lower crust rather than a prominent velocity increase.

SEISMIC SUMMARY

Based on data from the above seismic surveys, comparisons can now be made of upper lithospheric structure across Proterozoic and Phanerozoic provinces in northern and eastern Australia. The velocity/depth interpretations and the character of the vertical reflecting horizons across the continent are summarised in Figs. 3, 4 and 6 . These have been compiled

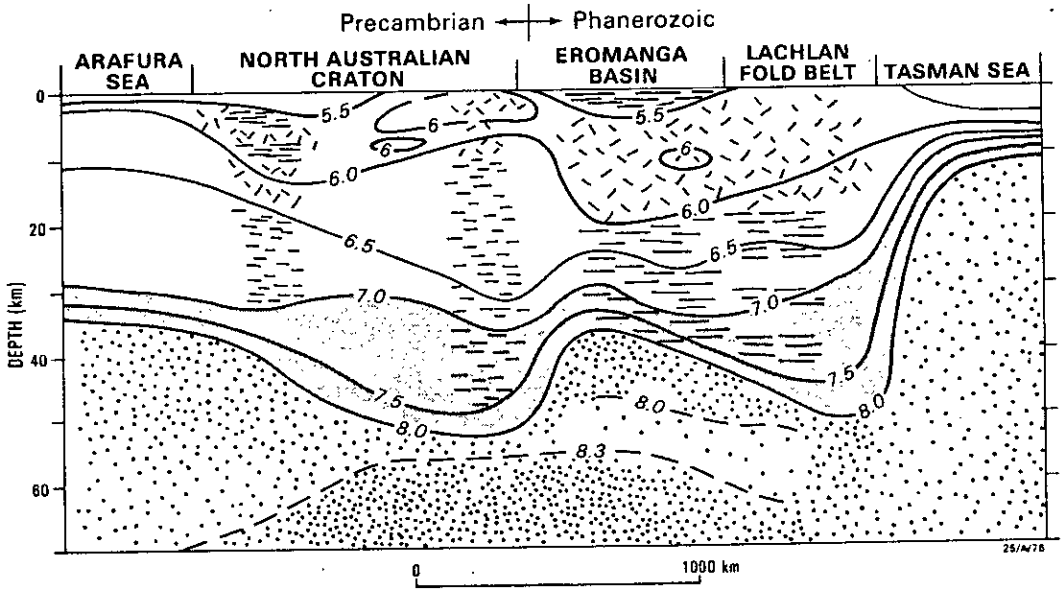

8. Diagramatic lithospheric transect between the Arafura Sea and the Lachlan Fold Belt. Iso-velocity lines are shown in km/s. The legend for features in the section is the same as in Figure 3.

into a lithospheric section in Fig. 8 .

The interpretation of the deep seismic data in meaningful geological terms is somewhat speculative but there are now some constraints which are recognised. These are,

1. The greater depth to the crust/mantle boundary under outcropping igneous, metamorphic and fold belt provinces than under the major basins.
2. The sharper velocity changes under the major basins contrasting with more complex velocity gradients under outcropping igneous, metamorphic and fold belt provinces.
3. The greater thickness of lower crust with velocity over 7 km/s under the outcropping igneous, metamorphic and fold belt provinces than under the major basins.
4. The complexity and variability displayed in both velocity and reflection charecter in the upper 20 km of crust.
5. The ubiquitous lower crustal reflecting horizons, with horizons under the Phanerozoic provinces being stronger, more coherent and more extensive than under the Proterozoic provinces.
6. The subcrustal lithosphere displays few, if any, seismic reflecting horizons but still has gross velocity/depth zonation, with a velocity greater than 8.3 km/s being observed at depths as shallow as 55 km.
7. The velocity below the crust/mantle boundary is greater than 8.0 km/s under both Proterozoic and Phanerozoic provinces with the averages being 8.15 km/s and 8.06 km/s respectively.
8. In the Proterozoic North Australian Craton there is no obvious difference between upper mantle velocities measured north-south and those measured east-west.

A question sometimes raised is whether the reflection and refraction horizons seen on records are merely an artifact of the recording methods

(Mereu & Ojo, 1981). However, the extent of some sub/super-critical reflections seen on long-line refraction record sections and the continuity and coherence on some multifold seismic reflection profiling sections strongly suggests that the gross features of the interpretations are real structural features.

AUSTRALIAN CONTINENTAL LITHOSPHERE

The structure determined from seismic data can be viewed in terms of some of the tectonic models currently being considered for continental Australia. In southeast Australia there is a substantial body of information on lower crustal compositions based on the study of xenoliths in kimberlitic and basaltic host rocks.

Wass & Hollis (1983) propose a model including multiple intrusive, metamorphic and metasomatic events at the crust/mantle boundary. This indicates that the Moho is probably not a discrete sharp feature but is represented by a transition zone up to 20 km thick. They conclude that underplating by continental basaltic magmas could be an important alternative or addition mechanism to the andesite model for crustal accretion. In eastern Queensland, Ewart, Baxter & Ross (1980) have proposed a model of crustal underplating based on the analysis of megacryst composition in Tertiary mafic lavas. The results are interpreted in terms of a model of intrusion and fractionation within the crust/mantle interface region (Fig. 9). The crustal thickening may amount to about 40% of the depth to the upper mantle.

Ferguson, Arculus & Joyce (1979), using the analyses of kimberlitic xenoliths, indicate that a basaltic lower crust in the granulite facies produces a multiplicity of mineralogical phase changes that is consistent with a gradational P-wave velocity transition to upper mantle values under southeast Australia. Manghnani et al (1974) have shown that the elastic

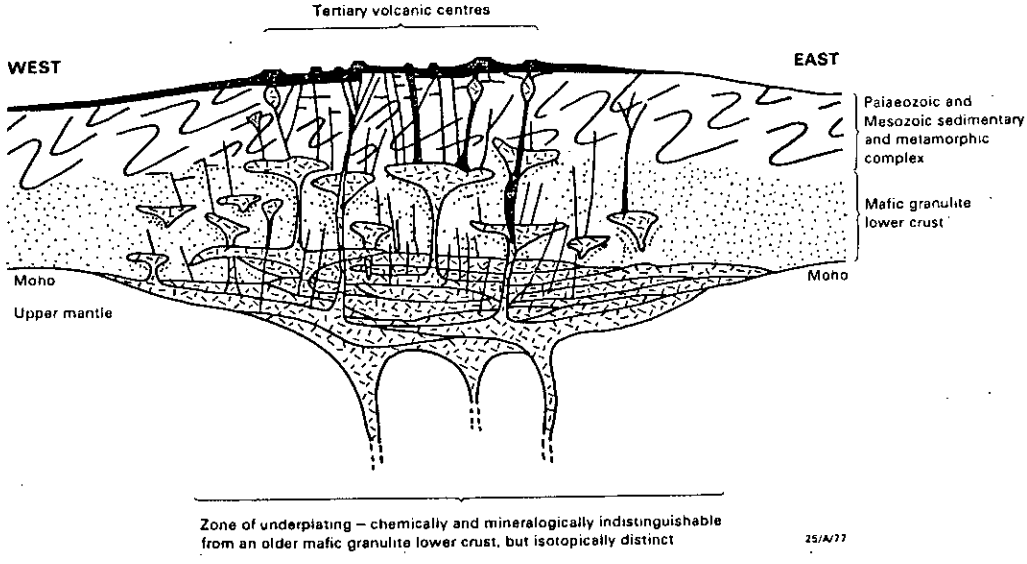

9. Schematic cross-section of the crust under southeastern Queensland (from Ewart et al., 1980), illustrating the concept of crustal underplating and thickening by multiple basaltic intrusion and fractionation.

properties of garnet granulite are compatible with velocities of 7.1-7.8 km/s in the lower crust. This velocity range is measured in the lower crust of southeast Australia; Ferguson, Arculus & Joyce (1979) indicate that such a composition is possible, but they also emphasise the heterogeneity of the lower crust which is contributing to the bulk velocities determined by seismic refraction methods.

Hale & Thompson (1982) have examined the reflection character of the continental Moho under conterminous USA and discussed the possible structures/rock types leading to multiple reflections in the lower crust. These include granulite facies gneisses of sedimentary and volcanic orogin, but they also emphasise that cumulate layering is a more reasonable explanation for reflection zones in magmatically active areas where extensive crustal melting would be expected. Smithson (1978) has emphasised the highly variable composition of the lower crust, being a region where igneous and metamorphic conditions overlap.

It therefore seems quite reasonable to recognise that, under a variety of different circumstances, underplating can produce a range of lower crustal velocity/depth distributions and it is the intrusive nature of the process that we see in the character of some deep vertical reflections. The geochemical modelling envisages episodes of crustal magma intrusion, crystallisation and fractionation accompanied by underplating and crustal accretion with metamorphic equilibration and possible deformation. (Fig. 10). These processes would be repeated at times of high thermal flux from the mantle. Hence in the Australian continental crust there may have been episodes of crustal accretion at continental margins by island arc volcanism and back-arc spreading/basin formation as discussed earlier, but it seems likely that episodes of lower crustal intrusion and reworking play an important part in determining the present-day character of the lower crust.

There is no reason to believe that such cumulative processes are

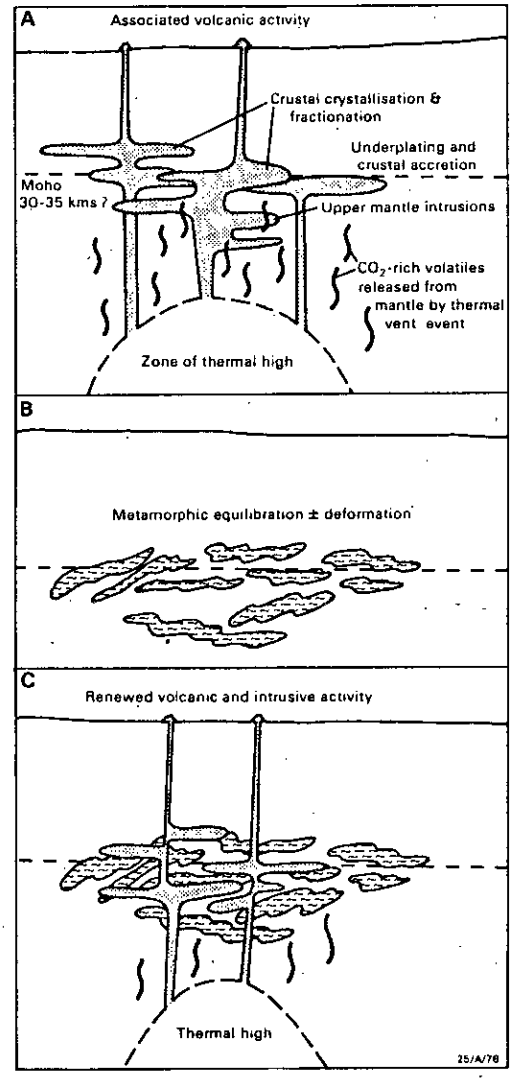

10. Crustal accretion model of Wass & Hollis (1983) for southeastern Australia. A, B and C represent successive stages which may be repetative.

exclusive to Phanerozoic Australia. Thus under the areas considered in this paper such a process probably accounts for the greater thickness of crust as well as the high lower-crustal velocities, measured under outcropping igneous, metamorphic and fold belt regions. The stronger, more coherent, lower crustal reflections evident in Phanerozoic Australia are probably a function of their relative youth compared to the long time span since such processes began in Proterozoic provinces, with consequent degradation of reflecting horizons by later thermal and tectonic events. With the intrusive/underplating model envisaged, it would be unreasonable to expect seismic reflecting horizons to be coherent over more than a few kilometers in the lower crustal reflecting zones.

Under the major continental basins (Eromanga,Murray) the character of the vertical seismic reflections is very different in the lower and upper crust, the latter being almost seismically transparent. The prominent mid-crustal velocity increase under the Eromanga Basin strengthens the argument that the tectonic development of the upper and lower crust may have occurred by different processes, possibly temporally separate. Rutland (1982) has put forward arguments in favour of the continental lithosphere developing through successive thermal stages (chelogenic cycles), newer crust incorporating older crust at middle and lower levels, formed from reworked rocks of the preceeding chelogenic cycle. The geochemical models for southeastern Australian tectonics certainly support the presence of reworked Precambrian rocks (Compston & Chappell,1979). However, Precambrian rocks need not underlie the entire region east of the Precambrian craton boundary (Fig. 1). There are many analogues in southeastern Asia,Japan and Europe (Ziegler,1981) of cratonic fragmentation and dispersal. In the Eromanga Basin the character of the lower crustal reflection horizons strongly suggests that it was affected by intrusive layering or metamorphic 'fronts'. Mathur (1983b) suggests the strong, coherent reflecting segments in the lower crust are produced by intrusive basaltic sills and that attenuation of

Precambrian crust took place during the development of a back arc marginal sea. However the possibility of other mechanisms cannot be discounted.

Oliver, Cook & Brown (1983) have reviewed some of the major findings of COCORP deep reflection profiling in conterminous USA with respect to tectonic processes which are likely to apply to all continents, including Australia. The outstanding finding is that the continental lithosphere is extremely complex and consequently trying to generalise from data at any one site is fraught with danger. They recognised that different regions of the upper, middle and lower crust in any area may have undergone quite separate tectonic histories before their present-day configuration was achieved. Consequently we should not be surprised at the contrast in the character of reflections from different levels of the crust in continental Australia.

Another point made was that Precambrian and Phanerozoic sediments can occur with a thickness corresponding to a substantial fraction of the total crustal thickness (15-20 km). These may either be layered and hence seen by seismic reflection profiling or highly deformed and consequently seismically transparent (an interpretation preferred for the Eromanga Basin results). However, within the continental crust, Oliver, Cook & Brown (1983) emphasise that the 'creation of new continental material may be of minor significance. Rather the process is primarily one of reshuffling of existing sialic crust'.

In Australia, the differences between the sub-crustal lithospheric structure under the various geological provinces are more difficult to see. The strongest evidence for lithospheric differences in the mantle between Precambrian and Phanerozoic provinces comes from teleseismic travel-time differences. Cleary (1967) and Cleary, Simpson & Muirhead (1972) have highlighted the general trend towards earlier arrivals on the Precambrian craton compared to the eastearn Australian coast (by about 1.1 s). Finlayson (1982b) has argued that this time difference cannot be accommodated in current velocity/depth models to depths of 200 km; consequently deeper anomalies

must exist. Dziewonski & Anderson (1983) have more recently re-emphasised this difference and also the dependence of that difference on source azimuth.

CRUSTAL GROWTH

There are a number of features in the seismic refraction and reflection data which, taken together with the analyses of crustal and upper mantle xenoliths, contribute to a better understanding of lithospheric structure and growth in continental Australia.

The first feature to note is that the lower crustal reflections, seismic velocities and rock compositions encourage the view that underplating and lower crustal intrusion are significant factors in any model of crustal growth. The greater depth to the crust/mantle boundary under outcopping igneous, metamorphic and fold belt regions can be attributed to lower crustal accretion. The deep reflections suggest strongly a process of thermal alteration from below by intrusion and/or by metamorphism. The mechanisms by which underplating and intrusion occur lead naturally to the strong possibility of reworked older terrains in northern and eastern Australia.

A second feature worth noting is that, under the major basins bordering the Australian Proterozoic craton, there are significant differences in the character of the reflections from the upper and lower parts of the crust and these parts are separated by a prominent velocity horizon. This suggests that the dominant tectonic processes affecting the two parts of the crust could be separated spacially and/or temporally. The lower crustal reflections are perhaps indicative of thermal effects from the mantle (either intrusive or metamorphic). The preferred interpretation for the lack of reflections in the upper crust is that it is composed of highly deformed/folded metamorphic rocks, but it must be noted also that a granitoid basement is recognised in some parts of the Eromanga Basin.

The gravity trends in the major basins bordering the Proterozoic

craton run strongly parallel to the craton boundary. These trends are linear and are evident in the morphology of the older depositional sequences under the Murray and Eromanga Basins (Wellman, 1976). It therefore seems likely that the lower crustal reflections under these basins are symptomatic of the thermal event(s) which rifted an earlier crust, a process similar to that described by Ziegler (1981) for the basins of central and western Europe.

ACKNOWLEDGEMENTS

The authors wish to acknowledge the contribution to the understanding of the seismic structure of the Australian continental lithosphere by their colleagues in BMR. This paper is published with the permission of the Director, Bureau of Mineral Resources, Geology & Geophysics, Canberra.

REFERENCES

Armstrong, J.D. & Barr, T.M., 1982. The Eromanga Basin. In, Eromanga Basin Symposium summary papers (editors P.S. Moore & T.J. Mount), Petrol. Expl. Soc. Aust. & Geol. Soc. Aust., Adelaide, 20-42.

Black, L.P., 1977. A Rb-Sr geochronological study in the Proterozoic Tennant Creek Block, central Australia. BMR J. Aust. Geol. & Geophys., 2, 111-122.

Branson, J.C., Moss, F.J. & Taylor, F.J., 1976. Deep crustal reflection seismic test survey, Mildura, Victoria, and Broken Hill, NSW, 1968. Bur. Miner. Resour. Geol. & Geophys., Report 183.

Cleary, J.R., 1967. P times to Australian stations from nuclear explosions. Bull. Seism. Soc. Am., 57, 773-781.

Cleary, J.R., Simpson, D. & Muirhead, K.J., 1972. Variations in Australian upper mantle structure from observations of the Cannikin explosion.

Nature, 236, 111-112.

Collins, C.D.N., 1978. Crustal structure of the central Bowen Basin, Queensland. BMR J. Aust. Geol. & Geophys., 3, 203-210.

Collins, C.D.N., 1983. Crustal structure of the southern McArthur Basin from deep seismic sounding. BMR J. Aust. Geol. & Geophys., 8, 19-34.

Collins, C.D.N. & Lock, J., 1983. A seismic refraction study of the Quilpie Trough and adjacent basement highs, Eromanga Basin, Queensland, Australia. Tectonophysics, 100, in press.

Compston, W. & Chappell, B.W., 1979. Sr-isotope evolution of granitoid source rocks. In, The Earth, Its Origin, Structure and Evolution (editor M.W. McElhinney), Academic Press, 377-426.

Cook, P.J., 1982. The Cambrian palaeogeography of Australia and opportunities for petroleum exploration. Aust. Petrol. Expl. Ass. J., 22(1), 42-64.

Crawford, A.J., 1983. Construction of the continental crust of south-eastern Australia and the orogin of Phanerozoic fold belts. Nature, in press.

Crook, K.A.W., 1980. Fore-arc evolution in the Tasman Geosyncline: the orogin of the southeast Australian continental crust. J. Geol. Soc. Aust., 27, 215-232.

Crook, K.A.W. & Powell, C.M., 1976. The evolution of the southeastern part of the Tasman Geosyncline. 25th Int. Geol. Cong. Field Guide 17A.

Curray, J.R., Shor, G.G., Raitt, R.W. & Henry, M., 1977. Seismic refraction and reflection studies of crustal structure of the eastern Sunda and western Banda arcs. J. Geophys. Res., 82, 2479-2489.

Doutch, H.F. & Nicholas, E., 1978. The Phanerozoic sedimentary basins of Australia and their tectonic implications. Tectonophysics, 48, 365-388.

Dziewonski, A.M. & Anderson, D.L., 1983. Travel time and station corrections for P waves at teleseismic distances. J. Geophys. Res., 88, 3295-3314.

Ewart, A., Baxter, K. & Ross, J.A., 1980. The petrology and petrogenesis of the Tertiary anorogenic mafic lavas of southern and central Queensland, Australia - possible implications for crustal thickening. Contr. Mineral. Petrol., 75, 129-152.

Ferguson, J., Arculus, R.J. & Joyce, J., 1979. Kimberlite and kimberlitic intrusives of southeastern Australia: a review. BMR J. Aust. Geol. & Geophys., 4, 227-241.

Finlayson, D.M., 1981. Reconnaissance of upper crustal velocities in the Tennant Creek Block, Northern Territory. BMR J. Aust. Geol. & Geophys., 6, 245-252.

Finlayson, D.M., 1982a. Seismic crustal structure of the Proterozoic North Australian Craton between Tennant Creek and Mount Isa. J. Geophys. Res., 87, 10569-10578.

Finlayson, D.M., 1982b. Geophysical differences in the lithosphere between Phanerozoic and Precambrian Australia. Tectonophysics, 84, 287-312.

Finlayson, D.M., 1983. The mid-crustal horizon under the Eromanga Basin, eastern Australia. Tectonophysics, 100, in press.

Finlayson, D.M., Prodehl, C. & Collins, C.D.N., 1979. Explosion seismic profiles, and implications for crustal evolution, in southeastern Australia. BMR J. Aust. Geol. & Geophys., 4, 243-252.

Finlayson, D.M., Collins, C.D.N. & Denham, D., 1980. Crustal structure under the Lachlan Fold Belt, southeastern Australia. Phys. Earth & Plan. Int., 21, 321-342.

Finlayson, D.M. & Collins, C.D.N., 1980. A brief description of BMR portable seismic tape recording systems. Aust. Soc. Expl. Geophys. Bull., 11, 75-77.

Finlayson, D.M. & McCracken, H.M., 1981. Crustal structure under the

Sydney Basin and Lachlan Fold Belt, determined from explosion seismic studies. J. Geol. Soc. Aust., 28, 177-190.

Finlayson, D.M., Collins, C.D.N. & Lock, J., 1983. P-wave velocity features of the lithosphere under the Eromanga Basin, eastern Australia, including a prominent mid-crustal (Conrad?) discontinuity. Tectonophysics, in press.

Frey, H., 1982. MAGSAT scalar anomaly distribution: the global perspective. Geophys. Res. Letts., 9, 277-280.

Hale, L.D. & Thompson, G.A., 1982. The seismic character of the continental Mohorovicic discontinuity. J. Geophys. Res., 87, 4625-4635.

Hales, A.L. & Rynn, J.M.W., 1978. A long-range, controlled source seismic profile in northern Australia. Geophys. J. Roy. Astro. Soc., 55, 633-644.

Hales, A.L.,Muirhead, K.J. & Rynn, J.M.W., 1980. A compressional velocity distribution for the upper mantle. Tectonophysics, 63, 309-348.

Harrington, H.J., 1974. The Tasman Geosyncline in Australia. In, The Tasman Geosyncline (editors A.K. Denmead, G.W. Tweedale & A.F. Wilson), Geol. Soc. Aust. (Qld Div.), 383-407.

Leven, J.H., 1980. The application of synthetic seismograms to the interpretation of crustal and upper mantle structure. Ph.D. Thesis, Aust. Nat. University.

Lock, J., Collins, C.D.N. & Finlayson, D.M., 1983. Basement structure and velocities under the central Eromanga Basin from seismic refraction studies. In, Eromanga Symposium Papers, Adelaide, Nov. 1982 (editor P.S. Moore) Geol. Soc. Aust. Special Publication.

Manghnani, M.H., Ramananantoandro, R. & Clark, S.P., 1974. Compressional and shear wave velocities in granulite facies rocks and eclogite to 10 kbar. J. Geophys. Res., 79, 5427-5446.

Mathur, S.P., 1983a. Deep reflection probes in eastern Australia reveal differences in the nature of the crust. First Break, in press.

Mathur, S.P., 1983b. Deep crustal reflection results from the central Eromanga Basin, Australia. Tectonophysics, 100, in press.

Mereu, R.F. & Ojo, S.B., 1981. The scattering of seismic waves through a crust and upper mantle with random lateral and vertical inhomogeneities. Phys. Earth & Plan. Int., 26, 233-240.

Mooney,W.D., Andrews,M.C., Ginzberg,A., Peters,D.A. & Hamilton,R.M., 1983. Crustal structure of the northern Mississippi Embayment and a comparison with other continental rift zones. Tectonophysics, 94, 327-348.

Moore, P.S. & Mount, T.J. (editors), 1982. Eromanga Basin symposium: survey papers. Petr. Expl. Soc. Aust. & Geol. Soc. Aust., Adelaide, Nov. 1982.

Moss, F.J. & Wake-Dyster, K.D., 1983. Australian Central Eromanga Project, an introduction. Tectonophysics, 100, in press.

Muirhead, K.J., Cleary, J.R. & Finlayson, D.M., 1977. A long-range seismic profile in south-eastern Australia. Geophys. J. Roy. Astr. Soc., 48, 509-519.

Murray, C.G. & Kirkegaard, A.G., 1978. The Thomson orogen of the Tasman orogenic zone. Tectonophysics, 48, 299-325.

Oliver, J., Cook, F. & Brown, L., 1983. COCORP and the continental crust. J. Geophys. Res., 88, 3329-3347.

Pinchin, J., 1980. Intracrustal seismic reflections from the Lachlan Fold Belt near Canberra. BMR J. Aust. Geol. & Geophys., 5, 305-309.

Plumb, K.A., 1979a. The tectonic evolution of Australia. Earth Sci. Rev., 14, 205-249.

Plumb, K.A., 1979b. Structure and tectonic style of the Precambrian shields and platforms of northern Australia. Tectonophysics, 58, 291-325.

Rutland, R.W.R., 1982. On the growth and evolution of continental crust:

a comparative tectonic approach. J. & Proc. Roy. Soc. of NSW, 115, 33-60.

Rynn, J.M.W. & Reid, I.D., 1983. Crustal structure of the western Arafura Sea from ocean bottom seismograph data. J. Geol. Soc. Aust., 30, in press.

Scheibner, E., 1973. A plate tectonic model of the Palaeozoic tectonic history of New South Wales. J. Geol. Soc. Aust., 20, 405-426.

Smithson, S.B., 1978. Modeling continental crust: structural and chemical constraints. Geophys. Res. Letts., 5, 749-752.

Veevers, J.J., Jones, J.E. & Powell, C.M., 1982. Tectonic framework of Australia's sedimentary basins. Aust. Petrol. Expl. Ass. J., 22(1), 283-300.

Wass, S.Y. & Hollis, J.D., 1983. Crustal growth in south-eastern Australia - evidence from lower crustal eclogitic and granulitic xenoliths. J. Metamorphic Geol.,1, 25-45.

Wellman, P., 1976. Gravity trends and the growth of Australia: a tentative correlation. J. Geol. Soc. Aust., 23, 11-14.

White, A.J.R., Williams, I.S. & Chappell, B.W., 1976. The Jindabyne Thrust and its tectonic, physiographic and petrogenetic significance. J. Geol. Soc. Aust., 23, 105-112.

Ziegler,P.A.,1981. Evolution of sedimentary basins in north-west Europe. In, Petroleum Geology of the Continental Shelf of North-West Europe, Inst. Petrol., 3-39.

SEISMIC RAY TRACING THROUGH THE ZURICH-I MODEL

D.M.Finlayson & C.D.N.Collins

Bureau of Mineral Resources, Geology & Geophysics, Canberra

INTRODUCTION

The theme of the workshop meeting of the Commission on Controlled Source Seismology at Zurich/Einsiedeln during August 1983 is "Interpretation of Seismic Wave Propagation in Laterally Heterogeneous Structures". Prior to the meeting a set of data was distributed consisting of a series of synthetic record sections generated by V.Cerveny and I.Psencik in a laterally varying velocity model (here called the ZURICH-I model). The objective was to have participants at the meeting interpret the data by whatever means at their disposal prior to arrival in Switzerland. Thus, at the meeting, the constraints that various methods of analysis can place on interpretations can be assessed.

This paper presents a seismic ray tracing interpretation of the Zurich-I data.

ZURICH-I DATA

Synthetic seismic record sections were generated by the ray theoretical method (Cerveny, 1979) from four shot points along the ZURICH-I model which was 520 km long and 60 km deep. Both forward and reversed sections were available from two of the shot points in the central part of the model; thus a total of six record sections were generated for interpretation. The sections were available with two normalising criteria; the first with the maximum amplitudes of all traces the same, and the second with the trace amplitudes multiplied by a factor, A, given by the relation,

$$A = 0.15(x - x')/SMAXIM$$

where (x-x') is the epicentral distance and SMAXIM is the maximum amplitude of the whole section. In two sections from the shot point at x = 320 km the scaling factor was taken as 0.5A.

A reduced time was used on the time axis of the record sections; the

velocity of reduction was 8.0 km/s. In a few cases extra sections were supplied with a velocity of reduction of 6.0 km/s. The seismic waves considered in the section were refracted (diving) waves and all types of primary reflections including converted phases (conversion at the reflection point).

The seismic source was taken to be a point source of P-waves with a symmetric radiation pattern. The record sections were generated close to the surface at four distances along the model, 20 km, 170 km, 320 km, and 470 km. The source corresponded to the far field approximation given by the expression,

$$f(t) = \exp\left[-(2\pi Fm.t/\gamma)^2\right] \cdot \cos(2\pi Fm.t + \vartheta)$$

with Fm = 4 Hz, γ = 4 and ϑ = 0.

The source time-function has a Gaussian envelope and the time zero corresponds to the maximum of the envelope. This feature remains valid even when the signal is deformed due to phase shifts. There is therefore a time difference of approximately 0.3 s between the first onset and the maximum amplitude corresponding to the true arrival time. Ideal recording equipment only was considered, i.e. possible signal distortion on recording was not considered. The vertical component of the displacement vector was shown in the record sections.

The information was given that the model was a two-dimensional inhomogeneous layered structure with smooth changes of velocity inside the layers.

RAY TRACING

Inspection of the synthetic seismic record sections revealed a number of prominent seismic phases. These were as follows:

- Pg - P-waves propagating through the upper crustal basement with a velocity of over 6.3 km/s.
- Pc - super-critical reflections from a boundary at mid-crustal levels with a lower velocity of about 7 km/s.
- PP7 - sub-critical reflections from the mid-crustal boundary.
- PmP - super-critical reflections from the crust/mantle boundary with upper mantle velocities in excess of 8 km/s.
- PP8 - sub-critical reflections from the crust/mantle boundary.

In addition it was evident that the velocity and thickness of the

uppermost crustal layer varied along the model. This layer could be interpreted as a weathered and sedimentary sequence.

Initial velocity/depth models were constructed for each record section based on estimates of the apparent velocities for the various seismic phases. The models were used in a ray-tracing computer program TTIME adapted by C.D.N.Collins from the program LAUFZEIT by G. Muller. This program assumes horizontal layering within the model, i.e. 1-D models. The velocity/depth profile was then varied iteratively until a reasonable fit of the travel-time data to the seismic arrivals was obtained.

The simple layered models were then used to construct a two-dimensional velocity/depth model 520km long. This model was tested using a program XIGHS developed by Collins (1980), which traces rays through laterally varying structures using Snell's law. The model was varied by trial-and-error until an acceptable fit of the calculated travel-times to the ZURICH-I model data was obtained. This was usually taken to be when arrivals which were within 0.1 s of the given data.

The synthetic seismic record sections from the four shot points are shown in Figures 1-6. The sections are labelled ZU20F, ZU170R, ZU170F, ZU3420R, ZU320F and ZU470R, the number indicating the shot point location and the last letter indicating whether the shooting was forward(F) or reversed(R). The upper part of each Figure contains the distance normalised section and the travel-time curve from the horizontally layered preliminary model. The lower part of each Figure contains the equal amplitude normalised section together with the travel-time curve for the laterally inhomogeneous model. The preferred 2-D model is shown in Figure 7 together with the 1-D velocity/depth models at each shot point. The depths to the iso-velocity lines under each shot-point are listed in Table 1.

Some features of the record sections deserve further comment because they are not all incorporated in the model shown in Fig. 7. In Fig. 1 the prominent variation in amplitude of events with an apparent velocity of about 6 km/s between 200 and 220 km is probably caused by the focussing of energy at the edge of the basin-type structure at 110-120 km.

In Fig. 5 the variation in amplitude of the PP8-PmP reflections between 380 and 410 km indicates some structural defocussing of rays at 350-365 km.

This effect probably indicates that the shallowest upper mantle probably is in the region 350-365 km rather than at 320 km as indicated in Fig. 7.

ACKNOWLEDGEMENTS

This paper is published with the permission of the Director, Bureau of Mineral Resources, Geology & Geophysics, Canberra.

REFERENCES

Cerveny, V., 1979 - Ray theoretical seismograms for laterally inhomogeneous structures. J. Geophys., 46, 335-342.

Collins, C.D.N., 1980 - Crustal structure of the central Bowen Basin from deep seismic sounding. MSc thesis, University of Queensland, Brisbane.

TABLE 1

Interpreted depths (km) to the iso-velocity horizons at the four shot points in the ZURICH-I model.

	Z20	Z170	Z320	Z470
4.0 km/s		surface	surface	
4.25	surface	0.4	1.0	surface
4.5	0.8	1.0	2.2	1.0
5.0	1.5	2.0	4.2	2.3
5.5	2.0	3.0	6.5	3.0
6.0	3.0	4.0	9.0	5.0
6.5	23.2	20.8	14.0	17.5
7.0	25.0	22.5	18.2	22.8
7.5	36.2	32.8	28.7	29.8
8.0	40.0	37.6	30.0	35.0
8.5	50.0	50.0	50.0	50.0

Fig. 1 a. Distance normalised forward record section from shot-point Z20 with superimposed the travel-time curve from the preferred 1-D velocity/depth model.

b. Trace normalised forward record section from shot-point Z20 with superimposed travel-times through the preferred 2-D velocity/depth model.

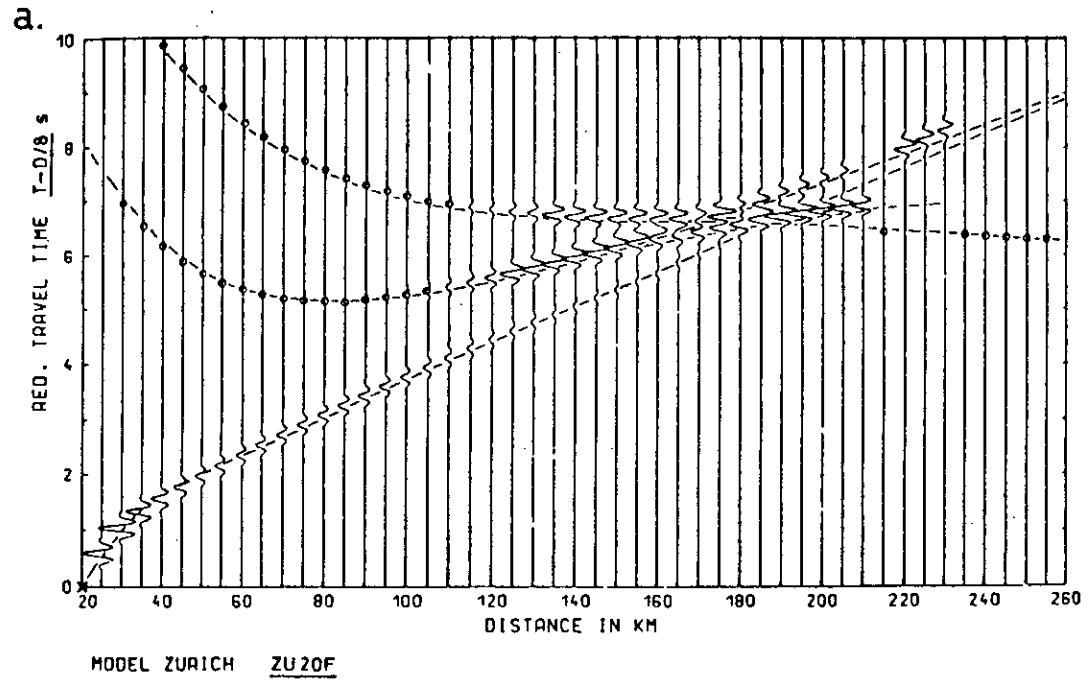

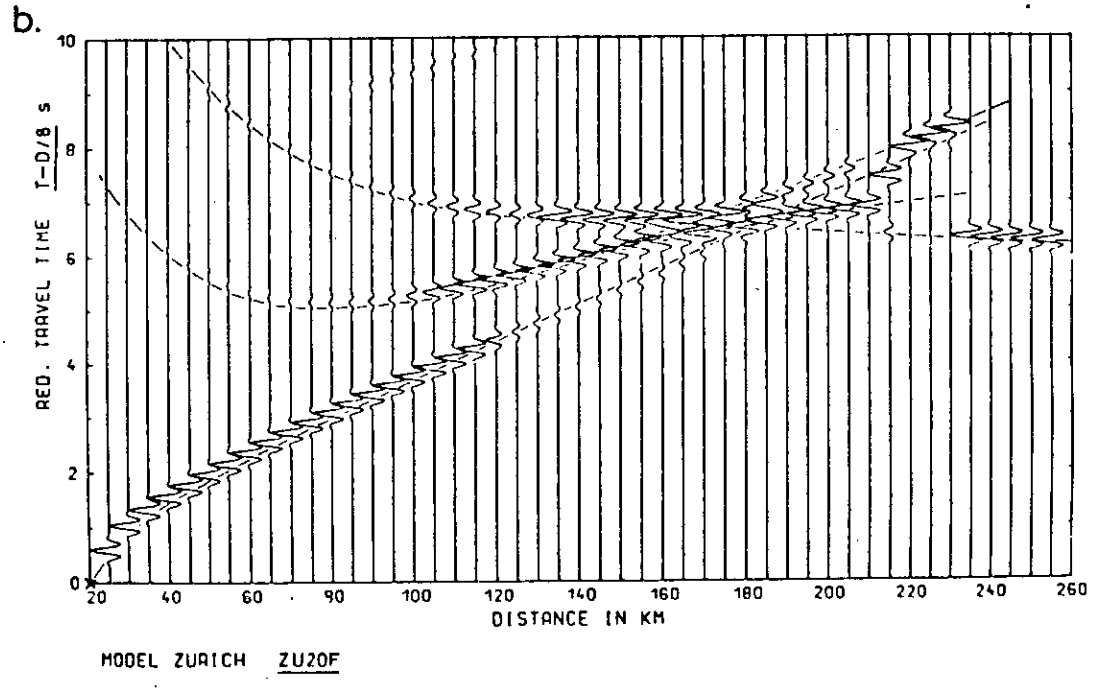

Fig. 2 a. Distance normalised reversed record section from shot-point Z170 with superimposed the travel-time curve from the preferred 1-D velocity/depth model.

b. Trace normalised reversed record section from shot-point Z170 with superimposed travel-times through the preferred 2-D velocity/depth model.

a.

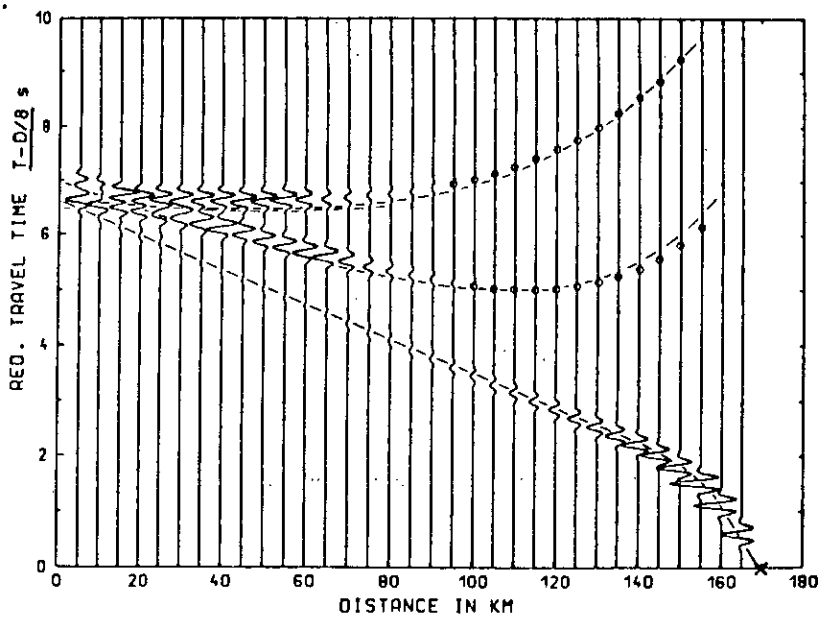

MODEL ZURICH ZU170R

b.

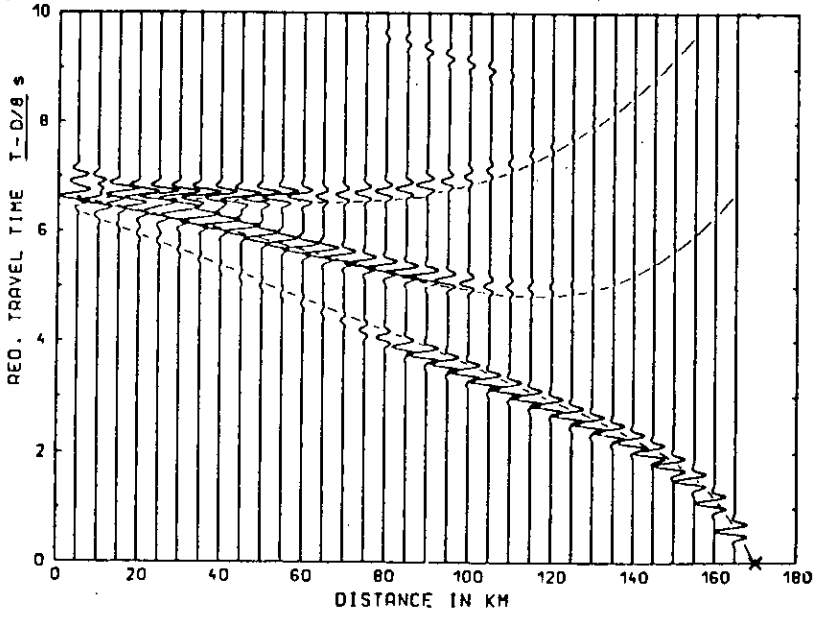

MODEL ZURICH ZU170R

Fig.3 a. Distance normalised forward record section from shot-point Z170 with superimposed the travel-time curve from the preferred 1-D velocity/depth model.

b. Trace normalised forward record section from shot-point Z170 with superimposed travel-times through the preferred 2-D velocity/depth model.

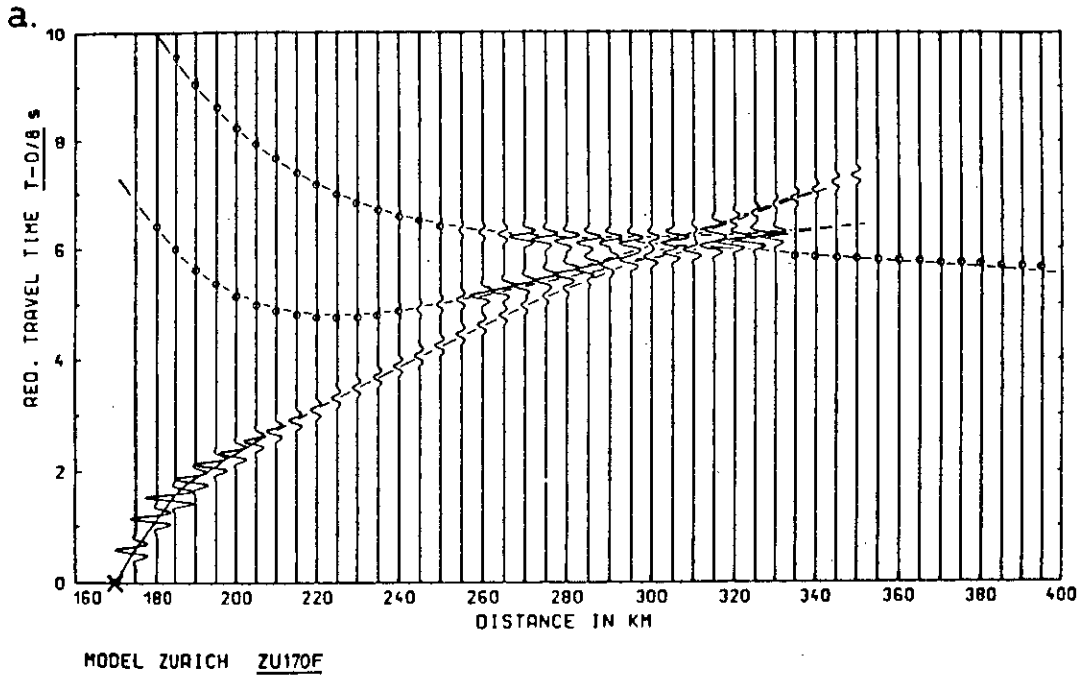

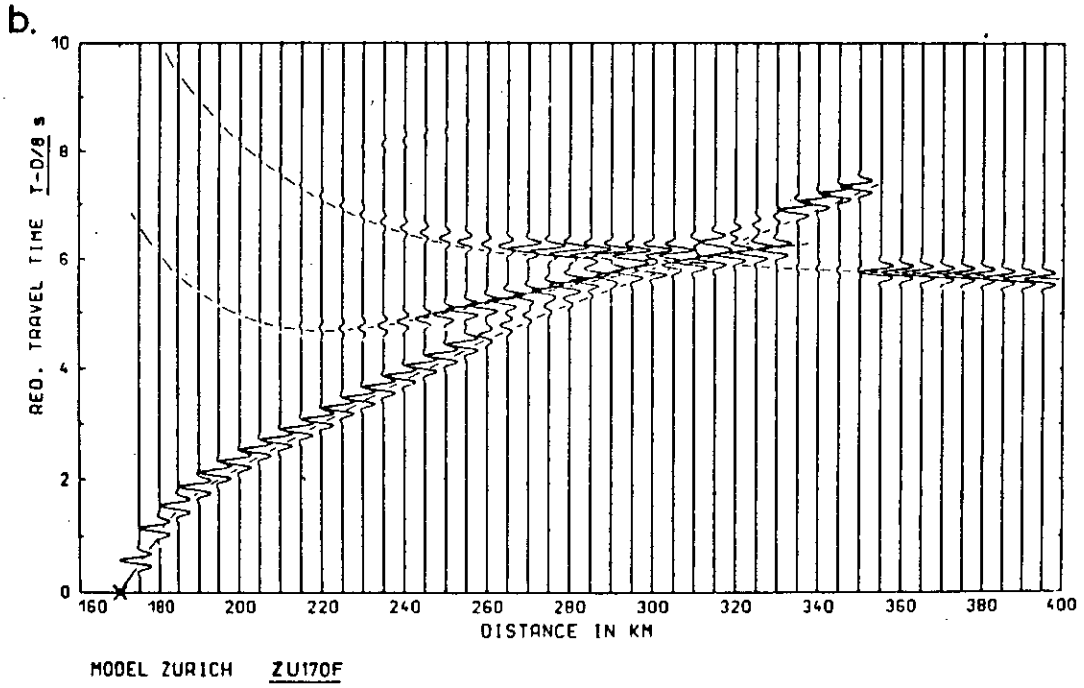

Fig.4 a. Distance normalised reversed record section from shot-point Z320 with superimposed the travel-time curve from the preferred 1-D velocity/depth model.

b. Trace normalised reversed record section from shot-point Z320 with superimposed travel-times through the preferred 2-D velocity/depth model.

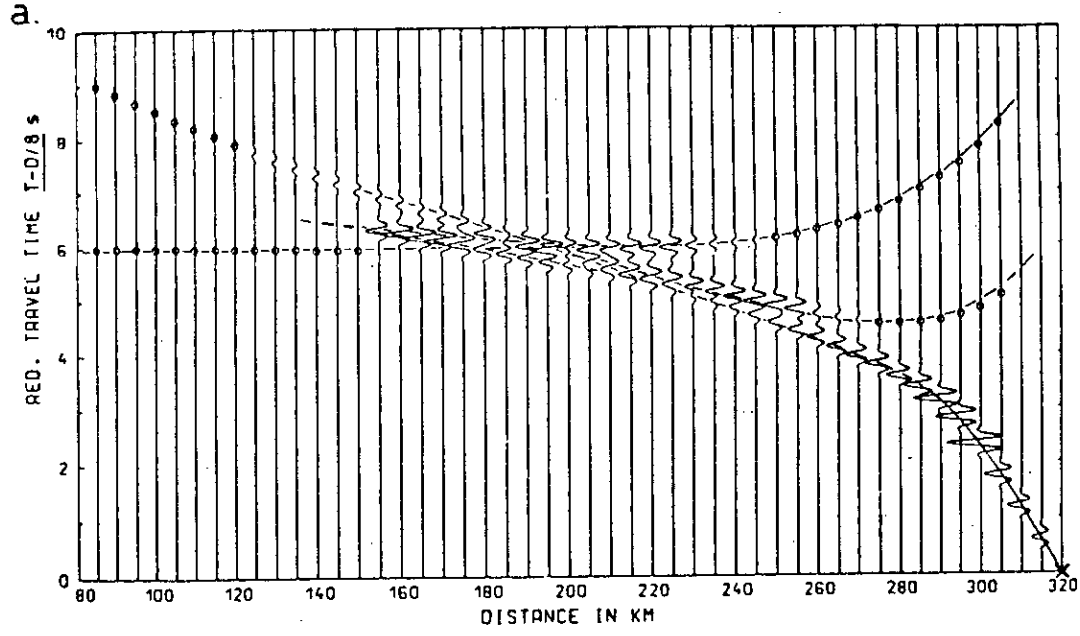

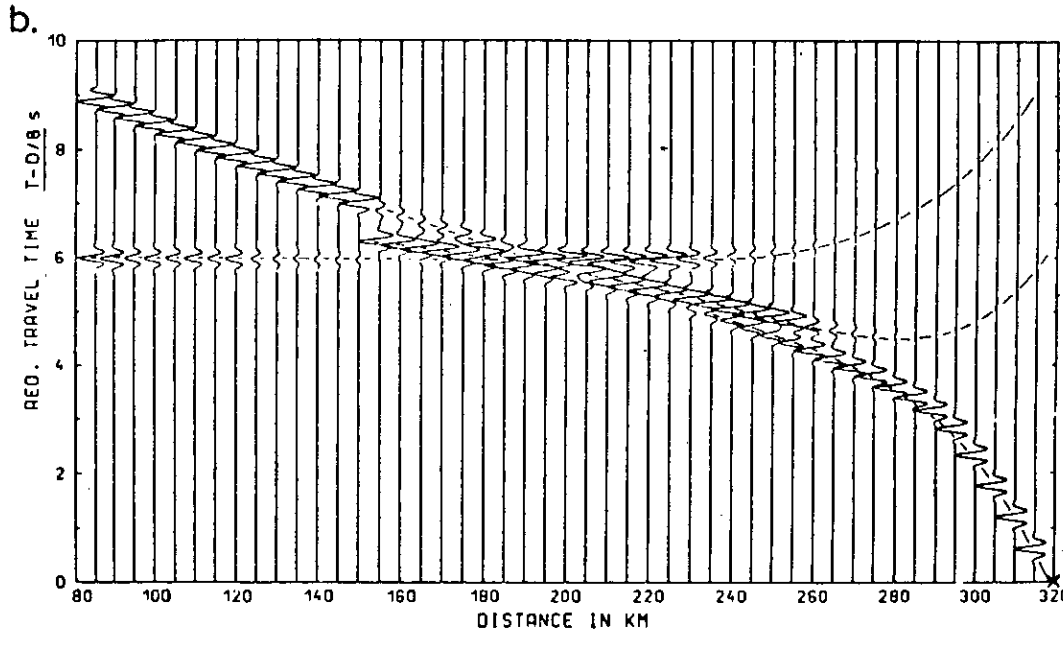

Fig.5 a. Distance normalised forward record section from shot-point Z320 with superimposed the travel-time curve from the preferred 1-D velocity/depth model.

b. Trace normalised forward record section from shot-point Z320 with superimposed travel-times through the preferred 2-D velocity/depth model.

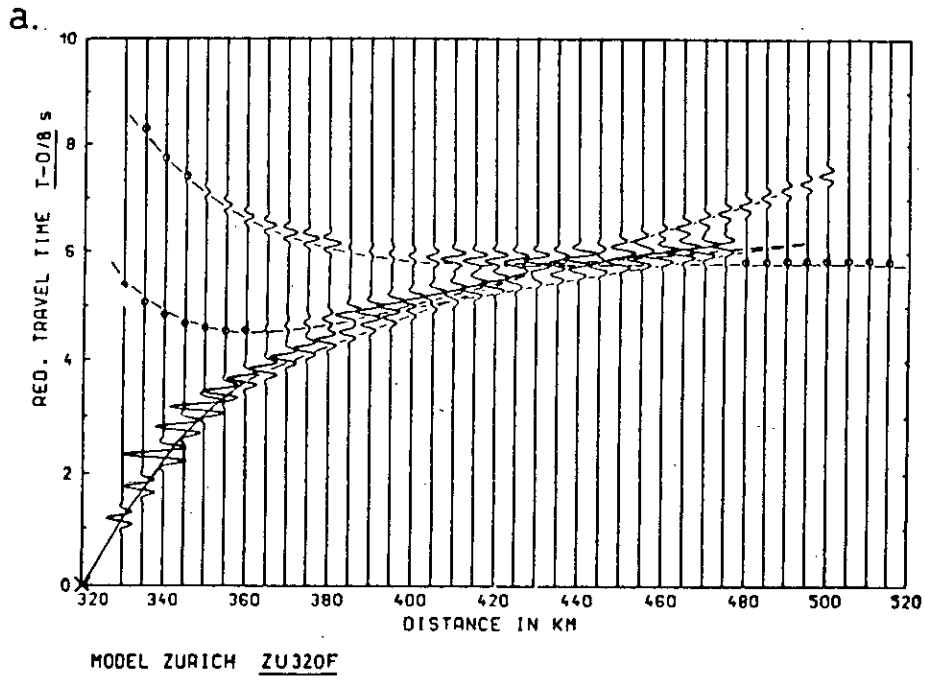

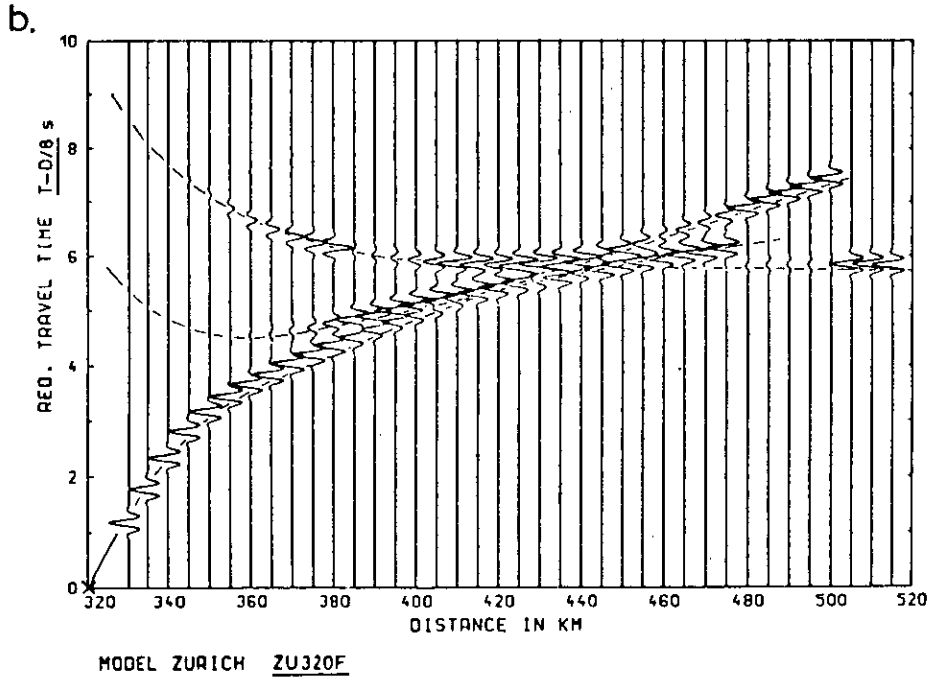

Fig.6 a. Distance normalised reversed record section from shot-point Z470 with superimposed the travel-time curve from the preferred 1-D velocity/depth model.

b. Trace normalised reversed record section from shot-point Z470 with superimposed travel-times through the preferred 2-D velocity/depth model.

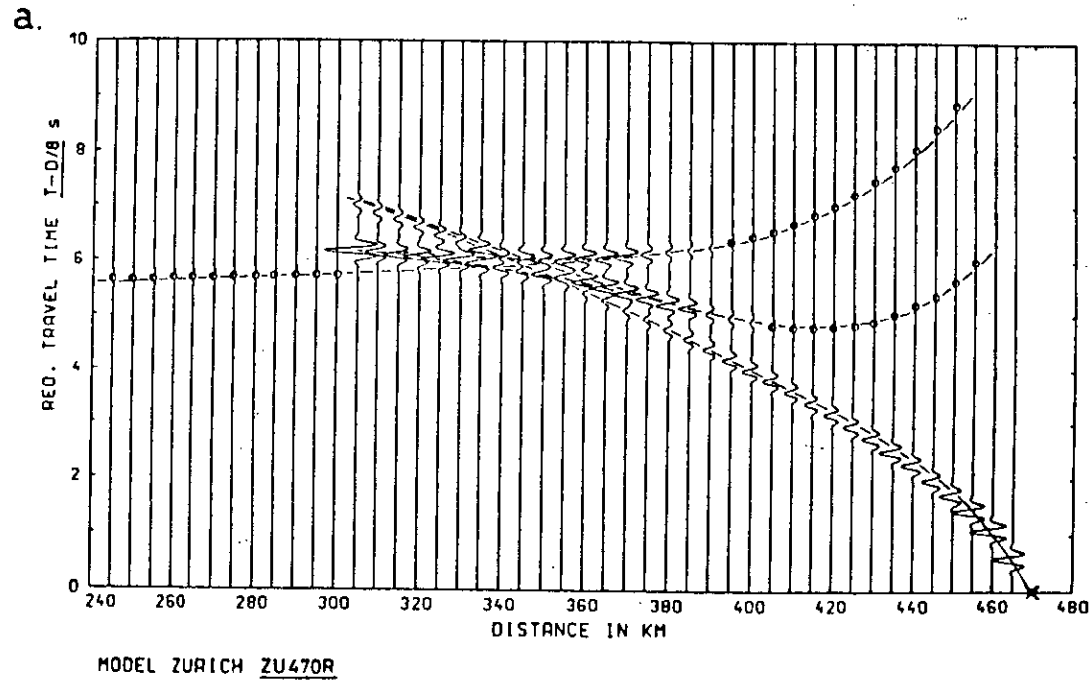

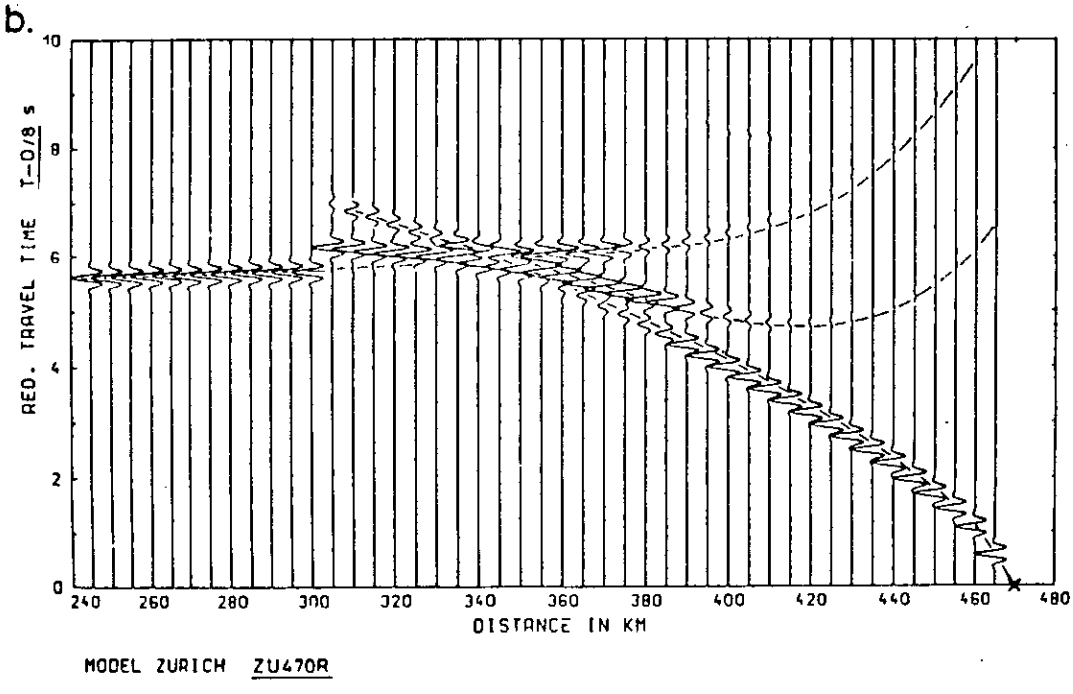

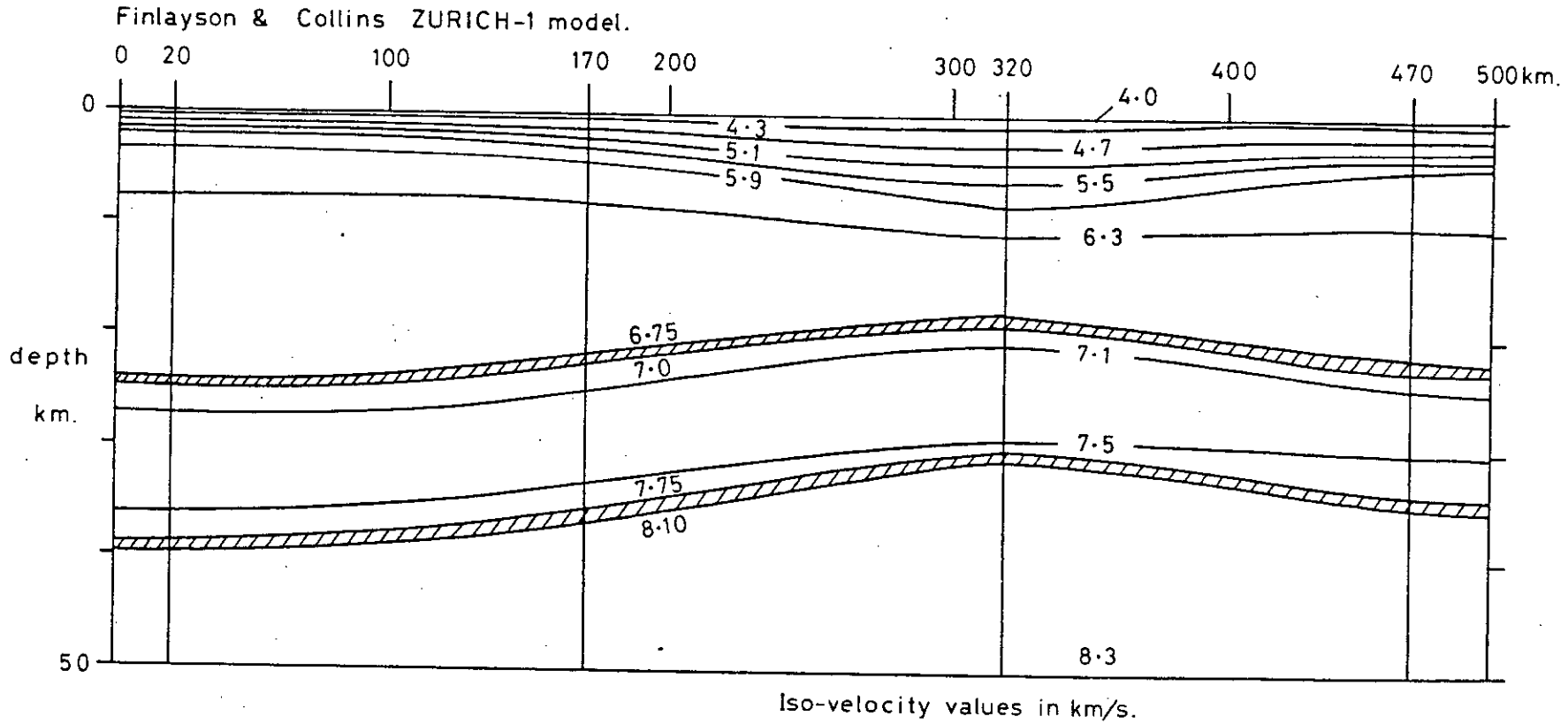

Fig. 7a Preferred 2-D velocity/depth model for the ZURICH-1 data.

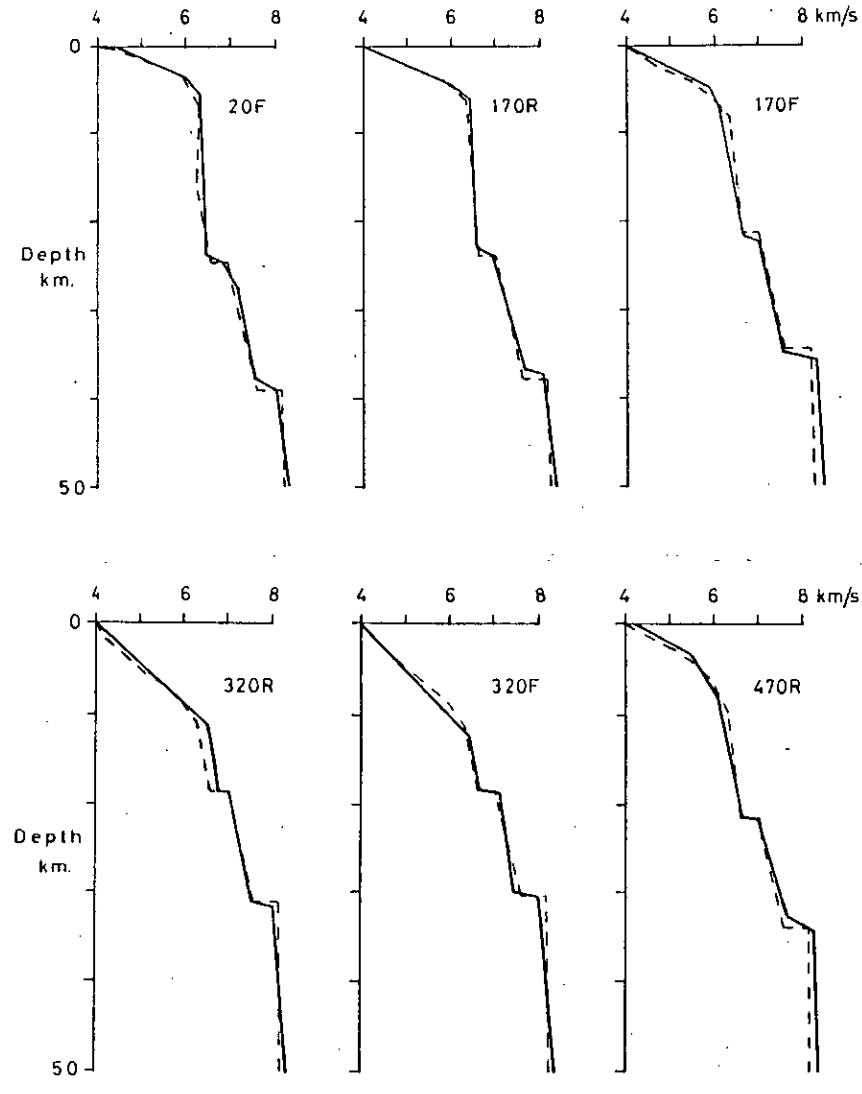

Fig. 7b 1-D velocity/depth models at each shot point (solid lines), together with the Cerveny & Psencik models (dashed lines).

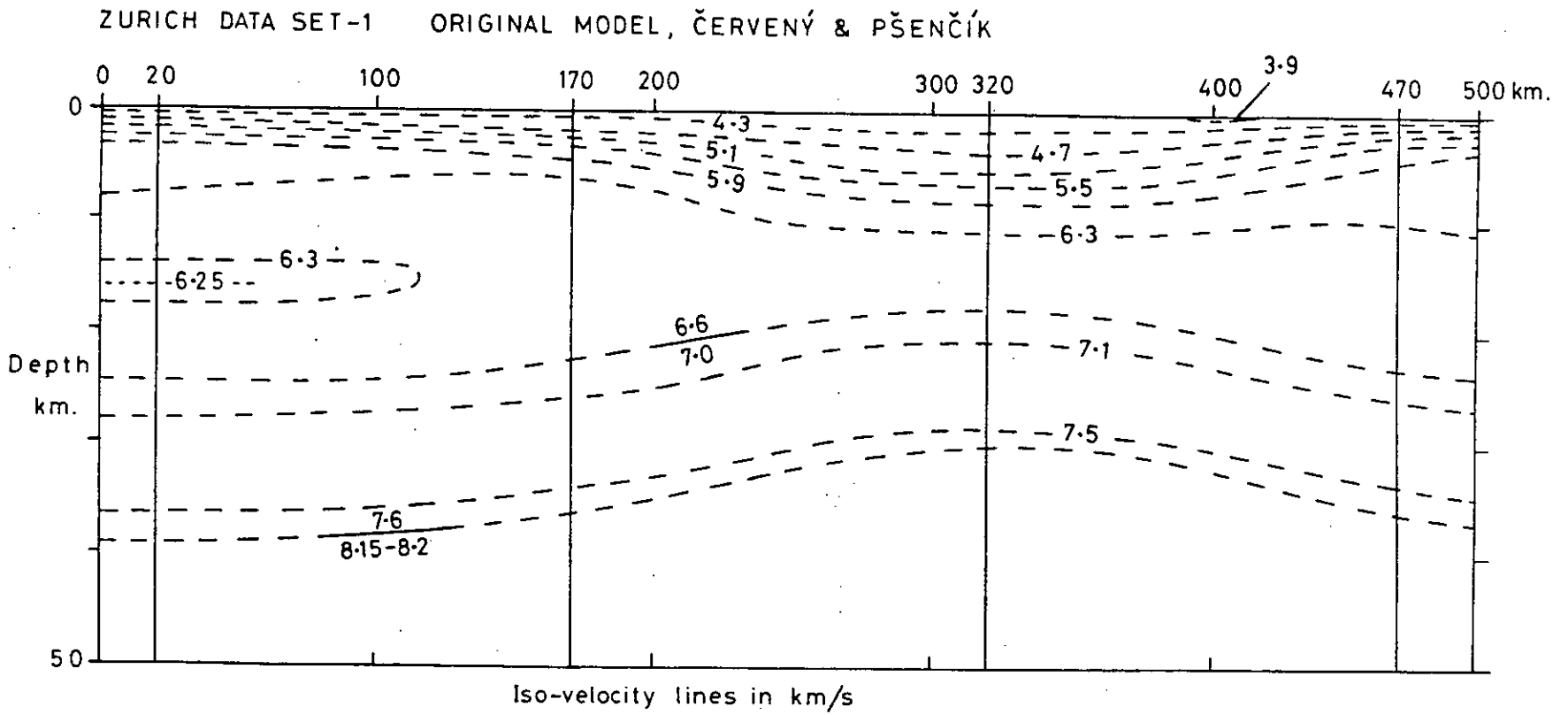

Fig. 7c Cerveny & Psencik model from which the synthetic data was generated.

REPORT 159

Isomagnetic Maps of the Australian Region for Epoch 1970.0

D. M. FINLAYSON

DEPARTMENT OF MINERALS & ENERGY
BUREAU OF MINERAL RESOURCES, GEOLOGY & GEOPHYSICS

REPORT 159

Isomagnetic Maps of the Australian Region for Epoch 1970.0

D. M. FINLAYSON

AUSTRALIAN GOVERNMENT PUBLISHING SERVICE
CANBERRA 1973

BUREAU OF MINERAL RESOURCES, GEOLOGY & GEOPHYSICS

DIRECTOR: N. H. FISHER

ASSISTANT DIRECTOR, GEOPHYSICAL BRANCH: L. S. PRIOR

Published for the Minister for Minerals & Energy,
the Hon. R. F. X. Connor, M.P.,
by the Australian Government Publishing Service.

ISBN 0 642 00128 6

Manuscript received: December 1970
Issued : May 1973

Printed by Advocate Press Pty. Ltd., Melbourne.

CONTENTS

SUMMARY

Isomagnetic maps of the Australian region for the epoch 1970.0 are presented for seven magnetic components and their respective annual rates of change.

The maps are based mainly on the results from magnetic surveys completed in the years 1966-70 but observations from all surveys completed since 1955 have been used at various stages in the map compilation.

INTRODUCTION

The Bureau of Mineral Resources, Geology and Geophysics (BMR) maintains a continuing program of regional magnetic surveying in the Australian region to meet the general needs of the mining and petroleum industries, land surveyors, and navigators (land, sea, and air). Australian regional magnetic surveys were started in 1911 by the Carnegie Institution of Washington (Bauer & Fleming, 1915: Bauer et al., 1921) and surveys by various institutes have continued up until the present time. An analysis of the early Australian results was included in Carnegie Institution Publication No. 578 (Vestine et al., 1948).

The first isogonic map of Australia was produced for the epoch 1944.5 (Rayner, 1944). Subsequent isogonic maps have been produced for epochs 1950.5 Holmes, 1951), 1955.5 (Wood & Everingham, 1953), 1960.5 (Parkinson, 1959), 1965.0 (van der Linden, 1965a), and 1970.0 preliminary (Finlayson, 1970a). The only complete set of isomagnetic maps for the Australian region published was for epoch 1957.5 (Parkinson & Curedale, 1960, 1961, and 1962).

Before the present series of maps all map compilations were based on second order magnetic survey data in which the corrections for diurnal variations in the field were derived from world-wide analysis (Vestine et al., 1948) or from the results of geomagnetic observatories as far off as 1 500 km. The desirability of making magnetic variograph recordings at each station to record not only diurnal variation but also other short period transient variations has always been recognized. This has been put into practice only with the setting up a network of first order magnetic stations, in the last three years.

Since 1955 a considerable amount of field work has been completed. Seventy-two first order regional magnetic stations have been established and surveyed to give precise data on the geomagnetic field and its rate of change in the Australian region (Finlayson, 1970b, 1971a, b, c; van der Linden 1965b, 1965c, 1968, 1969). In addition, a program of third order magnetic surveying has been undertaken which has been designed to map regional magnetic anomalies. At the time of production of the maps presented here, southern Queensland, New South Wales, and Victoria had been mapped in this way (van der Linden, 1970, 1971).

The maps presented in this report are derived mainly from the magnetic data obtained since 1955, but data from earlier surveys have been useful in defining trends.

Throughout this report centimetre-gram-second (CGS) units are used; the unit of magnetic intensity is 10^{-5} Oersted (= 1 gamma) and angular measurements are in degrees and minutes of arc. The magnetic components discussed and mapped are: horizontal intensity (H), north intensity (X), east intensity (Y), vertical intensity (Z), total intensity (F), inclination (I), declination (D), and their respective annual rates of change.

FIELD SURVEYS AND INSTRUMENTS

Any magnetic survey program must take into account both the spatial distribution of the geomagnetic field and its short and long term changes with time. Many aspects of mapping the spatial distribution of the field have been discussed by the World Magnetic Survey Board (WMS, 1967; Vestine, 1961). A power spectrum analysis of a single magnetic profile around the world indicates strong harmonic terms down to wavelengths of approximately 5 000 km, a weak spectrum between 3 000 km and 300 km, and an increase in power again in wavelengths from 150 km down to 15 km (Alldredge et al., 1963; Alldredge, 1965). The longer wavelengths are attributed to sources in the earth's core and the shorter wavelengths to sources in the earth's crust. The weak spectrum in the wavelength region 3 000 km to 300 km indicates a lack of geomagnetic field sources in the region of the earth from approximately 25 km to 2 900 km depth. Thus the magnetic field measured at the earth's surface is due mainly to the geophysical processes taking place in the earth's core (the main magnetic field) plus the effect of the earth's crust to a depth of approximately 25 km.

The changes with time that occur in the geomagnetic field can be separated broadly into long and short term changes. The majority of short term changes are caused by variations in the small contribution to the measured field due to ionospheric currents and have characteristic periods of 24 hours and less. Thus in field surveys they can be corrected for by making magnetic recordings for two or three days. The effects of magnetic storms, which may last for a week or more, can be estimated by referring to magnetic observatory records. The long term non-cyclic change (secular variation) is due to geophysical processes in the earth's core. The change is measured at magnetic observatories and at magnetic stations where magnetic observations are repeated every few years.

BMR has adopted two types of regional magnetic surveys for mapping purposes, with effective station intervals of approximately 500 km and 80 km, and thus should be able to resolve wavelengths greater than or equal to twice the station interval (Blackman & Tukey, 1958). The surveys should therefore be capable of mapping the regional components of the main magnetic field and the larger regional anomalies. Anomalies of smaller extent (local anomalies) can only be resolved by adopting more detailed survey methods.

First order magnetic surveys

Since 1965, BMR has established a network of 72 first order magnetic stations in the Australian region, which is designed so that repeat observations can be made for the foreseeable future (Plate 1). Many of the

stations are in the vicinity of earlier magnetic stations, thus providing valuable information on secular variation in the region.

The secular variation in the magnetic components is of the order of 10 gammas/year in intensity and 1 minute/year in arc (Plate 2), and thus the survey method must be capable of resolving such changes. BMR surveys achieve this by setting up a three-component fluxgate variograph (Seers, 1966) at each first order survey station visited and recording geomagnetic variations over a period of about 3 days, during which the associated control observations are made. Plate 3 illustrates the equipment used. The survey results give values of the H, D, and Z magnetic components which average out diurnal and other transient changes in the geomagnetic field over a 24 hour period. The systematic errors in the measurements of H and Z are within the limits $\pm$ 5 gammas and D within the limits $\pm$ 1.0 min.

Control observations in the first order surveys were made with the following types of instruments:

Horizontal Intensity (H) - La Cour Quartz Horizontal Magnetometer (QHM) or Horizontal Torsion Magnetometer (HTM). Both instruments operate on the same principles (La Cour, 1936). All instruments were compared before and after each survey against the Australian standard instruments kept by Toolangi magnetic observatory (van der Waal, 1966).

Total Intensity (F) - Elsec Proton Precession Magnetometer (PPM).

Crystal frequency is checked regularly. (Littlemore, 1960).

Declination (D) - Askania declinometer. (Askania, 1953). All instruments are compared against the Australian standard kept by Toolangi magnetic observatory. Azimuths were determined from sun observations and positions from data of the National Mapping Division of the Department of National Development and from the Department of Civil Aviation.

Control for the Z variograph record was derived from the H and F control observations mentioned above.

Third order magnetic surveys

Single readings of H, D, and F are made at 15 km intervals along road traverses so that on average there is a station within 40 km of all points in the region. The instruments used on the surveys are the same

as those used for control observations in first order survey work. In addition, a calibrated Wilde compass theodolite is often used for measuring declination (D). Azimuth control is obtained by making a single sun observation at each station and positions are read from 1:250,000 scale maps.

DATA PROCESSING AND CONTOURING

Data Preparation

The contoured values of the magnetic components on the maps accompanying this report are tied to the values of the field at the 81 stations listed in Table 1. Seventy of the stations are BMR first order magnetic stations, three are BMR magnetic observatories (Toolangi, Mundaring, and Port Moresby), two are magnetic observatories operated by the New Zealand government (Amberley and Apia), one is an observatory operated by the Indonesian government (Tangerang), and the remaining five (Djajapura, Honiara, Noumea, Ocean Island and Tibar) are stations from which comprehensive magnetic data are available. Two BMR first order stations (Rabaul and Aropa) have been omitted from the list because of the anomalous values of the field measured at these stations; however, they do provide valuable secular variation data. The locations of all these stations are shown in Plate 1.

Secular variation data are available at 65 of the stations in Table 1. Most of the BMR first order magnetic stations have a good record of re-occupation since 1955. Until 1968, the magnetic observations at these stations were of second order standard i.e. several observations of three magnetic components spread over one or two days but without variograph recording. Since 1968, all the stations have had a first order occupation as described above.

The H, D, and Z values observed since 1955 were plotted with respect to year of observation for all stations and a smooth curve drawn through the values of each component. These curves were extrapolated to give the 1970.0 values of H, D, and Z at all stations, and the gradients of the curves at 1970.0 were taken to be the secular variation for 1970.0.

From the H, D, and Z values for 1970.0 and their respective secular variations, the values for all other magnetic components were derived using the relations listed below.

Magnetic component:

$$X = H \cos D$$

$$Y = H \sin D$$

$$F = (H^2 + Z^2)^{\frac{1}{2}}$$

$$I = \arctan (Z/H)$$

Rate of change with time:

$$dX/dt = dH/dt.\ \cos D - H.\ \sin D.\ dD/dt$$

$$dY/dt = dH/dt.\ \sin D + H\ \cos D.\ dD/dt$$

$$dF/dt = (H.dH/dt + Z.dZ/dt)/F$$

$$dI/dt = (dZ/dt - (Z.dH/dt)/H)/H.(1 + Z^2/H^2)$$

Data from approximately 2 500 third order stations in eastern Australia have been used to produce detailed contouring in that region. Other data from approximately 250 second order survey stations throughout Australia which have been occupied since 1955 have been used to supplement the first order results. The year 1955 has been taken as the earliest from which data have been used in the production of the isomagnetic maps because good secular variation observations are available for updating to epoch 1970.0.

Data contouring

No internationally adopted procedures are laid down for the contouring and presentation of isomagnetic maps, although various suggestions regarding map scales and format have been made by the World Magnetic Survey Board (WMS, 1967; Vestine, 1961). BMR has adopted a Mercator projection base map on a scale 1:10,000,000 at the equator and has presented two sets of magnetic contours: (1) smoothed contours with detail dictated by the interval between first order magnetic stations, and (2) regional contours in eastern Australia with detail dictated by the effective interval between third order magnetic stations.

Secular variation maps

The H, D, and Z maps of secular variation are derived from data at 65 stations throughout the region (Table 1). Maps were hand-contoured for the epochs 1960.0 and 1970.0 and the data incorporated in a computer program used to update second and third order observed magnetic values to epoch 1970.0. The 1970.0 secular variation contours shown on the isomagnetic maps must be regarded as approximate because of the difficulty of accurate determination at stations which are not permanently occupied. The root mean square deviations of the observed values from the contoured values for H, D, and Z magnetic components are $\pm$ 5 gammas/year, $\pm$ 0.3 minutes/year and $\pm$ 4 gammas/year respectively. The secular variation values for the other magnetic components were derived from the H, D, and Z values.

Third order data contouring

The third order survey data were updated to epoch 1970.0 using secular variation data from first order surveys, and plotted by computer at scale 1:2,500,000 for all magnetic components. These plots were then hand-contoured, with the contours tied to the first order station data in the region. The resulting contours were then reduced to scale 1:10,000,000.

First order data contouring

The first order station data given in Table 1 were first contoured by hand for each magnetic component. Available supplementary information has been used to influence the contours. Thus in eastern Australia the contours were made consistent with the smoothed contours derived from equal area averaging of the third order data contours. In other regions, the contours were influenced by the 250 second order stations from which data were available. In the Tasman Sea and Arafura Sea regions, the D contours have been influenced by data from Qantas Airways Ltd (Qantas, 1968).

These contours were then tested against computer - contoured maps based on the first order station data. The computer contouring method has been developed by the BMR marine gravity group (Briggs, in prep.); it is based on fitting a two-dimensional spline through unevenly distributed data points. The hand-contoured maps were adjusted where necessary to be consistent with the computer contours. The computer-contouring program was not developed sufficiently to produce the final magnetic maps because of the uneven distribution of data in the oceanic areas around Australia.

The first order data were compared with the International Geomagnetic Reference Field (IGRF) for epoch 1970.0 (Cain et al., 1967). The results are tabulated in Table 2. The IGRF was also computer-contoured for all components and compared with the BMR contours. The ranges of differences are listed in Table 3.

Map presentation

The epoch 1970.0 isomagnetic maps for seven geomagnetic components and their annual rates of change are presented in the folio accompanying this Report.

By international agreement on the cartesian co-ordinate system used to define the magnetic components, the following sign conventions are observed.

F - positive everywhere

H - positive everywhere

X - positive everywhere except in polar regions

Y - positive easterly, negative westerly

Z - positive in northern hemisphere, negative in southern hemisphere

D - positive easterly, negative westerly

I - positive in northern hemisphere, negative in southern hemisphere

The colour convention adopted for the map series is as follows:

Positive magnetic field values - red contours

Negative magnetic field values - blue contours

Positive annual change values - red stippled contours

Negative annual change values - blue stippled contours

Examples of the application of the chart data to estimate values at another epoch are given below.

Town	Date	Magnetic Component	Field 1970.0	Secular Change	Field at date
Birdsville	1/1/72	H	+29450	-60	+29390 gammas
"	"	Z	-46050	-16	-46066 gammas
"	"	F	+54620	-22	+54598 gammas
"	"	X	+29180	-64	+29116 gammas
"	"	Y	+3320	+6	+3326 gammas
"	"	D	+6° 28'	+2'	+6° 30'
"	"	I	-57° 30'	-4'	-57° 34'

DISCUSSION OF RESULTS

The isomagnetic maps of the various magnetic components give regional values of the geomagnetic field and are not designed to highlight magnetic anomalies with linear dimensions less than the effective station spacing. The extent of regional anomalies can be gauged from the third order contouring in the east Australian region; similar departures from the smoothed contours can be expected in other regions. Local anomalies may produce further differences from the smoothed contour field values but these can only be mapped effectively by detailed magnetic surveys. Aeromagnetic surveys give very useful information on where such local anomalies occur.

Although the magnetic component data from all individual survey stations are mutually consistent, the contours have been derived independently with no attempt to make them mutually consistent in terms of electromagnetic theory. This is in accordance with the principle that they should represent observed data.

ACKNOWLEDGEMENTS

The author would like to thank all those who have assisted with the BMR regional magnetic survey and mapping program. In particular he would like to thank the Department of Civil Aviation, the New Zealand D.S.I.R., the Solomon Islands Protectorate Geological Survey, the Department of Supply for assistance at Woomera, Giles, and Gove, Comalco Pty Ltd (Weipa), the Bureau of Meteorology, Qantas Airways Ltd, and the BMR officers most closely connected with the work, P.M McGregor, J. van der Linden, and I. Briggs.

REFERENCES

ALLDREDGE, L.R., 1965 - Analysis of long magnetic profiles. J. Geomag. Geoelect., 17, 172.

ALLDREDGE, L R., VAN VOORHIS, G.D., and DAVIS, T.M., 1963 - A magnetic profile around the world. J. geophys. Res., 68, 3679.

ASKANIA, 1953 - The magnetic Travel - Theodolite. Askania Werke A.G., Berlin, Instrument handbook.

BAUER, L.A., FLEMING, J.A., 1915 - Land Magnetic observations 1911-1913. Publ. Carneg. Instn, 175, II.

BAUER, L.A., FLEMING, J.A., BARNETT, S.J., FISK, H.W., and PETERS, J.W., 1921 - Land magnetic observations 1914-1920. Publ. Carneg. Instn, 175, IV.

BLACKMAN, R.B., and TUKEY, J.W., 1958 - THE MEASUREMENT OF POWER SPECTRA. N.Y., Dover.

BRIGGS, I., in prep. - Computer contouring methods. Bur. miner. Resour. Aust. Rec.

CAIN, J.C., HENDRICKS, J., LANGEL, R.A., and HUDSON, W.V., 1967 - A proposed model for the International Geomagnetic Reference Field, 1965. J. Geomag. Geoelect., 19(4), 335.

FINLAYSON, D.M., 1970a - Preliminary isogonic map of the Australian region 1970.0. Bur. Miner. Resour. Aust. Rec. 1970/90 (unpubl.).

FINLAYSON, D.M., 1970b - First order regional magnetic survey at Cocos Island, Southern Cross and Augusta, 1970. Bur. Miner. Resour. Aust. Rec. 1970/101 (unpubl.).

FINLAYSON, D.M., 1971a - First order regional magnetic survey of eastern Australia, 1968. Bur. Miner. Resour. Aust. Rec. 1971/24 (unpubl.).

FINLAYSON, D.M., 1971b - First order regional magnetic survey of northern and western Australia, 1970. Bur. Miner. Resour. Aust. Rec. 1971/25 (unpubl.).

FINLAYSON, D.M., 1971c - First order regional magnetic survey of the Territory of Papua and New Guinea, 1969. Bur. Miner. Resour. Aust. Rec. 1971/26 (unpubl.).

FISK, H.W., 1927 - Land magnetic and electric observations 1918-1926. Publ. Carneg. Instn, 175, VI.

HOLMES, W.M., 1951 - A provisional isogonic map of Australia and New Guinea for the epoch 1950.5. Bur. Miner. Resour. Aust. Rec. 1951/44 (unpubl.).

LA COUR, 1936 - Le Quartz - Magnetometre QHM. Danish Met. Inst., Comm. Mag. Pub. 15.

LITTLEMORE, 1960 - The Elsec Proton Magnetometer. Littlemore Scientific Engineering Co., Oxford, U.K., Instrument Handbook.

PARKINSON, W D., 1959 - Isogonic map of Australia and New Guinea showing predicted values for the epoch 1960.5. Bur. Miner. Resour. Aust. Rep. 42.

PARKINSON, W.D., and CUREDALE, R.G., 1960 - Isomagnetic maps of Australia for the epoch 1957.5, Part 1 - Eastern Australia. Bur. Miner. Resour. Aust. Rep. 55.

PARKINSON, W.D., and CUREDALE, R.G , 1961 - Isomagnetic maps of Australia for the epoch 1957.5, Part 2 - Central and Western Australia. Bur. Miner. Resour. Aust. Rep. 62.

PARKINSON, W.D., and CUREDALE, R.G., 1962 - Isomagnetic maps of Eastern New Guinea for the epoch 1957.5. Bur. Miner. Resour. Aust. Rep. 63.

QANTAS, 1968 - Analysis of a accuracy of magnetic variation as used in calculating doppler magnetic tracks. Qantas Airways Ltd, internal report.

RAYNER, J.M., 1944 - Lines of equal magnetic declination as at June, 1942. Miner. Resour. Surv., Dep. Supply, Map "Q/Misc/9554A.

SEERS, K.J., 1966 - Three component fluxgate magnetometer, MFR1. Bur. Miner. Resour. Aust. Equipment Handbook M11.

VAN DER LINDEN, J., 1961 - Regional magnetic survey of Queensland and New South Wales, 1960. Bur. Miner. Resour. Aust. Rec. 1961/10 (unpubl.).

VAN DER LINDEN, J., and PARKINSON, W.D., 1963 - Regional magnetic surveys in Australia and Australian Antarctica, 1960-61. Bur. Miner. Resour. Aust. Rec. 1963/61 (unpubl.).

VAN DER LINDEN, J., 1965a - Isogonic Map of Australia and New Guinea for the epoch 1965.0. Bur. Miner. Resour. Aust. Rep. 98.

VAN DER LINDEN, J., 1965b - Regional magnetic surveys in Australia, Australian Antarctica, and the Territory of Papua and New Guinea during 1962. Bur. Miner. Resour. Aust. Rec. 1965/20 (unpubl.).

VAN DER LINDEN, J., 1965c - Regional magnetic surveys in Australia, Australian Antarctica and the Territory of Papua and New Guinea during 1963. Bur. Miner. Resour. Aust. Rec. 1965/218 (unpubl.).

VAN DER LINDEN, J., 1968 - Regional magnetic surveys in Australia, Australian Antarctica, and on some islands in the Pacific and Indian Oceans during 1964. Bur. Miner. Resour. Aust. Rec. 1968/2 (unpubl.).

VAN DER LINDEN, J., 1969 - Regional Magnetic Surveys in Australia, 1965 and 1966. Bur. Miner. Resour. Aust. Rec. 1969/5 (unpubl.).

VAN DER LINDEN, J., 1970 - Third order regional magnetic survey of southern Queensland, 1967. Bur. Miner. Resour. Aust. Rec. 1970/56 (unpubl.).

VAN DER LINDEN, J., 1971 - Third order regional magnetic surveys of eastern Australia, 1968-1969. Bur. Miner. Resour. Aust. Rec. 1971/29 (unpubl.).

VAN DER WAAL, C.A., 1966 - Corrections for absolute and semi-absolute magnetic instruments. Bur. Miner. Resour. Aust. Rec. 1966/207 (unpubl.).

VESTINE, E.H., 1961 - Instruction manual on World Magnetic Survey. Int. Un. Geod. Geophys., Monogr., 11, August 1961.

VESTINE, E.H., LAPORTE, L., LANGE, I., COOPER, C., and HENDRIX, W.C., 1948 - Description of the earth's main magnetic field and its secular change 1905-1945. Publ. Carneg. Instn, 578.

WALLIS, W.F., and GREEN, J.W., 1947 - Land magnetic observations 1927-1944. Publ. Carneg. Instn, 175, III.

W.M.S., 1967 - World Magnetic Survey, Report of colloquium held at Herstomonceux, 4-6/10/66. Geophys. J. Roy. Asstron. Soc., 12(5), 521-37.

WOOD, F.W., and EVERINGHAM, I.B., 1953 - A provisional isogonic map of Australia and New Guinea showing predicted values for the epoch 1955.5. Bur. Miner. Resour. Aust. Rep. 14.

TABLE 1: EPOCH 1970.0 FIRST ORDER MAGNETIC STATION AND MAGNETIC OBSERVATORY DATA

STATION	SITE	LAT.	LONG.	H	dH/dt	D	dD/dt	Z	dZ/dt	F	dF/dt	X	dX/dt	Y	dY/dt	I	dI/dt
ALBANY	C	-34 56.9	117 48.3	22060	-22	-2.98	0.0	55950	-7	60142	-15	22030	-22	-1147	1	68.48	1.0
ALICE BRIDGE		-34 9.6	115 31.8	22040	-18	-4.14	-0.4	55600	-4	59809	-10	21981	-16	-1606	-1	68.38	0.9
ALICE SPRINGS	D	-23 46.5	133 51.4	30440	-30	4.77	0.4	44240	4	53712	-14	30354	+10	2533	1	55.45	1.7
ALPHA		-23 39.3	146 35.2	30910		8.17		42550		52592		30594		4343		54.00	
AMBERLEY		-43 9.0	172 43.0	21790	-45	21.36	4.5	54700	-28	58880	-43	20297	-52	7926	10	68.28	1.8
APIA		-13 48.0	188 15.0	34470	-20	12.14	1.4	20270	-12	40161	-23	33895	-23	7291	10	30.31	-0.0
AYERS ROCK		-25 20.9	131 3.7	29220	-26	4.35	-0.9	46540	2	54953	-12	29136	-25	2216	-10	57.84	1.4
BIRDSVILLE	B	-25 54.8	139 21.1	29440	-44	6.27	0.8	46010	10	54623	-15	29264	-44	3215	2	57.39	2.7
BOULIA	B	-22 54.6	139 53.5	31150	-38	6.53	1.0	42250	23	52492	-4	30948	-39	3542	5	53.60	2.9
BOURKE	D	-30 3.1	145 57.1	27140	-33	9.08	1.2	49530	3	56478	-13	26800	-34	4283	4	61.28	1.8
CAMBRIDGE		-42 49.7	147 30.2	19000	-38	13.50	3.0	60100	-11	63032	-22	18475	-41	4435	7	72.44	1.8
CARNARVON	C	-24 52.9	113 39.9	28000	-11	-1.15	-1.1	46910	-6	54831	-11	27994	-11	-562	-9	59.17	0.4
CANBERRA		-35 17.3	149 18.0	24150	-30	11.70	1.9	53850	-5	59017	-17	23644	-32	4897	7	65.85	1.5
CARNEGIE		-25 48.2	122 56.7	28400	-14	1.87	-1.1	47460	-6	55308	-12	28385	-14	927	-10	59.10	0.6
CEDUNA	D	-32 7.8	133 42.8	25180	-25	4.89	0.6	53100	-3	58708	-13	25089	-25	2142	2	64.63	1.2
COCOS IS		-12 11.9	96 50.1	33030	0	-2.97	-0.9	33200	-12	46832	-4	32986	6	-1731	-9	45.15	-0.9
CONDOBOLIN	C	-33 6.0	147 8.1	25400	-36	9.75	1.6	52350	-1	58187	-17	25033	-37	4301	6	64.12	1.9
COOKTOWN	B	-15 28.5	145 15.0	34610	-16	6.44	1.0	32090	18	47198	1	34389	-17	3906	8	42.84	1.8
CHRISTMAS IS.		-10 25.1	105 40.6	35030	-3	0.67	0.4	30120	5	46199	1	35028	-3	410	4	40.69	0.4
CROYDON	A	-18 12.9	142 15.2	33520	-28	6.17	0.6	36260	14	49380	-9	33326	-28	3803	3	47.25	2.1
CUE	A	-27 25.3	117 52.5	26780	-16	-0.25	-1.4	49350	-6	56060	-13	26780	-16	-117	-11	61.46	0.7
DALY WATERS	B	-16 16.4	133 22.4	34350	-23	4.32	-1.0	34790	15	48890	-5	34259	-22	2587	-12	45.36	1.9
DARU	C	-9 5.2	143 12.3	36470	-16	5.32	0.8	23492	30	43341	1	36313	-19	3381	7	32.79	2.8
DARWIN	D	-12 26.8	130 50.0	35710	-12	3.55	-1.6	29740	15	46472	0	35641	-11	2211	-17	39.79	1.4
DERBY	B	-17 22.1	123 39.6	33390	-16	2.58	-1.3	37220	3	50052	-8	33356	-15	1503	-13	48.10	1.0
EMU		-28 36.9	132 13.2	27160	-31	4.58	0.5	49630	12	56576	-4	27073	-31	2169	1	61.31	2.0
ESPERANCE		-33 43.1	138 38.0	27710	-22	6.72	-0.4	49090	-3	56371	-13	27520	-21	3243	-6	60.56	1.1
EUCLA	B	-31 42.9	128 53.5	25080	-33	3.42	0.0	52770	-7	58427	-17	25035	-33	1496	-2	64.58	1.7
GERALDTON	C	-28 48.6	114 42.1	25670	-13	-1.95	-1.0	50760	-12	56882	-17	25655	-13	-873	-7	63.17	0.4
GILES		-25 2.1	128 17.8	29170	-20	3.40	-0.6	46290	0	54714	-11	29119	-20	1730	-6	57.78	1.1
GNANGARA		-31 47.0	115 57.0	23820	-22	-2.97	-1.2	53490	-2	58554	-11	23788	-22	-1234	-7	66.00	1.1
GOVE		-12 22.6	136 49.4	35960		4.83		98960		46171		35837		3028		38.85	
GRAFTON		-29 46.0	153 1.2	27700	-55	10.88	1.6	47930	3	55349	-24	27202	-56	5228	2	59.98	3.1
GRANITES	B	-20 33.5	130 19.5	32020	-23	3.42	-0.5	40310	8	51480	-8	31963	-23	1910	-6	51.54	1.5
GURNEY		-11 18.7	150 20.3	36120	-17	6.71	1.2	23930	23	43328	-1	35873	-16	4220	11	33.93	2.3
HALLS CK	C	-18 14.1	127 40.0	33230	-15	2.73	-1.2	37990	10	50472	-2	33192	-14	1583	-12	48.82	1.2
HOLLANDIA		-2 34.3	140 30.8	37190		4.13		14800		40027		37093		2678		21.70	
HONIARA		-9 25.4	160 2.8	35810		8.95		20660		41342		35374		5571		29.98	
INGHAM	B	-18 39.6	146 8.9	33240		7.18		36560		49412		32979		4155		47.72	
LAE	B	-6 43.7	147 0.1	36750	-19	6.03	1.5	19400	27	41556	-4	36547	-21	3861	14	27.83	2.7
LAVERTON	A	-28 25.5	122 24.7	26460		1.04		56840		57433		26676		484		62.32	
MACKAY	B	-21 10.1	149 10.9	32320	-21	8.40	1.2	39170	7	50763	-8	31973	-22	4721	8	50.47	1.4
MARYBOROUGH	B	-25 30.8	152 43.1	30700	-41	10.00	1.6	43640	8	53071	-17	29741	-43	5244	7	55.39	2.5
MEEKATHARRA		-26 36.8	118 32.7	27240		1.31		49030		56089		27233		623		60.94	
MILDURA	B	-34 14.3	142 5.1	24340	-30	8.53	1.9	54080	-2	59305	-14	24071	-32	3610	9	65.77	1.5
MOMOTE		-2 4.8	147 25.4	37010	-13	5.09	0.5	12880	30	39187	-2	36864	-13	3284	4	19.19	2.9
MOREE	C	-29 30.0	149 53.0	27620	-50	10.08	1.9	48620	12	55918	-14	27194	-52	4834	6	60.40	3.0
MT VERNON		-24 13.8	118 14.2	28940	-14	0.63	-0.8	45880	0	54245	-7	28938	-14	318	-7	57.76	0.8
NAURU		-0 33.3	166 55.2	35240		9.53		7100		35948		34754		5834		11.39	
NEALE		-28 17.3	125 49.0	27080		2.15		48220		55304		27061		1016		60.68	
NEWCASTLE		-32 47.8	151 50.0	25870	-37	11.50	1.7	51400	-5	57543	-21	25351	-40	5158	5	63.78	1.8
NORFOLK IS		-29 2.5	167 56.2	29070		14.57		43760		52536		28135		7313		56.40	
OCEAN IS		-0 50.9	169 32.0	35610		9.62		6100		36129		35109		5951		9.72	
ONSLOW		-21 38.2	115 6.3	30100	-11	0.42	-0.2	43610	-3	52989	-9	30099	-11	221	-2	55.39	0.5
OODNADATTA	B	-27 33.6	135 27.2	28360		5.35		48400		56097		28236		2644		59.63	
PARAFIELD		-34 47.5	138 38.6	23590	-30	7.57	1.7	55200	-2	60029	-14	23384	-31	3108	8	66.86	1.5
PORT HEDLAND	C	-20 18.8	118 36.7	31410	-10	1.18	-1.0	41500	7	52046	-0	31103	-10	647	-9	52.88	0.8
PORTLAND	B	-38 23.1	141 37.4	21570	-28	8.92	1.4	57460	-5	61469	-15	21309	-29	3345	4	69.46	1.4
PORT LINCOLN	C	-34 36.5	135 52.4	23730	-27	5.08	1.5	55620	2	60471	-9	23637	-28	2101	8	66.89	1.5
PORT MORESBY		-9 24.5	147 9.2	36210	-26	6.22	1.1	23930	33	43403	-3	35997	-27	3923	9	33.46	3.3
QUILPIE		-26 36.5	144 15.2	29170	-36	7.77	0.9	46190	11	54030	-10	28902	-37	3944	8	57.73	2.3
ROMA	B	-26 33.7	148 46.7	29500	-40	9.05	2.0	45340	10	54092	-13	29133	-42	4640	11	56.95	2.5
SWINDELLS		-21 4.9	123 25.3	31270		2.21		42020		52378		31247		1206		53.34	
TANGERANG		-6 10.0	106 38.0	37170	-5	1.05	-1.2	23900	1	44191	-4	37164	-9	881	-13	32.74	0.3
TIBAR		-8 34.0	125 28.0	36800				24500		44210						33.65	
TIBOOBURRA		-29 26.9	142 3.2	27400	-39	7.91	1.2	49610	6	56674	-14	27159	-40	3771	4	61.09	2.2
TOOMORDEN		-27 8.4	134 45.2	28600	-34	5.00	0.5	47870	-2	55763	-19	28491	-34	2493	1	59.14	1.7
TOOLANGI		-37 32.0	145 28.0	22400	-32	10.02	1.8	56390	-5	60676	-16	22016	-34	4126	6	68.34	1.6
VANIMO		-2 41.9	141 18.3	37230	-8	4.28	0.4	14520	33	39961	5	37126	-8	2778	4	21.31	2.9
WARAG		-5 29.5	143 43.6	36880	-10	5.03	0.7	18068	30	41073	4	36738	-11	3254	7	24.12	2.6
WARRACKNABEAL		-36 15.1	142 24.3	23030	-32	9.28	1.1	55740	-3	60310	-15	22729	-33	3714	2	67.55	1.6
WEIPA		-12 41.1	141 54.4	35970		5.43		29520		46532		35809		3404		39.38	
WEWAK	D	-3 35.2	143 40.1	37230	-10	4.70	0.2	15630	30	40378	2	37105	-10	3051	1	22.77	2.7
WILCANNIA	D	-31 30.9	143 22.7	26120	-32	8.58	1.2	51380	6	57638	-7	25828	-33	3897	4	63.05	1.9
WILLIS IS		-16 17.8	149 58.5	34310	-25	7.70	1.3	32400	18	47190	-6	34001	-27	4597	10	43.36	2.2
WINTON	B	-22 23.9	143 3.5	31390	-35	7.02	0.6	41340	10	51907	-13	31154	-35	3836	1	52.79	2.2
WONARAH		-19 53.7	134 20.3	32530	-25	5.12	0.5	39230	15	50963	-4	32400	-25	2903	2	50.33	1.9
WONKERA		-31 6.1	136 46.9	25910	-37	6.12	1.3	51770	10	57892	-8	25762	-36	2782	6	63.41	2.2
WYNDHAM	C	-15 30.6	128 8.8	34380		3.05		34460		48677		34331		1829		45.07	
ZANTHUS	B	-31 2.2	123 34.1	25080	-26	1.15	0.4	52610	-6	58282	-17	25175	-26	583	2	64.51	1.2

Units:— H,Z,F,X,Y, — gamma
D,I — degrees
dH/dt, dZ/dt, dF/dt, dX/dt, dY/dt — gamma/year
dD/dt, dI/dt — min/year

TABLE 2: COMPARISON OF OBSERVED MAGNETIC DATA AND IGRF VALUES FOR EPOCH 1970.0

STATION	LAT.	LONG.	OBS H	CALC H	DIFF H	OBS D	CALC D	DIFF D	OBS Z	CALC Z	DIFF Z
ALBANY	C-34 56,9	117 48,3	22060	21931	129	-2,98	-2,91	-0,07	55950	56454	-504
ALEX BRIDGE	-34 9,8	115 11,8	22040	22210	-170	-4,18	-4,12	-0,06	55600	55729	-129
ALICE SPRINGS	D-23 46,5	133 51,4	30460	30594	-134	4,77	4,91	-0,14	44240	44251	-11
ALPHA	-23 39,3	146 35,2	30910	31082	-172	8,17	8,06	0,11	42550	42348	202
AMBERLEY	-43 9,0	172 43,0	21790	21890	-100	21,33	21,24	0,09	54700	54746	-46
APIA	-13 48,0	188 13,0	34670	34601	69	12,14	11,72	0,42	20270	19146	1124
AYERS ROCK	-25 20,9	131 3,7	29220	29530	-310	4,35	4,25	0,10	46540	46388	152
BIRDSVILLE	B-25 54,6	139 21,1	29440	29610	-170	6,27	6,53	-0,26	46010	46080	-70
BOULIA	B-22 54,8	139 53,5	31150	31288	-138	6,53	6,29	0,24	42250	42469	-219
BOURKE	D-30 3,1	145 57,1	27140	27449	-309	9,08	9,19	-0,11	49530	49569	-39
CAMBRIDGE	-42 49,7	147 30,2	19000	19141	-141	13,50	13,79	-0,29	60100	60080	20
CARNARVON	C-24 52,9	113 39,9	28000	28174	-174	-1,15	-0,87	-0,28	46910	47017	-107
CANBERRA	-35 17,3	149 18,0	24150	24375	-225	11,70	11,72	-0,02	53850	53942	-92
CARNEGIE	-25 48,2	122 56,7	28400	28635	-235	1,87	1,94	-0,07	47460	47563	-103
CEDUNA	D-32 7,8	133 42,8	25180	25351	-171	4,88	5,31	-0,43	53100	53296	-196
COCOS IS	-12 11,9	96 50,1	33030	33215	-185	-2,97	-2,64	-0,33	33200	33234	-34
CONDOBOLIN	C-33 6,0	147 8,1	25400	25620	-220	9,75	10,34	-0,59	52350	52355	-5
COOKTOWN	B-15 28,5	145 15,0	34610	34626	-16	6,48	6,49	-0,01	32090	32055	35
CHRISTMAS IS.	-10 25,1	105 40,6	35030	35238	-208	0,67	0,43	0,24	30120	30172	-52
CROYDON	A-18 12,9	142 15,2	33520	33569	-49	6,17	6,23	-0,06	36260	36170	90
CUE	A-27 25,3	117 52,5	26780	27072	-292	-0,25	-0,08	-0,17	49250	49545	-295
DALY WATERS	B-16 16,4	133 22,4	34350	34295	55	4,32	4,38	-0,06	34790	34694	96
DARU	C -9 5,2	143 12,3	36470	36434	36	5,32	5,31	0,01	23492	23399	93
DARWIN	D-12 26,8	130 50,0	35710	35743	-33	3,55	3,80	-0,25	29740	29674	66
DERBY	B-17 22,1	123 39,6	33390	33429	-39	2,58	2,83	-0,25	37220	37236	-16
EMU	-28 38,9	132 13,2	27160	27552	-392	4,58	4,66	-0,08	49630	49924	-294
ETADUNNA	-28 43,1	136 38,0	27710	27868	-178	6,72	6,69	0,03	49090	49274	-184
ESPERANCE	-33 41,0	121 49,2	23190	23233	-43	-0,15	-0,14	-0,01	55430	55419	11
EUCLA	B-31 42,9	128 53,5	25080	25260	-180	3,42	3,42	0,00	52770	53305	-535
GERALDTON	C-28 48,6	114 42,0	25670	25780	-110	-1,95	-1,86	-0,09	50760	50980	-220
GILES	-25 2,1	128 17,8	29170	29540	-370	3,40	3,51	-0,11	46290	46284	6
GRANGARA	-31 47,0	115 57,0	23820	23931	-111	-2,97	-2,50	-0,47	53490	53739	-249
GROVE	-12 22,6	136 49,4	35960	35743	217	4,83	4,62	0,21	28960	28877	83
GRAFTON	-29 46,0	153 1,2	27700	27981	-281	10,88	11,15	-0,27	47930	47938	-8
GRANITES	B-20 33,5	130 19,5	32020	32177	-157	3,42	4,00	-0,58	40310	40666	-356
GURNEY	-10 18,7	150 20,3	36120	35946	174	6,71	6,84	-0,13	23930	24079	-149
HALLS CK	C-18 14,1	127 40,0	33230	33223	7	2,73	3,48	-0,75	37990	37949	41
HOLLANDIA	-2 34,3	140 30,8	37190	37447	-257	4,13	4,07	0,06	14800	14320	480
HONIARA	-9 25,4	160 2,8	35810	35840	-30	8,95	8,76	0,19	20660	20904	-244
INGHAM	B-18 39,6	146 8,9	33240	33406	-166	7,18	7,13	0,05	36560	36164	396
LAE	B -6 43,7	147 0,1	36750	36654	96	6,03	5,71	0,32	19400	19521	-121
LAVERTON	A-28 25,5	122 24,7	26680	26898	-218	1,04	1,35	-0,31	50860	50399	461
MACKAY	B-21 10,1	149 10,9	32320	32342	-22	8,40	8,23	0,17	39170	38854	316
MARYBOROUGH	B-25 30,8	152 43,1	30200	30302	-102	10,00	9,98	0,02	43640	43379	261
MEEKATHARRA	-26 36,8	118 32,7	27240	27670	-430	1,31	0,97	0,94	49030	48677	353
MILDURA	B-34 14,3	142 5,1	24340	24528	-188	8,53	8,82	-0,29	54080	54230	-150
MOMOTE	-2 4,0	147 25,4	37010	36947	63	5,09	5,18	-0,09	12880	12850	30
MOREE	C-29 30,0	149 53,0	27620	27978	-358	10,08	10,21	-0,13	48620	48289	331
MT VERNON	-24 13,8	118 14,2	28940	29132	-192	0,63	0,81	-0,18	45880	46097	-217
NAURU	-0 33,3	166 55,2	35240	35607	-367	9,53	9,14	0,39	7100	7090	10
NEALE	-28 17,3	125 49,0	27080	27301	-221	2,15	2,56	-0,41	48220	50062	-1842
NEWCASTLE	-32 47,8	151 50,0	25670	26115	-249	11,50	11,73	-0,23	51400	51174	226
NORFOLK IS	-29 2,5	167 56,2	29070	29142	-72	14,57	14,17	0,40	43760	43585	175
OCEAN IS	-0 50,9	169 32,0	35610	35502	108	9,62	9,60	0,02	6180	6784	-604
ONSLOW	-21 38,2	115 6,3	30100	30329	-229	0,42	0,48	-0,06	43610	43333	277
OODNADATTA	B-27 33,6	135 27,2	28360	28435	-79	5,35	5,60	-0,25	48400	48410	-10
PARAFIELD	-34 47,5	138 38,6	23590	23896	-306	7,57	7,56	0,01	55200	55199	1
PORT HEDLAND	C-20 18,8	118 36,7	31410	31474	-64	1,18	1,60	-0,42	41500	41479	21
PORTLAND	B-38 23,1	141 37,4	21570	21643	-73	8,92	9,56	-0,64	57560	57792	-232
PORT LINCOLN	C-34 36,5	135 52,4	23730	23808	-78	5,08	6,37	-1,29	55620	55362	258
PORT MORESBY	-9 24,5	147 9,2	36210	36226	-16	6,22	6,08	0,14	23930	23309	621
QUILPIE	-26 36,5	144 15,2	29170	29405	-235	7,77	7,99	-0,22	46190	46153	37
ROMA	B-26 33,7	148 46,7	29500	29602	-102	9,05	9,20	-0,15	45340	45326	14
SWINDELLS	-21 4,9	123 25,3	31270	31471	-201	2,21	2,56	-0,35	42020	41995	25
TANGERANG	-6 10,0	106 38,0	37170	37223	-53	1,05	1,12	-0,07	23900	24036	-136
TIBAR	-8 34,0	125 28,0	36800	36984	-184		3,07		24500	24728	-228
TIBOOBURRA	-29 26,9	142 3,2	27400	27616	-216	7,91	7,87	0,04	49610	49567	43
TODMORDEN	-27 8,4	134 45,2	28600	28654	-54	5,00	5,36	-0,36	47870	48026	-156
TOOLANGI	-37 32,0	145 28,0	22400	22577	-177	10,62	11,00	-0,38	56390	56521	-131
VANIMO	-2 41,9	141 18,3	37230	37380	-150	4,28	4,21	0,07	14520	14424	96
WABAG	-5 29,5	143 43,6	36880	36977	-97	5,03	4,96	0,07	18080	18177	-97
WARRACKNABEAL	-36 15,1	142 24,3	23030	23191	-161	9,28	9,40	-0,12	55740	55943	-203
WEIPA	-12 41,1	141 54,4	35970	35569	401	5,43	5,50	-0,07	29520	28673	847
WEWAK	D -3 35,2	143 40,1	37230	37154	76	4,70	4,70	-0,00	15630	15450	180
WILCANNIA	D-31 30,9	143 22,7	26120	26393	-273	8,58	8,70	-0,12	51380	51460	-80
WILLIS IS	-16 17,6	149 58,5	34310	34313	-3	7,70	7,61	0,09	32400	32388	12
WINTON	B-22 23,9	143 3,5	31390	31636	-246	7,02	6,98	0,04	41340	41387	-47
WONARAH	-19 53,7	136 20,3	32530	32718	-188	5,12	5,19	-0,07	39230	39140	90
WOOMERA	-31 6,1	136 46,9	25910	26252	-342	6,12	6,36	-0,24	51770	51958	-188
WYNDHAM	C-15 30,6	128 8,8	34380	34494	-114	3,05	3,54	-0,49	34460	34247	213
ZANTHUS	B-31 2,2	123 34,1	25080	25253	-173	1,15	1,32	-0,17	52610	52948	-338

Units:- H,Z -gamma
D -degrees

TABLE 3: DIFFERENCE BETWEEN 1970.0 IGRF AND BMR ISOMAGNETIC MAPS

The values listed are the range of corrections to be applied to IGRF maps to fit BMR maps.

Magnetic Component	Correction Range	Comments
H	-100 to -300 gammas	agreement in TPNG region
D	0 to -0.7°	approx. +1.0° Tasman Sea region
Z	+400 to -400 gammas	
X	-100 to -300 gammas	agreement in TPNG, Vic, Tas regions
Y	0 to -200 gammas	
F	0 to -300 gammas	
I'	0 to +0.5°	agreement in Southern Australia

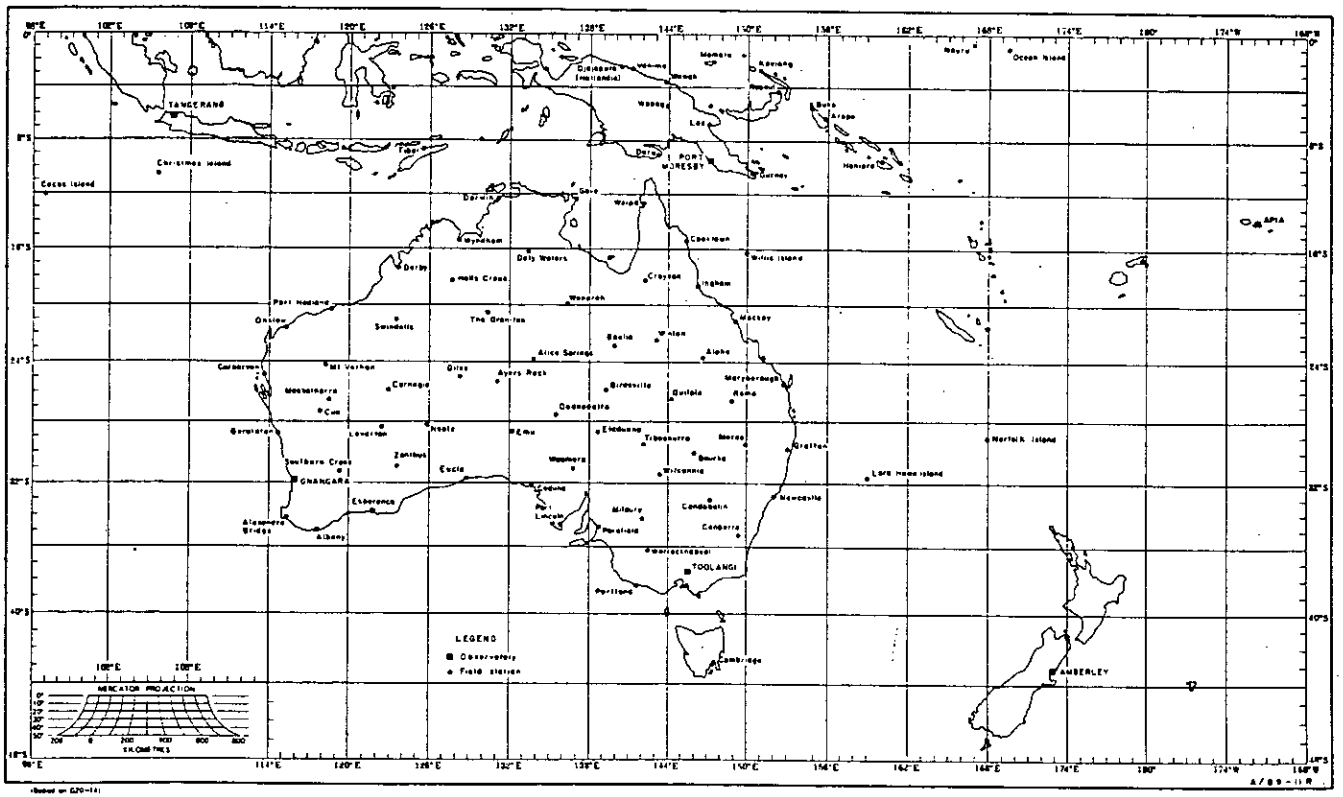

Plate 1 - Australian region magnetic observatories and principal field stations.

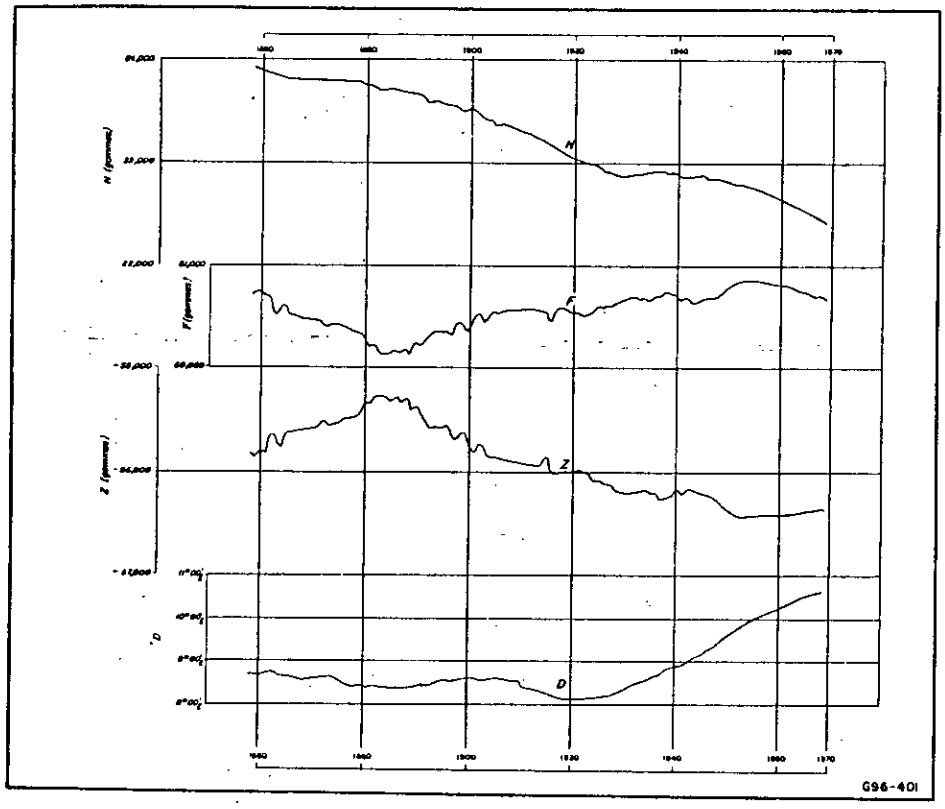

Plate 2 - Secular variation at Melbourne/
Toolangi Observatory, 1858-1969.

PLATE 3

FIELD INSTRUMENTS USED ON FIRST ORDER GEOMAGNETIC SURVEYS

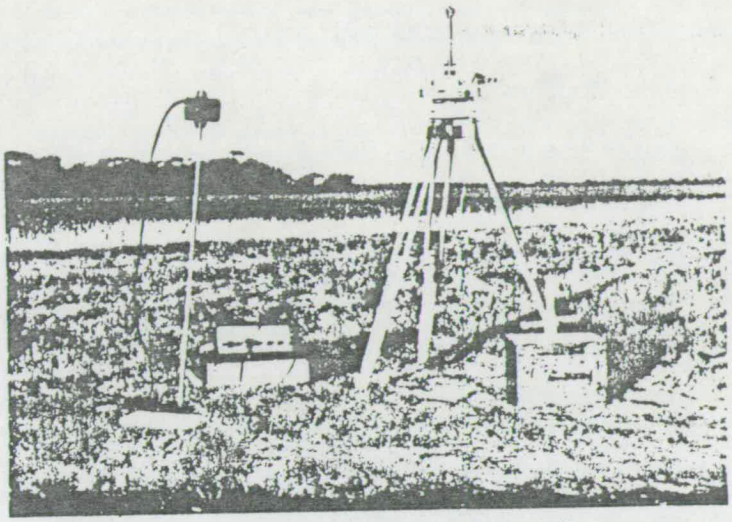

Elsec proton precession magnetometer, Askania declinometer and QHM magnetometer

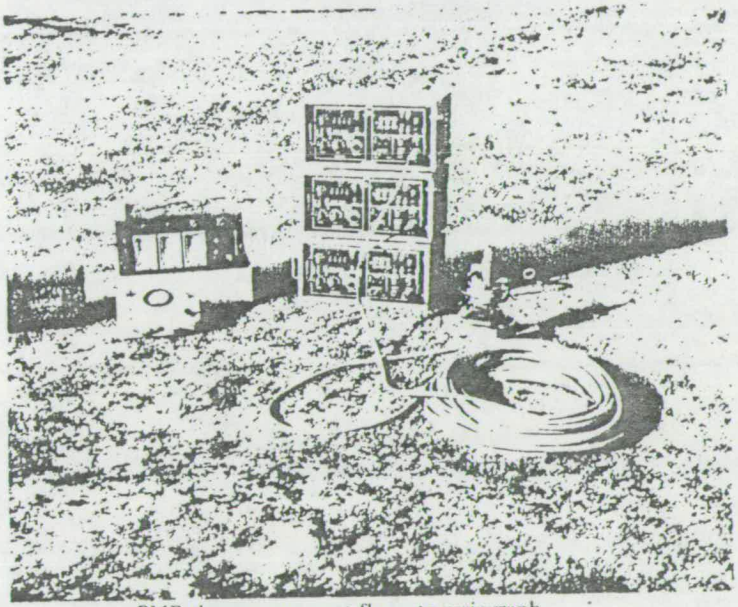

BMR three-component fluxgate variograph